Inhibitors of Sulf-2 and ERK5; Modulators of Cell Signalling Pathways, as Potential Cancer Therapeutics

---

Duncan Miller

This thesis is submitted to Newcastle University
for the degree of Doctor of Philosophy

December 2013

Declaration

The work carried out contributing to this thesis was conducted between October 2010 and September 2013 in the Medicinal Chemistry laboratories, Bedson Building, Northern Institute for Cancer Research at the Newcastle Cancer Centre, Newcastle University, Newcastle upon Tyne, NE1 7RU. The research was conducted in collaboration with scientists at the Paul O'Gorman Building, Newcastle Cancer Centre, and at Cancer Research Technology Discovery Laboratories, The Cruciform Building, Gower Street, London, WC1E 6BT, the Beatson Institute for Cancer Research, Garscube Estate, Switchback Road, Bearsden, Glasgow, G61 1BD and the Babraham Institute, Babraham Research Campus, Cambridge, CB22 3AT.

All of the research presented in this thesis is original in context, and does not include any material or ideas previously published or presented by other authors except where due reference is given in the text.

No part of this thesis has been previously submitted for a degree, diploma or any qualification at any other university.

Acknowledgements

Abstract

The majority of modern targeted cancer therapeutics are directed against components of cell signalling pathways. In this thesis inhibitors of two enzymes involved in cell signalling are investigated.

Sulfatase-2 is a heparan sulfate processing enzyme which has been implicated as a tumour promoter in multiple cancer cell lines, with high Sulf-2 expression being an indicator of a poor clinical prognosis. A monosaccharide sulfamate inhibitor **25**, based on the structure of the endogenous substrate and having an IC_{50} of 130 μM against Sulf-2, has been published. Multiple strategies were pursued in parallel in order to attempt to identify compounds with an IC_{50} against Sulf-2 of < 100 μM for use as chemical tools in target validation studies. These strategies included the preparation of **25**, and of a set of analogues of the generic structure **A**, with variation of substituents at R^1, R^2, R^3 and R^4.
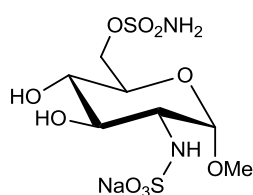
25	**A**	**64**
Sulf-2; IC_{50} 130 μM		
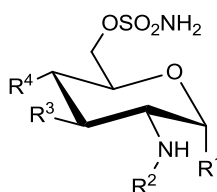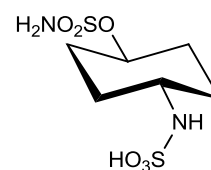
Access to these targets was facilitated by the development of a procedure for regioselective sulfamoylation of the O^6-position of the template. Analysis of this reaction on a model substrate resulted in an increased understanding of the factors which affect the success of sulfamate formation, enabling the reaction to be used with greater efficiency on complex intermediates, and longer reaction sequences to be undertaken to provide the desired test compounds.

Sets of phenolic, benzylic, and cyclic aliphatic sulfamates such as **64** were also designed in an attempt to identify a non-saccharide scaffold which could mimic the spatial arrangements of groups believed to be important for binding of the endogenous substrate to Sulf-2.

Preliminary sulfatase inhibition data has been generated, indicating that analogues of **25** with superior inhibition of Sulf-2 have been identified.

ERK5 is a soluble serine/threonine protein kinase component of a non-classical MAP kinase pathway, which has been implicated in tumour development. Breast cancer patients with high ERK5 levels have decreased disease-free survival, and ERK5 has been shown to have a role in cellular invasion and metastatic spread through affecting cell migration and attachment to the extracellular matrix. A pyrrole carboxamide series of ERK5 inhibitors was optimised from lead compounds including **212**, which suffered from high clearance and low membrane permeability *in vitro*, and translated to poor oral bioavailability *in vivo*.

212 ERK5; IC$_{50}$ 199 nM   **305** ERK5; IC$_{50}$ 7 nM
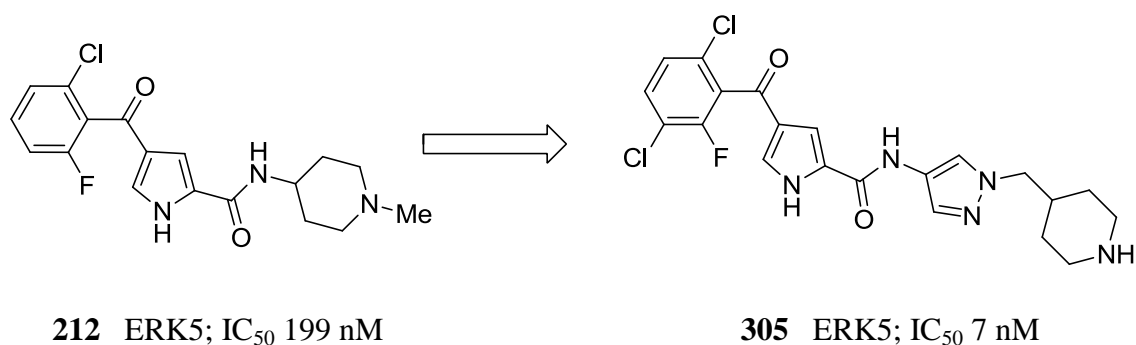
The focus of optimisation studies was to improve ERK5 inhibitory activity and pharmacokinetic parameters to deliver compounds suitable for *in vivo* target validation studies. Analysis of medicinal chemistry design tactics and physicochemical properties, which had previously led to the development of successfully approved kinase drugs was used to guide compound design. The amide substituent was explored and developed into three sub-series. The first analogues prepared suffered from instability in human and mouse liver microsomes and activity against the hERG cardiac ion channel. These flaws were successfully overcome leading to compounds such as **305**, which achieved an ERK5 inhibition improvement of over 20-fold, with good microsomal stability and low hERG activity. Docking of compounds into a recently published co-crystal structure of a small molecule inhibitor bound to ERK5 has provided information on the possible binding mode of the pyrrole carboxamide series.

Abbreviations

5-FU	5-Fluorouracil
ADME(T)	Absorption, distribution, metabolism, excretion, (toxicology)
AIBN	Azo *bis*(isobutyronitrile)
ALK	Anaplastic lymphoma kinase
APC	Adenomatous polyposis coli
app	Apparent
ARS	Aryl sulfatase
ASAP	Atmospheric solids analysis probe
ATP	Adenosine triphosphate
Bcl-2	B-cell leukaemia/lymphoma 2
BCRP	Breast cancer resistance protein
Calcd	Calculated
CAM	Ceric ammonium molybdate
cat	A catalytic amount
CDI	Carbonyldiimidazole
CK1	Casein kinase 1
Cl	Clearance
Cl_{int}	Intrinsic clearance
Cl_u	Unbound clearance
CML	Chronic myeloid leukaemia
c-Pr	Cyclopropyl
CRD	Cysteine-rich domain
DEAD	Diethyl azodicarboxylate

DIBAL	Diisobutylaluminium hydride
DMA	Dimethylacetamide
DMAP	4-(Dimethylamino)pyridine
DMI	1,3-Dimethylimidazolidinone
EGF	Epidermal growth factor
EMATE	Estrone sulfamate
ER	Efflux ratio in the Caco-2 permeability assay
ERK	Extracellular signal-related kinase
ES^+	Electrospray ionisation positive mode
ES^-	Electrospray ionisation negative mode
eq	Equivalents
F	Oral bioavailability
FDA	Federal drug administration
FGE	Formylglycine generating enzyme
FGF	Fibroblast growth factor
F. heparinium	*Flavobacterium heparinium*
F_u	Fraction unbound in plasma
GAG	Glycosaminoglycan
GIST	Gastrointestinal stromal tumour
GlcN	Glucosamine
GlcNAc	Glucosamine-2-acetate
GlcNS	Glucosamine-2-sulfate
GlcNS(6S)	Glucosamine-2,6-disulfate
GOF	Gain of function
GSK	Glycogen synthase kinase
GF	Growth factor
GFR	Growth factor receptor
H2L	Hit-to-lead

HBA	Hydrogen bond acceptor
HBD	Hydrogen bond donor
HCC	Hepatocellular carcinoma
hERG	Human ether-a-go-go-related gene
HexA	Hexuronic acid
HLM	Human liver microsomes
HPLC	High performance liquid chromatography
HRMS	High resolution mass spectrum
HSPG	Heparan sulfate proteoglycan
HTS	High throughput screening
Hünig base	Ethyl diisopropylamine
IC$_{50}$	Concentration for inhibition of 50% of the maximal response
IdoA	Iduronic acid
IdoA(2S)	Iduronic acid 2-sulfate
inh	Inhibition
Jak	Janus kinase
kDa	Kilodalton
IR	Infra-Red
LAH	Lithium aluminium hydride
LE	Ligand efficiency
LipE	Lipophilic efficiency
LOF	Loss of function
MAPK	Mitogen-activated protein kinase
MLM	Mouse liver microsomes
mTOR	Mammalian target of rapamycin
mRNA	Messenger ribonucleic acid
MS	Mass spectrum

Mukaiyama reagent	2-Chloro-1-methylpyridinium iodide
MW	Molecular weight
μW	Microwave irradiation
m/z	Mass charge ratio
NDA	New drug application
NMP	*N*-methyl pyrrolidinone
NSCLC	Non-small cell lung cancer
P_{app}	Apparent permeability rate in Caco-2 cell assay
PARS	*Pseudomonas aeruginosa* sulfatase
PDB	Protein databank
PDGF	Platelet-derived growth factor
P-gp	P-glycoprotein
PH	Plekstrin homology domain
PI3K	Phosphatidylinositol-3-kinase
PIP_2	Phosphatidylinositol diphosphate
PIP_3	Phosphatidylinositol triphosphate
PKC	Protein kinase C
Ppb	Plasma protein binding
ppm	Parts per million
PR	Proline-rich domain
Ptc	Patched
PTEN	Phosphatase and tensin homologue
py	Pyridine
PyBrOP	Bromotri(pyrrolidin-1-yl)phosphonium hexafluorophosphate
RCC	Renal cell carcinoma
ret. t.	Retention time
R_f	Retention factor

RP	Reverse phase
RT	Room temperature
SAR	Structure-activity relationship
Shh	Sonic hedgehog
shRNA	Short hairpin ribonucleic acid
siRNA	Short interfering ribonucleic acid
Smo	Smoothened
STAT	Signal transducer and activator of transcription
STS	Steroid sulfatase
Sulf	Sulfatase
$t_{1/2}$	Half-life
TCF-LEF	T-cell factor/lymphocyte enhancer factor
TFA	Trifluoroacetic acid
TLC	Thin layer chromatography
Tol	Toluene
tPSA	Topological polar surface area
UA	Uronic acid
V_d	Volume of distribution
VEGF	Vascular Endothelial Growth Factor
wnt	Wingless/int protein

Table of Contents

Chapter 1: Introduction

1.1 The Genetic Basis of Cancer

According to the clonal evolution model, cancer is believed to arise through a Darwinian evolution process on a cellular level in multi-cellular organisms.[1] Random introduction of genetic variation may confer an advantage in proliferation or cell survival, which is passed on to subsequent generations of cells through a process analogous to natural selection. The causes of genetic variance range from substitutions, deletions or insertions of single or multiple nucleotide bases, through chromosomal rearrangements, to an increase or decrease in copy number of whole chromosomes.[1] The human genome contains 22,000 protein-coding genes, and mutations have been reported which link over 1.6% of these to cancer development.[2] Mutations found in cancer can be broadly classified as either driver or passenger mutations.[3] Driver mutations affect key pathways associated with cancer development, whereas passenger mutations confer little phenotypic advantage, but may be carried through to later cell generations by being present in cells bearing driver mutations.[1]

In cancer, tumours develop due to abnormal cell proliferation and such malignancies acquire the ability to invade other tissues, forming secondary tumours or metastases. In a seminal paper,[4] six hallmarks of cancer were identified (Figure 1.1).
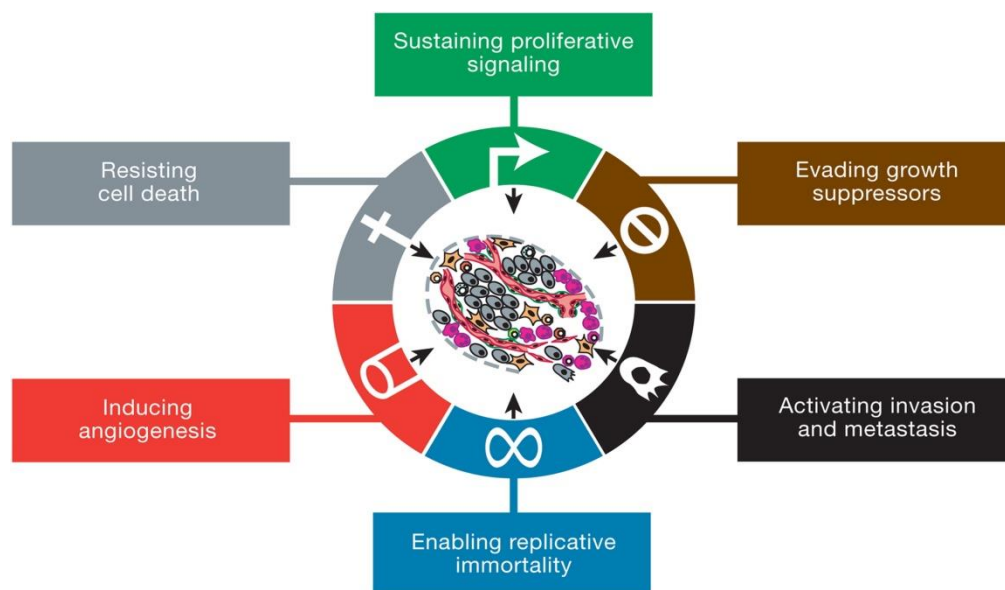
Figure 1.1: The six hallmarks of cancer.[5]

In a recent update, two further emerging hallmarks were suggested; the avoidance of immune destruction, and reprogramming of energy metabolism.[5] For a cell to become cancerous, it must accumulate mutations that confer most or all of these characteristics, and it is thought that between five and seven driver mutations may be required in epithelial cancers such as breast, colorectal and prostate.[1] Under normal conditions it has been estimated that each cell experiences over ten thousand DNA replication errors every day.[6] Genetic defects may be further accumulated with age, through an inherent genetic susceptibility, or following exposure to mutagens such as tobacco smoke or ultra-violet radiation. Viral infections which introduce foreign DNA into a cell, such as the Epstein Barr or hepatitis B viruses, can also disrupt the genetic material of a host cell, contributing to the development of a cancer phenotype.[7]

Genetic alternations may confer gain of function (GOF) or loss of function (LOF) on proteins coded by the affected genes. GOF mutations in oncogenes lead to constitutive activation of pathways, whereas transformations of tumour suppressor genes imparting LOF result in a decrease in regulatory signals. Diverse mechanisms have been identified which underlie each of the functional hallmark capabilities required for a cell to become cancerous, leading to complex heterogeneity in the genetic make-up of tumours between patients, organs, tissues, and even between regions in a single tumour.[8] Cataloguing of DNA mutations present in cancer has revealed that hundreds of genes may be transformed in each cancer subtype.[6]

Genome instability leading to an increased mutation rate has been identified as an additional enabling characteristic, with the development of a 'hyper-mutatable' phenotype facilitating the acquisition of the set of mutations required for a cell to become malignant.[5] In addition to the progressive accumulation of mutations as a tumour matures, it may enter a phase where much more fundamental chromosomal changes are acquired. This phenomenon has been described as genome chaos, and often leads to rapid development of drug resistance and a resultant poor prognosis.[9]

An alternative to the clonal evolution model of cancer development is the cancer stem cell (CSC) model, in which normal cells acquire the properties of stem cells. It is proposed that these cells sustain the tumour and generate heterogeneity through differentiation.[10] It is likely that aspects of both the clonal evolution model, the cancer stem cell model, and genome chaos are active in the replicative cycle of most cancers,

and that effective therapeutic strategies will be required that target pathways involved in each of these models.

1.2 Early Cancer Chemotherapy – Cytotoxic Agents

The advent of cancer chemotherapy can be traced to the observation that nitrogen mustards used on the battlefields of World War I depleted bone marrow and lymph, leading scientists at Yale to find that they could cause regression in lymphoma patients.[11] Chlorambucil (**1**) and cyclophosphamide (**2**) were subsequently introduced as orally available alkylating agents, often providing short-lived beneficial effects in cancer patients.

1   **2**
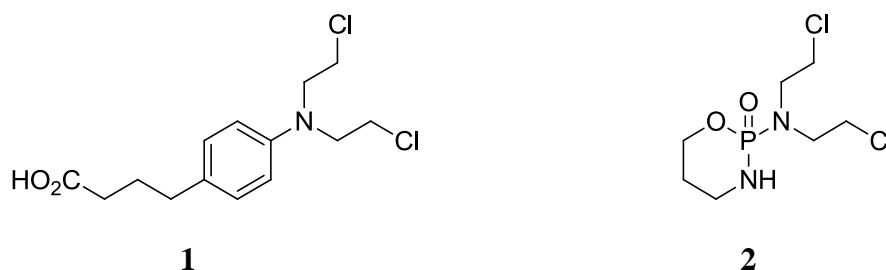
These agents act by cross-linking DNA, leading to cytotoxicity and cell death. Even at this early stage in the development of cancer chemotherapeutics, the issue of selectivity for malignant tissue over healthy cells was apparent. In the case of cyclophosphamide, elevated levels of phosphoramidase in certain tumour types were expected to generate the active nitrogen mustard, imparting a degree of selectivity.[12] However, it was subsequently found that hepatic oxidation by cytochrome P_{450}s could generate the active species, and that the moderate therapeutic index achieved may be attributable to the action of aldehyde dehydrogenase in healthy tissues which converts cyclophosphamide into an inactive metabolite.[12] Resistance to cyclophosphamide treatment occurs through several mechanisms including the development of elevated aldehyde dehydrogenase expression, and increased glutathione production in resistant tumours.[12]

In the 1940s the anti-metabolite class of chemotherapeutics was discovered. Treatment with antifolates such as aminopterin and methotrexate (**3**) led to remission in leukaemia patients,[11] and, subsequently, 5-fluorouracil (5-FU, **4**) was found to be active against solid tumours.[13] Dihydrofolate reductase, an enzyme that converts dihydrofolate to tetrahydrofolate, is inhibited by methotrexate. Tetrahydrofolate is a

co-enzyme required for C1-metabolism in the synthesis of nucleic acid bases required for DNA replication.[14,15] 5-FU is an inhibitor of thymidylate synthase, another enzyme required for nucleotide synthesis.[16] A second mechanism of 5-FU mediated cytotoxicity is through incorporation of fluoronucleotides during DNA and RNA synthesis.[16] Selectivity for tumour cells was anticipated due to their requirement for a higher DNA synthesis rate to support rapid proliferation. In practice, these treatments are accompanied by significant side-effects related to their effects on healthy cells. For example, expression of thymidylate synthase is often higher in tumour cells than in healthy tissue, and healthy cells with lower levels are consequently more sensitive to 5-FU treatment.

3 **4** **5**
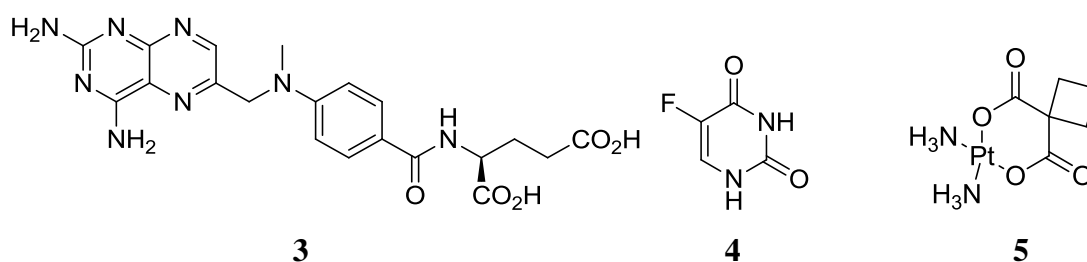
Cisplatin, a platinum complex, was discovered in 1965 and proved to have efficacy in testicular cancer.[17] Carboplatin (**5**) was subsequently developed, providing broader anti-tumour activity and reduced nephrotoxicity as compared to cisplatin.[18] The platinum drugs act by complexing to DNA bases, in particular guanidine, and cross linking DNA strands, resulting in an anti-mitotic effect. A further class of anti-mitotic agents acting through disrupting mitotic spindle formation have also proved effective, such as the vinca alkaloids,[19] and paclitaxel (*Taxol*).[18]

In order to achieve their effects, most cytotoxic anti-cancer drugs require high doses. Throughout their development, toxicity caused by non-specific cytotoxic or anti-mitotic effects has limited the utility and dose that can be administered due to concomitant adverse reactions. Multi-agent approaches are often used to improve outcomes; for example the response rate was improved from 24-26% to 48-92% by the dual use of carboplatin and 5-FU compared to single agent carboplatin therapy in squamous cell carcinomas of the head and neck.[20] However the use of multiple drugs at high concentrations also often leads to significant adverse effects.[21] Cytotoxic drugs can also increase the risk of developing secondary tumours later in life, an issue of particular concern when used in the treatment of childhood cancer.[22]

1.2.1 Resistance to Cytotoxic Chemotherapy

There are many mechanisms whereby tumours may develop resistance to cytotoxic agents. For example, sub-populations of tumour cells often over-express membrane associated efflux pumps, which reduce the access of a drug to its intracellular site of action.[23] In the presence of cytotoxic agents these cellular sub-types gain a survival advantage, and may rapidly become the predominant tumour cell type. Over-expression of promiscuous efflux pumps such as P-glycoprotein (P-gp) often results in such tumours becoming resistance to multiple drugs.[23] Tumour cells may develop other mechanisms to reduce a drug's access to its site of action. Resistant cell types have been found to have altered pH gradients across the membrane of certain intracellular organelles, resulting in sequestration of weakly basic drug molecules in the acidic environment of these organelles prior to secretion.[23] The action of many cytotoxic agents relies on their ability to impede DNA synthesis in a rapidly dividing malignant cell population. Alterations in the DNA damage repair machinery of a tumour cell may allow it to overcome the action of the drug. For example, temozolomide is a DNA alkylating agent that methylates guanine residues, leading to DNA replication errors and cell death. Resistance to temozolomide can develop through the over-expression of the DNA repair enzyme, O^6-methylguanine-DNA methyltransferase (MGMT), which allows the cell to repair the damage caused by temozolomide, thus reducing its cytotoxic efficacy.[23]

1.3 Targeted Therapies

The concept of oncogenes, tumour suppressor genes, and signalling pathways emerged in the 1960s, leading to the idea of cancer therapies targeted at altering the function of specific proteins responsible for driving tumour progression.[11] If the activity of a protein is specific to tumour cells, its selective modulation should result in reduced effects in healthy tissue, leading to fewer dose-limiting adverse events. An early example of a targeted therapy was tamoxifen (**6**), a selective oestrogen receptor modulator (SERM) for the treatment of oestrogen-dependent breast cancer. Tamoxifen was initially developed as an anti-oestrogenic compound primarily for use in the control of fertility and the menstrual cycle.[24] Oestrogens were known to enhance breast cancer tumourigenesis, with increases in oestrogen sensitivity correlating with susceptibility.[24] Tamoxifen subsequently became the agent of choice for endocrine

treatment of breast cancer, and it is estimated that its use has contributed to the survival of over 400,000 female cancer patients.[24] Further generations of SERMs have been developed with reduced side-effect profiles, such a raloxifene (**7**).[25]

6   **7**
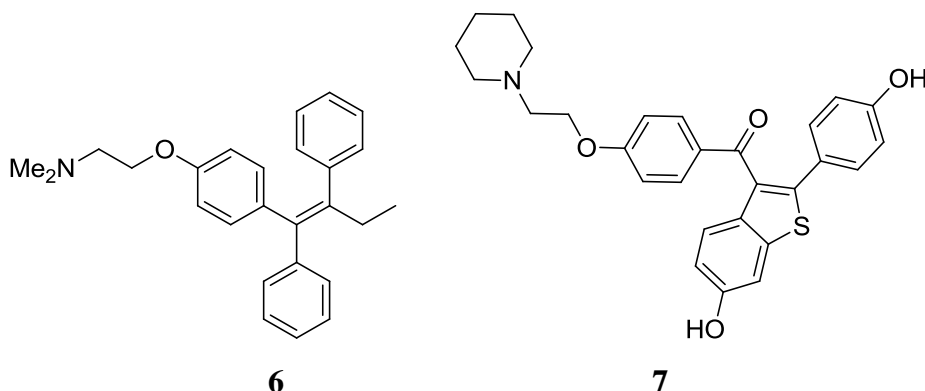
New cell biology techniques have identified signalling networks responsible for the regulation of cellular processes including cell survival and proliferation, which have expanded the scope for possible targeted therapies. Specific components of these signalling networks were recognised as promising biological targets for drug discovery, including targeting growth factors and their receptors, cell cycle modulators, and proteins involved in the regulation of apoptosis.[18] These discoveries have led to a concerted effort to rationally design drugs against a specific protein target for the treatment of cancer.

1.3.1 Cell Signalling Pathways and Targeted Cancer Chemotherapy

Over two hundred cell signalling pathways have been identified which transmit signals from the extracellular environment, transduce them through the cell membrane and cytosol, and cause an intracellular response.[26] Extracellular signals take a variety of forms including hormones, growth factors, cytokines, or extracellular stress signals such as osmotic stress. Intracellular effects may occur in the nucleus, such as the activation of transcription of certain genes, or may be due to activation of enzymes, for example by phosphorylation. Aberrant signalling through these pathways is often a feature of cancer. This can occur through increased production of extracellular growth factors, constitutive activation or amplification of expression of a component protein, or loss of function or expression of a regulatory protein affecting a pathway, resulting in uncontrolled cell growth, proliferation and survival.[27] In a substantial proportion of cancers, mutations are found in genes associated with cell signalling.[26] For example, in

pancreatic cancer between 67% and 100% of cancers have been found to have mutations in genes coding for members of 12 signalling pathways, comprising a total of 63 genetic alterations.[28] Mutational analysis has found that the majority of glioma cases have at least one mutation of a gene encoding for a component of a signalling pathway.[26] The mutation frequency for most somatic genes in tumours is approximately 2%, whereas certain genes have much higher frequencies. For example, mutations in the gene coding for the tumour suppressor protein p53 are present in 41% of cancers, and components of key signalling pathways such as Ras and phosphatidylinositol-3-kinase (PI3K) have 15% and 10% mutation frequency, respectively.[26] The cell signalling cascades are often depicted as independent linear sequences. In reality they comprise a vast, complex, interconnected signalling network (Figure 1.2), often involving regulatory feedback effects between apparently independent pathways, making the effect of blocking one pathway difficult to model.[29] However, certain key pathways have been identified as having potential for intervention, and many of the approved targeted anti-cancer therapeutics modulate these.
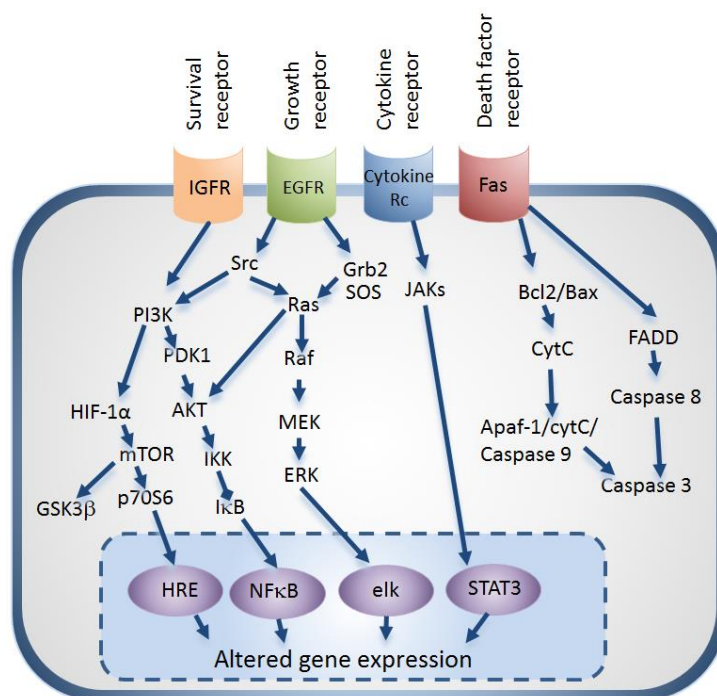
Figure 1.2: Representation of some of the complex interactions which form a cellular signalling network (adapted from reference 30).

The decision as to which pathway component to target for intervention with a small-molecule drug is complex, and will influence the efficacy, side effects, development of resistance, and the patient population that may respond to the drug. For example,

targeting a protein early in a pathway, such as a growth factor receptor, is likely to affect multiple downstream signalling outcomes.[31] This may lead to enhanced efficacy, but may also cause unwanted adverse effects, such as cardiotoxicity.[32] In patients where constitutive activation of an enzyme later in the sequence is driving tumourigenesis, blocking a component upstream of this target is unlikely to be effective.[33] In these cases blocking the aberrant protein itself, or inhibition downstream in the signalling cascade is preferable.[33] However, inhibition of a single downstream element may have limited efficacy if there are multiple parallel downstream pathways. There are also likely to be opportunities for the cell to develop alternative mechanisms to bypass the inhibition of a downstream target, *via* diversion of signal transduction through other pathways.[34] The options for effective combination with other targeted therapies also differ depending on the position in the pathway that is blocked.[34] Thus, the advantages of drugs targeting upstream or downstream pathway components will largely depend on the driver mutations present in a specific tumour.

The classical mitogen-activated protein kinase (MAPK) pathway is an important cell signalling pathway in which gain of function or loss of function of constituent proteins has been implicated in tumour development, and will be discussed in the following sections.

1.3.1.1 The MAP Kinase Signalling Pathways

The MAP kinases are a family of serine/threonine kinases involved in a signalling sequence that transduces extracellular stimuli, leading to intracellular responses such as activation of the transcription of genes.[35] The MAP kinase pathway involves three sequentially activated protein kinases (Figure 1.3).[28]
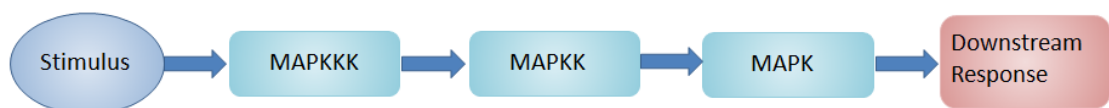
Figure 1.3: General representation of a MAP kinase signalling pathway.

The MAP kinase is activated by phosphorylation by a MAP kinase kinase (MAPKK), which in turn is activated by a MAP kinase kinase kinase (MAPKKK). The MAPKKK is itself activated in response to an extracellular signal such as an increase in growth

factor levels, cytokines, or as a stress response. The MAP kinases phosphorylate transcription factors, protein kinases, structural proteins, cytoplasmic enzymes and phospholipids, leading to diverse downstream events including inflammation, apoptosis, cell differentiation and growth.[36] There are 14 MAP kinases in eukaryotes that are categorised as conventional MAP kinases or atypical MAP kinases. Extracellular signal-related kinase (ERK) 1, 2, and 5, c-Jun amino (*N*)-terminal kinase (JNK), and p38 are classed as conventional MAP kinases, whereas ERK3/4, ERK7 and Nemo-like kinase (NLK) are classed as atypical.[37] The conventional MAP kinases are characterised by having a conserved T-X-Y phosphorylation motif, which is not conserved in the atypical MAP kinases.[28]

1.3.2 The Classical MAPK Pathway

The pathway involving Raf, MEK1/2 and ERK1/2 is referred to as the classical MAPK pathway, and is involved in the control of a number of cellular processes including cell proliferation, differentiation, survival, and motility.[38] Of the MAP kinase pathways, the classical pathway has received the most attention as a target for modulation in cancer chemotherapy.
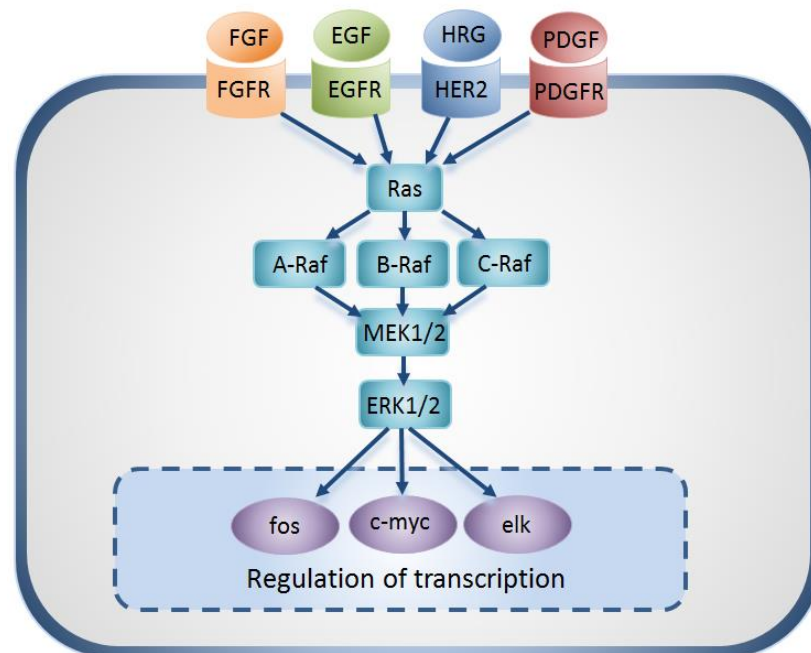
Figure 1.4: The classical MAP kinase pathway (adapted from reference 39).

In response to a growth factor binding to a receptor tyrosine kinase such as the fibroblast growth factor (FGF) receptor, a member of the Ras family of proteins (H-Ras, K-Ras or N-Ras) is activated (Figure 1.4). The Ras protein then activates a MAPKKK of the Raf kinase family (A-Raf, B-Raf or C-Raf), which in turn phosphorylates one of the MAPKK proteins, MEK1 or MEK2, which themselves phosphorylate the MAP kinase ERK1/2 proteins. ERK1/2 is phosphorylated by MEK1/2 on threonine and tyrosine in a Thr-Glu-Tyr (TEY) triad of amino acids. This results in activation of ERK1/2, leading to phosphorylation of downstream targets such as protein kinases, and transcription factors including Elk-1 and c-Myc.[40]

Unregulated activation of this pathway can occur through several mechanisms, including abnormally increased external growth factor availability or mutations conferring increased constitutive activity of a member of the pathway, allowing signalling to occur in the absence of growth factors.[41] Mutations in tyrosine kinase receptors upstream of the classical MAPK pathway such as Epidermal Growth Factor Receptor (EGFR), Fibroblast Growth Factor Receptor (FGFR) 1-3, Platelet Derived Growth Factor Receptor (PDGFR) A & B, and ERBB2, are found in many cancers,[35] as are mutations in the cytoplasmic components including H-Ras, K-Ras, N-Ras, B-Raf, and MEK1 (Table 1.1).[41]

Gene	Tumour type	Frequency
K-Ras	Pancreas	69%
	Lung	16%
	Colon	35%
	Breast	3%
N-Ras	Melanoma	19%
	Colon	2%
	Breast	2%
H-Ras	Breast	1%
B-Raf	Melanoma	41%
	Thyroid Cancer	45%
	Colon	14%
MEK1	Melanoma	3%
	Colon	2.2%

Table 1.1: Frequency of mutations of components of the MAP kinase signalling pathway across cancer types.[41]

1.3.3 Inhibitors of the Classical MAPK Pathway

1.3.3.1 *Inhibitors of the Raf protein family*

There are three functional Raf proteins in humans, termed A-Raf, B-Raf and C-Raf. B-Raf has significantly higher basal kinase activity than A-Raf or C-Raf, and elevated levels have been reported in 60% of malignant melanoma cases, with moderate to high frequency in ovarian, papillary thyroid and colorectal cancers.[42] In melanoma, 80% of cases where Raf is mutated contain a specific substitution of a glutamate residue for a valine (V600E).[43] The resulting sustained signalling through the classical MAPK pathway, in the absence of growth factor signals from the extrinsic environment, leads to a cellular phenotype characterised by uncontrolled proliferation, resistance to apoptosis and increased potential for invasion of other tissues.[43] The marketed kinase inhibitors sorafenib (**8**) and vemurafenib (**9**) include inhibition of B-Raf in their pharmacologic profile. Vemurafenib, which targets the B-Raf V600E mutation, has proven effective in drug-resistant metastatic melanoma patients.[43] Sorafenib is a multi-kinase inhibitor marketed for renal and liver cancer, with potent inhibitory activity against Vascular Endothelial Growth Factor Receptor (VEGFR) 2, PDGFR, and c-kit, in addition to C-Raf (IC_{50} = 6 nM) and B-Raf (IC_{50} = 22 nM).[44]

8   **9**
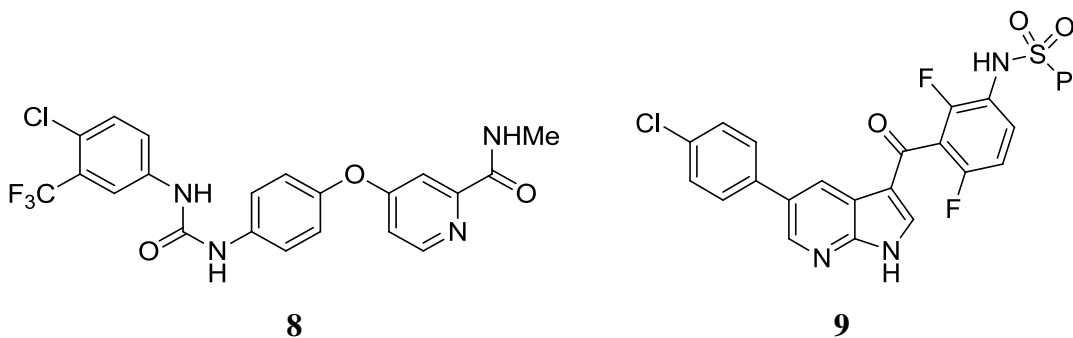
1.3.3.2 *Inhibitors of MEK1/2*

The first MEK inhibitor to enter the clinic, CI-1040 (**10**) suffered from poor bioavailability, resulting in insufficient plasma levels being achieved to validate the target.[45] This was followed by PD-325901 (**11**), which is currently undergoing Phase II trials for melanoma and breast, colon and non-small cell lung cancer (NSCLC).[46] Selumetinib (**12**) from AstraZeneca is a dual MEK1/2 inhibitor with an IC_{50} against MEK1 of 14 nM.[47] In preclinical studies the drug demonstrated potent anti-melanoma

activity in *in vitro* and *in vivo* models. Clinical studies are currently on-going but efficacy outcomes have been modest thus far.[47]

10   **11**   **12**
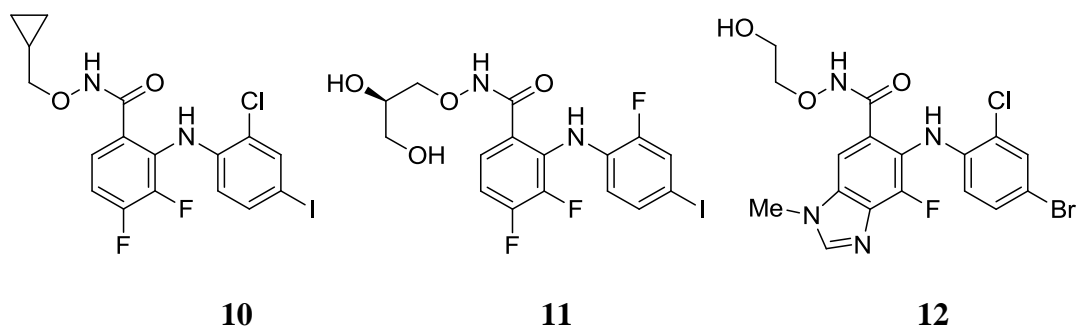
1.3.3.3 ERK1/2 inhibitors

To date no inhibitors of ERK1 or ERK2 have entered clinical trials. However, several chemotypes have been identified which provide potent inhibition of these kinases.

13
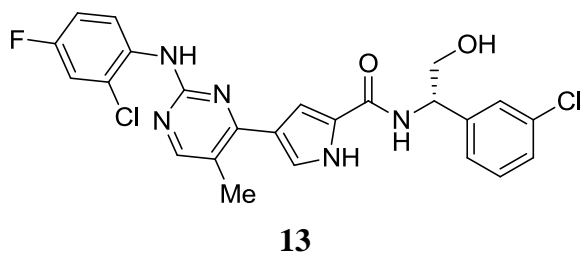
Compound **13** is a potent inhibitor of ERK2 ($IC_{50} < 2$ nM) based on a pyrrole carboxamide scaffold, with over 200-fold selectivity against a panel of kinases.[38] The compound exhibits good oral bioavailability in rat (F = 65%) and mouse (F = 67%), and was shown to be active in a cell proliferation assay in the HT29 human colorectal cancer cell-line with a GI_{50} of 48 nM.

14   **15**
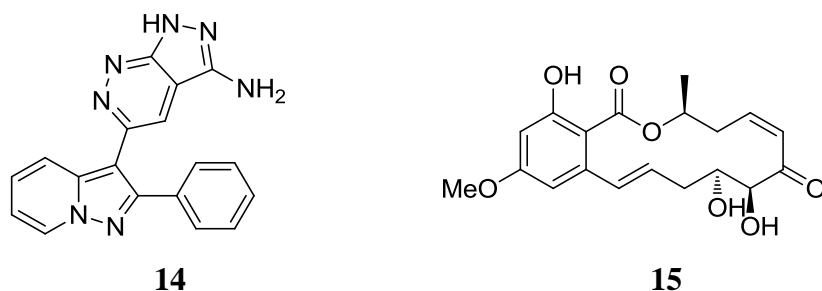
FR180204 (**14**) is an ATP-competitive inhibitor of ERK1 ($IC_{50} = 0.51$ μM) and ERK2 ($IC_{50} = 0.33$ μM).[48] The benzoxacyclotetradecine derivative FR148083 (**15**) is an ERK2 inhibitor ($IC_{50} = 80$ nM) which acts *via* an irreversible mechanism, whereby a cysteine residue in the active site of ERK2 covalently binds to the enone Michael acceptor functionality.[49] The covalent mechanism confers selectivity over other MAP

kinases such as JNK and p38, in which the ATP-binding site cysteine residue is not conserved.[48]

1.3.4 Other Cancer Chemotherapeutics Targeting Signalling Pathways

Imatinib (*Glivec*) (**16**), the first molecularly targeted cancer therapy to reach the market, was designed to block sustained proliferative signalling in chronic myeloid leukaemia (CML) caused by a t(9:22) gene translocation. This genetic defect, also known as the Philadelphia chromosome, produces a fusion of the Bcr and Abl gene products,[50,51] lacking the regulatory control elements of Abl kinase resulting in constitutive signalling, which affects multiple downstream signalling pathways.[52] Phenotypic effects of this activity include increased proliferation, resistance to apoptosis, and altered adhesion properties.[53] Inhibition by imatinib of the Bcr-Abl kinase is largely responsible for its efficacy in the treatment of Philadelphia chromosome positive CML.[52] Since this fusion protein is present only in tumour cells, selectivity over healthy tissue can be achieved. Imatinib is also used for the treatment of gastrointestinal stromal tumours (GIST), where it acts through a different mechanism. GIST, a form of soft tissue sarcoma, is often driven by mutations resulting in constitutive activation of the c-Kit kinase, or of the platelet derived growth factor receptor (PDGFR) kinase. Imatinib potently inhibits both c-Kit and PDGFR,[50] and GIST patients dosed with imatinib show a response rate of 38% compared with 0-5% on previous chemotherapy regimes.[54]
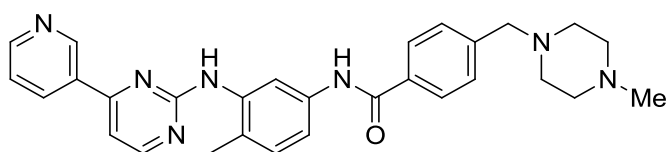
16

Clinical responses in both CML and GIST correlate with the presence of Bcr-Abl, and mutations in c-Kit or PDGFR, respectively. In the treatment of chronic phase CML, imatinib results in 90% remission rates.[26] However, there is a high incidence of resistance arising during treatment. The principal mechanisms for acquisition of resistance to imatinib is the development of sub-clones of tumour cells bearing single amino acid changes in the drug-binding site, which reduce its binding affinity. Drug treatment results in selective growth advantage of the resistant sub-clones.[50]

Nevertheless, the advent of imatinib treatment has greatly improved the prognosis and survival of CML and GIST patients, and provided a positive proof of concept for targeted cancer therapies. The second generation agents, dasatinib (*Sprycel*) and nilotinib (*Tasigna*), have been designed to have broad spectrum Bcr-Abl activity against a wide range of known imatinib resistant mutant cell lines and ponatinib (*Iclusig*), a third generation Bcr-Abl inhibitor which is active against dasatinib and nilotinib resistant mutants, has also recently been approved.[55]

The binding of growth factors to their receptors is one of the common methods by which cell signalling pathways are activated, and therapies which directly target growth factor receptors have been developed. Activation of a single class of receptor can initiate signal transduction through multiple pathways, leading to diverse intracellular responses. Increased growth factor availability, or mutations leading to constitutive activation of growth factor receptors are common drivers of tumour development, and some of the most successful marketed targeted anti-cancer agents act on these receptors.

Gefitinib (**17**) and erlotinib (**18**) are examples of agents that directly target the EGFR growth factor receptor tyrosine kinase, and which have proven effective in the treatment of non-small cell lung cancer (NSCLC) in cases where mutations in EGFR are present.[56] These account for around 10% of NSCLC cases, and in these cases the response rate to gefitinib is 75%, compared to 30% using cytotoxic drugs, with a doubling of progression-free survival from five to eleven months.[56] However, resistance to gefitinib treatment usually arises within two years of the commencement of treatment.

17   **18**
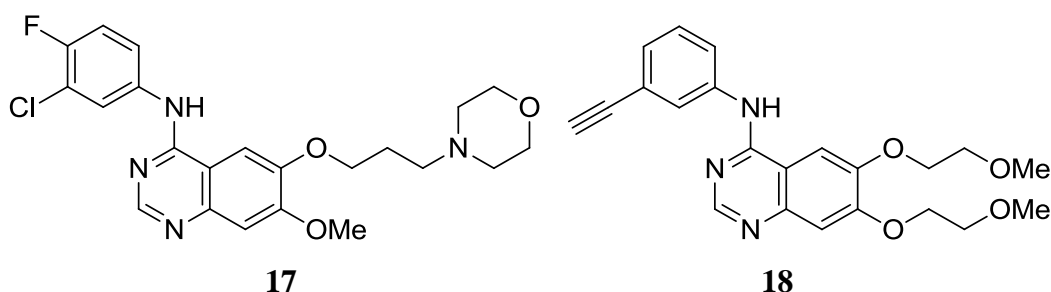
In addition to targeted small molecule inhibitors, antibody therapies have also emerged as injectable biologic treatments. Examples of these therapies are trastuzumab (*Herceptin*) an antibody targeted at the Human Epidermal Growth Factor Receptor (Her-2), and bevacizumab (*Avastin*) targeted at the VEGF Receptor.[57] These bind to

their respective receptors, preventing interaction with the endogenous growth factor ligands, or promoting receptor internalisation, thereby reducing downstream signalling.[57]

The majority of small-molecule targeted therapies which have been approved for use in human cancers are directed towards the inhibition of kinase enzymes in signalling pathways. Analysing the design and discovery of those kinase inhibitors which have reached the market can provide useful insights into the challenges and successful tactics that have been used. This will be explored further in chapter 6 in the formulation of strategies for the optimisation of inhibitors of ERK5.

1.3.5 Alternative Approaches to Targeted Therapy

In addition to drugs affecting cell signalling pathways, targeted cancer therapeutics which act on components of other cellular processes have also been developed. For example, the 26S proteasome has been targeted, which is involved in the degradation of poly-ubiquitin tagged proteins, including many involved in the cell cycle such as the tumour suppressor p53, and the endogenous cyclin-dependent kinase inhibitors p21 and p27.[58] In tumour cells the level of the 26S proteasome is often up-regulated, and its inhibition was found to induce apoptosis, arrest growth, and increase sensitivity to cytotoxic agents and radiotherapy, with little effect on healthy cells. Bortezomib (*Velcade,* **19**) is a boronic acid based inhibitor of the 26S proteasome which is approved for the treatment of multiple myeloma.[58] The exact mechanism of action of **19** is likely to be complex due to the number of proteasomal substrates affected by the activity of the drug.[59] In addition to stabilising the tumour suppressor p53, effects on the NF-κB pathway and an increase of pro-apoptotic factors derived from the B-cell leukaemia/lymphoma 2 (Bcl-2) family of proteins, have been implicated in its functional response.[59]
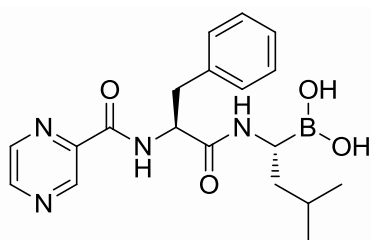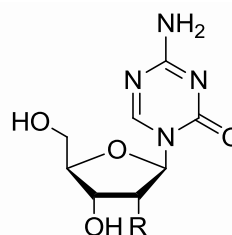
19   **20** R = H   **21** R = OH

A reduction of susceptibility to apoptosis is a common mechanism of tumour resistance to both cytotoxic and targeted agents. The Bcl-2 protein family has pro-apoptotic functions, and new targeted therapies that affect this apoptotic pathway are under investigation, such as ABT-263.[60] Epigenetic changes which allow tumour cells to transiently tolerate drug treatment have also been proposed, with a change in the methylation state of the promoter region of many genes which affects their transcription being observed in cancer. Histone deacetylase inhibitors have shown activity against drug-tolerant cancer cells,[61] and two DNA-methyltransferase inhibitors, decitabine (*Dacogen*, **20**) and azacitidine (*Vidaza*, **21**) have been approved for myelodysplastic syndrome,[62,63] and are undergoing clinical trials for acute myeloid leukaemia.[8,64,65]

1.4   Resistance to Targeted Therapies

The benefits of targeted agents have often proven to be short lived due to rapid emergence of drug resistance. In addition to the mechanisms discussed in section 1.2.1, such as the action of efflux pumps reducing a drug's access to its site of action, resistance to targeted therapies may arise through mutations in the drug target itself, reducing the binding affinity of the drug. These may be single point changes affecting a single amino acid in the protein sequence, or may be through changes in the splicing pattern, as is the case for some resistance to vemurafenib.[66] These resistance mutations may arise during drug treatment (acquired), or may be present in a small number of tumour cells prior to drug treatment (intrinsic).[8] Resistance may also develop through mutations that lead to a switching of pathway dependency in a sub-population of tumour cells. The approach of employing combinations of targeted agents against components of different signalling pathways, or single agents having activity against multiple targets may provide an approach to reducing the rate of development of resistance through such mechanisms.[67] While the development of new agents as stand-alone therapies is important, there is also likely to be significant benefit in developing agents which expand the options for combination therapy, affecting parallel pathways that may confer resistance to existing therapies.

1.5 Stratified Medicine

Targeted therapies, by their nature, only produce a response in patients having the underlying genetic defect for which the targeted drug aims to compensate. This led to the emergence of the paradigm of personalised or stratified medicine, whereby genetic testing or biomarker assessment is used to identify patient populations harbouring specific driver mutations that are therefore likely to be responsive to a specific drug.[68] Those with non-responsive genotypes can be directed to a more appropriate therapeutic strategy (Figure 1.5).
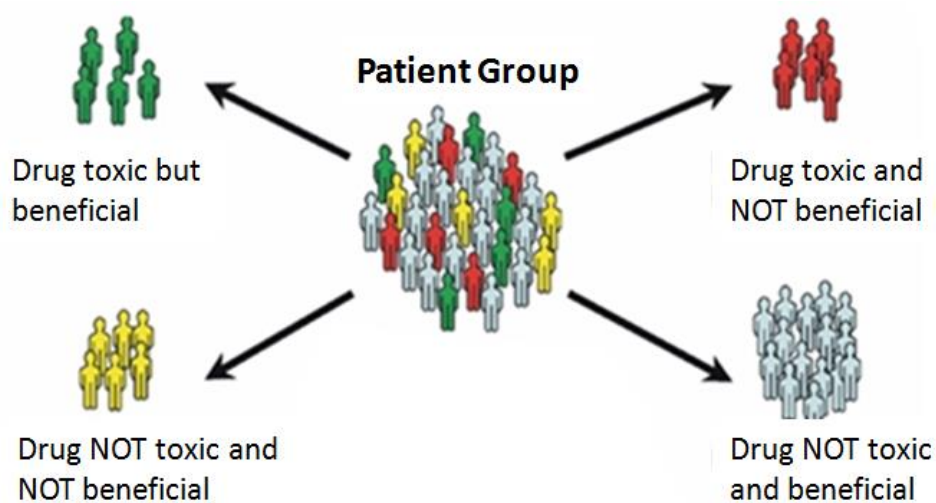
Figure 1.5: Personalised medicine allows only patients who will benefit, and experience low toxicity to be selected for treatment with a targeted agent.[69]

Personalised medicine requires the development of methods for screening for the presence of the genetic defect which is susceptible to inhibition by the targeted agent, to allow selection of patients who will be responsive to the drug. For example, tests have been developed to identify CML patients with the Bcr-Abl fusion protein who may respond to imatinib treatment, melanoma patients having the V600E mutation responsive to treatment with vemurafenib, and EGFR mutations for erlotinib and gefitinib in non-small-cell lung cancer.[70] However, there is still a need to improve the sophistication of the screening used to identify responsive patient populations, as the genetic instability and associated heterogeneity in the tumour cell genome often leads to the development of redundancy in reliance on a particular driver mutation or pathway.[8]

1.6 The Drug Discovery Process

The current prevalent drug discovery paradigm involves identification of a biological target, the modulation of which is hypothesised to affect the progression of a disease. A process of validation of the target follows, with biological studies designed to examine the effects of altering the activity of the target on the phenotype of cells, tissues or whole organisms.[71]
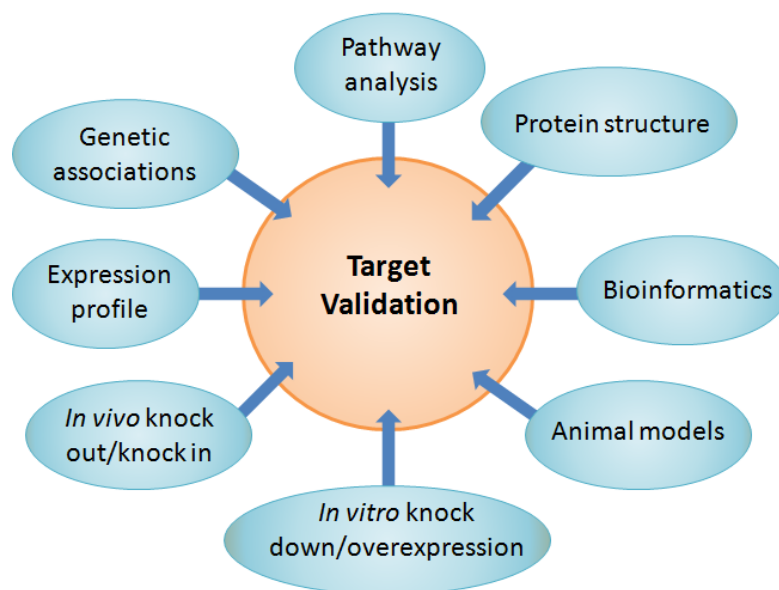
Figure 1.6: Factors involved in validation of a biological target (adapted from ref. 72).

This may be achieved through multiple diverse experiments, including examination of organisms genetically engineered to lack the gene coding for the target of interest (knock-out animals), the application of tools such as short interfering RNA (si-RNA) to block transcription of the gene of interest, or the use of small molecules that interact with the target to modulate its activity (Figure 1.6). One role of the medicinal chemist in this target validation phase is to identify 'tool' compounds that selectively modulate the target, initially for use in *in vitro* studies. The key criteria for an *in vitro* tool are potency and selectivity, with sufficient compound solubility to achieve a concentration to effectively modulate the target in the biological studies.

Once evidence for the role of a target in a disease has been established *in vitro*, tool reagents suitable for *in vivo* evaluation are required. In addition to potency and selectivity, the design of these compounds requires a consideration of ADMET (Absorption, Distribution, Metabolism, Excretion, Toxicology) parameters to ensure

sufficient free compound levels are maintained for the duration of the experiment.[73] Depending on the disease under investigation, sub-optimal pharmacokinetics may be overcome by the use of non-oral routes of administration such as intravenous bolus injection or infusion, or intraperitoneal injection.[74]

When the potential benefit of modulation of the target in the treatment of the disease has been established, a full drug discovery project is initiated (Figure 1.7). A hit-to-lead (H2L) program ensues, which may take the chemical tool as a starting point, or may require the identification of alternative chemical hits. New hit matter is often generated using high-throughput screening (HTS) techniques, where large libraries of chemically diverse templates are screened against the target. Alternatively, fragment-based approaches may be employed,[75] or compounds may be designed based on known inhibitors of the target or close family members. *De novo* design based on the endogenous ligand is a further possible approach. In practice, the drug discovery process is often initiated in parallel with the target validation and tool identification studies.[76]
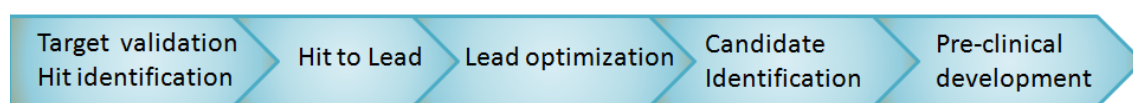
Figure 1.7: Phases in the pre-clinical drug discovery process (adapted from ref. 77).

In the H2L phase the structure-activity relationships (SARs) of initial hits are explored to ascertain functional groups required for activity, and those that may be varied to improve potency. The potential for oral absorption (assuming the intended route of delivery is oral), and pharmacokinetic parameters are also assessed in *in vitro* assays. Attempts are made to replace structural alerts which have been implicated in toxic outcomes in the clinic.[78] Lead criteria are defined that reflect the progression of a hit structure into a lead, which has clear potential to be developed into a drug.

The lead optimisation (LO) process involves combining all of the desired properties into a single agent suitable for progression into clinical trials. Thus, in addition to good potency against the primary target and selectivity over relevant secondary targets, the candidate molecule must demonstrate *in vivo* pharmacokinetics, safety, and pharmaceutical properties suitable for entering clinical evaluation studies.[79]

1.7 The Sulfatase-2 and ERK5 Projects

The global incidence of new cancer cases is predicted to rise from 12.7 million in 2008 to 20.3 million by 2030.[80] Despite the advent of new targeted agents and antibody therapies, cancer related deaths are expected to increase from 7.6 million in 2008 to 13.2 million by 2030.[80] Thus, the need for new cancer treatments is clear. Inhibition of components of cell signalling pathways has provided targeted therapies which are efficacious in the treatment of cancer, and further opportunities exist for modulators of components of signalling cascades. This approach is a current area of focus for anti-cancer drug discovery efforts, and the two projects described in this thesis centre on attempts to develop small molecules that modulate key signalling pathways. However, the approaches taken in the two projects differ significantly. In the sulfatase-2 (Sulf-2) project the aim is to affect both the availability of growth factors, and the activation of certain growth factor receptors, and can be thought of as an "upstream" approach *i.e.* modulating a pathway early in the signalling sequence. This approach is likely to affect multiple signalling pathways. In contrast, the ERK5 project aims to identify selective inhibitors of a non-classical MAP kinase pathway, where targeting the ERK5 MAP kinase directly affects its transcriptional activation and phosphorylation roles. This approach can therefore be considered as a "downstream" approach, affecting a signalling pathway at a late point in its signalling cascade.

The two projects described in this thesis cover different stages of the drug discovery process. The Sulf-2 project is at the target validation stage. Hence the focus of medicinal chemistry design efforts are on identifying chemical tools for use in *in vitro* and *in vivo* models to assess the effect of inhibition of Sulf-2 on cellular phenotypes and tumour growth. The initial aim of this project was improving potency and achieving selectivity to provide a fit-for-purpose tool molecule.

The ERK5 project is at a more mature stage, entering the lead optimisation phase. In addition to primary potency and selectivity, compound design was required to incorporate multiple parameters including parallel optimisation of ADMET properties and pharmacology.

Chapter 2: Introduction to the Sulf-2 Project

Sulf-2 is an extracellular enzyme that affects multiple signalling pathways, and has been implicated in the progression of several cancers including hepatocellular carcinoma.[81] Literature reports and earlier work at the Northern Institute for Cancer Research suggest that modulation of Sulf-2 activity by small molecules may be beneficial in the treatment of cancer.

2.1 The Human Sulfatase Family

Seventeen human sulfatases have been identified and are categorised into two classes (Tables 2.1 and 2.2).[82] The first category comprises arylsulfatases, which catalyse the removal of a sulfate from a phenol in a substrate. The most widely explored of these is arylsulfatase C (ARSC), which removes sulfate from steroids such as oestrone sulfate, **22** (Scheme 2.1).
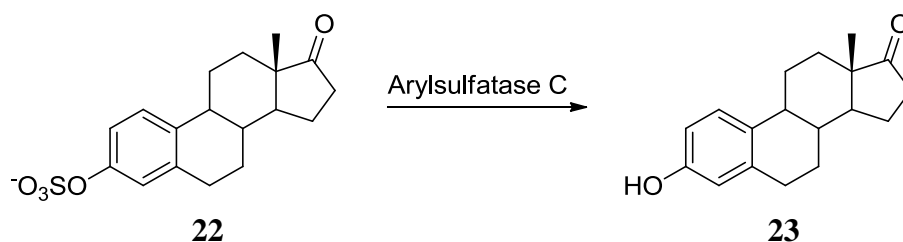
Scheme 2.1: The action of arylsulfatase C on its endogenous substrate, oestrone sulfate.

The second category catalyse removal of sulfate groups from alcohols in saccharides (Table 2.2). In the endogenous substrates, the saccharide to be de-sulfated is usually contained within a polysaccharide, which may be part of a larger proteoglycan such as a heparan sulfate proteoglycan (HSPG). The members of the sugar sulfatase family have different specificities for sulfate removal, either from distinct sites on a single sugar, or from different sugar residues.[83] Sulfatase-1 (Sulf-1) and sulfatase-2 (Sulf-2) are the only family members reported to have the ability to function as endosulfatases, removing sulfates from the O^6-position of glucosamine residues internal to the heparan sulfate structure.[82] This is in contrast to lysosomal sulfatases such as glucosamine-6-sulfatase, which remove sulfates exclusively from the O^6-position of glucosamine residues at the non-reducing end of heparin during its degradation in the lysosome.[83]

Sulf-1 and Sulf-2, were first cloned in 2002,[84] with the genes coding for them being located on human chromosomes 8 and 20, respectively.[85]

Sulfatase	Synonyms	Endogenous Substrate	Removes Sulfate from	Site of Action
Arylsulfatase A	ARSA	Sulfatide (a sulfated galactosylceramide)	Phenol, saccharide	Lysosome
Arylsulfatase B	ARSB	Dermatan sulfate, Chondroitin sulfate	Phenol, saccharide	Lysosome
Arylsulfatase C	ARSC Steroid sulfatase, STS Oestrone sulfatase	Steroid sulfates	Phenol	ER[a]
Arylsulfatase D	ARSD	Unknown	Phenol	ER[a]
Arylsulfatase E	ARSE	Unknown	Phenol	Golgi apparatus
Arylsulfatase F	ARSF	Unknown	Phenol	ER[a]
Arylsulfatase G	ARSG	Unknown	Phenol	ER[a]

[a] Endoplasmic reticulum

Table 2.1: The arylsulfatase family.

Sulfatase	Endogenous substrate	Removes sulfate from	Site of Action
Galactosamine-6-sulfatase	Chondroitin sulfate, Keratan sulfate	Terminal O^{6-} galactosamine	Lysosome
Glucosamine-3-sulfatase	Heparan sulfate	Terminal N^{2-} glucosamine-	Lysosome
Glucosamine-6-sulfatase	Heparan sulfate, Keratan sulfate	Terminal O^{6-} glucosamine-	Lysosome
Glucuronate-2-sulfatase	Heparan sulfate	Terminal O^{2-} glucuronic acid	Lysosome
Heparan-*N*-sulfatase	Heparan sulfate	Terminal N^{2-} glucosamine	Lysosome
Iduronate-2-sulfatase	Heparan sulfate, Dermatan sulfate	Terminal O^{2-} iduronic acid	Lysosome
Sulfatase-1	Heparan sulfate	Non-terminal or terminal O^{6-} glucosamine	Extracellular
Sulfatase-2	*Heparan sulfate*	*Non-terminal or terminal O^{6-} glucosamine*	*Extracellular*

Table 2.2: The sugar sulfatase family.

2.2   Heparan Sulfate Proteoglycans: Endogenous Substrates of Sulf-2

Heparan sulfate proteoglycans (HSPGs) consist of a protein core conjugated to multiple heparan sulfate polysaccharide chains. HSPGs comprise five protein classes, the syndecans, glypicans, perlecans, agrins, and type XVIII collagens.[86] The polysaccharide chains are composed to a large extent of repeating disaccharide units of hexuronic acids (glucuronic acid or iduronic acid) and glucosamine (Figure 2.1).[87] Heparin is a closely related polysaccharide with no protein component, and consists predominantly of the same repeating disaccharide unit.
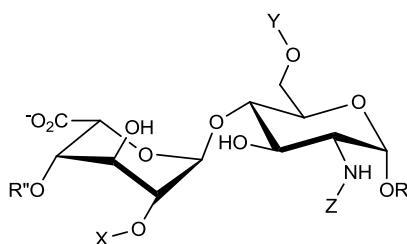
Figure 2.1: The basic repeating disaccharide unit of heparan sulfate chains. R' and R'' denote points of attachment to further disaccharide motifs. X & Y may be independently H or sulfate, and Z may be H, sulfate or acetate.

Mature heparan sulfate oligosaccharide chains are typically between 50 and 200 residues long. Both HSPGs and heparin contain considerable heterogeneity driven by C^5-epimerisation, sulfation of the O^6- or N^2-position of the glucosamine subunit, acetylation of the glucosamine N^2-position, and the sulfation state of the O^2-position of iduronic acid.[82] Through compositional analysis, at least twelve disaccharide units having different sulfation and acetylation patterns have been identified.[88] Heparin and heparan sulfates differ in the density of sulfation, with heparin being much more highly sulfated. In heparin the trisulfated disaccharide unit (Figure 2.1, X, Y, Z = SO_3^-) is predominant, whereas the polysaccharide chains of HSPGs contain much greater heterogeneity in their sulfation pattern, with regions of high sulfation[89] comprising 2-8 highly sulfated disaccharide units[90,91] separated by more flexible regions of lower sulfation (Figure 2.2).[90] In bovine kidney HSPGs the trisulfated disaccharides have been show to account for 6.4% of the total disaccharide content of the proteoglycan.[88]
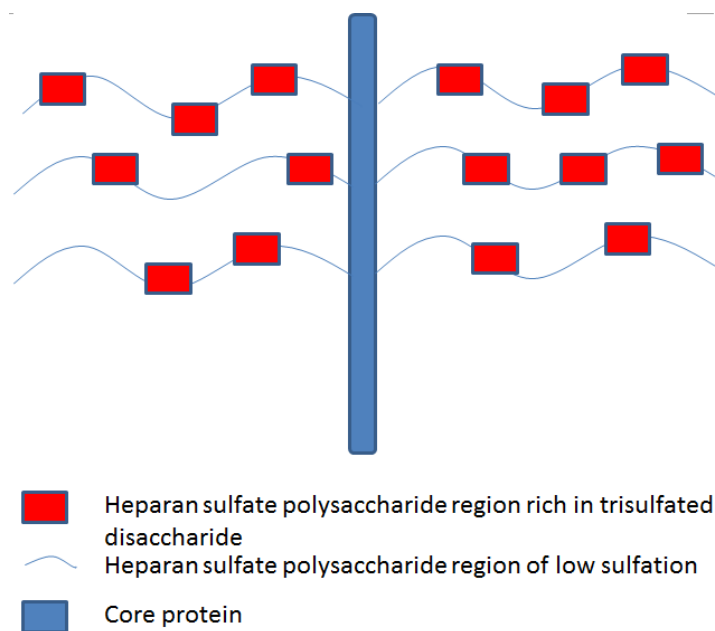
Figure 2.2: Schematic representation of the structure of an HSPG.

Sulf-1 and Sulf-2 preferentially recognise the highly sulfated sub-domains of HSPGs. They have highest enzymatic activity against the trisulfated disaccharide units, hydrolysing O^6-sulfate groups from glucosamine residues, resulting in an increase in the disulfated disaccharide motif.[88]

2.3 Rationale for Sulf-2 Inhibitors as Potential Cancer Therapeutics

Sulf-1 and Sulf-2 mRNA levels have each been shown to be up-regulated in human breast cancer cell lines.[92,93] In hepatocellular carcinoma (HCC) patients, high Sulf-2 mRNA expression correlates with a poor prognosis.[94] In a separate study, eleven hepatic cancer cell lines were examined for Sulf-2 levels, with eight showing increased Sulf-2 expression.[81] The Sulf-2 protein has also been shown to be over-expressed in non-small-cell lung carcinomas.[95] Gastric cancer tissue samples have significantly higher expression of both Sulf-1 and Sulf-2 compared to healthy tissue, which correlates with hypo-methylation of the gene promoter sequences.[85] Sulf-2 levels have been found to be elevated in 50% of glioblastoma tumours, whereas Sulf-1 levels were not.[96] Furthermore, a correlation was found between overall survival and the number of cells staining for Sulf-2 expression in a study of 100 oesophageal cancer patients.[97]

Overexpression of Sulf-2 mRNA and protein has been shown to increase proliferation and migration in a lung cancer cell-line.[95,98] Conversely, in pancreatic cancer, shRNA knockdown of Sulf-2 resulted in decreased proliferation.[98]

Stable transfection of Sulf-2 into HCC cell-lines has been shown to promote the growth of tumours *in vivo*. Pancreatic carcinoma cells transfected with Sulf-2 shRNA exhibited inhibition of tumour growth,[98] and this has also been demonstrated in lung cancer cell lines.[98] In the AGS gastric cancer cell line, transfection with Sulf-1 or Sulf-2 resulted in increased tumour growth relative to control (Figure 2.3).[85] However, forced expression of Sulf-1 and Sulf-2 has also been reported to *reduce* tumour growth *in vivo* suggesting that both may have tumour suppressor functions under certain circumstances.[99]
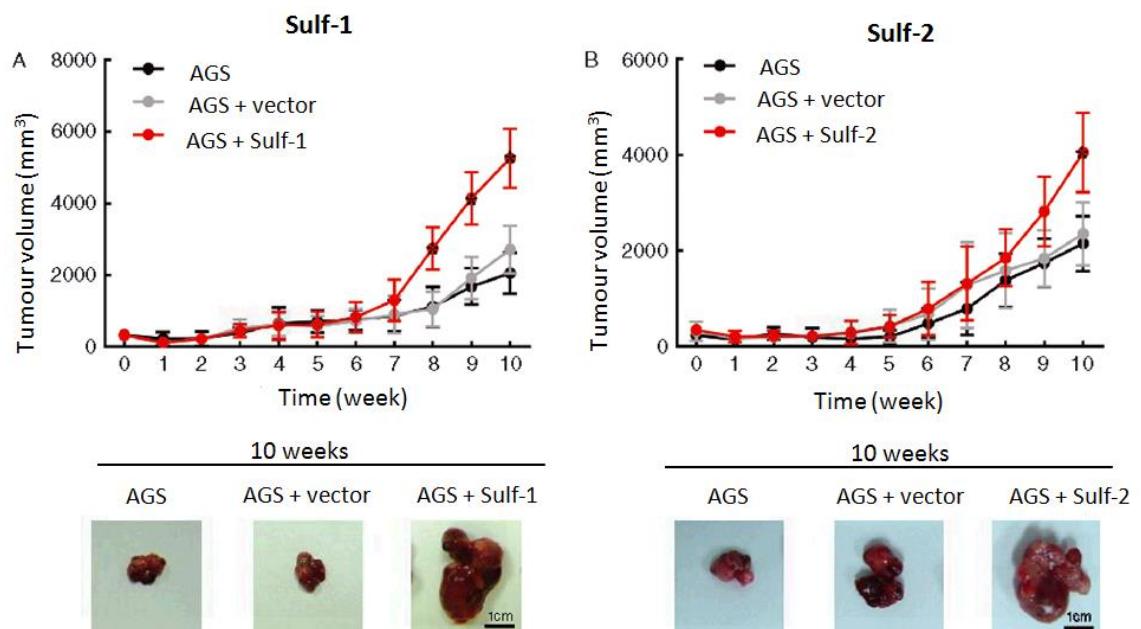
Figure 2.3: Nude mouse xenograft tumour growth model for AGS clones stably expressing (A) Sulf1 or (B) Sulf2. Tumour volumes represented as means $\pm$ SD. AGS: parental cell line; AGS_V: AGS cell line transfected with empty vector; AGS + Sulf1: AGS cell line transfected with *SULF1* expression vector; AGS + Sulf2: AGS cell line transfected with *SULF2* expression vector.[85]

In gastric cancer, overall survival and higher recurrence correlated significantly with high Sulf-1 expression.[85] However, this was not the case for *in vitro* assessments,[99] and contrasting reports provide evidence that Sulf-1 may have a tumour suppressor function.[100] In these studies Sulf-2 continued to appear to act as a tumour promoter.[95] Another study suggests that, in HCC, a wide spectrum of splice variants are present,

particularly of Sulf-1 and to a lesser extent of Sulf-2, that may confer the potential to regulate growth.[101]

2.4   The Signalling Pathways Influenced By Sulf-2

The activity of Sulf-2 is believed to affect signalling through multiple pathways that have been implicated in cell proliferation. The mechanisms whereby Sulf-2 is thought to affect three key pathways, the classical MAP kinase pathway, the wnt pathway, and the hedgehog signalling pathway, are outlined in the following sections.

2.4.1   Sulf-2 and the Classical MAP Kinase Pathway

Sulf-2 interacts with HSPGs resulting in their partial desulfation. Desulfated HSPGs exhibit decreased affinity for HSPG-binding proteins, resulting in their release into the extracellular matrix. This increases the availability of HSPGs to interact with growth factor receptors such as the FGF receptor. The interaction between the FGF receptor and an HSPG facilitates dimerization of the receptor into its active form. Various models have been proposed for the mechanism whereby HSPGs assist in this dimerization, and all invoke formation of a ternary complex between HSPGs, two FGF receptors, and one or two FGF ligands (Figure 2.4).[102]
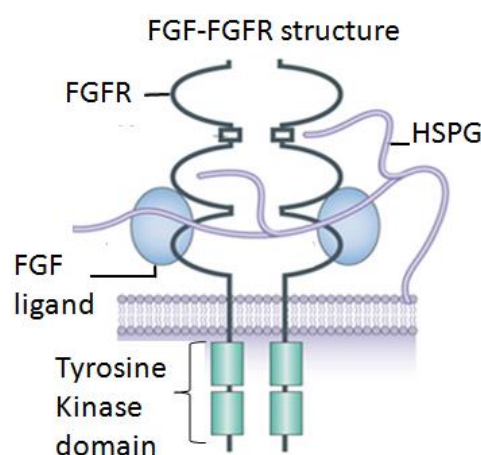
Figure 2.4: The FGF:FGFR:HS ternary complex (adapted from reference 103).

Formation of these complexes increase the affinity of the receptor for its agonist, FGF.[104] A disaccharide digestion analysis of the product of Sulf-2 activity on heparan

sulfate suggested that the enzyme has greater activity against the non-reducing end residues than internal residues, and this residue has been implicated as important for formation of the ternary complex. Thus, Sulf-2 exosulfatase activity may be of highest relevance for its effect on FGF signalling.[105] Activation of the FGF receptor increases signalling through the classical MAP kinase pathway, which is known to promote cell proliferation, invasion, migration and angiogenesis.[41,103] Inhibitors of Sulf-2 would be expected to affect this pathway, enabling HSPG binding proteins to sequester HSPGs, thus reducing the availability of free HSPGs to promote FGF receptor dimerisation.

2.4.2 Sulf-2 and the Wnt Signalling Pathway

Wnt (wingless/int) family proteins are involved in embryogenesis and development, affecting mitogenic stimulation and cell differentiation.[106] The primary wnt signalling pathway is referred to as the canonical pathway, and involves signalling through the cell surface frizzled receptor, a seven transmembrane domain protein with an extracellular *N*-terminal cysteine-rich domain (CRD).
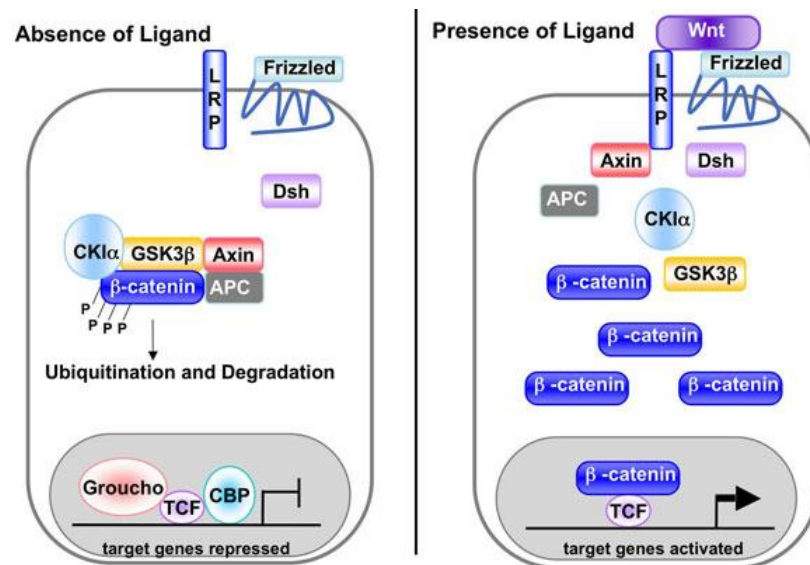
Figure 2.5: The canonical wnt signalling pathway.[106]

In the absence of wnt ligand bound to the frizzled receptor, β-catenin is phosphorylated through the action of a destruction complex comprising the structural proteins axin, adenomatous polyposis coli (APC), casein kinase 1 (CK1) and GSK3. The phosphorylation of β-catenin leads to its ubiquitinylation and subsequent proteasomal degradation.[107]

28

Signalling cells secrete wnt peptides, which bind to HSPGs for transport to their site of action. On binding of wnt ligands to the CRD of the frizzled receptor, a signal is transduced through dishevelled, and a complex series of further interactions results in inactivation of the destruction complex, thereby suppressing phosphorylation of β-catenin. This leads to reduced proteasomal degradation of β-catenin,[28] increasing its availability for translocation to the nucleus,[82] where it forms a complex with TCF-LEF (T-cell factor/lymphocyte enhancer factor) that activates transcription of genes associated with cell proliferation and apoptosis, including cyclin D1 and c-myc. Cyclin D1 is a regulator of cell-cycle progression through activation of cyclin-dependent kinases (CDKs), while c-myc is an oncogene that regulates cell-cycle progression and apoptosis. Other genes affected by the β-catenin/TCF-LEF complex include those coding the c-jun and fra-1 transcription factors. Accumulation of β-catenin and activation of TCF-LEF1 have been found in several human tumour types linked to mutations in β-catenin, axin, or APC.[28] Thus, activation of the wnt/β-catenin pathway is implicated in cell growth and proliferation.[108] Dysregulation of wnt/β-catenin signalling has been linked to colon cancer.[109,110] Si-RNA silencing of the wnt pathway,[111] and antibody approaches have shown efficacy in HCC and sarcoma cells.[112] Conversely, wnt signalling has been suggested to have anti-oncogenic effects in melanoma.[28]

The wnt signalling pathway differs from the previously discussed pathways in that it has few enzymic components that could be targeted for modulation by drugs. Mutations in APC are prevalent in the majority of colorectal cancers, and it has been suggested that inhibitors acting downstream of APC would be required to influence the disease state in this patient population.[33] However, approaches to identifying drugs to affect this pathway have explored targeting components both upstream and downstream of APC. Downstream approaches include developing compounds which bind to and stabilise axin, thus stabilising the β-catenin destruction complex, while upstream approaches include identifying compounds which reduce secretion of, or sequester, the wnt ligand. No inhibitors of the wnt signalling pathway have yet progressed to the clinic.[33]

Glypican 3 is an HSPG which binds to the wnt signalling peptide in the extracellular matrix. The action of Sulf-2 in desulfating sugar residues in glypican 3 reduces the affinity of glypican 3 for the wnt peptide. This results in the release of wnt from glypican 3, increasing its availability for interaction with the cell surface frizzled

receptor, leading to increased signalling through frizzled and dishevelled and ultimately to increased β-catenin levels in the nucleus.[82] Inhibitors of Sulf-2 should allow HSPGs to remain tightly bound to wnt, reducing signalling through this pathway. A schematic representation of the effects of Sulf-2 on both the classical MAPK and wnt signalling pathways is presented in Figure 2.6.
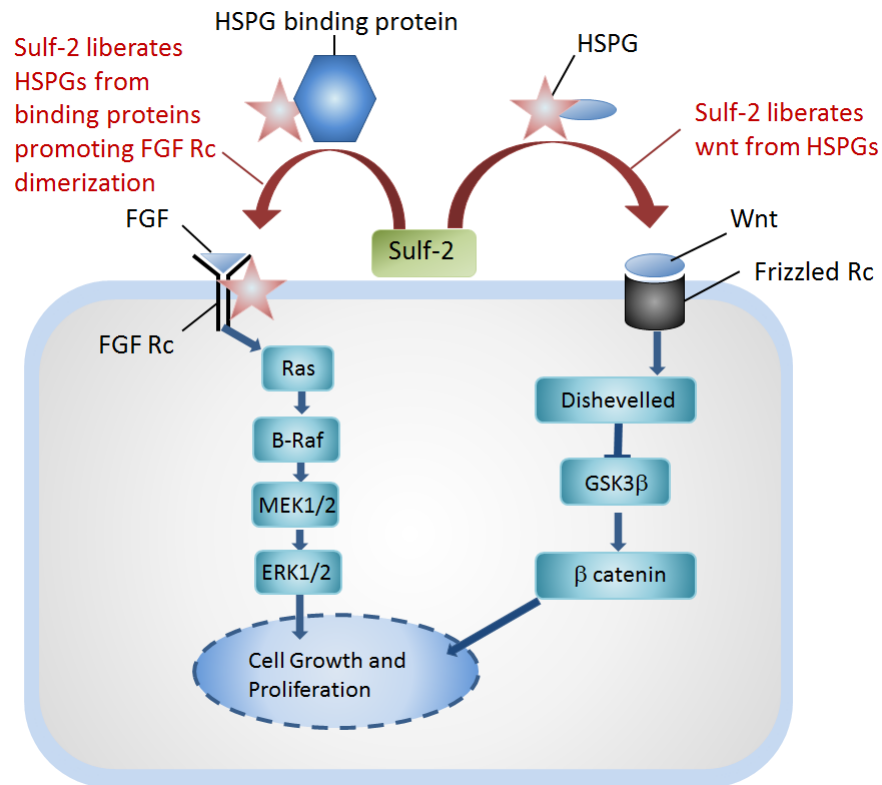
Figure 2.6: Summary of the role of Sulf-2 in the classical MAP kinase and wnt-signalling pathways (adapted from reference 17).

2.4.3 The Role of Sulf-2 in Other Signalling Pathways

HSPGs bind to and regulate the activity of other growth factors including platelet derived growth factor (PDGF), vascular endothelial growth factor (VEGF), glial cell-line-derived neurotrophic factor (GDNF), sonic hedgehog (Shh) and noggin.[96] In the U251 glioblastoma cell line the activity of platelet derived growth factor α (PDGFRα), and insulin-like growth factor receptor β (IGF1Rβ) were reduced by over 50% when Sulf-2 expression was knocked down with shRNA, whereas other receptor tyrosine kinase activities such as PDGFRβ were unaffected.[96] The reduction of PDGFRα signalling in the presence of PDGF was confirmed.

Hedgehog (Hh) proteins are signalling molecules which have a function in embryonic development.[113] Three homologues have been identified in vertebrates, designated Sonic (Shh), Indian (Ihh) and Desert (Dhh). During development, accumulation of Shh protein at the cell surface has been shown to be attributable to the action of Sulf-1. In several human cancers, aberrant signalling through the Shh-mediated pathway has been implicated. In this pathway, Shh protein interacts with the 12-transmembrane cell surface patched (Ptc) protein. In the absence of Shh, Ptc inhibits smoothened (Smo), a 7-transmembrane domain protein. Shh binding to Ptc reduces the Ptc-driven inhibition of Smo, leading to pathway activation. A membrane bound HSPG (Dally-like protein, Dlp) modulates Hh signalling. Although the mechanism for this modulation has not been elucidated, the participation of Sulf-1 and Sulf-2 is possible.[114] Inhibition of hedgehog signalling as an anti-cancer approach has been strengthened by the recent approval of vismodegib (*Erivedge*, **24**), a competitive inhibitor of the smoothened receptor, for the treatment of basal cell carcinoma.[115]

24
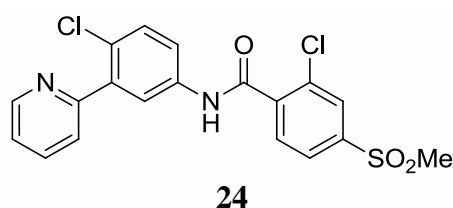
At present, the greatest body of evidence for the potential of Sulf-2 inhibitors in cancer therapy involves their effects on modulating signalling through the classical MAP kinase and wnt signalling pathways. It is not clear at present which of these pathways is affected to the greatest extent by Sulf-2 over-expression.

2.4.4 The Roles of Sulf-1 and Sulf-2 in Cancer

A recent report suggests that Sulf-1 may be anti-proliferative and anti-angiogenic, acting by negatively regulating VEGFR2 signalling.[116] A microarray analysis of genes associated with expression of Sulf-1 and Sulf-2 suggested that some gene associations were common to both. The common genes were associated with cell adhesion, cytoskeletal remodelling, blood coagulation, wnt/β-catenin, and epithelial-mesenchymal transition signalling pathways. However, Sulf-2 had a higher association with neoplastic processes than Sulf-1. The association of Sulf-1 to prognosis was found to be complex, with those patients having very high or very low expression of Sulf-1 having a poorer prognosis than those with moderate Sulf-1 expression.[117]

Reports suggest that Sulf-1 may have a similar effect to Sulf-2 on the wnt pathway, but an inhibitory role on MAP kinase signalling.[98] This might explain the conflicting evidence on the effect of Sulf-1 on cell proliferation. It may be that, in cancers where over-activity of the wnt signalling pathway is driving proliferation, inhibitors of both Sulf-1 and Sulf-2 could prove beneficial. However, in cancers where over-activity of the MAPK pathway is a significant contributory factor, inhibition of Sulf-1 may be detrimental, and a selective Sulf-2 inhibitor would be preferable.

An added complication is the recent identification of splice variants of Sulf-1 and Sulf-2.[101] It has been suggested that full length Sulf-1 and Sulf-2 may promote wnt signalling, while shorter variants might be associated with growth factor signalling *via* the FGF, VEGF and EGF receptor pathways.[101] A further layer of complexity arises from potential cross-talk between the wnt and MAPK pathways, which differ between tumour types. For example, in colorectal cancer, activation of the wnt pathway results in stabilisation of Ras, leading to activation of the MAPK pathway,[28] whereas, in melanoma, activation of the MAPK pathway leads to down-regulation of the wnt pathway.[28]

It is therefore unclear whether a Sulf-2 inhibitor with selectivity over Sulf-1 will have the widest utility, or if a dual Sulf-1/Sulf-2 inhibitor may be beneficial. Sulf-1 and Sulf-2 have 64% sequence identity, with the amino acid residues in the active-site being highly conserved.[84] This suggests that it may be a considerable challenge to identify a compound with selectivity for Sulf-2 over Sulf-1. The overall aim of this project was to develop both dual Sulf-1/Sulf-2 inhibitors and selective Sulf-2 inhibitor tool compounds, to allow further study of the implications of inhibiting these endosulfatases.

2.5 The Mechanism of Desulfation by Sulfatase Enzymes

Sulf-2 is translated as a pre-proenzyme, requiring two major post-translational modifications for its correct localization and activation. The first modification requires the translated 125 kDa pre-proenzyme to be cleaved into 75 kDa and 50 kDa domains,[84] which are subsequently linked by a disulfide bridge. If this does not occur the enzyme retains catalytic activity, but is no longer targeted to the lipid rafts of the cell membrane, resulting in a much higher proportion of secreted enzyme and a reduction in membrane associated sulfatase. Membrane localisation appears to be important for functional activity.[123]

The second post-translational modification conserved across the entire sulfatase family involves conversion of a cysteine residue into a formylglycine (FG), and is essential for catalytic activity (Figure 2.7). This modification is governed by formylglycine generating enzyme (FGE),[124] and occurs before the protein adopts its folded tertiary structure.[125]
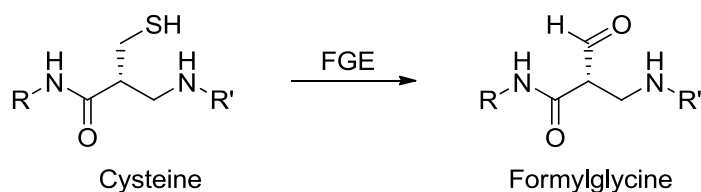
Figure 2.7: The post-translational modification mediated by FGE.

A highly conserved twelve amino acid signature sequence (C/S-X-P-S/X-R-X-X-L/X-T/X-G/X-R/X) is present in all hydrolytically active sulfatases, and is a key recognition element for FGE.[82] A second twelve amino acid signature sequence (G-Y/V-X-S/T-X-X-X-G-K-X-X-H) contains residues essential for catalytic activity, including key lysine and histidine amino acids.

Two mechanisms were originally proposed for the desulfation of substrates by sulfatases, each of which utilise the key active-site formylglycine in the desulfation step, with the mechanism outlined in figure 2.8 now generally accepted.[126] In this mechanism, the formylglycine is hydrated to hydroxyformylglycine which acts as a nucleophile, attacking the sulfate sulfur atom to liberate the alcohol or phenol. The sulfate is then released through a geminal elimination mechanism.
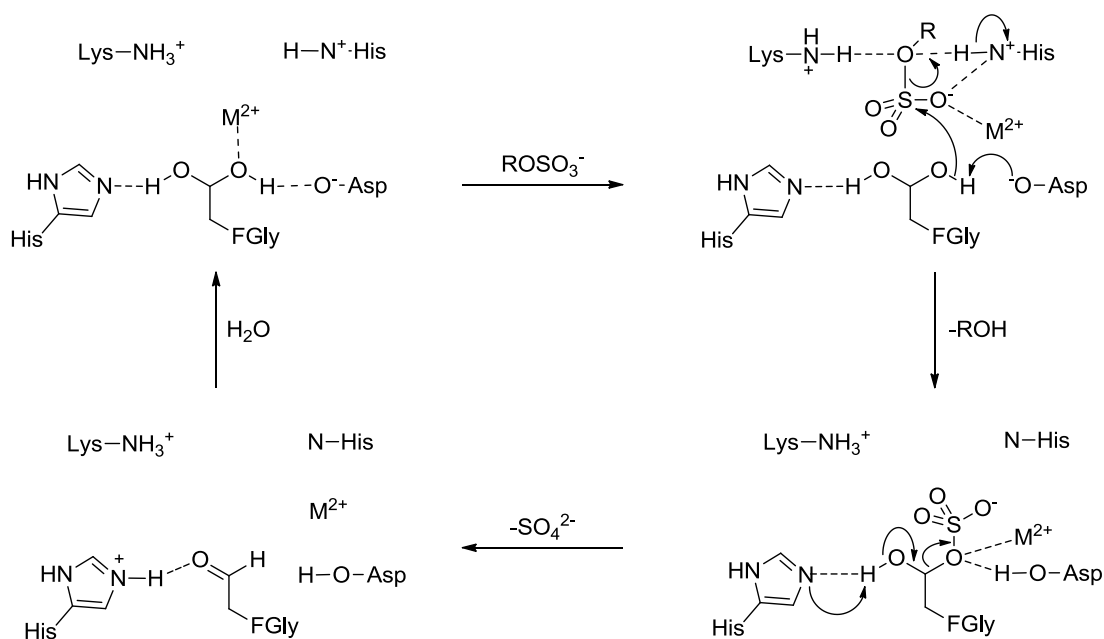
Figure 2.8: A proposed mechanism for sulfatase-mediated desulfation; FGly denotes the backbone atoms of the formylglycine residue.(adapted from reference 82).

Amino acid residues in the active-site, and co-ordination to a metal ion, facilitate the desulfation. For example, it has been proposed that an interaction between an aspartic acid residue and the hydrated aldehyde renders one of the hydroxyformylglycine oxygen atoms more nucleophilic, thereby facilitating attack on the sulfate group.

2.6   Structural Biology of the Sulfatases

The tertiary structure of all sulfatase family members contains four domains (A-D), with domain A being found at the *N*-terminus, and domain D at the *C* terminus.[127] Domain B contains the active-site, and is highly conserved with over 90% sequence similarity across the human sulfatase family.[128] The D domain is the major site of sequence variation between sulfatase family members. At the outset of this project four sulfatase crystal structures (ARSC (PDB accession code 1p49), ARSA (PDB accession code 1auk), ARSB (PDB accession code 1fsu) and PARS (PDB accession code 1hdh)) had been deposited.[124,129] Figure 2.9 shows a published overlay of these structures.
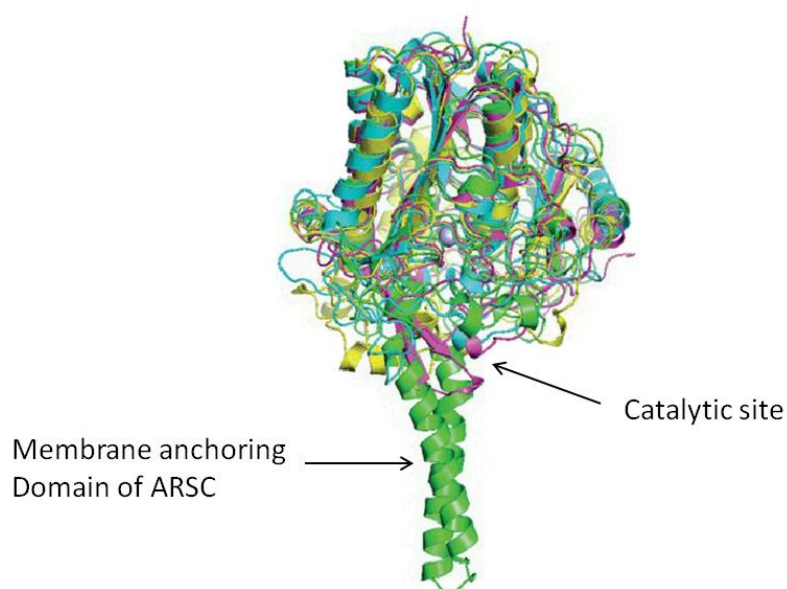
Figure 2.9: Superposition of the crystal structures of members of the sulfatase family. Human placental ARSC (green), ARSA (cyan), ARSB (magenta) & PARS (yellow). The Ca^{2+} ion is shown as a sphere.[124]

All four sulfatases have a similar active-site which can be closely overlaid. In three of the structures the active-site metal was found to be a calcium ion, with the fourth crystal structure (ARSA) containing magnesium. It is not certain whether this is the metal ion that is bound under physiological conditions, or an artefact arising from the high magnesium concentration used during the enzyme purification.[82] In the ARSC structure, a sulfate ion was present and covalently linked to the hydroxyformyl glycine residue, which led to a proposal that the resting state of the enzyme may retain the sulfate after cleavage from the substrate.[124] However, there is no evidence that this is

the case under physiological conditions. Across all four crystal structures, nine of the ten residues believed to be involved in catalysis are conserved.[124] There are significant differences in other residues in the substrate binding cavity, which may be responsible for substrate recognition. The ARSC structure contains two hydrophobic α helices which constitute a membrane anchoring domain. In the other three crystal structures no such domain exists, and the sequence of Sulf-2 suggests that it also lacks these hydrophobic α helices. In contrast to ARSC, Sulf-2 contains a hydrophilic domain of 300-320 amino acid residues, which has been implicated in both membrane anchoring, and in the binding of heparan sulfate to the enzyme.[84] Mutant forms of Sulf-2 lacking regions of the hydrophilic domain have higher extracellular secretion and lower membrane localization.[123] The membrane anchoring of Sulf-2 may involve a region of positively charged amino acids in the hydrophilic domain, which interact with the negatively charged head groups of membrane phospholipids.[130]

No crystal structures of a sulfatase with its substrate bound have been published to date. However, construction of an homology model has been reported for bacterial heparan sulfate 6-*O*-sulfatase from *F. heparinium* based on the known sulfatase crystal structures, into which a disulfated monosaccharide has been docked (Figure 2.10).[131]
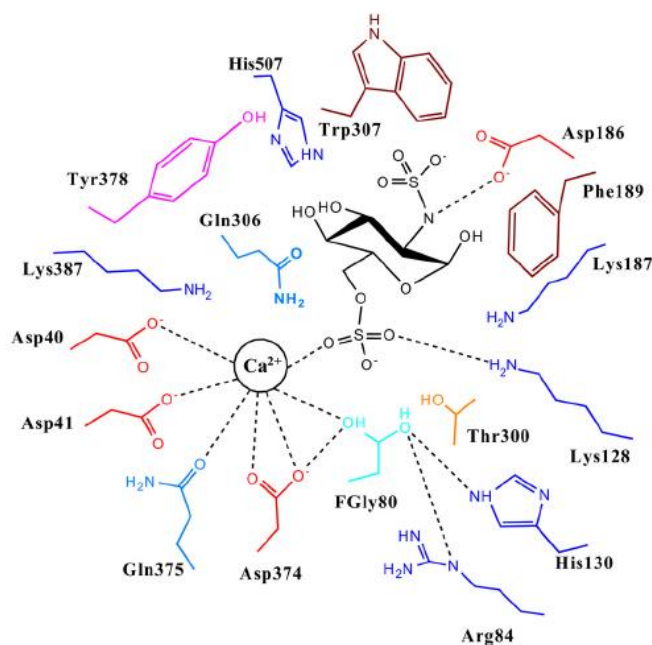
Figure 2.10: Schematic diagram of the proposed active-site interactions of *F. heparinium* sulfatase and a sulfated monosaccharide substrate.[131]

Many of the polar residues lining the active-site in this model are not conserved in arylsulfatases. It has been proposed that the calcium ion in the active-site co-ordinates to both the sulfate to be hydrolysed and the hydrated formyl glycine residue, and that an aspartate residue interacts with the *NH* from the glucosamine *N*-sulfate motif.[131] This implies that the role of the *N*-sulfate may be to increase the hydrogen bond donor ability of the glucosamine *NH* to facilitate this interaction. The authors state that the catalytic site residues proposed in this model would not allow for endosulfatase activity, which would require space for adjacent sugar chains to occupy or exit the active-site. Therefore, caution should be adopted in the use of this model to inform design for inhibitors of an endosulfatase.

2.7 Precedent for Small-Molecule Sulfatase Inhibitors

2.7.1 Inhibitors of Sulf-1 and Sulf-2

At the start of this project no small molecule inhibitors of either Sulf-1 or Sulf-2 had been reported in the literature. A study in 2005 had investigated the compositional profile of heparan sulfate and the ability of different fragments of heparin to interact with Sulf-2.[88] The investigators determined, through enzymatic digestion and mass spectrometry analysis, that the major component disaccharide present in bovine kidney heparan sulfate was the unsulfated disaccharide UA-GlcNAc. However, it was determined that the trisulfated disaccharide motif of heparan sulfate (Figure 2.11) is the primary motif for desulfation by human Sulf-2.
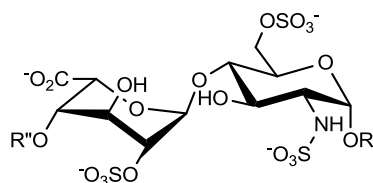
Figure 2.11: The trisulfated disaccharide unit, IdoA2S-GlcNS6S.

The length of sulfated polysaccharide required for recognition and Sulf-2 mediated desulfation was also investigated, with a decasaccharide containing trisulfated disaccharide units suffering a 47% decrease in O^6-sulfation by the action of Sulf-2. A tetrasaccharide had a 14% decrease, whereas no desulfation was observed for a single trisulfated disaccharide.[88] This may suggest that recognition elements distal to the

enzyme active-site are required for substrate recognition, and that high molecular weight inhibitors may therefore be necessary.

However, the first small molecule Sulf-2 inhibitors were reported soon after the commencement of this project.[132] These compounds were derived from the monosaccharide of the substrate glucosamine residue, bearing a primary, or a methylated tertiary sulfamate at the O^6-position, and an acetate or sulfate group at the N^2-position. The most potent analogue from this series was **25** with an IC_{50} against Sulf-2 of 130 μM (Table 2.4).
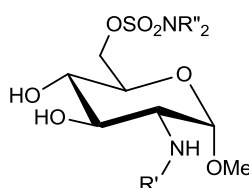
Cmpd	R'	R"	Sulf-2 IC_{50} μM (or % inhibition)	Sulf-1 IC_{50} μM (or % inhibition)
25	SO_3Na	H	130	95
26	SO_3Na	Me	240	180
27	Ac	H	(30% @ 5 mM)	(40% @ 5 mM)
28	Ac	Me	(45% @ 5 mM)	(50% @ 5 mM)

Table 2.4: Reported Sulf-2 inhibitory activity of monosaccharide sulfamates.[132]

Compounds **27** and **28** bearing an *N*-acetyl group were an order of magnitude less potent than **25** and **26**, suggesting that the *N*-sulfonyl substituent plays an important role in substrate binding. All compounds tested had no selectivity for Sulf-2 over Sulf-1. Although these compounds were not sufficiently potent for use in biological target validation studies, the results provided encouragement that viable Sulf-2 inhibition was possible with low molecular weight compounds. In the same paper two simple arylsulfamates (**29** and **30**) were also tested against Sulf-1 and Sulf-2 (Table 2.5), and found to be markedly weaker inhibitors than **25** and **26**. Both **25** and **26** were shown to be reversible inhibitors, whereas phenol sulfamate **29** was reportedly an irreversible inhibitor of Sulf-2.[132]
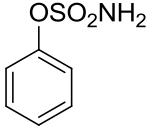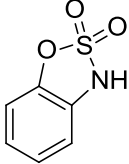
Compound	Structure	Sulf-2 % inhibition
29	OSO_2NH_2 (phenyl sulfamate)	30% @ 5 mM
30	(benzo-fused cyclic sulfamate)	50% @ 5 mM

Table 2.5: Reported Sulf-2 inhibitory activity of non-saccharide sulfamates **29** and **30**.

The alkyl nitrone OKN-007 (**31**) has also been suggested to be an inhibitor of Sulf-2.[133] Compound **31** (also known as disufenton sodium, NXY-059, and *Cerovive*) has previously been investigated in Phase II clinical trials for ischaemia due to stroke, with a proposed mechanism of action arising through its ability to scavenge free radicals.[134] No inhibition data against isolated active Sulf-2 have been published.

31
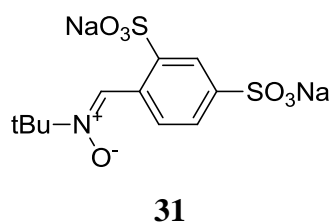
In a HuH-7 HCC cell-line expressing high levels of Sulf-2, **31** showed a dose-dependent increase in apoptosis, with some effects on cell migration but little influence on proliferation and cell viability.[133] In Sulf-2 shRNA-silenced Huh-7 cells, **31** had a reduced effect on apoptosis. In a low Sulf-2 expressing cell line (Hep3B) with Sulf-2 expressed to high levels, treatment with **31** resulted in a 60% increase in apoptosis compared with a 22% increase in the untransfected control cells.[133] In Huh-7 cells **31** inactivated TGFB1/SMAD2 and hedgehog/GLI1 signalling pathways, suggesting that Sulf-2 may play a role in the regulation of these pathways. However, while there is circumstantial evidence that **31** is an inhibitor of Sulf-2, the absence of isolated enzyme inhibition data offers the potential for other pharmacological effects, which may be responsible for at least some of the observed anti-tumour activity.

2.7.2   Inhibitors of Arylsulfatase C

ARSC inhibitors are believed to interact with its membrane anchoring domain, which is not present in Sulf-2. Therefore, SARs for inhibitors of ARSC are unlikely to transfer between the two targets. However, the conserved catalytic mechanism would suggest that SARs for sulfate isosteres may have relevance for the design of Sulf-2 inhibitors.[129] A brief review of ARSC inhibitors follows, with an emphasis on SARs around the sulfate warhead and the A ring of the steroid, which may inform Sulf-2 inhibitor design.

2.7.2.1   Steroid-Based ARSC Inhibitors

In 1994 the Potter group disclosed inhibitors of oestrone sulfatase based on a steroid template.[135] They explored oestrones substituted on the phenol and prepared oestrone sulfamate (EMATE, **32**), oestrone *N*-methylsulfamate (**33**), and oestrone *N,N*-dimethylsulfamate (**34**) (Table 2.6). Irreversible inhibition was observed for **32**, whereas the secondary and tertiary methylated sulfamates were reversible inhibitors. Increasing the size of the *N*-substituents resulted in a further loss of potency.[136]
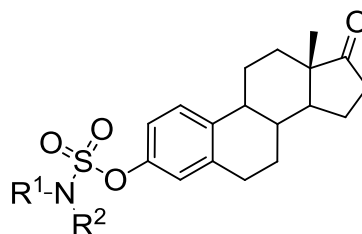
Cmpd	R^1	R^2	ARSC inhibition	Modality
32	H	H	IC_{50} = 65 pM	Irreversible
33	Me	H	87% inh @ 1 μM	Reversible
34	Me	Me	87% inh @ 1 μM	Reversible

Table 2.6: ARSC inhibitory activity for simple primary, secondary, and tertiary sulfamate derivatives of oestrone.[135]

ARSC inhibition data have also been reported for a wide range of sulfamate isosteres, including   sulfonates,[137]   alkylsulfones   and   sulfonamides,[138]   sulfonylureas,[139]

carbamates, and esters,[140] which universally led to significant potency loss. By contrast, cyclic sulfamate isosteres gave potent ARSC inhibition (Table 2.7).[138]
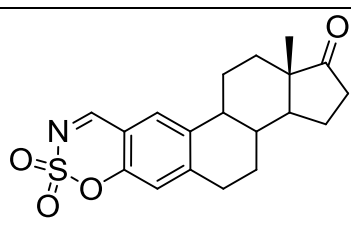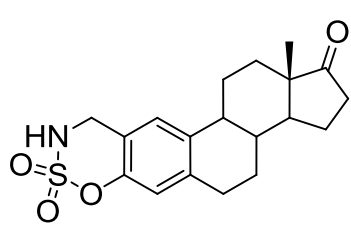
Cmpd	Structure	ARSC IC$_{50}$ nM
35		9
36		360

Table 2.7: ARSC inhibitory activity data for analogues of EMATE (**32**) containing cyclic sulfamate isosteres.[138]

2.7.2.1.1 A-Ring Substituted Steroid Sulfamates

Substitution on the A ring of **32** *ortho* to the sulfamate exhibited remarkable SARs with small structural changes resulting in potency differences of over one hundred thousand fold (Table 2.8).[141] These SARs are unlikely to be due solely to electronic effects on the leaving group ability of the steroid phenol, and may suggest that A-ring substituents participate in binding interactions within the sulfatase active-site. This is further supported by the difference in potency between the 2- and 4-nitro analogues, **40** and **41**, which would have broadly similar electronic properties.
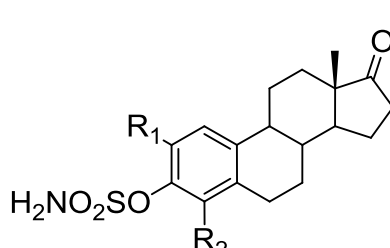
	Cmpd	R$_1$	R$_2$	ARSC IC$_{50}$ nM
	37	Cl	H	3.4
	38	Me	H	11,000
	39	CF$_2$H	H	0.1
	40	NO$_2$	H	70
	41	H	NO$_2$	0.8

Table 2.8: ARSC inhibitory activity of primary sulfamate analogues of oestrone bearing substituents on the steroid A-ring.

2.7.2.2 Non-Steroidal ARSC Inhibitors

The most advanced ARSC inhibitor in development is 667-coumate (STX-64, **42**), which is reported to bind irreversibly to the enzyme,[142] and completed phase I trials with few adverse events, prior to entering Phase II clinical trials for breast cancer.[143] Four patients with hormone-independent breast cancer exhibited stabilisation of disease for 2.75 to 7 months during treatment with **42**.[143] The lack of significant adverse events in the phase I study provides encouragement that compounds containing a phenolic primary sulfamate have no inherent toxicological liability.
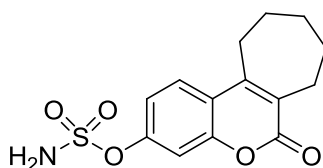
42

While the vast majority of ARSC inhibitors contain a sulfamate group or an obvious sulfamate isostere, there are a limited number of non-sulfamate inhibitors, for example **43**, **44** (Naringenin),[144] and **45**.[145] These compounds indicate that a sulfamate, or a sulfamate isostere, is not an absolute requirement for inhibition of a sulfatase.
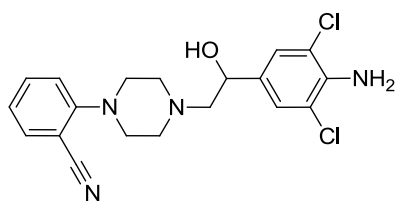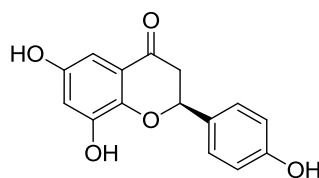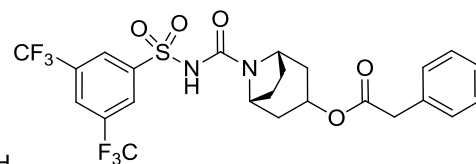
43	**44**	**45**
ARSC; IC_{50} = 48 nM	ARSC; 50% inh @ 10 μM	ARSC; IC_{50} = 76 nM

2.8 Further considerations for the Design of Sulfatase Inhibitors

In this section, a wider consideration of the literature that may provide information relevant to the synthesis of inhibitors for Sulf-2 is examined, including a discussion of known saccharide sulfate and sulfamate drugs and alternative approaches to heparin mimetics. Potential issues that may arise in the development of saccharide-based sulfatase inhibitors will also be discussed.

2.8.1 Saccharides as Drugs

The primary aim of the project at the present time is the identification of probe molecules to support *in vitro* target validation studies. However, the potential of a tool series for development into suitable *in vivo* tools, and ultimately compounds amenable for clinical development, should be considered. The physicochemical properties of saccharides have limited their application as oral therapies, as the high polar surface area and hydrogen bonding potential render them unlikely to diffuse passively through membranes. Exploiting active uptake *via* saccharide transporters is a potential approach for obtaining oral bioavailability. Advances in formulating low molecular weight heparin to improve bioavailability have also been made through co-administration with additives, which improve absorption by mechanisms such as targeting for active transport, or enlarging the pores in the gut epithelium to allow absorption by the paracellular route. An alternative prodrug strategy has also had some success, masking the saccharide hydroxyl groups as acyl esters which have sufficient stability in the stomach, and are absorbed in the lower intestine. The active component is then liberated in the plasma by the action of esterase enzymes.[146] This prodrug approach may have limited utility for intracellular targets, as, once liberated, the polar active species would be unlikely to cross plasma membranes to reach the site of action. However, this approach may be viable for Sulf-2, with its proposed extracellular site of action. Topiramate (**46**) is a monosaccharide derived primary sulfamate which has been employed as an anticonvulsive treatment for epilepsy,[147] the mode of action of which is yet to be established. However, it is known to have pharmacological activity against voltage-dependent sodium channels, GABA-A receptors, the AMPA/kainate subtype of the glutamate receptor, and carbonic anhydrase enzymes. Topiramate has high oral bioavailability (80%) and a long duration of action ($t_{1/2}$ 18-23 h).[148] The clinical precedence and widespread use of

topiramate lend further support to the safety of primary alkyl sulfamates, and the potential for developing saccharide-based inhibitors as oral drugs.
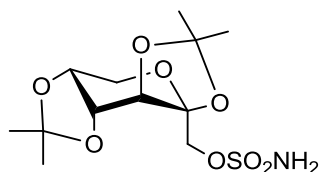
46

PI-88 (**47**) is a phosphosulfomannan oligosaccharide inhibitor of tumour growth and metastases currently in Phase III clinical trials. The compound was developed as an inhibitor of heparanase, but may act through multiple mechanisms including preventing the formation of the FGFR ternary complex.
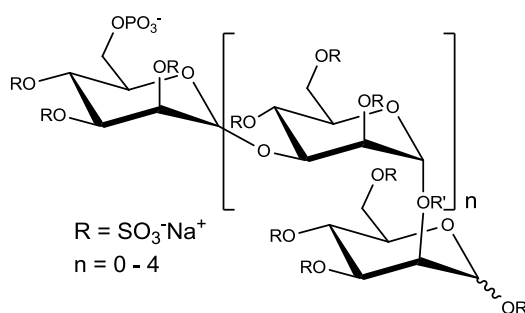
47

PI-88 has reported inhibitory activity against Sulf-1 and Sulf-2, with IC_{50} values of 2.6 μg/mL against Sulf-1, and 1.2 μg/mL against Sulf-2,[149] and it has been proposed that some of the antitumour activity exhibited by **47** may be attributable to inhibition of sulfatases. Owing to poor oral bioavailability, **47** is administered intravenously.

2.8.2 Carbonic Anhydrase Inhibition

Small molecule sugar sulfamates including **46** have been shown to potently inhibit carbonic anhydrase.[146] Inhibitors of this enzyme class have been approved for human use, for example acetazolamide for the treatment of glaucoma.[150] However, carbonic anhydrase inhibition can result in acidosis leading to the formation of kidney stones.[151] Carbonic anhydrase inhibitors also often partition into red blood cells, complicating the analysis of a compound's pharmacokinetics.[152] Thus, a sulfamate-based Sulf-2 inhibitor which also inhibits carbonic anhydrase may be viable for progression to clinical studies, but monitoring of the carbonic anhydrase inhibition during later stages of the development process would be advisable.

Chapter 3: Design of Potential Sulf-2 Inhibitors

3.1 Considerations in the Design of Chemical Tools for Target Validation

With the advent of the discipline of chemical biology, it has become widely accepted that the design of chemical tools for use in validating a novel target in a disease area will usually differ from the methods used for the design of potential drugs for clinical development.[76,153] Validation of a novel target is a high risk endeavour, with a good chance that the outcome will be a negative result, *i.e.* that the target of interest is unsuitable for a small-molecule drug discovery program.[154,155] This may be for a variety of reasons, including unsuitability of the target for efficient binding by a small molecule,[156] evidence that selectivity against key safety targets may not be achievable, or failure of modulation of the target to have the desired efficacy in disease models.[157]
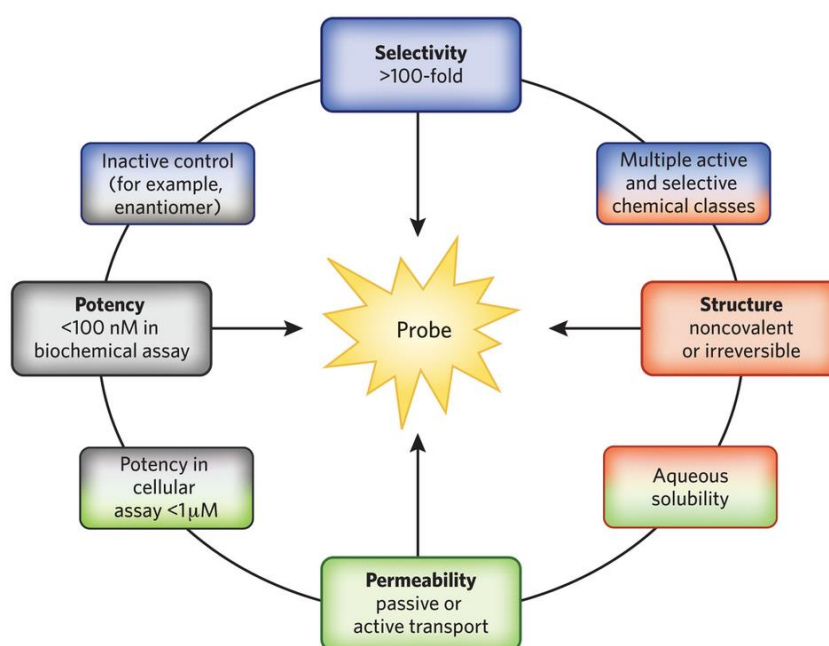
Figure 3.1: Criteria for consideration in the design of a chemical tool.[157]

Several recent commentary articles provide interesting discussions on how design criteria for tool compounds may differ from those for designing potential drug candidates. Kodadek[153] suggests that achieving potency against the target of interest is the unifying criterion in both cases. Drugs require optimization of oral bioavailability, pharmacokinetic half-life and cost of goods. While selectivity for the target of interest is often advantageous to a drug for reasons of safety, it is not a prerequisite. In

contrast, for a high quality tool compound to evaluate a mechanism, selectivity is important to ensure off-target pharmacology is not responsible for any effects observed, or, conversely, that off-target activity does not interfere with the ability to detect the effect of the primary pharmacology. Ensuring complete selectivity is usually not possible, as it is not practical to screen against all other biological targets that may affect the functional outcome. Indeed, often it is not practically or technically possible to screen against all of the close family members of the target of interest. One strategy to mitigate the risk of unknown selectivity is to identify more than one structural class of probe molecule, which are less likely to have similar off-target pharmacology profiles. Use of a control compound of similar structure to the probe molecule but with low activity against the target of interest, such as an inactive enantiomer, can also provide useful information about off-target effects.[157] For intracellular targets, cell permeability is important to enable the probe molecule to access the biological target.[157] Frye outlines several principles to be considered for a high quality tool, including sufficient potency and selectivity to allow a confident link between *in vitro* and *in vivo* activity, evidence for the mechanism of action, dose-dependent cellular activity, and chemical stability.[76] However, the nature of each target will dictate specific requirements for a chemical probe, and defining the rules can often only be achieved in hindsight once a probe molecule has been developed.[76] A set of 'fitness factors' for chemical tools has been described which summarize the aspects of the chemistry, potency, selectivity and biological context of the target which should be considered in the design and selection of a tool compound.[158]

3.2   The Design of Potential Chemical Tools for Sulf-2 Inhibition

As discussed in section 2.8, the first small-molecule Sulf-2 inhibitors were reported soon after the commencement of this project.[132] These compounds were derived from the glucosamine monosaccharide unit of HSPGs, bearing a primary or tertiary methylated sulfamate at the O^6-position, and an acetate or sulfate group on the N^2-position. The most potent analogue from this series was **25** with an IC$_{50}$ of 130 μM.
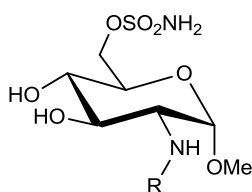
25 R = SO$_3$H
27 R = Ac

The initial aim of the Newcastle Sulf-2 project was to identify a tool compound for use in *in vitro* experiments to address the following questions:-

1. Is an IC_{50} of < 100 μM against Sulf-2 achievable with a small-molecule (MW < 500) inhibitor?

2. Is selectivity over Sulf-1, and over other human sulfatases, achievable?

3. Does inhibition of Sulf-2 alone, or dual Sulf-1/Sulf-2 inhibition, by a small-molecule inhibit the growth of cancer cell lines *in vitro*?

In order to answer these questions as rapidly as possible, the project's initial focus was on identifying probe compounds that aim solely to modulate the target *in vitro*, with improved potency, and sufficient solubility to allow the compounds to be tested in the relevant assays. Active compounds would subsequently be assessed for selectivity over other sulfatases. Inhibitors selective for Sulf-2, and dual Sulf-1/Sulf-2 inhibitors, were sought. In this phase of the project, *in vivo* properties that would be considered for a lead development or drug discovery program, such as pharmacokinetic and toxicological liabilities, were not high priority considerations for compound design.

Literature evidence suggests that the active-site of Sulf-2 is extracellular.[90] It follows that there is no requirement to achieve high cell permeability for a tool compound to effectively modulate this target. Indeed, lack of cell penetration may provide an alternative method to confer selectivity over off-target intracellular sulfatases.

There are no published crystal structures of Sulf-1 or Sulf-2, and attempts to build homology models based on the known sulfatase crystal structures resulted in structures with low confidence levels in key regions around the active-site, rendering them unsuitable for use in compound design. Ligand based approaches were thus pursued for the identification of improved tool compounds. The approaches taken are summarised below:

1. Synthesize compound **25** for use in assay development.

2. Prepare analogues of **25** to generate Sulf-1 and Sulf-2 SARs.

3. Prepare non-saccharide templates based on:

   a. Inhibitors of other sulfatase family members.

   b. *De novo* design based on the structure of the endogenous substrates of Sulf-2.

Generation of an assay for Sulf-2 inhibition was complicated by issues in the isolation of catalytically active Sulf-2 protein, due in part to the requirements for post-translational modification of the cysteine into a formylglycine residue. Consequently, a viable Sulf-2 biological assay has only recently become available. In the absence of a biological assay to allow a high-throughput screening campaign, and with no crystal structure of Sulf-2 on which to investigate structure-based design approaches, the structures of the endogenous HSPG substrates were considered as a potential starting point for analogue design. No crystal structures of HSPGs were available, so attention focussed on understanding the features of the related biomolecule, heparin, and its low molecular weight fragments. Heparin is highly sulfated, and may therefore reflect the structure of the oligosaccharide regions of HSPGs which are de-sulfated by Sulf-2. Gaining an understanding of the conformations, surface features and interactions made between heparin and its protein binding partners allowed analogue and *de novo* ligand-based design by overlaying prospective designs with key features of the substrate which were likely to contribute to binding.

3.3   Structural Characteristics of Heparan Sulfate Oligosaccharides

The primary structure of heparan sulfate oligosaccharides consists largely of the repeating disaccharide unit $[-4IduA\beta(1,4)-GlcNS\alpha1-]_n$.[87] The lowest energy conformation of glucosamine is the $^4C_1$ chair form, with all substituents occupying equatorial positions, and it would be expected that this form would predominate in the oligosaccharide structure. However, iduronic acid can adopt two low energy conformations of similar energy, the $^1C_4$ chair and the $^2S_0$ skew boat conformations (Figure 3.2).[159]
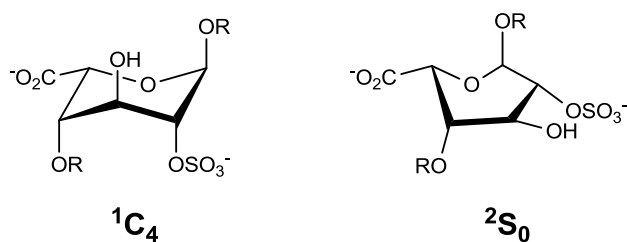
Figure 3.2: The most abundant forms of O^2-sulfated iduronic acid in heparin (adapted from reference 160).

The oligosaccharides also have considerable flexibility in the linkage between the monosaccharide sub-units, with the carbon-oxygen bonds in the ether linkers having low energy barriers to rotation. Consequently, heparan sulfate oligosaccharides could adopt a large number of secondary structures. However, two published modelled structures of heparin based on NMR and molecular modelling studies on a heparin dodecasaccharide consisting of the repeating trisulfated disaccharide unit suggest a helical rod-like secondary structure is likely to predominate in aqueous solution.[161] The first model assumes that the iduronic acids all adopt the $^1C_4$ form, whereas in the second all iduronic acids are modelled in the $^2S_0$ skew boat conformation. While it is likely that, in reality, the iduronic acid conformations may be heterogeneous along the length of an oligosaccharide, it is notable that remarkably similar helical structures appear favoured, regardless of the iduronate conformation.

The computed solution structure models were found to be closely related to the reported solid state X-ray crystal structure.[161] The proposed helical structures suggest that clusters of sulfate groups are presented at regular intervals of approximately 17 Å on either side of the helix.[161] A comparison of space-filling representations based on van der Waals atomic radii of the two modelled structures (Figure 3.3), clearly indicates a large number of negatively charged sulfate and carboxylate groups that dominate the accessible surface. These are likely to be important in the binding of heparin and heparan sulfate to biological targets.
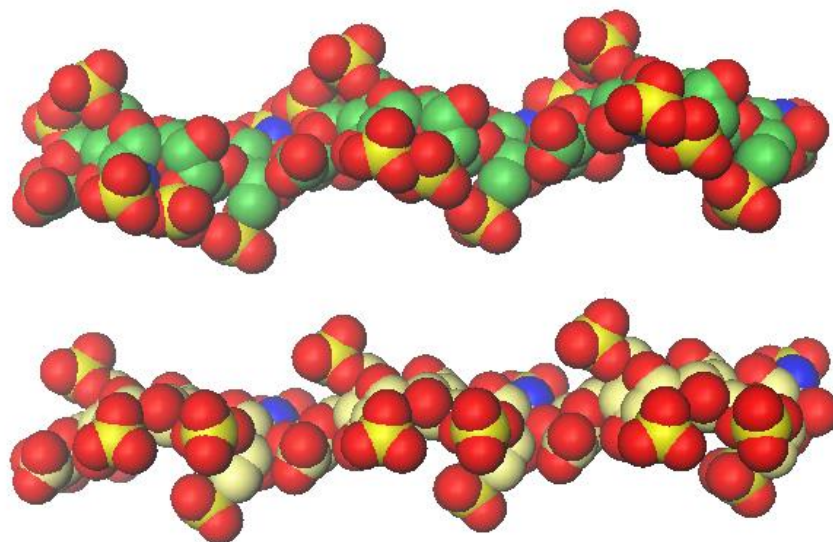
Figure 3.3: Space filling representations of the models of the heparan sulfate oligosaccharides (PDB accession code 1hpn).[162] Green: All iduronate residues in $^1C_4$ conformation; White: All iduronate residues in $^2S_0$ conformation.

3.4 General Observations on the Interactions between Oligosaccharides and Proteins

A review of carbohydrate mimetic strategies concluded that polysaccharide-protein interactions often involve a mixture of hydrogen bonding, hydrophobic, and ionic interactions.[163] Hydrogen bonding interactions between *NH* and carbonyl groups on the peptide backbone, and the saccharide hydroxyl groups dominated the hydrogen bonding contributions in the interactions surveyed. Far fewer hydrogen bond interactions were observed between serine and threonine side chains and the sugar hydroxyl groups.[163]

Hydrophobic interactions between the faces of the pyran rings of the saccharide core and lipophilic amino acid side chains were also found to play a significant role in protein-saccharide interactions. An example can be seen in the binding of a disaccharide to the maltose binding protein, where both saccharide rings are sandwiched between tryptophan and tyrosine aromatic side chains of the protein partner.[164] Thus while saccharide-binding sites are likely to contain more hydrophilic amino acids than in other binding site classes, the potential for hydrophobic interactions should also be considered in inhibitor design.

3.5   Interactions between Heparin Oligosaccharides and Proteins

Heparin oligosaccharides differ from the majority of other oligosaccharides in that they are highly sulfated. The presence of such polar groups would be expected to affect the interactions observed on the binding of a heparan sulfate derived saccharide to a protein. The first study to investigate heparin-protein interactions concentrated on the features of protein partners that confer heparin binding ability.[165] This study compared four proteins which interact with heparin (apolipoprotein B, apolipoprotein E, vitronectin, and platelet factor 4) and found certain primary sequence motifs rich in basic amino acid residues which are conserved across the heparin binding domains of these proteins. These conserved sequences were XBBXBX and XBBBXXBX where B are basic and X are hydropathic i.e. neutral or hydrophobic amino acid residues. Molecular modelling suggested that if these sequences formed an α helix, the basic residues would be aligned on one face of the helix and the hydrophobic residues on another face (Figure 3.4).
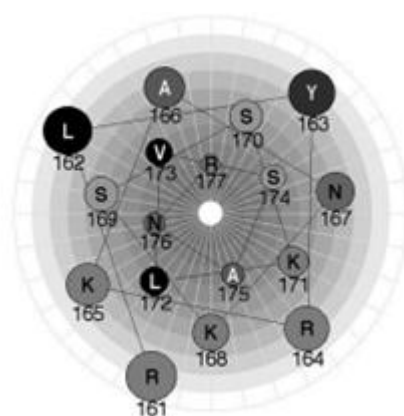
Figure 3.4: Helical wheel diagram of residues 161-177 of apolipopotein B.[166]

The face displaying the basic residues is likely to interact with the acidic sulfate and carboxylate groups on the surface of heparin. It has also been noted that basic residues distant from each other in the primary sequence could, on protein folding, form regions dense in positively charged residues that could bind to the negatively charged heparin surface.[166]

The structure of a heparin tetrasaccharide bound to the enzyme 3-O-sulfotransferase (Figure 3.5) is the closest protein in function to Sulf-2 with a published crystal structure bound to a heparin derived oligosaccharide.[168] Analysis of this structure

shows that the heparin oligosaccharide binds in a clear pocket in the protein, and that the major polar interactions between the protein and the oligosaccharide involve sulfate and carboxylate groups of the saccharide, and basic amino acids and backbone amide groups of the protein. Only a limited number of saccharide hydroxyl groups appear to make interactions with the protein, and none of the tetrahydropyran core oxygen atoms, or the linking ether oxygen atoms appear to contribute to binding. Several water molecules also occupy the pocket in the bound structure, and interactions between the ligand, the water molecules and the protein may also contribute to binding.
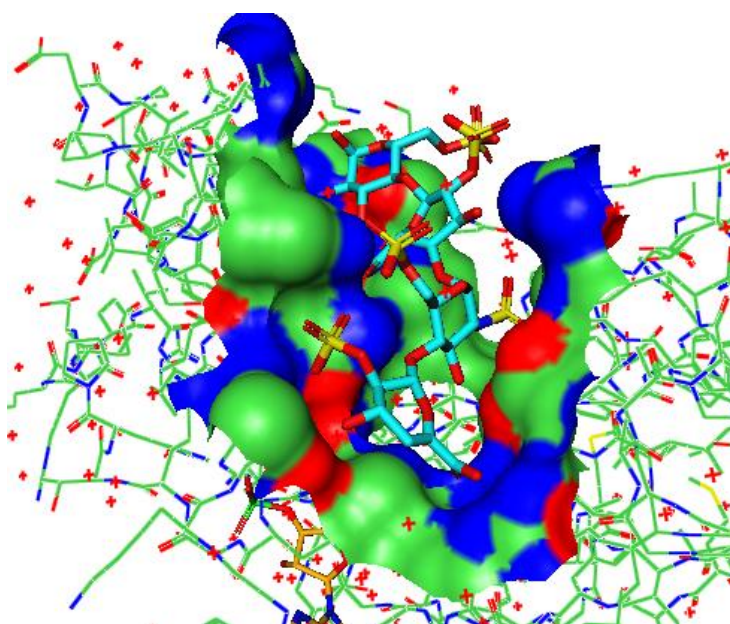
Figure 3.5: The binding surface of 3-*O*-sulfotransferase with a heparin-derived tetrasaccharide bound (PDB accession code 1t8u).[168]

From these analyses it can be concluded that interactions of the charged sulfate and carboxylate groups on the heparin oligosaccharide with basic residues on the protein are often the critical interactions responsible for binding. Attempting to mimic some of these interactions was a key consideration when designing potential inhibitors of Sulf-2. Interactions between the tetrahydropyran ring oxygen atoms or the linking ether atoms and the protein partner, either directly or through bridging water molecules, appear to be relatively uncommon. The saccharide scaffold may act principally as a template to display the charged and polar groups in the correct orientations for interaction with the protein. Mimicking of the spatial orientation of the pyran oxygen atoms may not therefore be necessary in inhibitor design.

It has been reported for heparin oligosaccharides bound to FGF that the helical parameters and glycosidic bond conformations of the bound oligosaccharide closely mimic those of heparin in the unbound solution state.[165,166] Similarly, in a crystal structure of heparin bound to angiotensin II, the bound structure in the crystal was found to closely resemble the solution structure. Comparison of the solution structure of heparin, and the conformation of four crystal structures of heparin oligosaccharides bound to proteins, revealed that the secondary structure was similar in all cases. This increased confidence that the solution structure could be used as a template for ligand-based design by superposition, in order to select templates which may mimic the heparin-protein binding interactions. The results of this analysis were used to inform both the design of analogues of monosaccharide Sulf-2 inhibitor (**25**), and the attempted *de novo* design of non-saccharide based Sulf-2 inhibitors.

3.6 Monosaccharide Sulfamate Inhibitors of Sulf-2

The reported Sulf-1/Sulf-2 dual inhibitors, **25** and **27**,[132] were successfully prepared for use in the development of a Sulf-2 primary pharmacology assay, using the novel synthetic route described in Section 4.1.

3.6.1 Design of Analogues of Compound 25

Analogues of **25** were targeted to develop SARs in order to build an understanding of features required for binding, and structural changes affecting selectivity. A program of work was thus undertaken to systematically vary the substituents around the monosaccharide core (Figure 3.6). The key design questions and rationale that guided the selection of analogues for synthesis are presented in the following sections.
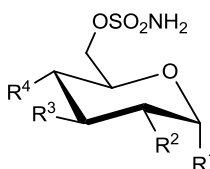
Figure 3.6: Exploration of monosaccharide SARs by variation of R^1 to R^4

3.6.1.1 Variation of the 2-Substituent of Compound 25

The *N*-sulfate is a highly polar group, contributing to the overall hydrophilic nature of **25** (clogP -2.7). Due to its acidic nature, the sulfate is likely to be deprotonated in the active-site, bearing a net negative charge on oxygen that may participate in a charge-charge interaction with basic residues in the binding site of Sulf-2. A report on an homology model of *F. heparinium* sulfatase suggested that the N^{2-}sulfate may instead influence binding by enhancing the hydrogen bond donor ability of the N^2-*H*.[131] Analogues were designed to explore the possible N^2-sulfate/protein interactions. The first targets (**25**, **27**, **48**, and **49**) explored the effect of variation of the *N-H* pK_a on Sulf-2 inhibition (Table 3.1), as a potential surrogate for the hydrogen bonding ability of the *N-H* hydrogen atom.
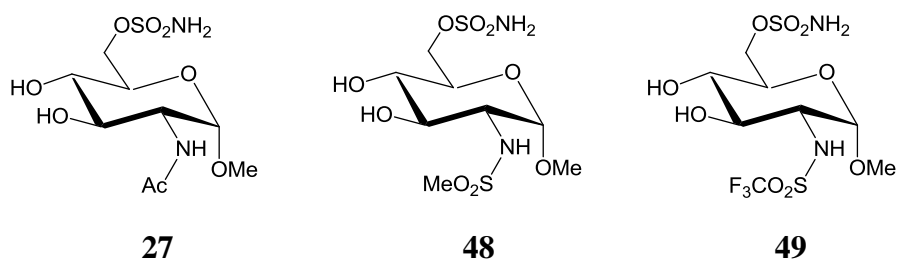
27 **48** **49**

Compound	25	27	48	49
Calculated *N-H* pK_a	14.1	16.2	11.0	6.9

Table 3.1: *N-H* pK_a values for potential novel *N*-substituted analogues (calculated using ACD labs software).[169]

Methanesulfonamide **48** resulted in an increase in *N-H* acidity of three pK_a units relative to **25**. Trifluoromethylsulfonamide (**49**) further acidifies the *N-H*, and would be expected to be significantly ionised at physiological pH.

Glucose- and mannose-based analogues, **50** and **51**, were prepared to assess whether the *N*-sulfate could be replaced with a hydroxyl group. Mannopyranoside **51** positions the 2-hydroxyl group in the axial position, which may enable it to participate in alternative hydrogen bonding interactions in the active-site.

50 **51** **52**
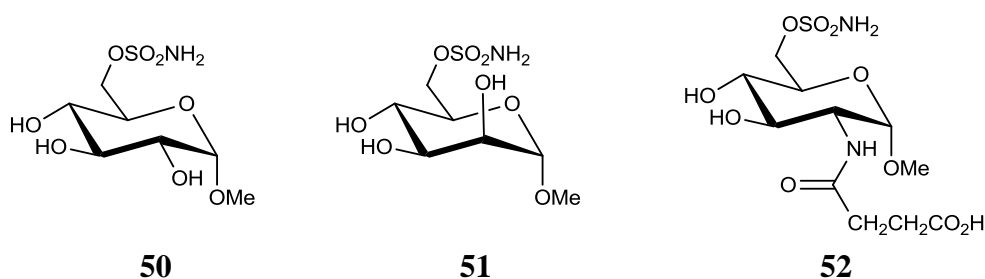
The final N^2-sulfate replacement prepared, **52**, incorporates an *N*-succinamide, providing a flexible link to a carboxylic acid which might be able to interact with basic residues in the active site. The amide carbonyl of **52** may also be able to mimic the sulfonyl group in the N^2-sulfate of compound **25**.

3.6.1.2 Variation of the O^1 Substituent of Compound 25

The O^1-position of glucosamine residues in HSPGs is linked to a hexuronic acid residue. Analogues were prepared to explore whether substitution at this position with polar or lipophilic residues would improve potency by mimicking possible interactions between the O^1-hexuronate and the Sulf-2 active site. Analogues were selected for synthesis based on overlay analyses with a heparin disaccharide template derived from the modelled solution structure.

53 R = $(CH_2)_2OH$ **56** R = i-Pr

54 R = $(CH_2)_3OH$ **57** R = n-Pr

55 R = CH_2CO_2H **58** R = $(CH_2)_3OBn$
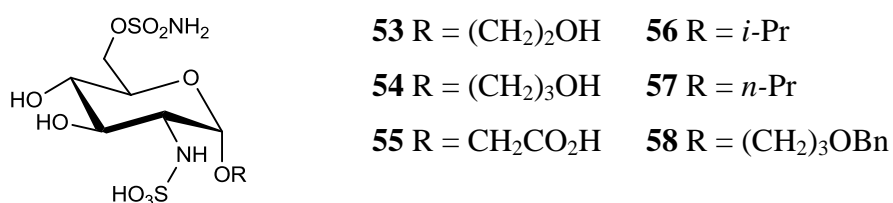
Figure 3.7 demonstrates this superposition for **53**, confirming the potential for O^1 substituents to mimic polar functionality of the O^1-iduronate residue, and suggesting that these substituents may occupy similar regions of space to hydrogen bonding groups in the endogenous substrate.
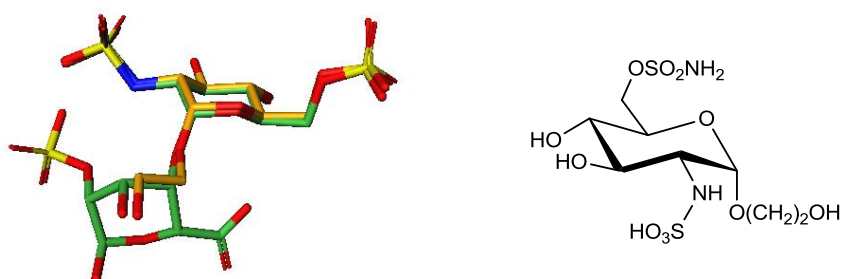
Figure 3.7: Superposition of **53** (orange) with a template disaccharide derived from the modelled solution structure of heparin (green).

The pyran ring of saccharides may also engage in hydrophobic interactions with lipophilic amino acid side chains, which can contribute to binding of saccharides to proteins. Identification of regions of the template where lipophilicity can be productively incorporated would also be useful to improve drug-like properties, for any future programs to identify an orally bioavailable Sulf-2 inhibitor based on this template. A set of analogues with lipophilic anomeric substituents was prepared (**56-58**) to investigate whether increased lipophilicity at this position might improve the binding affinity. Figure 3.8 shows the superposition of analogue **56** with the

disaccharide template, demonstrating the overlay of the isopropyl substituent with the pyran core of the neighbouring iduronic acid residue.
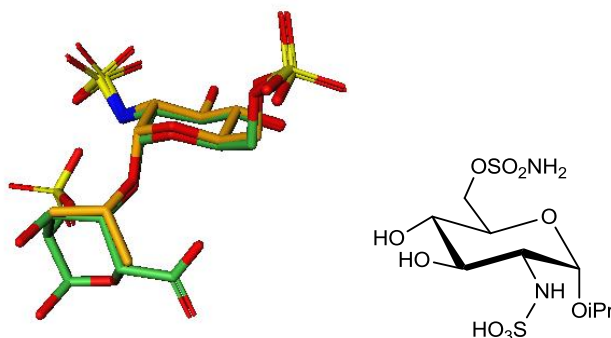
Figure 3.8: Superposition of **56** (orange) with a template disaccharide derived from the modelled solution structure of heparin (green).

To provide further information on the role of the O^1-substituent on the inhibition of Sulf-2 by **25**, β-anomer **59**, and analogue **60**, lacking an O^1-substituent, were also prepared.
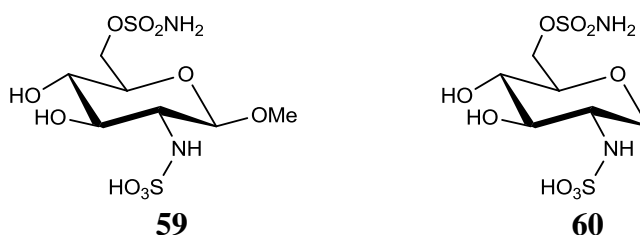
3.6.1.3 Variation of the Substituents at the 3- and 4- Positions of Compound 25

In the endogenous HSPG substrates, the O^4-position of glucosamine residues is substituted with a hexuronic acid residue. The carbohydrate substrates for exosulfatase family members, such as glucosamine-6-sulfatase and galactosamine-6-sulfatase, are unsubstituted at this position. Substitution at O^4 may therefore introduce selectivity for Sulf-1 and Sulf-2 over exosulfatases. The synthesis of analogues incorporating O^4-substituents proved challenging, with the O^4-benzyl ether **61**, being the only analogue prepared. An investigation of a wider range of polar and lipophilic groups at this position would be of interest for future studies.

To explore whether the 3- and 4-hydroxy groups participate in interactions with the active site of Sulf-2, **62** and **63** were prepared, whereby each of these groups was deleted.

61   **62**   **63**
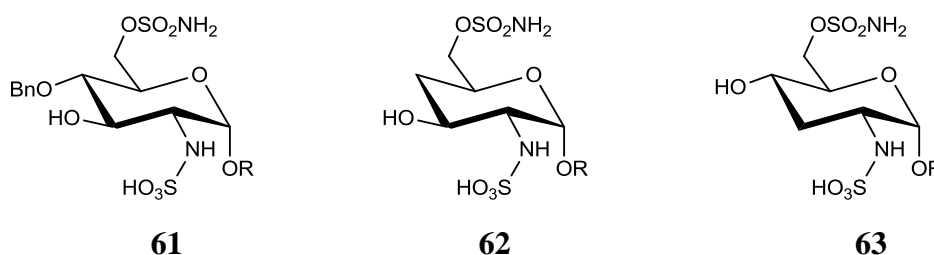
Thus, analogues varying each of the O^1-, N^2-, O^3- and O^4-positions of the template have been designed and prepared.

3.6.2 Sulfatase Inhibition Data for Monosaccharide Sulfamates

Preliminary sulfatase activity against Sulf-2 has recently been generated by Dr Gary Beale and Sari Alhasan on a subset of the compounds prepared. Inhibition of aryl sulfatases A (ARSA) and B (ARSB) was also assessed to determine if the compounds were non-selective inhibitors of the sulfatase enzyme class. Compounds were assayed for their ability to inhibit the desulfation of 4-methylumbelliferyl sulfate (4-MUS) to the fluorescent phenol, 4-methylumbelliferone (4-MU), at a single concentration of 1 mM. In this assay format, lead monosaccharide sulfamate **25** exhibited 38% inhibition of Sulf-2 activity, with no inhibition of ARSA or ARSB. The measured Sulf-2 inhibition of **25** was considerably reduced relative to the reported literature value (IC_{50} = 130 μM), which may reflect differences in the assay procedures. Data for derivatives are therefore considered relative to the activity of compound **25**.

4-MUS   **4-MU**
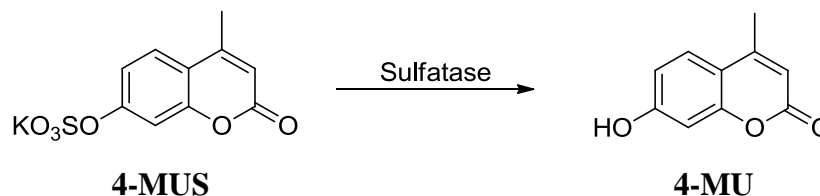
Scheme 3.1: The action of sulfatases in converting 4-MUS to 4-MU.

At the anomeric position, removal of the anomeric alkoxy substituent (**60**) led to a moderate improvement in Sulf-2 inhibition (Table 3.2). The β-methoxy anomer (**59**), and analogues incorporating larger polar or lipophilic α-alkoxy substituents (**53**-**57**)

58

exhibited low Sulf-2 inhibition. However, compound **59** was one of the most potent inhibitors of ARSA and ARSB in the monosaccharide-based set.

Substitution on the N^2-position was not tolerated (**48**, **52** and **104**), but the N^2-primary amine (**105**) retained encouraging Sulf-2 inhibitory activity, indicating that an N^2-sulfate is not essential. This compound was the most potent inhibitor of ARSA tested, but exhibited selectivity over ARSB. Replacement of the amine with an equatorial (**50**) or axial (**51**) hydroxyl group abolished Sulf-2 activity. This may indicate that a similar interaction between the amino substituent and an active site aspartate residue to that proposed in the homology model of *F. Heparinium* sulfatase[131] (see section 2.6) may be conserved in Sulf-2. Investigation of alternative basic groups at this position may therefore be of merit.

Cmpd	Sulf-2 % inh @ 1 mM	ARSA % inh @ 1 mM	ARSB % inh @ 1 mM	R^1	R^2	R^3	R^4
25	38	0	0	α-OMe	$NHSO_3Na$	OH	OH
60	58	0	32	H	$NHSO_3NH_4$	OH	OH
59	13	70	67	β-OMe	$NHSO_3Na$	OH	OH
53	0	0	0	α-O(CH$_2$)$_2$OH	$NHSO_3Na$	OH	OH
54	0	0	0	α-O(CH$_2$)$_3$OH	$NHSO_3NH_4$	OH	OH
55	0	0	0	α-CH$_2$CO$_2$H	$NHSO_3Na$	OH	OH
56	9	0	19	α-O^{i}Pr	$NHSO_3NH_4$	OH	OH
57	3	0	0	α-O^{n}Pr	$NHSO_3NH_4$	OH	OH
48	0	0	12	α-OMe	$NHSO_2Me$	OH	OH
52	9	0	33	α-OMe	NHCO(CH$_2$)$_2$CO$_2$H	OH	OH
104	5	0	44	α-OMe	NHCbz	OH	OH
105	53	86	3	α-OMe	NH_2	OH	OH
50	0	0	11	α-OMe	OH^{eq}	OH	OH
51	0	0	14	α-OMe	OH^{ax}	OH	OH
63	0	0	12	α-OMe	$NHSO_3Na$	H	OH
62	65	0	21	α-OMe	$NHSO_3Na$	OH	H
61	59	0	0	α-OMe	$NHSO_3Na$	OH	OBn

Sulfatase inhibition data are reported as the mean of two determinations

Table 3.2: Preliminary sulfatase inhibition data for monosaccharide sulfamates.

Compound **63**, lacking the 3-hydroxyl group did not inhibit Sulf-2 activity. In contrast, removal of the 4-hydroxyl group (**62**), gave the most potent compound in this set of analogues. The O^4-benzyl ether (**61**) also displayed encouraging levels of Sulf-2 inhibition.

Thus, it appears that substitution at C^1 is not tolerated for Sulf-2 inhibition and a sulfate on the N^2 position is not essential. Variation at the 4-position appears to be tolerated, and this may be a productive area for future investigation.

3.7 Simplified Cyclic Aliphatic Scaffolds

To further explore the structural requirements for inhibition of Sulf-2, simplified aliphatic scaffolds were designed, aiming to mimic the position of the sulfamate and *N*-sulfate groups in **25**, while minimizing other functional groups present. Three cyclic aminoalcohol scaffolds were selected for synthesis based on cyclohexane and piperidine templates (**64**-**66**). The primary sulfamate of pyran-2-methanol (**67**) was also prepared to explore the role of the *N*-sulfate in Sulf-2 inhibitor binding.
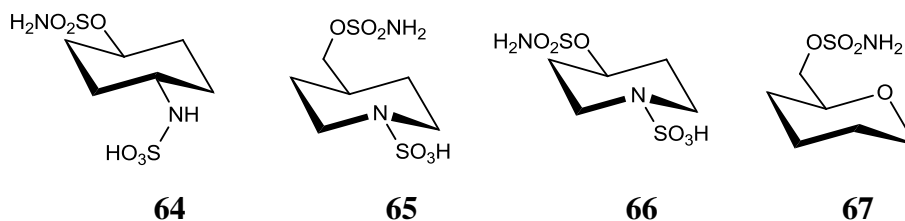
These compounds investigate the contribution of the sulfamate and sulfate moieties to inhibitor binding, and the effect of varying the spatial separation of these groups. Superposition of compounds **64** and **66** with monosaccharide **25** (Figure 3.9) indicated that the sulfamate and sulfate groups can be overlaid in each template.
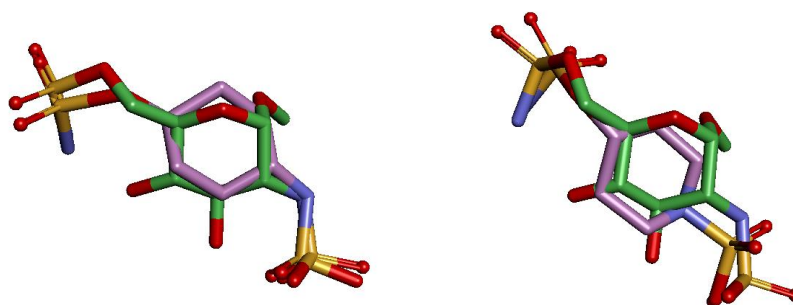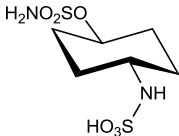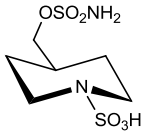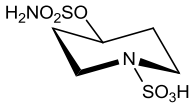
Figure 3.9: Superposition of cyclohexane **64** and piperidine **66** (purple) with monosaccharide **25** (green).

3.7.1 Sulfatase Inhibition Data for Inhibitors Based on Cyclic Aliphatic Sulfamate Scaffolds

Preliminary sulfatase inhibition data have been generated on cyclic aliphatic sulfamates **64-66** (Table 3.3). The cyclohexane (**64**) and piperidine methanol (**65**) scaffolds demonstrated weak Sulf-2 inhibition at 1 mM concentration, with no inhibitory activity against ARSA or ARSB. However, the 4-piperidinol template (**66**) displayed no Sulf-2 inhibition, possibly indicating that there is an optimal distance and orientation of the sulfamate and sulfate moieties.

Structure	Cmpd	Sulf-2 % inh @ 1 mM	ARSA % inh @ 1 mM	ARSB % inh @ 1 mM
	64	19	0	0
	65	23	0	0
	66	0	39	0

Sulfatase inhibition data are reported as the mean of two determinations

Table 3.3: Preliminary sulfatase inhibition data for cyclic aliphatic sulfamates.

3.8 Non-Saccharide Aromatic Heparan Sulfate Mimics

As discussed in chapter 2, aryl sulfamates have been extensively explored as inhibitors of ARSC. A report identified 3-nitrophenylsulfamate as the most potent of the monocyclic aryl sulfamate ARSC inhibitors prepared (ARSC; IC_{50} = 120 μM).[170] In general, ARSC inhibitory activity was found to increase with the electron-withdrawing nature of the aromatic substituent. The parent phenyl sulfamate **29** has also been reported to have weak Sulf-2 inhibitory activity,[132] but other simple aryl sulfamates have been examined for their inhibitory activity against Sulf-2.

Thus, in parallel with the synthesis of monosaccharide-based inhibitors, a set of 16 phenol-derived primary sulfamates (**29**, and **68**-**82**) was designed and prepared to explore the electronic and steric effects of substituents on the aryl ring on Sulf-2 inhibition. This compound set has yet to be profiled for Sulf-2 inhibition.
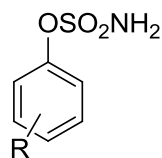
R	H	CF$_3$	CN	NO$_2$	OMe	Ph
Ortho	-	68	71	74	77	80
Meta	29	69	72	75	78	81
Para	-	70	73	76	79	82

From the analysis of heparin-protein interactions presented in chapter 2, it was clear that the sulfate and carboxylate groups often provide important binding contributions. A second generation of phenol-based templates was designed to position the sulfamate and a second polar group in similar regions of space to those adopted in the heparin solution structure. Literature examples where similar non-saccharide heparin mimetic strategies have been successful include suramin (**83**) and its analogues.[171] These high molecular weight compounds are believed to interact with the heparin-binding domain of FGF, with significant contributions to binding arising *via* interactions between the naphthalenesulfonic acid functionalities and basic amino acid residues in the heparin binding domain.

83
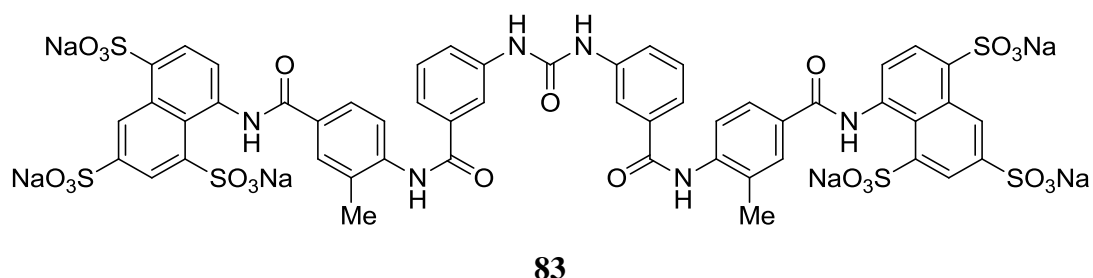
An investigation of lower molecular weight non-saccharide heparin mimics as inhibitors of hepatocyte growth factor/scatter factor activity has also been described, with the sulfate and carboxylic acid being appended to a benzoic acid scaffold.[172] Two compounds obtained through this strategy (**84** and **85**) were able to completely inhibit hepatocyte growth factor/scatter factor activity at concentrations of 100 μg/mL.

84 R = H
85 R = OSO$_3$H
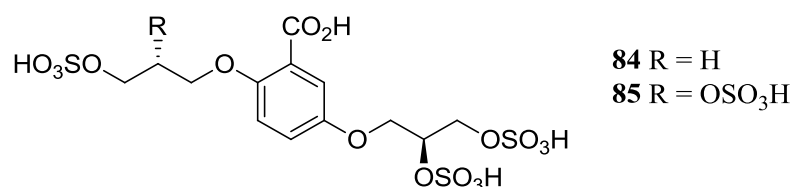
The first template explored for the design of potential Sulf-2 inhibitors using this strategy was based on a biphenyl sulfamate scaffold, with polar groups incorporated on the B-ring (Figure 3.10).

R = CO$_2$H, CO$_2$Me, CONH$_2$,
NH$_2$, NHAc, NHSO$_3$H
R' = H, Me
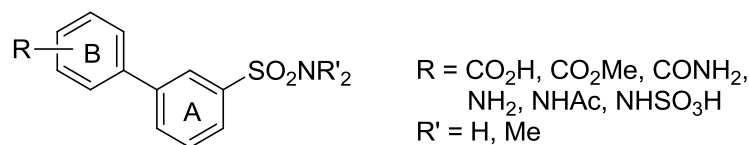
Figure 3.10: General structures for analogues designed in the biphenyl template.

The aim was to mimic the spatial orientation of hydrogen bonding groups of the neighbouring iduronate residues in the endogenous substrate. The designs were minimised in the gas phase, and overlaid onto a heparin-derived truncated trisaccharide template, in order to identify compounds that may allow the correct three dimensional orientations of polar functionalities. Representative overlay diagrams are shown in figure 3.11. The trisaccharide template was taken from the reducing end of the modelled heparin structure incorporating iduronic acid residues in the $^1C_4$ conformation. In addition to specific rationally designed analogues, this template was used to probe the active-site for polar interactions through incorporation of polar functional groups with diverse hydrogen bonding and charge characteristics into the 2', 3' and 4' positions of the B ring. This strategy could provide lead compounds with improved physicochemical properties relative to the saccharide based series, and amenable to more rapid analogue synthesis. The biaryl analogues described in this section were prepared by other colleagues working on the project. Sulf-2 inhibition data has not yet been generated on this compound set.
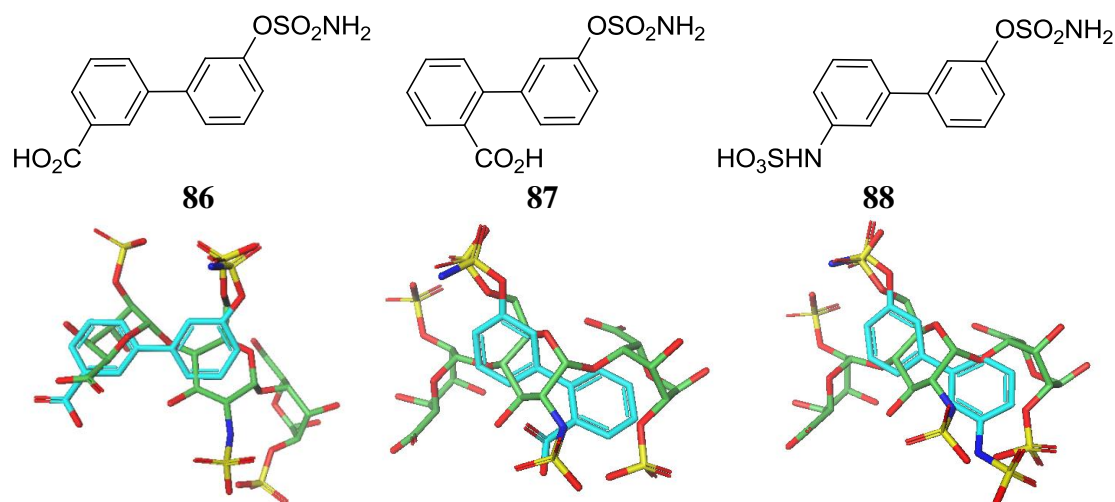
Figure 3.11: Representative overlays of biaryl targets **86**, **87**, and **88** (cyan) with a heparin trisaccharide template (green).

3.9   Benzylic Sulfamates

Benzylic sulfamates **89-92** were also investigated, incorporating the sulfamate functionality on an sp^3 hybridised carbon atom, which mimics the hybridisation-state of the linking-atom in the endogenous substrate of Sulf-2.

89 R = NO$_2$ **91** R = NO$_2$
90 R = NHSO$_3$H   **92** R = NHSO$_3$H
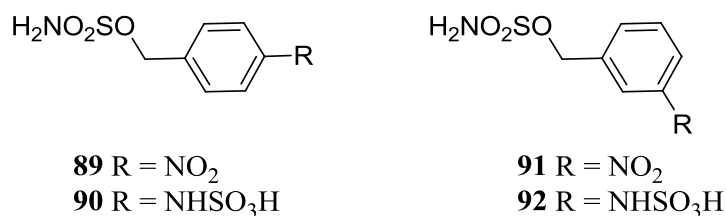
Superposition of benzylic sulfamate **90** with monosaccharide **25** demonstrates the overlap of both the sulfamate and sulfate groups in these templates (Figure 3.12). However, due to synthetic chemistry issues, only nitro intermediates **89** and **91** were successfully prepared, with evidence of potential chemical instability being observed for compound **90** (See section 4.6). Sulf-2 inhibition data has not yet been generated on compounds **89** and **91**.
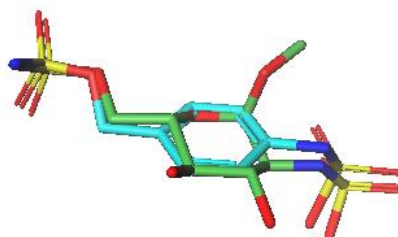
Figure 3.12: Overlay of benzylic sulfamate **90** (cyan) with monosaccharide **25** (green).

3.10 Sulf-2 Design and Biological Data Summary

In order to attempt to identify tool compounds for use in biological target validation studies, two approaches were investigated. Analogues of the literature monosaccharide inhibitor, **25**, were designed and prepared, incorporating structural changes in the substituents around the pyran core to build knowledge of the SARs. The aim was to identify features that improve Sulf-2 inhibitory potency, and explore how these changes affect selectivity over other sulfatase family members. Preliminary sulfatase inhibition data indicated that larger substituents at C^1 and N^2 were not tolerated. The C^1-methylene (**60**) and N^2-primary amine (**105**) derivatives exhibited improved Sulf-2 inhibition relative to **25**, indicating that simplification of the template is possible. Variation at the C^4-position (compounds **61** and **62**) was also tolerated, and would merit further investigation.

The second approach employed a *de novo* design strategy, based on an analysis of functional groups in the endogenous substrate HSPGs, which may be important for binding in the active site of Sulf-2. Non-saccharide aryl sulfamate scaffolds were selected that allowed superposition of sulfamate and other polar groups with those present in the HSPG template. Sulfatase inhibition data has not yet been generated on these compounds.

Chapter 4: Synthesis of Potential Sulf-2 Inhibitors

4.1 Synthesis of Monosaccharides 25 and 27

The literature monosaccharide-based inhibitors of Sulf-2, **25** and **27** were the first two compounds targeted. The published synthesis of **27** comprises nine steps starting from glucosamine (**93**) with an overall 8.5% yield (Scheme 4.1).[132]
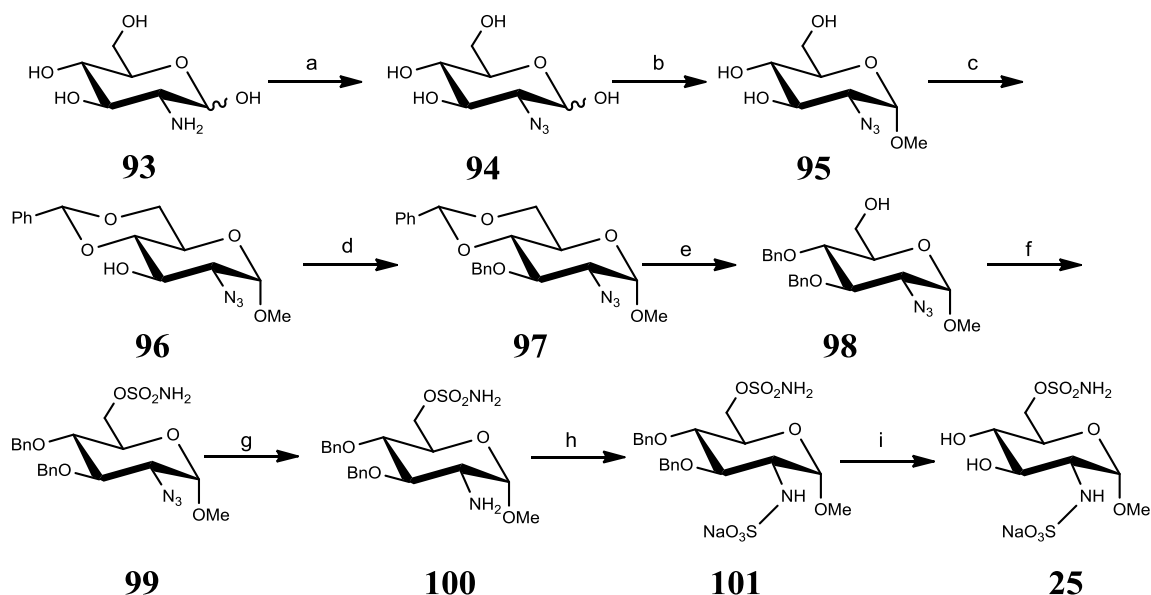
Scheme 4.1: *Reagents and conditions* a) TfN$_3$; NaOMe, DMAP/MeOH, CH$_2$Cl$_2$/20 °C; b) HCl/MeOH; c) PhCH(OMe)$_2$, TsOH, DMF, 51% over 3 steps; d) BnBr, NaH, THF, 85%; e) BF$_3$, Bu$_2$OTf, 0 °C, 2 h, 69%; f) NaH, ClSO$_2$NH$_2$, THF, r.t. 24 h, 88%; g) H$_2$/10% Pd/C, MeOH, r.t. 4 h, 65%; h) Py.SO$_3$, pyridine, r.t. 2 h, 65%; i) H$_2$/10% Pd/C, EtOH, r.t. 36 h, 77%.

Six of the nine steps of the published synthetic route involve protecting group manipulations to enable regioselective introduction of the O^6-sulfamate. In the first step, the N^2-position of glucosamine (**93**) is protected as an azide (**94**), introduced using triflic azide, a reagent with a well-documented explosion hazard.[173] This reaction is performed in dichloromethane, leading to a combination of reagents which can readily form diazidomethane, another high energy compound that has been implicated in several laboratory explosion incidents.[174] After introduction of the anomeric methoxy substituent, selective protection of the 3- and 4-positions is achieved using a 3-step procedure which starts with protection of the 4- and 6-positions as a benzylidene acetal, **96**. The remaining alcohol group at the 3-position is protected as

benzyl ether **97**, and regioselective reductive cleavage of the acetal provides **98** as the substrate for sulfamate formation. Chemoselective reduction of azide **99** gives amine **100**, which is sulfated before a final double debenzylation reaction to provide **25**. The length of the synthesis and low overall yield would require the potentially hazardous first step to be performed on a large scale to enable sufficient quantities of intermediate **94** to be prepared to allow analogue synthesis. The number of synthetic steps required for each analogue was also considered sub-optimal. For example, introduction of alternative groups at the anomeric position would be achieved in step two, with seven further steps required to progress each analogue to the target compound. Thus an alternative route was sought.

4.1.1 Development of a Novel Route to Monosaccharides 25 and 27

A more efficient synthesis was envisioned through minimising the number of protecting group manipulations. A route was designed seeking to investigate whether the reactivity difference of primary and secondary alcohols with electrophiles could be exploited to develop a regioselective sulfamoylation process, which would allow access to **25** in just five steps (Scheme 4.2). A similar approach for the regioselective mono-methylsulfonylation of the O^6-position of *N*-acetylglucosamine had been reported to proceed in over 70% yield.[176]
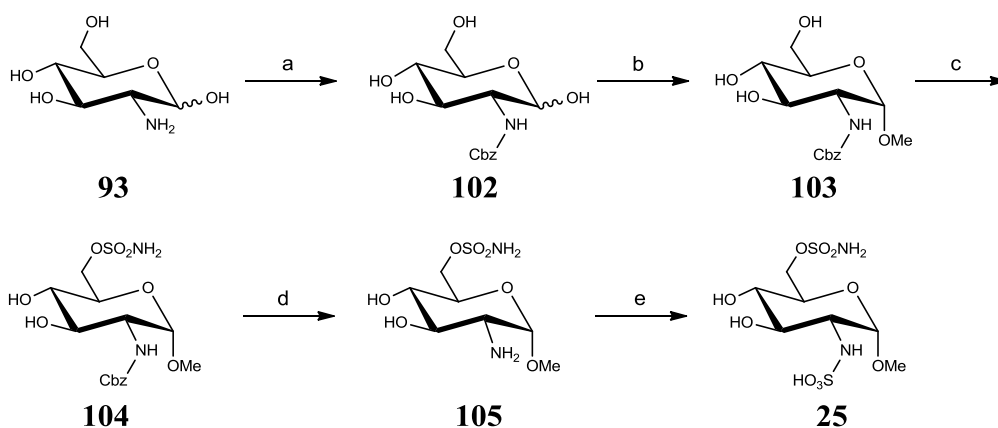
Scheme 4.2: Proposed route employing a regioselective sulfamoylation for the preparation of **25**. *Reagents:* a) CbzCl, NaHCO$_3$, H$_2$O; b) HCl/MeOH; c) ClSO$_2$NH$_2$, DMA/Tol; d) H$_2$/Pd/C, MeOH; e) PySO$_3$, pyridine.

For an initial investigation of the key regioselective sulfamoylation reaction, a readily available pyranoside monosaccharide template was required. The commercial availability of *N*-acetyl glucosamine (**106**) led to the selection of **107** as the first template in which to explore this concept. This would also lead to the preparation of **27**, an analogue of **25** with reportedly weak inhibitory activity against Sulf-2.[132]
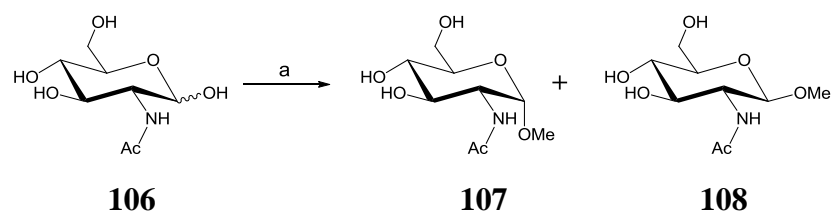
Scheme 4.3: Synthesis of **107** as a substrate for regioselective sulfamoylation studies. *Reagents and conditions*: a) Amberlite IR120 H$^+$, MeOH, 69 °C, 18 h, (**107**: 44%.)

Treatment of *N*-acetylglucosamine (**106**) with Amberlite IR120 H$^+$ ion exchange resin in methanol at reflux allowed introduction of the anomeric methoxy group. A 4:1 mixture of anomers was obtained, favouring the desired α anomer (**107**), and consistent with the stabilisation of the axial-isomer by the anomeric effect (Scheme 4.3). The major isomer had a coupling constant of 3.6 Hz between H^1 and H^2, in keeping with the α anomer; the minor anomer (**108**) had a larger coupling constant (*J* = 7.9 Hz) consistent with the vicinal diaxial arrangement of the β anomer.[177] Separation of **107** and **108** was not possible by normal or reversed phase chromatography, but isolation was achieved using a quaternary ammonium ion exchange column converted to the hydroxide form.[178]

4.1.1.1 Studies on the Formation of Sulfamoyl Chloride (H₂NSO₂Cl)

Literature procedures for the preparation of primary sulfamates generally involve reaction of a phenol or alcohol with sulfamoyl chloride (**112**, R = SO₂Cl), prepared *in situ* by the reaction of formic acid with chlorosulfonyl isocyanate **109** (R = SO₂Cl).[179] The proposed mechanism for the formation of sulfamoyl chloride in this reaction is shown in scheme 4.4.[180,181,182]
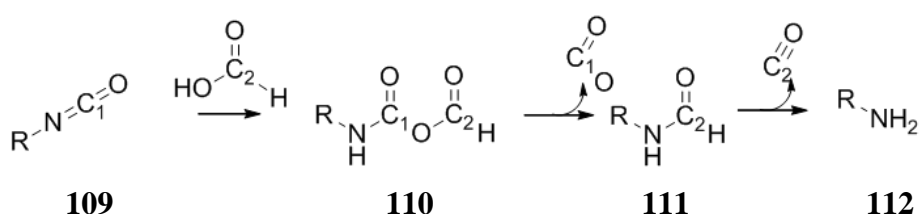
Scheme 4.4: Probable mechanism for the formation of sulfamoyl chloride from the reaction of chlorosulfonyl isocyanate with formic acid.

In support of this mechanism, gas evolution studies when R is aryl have confirmed that two mole equivalents of gas are liberated,[181] with radio-tracer studies establishing that the first is released as CO_2.[180] In the same study the carbon of the CO_2 was found to derive from the isocyanate (C_1), and formamide intermediate **111** contained the carbon from formic acid (C_2).[180] The second step of the mechanism can be considered as an intramolecular transacylation,[182] with subsequent loss of carbon monoxide to give **112**. Dichloromethane is the most commonly used solvent for the formation of sulfamoyl chloride.[159] However, in the current work the reagent formed as a suspension in this solvent, complicating its addition to the alcohol substrate. Reaction of formic acid with chlorosulfonyl isocyanate under solvent-free conditions, with subsequent addition of toluene to prepare a stock homogeneous sulfamoyl chloride solution[170] proved superior, and this method was used in the synthesis of the first analogues prepared. Dissolution of sulfamoyl isocyanate in toluene prior to the addition of formic acid led to inferior conversion when used in sulfamate formation reactions. An improved process was subsequently developed later in the project, employing MeCN as solvent for the sulfamoyl chloride formation, and was used for the synthesis of further analogues. This method gave a homogeneous solution, and provided superior control of gas evolution, which would be of particular value for future scale-up. The shelf-life of the acetonitrile sulfamoyl chloride solution was assessed by investigating its effectiveness in the sulfamate formation reaction on 2-(4-nitrophenyl)ethanol (**113**) over a 28 day period (Table 4.1).
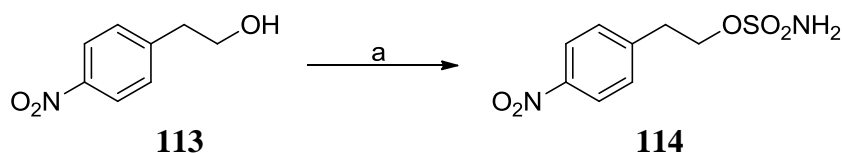
Time days[a]	113 %[b]	114 %[b]
0[c]	0	100
1	0	100
4	4	96
7	8	87
14	12	82
28	19	72

[a] Number of days of storage of the sulfamoyl chloride solution at r.t. under nitrogen prior to being used in the sulfamate formation reaction; [b] Percentages of **113** and **114** were estimated from LC-MS UV traces; [c] Solution used immediately after preparation.

Table 4.1: Investigation of the stability of a solution of sulfamoyl chloride in acetonitrile. *Reagents and conditions*: a) $ClSO_2NH_2$ (1 M in MeCN, 3 eq.), DMA, r.t., 30 min.

On storage for 24 h, the sulfamoyl chloride solution retained the ability to effect rapid sulfamoylation of **113**. A steady fall in conversion of **113** into **114** was seen when the reagent was stored for longer periods. Between days 4 and 7, material was observed to precipitate from the solution, and this could not be redissolved using sonication. Thus, freshly prepared sulfamoyl chloride solution was used in the preparation of sulfamate target compounds.

4.1.1.2 Regioselective Sulfamate Formation

Amide solvents such as DMA, NMP, or DMF have been reported as optimal for sulfamoylation of alcohols and phenols.[183] DMF has been found to form adducts with the sulfamate products, reducing the yield,[184] leading to the selection of DMA as solvent for our initial studies. The effect of sulfamoyl chloride stoichiometry on the sulfamate formation was studied for the conversion of **107** into **27** (Table 4.2).

107 → **27**
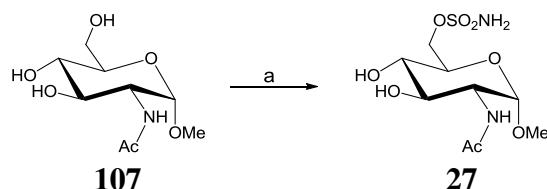
Expt	ClSO$_2$NH$_2$ Eq.	Temp °C	Time h	27[a] %	107[a] %
1	1	8	72	12	70
2	1.5	8	2	20	80
3	1.8	8	18	40	60
4	3	8	3	40	0

[a] Percentages of **107** and **27** were estimated from LC-MS UV traces.

Table 4.2: *Reagents and conditions*: a) ClSO$_2$NH$_2$ (1 M in MeCN), DMA, 8 °C.

Reactions were performed at an internal reaction temperature of 8 °C. Low conversion was obtained with one equivalent of sulfamoyl chloride, even on extended reaction times. Increasing the number of equivalents of sulfamoyl chloride improved conversion, with 1.8 equivalents proving optimal. Use of 3 equivalents led to a similar isolated yield, with complete consumption of starting material. In addition to formation of **27**, two derivatives, the O^3,O^6-*bis*(sulfamate) (**115**) and O^4,O^6-*bis*(sulfamate) (**116**) were also isolated.
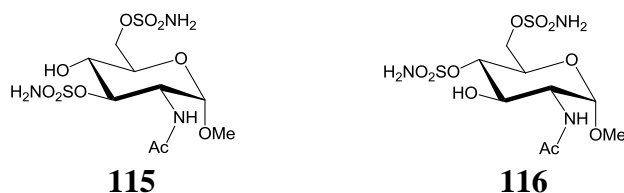
The regiochemistry of sulfamoylation of **27**, **115** and **116** was determined from the chemical shifts of the C*H*OSO$_2$NH$_2$ protons which could be unambiguously assigned from 2-dimensional homonuclear COSY NMR experiments. These protons experienced a downfield shift of between 0.3 and 0.6 ppm on sulfamate formation of the respective alcohols. This study provided proof of principle that regioselective sulfamoylation of glucosamine monosaccharide templates was achievable, and attention was turned to the synthesis of substrate **103**, required for the synthesis of **25**.

4.1.1.3 The Synthesis of 103
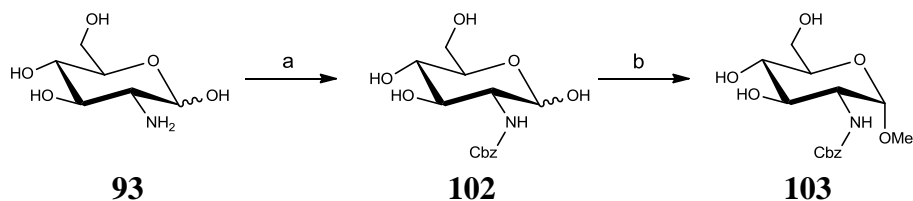
Scheme 4.5: *Reagents and conditions*: a) CbzCl, NaHCO$_3$, H$_2$O, r.t., 18 h, 92%; b) 1.25 M HCl in MeOH, 65 °C, 18 h, 73%;

A literature procedure was successfully employed for the preparation of benzyl carbamate **102** from D-glucosamine (**93**, Scheme 4.5).[185] Precipitation of **102** from the reaction mixture allowed its isolation by simple filtration as a white solid in 92% yield. Introduction of the anomeric methoxy group using Amberlite IR-120 resin resulted in formation of multiple minor by-products, complicating isolation of **103**. Heating at reflux for 18 h resulted in a 1:1 mixture of α:β anomers, which equilibrated to 5α:1β on prolonged heating (72 h), and remained constant on further extension of the reaction time. A cleaner profile was obtained by heating at reflux in a 1.25 M solution of HCl in methanol, with a stable product ratio of 5α:1β being achieved after 18 h. In this case, the anomers were readily separable by chromatography on silica to give **103** in a 73% yield. As described previously for **107**, the anomeric stereochemistry was assigned from the coupling constant of the H^1 proton.

4.1.1.4 Regioselective Sulfamoylation of 103
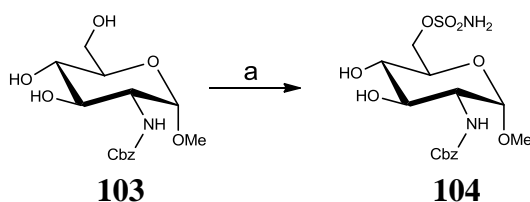
Scheme 4.6: *Reagents and conditions*: a) ClSO$_2$NH$_2$ (2.25-3 eq.), DMA, -15 °C, 18 h, 37-43%; b) H$_2$/10% Pd/C, MeOH/CH$_2$Cl$_2$, 40 °C, 1 h, 100%.

The key regioselective sulfamoylation was performed at room temperature in DMA, giving a 15% yield of **104**, with LC-MS analysis indicating significant formation of *bis*-sulfamate by-products. When the reaction was performed at -15 °C, *bis*-sulfamoylation was reduced, leading to an improved yield of **104**. The freezing point of DMA (-20 °C) prevented further reduction of the reaction temperature. To achieve

complete consumption of **103**, 2.25-3 equivalents of sulfamoyl chloride were required, with variability observed between batches of sulfamoyl chloride. Careful reaction monitoring and titration of sulfamoyl chloride was required to achieve optimal conversion leading to isolated yields of **104** of 37-43%. This method is referred to as sulfamoylation method 1. The regiochemistry was ascertained from 2D ^{1}H NMR, with coupling of the C^3-H and C^4-H protons to the O^3-H and O^4-H protons, respectively, confirming that these hydroxyl groups remained unsubstituted. No coupling was observed between the C^6- and O^6-protons, indicating that this position had been sulfamoylated. The proton NMR signals for the C^6-protons of **104** also experienced a downfield shift of between 0.5 and 0.6 ppm, consistent with the addition of the electron-withdrawing sulfamate group to the O^6-oxygen atom. The C^3- and C^4-protons experienced no such downfield shift.
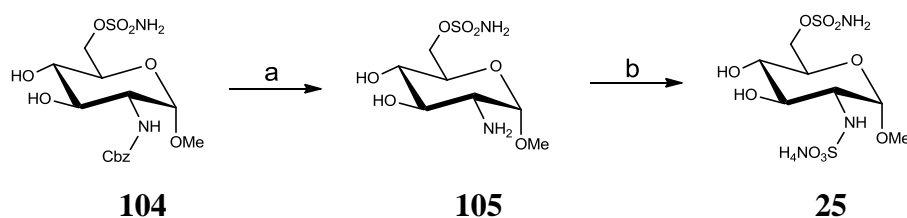
Scheme 4.7: *Reagents and conditions* a) H$_2$/10% Pd/C, MeOH/CH$_2$Cl$_2$, 40 °C, 1 h, 100%; b). SO$_3$.Py, H$_2$O, pH 9-10, r.t. 2.5 h, 43%.

The Cbz protecting group was removed in quantitative yield using flow hydrogenation over 10% palladium on carbon to give **105** (Scheme 4.7). Sulfation of the amino group of **105**, in the presence of the unprotected secondary alcohol groups, proved to be non-selective using sulfur trioxide-pyridine complex in anhydrous pyridine, affording a mixture of 2,3- and 2,4-*bis* sulfated products. A literature procedure for selective sulfation of an amino group in the presence of unprotected alcohols under pH controlled conditions was successfully applied.[186,187] Maintaining a pH of 9-10 during the addition of sulfur trioxide-pyridine complex, resulted in chemoselective sulfation on the amino group. Buffering was achieved by adjusting the pH of the reaction with 2 M aqueous NaOH after each portionwise addition of the sulfating reagent, resulting in isolation of **25** in a 43% yield after column chromatography.

No explanation as to the origin of the observed chemoselectivity of the sulfation reaction under the buffered conditions is given in the literature. It is possible that sulfate esters formed on the alcohol groups may be unstable at the basic reaction pH. At higher basicities, sulfur trioxide-pyridine complex is known to be unstable,

degrading to a "red complex",[188] dictating the narrow optimum pH range for the reaction. This step was the lowest yielding in the synthesis of **25**, and was later found to be substrate-dependent, with optimal yields of 40-45% being obtained. An alternative *N*-sulfation process *via* a trichloroethyl protected sulfate (**117**) provided **25** in a superior yield of 56% over two steps (Scheme 4.8). Incorporation of this sulfation protocol into the synthesis of **25** improved the overall yield for the preparation of this key Sulf-2 inhibitor to 16% over six steps.
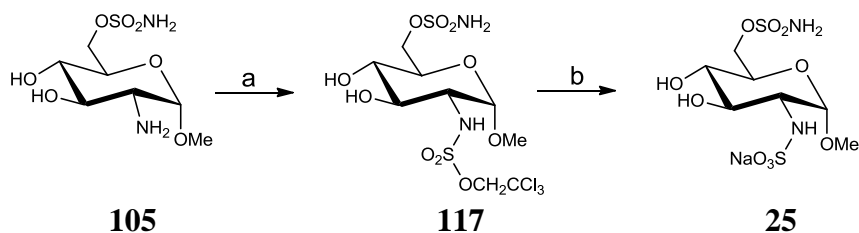
Scheme 4.8: *Reagents and conditions*: a) 1,1,1-trichloroethylsulfonyl imidazolium tetrafluoroborate (1 eq.), THF, 60 °C, 18 h, 61%; b) i) Zn (15 eq.), MeOH, H$_2$O, 60 °C. 1 h; ii) Ion exchange chromatography on Dowex 50W8x200 Na form, H$_2$O, 93%.

4.1.2 Optimisation of the Sulfamoylation Reaction

Sulfamoylation method 1 was used for the synthesis of a number of analogues of compound **25**, which will be described later. However, during the course of these syntheses it became apparent that the yields for this reaction were substrate-dependent, varying from 15-43%. Thus, in parallel with preparing analogues of **25** using this procedure, attempts were also made to further improve the overall regioselectivity, yield, and cross-substrate reliability of this reaction.

4.1.2.1 Studies with Alternative Sulfamate Transfer Reagents

Increased steric bulk around the electrophilic sulfur centre of sulfamoyl chloride was investigated in the hope of improving the regioselectivity for sulfamate formation on the less hindered O^6-primary alcohol. A small program of work was undertaken to investigate additives that might exchange with the chloride leaving group of sulfamoyl chloride, resulting in a more sterically constrained sulfamoyl transfer reagent (Scheme 4.9).
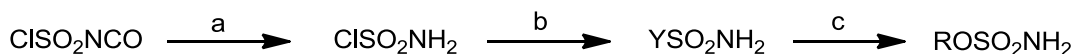
Scheme 4.9: Introduction of a bulky leaving group (Y) to form an alternative sulfamoyl transfer reagent. *Reagents and conditions*: a) HCO_2H (1 eq.), MeCN; b) Additive (1 eq.); c) ROH (0.5 eq.), DMA, -15 °C.

In situ generation of potential sulfamate transfer reagents **118a-d** was explored by addition of imidazole, pyridine, DMAP and sodium iodide, respectively, as additives to the stock solution of sulfamoyl chloride.

118a   **118b**   **118c**   **118d**
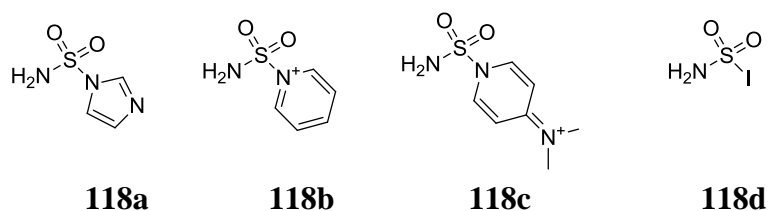
These reagents were first investigated for the sulfamoylation of model substrate **113**, with the high UV activity of **114** allowing facile reaction monitoring and purification. Only adduct **118d**, prepared by addition of one equivalent of sodium iodide to the sulfamoyl chloride solution, resulted in successful conversion to **114**, but with an inferior isolated yield to that obtained in the absence of additives. The iodide adduct was subsequently reacted with **103**, giving an isolated yield of 36% of **104** as compared to 43% using sulfamoylation method 1.

A modified Burgess reagent (**119**) was subsequently reported to provide successful sulfamoylation of alcohols and phenols.[189,190] This reagent was prepared in two steps from chlorosulfonyl isocyanate (Scheme 4.10).
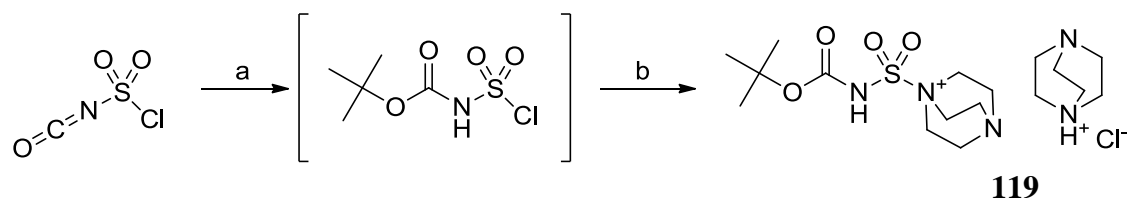
Scheme 4.10: The synthesis of **119**. *Reagents and conditions:* a) ^tBuOH, toluene; b) DABCO

Reaction of **119** with alcohols and phenols was reported to proceed in high yield, and give selectivity for primary alcohols over secondary alcohols. On preparation, **119** was

found to be moisture sensitive, hydrolysing in less than ten minutes in CD_3CN containing trace water during NMR studies. Reaction of **119** with **103** under anhydrous conditions gave multiple products with low regioselectivity. As these reagents require an extra acidic deprotection step to liberate the free primary sulfamate, which may not be compatible with the anomeric acetal in **103**, this approach was not investigated further.

4.1.2.2 Model Studies on the Sulfamate Formation Reaction

The identification of 4-nitrophenethyl alcohol (**113**) as a substrate that undergoes rapid conversion into sulfamate **114**, and can easily be monitored by LC-MS, provided a useful model system to enable detailed investigation of factors affecting the sulfamate transfer reaction. All reactions in the following section were performed by adding 2 equivalents of sulfamoyl chloride (1 M in MeCN) to 1 equivalent of **113** in DMA at the specified temperature. Conversions were monitored by analysis of the LC-MS UV trace. The extinction coefficients of **113** (ε = 3,499 $M^{-1}cm^{-1}$) and **114** (ε = 10,546 $M^{-1}cm^{-1}$) at 254 nm were determined using the Beer-Lambert law from a 3-point concentration-absorbance curve measured in ethanol, and indicated that the absorbance of product **114** was approximately 3-fold greater than that of substrate **113** at this wavelength. The percentages %**113** and %**114** in the following tables are corrected from the integral of the UV trace for this difference in extinction coefficients using equations 1 and 2. Where %**113** and %**114** do not sum to 100%, the remaining percentage was accounted for by one or more by-product peaks in the UV trace.

Equation 1:

$\%113_{corr} = ((\%113_{meas} \times 3.014)/((\%113_{meas} \times 3.014) + \%114_{meas})) \times (\%113_{meas} + \%114_{meas})$

Equation 2:

$\%114_{corr} = ((\%114_{meas}/3.014)/((\%114_{meas}/3.014) + \%113_{meas})) \times (\%113_{meas} + \%114_{meas})$

4.1.2.3 Investigation of the Effect of Solvent on Sulfamate Formation

The use of DMA as solvent in the sulfamoylation reaction has several disadvantages. The high freezing point precludes the use of temperatures below -15 °C, and its high boiling point complicates reaction work-up. TLC analysis was also complicated by the presence of DMA, owing to a large solvent spot having similar R_f to **103** and **104**. Substitution of DMA for alternative solvents at -15 °C was therefore investigated (Table 4.3).
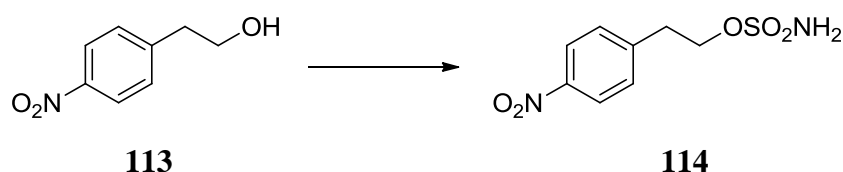
Entry	Solvent	5 min		3 h		24 h	
		%113	%114	%113	%114	%113	%114
1	DMA	11	89	9	91	6	94
2	DMF	8	76	11	60	11	60
3	Dioxane	80	0	75	4	75	4
4	MeCN	85	0	75	4	74	4
5	THF	87	1	75	13	75	13
6	CH₂Cl₂	87	0	78	2	78	2
7	EtOAc	82	0	70	4	70	4

Table 4.3: Investigation of the effect of solvent on the conversion of **113** into **114**.

Reaction in DMF (entry 2) gave a similar initial conversion to DMA (entry 1), but extended reaction times resulted in by-product formation, consistent with reports of the formation of DMF adduct **120** with primary sulfamates.[184]

120
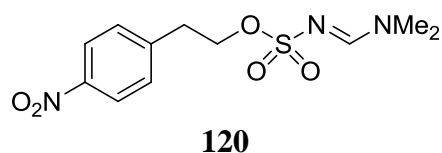
All other solvents investigated resulted in a slow reaction, coupled to the formation of multiple side products. The poor reactivity in ethyl acetate suggests that amide containing solvents have a unique effect on the reaction, which cannot be mimicked by an ester group. The cyclic ethers, THF and dioxane, were the next most successful solvents, with no starting material remaining after 24 h, and moderate conversion to product. The use of THF as a co-solvent allowed the amount of DMA to be reduced,

conversion in 10% DMA in THF proving similar to the reaction in 100% DMA (Table 4.4), with only a small retardation of the reaction. Further reduction of the DMA concentration led to a significantly slower reaction and by-product formation. Other amide or urea additives gave inferior results.
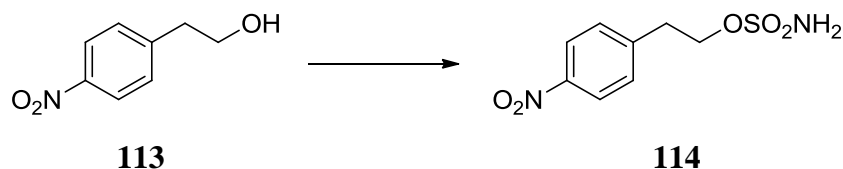
Solvent	5 min		30 min		3 h	
	%113	%114	%113	%114	%113	%114
100% DMA	11	89	n.d.	n.d.	9	91
10% DMA/THF	16	77	0	100	n.d.	n.d.
5% DMA/THF	43	41	20	65	n.d.	n.d.
1% DMA/THF	33	53	0	45	n.d.	n.d.
10% DMF/THF	20	65	n.d.	n.d.	34	58
10% NMP/THF	58	42	n.d.	n.d.	40	55
10% DMI†/THF	46	16	n.d.	n.d.	15	53

† DMI = 1,3-dimethylimidazolidinone; n.d. = not determined

Table 4.4: Investigation of the effect of solvent mixtures on the conversion of **113** into **114**.

4.1.2.4 Investigation of Sulfamate Formation at Reduced Temperature

DMF and 10% DMA in THF were selected as solvents for an investigation of the effect of reducing the reaction temperature. The freezing point of DMF (-61 °C) enables studies at lower temperatures than in DMA. At -40 °C in 100% DMF, the reaction proceeded cleanly, and with significant conversion after 24 hours (Table 4.5). Furthermore, at this temperature, formation of undesired DMF adduct **120** was completely suppressed.

Entry	Time h	%113	%114
1	0.08	95	5
2	0.5	92	8
3	1.5	86	14
4	4	75	23
5	18	62	38
6	24	69	31

Table 4.5: Investigation of conversion of **113** into **114** at -40 °C in DMF

The reaction progressed more slowly in 10% DMA in THF at -40 °C, with only 19% of **114** being obtained after 24 h, and multiple by-products being observed (Table 4.6).

Entry	Time h	%113	%114
1	0.08	63	1
2	1	63	1
3	4	60	2
4	24	32	19

Table 4.6: Investigation of conversion of **113** into **114** at -40 °C in 10% DMA/THF

Other solvent mixtures were re-investigated for the low temperature reaction, to ensure that the optimal solvent systems for application to the monosaccharide synthesis were selected (Table 4.7).

Solvent	5 min		3 h		18 h	
	%113	%114	%113	%114	%113	%114
DMA	97	3	75	25	33	67
10% DMA/THF	100	0	89	11	54	46
10% DMA/MeCN	91	9	61	39	25	75
DMF	93	7	47	53	0	95
10% DMF/THF	100	0	96	4	78	18

Table 4.7: Investigation of solvent systems for conversion of **113** into **114** at -40 °C.

In contrast to the results in MeCN at room temperature (Table 4.3), the use of 10% DMA in MeCN at low temperature gave high conversion and a similar reaction profile to that in neat DMF. These two solvent systems were therefore selected as the solvents of choice for an investigation of the regioselectivity of the sulfamoylation reaction with primary and secondary alcohols at low temperature. The reaction in DMF will be referred to as sulfamoylation method 2, and in 10% DMA/MeCN as method 3.

4.1.3 Application of Low Temperature Conditions to the Formation of Monosaccharide 25

The optimised low temperature conditions were applied directly to monosaccharide **103**. After 24 hours at -40 °C, TLC analysis suggested that starting material (**103**) was the major component present in both reactions. A further equivalent of sulfamoyl chloride was added to each reaction, with stirring at -40 °C for a further 72 hours. Isolated yields after chromatography are presented in Table 4.8.
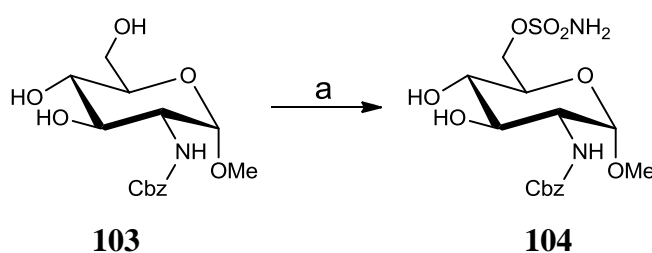
	104	Mixed by-products[a]
	%	%
Method 2	55	15
Method 3	19	42

[a] Isolated yield of mixed *bis*-sulfamoylated by-products.

Table 4.8: Isolated yields from the low temperature sulfamoylation of **103** to give **104**. *Reagents and conditions*: a) Method 2: ClSO$_2$NH$_2$ (1 eq., 1 M in MeCN), DMF, -40 °C, 24 h; Method 3: ClSO$_2$NH$_2$ (1 eq., 1 M in MeCN), 10% DMA/MeCN, -40 °C, 24 h.

Sulfamoylation method 2 proved superior to method 3, giving the highest isolated yield (55%) yet achieved for this reaction. The relatively poor results obtained with method 3 may have arisen from the reaction becoming viscous due to the temperature approaching the freezing point of MeCN (mp -46 °C). Reduced efficiency of mixing could result in high local concentrations of sulfamoyl chloride, which may lead to an increase in *bis*-sulfamoylation. The reaction using method 2 remained as a free flowing homogeneous solution throughout. The yield obtained for the sulfamoylation of **103** resulted in an improvement in the overall yield of the six step synthesis of **25** to 21%, which compares favourably with the 9% yield obtained in the literature 9 step synthesis of **25**. Analogues of **25** requiring regioselective sulfamoylation were subsequently prepared using method 2.

4.2 Preparation of Analogues of 25

4.2.1 Variation of the 2-Amino Substituent of 25

From the homology model of *F. heparinium* sulfatase, it was proposed that the sulfate on N^2 of the glucosamine residue in heparan sulfate may affect binding solely by enhancing the hydrogen bond donor ability of the N^2-hydrogen atom.[131] In order to explore this hypothesis for Sulf-2, sulfonamide derivatives **48** and **49** that would further acidify the *NH* were synthesised. The reaction of amine **105** with the respective sulfonyl chlorides provided **48** and **49**, as described in Scheme 4.11. Optimisation of these conditions was not investigated.
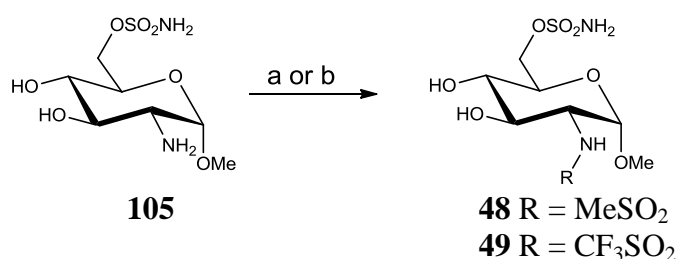
Scheme 4.11: *Reagents and conditions*: a) R = MeSO$_2$: MeSO$_2$Cl, Et$_2$iPrNH, CH$_2$Cl$_2$, 0 °C-r.t., 1 h, 28%; b) R = CF$_3$SO$_2$: (CF$_3$SO$_2$)$_2$O, Et$_3$N, CH$_2$Cl$_2$/dioxane, 0 °C, 1 h, 33%.

Slow evaporation of a dilute methanolic solution of **48** provided a crystal suitable for small molecule X-ray crystallography. The structure generated (Figure 4.3) unequivocally confirmed the assignment of the O^6-sulfamate regiochemistry.
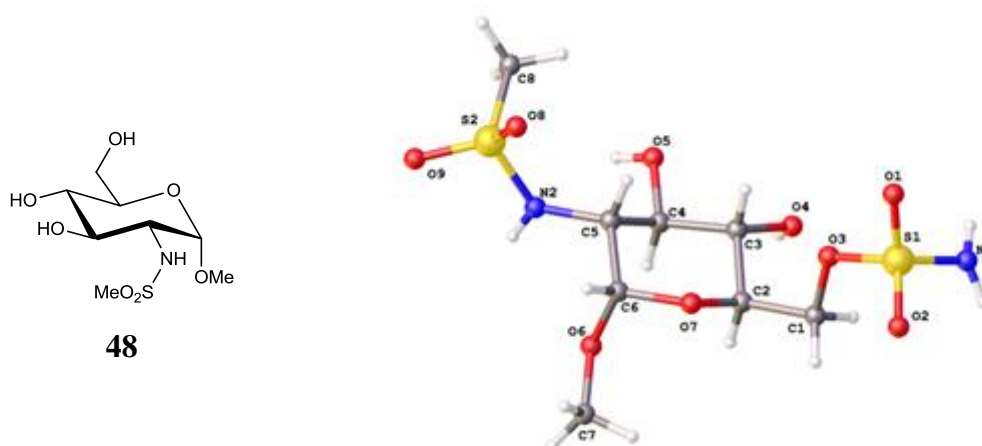
Figure 4.3: Small molecule X-ray crystal structure of **48**.

81

4.2.1.1 Glucose- and Mannose-Based Analogues of 25

To assess whether the *N*-sulfate could be replaced by a hydroxyl group, analogue **50** was prepared in a single step from commercially available methyl-α-D-glucopyranoside (**122**) using sulfamoylation method 2 (Scheme 4.12). The reaction did not proceed cleanly and an isolated yield of only 25% of **50** was obtained. Sulfamoylation of the 2-position is a likely confounding factor in this reaction, consistent with the empirically observed order of reactivity of the hydroxyl groups of glucopyranosides (6 > 2 > 3 > 4) in reactions with benzoyl chloride.[191]
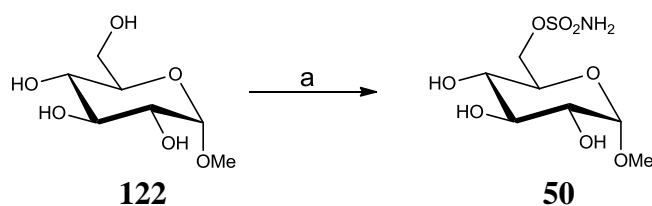
Scheme 4.12: *Reagents and conditions*: a) ClSO$_2$NH$_2$, DMF, -40 °C 18 h, 25%.

Target **51** was also prepared in low yield in a single step from commercially available methyl-α-D-mannopyranoside **123** using sulfamoylation method 2 (Scheme 4.13). The low yield is again likely to reflect the nucleophilicity of the axial hydroxy group at the 2-position.[191]
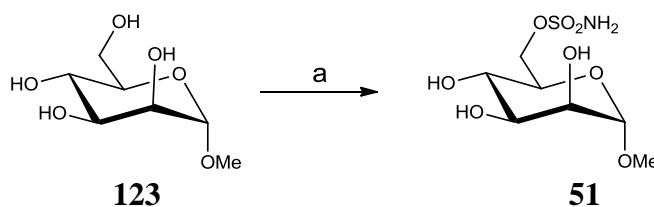
Scheme 4.13: *Reagents and conditions*: a) ClSO$_2$NH$_2$, DMF, -40 °C 18 h, 9%.

4.2.1.2 Preparation of the N²-Succinate Analogue of 25

Succinamide derivative **52** was prepared by reaction of **105** with succinic anhydride (Scheme 4.14). Separation of **52** from an unidentified impurity could not be achieved using column chromatography, but trituration in ethyl acetate allowed **52** to be isolated in high purity.
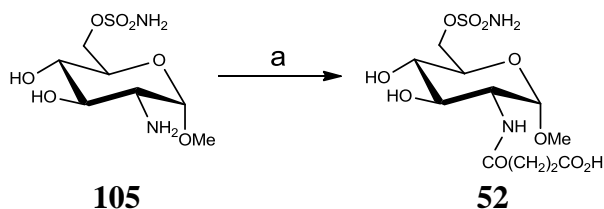
Scheme 4.14: *Reagents and conditions*: a) Succinic anhydride, H$_2$O/dioxane, r.t., 18 h, 18%.

4.2.2 Variation of the C¹-Substituent of 25

4.2.2.1 Preparation of the β-Anomer of 25

The importance of the anomeric stereochemistry of the monosaccharide template was investigated by preparing β anomer, **59** (Scheme 4.15). Significant quantities of **124** were obtained from reaction of **102** with a 1.25 M methanolic HCl solution at short reaction times. After 1 hour, a ratio of α to β anomers of approximately 3:2 was obtained, allowing isolation of a 37% yield of **103** and 22% of **124**. Sulfamoylation of **124** using method 1 gave a 19% yield of **125**, which was converted into target **59** with no evidence of epimerisation of the anomeric centre by proton NMR spectroscopy.
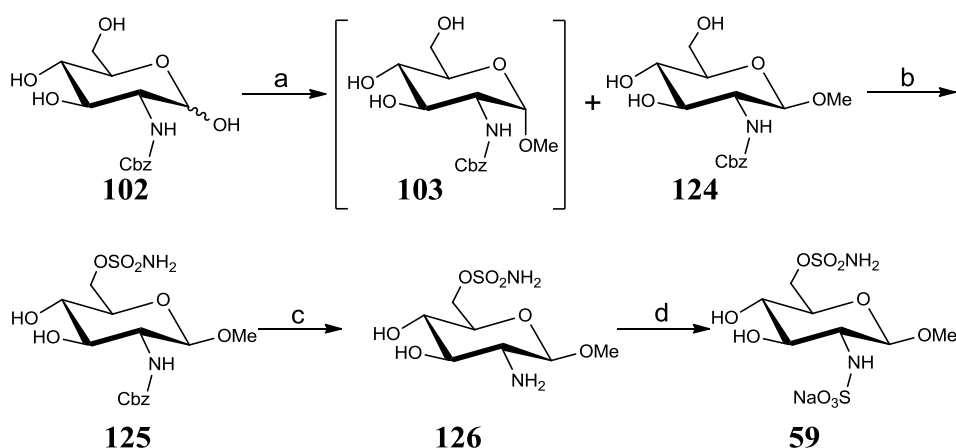
Scheme 4.15: Preparation of the β-anomer **59**. *Reagents and conditions*: a) HCl/MeOH, 70 °C, 1 h, **124** 21% (+ **103** 37%); b) ClSO$_2$NH$_2$, Tol/DMA, -15 °C, 2.5 h, 19%; c) H$_2$/10% Pd/C, MeOH/CH$_2$Cl$_2$, 40 °C, 1 h, 95%; d) SO$_3$.Py, H$_2$O, pH 9-10, r.t. 2.5 h, 29%.

4.2.2.2 Preparation of the C¹-Methylene Analogue of 25

Removal of the anomeric substituent of compound **25** was also investigated to determine whether a substituent at this position was required for activity (Scheme 4.15). Treatment of **102** with acetyl chloride in the absence of solvent at room temperature[192] introduced the α-chloro substituent at the anomeric position, with simultaneous protection of the 3-, 4-, and 6-hydroxy groups as their acetate esters to give **127**. Radical hydrodechlorination[192] with tributyltin hydride and AIBN gave a 47% isolated yield of **128**, with successful removal of contaminating tin residues achieved by purification through a SiO_2 column containing 10% K_2CO_3.[193] Tributyltin hydride was replaced by the less toxic tris(trimethylsilyl)silane,[194] resulting in a cleaner reaction profile and a more straightforward purification on a standard silica solid phase, leading to an improved isolated yield of 90% for **128**.
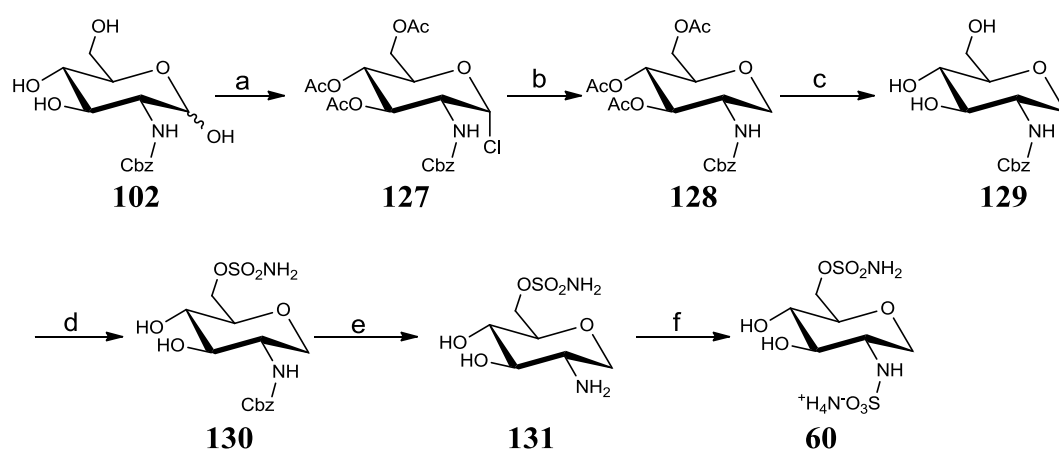
Scheme 4.16: *Reagents and conditions*: a) AcCl, r.t., 48 h, 55%; b) i) Bu$_3$SnH/AIBN, 110 °C, 1.5 h, 47%, or ii) (TMS)$_3$SiH/AIBN, 110 °C, 1.5 h, 92%; c) NaOMe (cat.), MeOH, r.t., 2 h, 85%; d) ClSO$_2$NH$_2$, Tol/DMA, -15 °C, 2 h, 34%; e) H$_2$/10% Pd/C, MeOH/CH$_2$Cl$_2$, 40 °C, 2 h, 98%; f) SO$_3$.Py, H$_2$O, pH 9-10, r.t., 2 h, 24%.

Deprotection of the alcohol groups of **128** under Zemplen conditions[195] proceeded in high yield giving triol **129**. The use of sulfamoylation method 1, gave a 34% yield of **130**, which was progressed using the standard conditions described for the previous analogues, to provide **60**.

From consideration of the structure of heparan sulfate, it was concluded that the binding site of Sulf-2 should be sufficiently large to accommodate further saccharide units at the reducing end of the monosaccharide template. In an effort to develop SARs for this region, alternative anomeric substituents were investigated.

4.2.2.3 Preparation of C^1-Isopropoxy Derivative 56

Reaction of protected glucosamine **102** with 4 M HCl/dioxane in isopropyl alcohol gave predominantly α-anomer **132** in 73% isolated yield. Sulfamoylation using method 1 resulted in a 37% isolated yield of **133**, which was progressed through the deprotection/sulfation steps as described previously (Scheme 4.17) to provide target **56**.
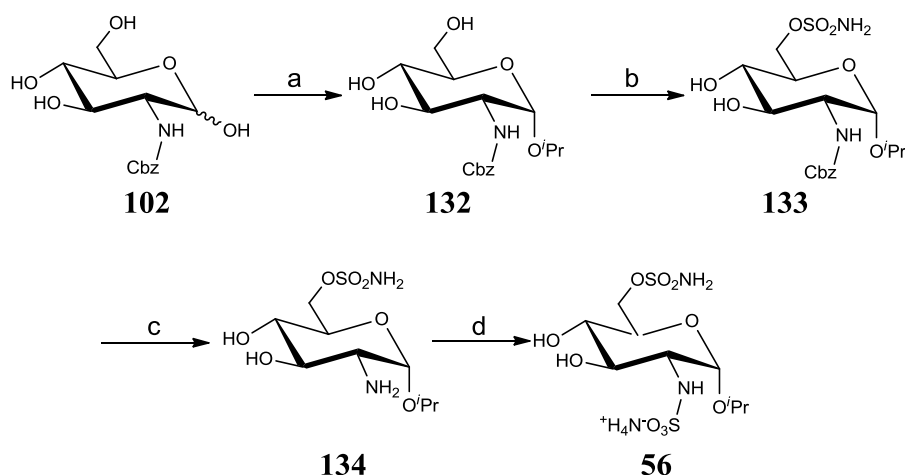
Scheme 4.17: *Reagents and conditions*: a) HCl/Dioxane, IPA, 60 °C, 4 h, 73%; b) ClSO$_2$NH$_2$, Tol/DMA, -15 °C, 2 h, 37%; c) H$_2$/10% Pd/C, MeOH/CH$_2$Cl$_2$, 40 °C, 1 h, 100%; d) SO$_3$.Py, H$_2$O, pH 9-10, r.t., 90 min, 27%.

4.2.2.4 A Divergent Approach to Further Diversification at the C^1-Position

Further elaboration of the anomeric *C*^{1}-substituent was desirable, particularly to allow investigation of the tolerance of polarity at this position. The anomeric position of glucosamine in HSPGs is linked to an iduronic acid residue, and it was hypothesised that polar groups at this position may be able to mimic interactions of the polar functionality of the iduronate residue with the Sulf-2 protein.

A divergent approach was adopted to probe for polar interactions in this region of space, with the versatility of the allyl group being exploited to enable late stage diversification, enabling the introduction of both polar and lipophilic functionality from a common intermediate. The allyloxy group was introduced into the anomeric position using allyl alcohol and 4 M HCl/dioxane at 70 °C for 18 h, to give a 52%

yield of the α anomer **135**, together with 20% of β anomer **136**, which were readily separable (Scheme 4.18).
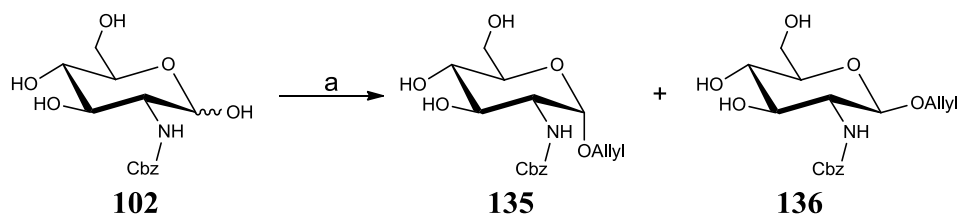
Scheme 4.18: *Reagents and conditions*: a) Allyl alcohol, HCl/Dioxane, 60 °C, 4 h, 52% (**135**) and 20% (**136**).

The first analogue prepared from intermediate **135** was *n*-propyl target **57**. Sulfamate formation using method 1 resulted in a 40% yield of **137**. Reduction of the alkene was achieved concurrently with hydrogenolysis of the Cbz-protected amine to give **138**, which was sulfated to provide target compound **57** (Scheme 4.19).
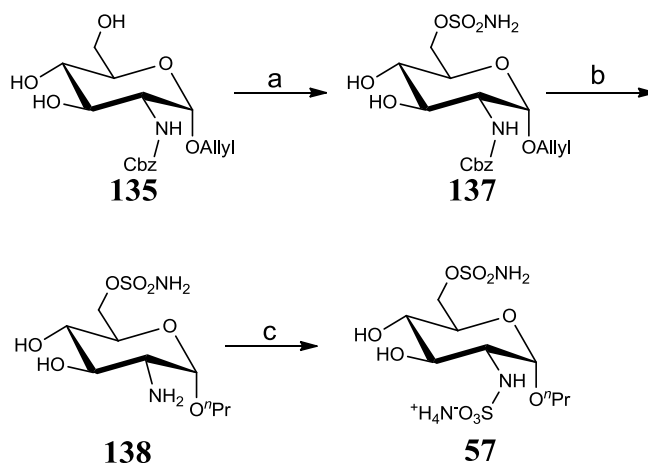
Scheme 4.19: *Reagents and conditions*: a) ClSO$_2$NH$_2$, Tol/DMA, -15 °C, 2.5 h, 40%; b) H$_2$/10% Pd/C, MeOH/CH$_2$Cl$_2$, 40 °C, 2 h, 100%; c) SO$_3$.Py, H$_2$O, pH 9-10, r.t. 90 min, 39%.

The hydroxyethyl derivative **53** was also obtained from allyl intermediate **137**. Ozonolysis of **137**, followed by reductive work-up, led to isolation of **139** (Scheme 4.20), which was carried through the standard deprotection/sulfation methodology to provide target **53**.
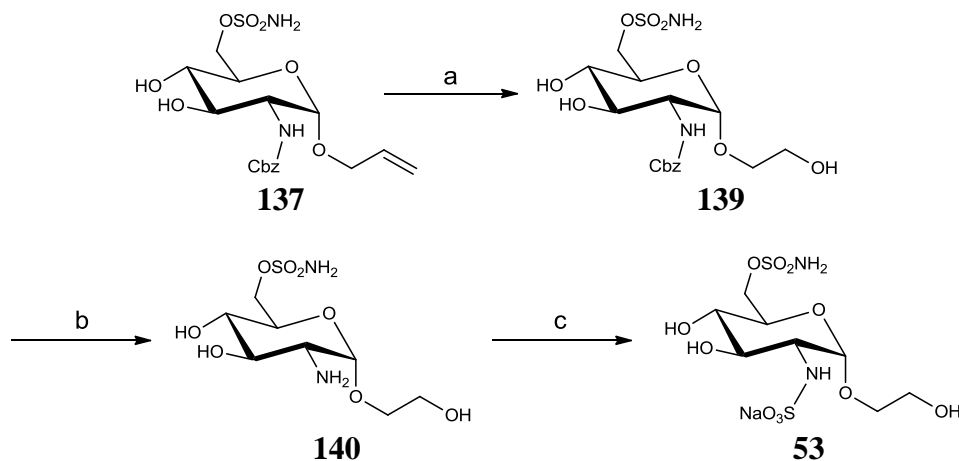
Scheme 4.20: *Reagents and conditions*: a) i) O_3/MeOH, -78 °C, 30 min; ii) $NaBH_4$, 1 h, 69%; b) H_2/10% Pd/C, MeOH/CH_2Cl_2, 40 °C, 3 h, 78%; c) SO_3.Py, H_2O, pH 9-10, r.t., 1 h, 30%.

4.2.2.1 Preparation of Carboxylic Acid 55

Subjecting C^1-allyloxy triacetate **141** to conditions reported for the ozonolysis of alkenes to methyl esters in the presence of sodium methoxide,[196] resulted in none of the desired methyl ester being obtained. An alternative method for oxidative cleavage of allyl groups to carboxylic acids has been documented using $NaIO_4$ with catalytic $RuCl_3$.[197] Dihydroxylation of the alkene is followed by cleavage of the resultant diol by ruthenium tetraoxide, generated *in situ* from $RuCl_3$, and the aldehyde product is further oxidised to the carboxylic acid under the reaction conditions. This approach was successful in converting **141** into **142** in good yield (Scheme 4.21).
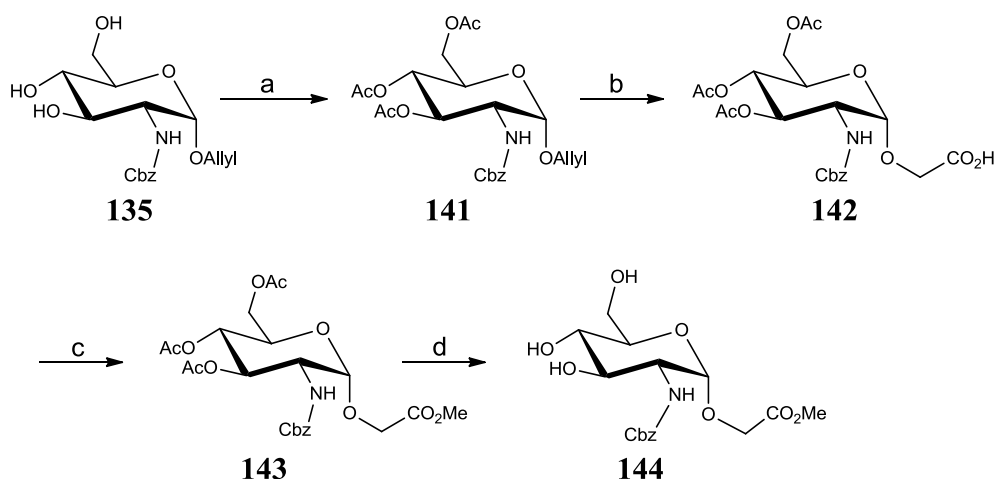
Scheme 4.21: *Reagents and conditions*: a) Pyridine, Ac$_2$O, r.t. 8 h, 96%; b) RuCl$_3$, NaIO$_4$, MeCN, CH$_2$Cl$_2$, H$_2$O, r.t. 30 min, 56-62%. c) MeI/Cs$_2$CO$_3$/CH$_3$CN, r.t., 18 h, 77-95%; d) NaOMe (cat), MeOH, r.t., 1 h, 100%.

Four sets of conditions were investigated for the transformation of **142** into methyl ester **143** (Table 4.9). The use of *N,N'*-diisopropyl-*O*-methylisourea resulted in low isolated yields of **143**, primarily due to issues with isolation of the product from the urea by-product. TMS-diazomethane also gave a disappointing conversion. Alkylation of the carboxylic acid with methyl iodide in the presence of cesium carbonate in acetonitrile proved optimal for this transformation.

Reagents	Solvent	Temp	Time	Yield
^{i}PrNHC(OMe)NH^{i}Pr	MeCN	135°C^a	5 min	< 20%
TMSCHN$_2$ (1.5 eq.)	MeOH/toluene 1:1	r.t.	2 h	50%
MeI (1.5 eq.), NaHCO$_3$ (3 eq.)	DMF	r.t.	18 h	57-75%
MeI (2 eq.), Cs$_2$CO$_3$ (2 eq.)	MeCN	r.t.	18 h	77-95%

^{a} With microwave heating.

Table 4.9: Studies on the formation of methyl ester **143**.

Deprotection of the alcohol groups using Zemplen conditions proceeded smoothly in high yield to furnish **144**, which was sulfamoylated in 67% yield using method 2 (Scheme 4.22). Hydrogenation of **145** was unsuccessful in methanol over 10% Pd/C, requiring addition of acetic acid to achieve quantitative conversion to acetate salt **146**.
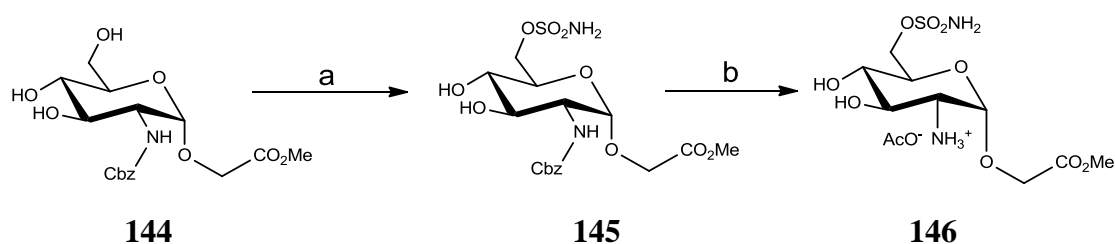
Scheme 4.22: *Reagents and conditions*: a) ClSO$_2$NH$_2$, DMF, -40 °C, 18 h, 67%; b) H$_2$/10% Pd/C, AcOH, 40 °C, 2 h, 100%.

Attempted sulfation of **146** under the pH buffered conditions led to a complex mixture of products. In addition to desired N^2-sulfate, there was evidence of partial hydrolysis of the methyl ester. In the mass spectrum, formation of a by-product with a mass consistent with δ-lactam **147** was evident, which could conceivably form through intramolecular nucleophilic attack of the liberated amine on the methyl ester.

147
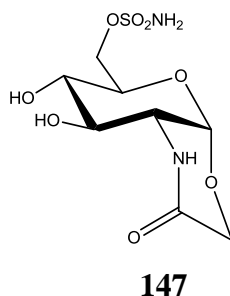
Hydrolysis of ester **145** to the corresponding carboxylic acid **148** prior to deprotection of the amino functionality avoided formation of these by-products, allowing the successful preparation of acid **55** (Scheme 4.23).
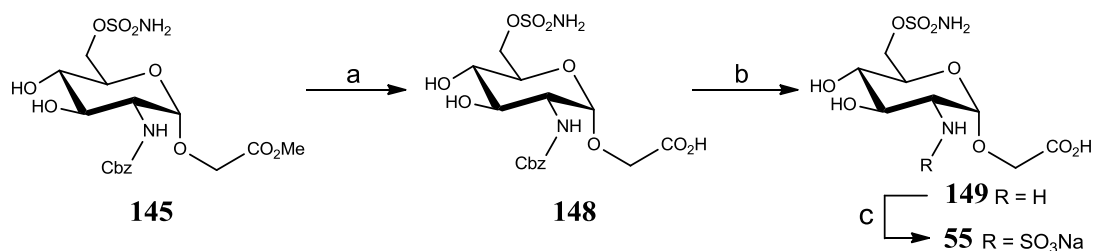
Scheme 4.23: *Reagents and conditions*: a) 2 M NaOH$_{(aq)}$, THF, r.t., 2 h, 82%; b) H$_2$/10% Pd/C, MeOH, 40 °C, 3 h, 100%; c) SO$_3$.Py, H$_2$O, pH 9-10, r.t., 24 h, 38%.

The synthesis of C^1-hydroxypropyl target **54** was investigated from allyl intermediate **141** employing hydroboration to introduce the hydroxypropyl functionality (Scheme 4.24). Hydroboration of 3,4,6 *tris*(acetate) ester **141** proved slow and low yielding with 9-BBN. The use of BH$_3$.THF resulted in a slightly improved yield of 35% of **150**.

However, a significant by-product was also formed, having a mass ion identical to the desired product, and this was proposed to be regioisomeric alcohol **151**, derived from Markovnikov addition of borane to the alkene. The expected ratios of anti-Markovnikov to Markovnikov product using borane are >95:5.[198] However, the ratio of **150** to **151** obtained was approximately 3:1 for this substrate. Co-ordination of the borane to the neighbouring carbamate may facilitate addition of boron to the more substituted end of the alkene, although this was not explored further.
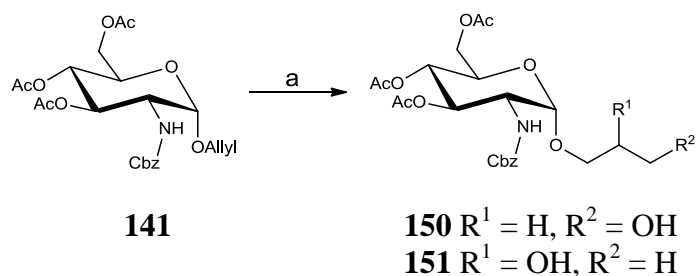
Scheme 4.24: *Reagents and conditions*: a) i). BH$_3$.THF, THF, 0 °C-r.t., 18 h; ii) H$_2$O$_2$, 35% **150**.

An alternative synthetic strategy to access **54** was also investigated, employing direct introduction of commercially available 3-benzyloxypropanol at the C^1-position of **102** to give a 31% yield of α anomer **152** (Scheme 4.25). Regioselective sulfamoylation using method 2 gave **153** in 57% yield. Palladium catalysed hydrogenation allowed deprotection of both *O*-benzyl and *N*-Cbz groups to give acetate salt **154**, which was subjected to the pH controlled *N*-sulfation conditions to give target **54**.
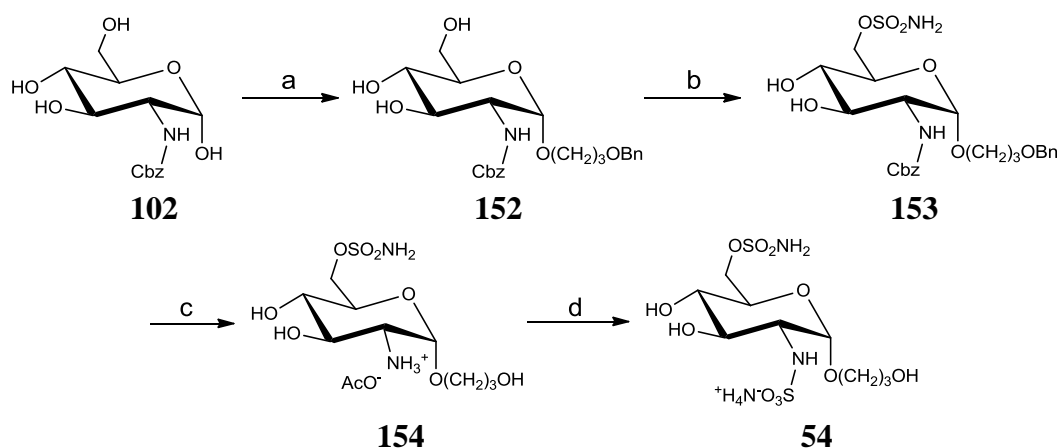
Scheme 4.25: *Reagents and conditions*: a) 3-(Benzyloxy)propan-1-ol, HCl/Dioxan, 75 °C, 5 h, 31%; b) ClSO$_2$NH$_2$, DMF, -40 °C, 18 h, 57%; c) H$_2$/5% Pd/C, AcOH, 20 °C, 1 h, 83%; d) SO$_3$.Py, H$_2$O, pH 9-10, r.t., 1 h, 41%.

Chemoselective methods for the removal of a Cbz group from an amine in the presence of a benzyl ether have previously been reported, using mild hydrogenation conditions on specific substrates.[199] Other systems appear to require the use of attenuated catalysts to achieve chemoselectivity, with amines such as triethylamine or pyridine being employed to partially poison the catalyst and impart selectivity.[200] Chemoselective removal of the carbamate from **153** was achieved by flow hydrogenation over 5% palladium on carbon at room temperature and 20 bar hydrogen pressure, providing **155**, which was sulfated using the pH-controlled sulfation conditions to give benzyloxypropyl derivative **58** in 62% yield (Scheme 4.26).
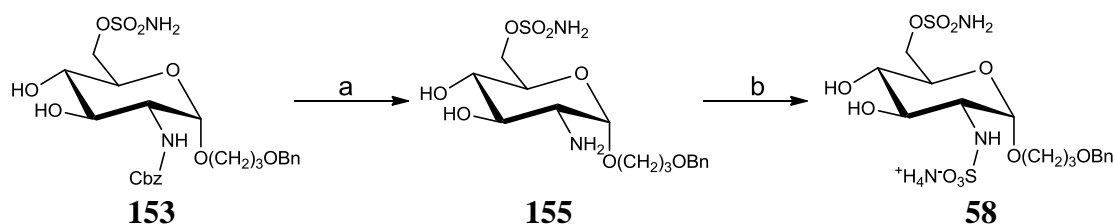
Scheme 4.26: *Reagents and conditions*: a) H_2/5% Pd/C, EtOH, 20 °C, 1 h, 75%; b) $SO_3.Py$, H_2O, pH 9-10, r.t., 18 h, 62%.

4.2.3 Preparation of C^3- and C^4-Methylene Derivatives of Compound 25

An approach employing Barton-McCombie radical deoxygenation to allow preparation of C^3- and C^4-methylene targets **63** and **62** was inspired by a similar strategy described for the synthesis of a series of activators of the glmS-riboswitch of *Staphylococcus aureus*.[201]

4.2.3.1 Preparation of C^3-Methylene Derivative 63
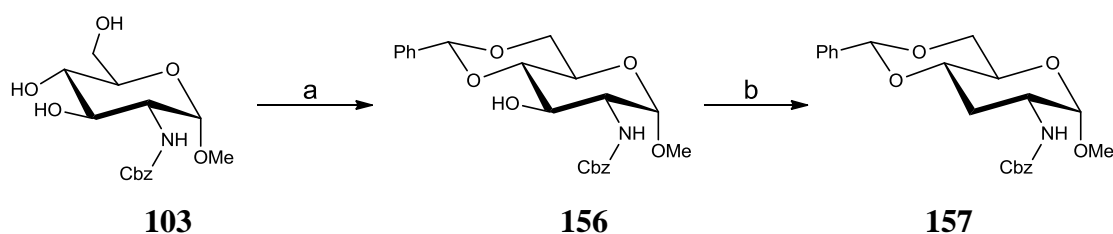
Scheme 4.27: *Reagents and conditions*: a) PhCH(OMe)$_2$, *p*-TsOH, DMF, 75 °C, 3 h, 79%; b) i) CS(Im)$_2$, toluene, 110 °C, 3 h; ii) TMS$_3$SiH, AIBN, 110 °C, 1 h, 83%.

The 4- and 6-positions of **103** were selectively protected as benzylidene acetal **156** (Scheme 4.27). Performing the benzylidene acetal formation in dioxane at room

temperature resulted in an isolated yield of only 35% of **156**, along with a significant by-product which was tentatively assigned as 3,4-benzylidene acetal **158**.

158
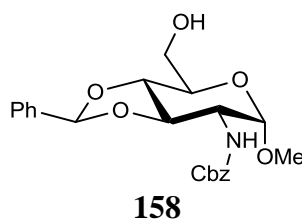
Following a literature procedure,[202] the reaction was repeated in DMF at 75 °C for 3 h, to give 4,6-benzylidine acetal **156** under thermodynamic control, in an isolated yield of 78%. Radical deoxygenation of **156** under modified Barton-McCombie conditions[203,204] using tris(trimethylsilyl)silane[194] gave **157** in 83% isolated yield. Regio- and chemo-selective cleavage of 4,6-benzylidene acetals to give 4-benzyl protected species has been reported for a range of differentially protected monosaccharides, using borane tetrahydrofuran complex in the presence of trimethylsilyl triflate.[205] A remarkable influence of the choice of borane complex is described; thus, borane.THF complex gave almost exclusive regioselectivity for the O^4-benzyl ether product, whereas both borane dimethysulfide and borane trimethylamine complexes resulted in predominant formation of the O^6-benzyl ether. Variation of the Lewis acid had little effect on the reaction outcome, with good yields being obtained with TMSOTf, Sc(OTf)$_3$, ZnI$_2$, AlCl$_3$, and BF$_3$·OEt$_2$. However, TMSOTf was reported to give the fastest reaction rates, with complete reaction in one hour, other Lewis acids requiring between 6 and 240 hours to achieve complete conversion. No rationale was offered for the observed regioselectivity, or for chemoselectivity over the anomeric acetal. An alternative procedure utilising Bu$_2$BOTf and BH$_3$.THF has also been published.[206] This method was employed in the literature synthesis of **25**, in this instance providing a 69% yield of 4-benzyloxy intermediate **98**.[132]

Subjecting **157** to TMSOTf/BH$_3$.THF resulted in a disappointing 22% yield of **159**. In contrast, with Bu$_2$BOTf and BH$_3$.THF a yield of 40% was achieved (Scheme 4.28). The regiochemistry of **159** was confirmed by ^{1}H NMR, with coupling observed between the hydrogen of the 6-hydroxy group to both protons on the C^6-carbon atom. The C^6-protons were readily identifiable by 2D COSY NMR.
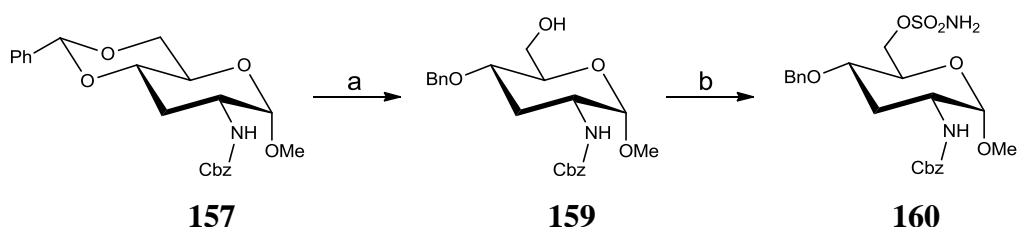
Scheme 4.28: *Reagents and conditions*: a) BH$_3$.THF (1 M), Bu$_2$BOTf, 0 °C, 1 h, 40%; b) ClSO$_2$NH$_2$, 10% DMA/CH$_3$CN, r.t., 15 min, 73%.

Sulfamoylation of **159** had no regioselectivity issues, and was therefore performed at room temperature in 10% DMA in MeCN to avoid the potential for DMF adduct formation at this temperature. Complete consumption of **159** was observed in 15 minutes and a yield of 73% of **160** was obtained. However, the benzyl ether of compound **160** proved resistant to catalytic hydrogenation at elevated temperature and pressure. An alternative route from intermediate **157** was therefore investigated.

Complete removal of the benzylidene acetal from **157** gave diol **161** (Scheme 4.29). Initial low yields for this transformation were found to be caused by *para*-toluenesulfonic acid catalysing the reverse reaction on evaporation of the reaction mixture prior to work-up. Direct basic aqueous work-up of the reaction with potassium carbonate was critical in preventing this reverse reaction, allowing isolation of **161** in high yield.
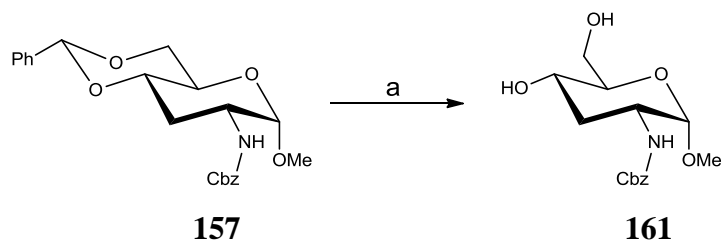
Scheme 4.29: *Reagents and conditions*: a) i) *p*-TSA (cat), MeOH/CH$_2$Cl$_2$, µW, 80 °C, 20 min; ii) 10% K$_2$CO$_3$ (aq), 72%.

Regioselective sulfamate formation using method 2 gave a 36% yield of **162** (Scheme 4.30). The relatively low yield obtained may be due to reduced steric crowding around the 4-hydroxyl group arising from removal of the 3-hydroxyl substituent. Hydrogenation of **162** to **163**, followed by *N*-sulfation, gave **63**.
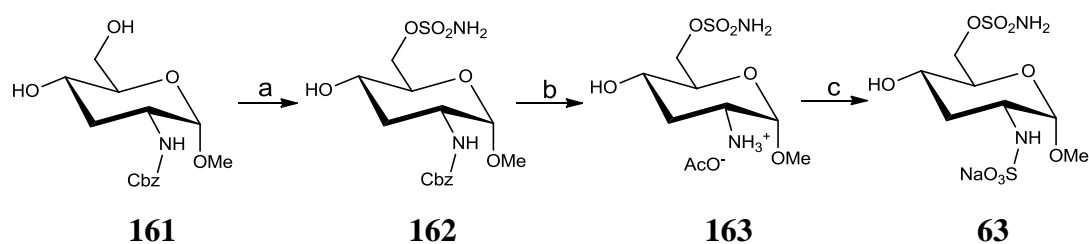
Scheme 4.30: *Reagents and conditions*: a) $ClSO_2NH_2$, Tol/DMA, -40 °C, 24 h, 36%; b) H_2/10% Pd/C, AcOH, 40 °C, 2 h, 97%; c) SO_3.Py, H_2O, pH 9-10, r.t., 2 h, 21%.

The synthesis of C^4-methylene derivative **62** required selective protection of the 3- and 6-hydroxyl groups. As discussed for the synthesis of **50**, the observed order of reactivity of the hydroxyl groups of methyl-D-glucopyranoside toward benzoyl chloride is 6 > 2 > 3 > 4.[191] This trend is conserved in D-glucosamine systems which is reported to enable selective protection at the 3- and 6-positions.[201] Using the literature conditions at room temperature resulted in no selectivity, with only 7% of **164** being obtained along with 69% of *tris*(benzoyl) product. Reducing the reaction temperature to -40 °C allowed **164** to be isolated in a 72% yield (Scheme 4.31).
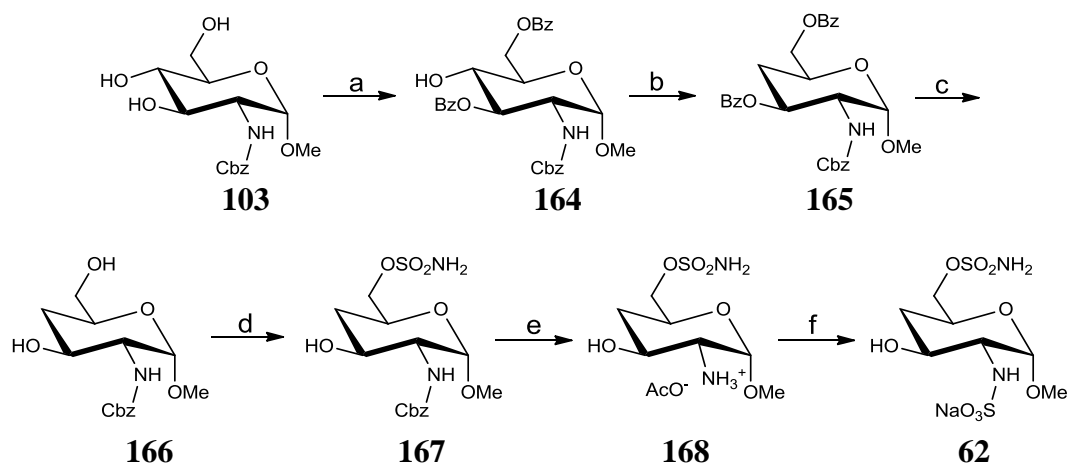
Scheme 4.31: *Reagents and conditions*: a) BzCl (2.2 eq.), CH_2Cl_2/pyridine, -40 °C, 3 h, 72%; b) i) $CS(Im)_2$, toluene, 110 °C, 3 h; ii) TMS_3SiH, AIBN, 110 °C, 1 h, 79%; c) NaOMe (cat), MeOH, r.t., 18 h, 68%; d) $ClSO_2NH_2$, Tol/DMA, -40 °C, 36 h, 51%; e) H_2/10% Pd/C, AcOH, 40 °C, 2 h, 70%; f) SO_3.Py, H_2O, pH 9-10, r.t., 2 h, 8%.

Radical deoxygenation of **164** provided **165**, which was deprotected under Zemplen conditions to give a 68% yield of diol **166**. Sulfamoylation using method 2 gave **167** in 51% yield, with subsequent *N*-deprotection and sulfate formation providing target **62**. The low isolated yield obtained for the final step reflected the presence of close-running impurities which hindered purification.

4.2.4 Substitution on the 4-Hydroxy Position of Monosaccharide 25

Introduction of alkoxy substituents at the 4-position of **25** was investigated starting from 3,6-dibenzoyl protected intermediate **164**. Benzylation of the 4-position of a similar substrate containing adjacent acyl protected alcohols has been reported to proceed with no acyl migration under basic conditions.[207] However, when applied to **164** a complex mixture formed.
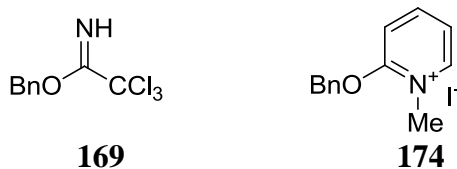
Benzyl ether formation under mildly acidic conditions using Bundle's reagent (benzyl-2,2,2-trichloroacetimidate, **169**) with catalytic triflic acid[208] has been successfully used on monosaccharide alcohol substrates bearing vicinal benzoyl protected alcohols with no acyl migration,[209] and successfully provided O^4-benzyl ether **170** in 75% yield. However, 6 equivalents of **169** were required for complete consumption of starting material, and on scale-up a yield of only 17% was achieved after addition of 12 equivalents of **169**. Conversion was improved by performing the reaction at 60 °C in dioxane, giving a 78% yield of **170** on a 500 mg scale (Scheme 4.32).
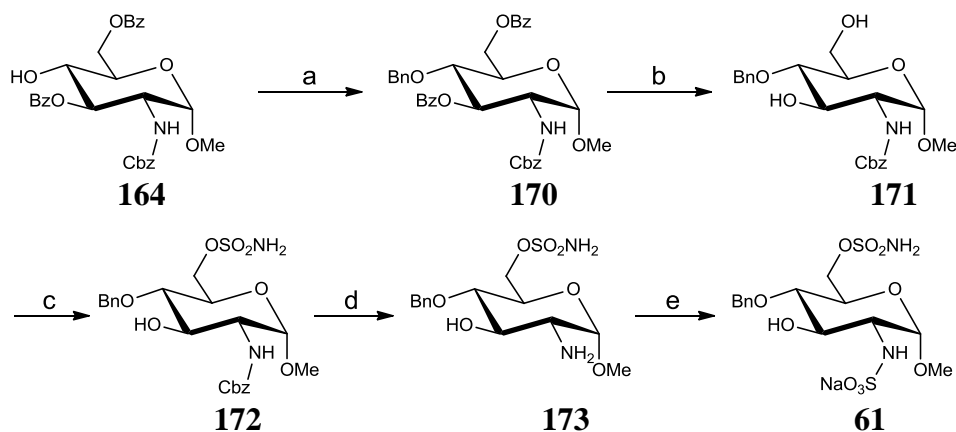
Scheme 4.32: *Reagents and conditions*: a) Benzyl-2,2,2-trichloroacetimidate (8 eq.) (**182**), TfOH, dioxane, 60°C, 4 h, 78%; b) 3 eq. LiAlH$_4$, 0 °C, 2 h, 69%; c) ClSO$_2$NH$_2$, Tol/DMA, -40 °C, 22 h, 52% d) 10 bar H$_2$/5% Pd/C, MeOH, r.t. 35 min, 100% e) SO$_3$.Py, H$_2$O, pH 9-10, r.t., 2 h, 25%.

Benzyl ether formation under neutral conditions was also investigated using 1-methyl 2-benzyloxypyridinium triflate (**174**), at room temperature in the presence of magnesium oxide, to give a 43% yield of **170**. Under microwave heating at 150 °C, the

reaction achieved high conversion in 30 minutes, with an improved isolated yield of **170** of 73%.

Removal of the benzoyl protecting groups from **170** under Zemplen conditions required more than one equivalent of sodium methoxide to achieve a 25% isolated yield of **171**. Attempts to cleave the benzoyl groups reductively with DIBAL in DCM gave exclusively starting material at -78 °C, and at room temperature only the 6-benzoyl group was removed. Access to the carbonyl group of the 3-benzoyl ester is hindered by the neighbouring benzyl ether, which may explain the low reactivity towards nucleophiles. Reaction of **170** with lithium aluminium hydride allowed isolation of **171** in 69% yield, the small size of the hydride reducing species, and non-coordinating mechanism, presumably aiding reaction with this sterically hindered substrate. Sulfamoylation using method 2 gave **172** in 52% yield, which was deprotected selectively in the presence of the benzyl ether under mild palladium-catalysed flow hydrogenation conditions, to give **173** which was successfully sulfated to provide **61**.

4.3 Synthesis of Cyclic Aliphatic Sulfamates

Sulfamoylation of racemic tetrahydropyran-2-methanol (**175**) was achieved at room temperature in DMA to yield **67** (Scheme 4.33).

175   **67**
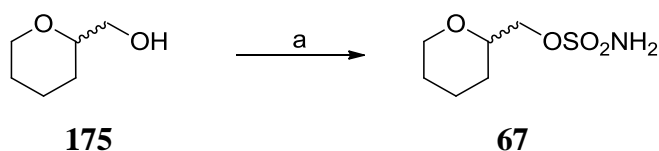
Scheme 4.33: *Reagents and conditions*: a) ClSO$_2$NH$_2$, DMA, r.t., 48%.

Sulfamoylation of Cbz protected *trans*-4-aminocyclohexanol (**177**) proceeded in high yield (Scheme 4.34). However, Cbz deprotection of **178** using palladium-catalysed hydrogenation resulted in none of the desired amine being isolated. A proposed pathway for decomposition involves intramolecular transannular S$_N$2 displacement of the sulfamate by the liberated amine, to give **180**. The hydrogenation was repeated in acetic acid, resulting in successful isolation of acetate salt **179**. However, attempts to prepare the *N*-sulfate from **179** were unsuccessful, which may be due to rapid

formation of **180** on liberation of the free amine under the basic conditions used for *N*-sulfate formation.
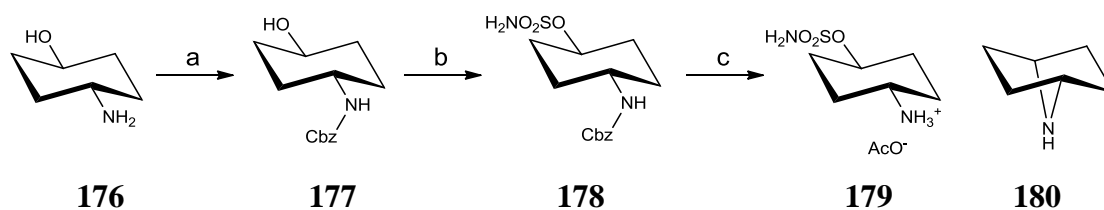
Scheme 4.34: *Reagents and conditions*: a) CbzCl (1.1 eq.), NaHCO$_3$ (7 eq.), H$_2$O, r.t., 18 h, 79% ; b) ClSO$_2$NH$_2$, DMF, - 40 °C, 18 h, 76%; c) H$_2$, 10% Pd/C, MeOH, 40 °C, 2 h, AcOH (2 eq.), 100%.

An alternative three-step route which avoided the possibility of formation of **180** was designed, employing a trichloroethyl protected sulfate, and successfully applied to the synthesis of **64** (Scheme 4.35). Protection of **176** was followed by sulfamate formation, and zinc-mediated deprotection of the sulfate provided **64**, which was isolated as the sodium salt after ion exchange chromatography.
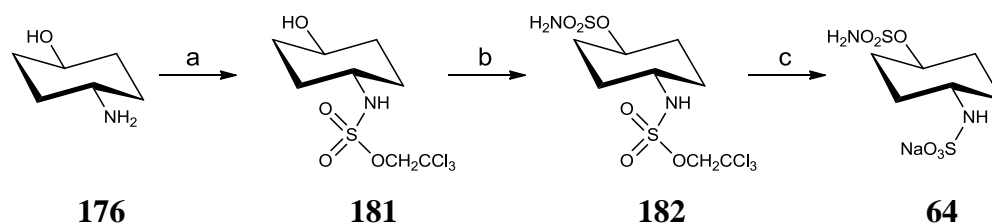
Scheme 4.35: *Reagents and conditions*: a) 1,1,1-trichloroethylsulfonyl imidazolium tetrafluoroborate (1 eq.), THF, r.t., 18 h, 73%; b) ClSO$_2$NH$_2$, DMF, - 40 °C, 18 h, 76%; c) i) Zn (15 eq.), MeOH, H$_2$O, r.t. 1 h; ii) Ion exchange chromatography on Dowex 50W8X200 Na form, H$_2$O, 95%.

Derivative **66** was prepared from piperidinol **183** using a similar reaction sequence (Scheme 4.36).
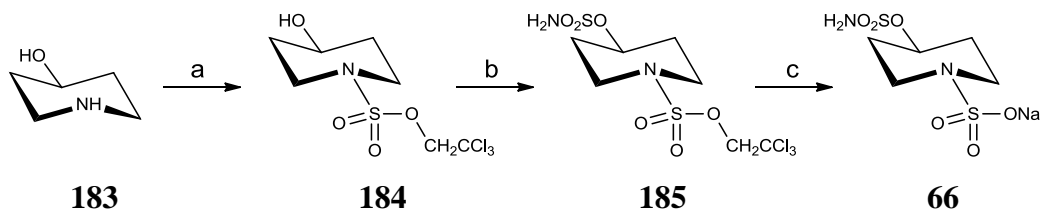
Scheme 4.36: *Reagents and conditions*: a) 1,1,1-trichloroethylsulfonyl imidazolium tetrafluoroborate (1 eq.), THF, r.t., 18 h, 83%; b) ClSO$_2$NH$_2$, K$_2$CO$_3$ (5 eq.), DMF, - 40 °C, 18 h, 92%; c) i) Zn (15 eq.), MeOH, H$_2$O, r.t. 1 h; ii) Ion exchange chromatography on Dowex 50W8X200 Na form, H$_2$O 99% .

Attempted sulfamate formation at room temperature resulted in degradation of **184**, and the low temperature sulfamoylation method 2 yielded **185** in only 19% yield with significant evidence of trichloroethanol as a by-product. A potential pathway for degradation was nucleophilic attack of the liberated chloride ion at the sulfur centre of the protected *N*-sulfate of **185**, to release trichloroethanol, thereby forming chloride **186** (Scheme 4.37).
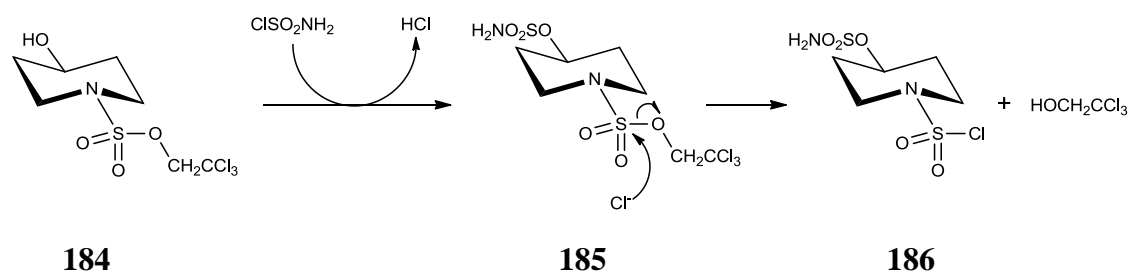
Scheme 4.37: Proposed pathway for liberation of trichloroethanol in the sulfamate formation reaction with **184**.

Addition of potassium carbonate to the reaction as an acid scavenger completely suppressed this side reaction, resulting in a 92% isolated yield of **185**. Sulfate deprotection was performed in the absence of ammonium chloride to avoid issues with purification. The zinc salt thus obtained was converted into the sodium salt of **66** by ion exchange chromatography, giving **66** in 99% isolated yield.

A similar route was applied to the synthesis of **65** from 4-piperidine methanol (**187**) as shown in scheme 4.38, again employing potassium carbonate in the sulfamate formation step to suppress degradation of the trichloroethyl protected *N*-sulfate.
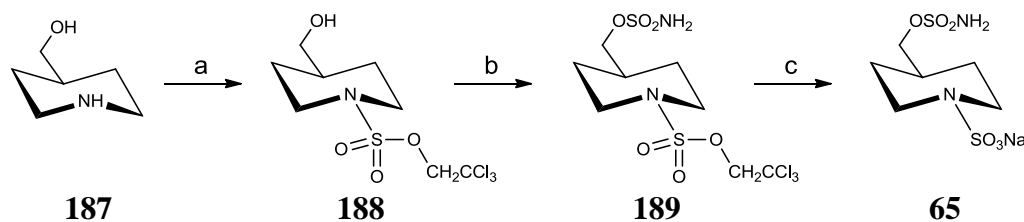
Scheme 4.38: *Reagents and conditions*: a) 1,1,1-trichloroethylsulfonyl imidazolium tetrafluoroborate (1 eq.), THF, r.t., 18 h, 94%; b) ClSO$_2$NH$_2$, K$_2$CO$_3$ (5 eq.), DMF, -40 °C, 18 h, 75%; c) i) Zn (15 eq.), MeOH, H$_2$O, r.t. 1 h; ii) Ion exchange chromatography on Dowex 50W8X200 Na form, H$_2$O 90%.

4.4 Synthesis of Aryl Sulfamates

Prior to the preparation of the aryl sulfamate compound set, a study was undertaken to confirm the effect of base and solvent on sulfamate formation for this class of substrates, using 3-trifluoromethylphenol (**190**) as a representative example. The results from these experiments are summarised in Table 4.10.
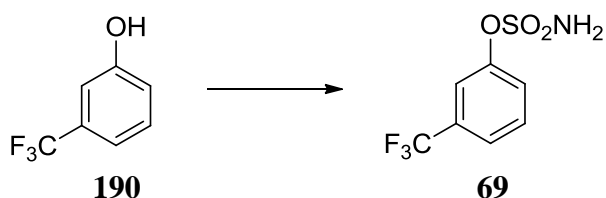
Entry	Base	Solvent	Outcome
1	None	MeCN	No product formation
2	None	NMP	Trace conversion
3	None	DMA	93% isolated yield
4	NaH (2 eq)	NMP	No conversion
5	NaH (3 eq)	DMF	New TLC component, not consistent with desired product
6	Cs_2CO_3 (1.2 eq)	MeCN	Trace product, mainly starting material

Table 4.10: Summary of conditions explored for reaction of phenols with sulfamoyl chloride. *Conditions*: 2 eq. of a freshly prepared sulfamoyl chloride (2 M in toluene) added to 3-trifluoromethyl phenol at 0°C, in the presence of the base stated above. The reaction was allowed to warm to room temperature over 18 h.

The presence of base resulted in either no significant conversion to product (Entries 4 and 6), or formation of unidentified compounds which were inconsistent with the formation of **69** (Entry 5). Primary aryl sulfamates have been reported to degrade under basic conditions *via* an E1cB mechanism, to regenerate the phenol (Scheme 4.39).
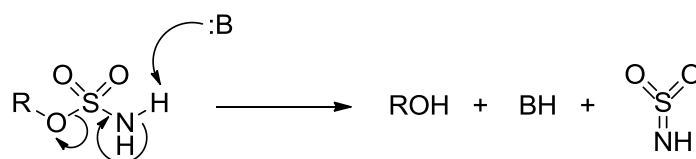
Scheme 4.39: Proposed E1Cb pathway for decomposition of primary arylsulfamates under basic conditions.

In the absence of base, the choice of solvent had a dramatic effect on the outcome of the reaction, with DMA again being confirmed as the optimal solvent for room temperature sulfamoylation.[183] This study led to the selection of DMA as solvent in the absence of a base for the synthesis of primary arylsulfamates. Isolated yields for the synthesis of a matrix of substituted phenyl sulfamates, are summarised in Table 4.11.
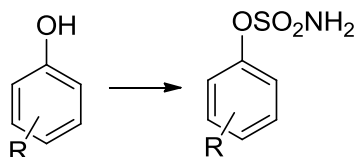
R	H	CF$_3$	CN	NO$_2$	OMe	Ph
Ortho		**68** (31%)	**71** (26%)	**74** (52%)	**77** (29%)	**80** (67%)
Meta	**29** (76%)	**69** (80%)	**72** (58%)	**75** (87%)	**78** (56%)	**81** (43%)
Para		**70** (60%)	**73** (21%)	**76** (48%)	**79** (53%)	**82** (67%)

Table 4.11: Isolated yields (%) for the synthesis of substituted phenyl sulfamates.

4.4.1 X-ray Crystal Structures of Representative Phenyl Sulfamates

Sepctroscopic data for 4-nitrophenyl sulfamate (**76**) and 4-methoxphenyl sulfamate (**79**) were inconsistent with literature NMR data.[210] Crystals of these products were grown by slow evaporation from water (**76**), and from acetonitrile (**79**). X-ray crystal structures were obtained, providing definitive structural confirmation (Figure 4.3).
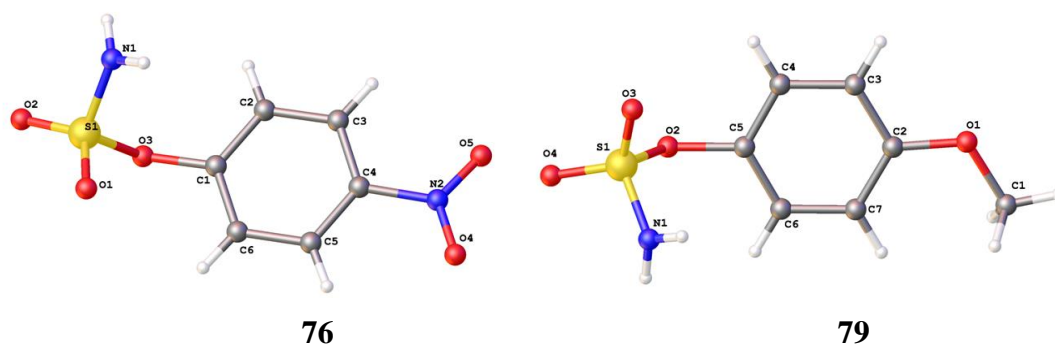
Figure 4.3: X-ray crystal structures of **76** and **79**.

In both crystal structures the C-O-S torsion angle is close to 90°, suggesting that it is unfavourable for the sulfur-oxygen bond to reside in the plane of the aromatic ring, presumably due to steric interactions between the sulfamate amino or sulfonyl functionalities and *ortho*-hydrogen atoms.

4.5   Stability of Primary Aryl and Aliphatic Sulfamates

Nitro-substituted phenyl sulfamates **74**-**76** were found to suffer from chemical instability in neat DMSO-d_6 during overnight acquisition of ^{13}C NMR spectra, with signals corresponding to both the expected product and phenolic starting material being present. No such degradation was observed with spectra obtained in CD$_3$OD. ^{1}H NMR stability studies were performed over 24 h at room temperature to explore the stability profile for a set of phenolic and aliphatic sulfamates in DMSO-d_6 (Table 4.12) and CD$_3$OD (Table 4.13). In DMSO-d_6, analogues **74** and **75**, bearing the strongly electron withdrawing nitro group at either the 2- or the 3-position, suffered significant degradation after 24 h. Over the same time period, between 10% and 20% degradation was seen with the moderately electron withdrawing groups, cyano and trifluoromethyl. The representative alkyl sulfamate tested (**67**) showed no evidence of degradation.

Compound	Time h				
	0	1.5	3	6	24
3-nitrophenyl sulfamate (**75**)	>99%[a]	>99%	97%	n.d.	55%
2-nitrophenyl sulfamate (**74**)	>99%	97%	91%	n.d.	53%
3-cyanophenyl sulfamate (**72**)	>99%	n.d.	97%	95%	80%
3-trifluoromethylphenyl sulfamate (**69**)	>99%	n.d.	98%	96.5%	86%
2-tetrahydropyranylmethyl sulfamate (**67**)	>99%	n.d.	>99%	>99%	>99%

[a] Percentages of sulfamate remaining were calculated by ^{1}H NMR from integrals of characteristic aromatic protons, which were identified from ^{1}H NMR of pure samples of the sulfamate and phenol; n.d. indicates value not determined..

Table 4.12: Stability studies on sulfamate compounds in DMSO-d_6.

In CD$_3$OD, **74** showed greater stability than in DMSO-d_6. The less electron-withdrawing **69** and the alkyl sulfamate **67** were stable in CD$_3$OD over 24 hours (Table 4.13).

Compound	Time h				
	0	**1.5**	**3**	**6**	**24**
2-nitrophenyl sulfamate (**74**)	>99% [a]	>99%	97%	95%	86%
3-trifluoromethylphenyl sulfamate (**69**)	>99%	>99%	>99%	>99%	>99%
2-tetrahydropyranylmethyl sulfamate (**67**)	>99%	n.d.	>99%	>99%	>99%

[a] Percentages of sulfamate remaining were calculated by ^{1}H NMR from integrals of characteristic aromatic protons, which were identified from ^{1}H NMR of pure samples of the sulfamate and phenol; n.d. indicates value not determined..

Table 4.13: Stability studies on sulfamate compounds in CD$_3$OD.

In contrast to the solution instability, all phenolic and aliphatic sulfamates proved stable for one year when stored at room temperature as solid samples, with no signs of degradation by ^{1}H NMR spectroscopy.

4.6 Synthesis of Benzylic Sulfamates

The sulfamoylation conditions were applied to the synthesis of 4-nitrobenzyl sulfamate (**89**), giving a 50% isolated yield. Diversification of **89** was anticipated to enable synthesis of the *N*-sulfate (**90**), acetamide (**192**) and methanesulfonamide (**193**) *via* aniline **191** (Scheme 4.40).
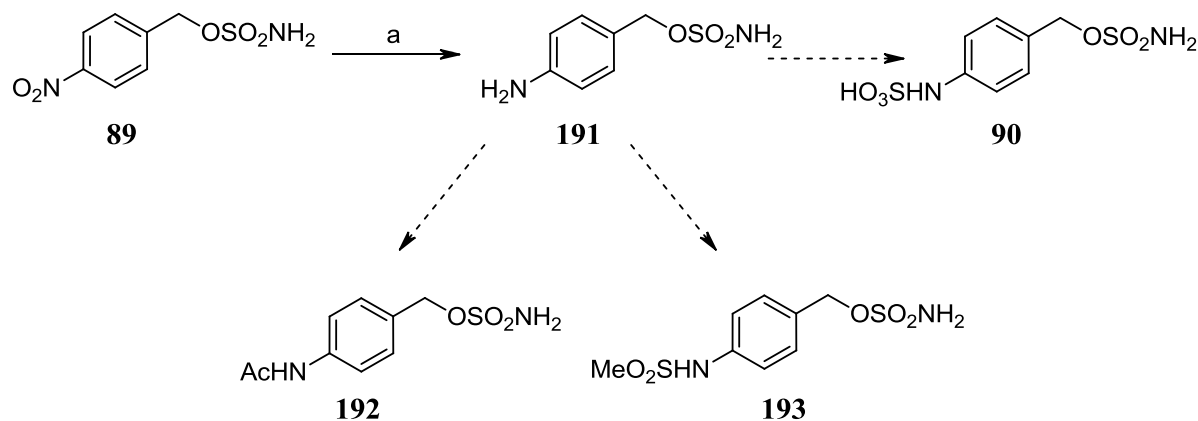
Scheme 4.40: Proposed synthetic route to substituted 4-aminobenzylsulfamate targets. *Reagents and conditions:* a) HCO$_2$NH$_4$, 10% Pd/C.

Catalytic transfer hydrogenation of **89** resulted in multiple products with no evidence of formation of **191**. Degradation of **191** is possible *via* a highly reactive aza quinone methide intermediate (**194**, Scheme 4.41), which may account for the observed reaction profile.
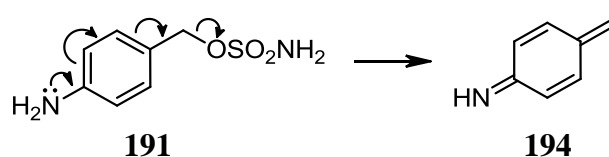
Scheme 4.41: Proposed mechanism for the degradation of **191** via a reactive aza quinone methide intermediate **194**.

In an attempt to decrease formation of **194**, the electron-withdrawing nitrogen substituents were introduced prior to sulfamate formation. Acetylation of **195** gave **196**, which, under the sulfamoylation conditions, formed a significant amount of benzylic chloride **197**, with no **192** being obtained (Scheme 4.42). Chloride **197** may arise either *via* an S$_N$1 mechanism, through an aza quinone methide intermediate, or by direct S$_N$2 displacement of the benzylic sulfamate formed by chloride.
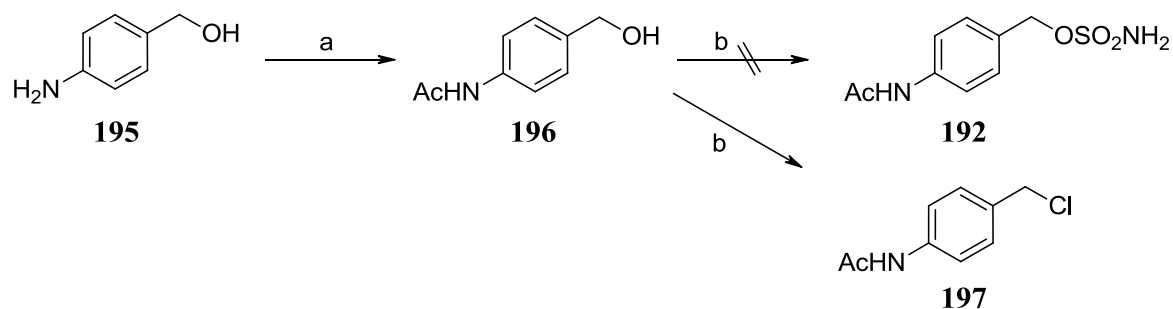
Scheme 4.42: Unexpected formation of 4-acetamidobenzyl chloride **197**. *Reagents and conditions*: a) Ac$_2$O (4.6 eq), MeOH, r.t., 5 h, 65%; b) ClSO$_2$NH$_2$, DMA, r.t.

No chloride by-product was formed in the preparation of **89**, where the aza quinone methide degradation pathway is not available. The electron-withdrawing nitro group of **89** would be expected to accelerate chloride displacement *via* an S$_N$2 mechanism. The S$_N$1 degradation pathway is therefore the more likely.

Methanesulfonamide formation employing 4-aminobenzyl alcohol was also attempted, resulting in a complex reaction mixture. Thus, 4-amino substituted benzyl sulfamates may suffer from inherent chemical instability and these targets were not pursued further. Future work investigating a similar synthetic strategy on substrates with nitrogen substituents *meta* to the benzylic sulfamate would be of interest. These substrates would be unable to participate in the proposed aza quinone methide degradation pathway, and would therefore provide further mechanistic insights.

4.7 Summary

A series of analogues of the literature monosaccharide Sulf-2 inhibitor **25** has been prepared, varied with respect to R^1-R^4 (Figure 4.4).
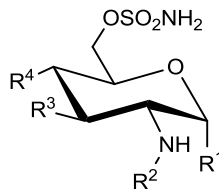
Figure 4.4: Generic structure of analogues of monosaccharide sulfamate **25** prepared.

Access to these targets was facilitated by the development of a procedure for the regioselective sulfamoylation of the O^6-position of the monosaccharide template. Analysis of a model substrate resulted in an increased understanding of the factors that influence the success of this reaction. The information gained from these model experiments allowed further improvements in the regioselectivity, reproducibility and hence in the isolated product yields. This enabled the reaction to be used with greater efficiency on more complex intermediates, and longer reaction sequences to be undertaken to provide more complex final compounds.

Variations of R^1 and R^2 were achieved using a diverse range of chemical transformations. The use of an allyl group as a versatile synthetic handle allowed the introduction of both lipophilic and hydrophilic functionality at the anomeric position. The R^3 and R^4 hydroxy groups were independently removed, and synthetic methodology for substitution at the R^4 position was developed.

Focussed libraries of phenolic, benzylic, and cyclic aliphatic sulfamates were also prepared in an attempt to identify non-saccharide based templates with inhibitory activity against Sulf-2.

Chapter 5: Introduction to the ERK5 Project

5.1 Protein Kinases

Protein kinases are a class of enzymes which catalyse the transfer of the γ-phosphate from adenosine triphosphate (ATP) to a substrate protein on a serine, threonine or tyrosine side chain.[211] The introduction of the charged phosphate group often induces a conformational change in the secondary, tertiary or quaternary structure of the substrate, affecting its biological activity.[211] Signal transduction in eukaryotic cells is mediated primarily by protein kinases.[212] Many other cellular processes, including metabolism, transcription, cell cycle progression, cytoskeletal rearrangement and cell movement, apoptosis, and differentiation are also mediated by protein kinases, and tumour formation has been linked to the loss of regulation of protein kinase activity.[27] This can occur through several mechanisms, including mutation or formation of fusion proteins leading to constitutive kinase activity, or the loss of negative regulators,[211] resulting in oncogenic signalling leading to increased tumour cell survival, proliferation, migration and angiogenesis.[213] Over five hundred protein kinases have been identified, representing approximately 1.7% of the human genome, and genes coding for 164 of the 518 human protein kinases are located in chromosomal regions implicated in cancer.[214]

Kinases can be classified by the residues that they phosphorylate. Typical kinases are divided into serine/threonine kinases and tyrosine kinases.[214] A third class encompass atypical kinases, which exhibit kinase activity but are structurally dissimilar to the typical kinase families. In the human kinome, 388 kinases are classed as serine/threonine kinases, 90 as tyrosine kinases, and 40 as atypical kinases.[214]
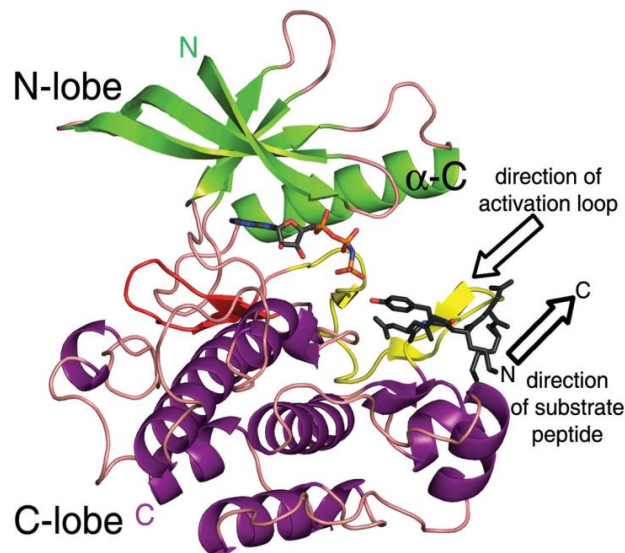
Figure 5.1: Ribbon diagram representing the main features of a prototypical kinase catalytic domain based on the structure of IRK. The N-lobe is shown in green, the C-lobe is shown in purple and the activation loop is colored yellow. The ATP binding site is coded in red. The substrate peptide, docked onto the activation loop, is shown in black, and an ATP analog is shown in blue and orange.[215]

Protein kinases may be integrated into the plasma membrane of a cell, or may be intracellular. Membrane-associated kinases can transduce an extracellular signal across the plasma membrane, allowing downstream intracellular signalling, which manifests in a variety of ways. For example, the enzymic activity of the substrate protein may be activated by kinase-mediated phosphorylation, allowing it to catalyse transformations of further downstream substrates. Phosphorylation may also influence the substrate's affinity for other proteins, resulting in their release or sequestration, and in so doing affecting their biological activity.

The catalytic domain of typical protein kinases consists of approximately 290 amino acid residues arranged into two distinct lobes connected by a linker (Figure 5.1). The vast majority of protein kinases utilise ATP as the phosphate source, and have highly conserved ATP binding pockets (Figure 5.2). ATP binds in a cleft at the hinge between the *N*-terminal and *C*-terminal lobes.[211] Selectivity is principally achieved through protein-protein interactions between the kinase and its substrate. Consequently, the mode of ATP binding is largely consistent across kinase families, with the N^1 and N^6 positions of the adenine ring system forming hydrogen bonds with the peptide backbone in the kinase hinge region.[216] This binding mode positions the γ-

phosphate group towards the substrate binding site.[211] Secondary interactions such as Van der Waals contacts contribute further to ATP binding.
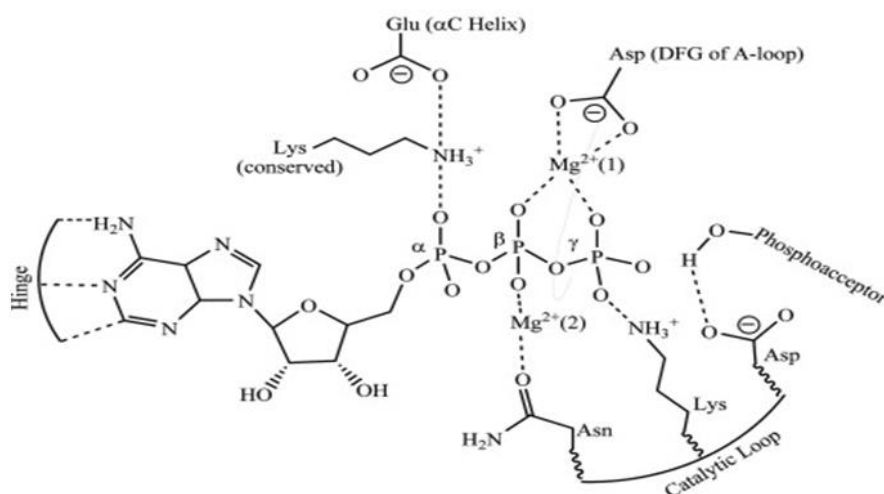
Figure 5.2: Simplified illustration of the molecular contacts between the substrates and conserved active site residues and cofactors involved in catalysis of phosphate transfer by kinases.[216]

Kinases exist in active and inactive forms, which may differ in their phosphorylation state.[213] In the inactive form of many kinases an activation loop blocks the ATP site, preventing ATP from binding. A change of conformation on phosphorylation of activation loop residues enables ATP to access the binding site, and the enzyme to become catalytically active.[213] Kinase inhibitors can be classified by their binding mode, and the kinase state that they inhibit.[217]

5.2 Classes of Kinase Inhibitor

Four main classes of kinase inhibitors have been defined (Types I-IV).[217] The majority of small-molecule kinase inhibitors that have been developed are Type I inhibitors, which directly compete with ATP for the active conformation of the kinase. These inhibitors usually utilise hydrogen bond donor and acceptor motifs which mimic the hydrogen bonding interactions of ATP to the kinase hinge residues. Further potency and selectivity are achieved through incorporation of groups occupying adjacent hydrophobic pockets.

a. Type I Inhibitor binding   b. Type II inhibitor binding
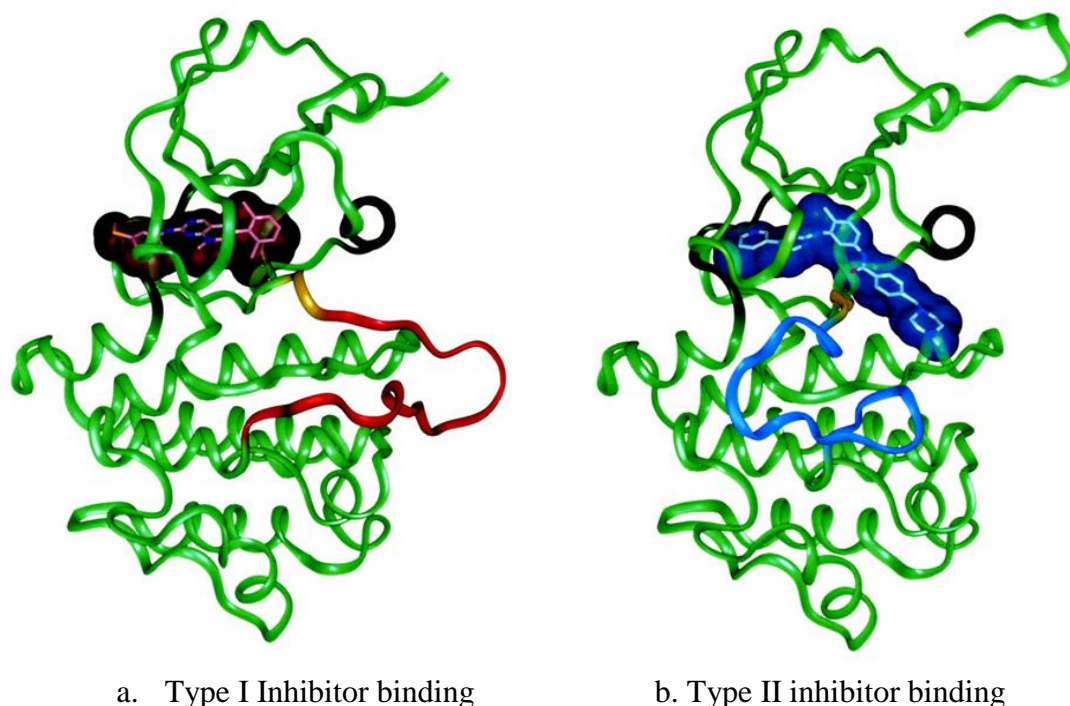
Figure 5.3: Ribbon diagram showing differences in the conformation of the activation loop on binding to Abl kinase of a). a type I inhibitor (PD173955) and b). a type II inhibitor (imatinib). The position of the activation loop is highlighted in red and blue, respectively.[218]

Type II inhibitors target the inactive form of the kinase which has reduced affinity for ATP, and usually utilise a pocket formed by a change in conformation of the activation loop. These inhibitors are often referred to as 'DFG-out', a reference to the movement of a conserved triad of amino acid residues (aspartate (D), phenylalanine (F) and glycine (G)) at the start of the activation loop.[219] In contrast, type I inhibitors are often referred to as 'DFG-in'.[219] Type II inhibitors are not directly ATP competitive, and thus their affinity is less susceptible to changes in intracellular ATP concentration.[219] Their use of the pocket formed by movement of the activation loop also allows the inhibitor to interact with the kinase protein in a region of lower sequence conservation, increasing options for achieving selectivity. Access to this pocket is controlled by a "gatekeeper" residue, which may vary in size and hydrophobicity, providing another mechanism of introducing selectivity into inhibitor design. Mutations of this residue can also significantly affect the binding affinity of Type II inhibitors, which can confer drug resistance.[213] Type III inhibitors bind to a site adjacent to, but distinct from the ATP-binding site, and thus may be considered allosteric binders.[220] While this may be advantageous, the identification of leads for Type III inhibitors requires alternative biological assay procedures from those which

109

have been historically used for the identification of kinase inhibitors.[217] Type IV inhibitors bind to distant sites distinct from the ATP-binding site, acting as true allosteric inhibitors,[220] which may impart higher selectivity. There are currently no marketed Type IV kinase inhibitors.
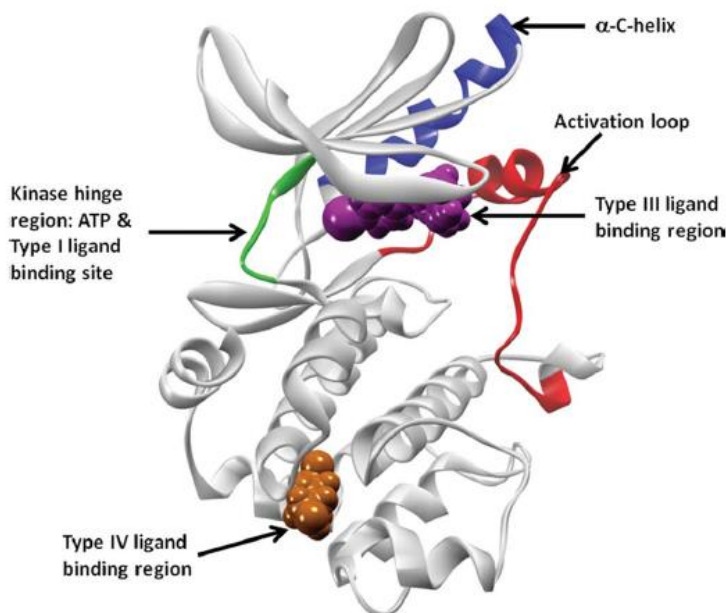
Figure 5.4: Examples of type III and IV kinase inhibitor binding sites. The cMET crystal structure in DFG-in, α-C-helix-out conformation (pdb id: 3eqg) is to used highlight these pockets. The protein kinase is shown in grey, with the hinge region connecting the N- and the C-loops in green. Type III inhibitor (PD-325089) binding at the allosteric pocket, adjacent to the ATP pocket, is represented by magenta van der Waals surface. The region where the Type IV inhibitor GNF-2 binds, the myristoyl pocket in cAbl, is shown in this cartoon representation using a russet surface. The activation loop between the DFG and PE sequences are colored in red, and the α-C-helix is represented in blue.[220]

Research has also been undertaken into the design of selective covalent kinase inhibitors, incorporating electrophilic functional groups which irreversibly interact with nucleophilic residues in the ATP-binding site (usually cysteines).[220] No covalent kinase inhibitors are currently on the market.[213] The purpose of this project is to develop an inhibitor of the ERK5 protein kinase, with the ultimate aim of identifying a drug that may be approved for human use as an anti-cancer therapy.

5.3   The MAP Kinase Pathways and the Role of ERK5

In addition to the classical MAP kinase pathway discussed in chapter 1, three other MAP kinase pathways have been identified.[35] Each of these has a similar composition, with the MAP kinase (MAPK) being activated by a MAP kinase kinase (MAPKK), which in turn is activated by a MAP kinase kinase kinase (MAPKKK). A distinct set of growth factor signals and stimuli, such as cellular stress and the release of cytokines, initiate signalling in these pathways. A schematic representation of the four pathways is shown in Figure 5.5.
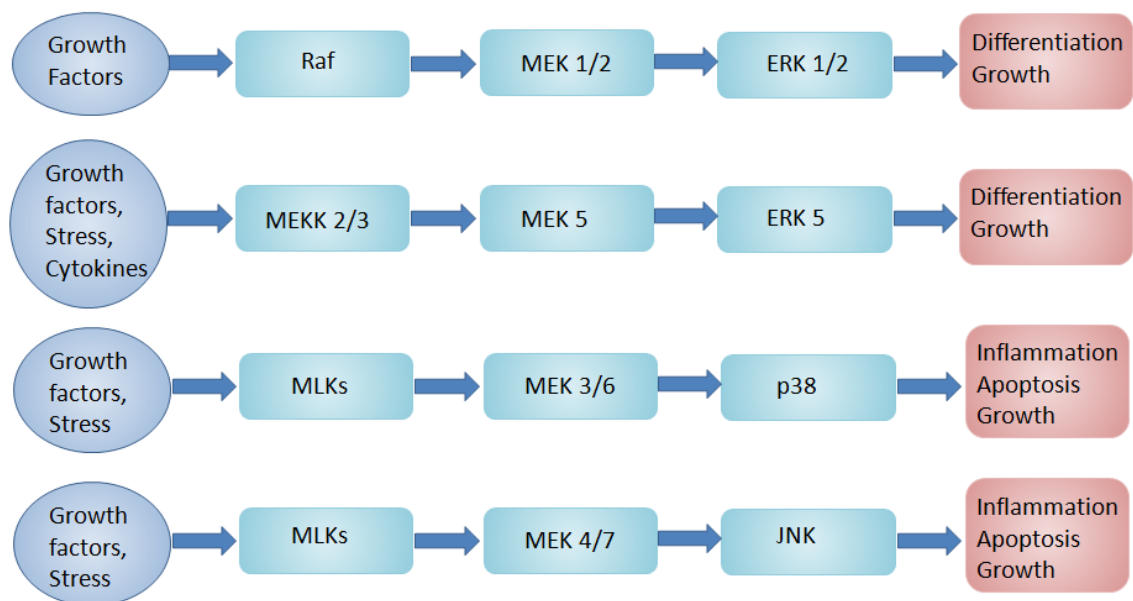
Figure 5.5: Schematic representation of the classical and non-classical MAP kinase pathways.

5.3.1   The Jnk and p38 MAP Kinase Pathways

The p38 and c-jun *N*-terminal kinase (Jnk) pathways are activated by pro-inflammatory cytokines such as interleukin 1-β (IL-1β) and tumour necrosis factor-α (TNF-α) in response to cellular stress.[35] These pathways have been the target of investigations into the treatment of inflammatory diseases such as rheumatoid arthritis, psoriasis and inflammatory bowel disease.[35] Neuronal apoptosis in neurodegenerative diseases such as Alzheimer's disease and Parkinson's disease have been linked to persistent activation of these pathways.[40] Inflammation has also been identified as a risk factor for tumour development, which may be in some part mediated by the p38 and Jnk MAP kinase pathways.[40] Elevated Jnk activity promotes proliferation in

mouse fibroblasts, and Jnk 1 has been shown to be over-activated in over a half of hepatocellular carcinoma (HCC) cases.[221] Increases in Jnk activity accelerated the development of chronic colitis-induced colorectal cancer, and has also been implicated in human prostate cancer.[40] p38α is an important regulator of differentiation of various cell types, and mouse embryonic fibroblasts deficient in p38α proliferate faster and exhibit increased G1/S and G2/M transitions as compared to control cells.[222] These observations lend further evidence to the critical roles of MAP kinase signalling pathways in cancer.

5.3.2   The ERK5 MAP Kinase Pathway

The ERK5 (extracellular signal-regulated kinase 5) pathway has been shown to be activated by a wide range of stimuli, including vascular endothelial growth factor (VEGF), epidermal growth factor (EGF), fibroblast growth factor (FGF2), platelet derived growth factor (PDGF), brain derived neurotrophic factor (BDNF), nerve growth factor (NGF), inflammatory cytokines such as interleukin 6 (IL-6) and osmotic and hypoxic stress.[36] MEK5 uniquely activates ERK5 by phosphorylation first of Thr[218] and subsequently of Tyr[220]. ERK5 does not interact with MEK1/2, indicating that the MEK5-ERK5 pathway is independent of the classical MAPK pathway.[223] MEK5 is activated by the closely related MAPKKKs, MEKK2 and MEKK3, which share 94% sequence identity.[36] The PB1 domain of MEK5 mediates the interactions between MEK5 and MEKK2 and 3, and between MEK5 and ERK5. It has been proposed that the PB1 domain of MEK5 has a role as a scaffold for a MEKK2-MEK5-ERK5 ternary complex.[224]

ERK5 double knock-out mice exhibit defects in development of the vasculature and cardiac systems, resulting in embryonic lethality at around day ten.[225] ERK5 is expressed in many tissues, with high levels evident in the brain during early embryonic development, and has been shown to facilitate neurone survival.[36] The role of ERK5 in cancer, and the effect of its inhibition on cancer progression, has still to be fully elucidated. The key data which support the inhibition of ERK5 as a potential cancer therapeutic strategy are outlined below.

5.3.3 The Role of ERK5 in Cancer

The ERK5 Pathway and Prognosis

In breast cancer, patients with high ERK5 levels have a decreased median disease-free survival time of 14 months compared with 34 months for patients with low ERK5 levels (Figure 5.6a).[226] In prostate cancer, MEK5 over-expression also correlates with poor survival (Figure 5.6b).[227]
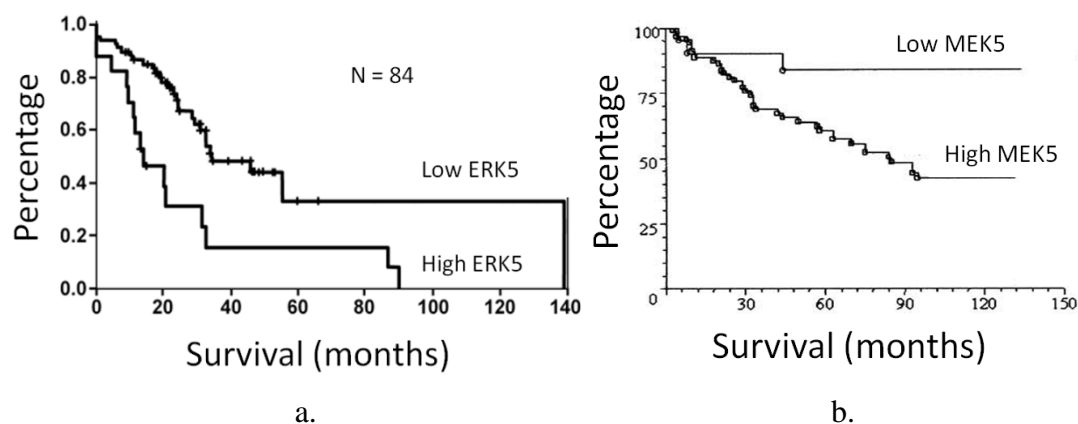
Figure 5.6: a) Kaplan-Meier plot of disease-free survival (DFS) with respect to ERK5 levels in 84 early stage breast cancer patients. Patients with high levels of ERK5 (n = 17) had a worse disease-free survival time (14.13 months; 95% CI: 3.78-24.48) compared with patients (n = 67) with low levels (34.33 months; 95% CI: 18.52-50.14).[226] b) Kaplan-Meier plot of DFS with respect to MEK5 levels in prostate cancer. Patients with moderate/strong MEK5 expression had a shorter mean disease-specific survival of 52 months compared to those exhibiting weak MEK5 expression (58 months).[227]

ERK5 Amplification and Overepression

ERK5 gene amplification is observed in approximately 50% of HCC tumours,[228] and overexpression of ERK5 has been detected in 20% of breast cancer patients.[226] ERK5 expression was also found to be significantly upregulated in high grade prostate cancer when compared to benign prostatic hyperplasia.[229]

ERK5 and In Vitro Cell Proliferation

Proliferation of the HeLa cervical cancer cell line has been shown to be ERK5-dependent.[230] Proliferation of MCF-7 and BT474 breast cancer cell lines is affected by ERK5 activity, and ERK5 also affects the expression of the p21 proliferation

modulator through suppression of promyelocytic leukaemia protein (PML) activity.[36] The MDA-MB-231 human breast cancer cell line has also been shown to be dependent on ERK5 for proliferation.[231]

The ERK5 Pathway and Metastatic Potential

ERK5 has been shown to play a role in cellular invasion and metastatic spread, affecting cell migration, and attachment to the extracellular matrix, through interactions with the $\alpha v\beta 3$ integrin and focal adhesion kinase (FAK).[36] Lymph node metastases in oral squamous carcinoma are associated with high ERK5 expression.[232] In a prostate cancer cell line, reduction of expression or inhibition of the MEK5/ERK5 signalling cascade resulted in reduced invasive capability, and ERK5 signalling promoted metastatic formation *in vivo*.[233] Hepatocyte growth factor (HGF) induced cell migration of MDA-MB-231 breast cancer cells has also been found to be dependent on ERK5 expression.[234] In prostate cancer, over-expression of constitutively active MEK5 leads to increased expression of matrix metalloproteases-2 and -9 through induction of expression of activator protein (AP)-1.[36] ERK5 expression correlates with prognosis in prostate cancer, having a significant link to bone metastases.[36] Figure 5.7 shows the results from another study of prostate cancer patients, which found that MEK5 over expression also correlates with higher metastatic potential.[227]
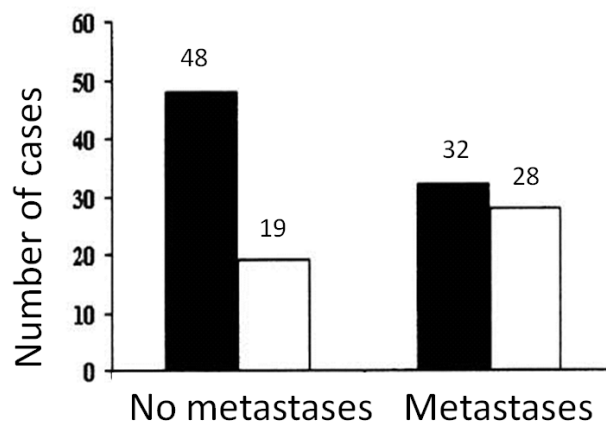
Figure 5.7: MEK5 expression level and presence of metastases.[227] White bars – high/moderate MEK5 expression, Black bars - low MEK5 expression.

ERK5 and Apoptosis

Multiple myeloma cells are protected from induced apoptosis by over-expression of ERK5, whereas over-expression of a catalytically inactive mutant of ERK5 leads to increased sensitivity to induced apoptosis.[235] Double MEK5 knockout in mouse embryonic fibroblasts resulted in sensitisation to osmotic stress induced apoptosis, suggesting that the MEK5/ERK5 pathway may have a role in protecting against apoptosis.[236]

The ERK5 Pathway and Angiogenesis

In human xenograft models, deletion of ERK5 reduced tumour growth in mice and inhibited development of tumour blood vessels.[36] VEGF-stimulated tubular morphogenesis in endothelial cells is mediated by ERK5,[237] and VEGF and FGF pro-angiogenic factors have been shown to stimulate ERK5 activation in HUVEC cells.[36]

Constitutive Activation of ERK5

Out of 900 samples sequenced, only one somatic mutation of ERK5 has been reported, suggesting that mutation of ERK5 into a constitutively active form is rare in cancer.[232] De-regulation of this pathway is therefore likely to occur through altered protein levels, as seen in HCC, with the 17p11 amplification being present in 50% of cases.[232] Sustained activation of upstream signalling may also result in dysregulation of ERK5 signalling.[232]

ERK5 Interactions with other Pathways Implicated in Tumour Development

ERK5 also regulates cyclin D1 expression, and regulates NF-κB activity, affecting cell cycle progression.[36] Ras is mutated in 20-30% of cancers, and Ras activity resulted in activation of ERK5 in PC12, C2C12 and COS7 cells.[36] Constitutive activation of signal transducer and activator of transcription (STAT) is often apparent in advanced breast cancer patients, and elevated STAT has been shown to result in up-regulation of MEK5.[232,238]

5.3.4 The Structure of ERK5

Two research groups independently discovered ERK5 in 1995.[223,239] The ERK5 MAP kinase consists of 816 amino acids and has a molecular weight of approximately 102 kDa, which is more than double that of other MAP kinases. ERK5 is consequently also known as Big Map Kinase-1 (BMK-1). The kinase domain resides towards the *N*-terminus, and has high similarity with ERK1/2 and the same TEY phosphorylation triad (Figure 5.8).[36]
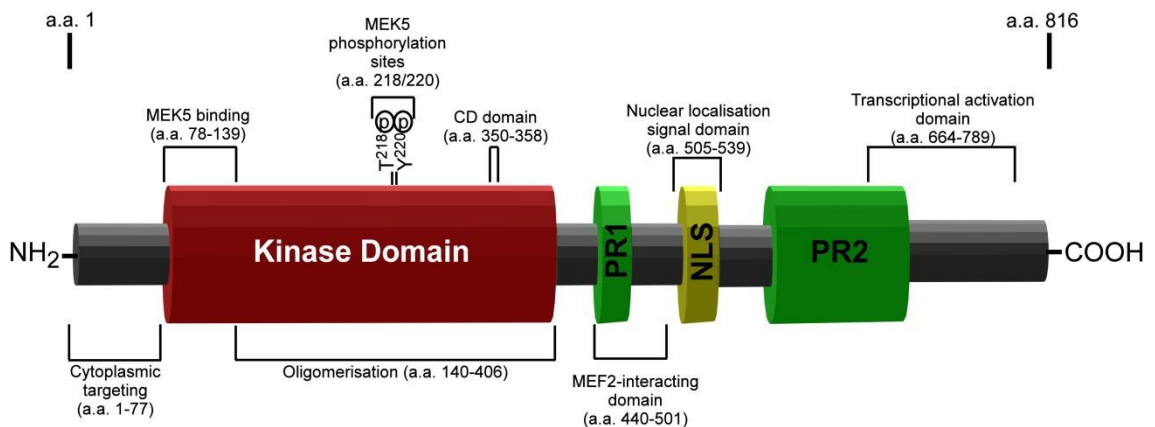
Figure 5.8: Schematic representation of the domain structure of ERK5.[36]

Amino acids 1-77 at the *N*-terminus are involved in targeting the protein to the cytoplasm, with residues 78-406 comprising the kinase domain, which shares 66% sequence identity with ERK2.[36] ERK5 has a unique 410 amino acid *C*-terminal tail, which may have an auto-inhibitory function, as truncation leads to increased kinase activity. The *C*-terminal amino acids also contain a nuclear localisation signal (NLS) domain (505-539), two proline rich domains (PR1, 434-465 and PR2, 578-701) and a transcriptional activation domain (664-789). The proline rich domains are believed to be involved in binding to proteins containing a Src-homology 3 (SH3) domain.[36]

5.3.5 Downstream Effects of ERK5

ERK5 and ERK1/2 require translocation to the nucleus in order to potentiate their signals, but the mechanism by which this translocation is controlled is different.[240] It has been proposed that in the inactive state of ERK5 the *C*- and *N*-termini interact, resulting in a folded conformation which is exported from the nucleus (Figure 5.9). Phosphorylation of the kinase domain disrupts this interaction leading to an extended

active conformation that can autophosphorylate multiple *C*-terminal residues, resulting in nuclear translocation.
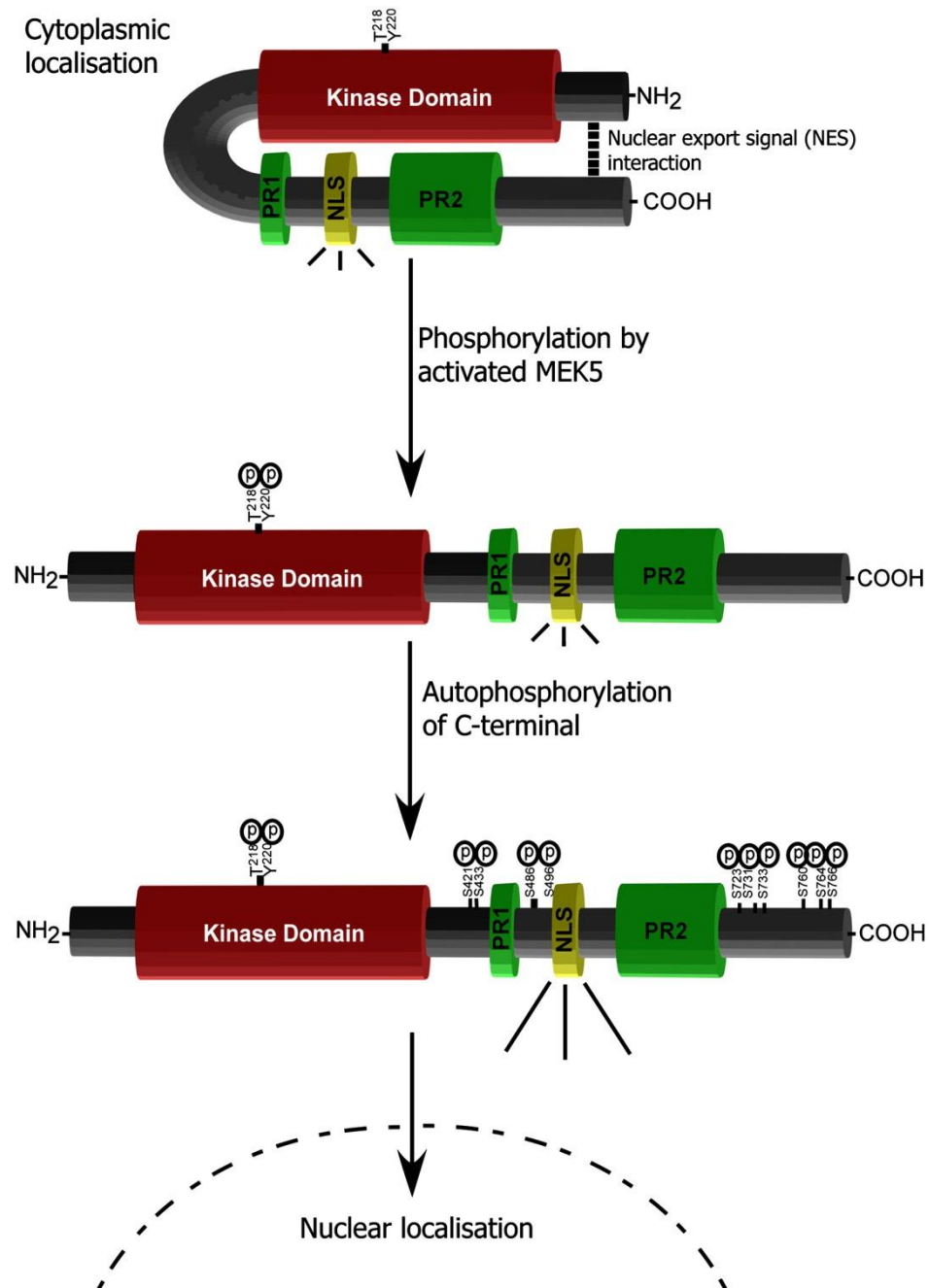
Figure 5.9: Schematic representation of the process of activation of ERK5 for nuclear localisation.[36]

ERK1/2 has a shorter *C*-terminal domain, with no nuclear import or export signalling role. Instead, MEK1/2 contains a nuclear export signal, and in its unphosphorylated form associates with ERK1/2, localising it to the cytoplasm.[240] The phosphorylation of ERK1/2 results in dissociation of the ERK1/2-MEK1/2 complex, enabling ERK1/2 to translocate to the nucleus by both passive diffusion and active transport.

The mechanism of control of transcription by ERK1/2 also differs from that of ERK5.[240] In addition to the activation of transcriptional factors, ERK5 itself has a *C*-terminal transcriptional activation region which is activated by autophosphorylation. ERK1/2, lacking the *C*-terminal domain, only acts by phosphorylation of other transcription factors.

There are some common downstream targets of phosphorylation by ERK5 and ERK1/2, including Sap1a, c-Myc, RSK, c-Fos and c-Jun. ERK5 also activates members of the MEF family of transcription factors which are involved in the modulation of apoptosis.[241] MEF2A and MEF2C are activated by both ERK5 and p38 MAP kinases, whereas MEF2D appears to be a specific substrate of ERK5. An ERK5 construct containing only the kinase domain (AAs 1-400) was unable to activate the lklf (lung kruppel-like factor) reporter gene, whereas a construct devoid of kinase activity, comprising only the *C*-terminal residues (400-806), constitutively activated lklf transcription. This suggests that the kinase domain may have a regulatory function,[242] and that activation of MEF transcription factors may be independent of the kinase activity of ERK5. Autophosphorylation of the *C*-terminal domain has been shown to increase the transcriptional activating activity of ERK5.[243] c-Fos is a transcription factor which has been implicated in proliferation, differentiation and apoptosis.[244] ERK5 and ERK1/2 both phosphorylate c-Fos.[240] However, only ERK5 subsequently phosphorylates further sites on c-Fos, allowing full c-Fos transcriptional activity. ERK5 also affects the transcription factors c-Myc, CREB and Sap1a, and indirectly affects AKT phosphorylation, all of which have been implicated in tumour development.[36]

5.3.6 Literature Inhibitors of ERK5

There are two classes of inhibitor of the MEK5/ERK5 pathway described in the literature; a diazepinone series,[245] and an oxindole series.[246] Both classes are selective for the MEK5/ERK5 pathway over the classical MAP kinase pathway.

5.3.6.1 The Diazepinone Series

A series of diazepinone ERK5 inhibitors has been described.[245] SARs around the polar aliphatic heterocycle have been published, showing little effect on potency through variation at this position (Table 5.1).
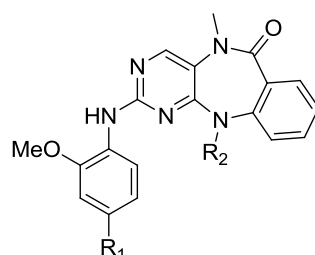
Cmpd	R$_1$	R$_2$	ERK5 IC$_{50}$ nM
198	-N⟩N−Me	Me	190
199	-N⟩NH	Me	230
200	-N⟩O	Me	260
201	-N⟩−OH	Me	240
202	-N⟩−N⟩N−Me	Me	200
203	-N⟩−N⟩	Me	130
204	-N⟩N−Me	c-Pent	200
205	O⟩−N⟩−N⟩N−Me	c-Pent	n.d.

n.d. = not disclosed

Table 5.1: Selected ERK5 inhibition data for the diazepinone class of ERK5 inhibitors.[245]

A co-crystal structure of **205** bound to ERK5 was recently published, using a kinase domain construct (residues 1-397), determined at a resolution of 2.8Å (Figure 5.10).[247] This construct was not phosphorylated on the activation loop. The structure confirms the key binding interaction between the aminopyrimidine of **205** and the hinge region of ERK5. The cyclopentyl group projects towards the glycine-rich loop, and the carbonyl of the diazepinone central ring forms a hydrogen bond through a water molecule to the backbone nitrogen of Asp200 in the DFG motif.

205
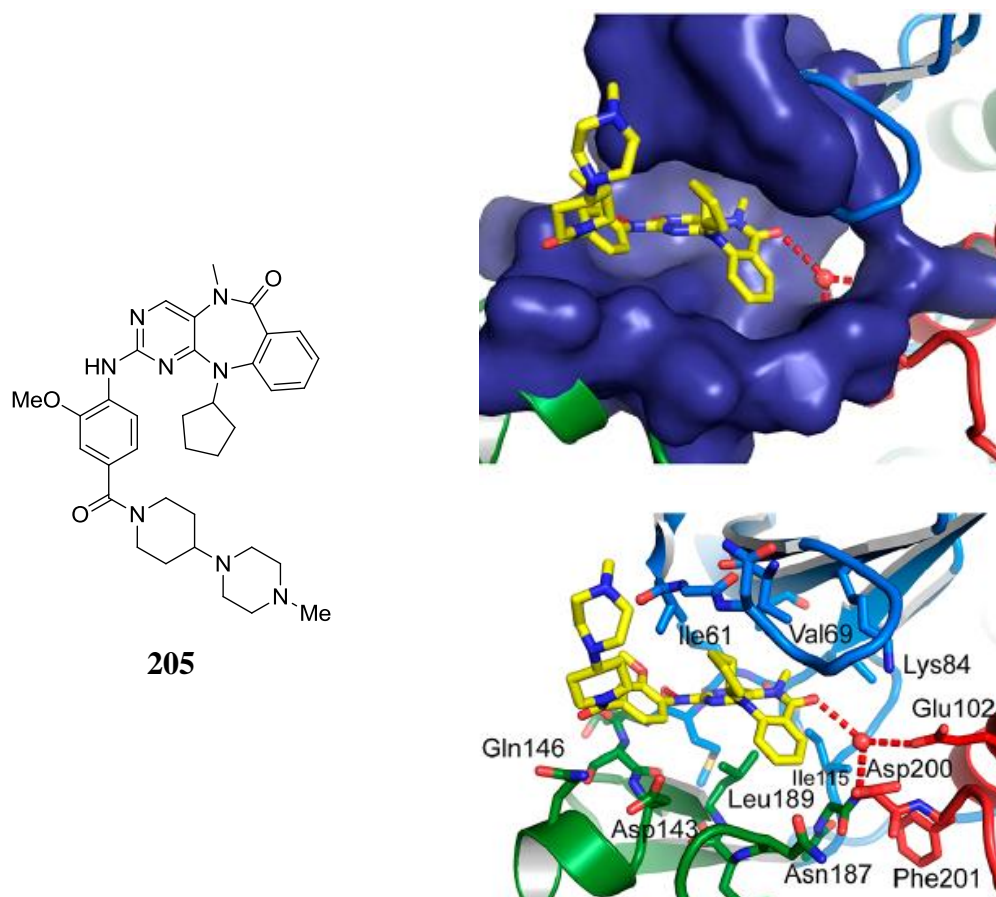
Figure 5.10: The X-ray co-crystal structure of **205** bound to ERK5.[247] The *N*-terminal lobe is colored blue. The *C*-terminal lobe is colored green. The activation loop and α*C* helix are colored red, and compound **205** is colored yellow. The surface of the ERK5 ATP-binding site around the inhibitor is shown in purple. (PDB accession code 4b99).

The piperidylpiperazine ring system points out of the ATP-binding site towards solvent and appears to lie close to the glycine-rich loop. The position of this group towards the solvent-exposed surface of the protein is consistent with the flat SAR published for analogues having diversity at this position.[245] Diazepinone **203** has shown anti-proliferative activity in HeLa cells,[248] and in *in vivo* tumour xenograft models this compound also exhibited growth inhibitory activity,[248] lending further
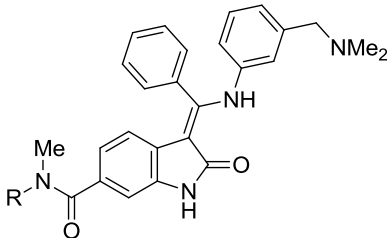
support to the hypothesis that inhibition of ERK5 may have a role in cancer therapy. Compound **203** has been profiled in an *in vivo* rat pharmacokinetic study, demonstrating good bioavailability and moderate clearance (Table 5.2).[248]

	$t_{1/2}$	Cl	V_d	F
	h	ml/min/kg	L/kg	%
203	2.6	18	5.4	87

Table 5.2: Rat *in vivo* pharmacokinetic parameters for **203**.[248]

5.3.6.2 Oxindole inhibitors

The oxindole compounds **206** and **207** inhibit both ERK5 and MEK5, with 50- to 200-fold greater activity against MEK5 than ERK5 (Table 5.3).[246] IC_{50} values against MEK1, MEK2 and ERK1 were all greater than 6 µM, and both compounds were over 100-fold selective for MEK5 against a panel of 87 kinases.[246]

Cmpd	R	MEK5 IC_{50}	ERK5 IC_{50}
		nM	nM
206	H	4.3	810
207	Me	1.5	59

Table 5.3: Published MEK5 and ERK5 inhibitory data for **206** and **207**.[246]

Neither **206** nor **207** affected phosphorylation of ERK1/2, p38 or Jnk1/2 MAP kinases in HeLa cells, but inhibited transcriptional activation of MEF2C, a downstream target of the MEK5/ERK5 pathway, supporting the hypothesis that their effects are due to inhibition of this pathway.[246]

5.4 The Pyrrole Carboxamide Series of ERK5 Inhibitors

The Newcastle pyrrole carboxamide series was identified from a high-throughput screen against ERK5, with the most potent hit in the series, **208**, having an IC_{50} of 0.7 µM. Seventeen members of this series demonstrated ERK5 inhibition ($IC_{50} < 33$ µM), with seven compounds having an IC_{50} of less than 10 µM. Four compounds had been re-synthesised and re-tested against ERK5 to validate the hits, with two of the resynthesised compounds failing to inhibit ERK5, and **208** showing only a 5-fold reduction in potency, the resynthesised sample having an IC_{50} of 3.7 µM.

208
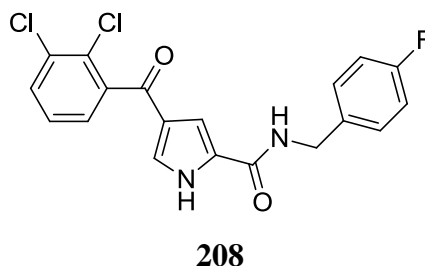
5.5 *In Silico* and *In Vitro* Tools for Assessing ADMET Properties

The *in vitro* assays used in the program to optimise the pyrrole carboxamide series were outsourced to Cyprotex, and are summarised in Table 5.3. An assessment of kinetic solubility was also performed at Cyprotex, using a turbidimetric method, which entails diluting a test compound solution prepared in DMSO with aqueous buffer, and determining precipitation as the end-point by measuring absorbance at 620 nm. An estimated precipitation range in µM is reported, and when this value is less than 1 µM, a compound is considered highly insoluble. In cases where the lower solubility limit is between 1 and 100 µM, a compound can be considered to be moderately soluble, and above 100 µM denotes high solubility.

Assay	Explanation
HLM (Human liver microsomes) MLM (Mouse liver microsomes).	A measure of the vulnerability of a compound to metabolism by cytochrome P_{450} in human or mouse. Figures are quoted as intrinsic clearance (Cl_{int}) in units of μL/min/mg protein, with lower figures representing low liability to cyp-mediated metabolism. A Cl_{int} of < 48 μL/ml/mg protein was targeted.
Caco-2	A measure of the rate of permeation of a compound across a monolayer of a Caco-2 cancer cell line, which contain efflux pumps. Intrinsic flux is measured by the B2A measurement, with recognition by efflux transporters being implied from the ratio of B2A over A2B. Two figures are quoted: Apparent permeability (P_{app}) is quoted as a rate in units of 10^{-6} cm/s; efflux ratio (ER) is a ratio with no units. A high B2A figure and low ER reflect that a compound is highly permeable with low propensity for efflux. An ER of below 2 was targeted.
Ppb	Ppb represents the extent of binding to plasma proteins in blood. It is reported as fraction unbound (F_u), and is a value between 0 and 1. An F_u of 0.1 indicates that, in blood, 90% of the compound is bound to proteins, with 10% free. A figure of > 0.005 was targeted.
Cyp inhibition	Inhibition of cytochrome P_{450}s can lead to drug-drug interactions, or a compound inhibiting its own metabolism leading to unpredictable accumulation. Inhibition of four isoforms of cytochrome P_{450} (2D6, 3A4, 2C9 and 2C19) were assessed, initially at a single concentration with results presented as per cent inhibition (% inh.). K_i values are generated on compounds showing evidence of Cyp inhibition.
hERG	The hERG (human ether-a-go-go-related gene product) ion channel is linked to cardiac arrhythmias leading to life-threatening Torsades de Pointes. A significant therapeutic window over hERG inhibition is required.

Table 5.3: Summary of the Cyprotex *in vitro* ADMET assays used in the ERK5 inhibitor optimisation program.

5.6 The Screening Sequence for the ERK5 Discovery Program

The initial screening sequence (Figure 5.11) started with generation of cell free IC_{50} data for ERK5 using an IMAP® format assay.[249] In this screening platform, the isolated kinase acts on a fluorescently labelled substrate, with subsequent addition of the IMAP binding system, which stops the enzymic reaction and binds to the phosphorylated substrate, relying on a specific, high affinity interaction between phospho-groups and metal-containing nanoparticles within the IMAP® binding system. This binding is detected by fluorescence polarisation to determine the extent of phosphorylation.
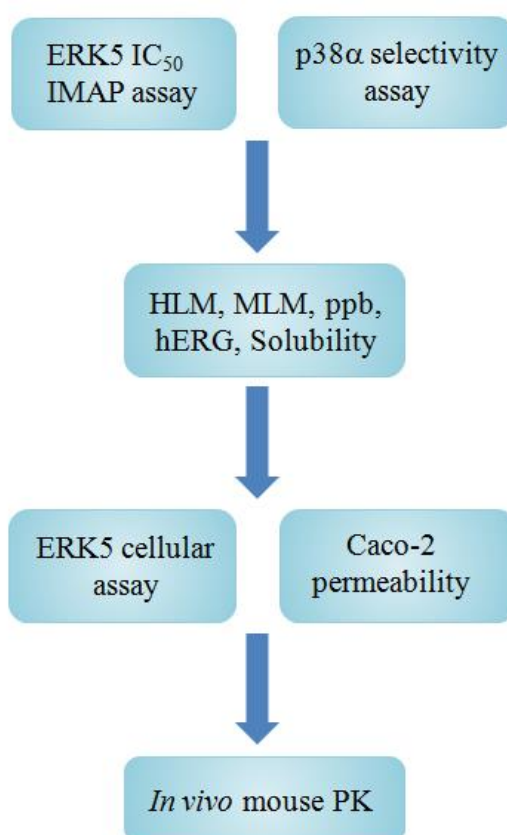
Figure 5.11: The initial screening sequence for the evaluation of ERK5 inhibitors.

In the early stages of SAR development, selectivity over the closely related p38α MAPK, was a significant issue for the pyrrole carboxamide series, and IC_{50} values against this counter-target were obtained in parallel with the primary pharmacology determination. Compounds with encouraging primary potency and selectivity data were progressed to a panel of *in vitro* pharmacokinetic screens. In the third tier of the cascade, the ERK5 cellular activity was measured in a MEF2D reporter gene assay in

HEK293 cells, and membrane permeability and transporter-mediated efflux were assessed in Caco-2 cells. Promising compounds were progressed to an *in vivo* pharmacokinetic study in mice, before profiling against a panel of kinases to assess the wider selectivity profile, and *in vivo* efficacy assessment in a tumour xenograft model in mouse.

As the project matured, structural features which conferred selectivity over p38α were identified, and p38α activity became less of a concern. Counter-screening against this target was moved to the second tier of the screening cascade. It became apparent that further mouse *in vivo* studies to support target validation would be required, and the screen sequence was adjusted to reflect this (Figure 5.12).
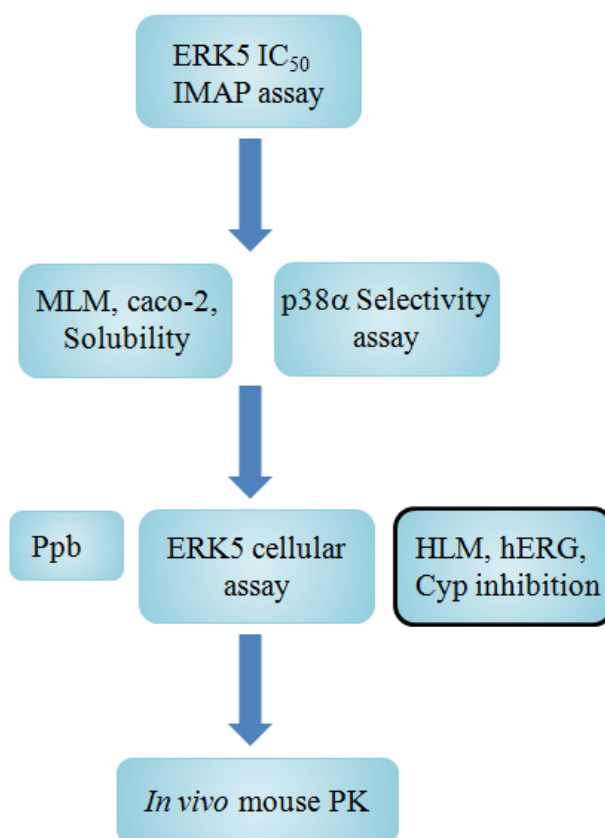
Figure 5.12: The second screening sequence for the evaluation of ERK5 inhibitors.

In vitro pharmacokinetic assays that would inform the selection of compounds for studies in mouse (mouse liver microsomes, Caco-2 permeability, and solubility) were prioritised in the second tier, with a further round of *in vitro* assays forming a third assay tier. Human liver microsomal (HLM) intrinsic clearance and inhibition of the hERG ion channel were determined, but were not considered to be on the critical path for selection of a compound for *in vivo* studies. Inhibition of cytochrome P_{450} (Cyp)

enzyme isoforms was assessed on an *ad hoc* basis when substituents with a known liability, such as potential haem-binding groups, were present.[250,251] In parallel, determination of ERK5 inhibition in an EGF-stimulated HeLa cell-line was assessed, using Western blotting to monitor ERK5 autophosphorylation, with quantification by densitometry enabling IC_{50} determination. Details of the protocols for the ERK5 isolated enzyme and cell-based assays, and for the p38α selectivity assay are included in Chapter 10.

5.7 Early SARs in the Pyrrole Carboxamide Series

Extensive structure-activity relationship studies[252,253] led to the identification of functionality in the template which was important for activity, and areas that may be amenable to further optimisation. The key SARs that had been generated prior to the start of this thesis are summarised in Figure 5.13.
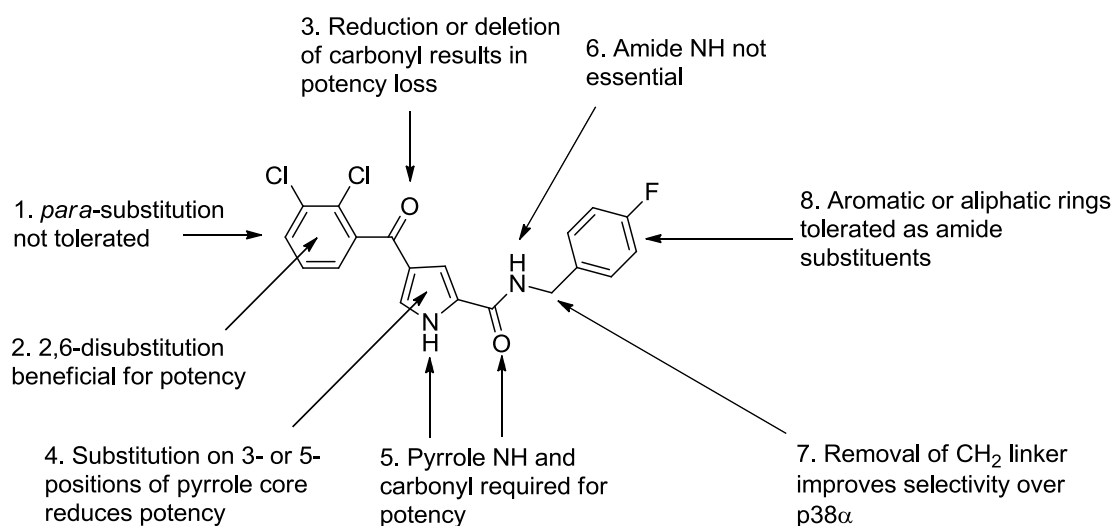
Figure 5.13: Summary of the key pyrrole carboxamide series SARs for ERK5 inhibition.

The pyrrole NH and amide carbonyl were essential for activity. Based on this observation it was hypothesised that these may be involved in binding to the key hinge region of the kinase. Both the aryl ketone and amide substituent were required for ERK5 inhibition, and fragments lacking each of these features resulted in an ERK5 IC_{50} of over 120 μM. Replacement of the 2,3-dichlorobenzoyl ring with a saturated cyclohexyl ketone resulted in inactive compounds. Substituents on this aryl ring are numbered with a prime suffix. An unsubstituted aryl ring gave a loss of potency (ERK5; $IC_{50} = 40$ μM), as did introduction of substituents at the 4'-position, including

Me, F, Cl, OMe, O^{i}Pr, OCF$_3$, and NO$_2$. Halogens at the 2'- and 6'-positions were optimal, with disubstituted benzoyl groups such as 2'-bromo-6'-fluoro- and 2'-chloro-6'-fluorobenzoyl being found to provide potent ERK5 inhibitors. Substitution at the 3'- and 5'- positions was tolerated, but had not been extensively studied

208
ERK5 IC$_{50}$ = 3.7 ± 0.8 μM
p38a IC$_{50}$ = 44 μM

209
ERK5 IC$_{50}$ = 2.0 ± 1.0 μM
p38a IC$_{50}$ = 10 μM

210
ERK5 IC$_{50}$ = 1.5 ± 1.0 μM
p38a IC$_{50}$ >120 μM

211
ERK5 IC$_{50}$ = 0.82 ± 0.07 μM
p38a IC$_{50}$ >120 μM

Class 1: Aliphatic heterocyclic amides

212
ERK5 IC$_{50}$ = 0.20 ± 0.07 μM
p38a IC$_{50}$ >120 μM

Class 2: Heteroaromatic amides

213
ERK5 IC$_{50}$ = 0.58 ± 0.24 μM
p38a IC$_{50}$ >120 μM

214
ERK5 IC$_{50}$ = 0.60 ± 0.27 μM
p38a IC$_{50}$ >120 μM

215
ERK5 IC$_{50}$ = 0.40 ± 0.09 μM
p38a IC$_{50}$ >120 μM

Figure 5.14: Summary of key SARs in the pyrrole carboxamide series.

Incorporation of a heteroatom into the benzylic amide, to give pyridylmethyl amide (**209**) was tolerated, and aliphatic heterocyclic amides also retained good ERK5 inhibitory activity (Figure 5.14). Replacing the benzylic amide with a heteroaryl amide (**210**) led to a significant and consistent improvement in selectivity over p38.

127

Exploitation of SAR knowledge for this template led to the identification of two key classes of lead compound with sub-micromolar potency against ERK5.

5.8 Lead Compounds in the Pyrrole Carboxamide Series

The most promising compounds in this series at the commencement of the work described in this thesis can be classified according to their amide substituent. The following section summarises the pharmacological, physicochemical, and pharmacokinetic properties of the lead compounds in each class.

5.8.1 Class 1: Aliphatic Heterocyclic Amides

The class 1 aminopiperidyl amide **212** was the most potent analogue at the start of my involvement in this project (ERK5; IC_{50} = 199 ± 68 nM, L.E. 0.38). This amide substituent introduces a basic centre into the template, with an estimated pK_a of 9.5, which would be expected to be protonated under physiological conditions.
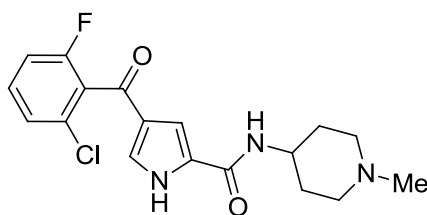
212

Compound **212** had low metabolic turnover in human and mouse liver microsomes (Table 5.4). However, **212** exhibited low flux and a high efflux ratio (ER) in the Caco-2 assay, suggesting it is slow to cross membranes, and is recognised by an efflux transporter.

MW	clogP	clogD	HLM Cl_{int}[a]	MLM Cl_{int}[a]	Caco-2 AB[b] (ER)
363	2.6	1.3	<5	8	3.8 (9)

[a] μL/min/mg protein. [b] P_{app} 10^{-6} cm s^{-1}.

Table 5.4: Physicochemical and *in vitro* ADME parameters of **212**.

Compound **212** was progressed into a mouse *in vivo* pharmacokinetic study (Table 5.5). This compound had low plasma protein binding, and was cleared at

approximately liver blood flow in mouse (mouse liver blood flow ~90-110 ml/min/kg).[254] The unbound clearance was moderate, consistent with low *in vitro* mouse microsomal clearance. The translation to high total plasma clearance was likely to be due to the high unbound fraction in plasma available to be metabolised. An alternative explanation is that the compound is cleared by non-cytochrome P_{450}-based mechanisms for which microsomal data would not be relevant. The volume of distribution was consistent with expectations for a basic compound. The bioavailability was low, which reflected the high total plasma clearance. The high efflux in the Caco-2 assay indicated that absorption may also be impaired.

F_u	Cl ml/min/kg	Cl_u ml/min/kg	V_d L/kg	$t_{1/2}$ min	F %
0.32	91	284	3.4	61	<10

Table 5.5: *In vivo* pharmacokinetic parameters for **212**. Dose 10 mg/kg *i.v.* and *p.o.*

In this series the target for the optimisation program was to further improve potency against ERK5 (target IC_{50} < 20 nM), decrease *in vivo* plasma clearance, and reduce transporter-mediated efflux in the Caco-2 assay.

5.8.2   Class 2: Heteroaromatic Amides

The structures of the key heteroaromatic amide lead compounds are shown in Table 5.6. The matched compound pair of **213** and **214** demonstrate that the postion of the pyridyl nitrogen has little effect on ERK5-inhibitory potency. However, unflanked pyridine nitrogen atoms are known to carry a risk of inhibition of cytochrome P_{450} enzymes,[255] and 4-pyridyl analogue **214** was found to be a potent cyp inhibitor, with an IC_{50} of 74 nM for the 2C19 isoform. The 5-aminopyrimidyl amide (**215**) was identified as an alternative to the pyridyl substituent that retained similar potency but exhibited no inhibition of cytochrome P_{450}s, although some evidence of efflux in the Caco-2 assay (efflux ratio = 3.3) suggested that this compound may be a transporter substrate. Substitution of the 2-position of the pyrimidyl ring with a methyl group (**217**) led to a small loss in potency.
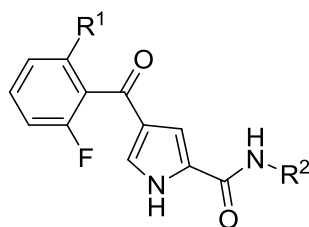
Compound	R^1	R^2	ERK5 IC_{50}[a] nM	Cyp Inhibition
211	Br		821 ± 73[a]	No cyp inhibition
213	Cl		583 ± 242	Weak ($IC_{50} > 6$ μM)
214	Cl		602 ± 266	Strong ($IC_{50} < 1.5$ μM)
216	Cl		400 ± 166	n.d.
215	Cl		404 ± 91	Weak ($IC_{50} > 11$ μM)
217	Cl		1185 ± 615	n.d.

[a] Determination $\pm$ standard deviation; n.d. = not determined.

Table 5.6: Primary pharmacology and Cyp inhibition profiles for key leads in the class 2 amide series.

In *in vitro* ADME studies, compound **211** had low turnover in mouse and human microsomes, with high flux and no evidence of efflux in the Caco-2 assay (Table 5.7).

MW	clogP	HLM Cl_{int}[a]	MLM Cl_{int}[a]	Caco-2 AB[b] (ER)
388	3.1	<5	20	34 (0.82)

[a]μL/min/mg protein. [b]P_{app} 10^{-6} cm s^{-1}.

Table 5.7: Physicochemical and *in vitro* ADMET parameters for **211**.

An *in vivo* pharmacokinetic study in mouse had been undertaken with **211** in order to benchmark the series, and provide information for use in *in vivo* target validation studies. The key *in vivo* pharmacokinetic parameters are shown in Table 5.8.

F_u	Cl ml/min/kg	Cl_u ml/min/kg	V_d L/kg	$t_{1/2}$ min	F %
0.06	27	459	1.2	65	68

Table 5.8: *In vivo* pharmacokinetic parameters for **211** in mouse. Dose 10 mg/kg *i.v.* and *p.o.*

Compound **211** was moderately protein bound in plasma, and after intravenous dosing it was cleared at approximately one third of liver blood flow in mouse. The compound had a moderate volume of distribution consistent with the presence of a weakly basic centre. The bioavailability after oral dosing is consistent with the clearance determined from the intravenous leg of the study, suggesting that the compound is well absorbed. Profiling of **211** against a panel of 130 kinases showed it to be a selective kinase inhibitor, with CDK2 being the only kinase with over 50% inhibition at 1 μM. Independently, **211** was found to inhibit MEK5, the upstream activator of ERK5, with an IC_{50} of 3.4 μM. Inhibition of two components of the pathway may provide an improved resistance profile, as single point mutations which reduce the binding affinity of the inhibitor would be required to occur simultaneously in both ERK5 and MEK5 in order for the efficacy of the drug to be reduced.

Compound **211** was assessed in an *in vivo* tumour xenograft model in CD1 mice subcutaneously inoculated with A2780 human ovarian carcinoma cells. Before compound treatment, tumours were allowed to develop for 7 days to an average volume of 72 mm^3. Mice were randomised to receive either vehicle, 100 mg/kg **211** *p.o.* or 50 mg/kg of the literature diazepinone ERK5 inhibitor, **203**, *i.p.* twice daily for 11 days. Tumour volumes were measured at days 0, 2, 4, 7, 9 and 11, and body weight was also assessed as a surrogate for toxicity. No weight loss was observed in animals dosed with **211**. However, one mouse in the **203**-dosed group showed weight loss (78% of original body weight) at day 10 of the study. Treatment with either **203** or **211** led to similar significant decreases in tumour growth compared with the vehicle control group (Figure 5.15).
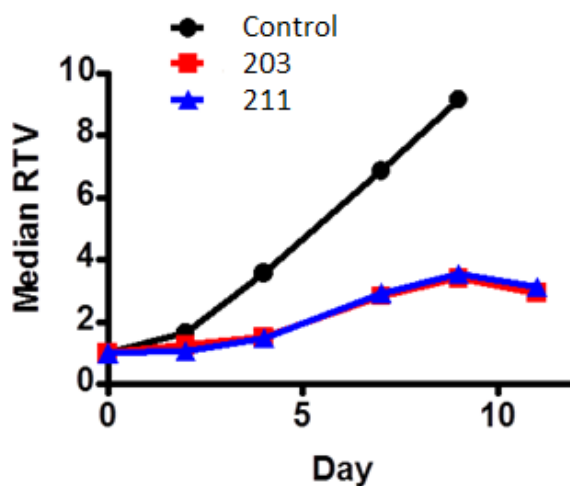
Figure 5.15: *B.i.d.* Treatment of CD1 mice bearing A2780 xenograft with **203** (50 mg/kg *i.p.*) or **211** (100 mg/kg *p.o.*)

In the heteroaromatic amide series the target for the optimisation program was to improve primary ERK5 inhibitory potency, while maintaining the attractive pharmacokinetic profile. To guide design, Susan Boyd at Cancer Research Technology modelled compound **213** in the ATP-binding site of ERK5 from the published protein co-crystal structure (PDB code 4b99) using the GOLD docking program.[256] The pyrrole amide was proposed to interact with the hinge region of the enzyme, through a hydrogen bond donor-acceptor motif as shown in figure 5.16.
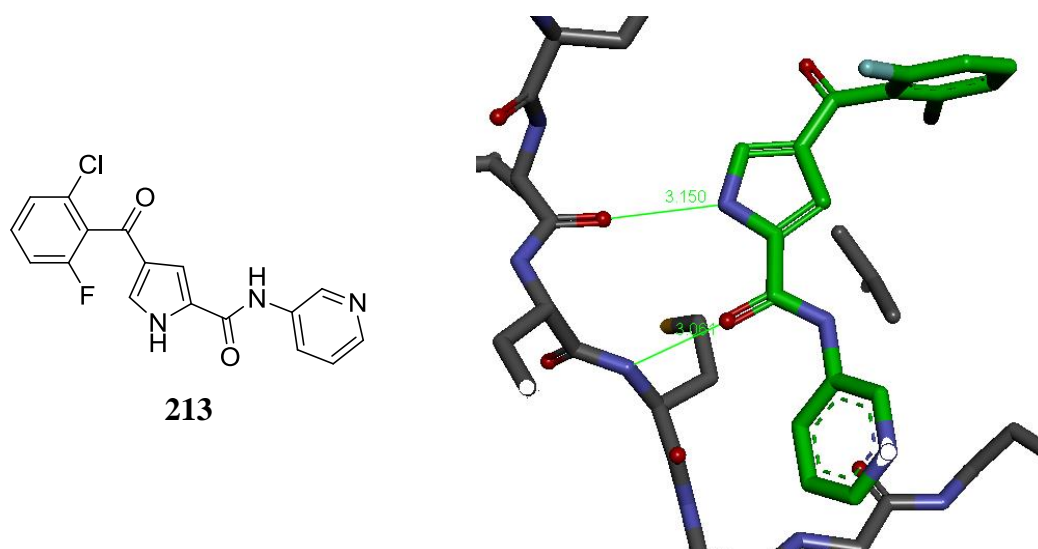
Figure 5.16: Docking of **213** into the published ERK5 crystal structure (PDB code 4b99)[247] to show the likely interaction between the inhibitor and the hinge region.

In the model of the bound inhibitor, the ketone and amide carbonyl groups are co-planar with the pyrrole ring, with the 2,6-disubstituted phenyl ring orthogonal to this plane, occupying a hydrophobic pocket (Figure 5.17). The pyridyl amide projects into the mouth of the binding pocket. The orientation of the phenyl and pyridyl rings was difficult to predict accurately.
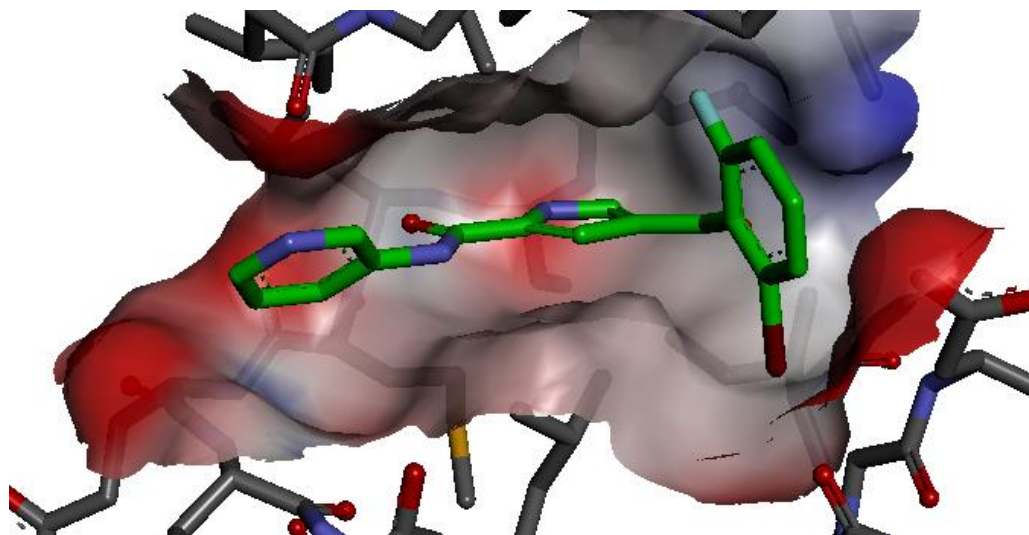
Figure 5.17: Possible binding pose of **213** modelled in the active site of ERK5 (PDB code 4b99).[247]

Further optimisation of the lead structures was directed towards two parallel aims:

1) Identification of *in vivo* tool compounds with improved potency relative to **211**, and

2) Identification of compounds with the potential for pre-clinical development, having sub-20 nanomolar potency against ERK5, selectivity over p38α, and a suitable ADMET profile.

In order to guide the optimisation program, and to gain general insights into the challenges, physicochemical properties and successful strategies that have been used in the development of kinase inhibitor drugs, the following chapter analyses marketed kinase inhibitors and compares their properties with those of the ERK5 lead compounds.

Chapter 6: Kinase Inhibitors in Clinical Use

The first kinase inhibitor to become a marketed drug, imatinib (*Glivec,* **16**), was approved in 2001, and in the ensuing years through to 2012 a further 14 kinase inhibitors have reached the market. Fourteen of the fifteen approved kinase inhibitors are indicated as cancer therapeutic agents, with the first kinase inhibitor developed for a non-cancer indication, tofacitinib (*Xeljanz*) being approved by the FDA for the treatment of rheumatoid arthritis in November 2012.

Understanding the molecular properties and medicinal chemistry design tactics that were used in the development of successfully marketed kinase inhibitors provided useful information to guide the optimisation of the pyrrole carboxamide series of ERK5 inhibitors. The following section briefly analyses the key medicinal chemistry decisions and breakthroughs that led to the identification of some of the approved first-in-class kinase inhibitor drugs. The profiles of these agents are discussed, with emphasis on the pharmacokinetic and safety parameters. A comparison of the molecular properties of lead compounds in the pyrrole carboxamide series with the properties of marketed kinase inhibitors is also presented, and its impact on the optimisation of the current series is discussed.

6.1 Inhibitors of the Bcr-Abl Fusion Gene Product

6.1.1 Imatinib

16
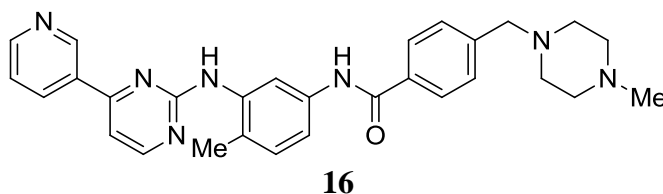
As discussed in Chapter 1, imatinib (**16**) is a Type II inhibitor of the Bcr-Abl fusion protein kinase with efficacy in the treatment of Philadelphia chromosome-positive CML.[52] Imatinib is also licensed for the treatment of GIST, acting in this indication through inhibition of c-Kit, and PDGFR kinases, and affecting downstream signalling through the classical MAPK pathway.[54]

The initial lead compound from which imatinib was developed was identified from a screen for protein kinase C inhibitors (PKC).[53] From the hits, phenylaminopyrimidine **218** was selected for follow-up due to its lead-like properties and synthetic tractability, having the potential for rapid SAR generation using simple chemistry. Substitution of the 3-position of the pyrimidine ring with a 3-pyridyl group (**219**) gave improved PKC potency, and adding an amide group to the phenyl ring (**220**) imparted increased potency against Bcr-Abl and receptor tyrosine kinases. Introduction of a methyl group at the 6-position of the central phenyl ring (**221**) significantly reduced PKC activity, while retaining activity against Bcr-Abl. The first members of this structural class of inhibitor had poor oral bioavailability and solubility. Addition of a polar *N*-methylpiperazine group improved these properties, resulting in the discovery of imatinib (**16**).[53]
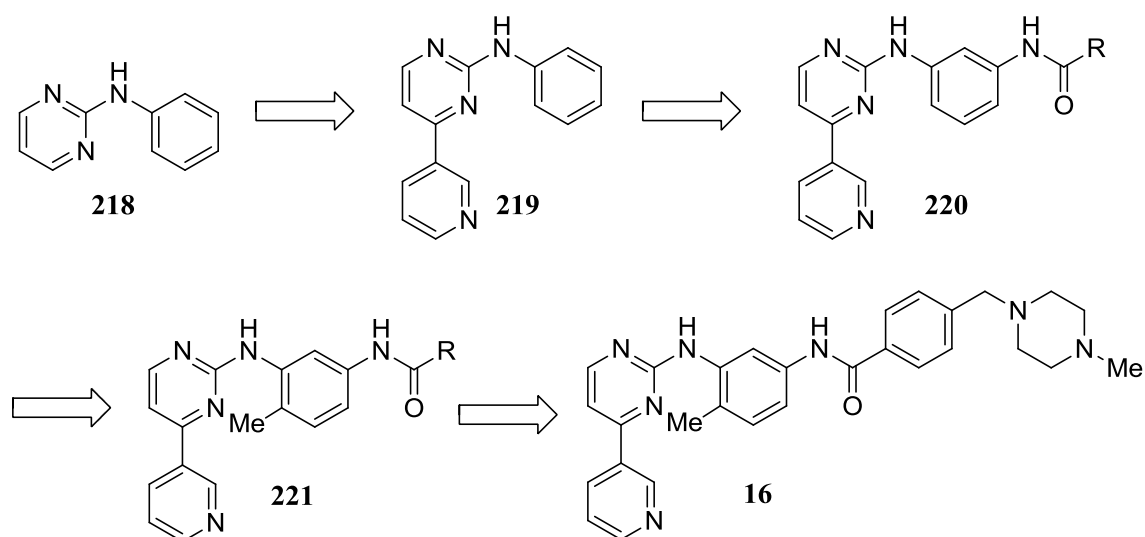
Figure 6.1: Key stages in the discovery of imatinib (**16**).

Table 6.1 outlines the molecular properties of imatinib, showing it to have sub-nanomolar potency against the isolated Bcr-Abl kinase, moderate lipophilicity, and a molecular weight close to 500. This results in good ligand efficiency (LE) and excellent lipophilic efficiency (LipE).
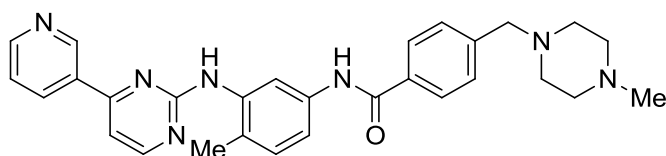
Bcr-Abl IC$_{50}$ nM	MW	clogP	clogD	tPSA Å^2	HBD	HBA	LE	LipE
0.2	494	3.6	3.3	85	2	8	0.37	7.2

Table 6.1: The molecular properties of imatinib (**16**).

6.1.2 Resistance and Second Generation Bcr-Abl Inhibitors

Although imatinib demonstrated impressive results in the clinic and validated the targeted therapy paradigm for cancer drug discovery, development of resistance to this kinase inhibitor has emerged as a significant issue. Between 15-25% of imatinib-treated CML patients show intrinsic resistance, and a further 7-15% lose their initial response to the drug through acquired insensitivity.[213] The principal resistance mechanism is the development of point mutations in the Bcr-Abl gene, with over thirty such resistance-inducing mutations having been observed in the clinic.[213] Other mechanisms such as gene amplification or over-expression, and up-regulation of downstream effectors also decrease the drug's effectiveness. For example, some imatinib-resistant CML cells show up-regulation of members of the MAPK and PI3K signalling pathways. Second generation Bcr-Abl inhibitors that have reached the market include dasatinib (*Sprycel*, **222**) and nilotinib (*Tasigna*, **223**). Dasatinib is 325-fold more potent against Bcr-Abl than imatinib, and has activity against 21 imatinib-resistant mutants.[257] Nilotinib and dasatinib both also inhibit c-kit and the PDGF receptor, with dasatinib having additional activity against Src.

222

223
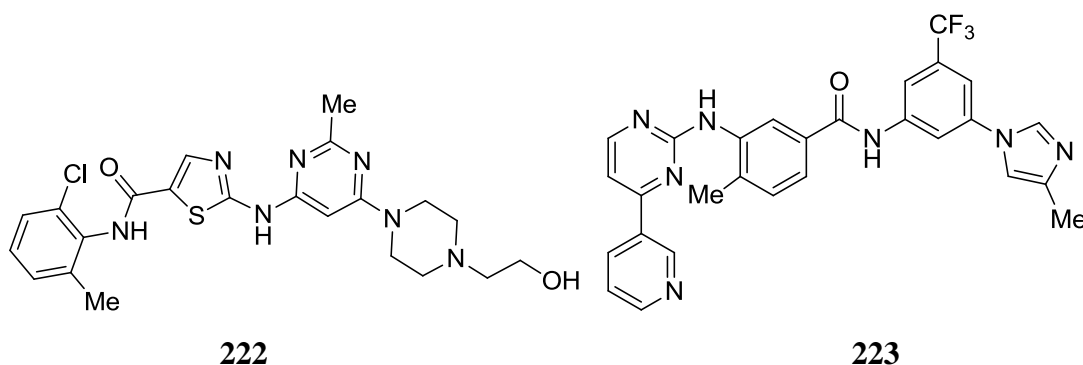
Bosutinib (*Bosulif*, **224**) is another second generation Bcr-Abl inhibitor that was approved for use in CML in September 2012,[258] with activity also against the c-Src

kinase. Its negligible inhibitory activity against c-kit or platelet-derived growth factor receptor kinase has been proposed to be advantageous in reducing haematological side-effects which can arise during treatment with imatinib and other second generation agents.[258] The first and second generation drugs are ineffective against the common T315I mutation of the gatekeeper residue of Bcr-Abl.[259] These agents all exploit a hydrogen bond with the native threonine gatekeeper residue as a key interaction, which contributes to their binding affinity.[260]

224   **225**
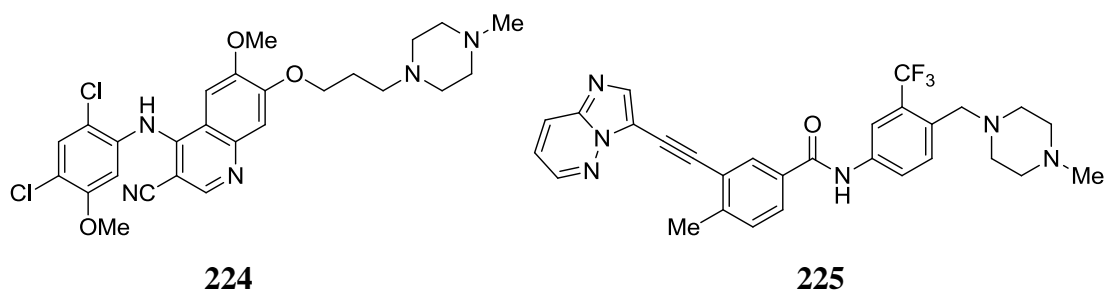
Ponatinib (*Iclusig,* **225**), a third generation Bcr-Abl inhibitor, was approved by the FDA in December 2012. This compound was developed to include inhibition of the T315I mutant kinase in its profile, utilising an acetylene linker to bypass interaction with the gatekeeper threonine residue.[260] Ponatinib potently inhibits the native enzyme and all other mutants tested.[260]

6.2 EGFR Inhibitors

A second group of marketed kinase inhibitors target EGF receptor kinases. Gefitinib (*Iressa*, **17***)* was approved in May 2003 for patients with NSCLC, followed in 2004 by erlotinib (*Tarceva,* **18**). These agents are Type I kinase inhibitors with selectivity for the EGFR receptor (ErbB1) kinase over Her-2, despite high sequence identity between these two sub-types.[261] The use of these agents has given an improvement of 25% in progression-free survival.[56] However, resistance is common, with treatment often providing benefit for only a matter of months.[262]

17   **18**
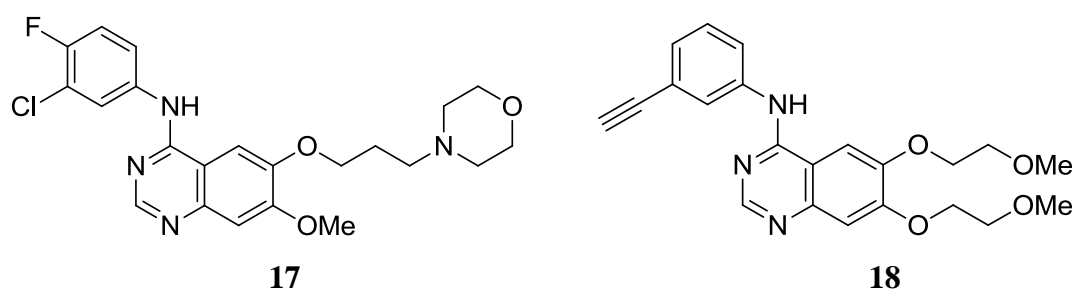
6.2.1 Medicinal Chemistry Leading to the Discovery of Gefitinib (17)

Gefitinib (**17**) was the first-in-class EGFR kinase inhibitor. The aminoquinazoline core was identified from a 3D computational search for structures that could satisfy a pharmacophore proposed for EGFR activity.[263] This was developed from a computational model of the enzyme active-site, with features from both the tyrosine and ATP substrates being incorporated.[264] Three features were selected based on their likely importance in the interaction between enzyme and substrate, and the confidence in their position in the model. Thus, the desired features were mimics of any of the non-bridging oxygen atoms of the ATP γ-phosphate, tyrosyl hydroxyl and tyrosyl aromatic ring. Once virtual hits had been identified, these were used to query a larger database using 2-dimensional molecular descriptors, which resulted in the discovery of 4-(3-chloroanilino)quinazoline (**226**) as a 16 nM inhibitor of EGFR (Figure 6.2). Key SARs for activity were identified as the presence of electron-donating substituents at the 6- and 7-positions of the quinazoline, a free NH at the 4-position, and a small lipophilic group at the 3-position of the aniline. Substitution at the 2-, 5-, and 8-positions of the quinazoline was detrimental. Replacement of the aniline chloro substituent by a methyl group and addition of two methoxy groups to the quinazoline core led to **227**, a 5 nM inhibitor with a cellular growth inhibition IC_{50} of 50 nM in KB oral carcinoma cells.[264] However, this compound was rapidly metabolised, resulting in a short pharmacokinetic half-life of one hour. Identification of the metabolites as arising from oxidation of the phenyl 4-position, and oxidation of the 3-methyl group on the phenyl ring led to the synthesis of analogues to block these metabolic routes, including **228**. Compound **228** had an isolated enzyme IC_{50} of 9 nM, an IC_{50} of 80 nM in the cell growth assay, and a pharmacokinetic half-life in mouse of three hours.[264]
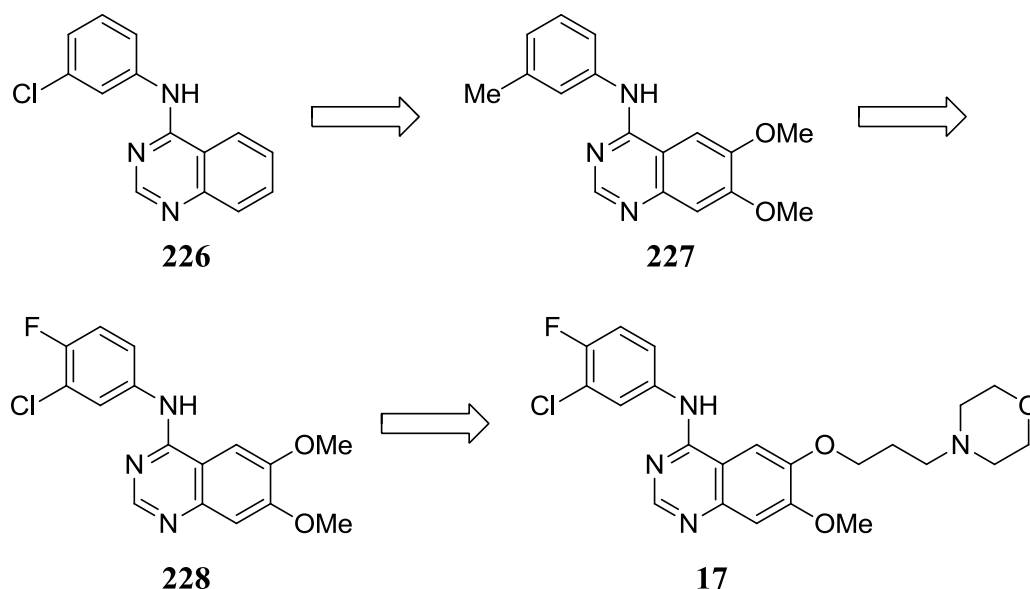
Figure 6.2: Key stages in the discovery of gefitinib (**17**).

In an attempt to improve the *in vivo* activity of **228**, modification of the alkoxy groups was investigated to tune the pharmacokinetic properties.[263] A range of alkoxy replacements were introduced, with focus on incorporation of pendant basic centres that varied the basicity, lipophilicity and solubility. *In vivo* pharmacodynamic experiments indicated that a 24 hour duration of action may be necessary for optimal efficacy. Compounds were thus assessed both for potency and plasma concentration at a 6 hour time-point after dosing. Alkoxymorpholine derivatives provided potent compounds which achieved high plasma levels after 6 hours. Gefitinib (**17**), while not the most potent analogue, allowed a compound concentration of 70-fold the IC_{50} value to be maintained for 24 hours after a single 200 mg/kg dose. Table 6.2 outlines the molecular properties of gefitinib, showing it to be a moderately lipophilic compound with good ligand and lipophilic efficiency.
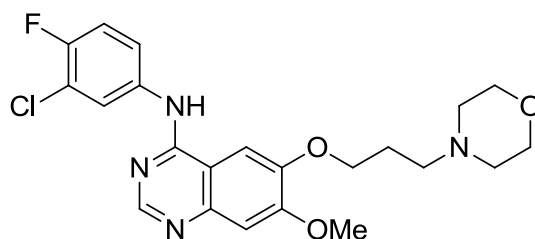
EGFR IC_{50} nM	MW	clogP	clogD	tPSA Å^2	HBD	HBA	LE	LipE
23	446	4.1	3.5	67	1	7	0.35	5.0

Table 6.2: Molecular properties of gefitinib (**17**).
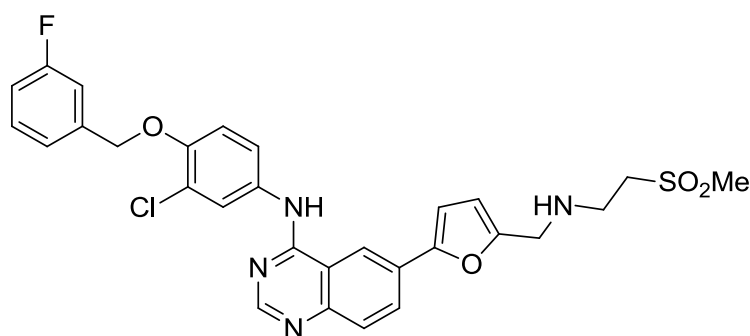
229

Lapatinib (*Tykerb*, **229**) is another 4-aminoquinazoline-derived kinase inhibitor, with dual activity against EGFR and Her-2 kinases, which is marketed for the treatment of breast cancer.[265] This dual inhibition results in reduced signalling through both the PI3K and classical MAPK pathways. Lapatinib exhibits slow offset binding kinetics from the target, with a binding half-life of five hours, in contrast to gefitinib and erlotinib which have dissociative half-lives of under 10 minutes.[266]

6.3 Inhibitors of VEGF, PDGF and Raf Kinases

Tumours require angiogenesis to grow beyond 1-2 mm, and a third major group of marketed kinase inhibitors target the pro-angiogenic growth factor receptors VEGFR and PDGFR. Over-expression of VEGF is associated with many cancers including pancreatic, lung, prostate, and breast cancers, renal cell carcinoma, and melanoma.[267]
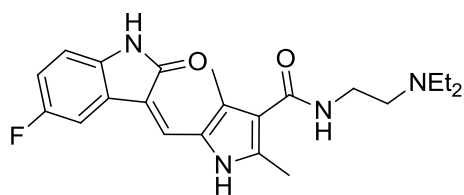
230
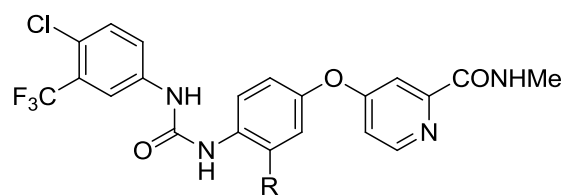
8   R = H
231 R = F

Sunitinib (*Sutent,* **230**) was designed as a multi-kinase inhibitor, with the hypothesis being that inhibiting the VEGF and PDGF receptor kinase sub-types could provide a greater benefit than inhibition of either VEGFR or PDGFR alone.[268] It is a Type II kinase inhibitor with an IC_{50} of less than 20 nM against VEGFR 1-3, PDGFR-β, c-Kit and Flt-3 kinases.[268] Sunitinib and erlotinib have been used in combination in NSCLC to provide triple inhibition of signalling through the VEGF, PDGF and EGF receptors.[268]

Sorafenib (*Nexavar*, **8**) is also a type II inhibitor of VEGFR-2 and 3 and PDGFR-β kinases, in addition to B-Raf, C-Raf, and c-Kit.[268] This drug was originally designed as an inhibitor of the raf enzyme isoforms, as aberrant signalling through the classical MAPK pathway, of which raf is a key component, is observed in approximately 30% of human cancers.[269] The inhibition of raf and VEGF family members by sorafenib results in its affecting the classical MAPK pathway at two distinct points in the signalling cascade. Regorafenib (*Stivarga,* **231**), a close analogue of sorafenib differing by a single fluorine atom, was approved by the FDA in September 2012. Despite the small structural difference, the spectrum of kinase activity differs markedly, with regorafenib being significantly more potent against VEGFR-2, c-Kit, ret and p38 kinases than sorafenib.[270,271] This leads to regorafenib having broader anti-angiogenic properties than sorafenib while having similar activity against the classical MAPK pathway.[270]

232   **233**
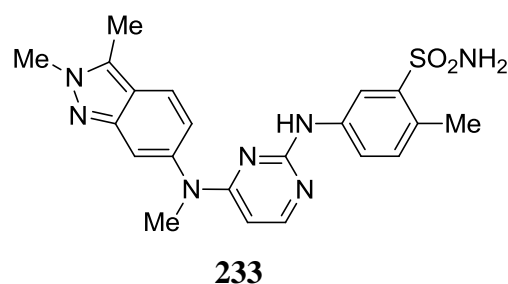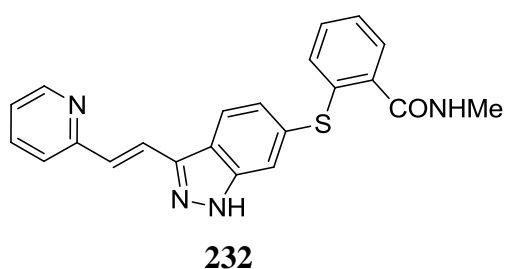
Axitinib (*Inlyta*, **232**) is a type I ATP-competitive inhibitor of VEGFR kinases 1-3, that also has activity against c-Kit and PDGFR-β kinases.[271] The inhibition of VEGFR 2 and 3 reduces Akt phosphorylation and signalling through the classical MAPK pathway.[271] Pazopanib (*Votrient*, **233***)* inhibits VEGFR kinases 1-3, PDGFR-α & β and c-Kit kinases, and is approved for renal cell carcinoma, while vandetanib (*Zactima*, **234**) is an inhibitor of VEGFR-2 and ErbB1 kinases.[268]

234   **235**
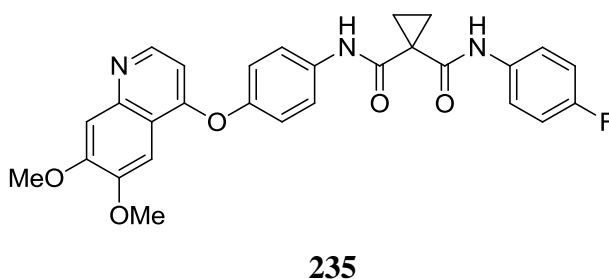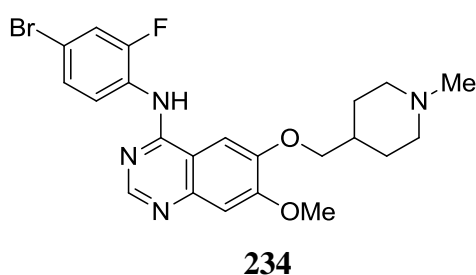
Carbozantinib (*Cometriq,* **235**) is an inhibitor of VEGFR2 and c-Met that also inhibits Ret, Kit, Axl, and Flt3 kinases, all of which have been implicated in tumour development. It was approved for the treatment of medullary thyroid cancer in

November 2012.[272] The simultaneous inhibition of multiple kinases from key tumour survival, metastasis, and angiogenesis pathways is thought to result in a greater reduction in invasiveness and metastases than single activity agents.[273]

6.3.1 Medicinal Chemistry Leading to the Discovery of Sorafenib (8)

An HTS of 200,000 compounds led to the identification of hit compound **236**, which inhibited Raf-1 with an IC_{50} of 17 µM (Figure 6.3).[269] Addition of a methyl group to the 4-position of the phenyl ring (**237**) resulted in a 10-fold potency improvement, but an analogue synthesis campaign failed to identify compound with an IC_{50} of below 1 µM. A one-thousand compound bis-arylurea library was screened, from which the isoxazole urea (**238**) emerged as an alternative template. Introduction of a nitrogen atom into the distal phenyl ring resulted in 4-pyridyl analogue **239**, which improved potency (IC_{50} = 230 nM). This compound was orally available in mice, and demonstrated *in vivo* inhibition of tumour growth in a tumour xenograft model using the HCT116 human colorectal carcinoma cell-line.[269]
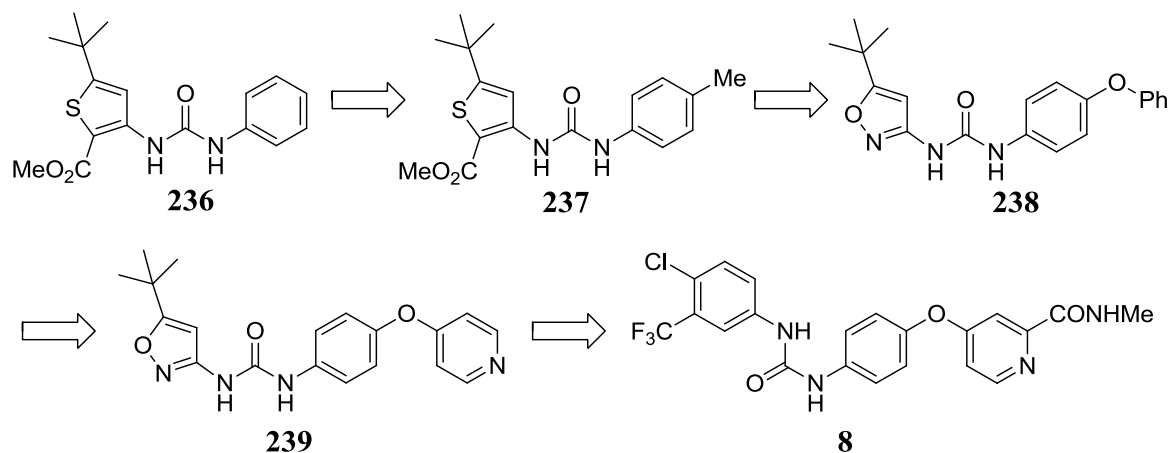
Figure 6.3: Key stages in the discovery of sorafenib (**8**).

Further SAR studies established that the urea was essential, but that the isoxazole heterocycle could be replaced. A disubstituted phenyl ring provided improved potency, and addition of a polar group to the pyridyl ring resulted in the discovery of sorafenib (**8**), having an IC_{50} against Raf-1 kinase of 6 nM. Sorafenib also inhibited wild type and V600E mutant B-raf kinase (IC_{50} = 38 nM). The VEGF1 (IC_{50} = 26 nM) and VEGF2 (IC_{50} = 90 nM) kinases were also inhibited along with p38 (IC_{50} = 38 nM), c-Kit (IC_{50} = 68 nM) and Flt-3 (IC_{50} = 33 nM).[269]

When sorafenib was co-crystallised with Raf, the pyridyl carboxamide was found to undergo a bidentate interaction with the hinge region of the kinase. The urea forms hydrogen bonds with the backbone of an aspartate residue in the DFG loop, and another with a glutamate side-chain. The terminal di-substituted phenyl group is buried in a hydrophobic pocket formed by two helices and regions of the DFG and catalytic loops.[269] Table 6.3 outlines the molecular properties of sorafenib, showing it to have relatively high lipophilicity, good ligand efficiency and moderate lipophilic efficiency.
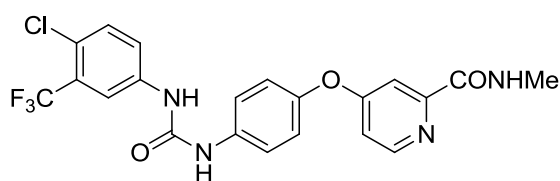
Raf-1 IC$_{50}$ nM	MW	clogP	clogD	tPSA Å^2	HBD	HBA	LE	LipE
6	464	3.9	3.9	92	3	7	0.36	3.4

Table 6.3: Molecular properties of sorafenib (**8**).

6.4 Other Classes of Marketed Kinase Inhibitors

The scope of the kinases targeted by marketed inhibitors has been expanded by the recent approval of four further drugs. Vemurafenib (*Zelboraf*, **9**) is an inhibitor of the V600E B-Raf mutant, and approved for non-resectable or metastatic melanoma.[274] The therapeutic effect is a result of direct inhibition of the classical MAPK pathway.

9   **240**
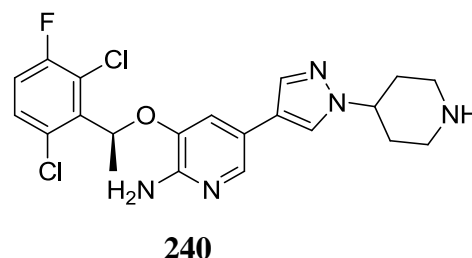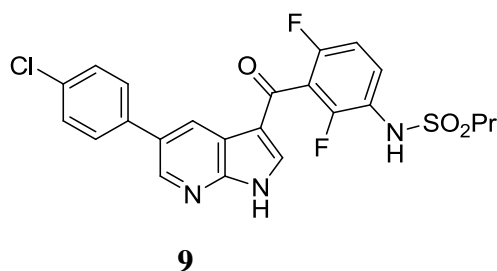
Crizotinib (*Xalkori,* **240)** is an inhibitor of the Alk and c-Met kinases approved for non-small cell lung carcinoma (NSCLC).[275] Over-expression of c-Met, also known as the hepatocyte growth factor receptor (HGFR), correlates with metastatic progression or poor prognosis in several cancers, and has also been found to affect cell survival, angiogenesis, and invasion.[275] Anaplastic lymphoma kinase (Alk) is a member of the insulin receptor family of receptor tyrosine kinases. Chromosomal rearrangements

forming several Alk fusion proteins have been observed in many cancers; for example a translocation forming an Alk-Npm (nucleophosmin) hybrid results in oncogenic signalling.[276]

Ruxolitinib (*Jakafi*, **241**) is an inhibitor of janus kinase 2 (Jak-2) approved in 2012 for myelofibrosis, and may be also used as a treatment for other myeloproliferative diseases where a V617F mutation in Jak-2 causes constitutive activation.[277] The structurally related Jak-3 inhibitor tofacitinib (*Xeljanz*, **242**) became the first kinase to be approved for a non-cancer indication in 2012.[278]

241   **242**
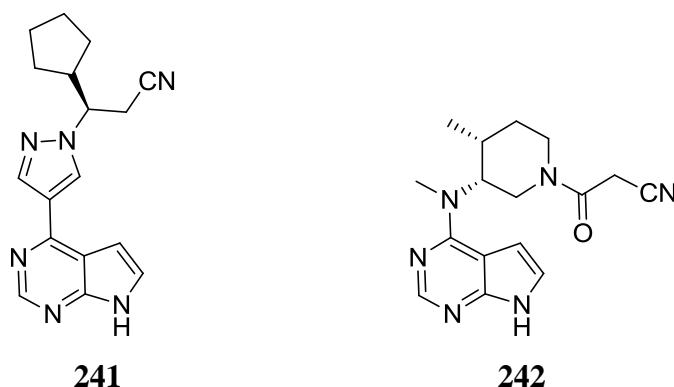
6.4.1 Medicinal Chemistry Leading to the Discovery of Crizotinib (240)

Crizotinib (**240**) was designed as an inhibitor of c-Met kinase. The starting point for the discovery program was a high molecular weight c-Met inhibitor based on an oxindole scaffold (Figure 6.4, **243**). This lead was a potent Met inhibitor (IC_{50} = 9 nM), but suffered from sub-optimal physicochemical properties, having a molecular weight of 641, poor solubility, high metabolic turnover and low membrane permeability.[276] Crizotinib was designed using a structure-based approach aiming to reduce lipophilicity and identify a lower molecular weight hinge binding motif to increase binding efficiency. Examination of co-crystal structures of leads bound to a Met kinase domain construct guided compound design. Lipophilic efficiency (LipE or LLE)[279,280] was also a key parameter which guided optimisation. An ambitious template re-design was undertaken based on the binding mode observed in the crystal structure, leading to an aminopyridine replacing the oxindole scaffold, that enabled positioning of the distal portions of the lead to be replicated by substitution from this simplified core.[276]
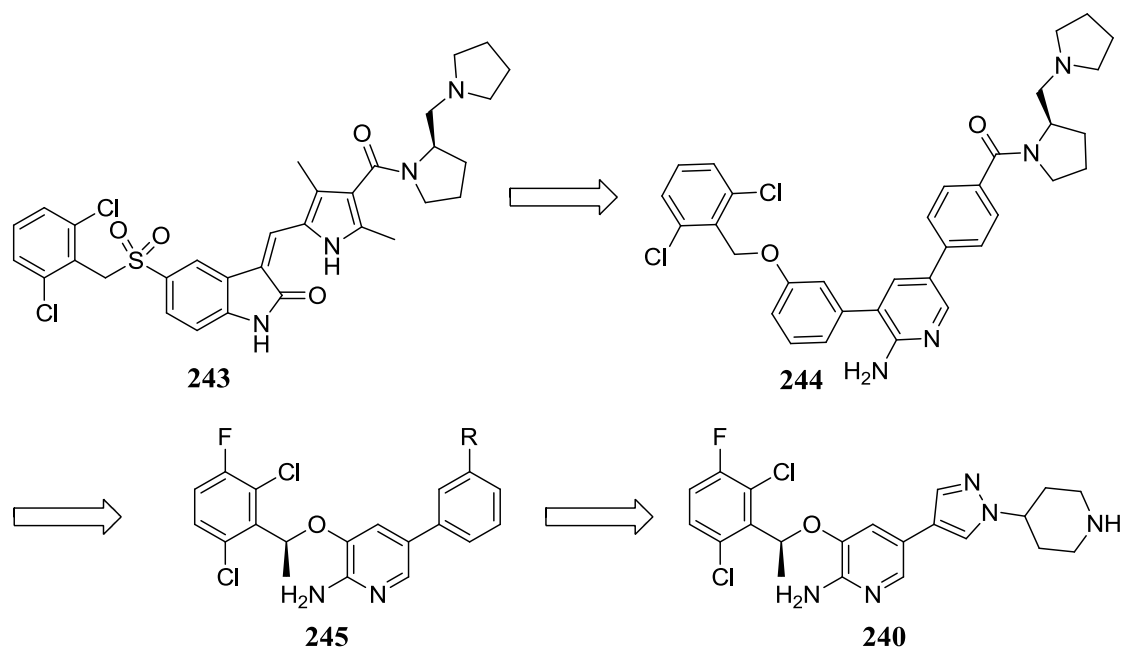
Figure 6.4: Key stages in the discovery of crizotinib (**240**).

From the first set of compounds prepared in this scaffold, **244**, a compound with 460 nM potency against Met was discovered. The substituents from this core were re-investigated, with an optimal tri-halogenated substitution pattern on the benzyl ring initially being identified. Structure-based design guided the incorporation of a small lipophilic methyl group on the benzyl linker, which provided a potency benefit (**245**). The pyridyl 5-substituent projected into the solvent exposed surface of the kinase, and a range of polar groups were introduced at this position, with pyrazolopiperidine **240**, (crizotinib), giving the best overall balance of properties.[276] Table 6.4 shows the molecular properties of crizotinib, confirming it as a potent, moderately lipophilic compound with excellent ligand efficiency and LipE.
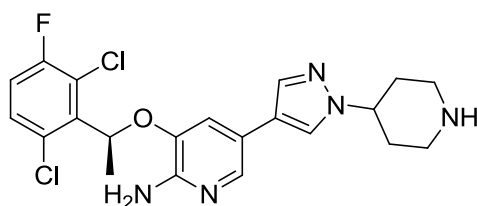
Met IC$_{50}$ nM	MW	clogP	clogD	tPSA Å^2	HBD	HBA	LE	LipE
2	450	4.7	2.3	75	3	6	0.41	6.4

Table 6.4: Molecular properties of crizotinib (**240**).

6.5 Summary

It is notable that high selectivity for the target for which the drug was initially designed is rarely achieved. Secondary off-target pharmacology in many agents has proven to be advantageous, providing wider scope for their use in other cancer types than those originally targeted. This is clearly dependent on the nature of the secondary targets inhibited, but indicates that during optimisation of a kinase inhibitor, activity against other kinase targets should be investigated further, and that the advantages and disadvantages of any observed polypharmacology should be carefully considered during compound selection. Second- and third-generation agents in each class have primarily attempted to address resistance developed to the first-in-class agent, often arising through point mutations in the drug's binding site in the kinase.

6.6 *In Vitro* ADMET Data and Human Pharmacokinetics of Approved Kinase Drugs

Examination of the new drug application (NDA) reports for the kinase inhibitors in clinical use (Table 6.5), in conjunction with the above analyses, reveals some interesting trends. A large proportion of these drugs contain a basic centre. This was often introduced to improve pharmaceutical properties including solubility, but also leads to high volumes of distribution which contribute to the long human pharmacokinetic half-lives often achieved.

Common metabolic pathways involve dealkylation of amines and phenols, or formation of *N*-oxide metabolites. Inhibition of cytochrome P_{450} enzyme isoforms is also common in the approved kinase drugs dataset. A significant number of the drugs are substrates for efflux transporters but this does not appear to substantially limit their oral bioavailability. However, this is a potential mechanism for the development of resistance through over-expression of the relevant transporter proteins. Many of the marketed agents also inhibit the hERG ion channel, and adversely affect the cardiac QT_c interval.

Table 6.5: Summary of ADMET properties of Approved Kinase Drugs.

Kinase Inhibitor	Human PK $T_{1/2}$ h	Human F %	hERG IC_{50} μM	QTc^a	Transporter Effects	Major metabolic route	Cyp inhibition
Imatinib[281]	18	98	n.a.	N	Caco-2 ER = 54	*N*-demethylation	-
Dasatinib[282]	3-6	14-34	14.3	Y	Caco-2 ER = 2	*N*-oxidation, *N*-dealkylation	Cyp 3A4 inhibitor
Nilotinib[283]	17	30	0.13	Y	P-gp substrate	Hydroxylation	Multiple Cyp inhibitor
Bosutinib[284]	19-30	n.a.	0.3	N	P-gp substrate	Oxydechlorination, *N*-demethylation and *N*-oxidation	-
Ponatinib[285]	24	n.a.	2.3	Y	P-gp and BCRP inhibitor	*N*-demethylation	-
Gefitinib[286]	25-85	60	ca. 1 μM	Y	Caco-2 ER = 12	*O*-demethylation	Cyp 2D6 inhibitor
Erlotinib[287]	36	59	IC_{20} = 3 μM	N	P-gp substrate	*O*-demethylation	Cyp 1A1, 3A4 and 2C8 inhibitor
Lapatinib[288]	6-24	<25	n.a.	Y	P-gp and BCRP substrate	Multiple oxidised metabolites	Cyp 3A4 and 2C8 inhibitor
Sunitinib[289]	40-60	n.a.	0.27	Y	n.a.	*N*-deethylation	-
Sorafenib[290]	25-48	n.a.	>10	N	n.a.	*N*-oxidation	Multiple Cyp inhibitor
Regorafenib[291]	14-58	n.a.	>10	N	Caco-2 ER = 0.8	*N*-oxidation	Multiple Cyp inhibitor
Axitinib[292]	2-5	58	>10	N	Caco-2 ER = 10 BCRP and P-gp substrate	*N*-glucuronide and sulfur oxidation	Cyp 1A2 and 2C8 inhibitor
Pazopanib[293]	18-53	14-39	>10	N	Caco-2 ER = 5 BCRP and P-gp substrate	Biliary clearance of parent	Multiple Cyp inhibitor

Table 6.5: Summary of ADMET properties of Approved Kinase Drugs (continued).

Kinase Inhibitor	Human PK $T_{1/2}$ h	Human F %	hERG IC$_{50}$ μM	QTc [a]	Transporter Effects	Major metabolic route	Cyp inhibition
Vandetanib[294]	19 d	n.a.	Metabolites inhibit hERG	Y	Caco-2 ER = 0.8	Demethylation and *N*-oxidation	Cyp 2D6 inhibitor, 1A2, 2C9, 3A4 inducer
Vemurafenib[295]	57	"Low"	1.25	Y	Caco-2 ER = 1.3	Biliary clearance of parent	Inhibitor and inducer of multiple Cyps
Crizotinib[296]	42	43	n.a.	Y	Caco-2 ER >20	Oxidation to lactam and *O*-dealkylation	Inhibitor and inducer of Cyp 3A isoforms

[a] Prolongation of cardiac QTc interval observed in pre-clinical or clinical setting; n.a. = Data not available from FDA new drug approval reports; FDA reports not available for carbozantinib, ruxolitinib and tofacitinib.

6.7 Comparison of the Molecular Properties of ERK5 Lead Compounds with Approved Kinase Inhibitors

Examining the physicochemical properties of kinase inhibitors that have reached the market may help define the chemical property space occupied by successful inhibitors of this target class. Comparison with the physicochemical properties of the pyrrole carboxamide lead compounds can inform the lead optimisation process, allowing potential targets to be assessed as to whether they fall inside or outside of precedented kinase drug space. While compounds outside of this chemical space are not destined to fail *per se*, and those that lie inside are not guaranteed to succeed, confidence in the likelihood of developing a successful kinase drug is increased if the optimised compounds have physicochemical properties in a similar range to those that have previously been successfully developed.

To this end, the physicochemical and structural properties of the kinase drugs marketed for cancer treatment from 2001-2012 were determined using the *Stardrop^{TM}* program. Properties selected were molecular weight (MW), clogP, clogD, number of hydrogen bond acceptors (HBA), number of hydrogen bond donors (HBD), topological polar surface area (tPSA), number of rings present, (ring count), and the rotatable bond count.

The value of a property for each drug was assigned to a bin, allowing a histogram of the distribution of each property across all of the drugs to be generated. For non-continuous parameters (HBA, HBD, ring count), the bins reflect the absolute values of the property.

The same physicochemical properties were then generated for the benchmark pyrrole carboxamide lead, **212** (Table 6.6).

212
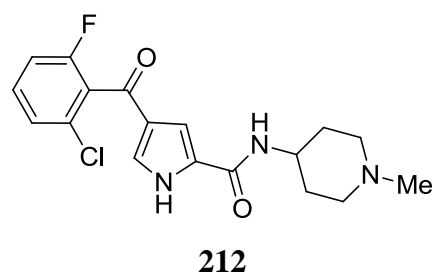
Property	Value
MW	363
clogP	2.6
clogD	1.3
tPSA ($\AA^2$)	65
HBA	5
HBD	2
Rotatable bonds	5
Ring count	3

Table 6.6: The molecular properties of benchmark pyrrole carboxamide **212**

The value of each property for compound **212** is overlaid onto each histogram as a red line. Thus, it can quickly be determined where the lead compound lies relative to precedented kinase drug chemical space, as defined by this process. For parameters where the property of the lead is towards the lower end of the range, confidence was gained that there was scope to design analogues where the value of this property was increased. The conclusions drawn from analysis of each of the properties follow:

6.7.1 Molecular Weight
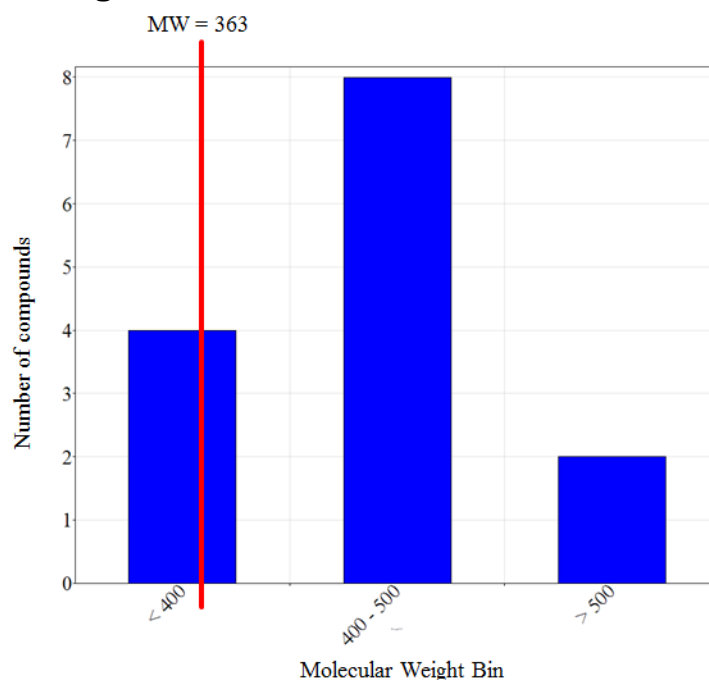
Figure 6.5: Histogram of molecular weights of marketed kinase inhibitor drugs. The red line indicates the molecular weight of pyrrole carboxamide lead **212**.

It is clear from figure 6.5 that the molecular weight of **212** is towards the lower end of the range for kinase drugs. The only two marketed kinase inhibitors having lower molecular weight are the recently approved Jak inhibitors, ruxolitinib (**241**, MW = 306) and tofacitinib (**242**, MW = 311). Minimising the molecular weight of a compound offers advantages for compound absorption,[297] and often correlates with an increased chance of progressing through the drug development pipeline.[298] However, it was clear that there was scope to increase the molecular weight of **212** during the optimisation process. Subsequent compound design was thus aimed at preparing 90% of future compounds having a molecular weight below 500, and attempting to reduce the molecular weight to a minimum where possible.

6.7.2 Lipophilicity

Two calculated measures of lipophilicity were examined, namely clogP and clogD. clogP is an estimate of the inherent lipophilicity of the unionised compound, whereas clogD incorporates the effect of the ionisation state of the compound at pH 7.4. Calculated values may not accurately reflect the experimentally measured logD values, but are useful in compound design as they can be determined computationally prior to compound synthesis.
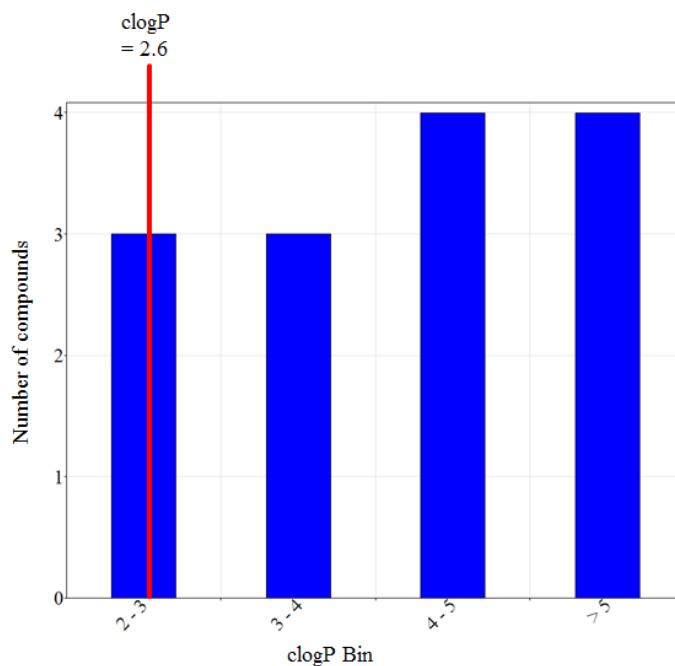
Figure 6.6: Histogram of the clogP values of marketed kinase inhibitor drugs. The red line indicates the clogP of pyrrole carboxamide **212**.

The marketed kinase drugs spanned a wide range of clogP values (figure 6.6), with no clear clustering of marketed drugs in any clogP bin. The clogP of 2.6 for **212** is at the lower end of the range covered by marketed inhibitors. However, the distribution of clogD values in the drug dataset (figure 6.7) showed that the majority of kinase drugs have a clogD between 2 and 4, with only 3 compounds lying outside of this range. Thus it appears that the clogD of a compound may be the more important lipophilicity measure to consider during compound optimisation; hence analogues with a clogD in the range 2 to 4 were targeted.
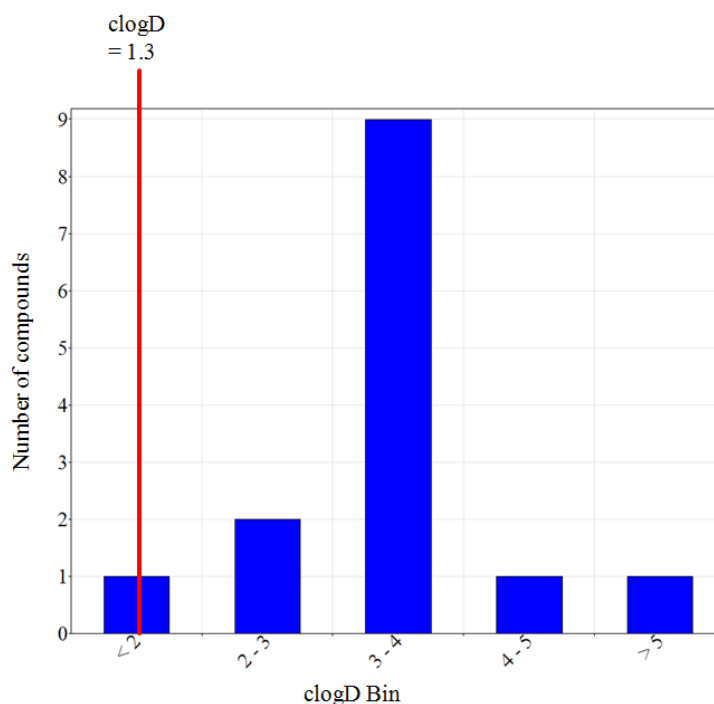
Figure 6.7: Histogram of the clogD values of marketed kinase inhibitor drugs. The red line indicates the clogD of pyrrole carboxamide **212**.

6.7.3 Hydrogen Bonding Groups

Three measures of hydrogen bond interactions were included in this analysis; tPSA, HBD and HBA. Relationships between the presence of hydrogen bonding groups and the ability to cross cell membranes have been observed in several studies.[299,300] With kinase targets having intracellular drug binding sites, attaining good cell penetration is essential for a successful drug. The tPSA is a simplified polar surface area calculation based on the 2 dimensional structure of a compound, which does not take into account 3-dimensional conformational effects.[299] However, it has been shown to correlate with the more time consuming calculation of polar surface area based on the 3-dimensional structure of a compound. tPSA is calculated computationally by adding together tabulated contributions of the polar fragments contained in a molecule. It is essentially an estimate of the total surface area of a molecule which is available to participate in hydrogen bonding with a polar solvent such as water.
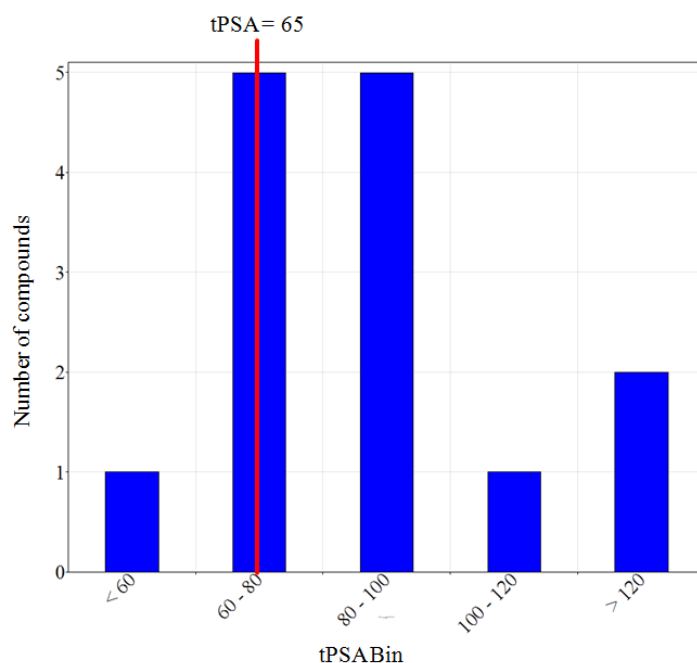
Figure 6.8: Histogram of the tPSA values of marketed kinase inhibitor drugs. The red line indicates the tPSA of pyrrole carboxamide **212**.

The majority of members of the kinase drug dataset have a tPSA between 60 and 100 Å^2 (figure 6.8), with only two examples having a tPSA above 120 Å^2. Compound **212** has a tPSA of 65 Å^2, which is towards the lower end of the range, suggesting that there is scope to introduce further heteroatoms and moderately increase the tPSA during compound optimisation.
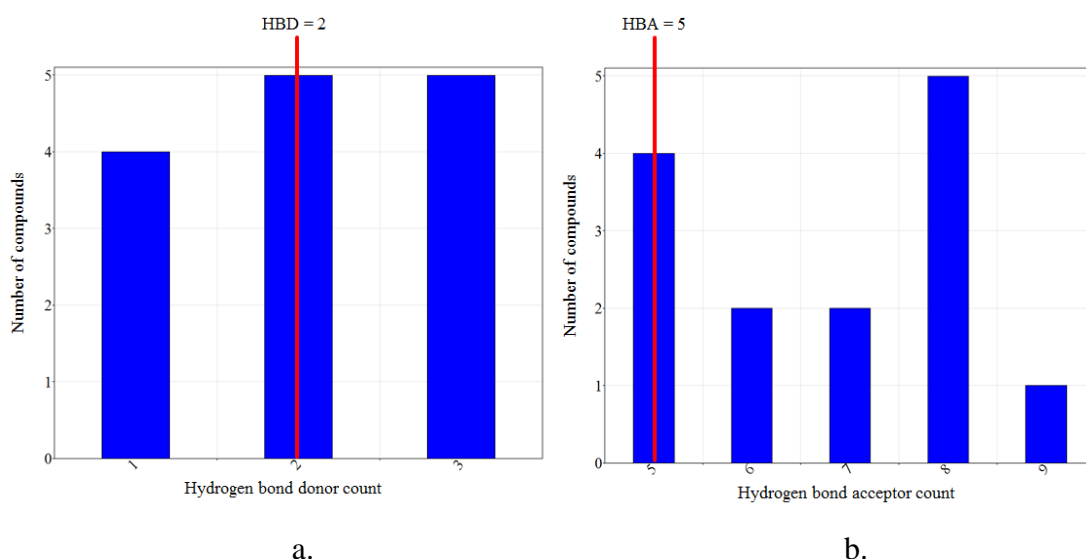
Figure 6.9: Histogram of the a) HBD and b) HBA parameters of marketed kinase inhibitor drugs. The red line indicates the respective values of pyrrole carboxamide **212**.

The majority of the marketed kinase inhibitor drugs have less than three hydrogen bond donors (Figure 6.9a). A design criterion was thus defined that minimising the hydrogen bond donor count was preferable, and the majority of targets would be limited to a maximum of three hydrogen bond donors. Lead **212** has two hydrogen bond donors, suggesting that no more than one further hydrogen bond donor should be added during compound optimisation.

The range of hydrogen bond acceptors varied more widely across the drug dataset (Figure 6.9b), with a maximum of nine and a minimum of five being represented. Pyrrole **212** has five hydrogen bond acceptors. This analysis suggests that increases in tPSA through introduction of hydrogen bond acceptors may be better tolerated than through additional hydrogen bond donors.

6.7.4 Ring Count and Rotatable Bond Count

Ring count and rotatable bond count are intended as surrogates for the flexibility of a molecule. A flexible molecule can access more conformations than a more rigid molecule of a similar molecular weight. The ability to readily achieve alternative conformations may increase the chance of a molecule being able to adopt a conformation whereby it can bind to secondary targets, increasing the probability of off-target effects. Flexibility may also be detrimental to the binding affinity of a compound, due to an entropic loss on binding.
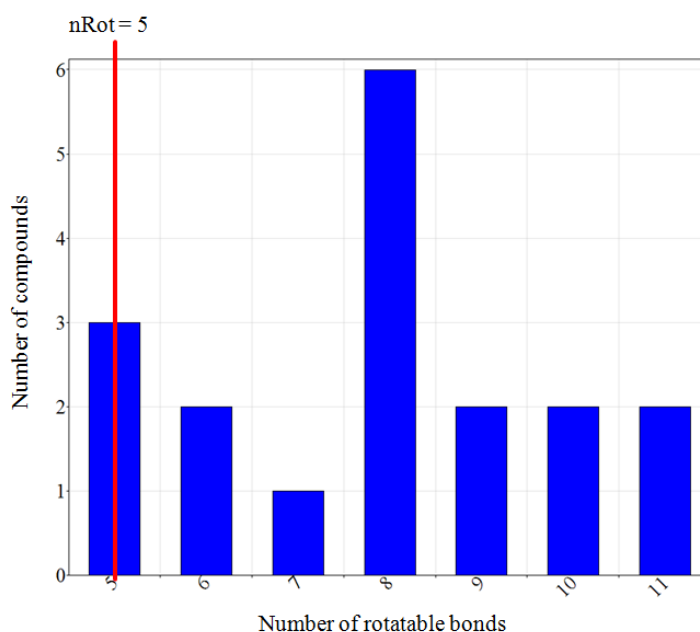
Figure 6.10: Histogram of the rotatable bond count of marketed kinase inhibitor drugs. The red line indicates the rotatable bond count of pyrrole carboxamide **212**.

154

The number of rotatable bonds in the drug dataset varied between 5 and 11 (Figure 6.10), with **212** again occupying the lower end of this range, indicating that it is relatively rigid for a kinase inhibitor, and that increased flexibility may be tolerated.
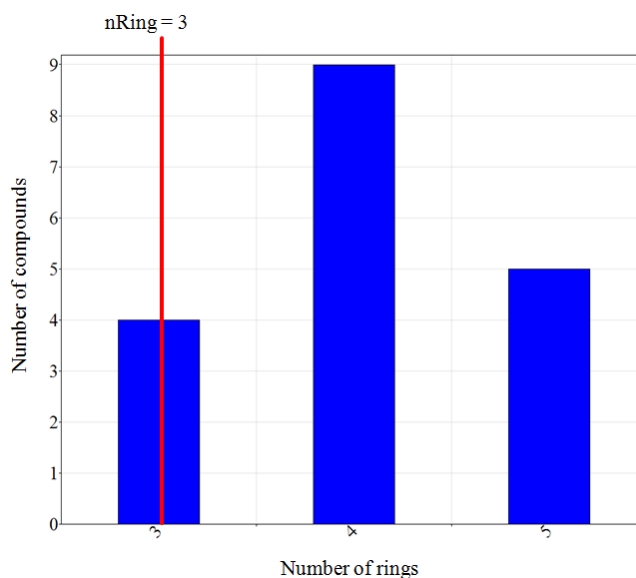
Figure 6.11: Histogram of the ring count of marketed kinase inhibitor drugs. The red line indicates the ring count of pyrrole carboxamide **212**.

The number of rings present in kinase drugs ranges from three to five (Figure 6.11), and this analysis indicates that addition of a further ring during optimisation may be possible.

6.8 Summary

The above analyses have been compressed into a spider plot (Figure 6.12), where the green area depicts the range of properties currently occupied by successful kinase drugs, with the properties of **212** superimposed in red. This clearly indicates scope for increasing the value of most of the parameters during the optimisation of the pyrrole carboxamide lead compounds.
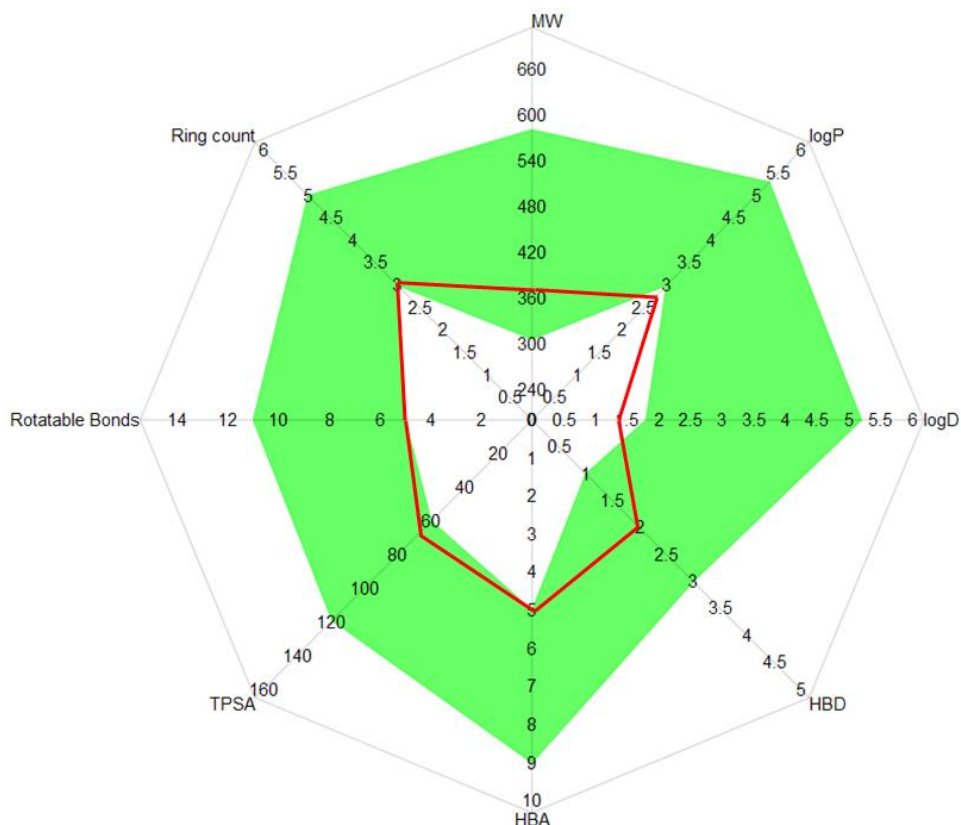
Figure 6.12: Spider plot of molecular properties of marketed kinase inhibitors (green area) in comparison with the properties of pyrrole **212** (red line).

The target physicochemical properties for the majority of analogues designed in the optimisation of the pyrrole carboxamide series were thus defined as shown in table 6.7.
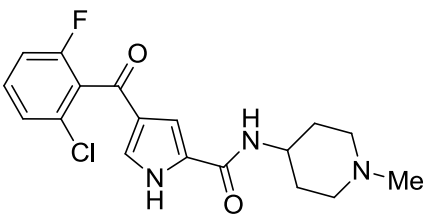
MW	clogD	tPSA Å^2	HBA	HBD	Rot bonds	Ring count
<500	2-4	60-100	≤ 3	≤ 9	≤ 11	≤ 5

Table 6.7: Target molecular properties for analogues during the optimisation of the pyrrole carboxamide series.

Chapter 7: ERK5 SARs and Biological Results

7.1   Class 1: Heterocyclic Aliphatic Amides

Compound **212** was the most potent analogue at the start of my involvement in the ERK5 project. A summary of the profile of this compound is given in Table 7.1.

ERK5 IC$_{50}$[a]	199 ± 68 nM
HLM Cl$_{int}$	<5 µL/min/mg
MLM Cl$_{int}$	8 µL/min/mg
Caco-2 AB	3.8×10^{-6} cm s^{-1}
Caco-2 ER	9
Cl	91 ml/min/kg
F	$<10\%$

212

[a] Determination $\pm$ standard deviation

Table 7.1: ERK5-inhibitory activity, and selected *in vitro* and *in vivo* pharmacokinetic parameters for **212**.

For the design of analogues of compound **212**, three parameters were selected for improvement: ERK5 potency, metabolic stability, and absorption. The docking of this compound into the ATP-binding site from the published ERK5 co-crystal structure[247] suggested that the piperidine *N*-substituent may project out of the binding pocket towards the solvent-exposed surface of the protein. Exploration of this region of the template had not previously been extensively undertaken, although two existing compounds, **246** and **247**, retained ERK5 potency, indicating that the binding site of ERK5 may accommodate larger substituents at this position. This was therefore investigated as a region where variation might allow modulation of pharmacokinetic parameters.
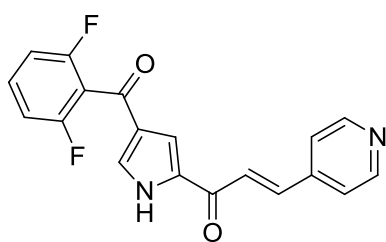
246
ERK5; IC$_{50}$ 1.5 µM
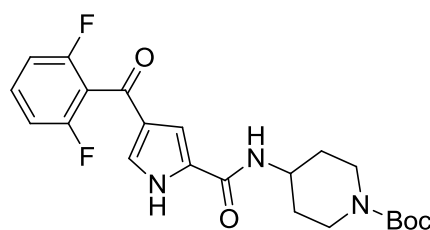
247
ERK5; IC$_{50}$ = 2.9 ± 0.7 µM

7.1.1 Reducing Metabolic Liability

The *in vitro* microsomal stability data (MLM Cl_{int} = 8 µL/min/mg protein), and the mouse *in vivo* unbound clearance (Cl_u = 284 ml/min/kg) of compound **212**, suggested that it was not highly susceptible to metabolism. However, *in vivo,* **212** was cleared with an extraction ratio of approximately 100% by the liver (Cl_p = 91 ml/min/kg; mouse liver blood flow = 90-110 ml/min/kg). The high free fraction in blood (F_u = 0.32) contributes to the high observed total plasma clearance. Thus, in order to improve the bioavailability, a further reduction in the unbound clearance would be beneficial.

Metabolite identification studies were not available to guide compound design. However, cytochrome P_{450} mediated *N*-dealkylation and *N*-oxidation are both known mechanisms of metabolism of tertiary amines, and were prevalent pathways observed in the metabolism of the tertiary amine containing kinase inhibitor drugs including imatinib,[301] ponatinib,[302] sunitinib,[303] and vandetanib.[294] Altering the steric character of the environment around the nitrogen atom may affect the propensity for metabolism at this position.[304] Variation of the *N*-substituent was therefore of potential benefit in reducing metabolic turnover of **212**. Targets were thus designed to investigate the effect of sterically hindering the exocyclic α-carbon atom, and introducing nitrogen substituents that cannot undergo α-oxidation.

7.1.2 Strategies for Improving Membrane Flux

The Caco-2 cell-line used to assess membrane permeability *in vitro* is a colon cancer cell-line that expresses multiple transporters. The transporters vary between cell bank sources, but include P-glycoprotein (P-gp, multidrug resistance protein 1 (MDR1)), breast cancer resistance protein (BCRP), and peptide transporter 1 (PEPT1).[305] P-gp is a member of the ATP-binding cassette (ABC) family of proteins and is the most studied of these efflux transporters. It is localised on the apical membrane of gut epithelial cells and in the blood brain barrier (BBB), and has a physiological role to prevent undesirable compounds from passing through these membranes.[306]

Functional groups which contain hydrogen bond donor groups have been found to increase P-gp recognition, such as primary and secondary amides, sulfonamides, alcohols, carboxylic acids, and ureas.[307] One strategy to reduce P-gp mediated efflux is to minimise

the number of HBDs in the molecule. Another approach is to introduce hydrogen bond acceptor groups into positions that can form intramolecular hydrogen bonds with a hydrogen bond donor,[308] masking some of the hydrogen bonding character of the molecule. This strategy is limited by the structural topology of the template, and the tolerance of the primary pharmacology SARs to such structural modifications.

Topological polar surface area[299] (tPSA) is a further parameter that has been shown to have a relationship with P-gp recognition, and minimising tPSA is another strategy for reducing P-gp-mediated efflux.[307] Compounds with a tPSA below 60 $\mathrm{\mathring{A}}^2$ have been shown to have a high probability of good membrane penetration, with those having a tPSA of over 140 $\mathrm{\mathring{A}}^2$ having a low probability.[309] Compounds containing basic centres that are significantly protonated at physiological pH are more susceptible to P-gp-mediated efflux, and the tPSA threshold for recognition by P-gp may be lower in basic than in neutral compounds.[307] Thus, reducing the basicity of the template, or removing the basic centre, may mitigate the risk of P-gp-mediated efflux. An example of a successful implementation of this tactic is observed by a comparison of desloratidine (**248**) and loratidine (**249**) (Table 7.2).[307]
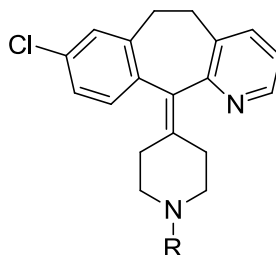
Cmpd	R	MW	clogP	pK_a	PSA $\mathrm{\mathring{A}}^2$	Caco-2 ER
248	H	310	6.8	10.3	25	9.1
249	CO$_2$Et	382	5.9	4.3	42	1.9

Table 7.2: An example of the effect of a basic amine on drug efflux.[307]

Desloratidine (**248**) has a basic pK_a of 10.3, and an efflux ratio of 9.1 in a Madin-Darby Canine Kidney (MDCK) cell line. Substitution of the secondary amine with an ethoxycarbonyl group in loratidine (**249**) renders the piperidine nitrogen essentially non-basic under physiological conditions, with a resultant reduction in efflux ratio to 1.9.[307]

Pyrrole carboxamide **212** has a low tPSA (65 $\mathrm{\mathring{A}}^2$), and contains two hydrogen bond donors. While only the pyrrole *NH* is essential for ERK5 activity, the amide *NH* cannot easily be

replaced, since methylation of the amide resulted in a 10-fold reduction in the ERK5 IC_{50} (**212** and **250**).
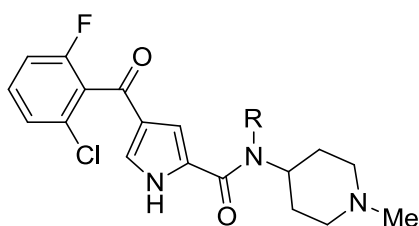
212 R = H   ERK5; $IC_{50} = 0.20 \pm 0.07$ μM
250 R = Me ERK5; $IC_{50} = 2.47 \pm 0.38$ μM

Thus, the first strategy employed in an attempt to reduce efflux in the Caco-2 assay was to introduce nitrogen substituents expected to reduce the pK_a of the basic centre.

7.1.3   Variation of the Piperidine N^1-Substituent of 212

The compounds in table 7.3 were designed and synthesised with the aim of addressing either or both of the issues of metabolic stability and membrane permeability, including derivatives increasing the steric bulk of the piperidine N^1-alkyl chain (**252-254**), and analogues which reduce the pK_a of the piperidyl nitrogen (**254-258**). Analogues **255-258** increase the number of hydrogen bond acceptors in the molecule, and consequently result in increased tPSA.
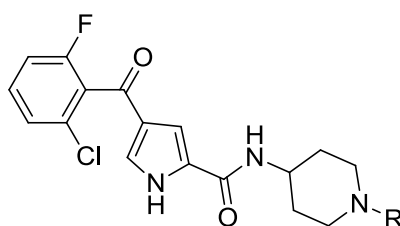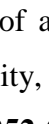
Cmpd	R	MW	clogP	clogD	tPSA Å^2	HBA	HBD
251	H	349	2.3	0.9	74	5	3
212	Me	363	2.6	1.4	65	5	2
252	Et	377	3.0	1.7	65	5	2
253	*i*-Pr	391	3.4	1.9	65	5	2
254	⊲	389	3.3	1.8	65	5	2
255	Ac	391	2.0	2.0	82	6	2
256	SO₂Me	427	1.9	1.9	99	7	2
257	pyrimidyl	427	3.4	1.8	86	7	2
258	Boc	449	*4.2*	*4.2*	92	7	2

Table 7.3: Structures and molecular properties of N^1-substituted piperidine amides.

Diverse substitution of the piperidyl nitrogen was found to have little effect on ERK5 inhibitory potency (Table 7.4), with the majority of N^1-substituted derivatives having an IC_{50} within 3-fold of **212**. The *tert*-butyl carbamate (**258**) was tolerated, resulting in only a 5-fold reduction in potency, consistent with the hypothesis that this substituent points towards the solvent exposed surface of the protein. However, these compounds did not achieve the IC_{50} threshold of 150 nM required to trigger generating Caco-2 and microsomal stability data.
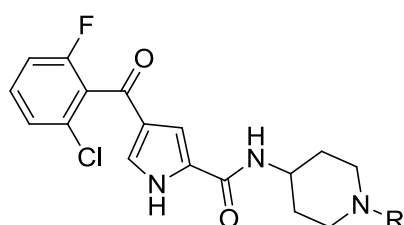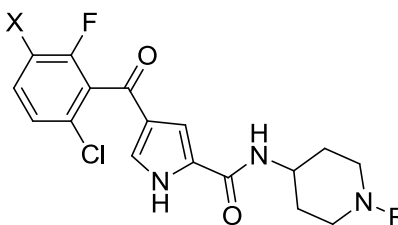
Cmpd	R	ERK5 IC_{50}[b] nM
251	H[a]	487 ± 40
212	Me[a]	198 ± 68
252	Et	437 ± 109
253	*i*-Pr	657 ± 85
254	⊲	360 ± 87
255	Ac	458 ± 182
256	SO_2Me	297 ± 29
257	pyrimidinyl	263 ± 57
258	Boc[a]	1078 ± 422

[a] Existing compounds previously prepared by Dr Stephanie Myers.
[b] Determination $\pm$ standard deviation

Table 7.4: ERK5 inhibitory activity of N^1-substituted piperidine amides.

However, in parallel with this work, a co-worker identified 2,5-dichloro-6-fluorobenzoyl as an alternative substituent at the pyrrole 4-position which conferred improved ERK5 inhibition relative to the 2-chloro-6-fluorobenzoyl group. Compounds containing a sub-set of the piperidine N^1-substituents in combination with the 2,5-dichloro-6-fluorobenzoyl-substituted pyrrole scaffold were prepared, resulting in a potency improvement of up to 10-fold (Table 7.5).

Cmpd	R	ERK5 IC_{50}[a] nM X = Cl	IC_{50} Ratio X=H/X=Cl
259	Me	115	1.7
260	H	82 ± 30	10
261	Ac	88 ± 53	5.8
262	SO_2Me	143 ± 60	3.5
263	Boc	1354 ± 683	1.3

[a] Determination ± standard deviation

Table 7.5: ERK5 inhibitory activity of N^1-substituted piperidine amides.

Compounds **259**-**262** were progressed to *in vitro* ADME assessment, exhibiting good stability in human and mouse liver microsomes, but increased plasma protein binding relative to **212** (Table 7.6). Acetamide **261** was assessed in the Caco-2 permeability assay, and found to have a high efflux ratio, suggesting that, despite the absence of a basic centre, the compound was still a substrate for transporter pumps.
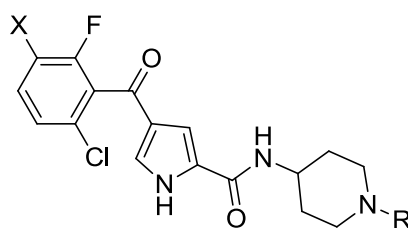
Cmpd	R	X	MLM Cl_{int}[a]	HLM Cl_{int}[a]	Ppb F_u	Sol μM	Caco-2 AB[b] (ER)
212	Me	H	<5	8	0.32	>100	4 (9)
259	Me	Cl	<5	<5	0.02	3-20	n.d.
260	H	Cl	<5	<5	0.04	>100	n.d.
261	Ac	Cl	<5	<5	0.02	>100	3 (16)
262	SO_2Me	Cl	<5	<5	0.02	30-100	n.d.

[a] μL/min/mg protein; [b] P_{app} 10^{-6} cm s^{-1}; n.d. = not determined.

Table 7.6: *In vitro* ADME data for *N*-substituted piperidine amides.

A literature review identified an example of replacement of an acetamide (**264**) with fluorinated amides (**265**-**268**) which affected Caco-2 efflux. The trifluoroacetamide (**265**)

resulted in a significant reduction in P-gp mediated efflux (Table 7.7).[310] This observation inspired the design and preparation of trifluoroacetyl-substituted piperidine **269**.
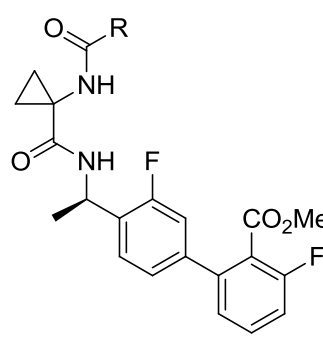
Cmpd	R	Caco-2 ER
264	Me	8.6
265	CF_3	2.3
266	CF_2CF_3	1.4
267	CHF_2	3.2
268	CH_2CF_3	8.6

Table 7.7: Case study of the effect of fluorination of an acetamide substituent on the Caco-2 efflux ratio.[310]

Introduction of a trifluoroacetamide group into the piperidine N^1-position of **212** proved successful in improving membrane permeability, with the efflux ratio in the Caco-2 assay for **269** being reduced to 1.1, and high membrane flux being observed. This observation is consistent with the effect reported for the literature series, and suggests that fluorination alpha to carbonyl groups may have a more general application for reducing a compound's efflux liability. It is possible that the electronic effect of the trifluoromethyl group on the hydrogen bond acceptor ability of the carbonyl group plays a part in reducing the recognition of the compound by efflux pumps. Unfortunately, the ERK5 inhibitory potency of **269** was significantly reduced relative to acetamide **261**.
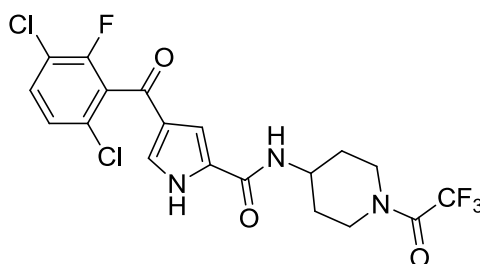
Compound	ERK5 IC$_{50}$ nM	MLM Cl$_{int}$[a]	Sol μM	Caco-2 AB[b] (ER)
269	521 ± 224	30	30-100	19 (1.1)

[a] μL/min/mg protein. [b] P_{app} 10^{-6} cm s^{-1}.

Table 7.8: ERK5 inhibitory activity and *in vitro* ADME data for **269**.

Due to the lack of success in achieving an acceptable balance of potency and low efflux in the Caco-2 assay, focus turned to optimisation of the heteroaromatic amide series.

7.2 Class 2: Heteroaromatic Amides

7.2.1 Pyrimidine Amide-Linked Analogues

In progressing the heteroaromatic amide series the main aim was to improve the potency of lead compound **215**.
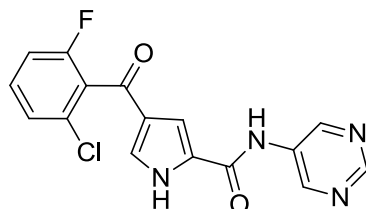
215 ERK5; $IC_{50} = 403 \pm 91$ nM

Diversification at the 2-position of the pyrimidine was synthetically amenable (see section 8.2) and was the first position explored. Previous SARs had shown that substitution of this position with a methyl group (**217**, table 5.6) led to a 3-fold reduction in ERK5 potency. Examination of **215** modelled in the ERK5 ATP-binding site from the literature co-crystal structure,[247] suggested that substituents at this position may project towards the solvent exposed surface of ERK5. A small library of heteroatom-linked 2-substituted pyrimidyl derivatives (**271**-**276**) was prepared to explore the effect of elaboration at this position on ERK5 inhibition. The molecular properties of these analogues are shown in Table 7.9.
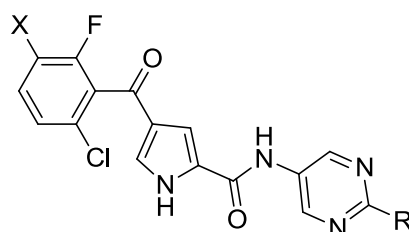
Cmpd	R	X	MW	clogP	clogD	tPSA Å^2	HBA	HBD
215	H	H	344	3.3	3.3	88	6	2
270	H	Cl	379	4.0	4.0	88	6	2
217	Me	H	358	3.6	3.6	88	6	2
271	OMe	H	374	3.2	3.2	97	7	2
272	NHMe	H	373	2.8	1.4	100	7	3
273	NMe_2	H	387	3.2	1.6	91	7	2
274	–N(pyrrolidine)	H	413	3.6	2.0	91	7	2
275	–N(piperazine)N–Me	H	442	2.8	1.9	94	8	2
276		Cl	477	3.4	2.4	94	8	2

Table 7.9: Structures and molecular properties of 2-substituted pyrimidine amides.

Substitution with methoxy (**271**) and small alkylamines (**272-274**) reduced ERK5 binding affinity (Table 7.10). Pyrrolidine analogue **274** also exhibited reduced aqueous solubility, with evidence of precipitation under the assay conditions. A breakthrough was made with *N*-methylpiperazine **275**, which resulted in a 6-fold increase in potency relative to **215**. Combination with the trihalogenated aromatic ring gave derivative **276**, having a further two-fold improvement in potency.
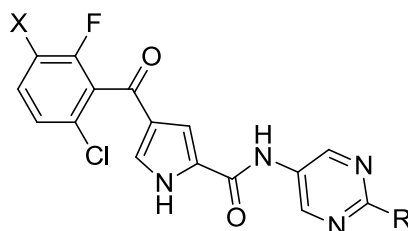
Cmpd	R	X	ERK5 IC_{50}[a] nM	L.E.	LipE
215	H	H	403 ± 91	0.37	3.1
270	H	Cl	315 ± 368	0.36	2.5
217	Me	H	1185 ± 619	0.33	2.3
271	OMe	H	790 ± 180	0.33	2.9
272	NHMe	H	1748 ± 212	0.31	4.4
273	NMe$_2$	H	3478 ± 169	0.28	3.9
274	-§-N⟨⟩	H	4109 ± 1354	0.26	3.4
275	-§-N⟨⟩N−Me	H	72 ± 10	0.32	5.2
276		Cl	37 ± 17	0.32	4.9

[a] Determination ± standard deviation

Table 7.10: ERK5 inhibitory activity of 2-substituted pyrimidine amides.

Possible binding interactions between the piperazine and the protein include the basic nitrogen interacting with an acidic amino acid side-chain (Asp or Glu) through a charge-charge interaction. Alternatively, the protonated amine may act as a hydrogen bond donor to side-chain or backbone hydrogen bond acceptors, or may interact with aromatic residues through π–cation interactions. Unprotonated piperazine may also serve as a hydrogen bond acceptor, interacting with a hydrogen bond donor in the protein. Analogues **279**-**282** were therefore designed and prepared to investigate the potential role of the basic piperazine nitrogen (Table 7.11).
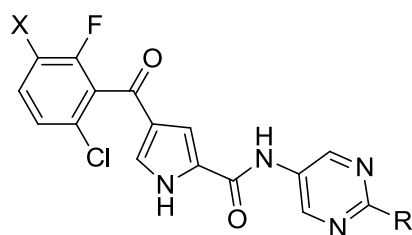
Cmpd	R	X	MW	clogP	clogD	tPSA $\mathring{A}^2$	HBA	HBD
275	-N⌐N−Me	H	442	2.8	1.9	94	8	2
276		Cl	477	3.4	2.4	94	8	2
279	-N⌐O	H	429	3.1	2.0	100	8	2
280		Cl	464	3.7	2.5	100	8	2
281	-N⌐OH	H	443	3.1	1.5	111	8	3
282		Cl	478	3.7	2.0	111	8	3
283	-N⌐OAc	H	485	3.7	1.9	117	9	2
284		Cl	520	4.3	2.4	117	9	2

Table 7.11: Structures and molecular properties of 2-substituted piperidine amides.

The ERK5 inhibitory activity of morpholine analogues **279** and **280** (Table 7.12) was significantly reduced relative to **275** and **276**, suggesting that the presence of a hydrogen bond acceptor at this position was not able to replicate the interactions of the piperazine. The 4-hydroxypiperidine analogues **281** and **282** position a hydrogen bond donor in the vicinity of the basic centre of **275**, and were also much less potent than the piperazine analogues. Acetoxypiperidines **283** and **284**, prepared as intermediates *en route* to **281** and **282**, probed the effect of an alternative hydrogen bonding motif in this region of space, and were again less potent than **275** and **276**. Thus, the improved potency observed for **275** and **276** appeared to be due to the basic nature of the piperazine nitrogen.
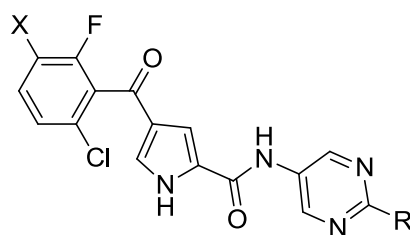
Cmpd	R	X	ERK5 IC_{50}^{a} nM	L.E.	LipE
275		H	72 ± 10	0.32	5.2
276		Cl	37 ± 17	0.32	4.9
279		H	2081 ± 226	0.30	4.4
280		Cl	1508 ± 230	0.29	3.8
281		H	2232 ± 427	0.29	4.9
282		Cl	536 ± 89	0.28	4.3
283		H	5385	0.26	4.4
284		Cl	9661 ± 7320	0.25	3.9

[a] Determination ± standard deviation

Table 7.12: ERK5 inhibitory activity data for 2-substituted pyrimidine amides.

This SAR contrasts with that described for the diazepinone class of literature ERK5 inhibitors described in chapter 5, where similar potency was achieved by morpholine, hydroxypiperidine and piperazine substituents, suggesting that the binding mode of these groups in the pyrrole carboxamide series is significantly different from that observed in the published co-crystal structure.[247] Comparison of a modelled pose of **275** with the X-ray structure of diazepinone **205** bound to ERK5 (Figure 7.1), suggests that the piperazine groups in each series are likely to adopt different exit vectors from the binding-site. The pyrrole carboxamide series may bind in a more planar conformation, with the *ortho*-substituents twisting the halogenated phenyl ring out of the plane of the remainder of the molecule.
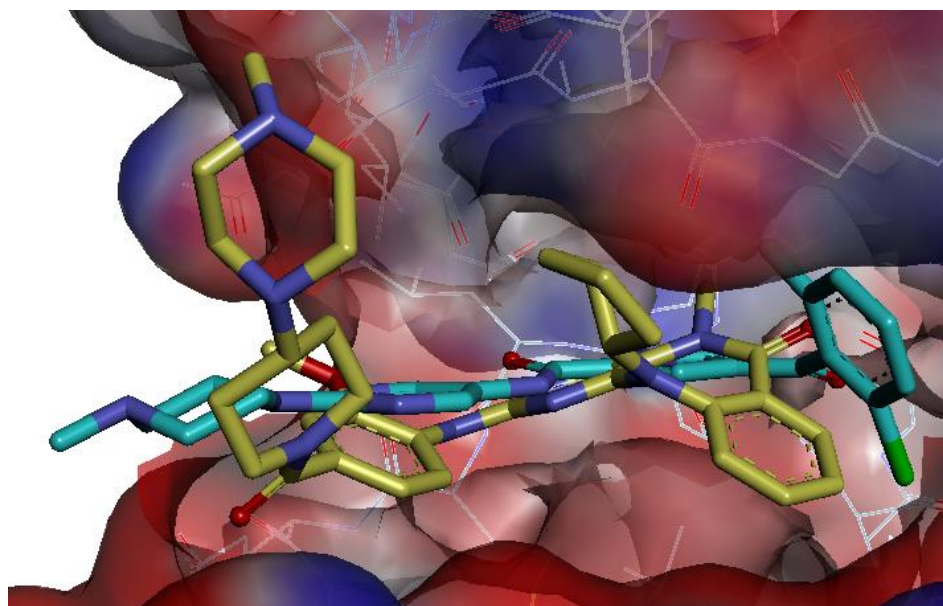
Figure 7.1: Comparison of the co-crystal structure of **205** (yellow) bound to ERK5 with a modelled structure of **275** (cyan) in the ATP-binding site.

In vitro human and mouse liver microsomal data for **275** and **276** indicated that they were both subject to rapid metabolism (Table 7.13). In an attempt to improve microsomal stability, *NH*-piperazine analogues **285** and **286** were prepared. Compound **285** was equipotent with **275**, and compound **286** had superior ERK5 inhibitory activity over **276**. The improved stability of **286** in both human and mouse liver microsomes relative to **276** supports the possibility of *N*-dealkylation as a major route of metabolism. As an alternative approach to reducing the potential for metabolic *N*-dealkylation, *N*-cyclopropylpiperazine derivative **287** was prepared. Cyclopropyl groups have been reported to confer resistance to oxidative metabolism,[311] although this group has also been implicated in covalent inactivation of cytochrome P_{450} enzymes.[312] Unexpectedly, **296** suffered a 24-fold reduction in potency relative to **287**, which may be due to a variety of factors including the cyclopropyl group reducing the basicity of the piperazine nitrogen, a possible adverse steric interaction between the cyclopropyl and the kinase ATP-binding site, or an effect of this more sterically demanding nitrogen substituent on the conformation of the piperazine ring.
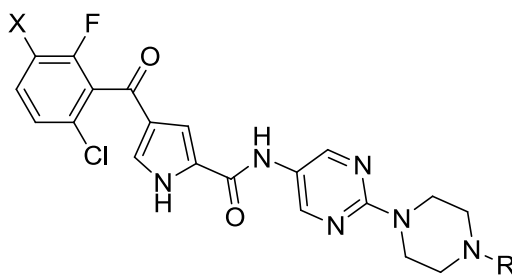
Cmpd	R	X	ERK5 IC$_{50}$[a] nM	MLM Cl$_{int}$[b]	HLM Cl$_{int}$[b]	Ppb F$_u$	Sol μM
275	Me	H	72 ± 10	51	200	0.11	> 100
276	Me	Cl	37 ± 17	75	252	0.028	30-100
285	H	H	89 ± 14	n.d.	n.d.	n.d.	n.d.
286	H	Cl	13 ± 5	13	31	0.066	> 100
287	⊲	Cl	1747 ± 1703	n.d.	n.d.	n.d.	n.d.

[a] Determination ± standard deviation; [b] μL/min/mg protein. n.d. = not determined.

Table 7.13: ERK5 inhibitory activity and *in vitro* ADME data for 2-substituted pyrimidine amides.

To investigate tolerance to variation of the position of the basic centre, the 4-aminopiperidines **288**-**290** were prepared (Table 7.14).
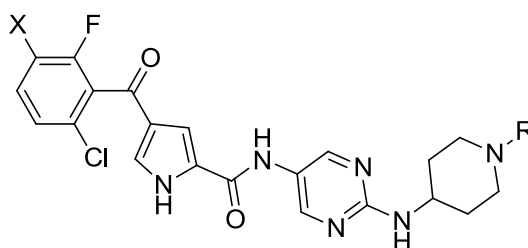
Cmpd	R	X	MW	clogP	clogD	tPSA Å^2	HBA	HBD
288	Me	H	456	3.8	2.4	103	8	3
289	Me	Cl	491	3.5	2.6	103	8	3
290	⊲	Cl	517	4.4	2.6	103	8	3

Table 7.14: Structures and molecular properties of 2-substituted pyrimidine amides.

Analogues **288** and **289** retained similar potency to **275** and **276**, respectively (Table 7.15). In contrast to **287**, in this template *N*-cyclopropyl analogue **290** exhibited good ERK5

inhibitory activity. The metabolic stability of *N*-methylpiperidine **289** (Table 7.15) was much improved relative to **276**, indicating that *N*-dealkylation is a slower metabolic process in this template. Interestingly, the microsomal stability of **290** was species-dependent, with higher turnover in mouse than in human liver microsomes. The solubility was also reduced for **290** relative to **289**, which may be due to increased lipophilicity and a reduction in the basicity of the piperidine nitrogen.
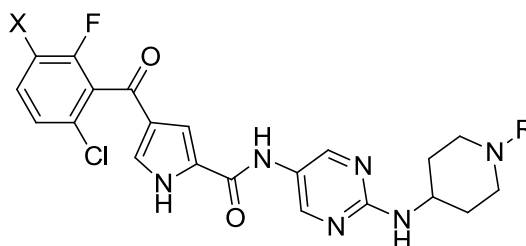
Cmpd	R	X	ERK5 IC_{50}[a] nM	MLM Cl_{int}[b]	HLM Cl_{int}[b]	Ppb F_u	Sol μM
288	Me	H	93 ± 20	n.d.	n.d.	n.d.	n.d.
289	Me	Cl	14 ± 3	19	6	0.067	10-100
290	⊲	Cl	50 ± 28	141	20	n.d.	3-20

[a] Determination ± standard deviation; [b] μL/min/mg protein; n.d. = not determined.

Table 7.15: ERK5 inhibitory activity and *in vitro* ADME data for **288**-**290**.

Further modelling of **276** in the ATP-binding site of ERK5 from the literature co-crystal structure suggested that the piperazine could adopt a conformation that would allow the protonated basic centre to participate in an ionic interaction with a glutamate residue on the exit of the binding-site (Figure 7.2). However, the glutamate residue is in a flexible region of the protein, and it is likely that some re-ordering of the protein might occur on binding of the basic group, leading to an alternative binding conformation.
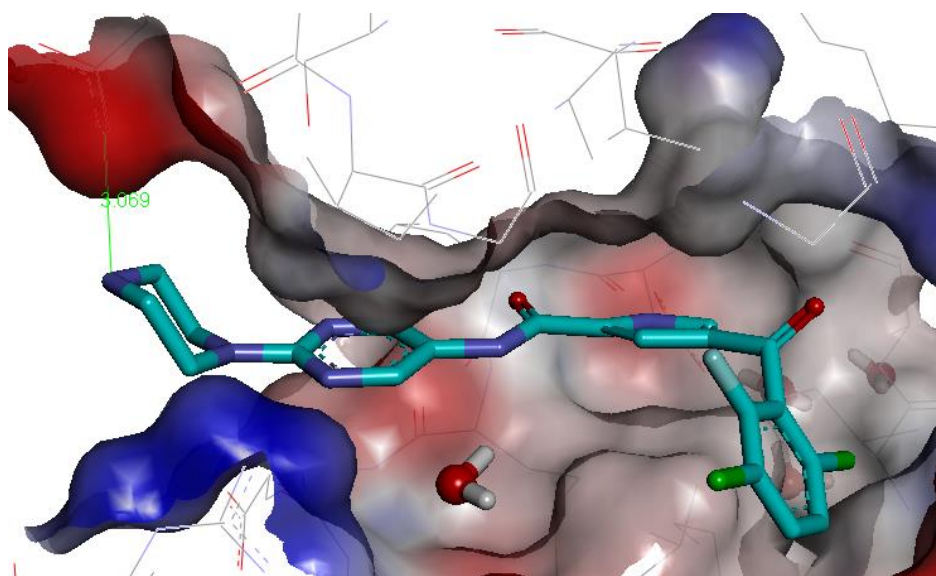
Figure 7.2: Modelling of **276** in the ATP-binding site of ERK5. The protein structure is taken from the ERK5 crystal structure.[247]

The presence of a basic centre in a molecule increases the probability of undesired activity against the hERG cardiac ion channel, and **276** was found to inhibit hERG with an IC_{50} of 2.63 μM (Table 7.16). In contrast, the hERG IC_{50} of both **286** and **289** was greater than 25 μM indicating the presence of subtle hERG SAR in this series, which enabled this undesirable activity to be avoided.
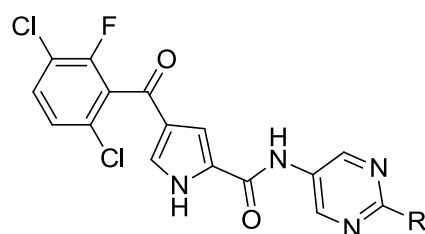
Cmpd	R	ERK5 IC_{50}^{a} nM	hERG IC_{50} μM	Caco-2 AB^{b} (ER)
276	-N⟮⟯N−Me	37 ± 17	2.63	n.d.
286	-N⟮⟯NH	13 ± 5	>25	0.6 (35)
289	HN⟮⟯N−Me	14 ± 3	>25	0.3 (99)
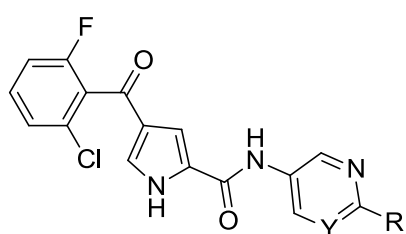
^{a} Determination $\pm$ standard deviation; ^{b} $P_{app} 10^{-6}$ cms^{-1}; n.d. = not determined.

Table 7.16: Inhibitory activity against ERK5, the hERG ion channel, and Caco-2 membrane permeability data for **276**, **286**, and **289**.

In the Caco-2 membrane permeability assay, both **286** and **289** were found to exhibit high efflux, suggesting significant recognition by active transporters (Table 7.16). The focus for further optimisation thus turned to reducing efflux liability while maintaining ERK5 inhibitory potency.

7.2.2 Pyridine-Amide Linked Analogues

Previous SAR had demonstrated that ERK5 inhibitory potency for pyridyl and pyrimidyl amides was broadly similar (Table 7.17).

Cmpd	Y	R	ERK5 IC$_{50}$ nM
213	CH	H	583 ± 242
215	N	H	403 ± 91
291	CH	Me	1030 ± 65
217	N	Me	1200 ± 619

[a] Determination $\pm$ standard deviation

Table 7.17: Comparison of ERK5 inhibitory activity for simple 3-pyridyl and 5-pyrimidyl amides.

Incorporation of a pyridine ring in place of the pyrimidine removes a hydrogen bond acceptor, and the resultant reduction in tPSA was considered of potential benefit for membrane permeability. This modification was therefore investigated in combination with the most potent basic substituents, to give **292** and **293** (Table 7.18).
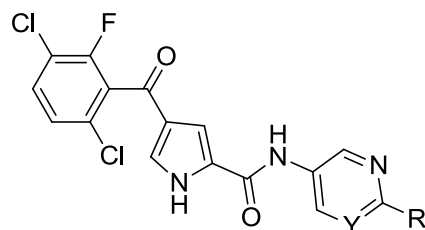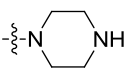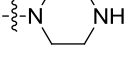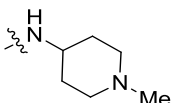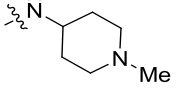
Cmpd	R	Y	MW	clogP	clogD	tPSA Å^2	HBA	HBD
286		N	463	3.1	2.1	103	8	3
292		CH	462	2.9	2.3	90	7	3
289		N	491	3.8	2.4	103	8	3
293		CH	490	3.5	2.6	90	7	3

Table 7.18: Comparison of the molecular properties of 2-substituted 5-pyridyl and 5-pyrimidyl amides that incorporate a basic centre.

ERK5 inhibition was found to be comparable for the pyrimidyl and pyridyl amide analogues (Table 7.19; **286** vs. **292**, and **289** vs. **293**). Good *in vitro* microsomal stability and low hERG activity were also maintained. However, undesirable high efflux ratios in the Caco-2 assay were retained in the pyridyl analogues.
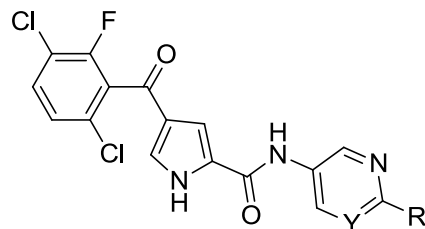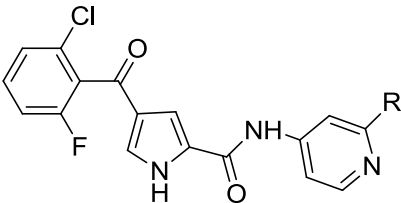
Cmpd	R	Y	ERK5 IC$_{50}$[a] nM	MLM Cl$_{int}$[b]	HLM Cl$_{int}$[b]	hERG IC$_{50}$ μM	Caco-2 AB[c] (ER)
286		N	13 ± 5	31	13	>25	0.6 (36)
292		CH	13 ± 6	25	19	>25	0.3 (105)
289		N	14 ± 3	19	6	>25	0.3 (99)
293		CH	24 ± 20	n.d.	n.d.	n.d.	n.d.
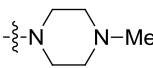
[a] Determination ± standard deviation; [b] μL/min/mg protein; [c] P_{app} 10^{-6} cm s^{-1}; n.d. = not determined.

Table 7.19: Comparison of ERK5 inhibitory activity and *in vitro* ADME parameters for 2-substituted 5-pyridyl and 5-pyrimidyl amides.

7.2.3 Analogues of 4-Pyridyl Amide Lead 214

The effect of a change in the shape of the molecule was investigated by appending substituents to the 2-position of 4-aminopyridine amide **214**. Compound **216** was the most potent 4-pyridyl amide previously prepared, having an ERK5 IC_{50} of 400 nM (Table 7.20). Introduction of the 2-methyl group on the pyridyl ring resulted in reduced cytochrome P_{450} inhibition relative to the unsubstituted analogue. In an attempt to improve the potency of this series, basic and neutral substituents were incorporated at the 2-position of the pyridine ring (Table 7.20).

Cmpd	R	ERK5 IC_{50}[a] nM
214	H	602 ± 266
216	Me	400 ± 166
294	Cl	2322 ± 267[b]
295	CF_3	n.d.[c]
296	OMe	1827 ± 170
297	-N(pyrrolidine)	523 ± 260[b]
298	-N(piperazine)N—Me	137 ± 65

[a] Determination $\pm$ standard deviation; [b] Evidence of precipitation in assay; [c] Insufficient solubility for data to be generated.

Table 7.20: ERK5 inhibitory activity data for 2-substituted 4-pyridyl amide analogues.

Compounds of this structural class generally suffered from poor solubility, affecting the ability to generate reliable IC_{50} values in the primary assay. Despite this, pyrrolidine **297** retained encouraging activity. The *N*-methylpiperazine **298** was more soluble under the assay conditions, and gave an ERK5 IC_{50} value of 137 nM, providing encouragement for further work in this area.

Incorporation of the trihalogenated phenyl group (**299**) again improved ERK5 inhibition (Table 7.21). The morpholine analogue **300** was also prepared in this series, providing further evidence of the importance of the basic centre for potent ERK5 inhibition in this regioisomeric series.
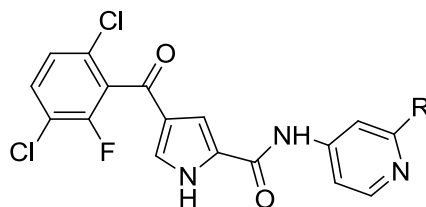
Cmpd	R	ERK5 IC$_{50}$^{a} nM	MLM Cl$_{int}$^{b}	Caco-2 AB^c (ER)	Sol μM
299	-§-N‾‾N–Me	36 ± 4	103	3.6 (3.6)	3-65
300	-§-N‾‾O	588 ± 55	n.d.	n.d.	n.d.

^{a} Determination ± standard deviation; ^{b} μL/ml/mg protein; ^{c} P_{app} 10^{-6} cm s^{-1}; n.d. = not determined.

Table 7.21: ERK5 inhibitory activity and *in vitro* ADME data for **299** and **300**.

In mouse liver microsomes **299** suffered from a high turnover, which may be due to *N*-demethylation. Caco-2 efflux for this compound was moderate (ER = 3.6). Despite the presence of the water-solubilising *N*-methylpiperazine, the turbidimetric solubility assay indicated that **299** was considerably less soluble than isomer compound **276**. Future work in this series should investigate the *NH*-piperazine **301**, which would be anticipated to have improved microsomal clearance and solubility.
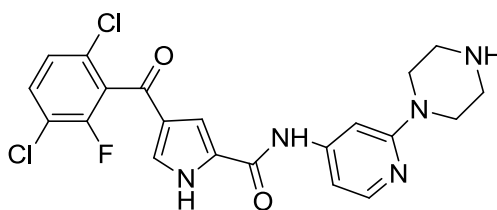
301

7.2.4 Pyrazole-Amide Linked Analogues

Another approach investigated was to replace the pyrimidyl ring of **289** with a pyrazole heterocycle. Removal of one heavy atom from the heteroaromatic amide reduces the molecular weight, and the pyrazole architecture enables carbon-linked substituents to be appended to the ring using facile synthetic chemistry. Such analogues result in a reduction in the tPSA compared to pyridyl and pyrimidyl analogues, which is of potential benefit in reducing efflux liability. The change from a 6-membered ring to a 5-membered ring also results in a subtle variation of the position of the basic centre, which may enable improvements in the binding interactions with ERK5, and may also affect recognition by the P-gp efflux pump. The set of pyrazole analogues **302**-**307** were therefore prepared, incorporating a basic centre on the pyrazole N^1-substituent (Table 7.22).

Cmpd	R	MW	clogP	clogD	tPSA Å^2	HBA	HBD
302	$-\xi-\langle\rangle-\text{NH}$	450	3.3	2.0	92	7	3
303	$-\xi-\langle\rangle-\text{N}-\text{Me}$	464	3.8	2.4	83	7	2
304	$-\xi-\langle\rangle\text{NH}$	422	2.7	1.8	92	7	3
305	NH	463	3.6	2.0	92	7	3
306	$\text{N}-\text{Me}$	478	4.2	2.4	83	7	2
307	$CH_2CH_2N(Et)_2$	466	4.1	2.1	83	7	2

Table 7.22: Structures and molecular properties of pyrazole analogues **302**-**307**.

ERK5 inhibitory activity for these pyrazole linked analogues was comparable with the most potent pyrimidine and pyridine linked compounds (Table 7.23). Compound **305** was the most potent analogue prepared, and the first to achieve a sub-10 nM ERK5 IC$_{50}$ value.

It exhibited good stability in mouse liver microsomes, and the Caco-2 efflux ratio was reduced significantly compared to **286**. However, the intrinsic flux across the Caco-2 monolayer was low ($P_{app} = 1.5 \times 10^{-6}$ cm/s). The only analogue prepared with an acyclic basic side-chain (**307**), surprisingly resulted in a 10-fold potency reduction, which may reflect the increased conformational flexibility resulting in an entropic penalty for binding. Increased steric crowding around the basic centre in **307** may also hinder the proposed charge-charge interaction with a glutamate residue in ERK5.
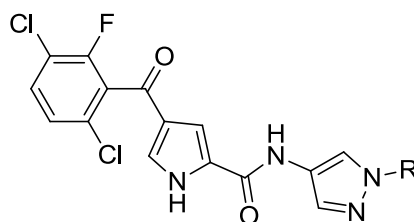
Cmpd	R	ERK5 IC$_{50}$[a] nM	MLM Cl$_{int}$[b]	HLM Cl$_{int}$[b]	hERG IC$_{50}$ μM	Caco-2 AB[c] (ER)	Sol μM
302	–⌇⟨NH⟩	19 ± 6	8.2	n.d.	n.d.	0.3/6 (18)	>100
303	–⌇⟨N–Me⟩	22 ± 6	103	n.d.	n.d.	1.3/19 (15)	30
304	–⌇⟨NH⟩	32 ± 12	3.7	n.d.	n.d.	0.2/4.0 (19)	10
305	⌇⟨NH⟩	7 ± 4	0.3	2.4	n.d.	0.2/1.5 (4.5)	>100
306	⌇⟨N–Me⟩	16 ± 7	5.9	10	>25	0.6/18 (32)	>100
307	CH$_2$CH$_2$N(Et)$_2$	207 ± 19	n.d.	n.d.	n.d.	n.d.	n.d.

[a] Determination ± standard deviation; [b] μL/min/mg protein; [c] P_{app} 10^{-6} cm s^{-1}; n.d. = not determined.

Table 7.23: ERK5 inhibitory activity and *in vitro* ADME parameters for pyrazole amides incorporating a basic centre.

The effect of modulation of the basicity of the basic centre on ERK5 inhibition and transporter recognition was next investigated. Fluorination beta to a basic amine has a significant effect on its basicity, as shown in table 7.24.[313]

Conjugate acid of amine	pK_a
$CH_3CH_2NH_3^+$	10.7
$FCH_2CH_2NH_3^+$	9.0
$F_2CHCH_2NH_3^+$	7.3
$F_3CCH_2NH_3^+$	5.7
$CH_3CH_2N(CH_3)_2H^+$	10.2
$F_3CCH_2N(CH_3)_2H^+$	4.8

Table 7.24: Effect on the measured pK_a of successive β-fluorination of an amine.[313]

Trifluoroethyl-substituted amine **308** was the first analogue prepared in an attempt to moderate the pK_a of the basic centre (Table 7.25). Another approach for pK_a moderation was incorporation of the basic centre within an aromatic heterocycle. Pyridyl analogues **309**-**311** and imidazole analogue **312** were selected for synthesis. The pK_a of pyridine (5.23) suggests that these analogues would be expected to be less than 1% protonated at physiological pH, which may be advantageous if the protonated form is recognised by efflux pumps. In the ERK5 ATP-binding site, the pyridine would be likely to be protonated in proximity to the glutamate residue, and the proposed charge-charge interaction contribution to the binding affinity may still be achieved. Imidazole (pK_a = 7.0) is of intermediate basicity, and **312** explores an alternative heteroaromatic basic group.
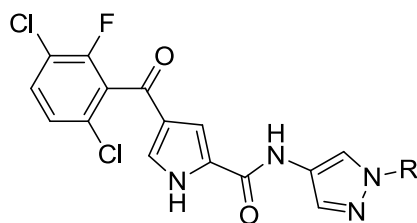
Cmpd	R	MW	clogP	clogD	tPSA Å^2	HBA	HBD
308		532	4.5	3.3	83	7	2
309		458	4.0	4.0	93	7	2
310		458	4.0	4.0	93	7	2
311		458	4.0	4.0	93	7	2
312		461	3.9	3.9	98	8	2

Table 7.25: Structure and molecular properties of pyrazole analogues containing weakly basic centres.

Compound **308** (Table 7.26) was over 100-fold less potent than the equivalent *N*-methyl analogue **303** (ERK5; $IC_{50} = 22 \pm 6$ nM). The 3-pyridylmethyl (**310**) and 4-pyridylmethyl (**311**) compounds retained good activity, while 2-pyridyl derivative **309** suffered a 4-fold loss of potency. In the Caco-2 assay **309** and **310** had efflux ratios above 5, indicating that incorporation of weakly basic heterocycles had not abrogated transporter recognition.

Cmpd	R	ERK5 IC$_{50}$[a] nM	MLM Cl$_{int}$[b]	Caco-2 AB[c] (ER)	Sol μM
308	(piperidine-CF_3)	2994 ± 386	n.d.	n.d.	n.d.
309	(2-pyridyl)	124 ± 10	40	6 (5.6)	10-65
310	(3-pyridyl)	34 ± 2	41	2.7 (15)	30-100
311	(4-pyridyl)	31 ± 1	n.d.	n.d.	n.d.
312	(N-Me-imidazole)	23 ± 6	n.d.	n.d.	n.d.

[a] Determination ± standard deviation; [b] μL/min/mg protein. [c] P_{app} 10^{-6} cm s^{-1}. n.d. = not determined.

Table 7.26: ERK5 inhibitory activity and *in vitro* ADME data for pyrazole analogues containing weakly basic centres.

In order to confirm whether the basic centre was providing a potency advantage in the pyrazole series, the parent *NH*-pyrazole (**313**) and the *N*-methylpyrazole (**314**) were prepared. These low molecular weight compounds lacking a basic centre have relatively low tPSA, and fewer hydrogen bonding groups than the basic analogues (Table 7.27).
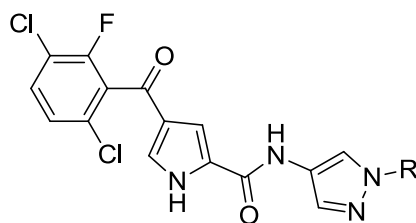
Cmpd	R	MW	clogP	clogD	tPSA $\mathring{A}^2$	HBA	HBD
313	H	367	3.1	3.1	91	6	3
314	Me	381	3.6	3.6	80	6	2
315	Et	395	4.0	4.0	80	6	2
316	CH$_2$CH$_2$OMe	425	3.7	3.7	90	7	2

Table 7.27: Structures and molecular properties of neutral pyrazole amide analogues.

Compound **313** retained ERK5 inhibitory potency similar to the unsubstituted 3-pyridyl analogue **213**, but suffered from higher microsomal turnover, and an efflux ratio of 9.4 in the Caco-2 cell assay (Table 7.28). Surprisingly, *N*-methyl pyrazole **314** was 3-fold more potent than **313**, having similar ERK5 inhibition to the most potent basic analogues. Furthermore, the mouse microsomal clearance of **314** was significantly lower than for **313**. More importantly, **314** exhibited no efflux in the Caco-2 assay, and thus had the best balance of ERK5 inhibitory activity and *in vitro* pharmacokinetic parameters of the compounds prepared. Due to the low molecular weight of **314**, this compound also achieved an impressive ligand efficiency of 0.43. Increasing the size of the neutral pyrazole substituent (**315** and **316**), did not result in any further improvement in ERK5 inhibition.

Cmpd	R	ERK5 IC$_{50}$^{a} nM	MLM Cl$_{int}$^{b}	HLM Cl$_{int}$^{b}	Caco-2 AB^c (ER)	Sol μM	LE
313	H	99 ± 40	85	n.d.	5.6 (9.4)	>100	0.42
314	Me	27 ± 10	28	13	27 (0.9)	>100	0.43
315	Et	92 ± 31	n.d.	n.d.	n.d.	n.d.	0.38
316	CH$_2$CH$_2$OMe	89 ± 36	n.d.	n.d.	n.d.	n.d.	0.35

^{a} Determination ± standard deviation; ^{b} μL/min/mg protein. ^{c} P_{app} 10^{-6} cm s^{-1}. n.d. = not determined.

Table 7.28: ERK5 inhibitory activity and *in vitro* ADME data for neutral pyrazole amides.

To follow up on the exciting result for **314**, a set of 5-membered aromatic heterocyclic amides was prepared as mimics of the *N*-methylpyrazole moiety (Table 7.29). A significant reduction in ERK5 inhibitory activity was apparent for compounds **317**-**320**, suggesting that the position of heteroatoms in the 5-membered ring is crucial to activity. In contrast to **314**, these analogues all contain a heteroatom in a position adjacent to the amine linker atom, which may influence the conformational preference of the heterocyclic ring.
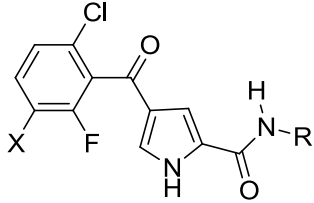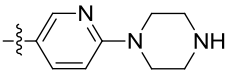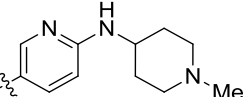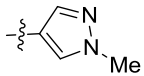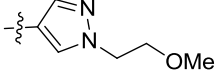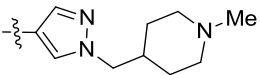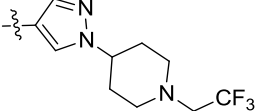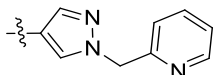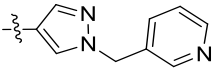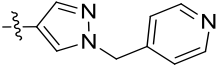
Cmpd	R	ERK5 IC$_{50}$ nM
314		27 ± 10
317		1235 ± 605
318		2482 ± 921
319		1038 ± 141
320		642 ± 154

^{a} Determination ± standard deviation

Table 7.29: Structures and ERK5 inhibitory activity data for compounds **317**-**320**.

182

7.3   Investigation of an Alternative Pyrrole 4-Substituent

During the course of the program to optimise the amide substituent, work in the research group was also being undertaken to investigate the SARs at the pyrrole 4-position. A colleague identified 2-fluoro-3-methoxy-6-chlorobenzoyl as a substituent that conferred similar ERK5 inhibitory potency to the 2-fluoro-3,6-dichlorobenzoyl substituent at the pyrrole 4-position. A selection of the optimised amide substituents was therefore prepared in combination with the 2-fluoro-3-methoxy-6-chlorobenzoyl group (Table 7.30). This confirmed that these benzoyl substitution patterns endowed similar ERK5 activity and ADMET properties.

| R | ERK5 IC$_{50}$[a] nM | |
	X = Cl	X = OMe
	292 13 ± 6	**321** 16 ± 2
	293 24 ± 20	**322** 27 ± 4
	314 27 ± 10	**323** 107 ± 26
	316 89 ± 36	**324** 107 ± 37
	306 17 ± 6	**325** 20 ± 3
	308 2994 ± 386	**326** 3546 ± 201
	309 124 ± 10	**327** 74 ± 4
	310 34 ± 2	**328** 23 ± 2
	311 31 ± 1	**329** 23 ± 1

[a] Determination ± standard deviation

Table 7.30: Comparison of ERK5 inhibitory activity for 2-fluoro-3,6-dichlorobenzoyl and 2-fluoro-3-methoxy-6-chlorobenzoyl pyrrole-4-substituents.

An analysis of a matched pair of compounds in mouse liver microsomes revealed that both chloro- (**292**; MLM Cl_{int} = 26 μL/min/mg protein) and methoxy- (**321**; MLM Cl_{int} = 20 μL/min/mg protein) benzoyl analogues exhibited similar levels of microsomal stability.

7.4   Evaluation of ERK5 Inhibitors in a Cell-Based Assay

Cellular activity was measured in HeLa cells by Lan-Zhen Wang. The cells were incubated with the ERK5 inhibitor for 1 hour, followed by stimulation with EGF. Cell lysis was followed by western blotting with an ERK5 antibody (Cell signalling #3372S). An IC_{50} value was generated from a seven point concentration response curve, using a densitometry measurement of the phospho-ERK5 band. An example western blot with a dose-response for an inhibitor is shown in Figure 7.4.

330
ERK5; IMAP IC_{50} 66 ± 33 nM
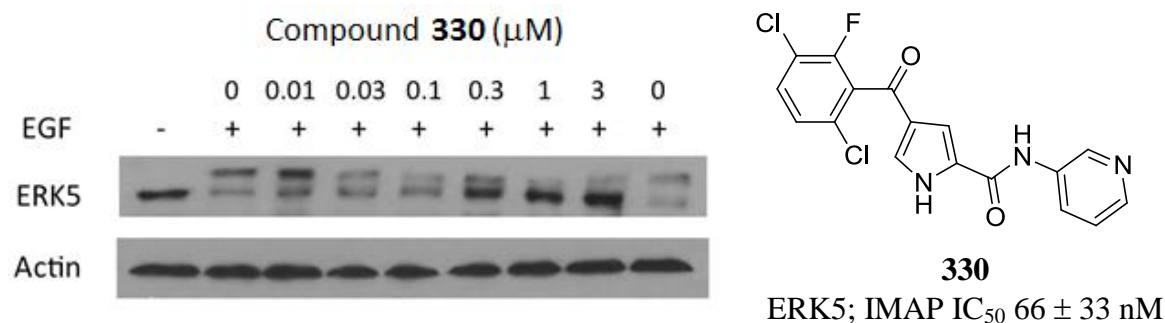
Figure 7.4: Inhibition of EGF-stimulated phospho-ERK5 formation by **330**. Upper figure shows the resolution of a phospho-ERK5 band (upper band) from non-phosphorylated ERK5 (lower band). The IC_{50} value for **330** was calculated as 90 ± 10 nM and is the mean from three independent experiments, following densitometry and an analysis of the ratio of phospho-ERK5 to total ERK5.

Western blotting is a semi-quantitative technique, and as such, the use of densitometry resulted in a high degree of variability in the ERK5 IC_{50} values generated using this assay. The IC_{50} values for the majority of the compounds tested were below one micromolar, which provides confirmation that this class of compound is able to affect ERK5 auto-phosphorylation in a cellular context (Table 7.31).
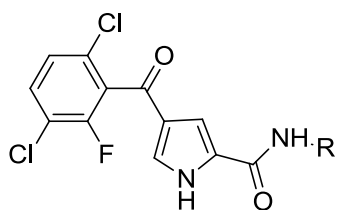
Cmpd	R	ERK5 IC$_{50}$[a] nM	HeLa IC$_{50}$[b] nM
286		13 ± 5	100 ± 10
289		14 ± 3	60 ± 40
302		19 ± 6	790 ± 520
304		32 ± 12	140[c]
305		7 ± 4	830 ± 1020
306		16 ± 7	2700[c]
314		27 ± 10	220 ± 120

[a] ERK5 inhibitory activity in the cell-free IMAP format assay;

[b] IC$_{50}$ determined by densitometry in the cell-based assay;

[c] Data from a single determination.

Table 7.31: Comparison of inhibition of ERK5 in the IMAP cell-free assay, with inhibition of ERK5 auto-phosphorylation determined by western blot densitometry in HeLa cells.

7.5 *In vivo* Pharmacokinetic Evaluation of 306 and 314

Compounds **306** and **314** from the pyrazole amide series were selected for pharmacokinetic evaluation in mouse. In vivo pharmacokinetic studies were performed by Dr Huw Thomas. Table 7.32 shows a comparison of the *in vitro* and *in vivo* pharmacokinetic parameters of the two compounds.

Cmpd	HLM Cl_{int}[a]	MLM Cl_{int}[a]	Caco-2 AB[b] (ER)	F_u	Cl ml/min/kg	Cl_u ml/min/kg	V_d L/kg	$t_{1/2}$ min	F %
306	2	0.3	0.2 (4.5)	0.10	10	100	0.1	132	1
314	13	28	27 (0.9)	0.08	14	175	0.6	80	42

[a] μL/min/mg protein. [b] P_{app} 10^{-6} cm s^{-1}.

Table 7.32: *In vitro* and *in vivo* pharmacokinetic parameters for **306** and **314**. *In vivo* studies were performed at a dose of 10 mg/kg *i.v.* and 10 mg/kg *p.o.* in mouse.

Compound **306** had low plasma clearance, but negligible bioavailability (F ~ 1%) suggesting that the oral dose was poorly absorbed. This is consistent with the low membrane permeability and moderate efflux observed in the Caco-2 assay. The low volume of distribution is surprising for a basic compound. Derivative **314** had low clearance, with a hepatic extraction ratio of approximately 15%. Oral bioavailability was determined to be 42%, implying that **314** suffered impairment of absorption (F_{abs} ~ 50%), which is not predicted from the Caco-2 and solubility data. However, the bioavailability was sufficient for this compound to be progressed into a tumour xenograft *in vivo* efficacy study. Data from this study are awaited.

7.6 Summary

Exploration of SAR around the amide substituent in the pyrrole carboxamide series of ERK5 inhibitors has resulted in the identification of groups which improve the potency. Combination with trisubstituted benzoyl 4-substituents provided a set of potent compounds with ERK5 inhibitory-activity below 20 nM. The most potent compounds incorporate a basic centre, which is hypothesised to interact with an aspartate residue on the exit to the active site. However, all compounds containing a basic centre suffered from efflux in the Caco-2 assay, and this translated to poor *in vivo* bioavailability in the case of compound **306**.
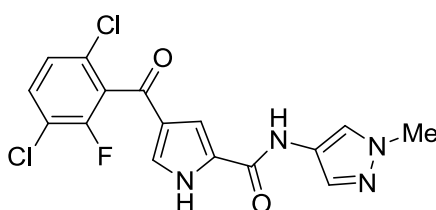
314 ERK5; IC$_{50}$ = 27 ± 10 nM
Caco-2 ER 0.9
L.E. 0.43
Mouse F = 42%

The neutral compound, **314** had the best balance of potency and *in vitro* ADME parameters, and inhibited ERK5 auto-phosphorylation in a cell-based assay. This compound had good bioavailability in a mouse pharmacokinetic study, and is currently being progressed into a tumour xenograft model to examine the effects of ERK5 inhibition *in vivo*.

Chapter 8: Discussion of ERK5 Inhibitor Synthesis

Knowledge of the SARs around the amide substituent on the pyridyl carboxamide scaffold was limited at the start of this program of work. Thus, robust, reliable, and relatively high-throughput synthetic methods were sought to enable rapid analogue preparation to facilitate elaboration of this region.

The carboxylic acids **336** and **337** were key building blocks for the synthesis of amide derivatives. These were prepared in two steps from commercially available materials, employing a Friedel-Crafts acylation followed by basic ester hydrolysis, which had been previously developed in our research group (Scheme 8.1).

331 X = H **333** **334** X = H **336** X = H
332 X = Cl **335** X = Cl **337** X = Cl
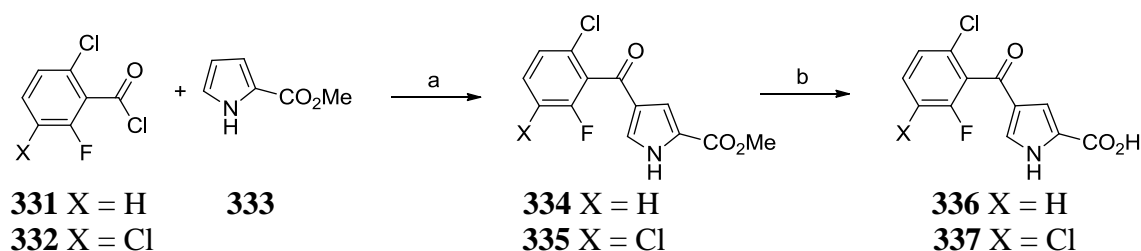
Scheme 8.1: *Reagents and conditions* a) Aryl acid chloride (2 eq.), $AlCl_3$ (2.5 eq.), CH_2Cl_2, 0 °C-r.t., 18 h, (X = H, 92%; X = Cl, 89%); b) LiOH (20 eq.), THF:H_2O (1:2) 65 °C, 48 h, (X = H, 99%).

8.1 Variation of the Piperidine 4-Substituent of 212
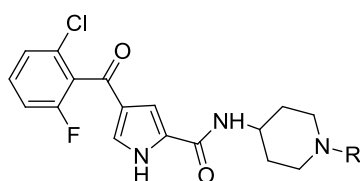
Two strategies were employed for the synthesis of analogues of **212** which varied the piperidine nitrogen substituent (R). Where the desired 4-aminopiperidine was commercially available at an acceptable price (R = *i*-Pr, *c*-Pr) this reagent was purchased and directly coupled to pyrrole carboxylate **336** using carbonyldiimidazole (CDI) as the coupling reagent (Scheme 8.2) to give targets **253** and **254**.

336

253 R = *i*-Pr
254 R = *c*-Pr
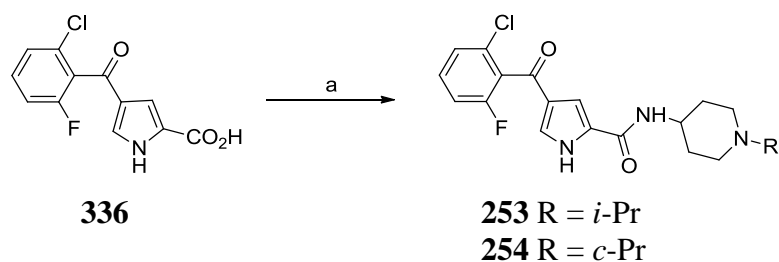
Scheme 8.2: *Reagents and conditions* a) i) CDI (2 eq.), THF, 70 °C, 3 h; ii) 1-*c*-Pr-4-aminopiperidine (2.2 eq), 50 °C, 3 h, 52%, or 1-*i*-Pr-4-aminopiperidine (2.5 eq.), 50 °C, 3 h, 60%.

For the second approach, unsubstituted piperidine amides **251** and **260** were prepared in two steps from pyrrole carboxylates **336** and **337** (Scheme 8.3).

336 X = H
337 X = Cl

258 X = H
263 X = Cl

251 X = H
260 X = Cl
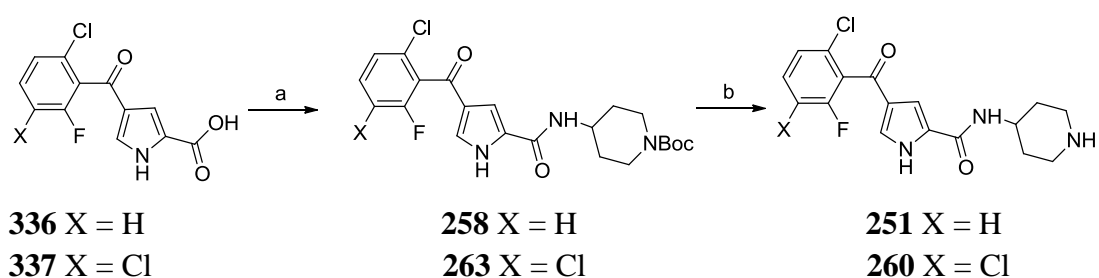
Scheme 8.3: *Reagents and conditions* a) i) CDI (2 eq.), THF, 70 °C, 3 h; ii) 1-Boc-4-aminopiperidine (2.2 eq) 50 °C, 3 h, (X=H, 75%; X = Cl, 79%); b) Et₃SiH, TFA/CH₂Cl₂, r.t., 2 h, (X = H, 99%; X = Cl, 75%).

The versatile secondary amine functionality of compounds **251** and **260** allowed the introduction of a diverse set of piperidine N^1-substituents at the final step of the synthesis. An array of synthetic transformations were employed including reductive alkylation, amide and sulfonamide formation, and nucleophilic aromatic substitution reactions as summarised in scheme 8.4.
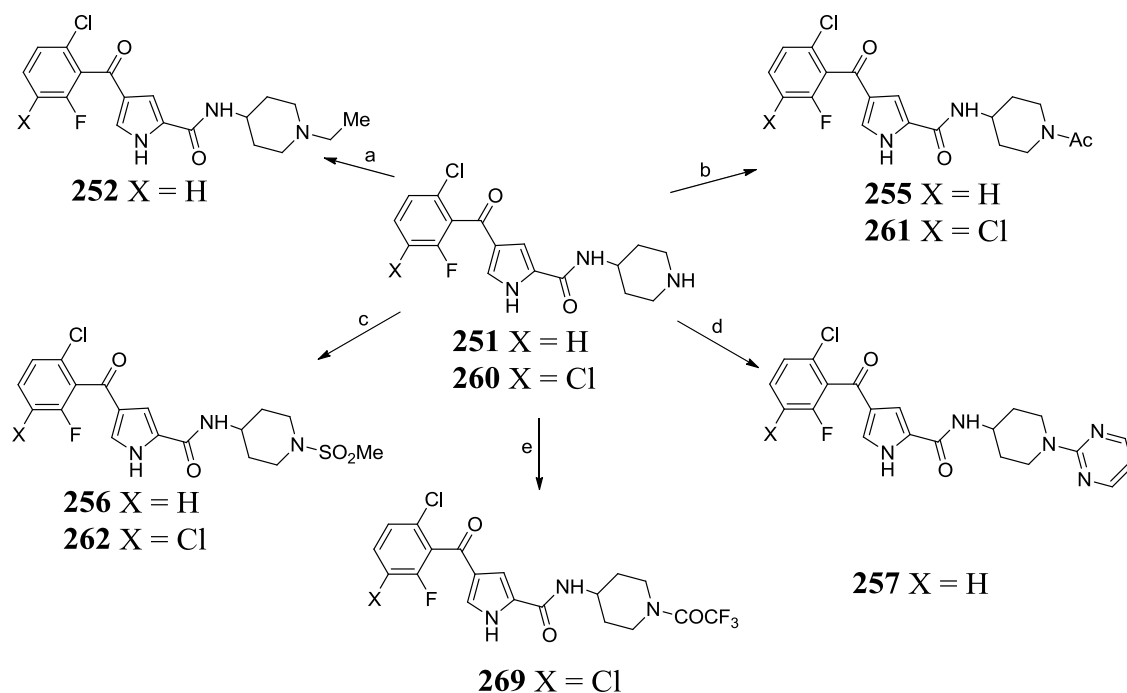
Scheme 8.4: *Reagents and conditions* a) i) MeCHO (2 eq.), AcOH (2 eq.), MgSO$_4$, MeOH, r.t., 1 h; ii) NaCNBH$_3$ (1.5 eq.), r.t., 18 h, (X = H, 16%); b) AcCl (1.1 eq.), Et$_3$N (1.2 eq), CH$_2$Cl$_2$, r.t., 1 h, (X = H, 48%; X = Cl, 52%); c) MeSO$_2$Cl (1.5 eq.), Et$_3$N (1.5 eq.), CH$_2$Cl$_2$, r.t., 1 h, (X = H, 27%; X = Cl, 35%); d) 2-chloropyrimidine (1 eq.), iPr$_2$EtNH (1.2 eq.), MeCN, μW, 150 °C, 1.5 h, (X = H, 23%); e) (CF$_3$CO)$_2$O (4.5 eq), Et$_3$N (1.2 eq.), CH$_2$Cl$_2$/dioxane, r.t., 3 h, (X = Cl, 41%).

8.2 Variation of the Pyrimidyl 2-Substituent of 215

Exploration of the pyrimidyl 2-position of **215** was achieved through preparation of the requisite aminopyrimidines from 2-chloro-5-nitropyrimidine (**338**). The first amine prepared was 2-(pyrrolidin-1-yl)pyrimidin-5-amine **340**. S$_N$Ar displacement of the 2-chloro group of **338** proceeded at room temperature to give **339**, which was cleanly reduced using palladium-catalysed hydrogenation to give **340**.
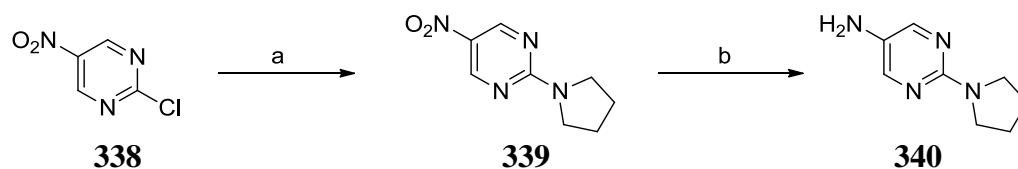
Scheme 8.5: *Reagents and conditions:* a) Pyrrolidine, Et$_3$N, THF, r.t. 18 h, 80%; b) H$_2$, 10% Pd/C, MeOH, CH$_2$Cl$_2$, 100%.

190

A previous investigation of amide coupling conditions of aromatic heterocyclic amines to carboxylic acid **336** conducted in our research group led to the identification of conditions employing PCl$_3$ under microwave heating at 150 °C as optimal. However, when these conditions were applied to the coupling of **340** with **336**, a complex mixture was formed. CDI-mediated coupling resulted in product formation along with several close-running impurities, which led to difficulties in purification. However, coupling using cyanuric fluoride allowed isolation of **274** in high purity and 42% yield (Table 8.1).

	336		**340**			**274**
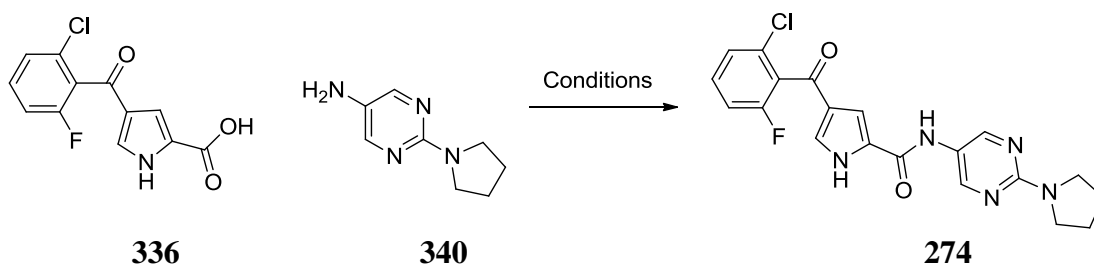
Entry	Reagent	Amine Equiv.	Solvent	Temp °C	Time h	Result
1	PCl$_3$	2.5	MeCN	150	0.5	Complex mixture[a]
2	CDI	2.5	THF	70	2	Product plus impurities[a]
3	Cyanuric fluoride	1.25	MeCN	r.t.	18	42% isolated yield

[a] Observations from TLC and LCMS analyses.

Table 8.1: Exploration of conditions for the coupling of **336** and **340**.

This three step scheme was applied to the synthesis of a small library of nitrogen-linked derivatives, introducing small cyclic and acyclic alkylamines. The yields for each step are summarised in Table 8.2.
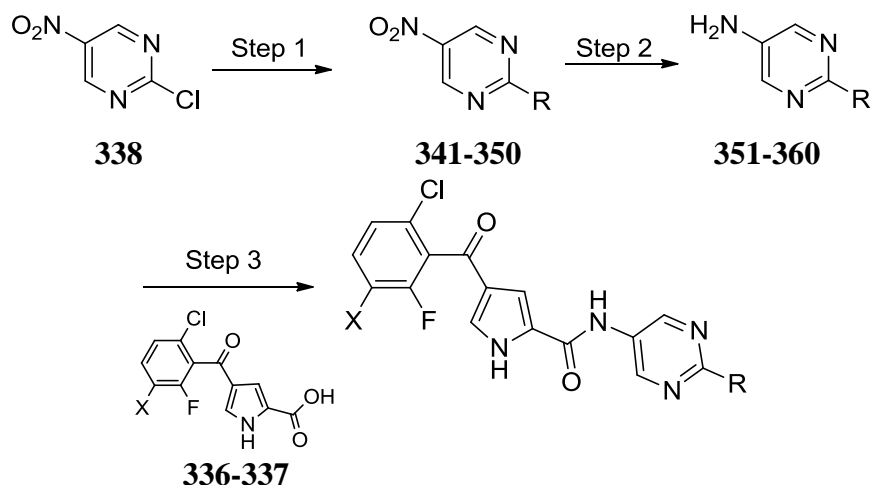
Entry	R	Step 1		Step 2		Step 3		
			Yield		Yield	X		Yield
1	NHMe	341	55%	351	100%	H	272	26%
2	NMe$_2$	342	87%	352	100%	H	273	34%
3	-ξ-N⟩⟨N−Me	343	82%	353	96%	H	275	50%
4						Cl	276	41%
5	-ξ-N⟩⟨N−◁	344	89%	354	98%	Cl	287	18%
6	-ξ-N⟩⟨N−Boc	345	68%	355	99%	H	361	49%
7						Cl	362	69%
8	-ξ-N⟩⟨O	346	73%	356	100%	H	279	50%
9						Cl	280	40%
10	-ξ-N⟩−OH	347	94%	357	72%	H	281	0%
11	-ξ-N⟩−OAc	348	97%	358	78%	H	283	47%
12						Cl	284	54%
13	N-H piperidine N−Me	349	83%	359	92%	H	288	35%
14						Cl	289	35%
15	N-H piperidine N−◁	350	95%	360	100%	Cl	290	15%

Table 8.2: Summary of yields for the three step synthesis of analogues of **215**; *Reagents and conditions:* Step 1: Amine, Et$_3$N, THF, r.t. 18 h; Step 2: H$_2$, 10% Pd/C, MeOH, CH$_2$Cl$_2$; Step 3: Amine (2.5 eq.), cyanuric fluoride (0.3-0.7 eq.), pyridine (1 eq), MeCN, r.t., 18 h.

t-Butyl carbamates **361** and **362** were deprotected using TFA/DCM in the presence of triethylsilane, which acted as a scavenger for the liberated *t*-butyl cation, preventing alkylation of the pyrrole ring. This provided secondary amine targets **285** and **286** (Scheme 8.5).

361 X = H
362 X = Cl

285 X = H
286 X = Cl
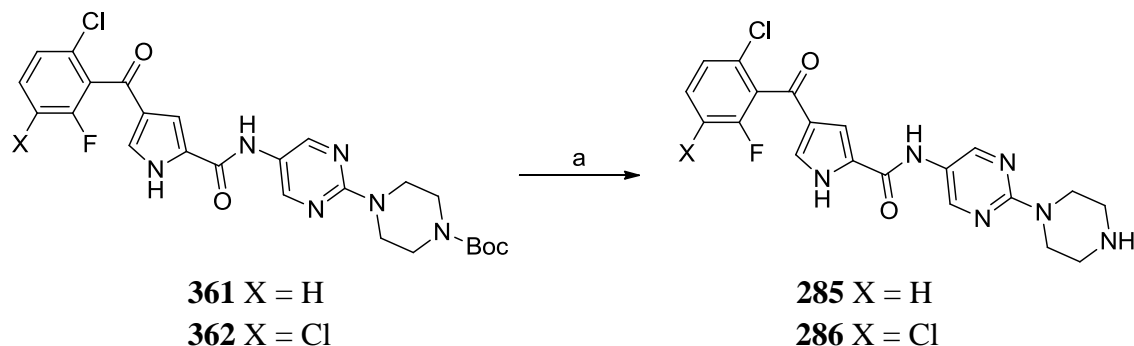
Scheme 8.5: *Reagents and conditions:* a) TFA, DCM, Et$_3$SiH (2.5 eq.) (X = H, 52%; X = Cl, 69%).

Amine **357** failed to react under the cyanuric fluoride coupling conditions, with evidence by LC-MS analysis of the unprotected alcohol participating in undesired side-reactions. The scheme was repeated with the alcohol protected as acetate ester **358**, allowing good yields to be achieved for the amide coupling. The acetate was removed under mild conditions to provide alcohols **281** and **282** (Scheme 8.6).

283 X = H
284 X = Cl

281 X = H
282 X = Cl
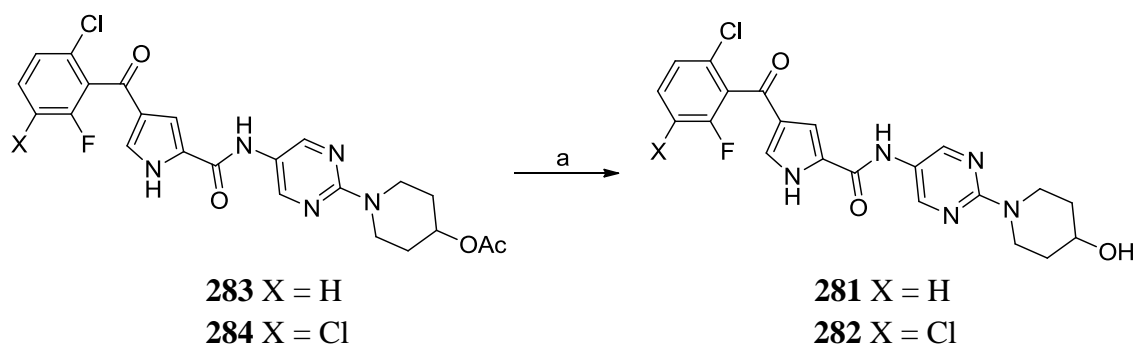
Scheme 8.6: *Reagents and conditions:* a) K$_2$CO$_3$ (2 eq.), THF, MeOH, H$_2$O, r.t., 18 h, X = H, 93%, X = Cl, 54%.

Methoxy-substituted pyrimidine **271** was prepared in a similar three step sequence from **338**, using freshly prepared sodium methoxide in the nucleophilic aromatic substitution reaction (Scheme 8.7).
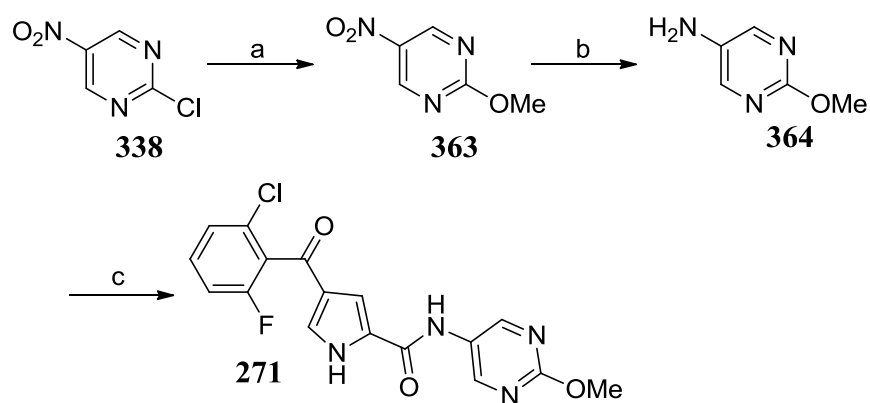
Scheme 8.7: *Reagents and conditions:* a) Na (1.2 eq.), MeOH, 65 °C, 1 h, 59%; b) H$_2$, 10% Pd/C, MeOH, CH$_2$Cl$_2$, 97%; c) Cyanuric fluoride (0.3-0.7 eq.), **336** (0.33 eq.), pyridine (1 eq), MeCN, r.t., 18 h, 43%.

8.3 Synthesis of Pyridyl Analogues of 286 and 289
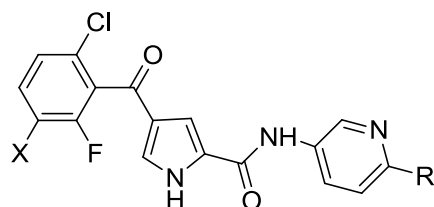
Compounds incorporating a pyridyl linker in place of the pyrimidine ring were also prepared. A similar reaction sequence was employed to that described for the pyrimidyl analogues above. The 2-chloro-5-nitropyridine starting material (**365**) reacted more slowly with amines than in the pyrimidine case, with incomplete conversion observed after 4 hours at room temperature. Increasing the reaction temperature to 80 °C enabled complete conversion to the desired products within 30 minutes. Hydrogenation and amide coupling (Table 8.3) was achieved in a manner analogous with the pyrimidyl targets discussed in the previous section.

Deprotection of **370** using TFA/DCM and triethylsilane gave secondary amine target **292** in 46% yield. Amine **369** failed to couple under the cyanuric fluoride conditions, but target **293** was successfully obtained by employing PyBrOP to activate the carboxylic acid. This reaction achieved high conversion in 2 hours, and had a further advantage of requiring only 1.5 equivalents of the amine. However, the overall yield was relatively low due to difficulties in isolating the product from close-running impurities.
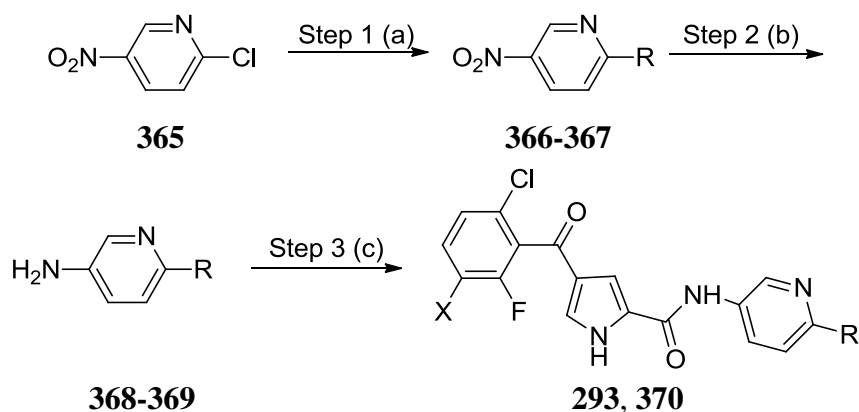
Entry	R	Step 1		Step 2		X	Step 3		
			Yield		Yield		Method		Yield
1	–N(piperazine)N–Boc	**366**	97%	**368**	100%	Cl	1	**370**	45%
2	–NH–(N-Me-piperidin-4-yl)	**367**	56%	**369**	95%	Cl	2	**293**	19%

Table 8.3: *Reagents and conditions:* a) Amine (2 eq.), K_2CO_3 (2 eq.), THF, 80 °C, 0.5-3 h; b) H_2, 10% Pd/C, MeOH; c) Method 1: Amine (2.5 eq.), cyanuric fluoride (0.3-0.7 eq.), pyridine (1 eq), MeCN, r.t., 18 h; Method 2: Amine (1.5 eq.), PyBrOP (1.3 eq.), pyridine (1 eq.), MeCN, r.t., 2 h.

8.4 Elaboration of the Pyridyl 2-Position of 214
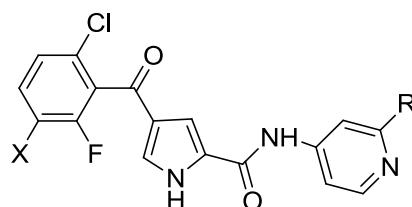
A literature report indicated that elaboration of the 2-position of 2-chloro-4-nitropyridines by reacting with nucleophiles is complicated by competing displacement of the 4-nitro group, and that selectivity for substitution of the chloro group can be achieved by performing the reaction on the equivalent pyridine *N*-oxides.[314] Reaction of 2-chloro-4-nitropyridine *N*-oxide (**371**) with pyrrolidine at reflux in IPA resulted in the formation of **372** (Scheme 8.6). Reduction of both the nitro group and the *N*-oxide was achieved in a single process, using palladium catalysed flow hydrogenation, to give **373**.
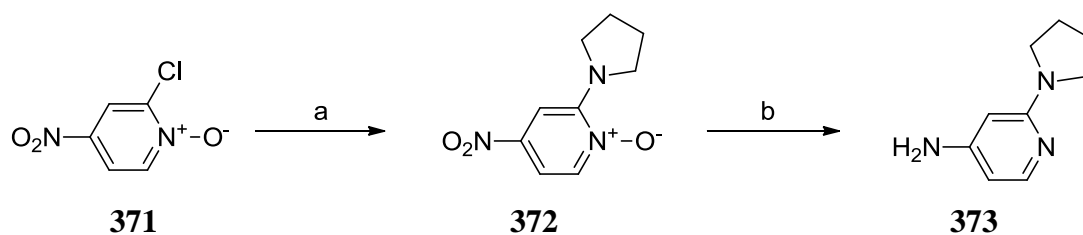
Scheme 8.6: *Reagents and conditions:* a) Pyrrolidine, NaHCO$_3$, IPA, r.t. 2 h, 88%; b) H$_2$, 20% Pd(OH)$_2$/C, MeOH, 89%.

However, coupling of this amine to carboxylic acid **336** under a range of conditions was unsuccessful (Table 8.4). A review of the literature revealed few examples of successful amide couplings with 2,4-diaminopyridines. A patent procedure for the coupling of 2,2-dimethylamino-4-aminopyridine to a carboxylic acid[315] utilised the Mukaiyama pyridinium coupling reagent to activate the acid,[316] but no yield was given for this reaction. Applying these conditions to the coupling of **336** with **373** led to isolation of target **297** in 20% yield.
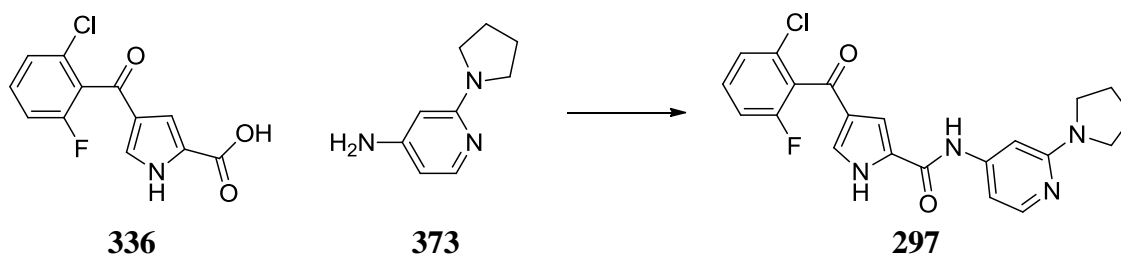
Entry	Amine Eq.	Reagents	Solvent	Temp °C	Time h	Result
1	2.5	PCl$_3$ (1 eq.)	MeCN	150	0.5	Degraded
2	2.5	Cyanuric fluoride (0.7 eq.), pyridine (1 eq.)	MeCN	r.t.	18	Trace conversion[b]
3	2	Mukaiyama reagent[a] (1.1 eq.), Et$_3$N (2.5 eq.)	DCM	50	2	20% isolated yield

[a] 2-chloro-1-methylpyridinium iodide; [b] Determined by LC-MS.

Table 8.4: Conditions investigated for the coupling of **336** and **373**.

In an attempt to improve both the yield and throughput for analogue synthesis, an alternative approach was investigated which would allow late-stage diversification of the 2-pyridyl substituent in this series (Scheme 8.7). Coupling of commercially available 2-chloro-4-aminopyridine **374** to carboxylic acid **336** using PCl$_3$ with microwave irradiation resulted in a 45% isolated yield of pyridyl 2-chloride **294**.
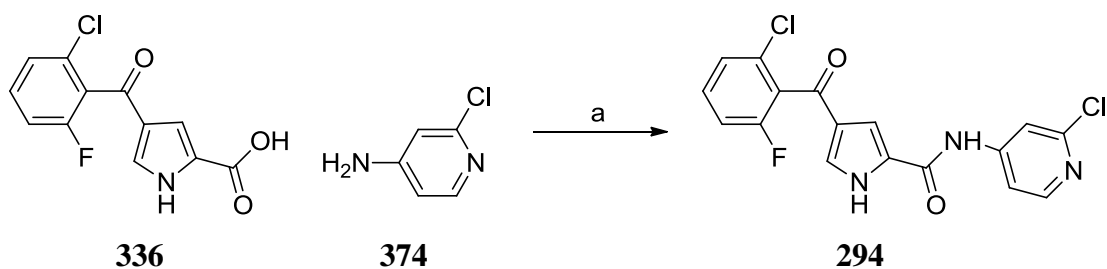
Scheme 8.9: *Reagents and conditions*: a) PCl₃, MeCN, 100 °C, 0.5 h, 45%.

Palladium-catalysed amination[317-319] of **294** was investigated using pyrrolidine as a representative amine (Table 8.5). No conversion was observed using conditions which had previously been successful on another project in the research group for carbon-nitrogen cross coupling (entry 1). The conditions recommended by the Buchwald group for coupling of aliphatic secondary amines[320] also gave no conversion (entries 2 and 3). The presence of unreacted starting material indicated that oxidative addition of palladium to the 2-chloropyridine was not occurring under these conditions.
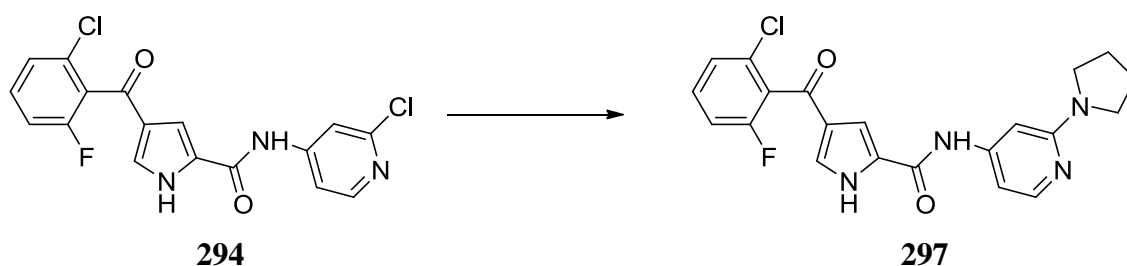
Entry	Conditions	Temp °C	Time h	Result[a]
1	Pd₂(dba)₃ (0.1 eq), Xphos (0.1 eq), pyrrolidine (1.25 eq.), K₂CO₃ (2.25 eq), MeCN	100	0.75	SM only
2	Pd₂(dba)₃ (0.1 eq), Xphos (0.1 eq), pyrrolidine (1.25 eq.), K₂CO₃ (2.25 eq), MeCN	120	2	SM only
3	Pd₂(dba)₃ (0.1 eq), Xphos (0.1 eq), pyrrolidine (1.25 eq.), K₂CO₃ (2.25 eq), MeCN	150	2	SM only

[a] Determined by LC-MS and TLC analyses.

Table 8.5: Summary of investigation of palladium-catalysed cross-coupling conditions employed for the synthesis of **297**.

Thermal displacement of the 2-chloropyridine with amines in the absence of catalyst was also investigated, with NMP as solvent (Table 8.6).
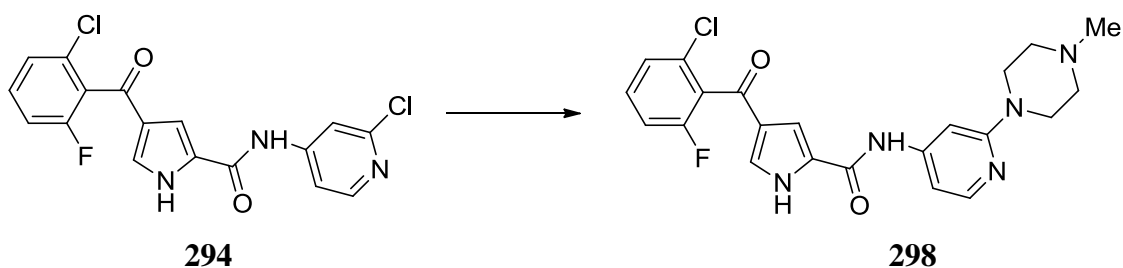
Expt	Pyrrolidine Equiv.	Temp °C	Time h	Product[a] %
1	4	200	0.5	<5
2	4	250	0.5	23
3	4	250	2	65
4	4	250	3	0
5	2	250	3	77

[a] Percentages from LC-MS UV trace.

Table 8.6: Summary of studies on the S_NAr reaction of 2-chloropyridine intermediate **294** with pyrrolidine. All reactions were performed in NMP.

Under microwave irradiation at 200 °C no discernible reaction occurred (entry 1). Increasing the temperature to 250 °C and extending the reaction time to 2 hours improved conversion to **298** (entries 2 and 3). Further extension of the reaction time (entry 4) led to product depletion due to competing substitution of the 2-fluoro group on the phenyl ring. Reducing the number of equivalents of pyrrolidine decreased this side-reaction. Scaling up of the conditions for entry 5 gave an isolated yield of 45% of **298**.

However, when these optimized conditions were applied to other amines, multiple by-products were formed from which the target compounds could not be isolated in high purity. It has been reported that the use of 1,2-ethanediol as solvent facilitates the displacement of 2-halopyridines by amines, enabling the use of lower reaction temperatures.[321] However, repeating the reaction in 1,2-ethanediol, using two equivalents of *N*-methylpiperazine at 150 °C under microwave irradiation led to a 1:1 mixture of starting material and 2-hydroxyethyl ester **375**.

375
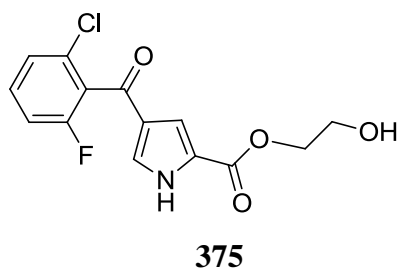
Displacement of the 2-chloropyridine of **294** with sodium methoxide[322] was also explored, resulting in methanolysis of the amide bond to form methyl ester **334** (Scheme 8.8). Thus it appears that the amide bond of **294** is unstable to nucleophilic reagents at elevated temperatures.

294   **305**   **334**
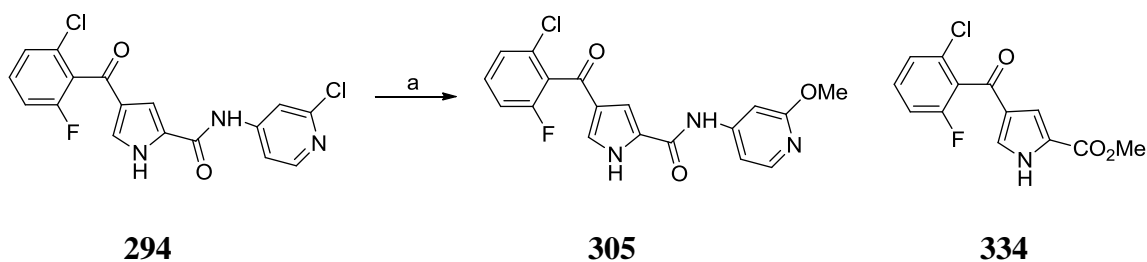
Scheme 8.8: *Reagents and conditions:* a) NaOMe, MeOH, μW, 125 °C, 30 min.

In order to develop a more efficient synthesis of amine analogues, several alternative routes were investigated. Oxidative addition of palladium catalysts is often facilitated by the use of aryl iodides and bromides in place of chlorides. A procedure for direct conversion of 2-pyridyl chlorides to 2-pyridyl iodides has been reported, using transient acylation of the pyridyl nitrogen with acetyl chloride to activate the ring to nucleophilic displacement.[323] However, applying these conditions to the synthesis of **376** led to an inseparable mixture of chloride **294** and iodide **376** (Scheme 8.9). The chloropyridine also proved resistant to S$_N$Ar reaction with sodium thiomethoxide in a sealed tube at 110 °C.

294   **376**
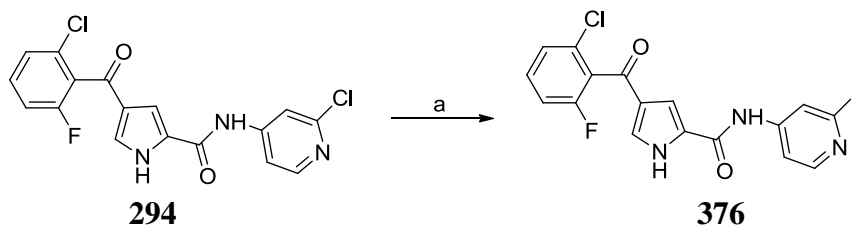
Scheme 8.9: *Reagents and conditions:* a) AcCl (1.5 eq.), NaI (10 eq.), MeCN, 80 °C, μW, 3 h.

Methods for the activation of pyridine *N*-oxides, which enable direct attack of nucleophiles at the pyridine 2-position under mild conditions, have also been described, including the

use of toluenesulfonic anhydride/*t*-butylamine,[324] and PyBrOP.[325,326] Pyridine *N*-oxide **378** was formed in two steps from **337** using the process outlined in scheme 8.10.
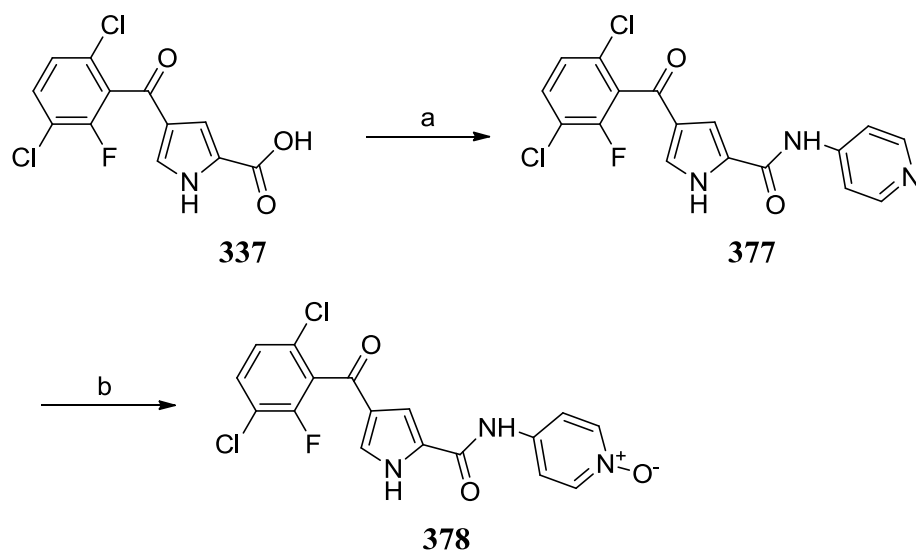
Scheme 8.10: *Reagents and conditions*: a) 4-aminopyridine (2.5 eq.), PCl_3, MeCN, 100 °C, 0.5 h, 58%; b) mCPBA (1.5 eq.), MeCN, r.t., 18 h, 72%.

Activation of *N*-oxide **378** with PyBrOP in the presence of either *N*-methylpiperazine or morpholine led to isolation in low to moderate yields of the desired products **299** and **300**, respectively, (Table 8.7).
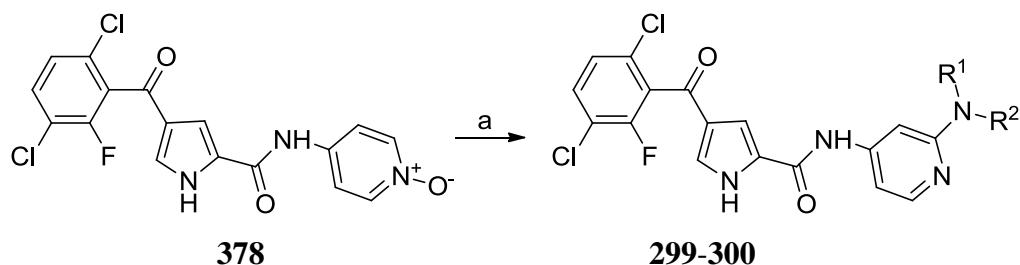
Entry	NHR^{1}R^2	Cmpd	Isolated yield
1	*N*-Methylpiperazine	**299**	35%
2	Morpholine	**300**	14%

Table 8.7: Yields for the amide coupling step in the synthesis of **299** and **300**. *Reagents and conditions*: a) PyBrOP (1.3 eq.), NHR_1R_2 (1.25 eq.), Hünig base (3.75 eq.), CH_2Cl_2, r.t, 18 h.

The final derivatives in this series, **295** and **296**, were prepared by coupling of commercially available amines using either PCl₃ or cyanuric fluoride coupling procedures (Table 8.8).
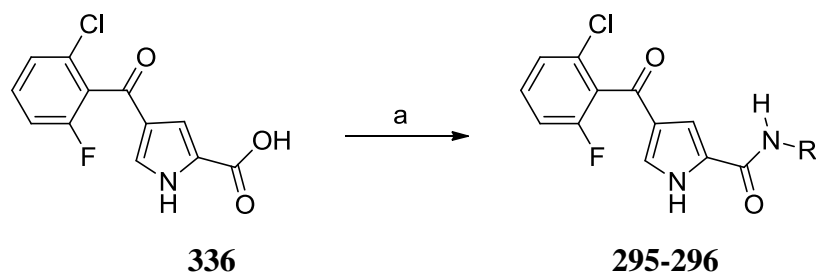
Entry	Amine	Cmpd	Isolated yield
1	2-trifluoro-4-aminopyridine[a]	**295**	45%
2	2-methoxy-4-aminopyridine[b]	**296**	33%

Table 8.8: *Reagents and conditions*: a) Amine (2.5 eq.), PCl₃, MeCN, 100 °C, 0.5 h or b). Amine (2.5 eq.), cyanuric fluoride (0.7 eq.), pyridine (1 eq), MeCN, r.t., 18 h

8.5 Pyrazole-Linked Amides

Replacement of the pyrimidine linker with a pyrazole ring was achieved using a 3-step route. The heterocyclic *NH* of 4-nitropyrazole has a pK_a of 9.64,[327] enabling participation in Mitsunobu reactions with alkyl alcohols.[328] This allowed access to the desired amine coupling partners in two steps from 4-nitropyrazole **379** and commercially available alcohols, as shown in Table 8.8.

Entry	R	Step 1		Step 2	
1	–piperidine N–Boc	**380**	67%	**393**	100%
2	–azetidine N–Boc	**381**	63%	**394**	99%
3	CH₂-piperidine N-Boc	**382**	82%	**395**	95%
4	CH₂-piperidine N-Me	**383**	34%	**396**	91%
5	–piperidine N–CH₂CF₃	**384**	54%	**397**	97%
6	Me	**385**	67%	**398**	98%
7	Et	**386**	54%	**399**	100%
8	CH₂CH₂N(Et)₂	**387**	43%	**400**	28%
9	CH₂-2-pyridyl	**388**	83%	**401**	96%
10	CH₂-3-pyridyl	**389**	40%	**402**	91%
11	CH₂-4-pyridyl	**390**	55%	**403**	99%
12	CH₂CH₂OMe	**391**	85%	**404**	91%
13	CH₂-imidazolyl N-Me	**392**	18%	**405**	96%

Table 8.8: Summary of yields for the synthesis of substituted pyrazole compounds; *Reagents and conditions:* a) PPh₃, DEAD, THF, r.t. 18 h; b) H₂, 10% Pd/C, MeOH.

The increased polarity imparted by the introduction of a basic centre resulted in certain products having a similar retention factor on silica to the reaction by-products of triphenylphosphine oxide or reduced diazocarboxylate. The use of a catch-and-release process on an SCX strong acid ion exchange resin, in conjunction with standard medium pressure column chromatography on silica, allowed successful isolation of these products. In order to avoid this issue, an alternative synthesis was developed for *N*-methylated aliphatic heterocycles *via* the *N*-Boc protected intermediates using an *in situ* deprotection/Eschweiler-Clarke methylation strategy (Scheme 8.11).[329,330]

382 **383**
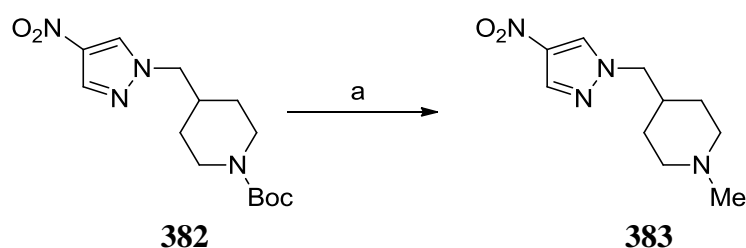
Scheme 8.11: *Reagents and conditions*: a) HCHO (4 eq.), HCO$_2$H, 95 °C, sealed tube, 2 h, 84%.

Preparation of **308** required the synthesis of 1-trifluoroethyl substituted piperidine (**409**), which was accessed in two steps from 4-hydroxypiperidine (Scheme 8.12), the initially formed *N,O-bis*(trifluoroacetyl) intermediate **407** being cleaved to trifluoracetamide **408** on treatment with weak base prior to work-up.

406 **407**

408 **409**
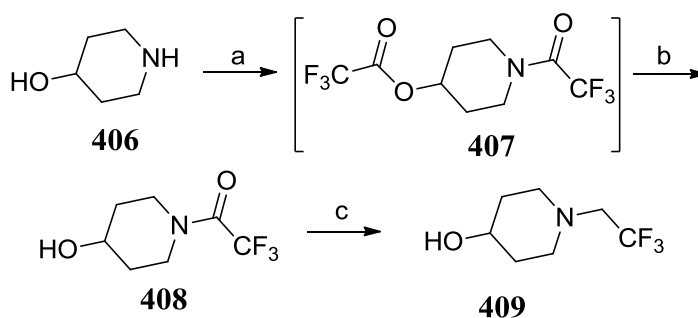
Scheme 8.12: *Reagents and conditions*: a) TFAA (1.1 eq.), pyridine (2 eq.), DCM, 0 °C to r.t., 18 h; b) NaHCO$_3$, H$_2$O, MeOH, r.t., 15 min, 47% over 2 steps; c) BH$_3$.THF (2.5 eq.), THF, 66 °C, 90 min, 67-71%.

Amine **410** was obtained in a single step by hydrogenation of 4-nitropyrazole (Scheme 8.13).
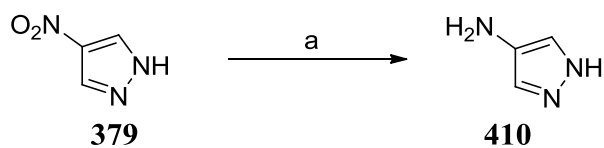
Scheme 8.13: *Reagents and conditions:* a) H_2, 10% Pd/C, MeOH, 40 °C, 2 h, 98%.

The Mitsunobu reaction utilised for the synthesis of **392** (Table 8.8, entry 13) was low yielding due to competing formation of a significant by-product. This was isolated and structure **411** was proposed based on spectroscopic data. The structure was confirmed by small molecule X-ray crystallography of a crystal grown by slow evaporation from ethyl acetate.
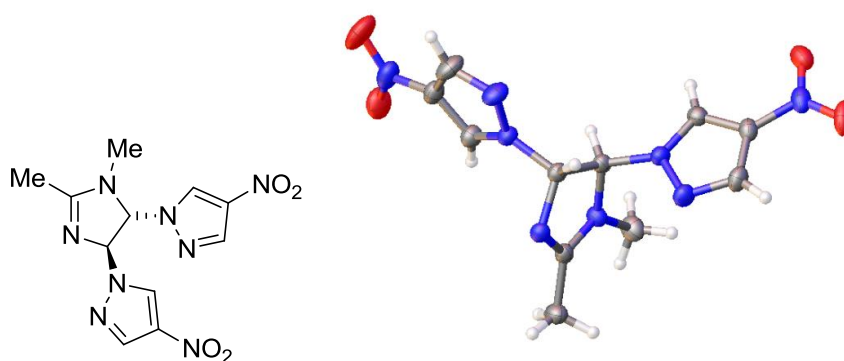
Figure 8.1: The X-ray crystal structure of side-product **411**.

The isolated yield of **411** was 18%. A proposed mechanism for the formation of **411** under the reaction conditions is shown in Scheme 8.14.
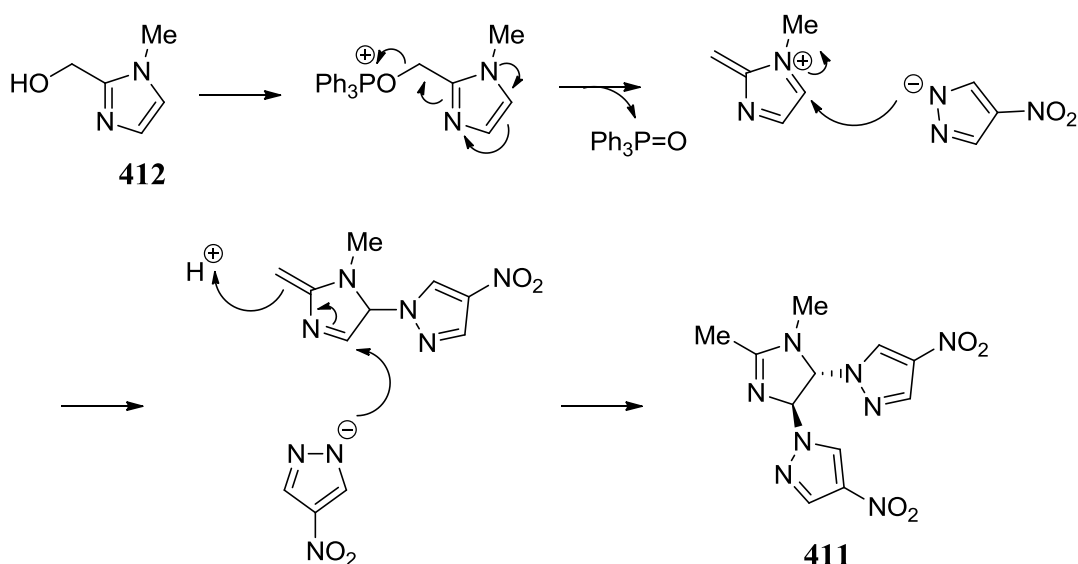
Scheme 8.14: Proposed mechanism for the formation of **411**.

A similar reaction has been reported when attempting a nucleophilic displacement of substituted 2-chloromethylimidazoles with amines (Scheme 8.15).[331] In this report the nucleophiles explored were aliphatic primary and secondary amines, with optimal yields of **413** when R^1 was *tert*-butyl. No examples have previously been described where R^1 = H, or with heteroaromatic nucleophiles.
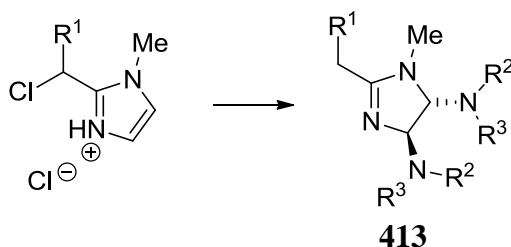
Scheme 8.15: Literature reaction of 2-chloromethylimidazoles with amines.[331]

To complete the synthesis of the pyrazole-linked amide targets, the substituted aminopyrazole intermediates **393**-**405** were coupled to the pyrrole carboxylic acid **337** using either the cyanuric fluoride or Mukaiyama coupling protocols (Table 8.11). During the course of this work, a transition was made to using the Mukaiyama coupling protocol as the method of choice, principally due to its requirement for a lower number of equivalents of the bespoke amine coupling component (1.25 equivalents) as compared to the 2.5 equivalents required to achieve high conversion in couplings employing cyanuric fluoride.

Entry	R	Amide Coupling Method		Yield %
1	−ξ−⟨piperidine⟩N−Boc	1	**414**	76
2	−ξ−⟨azetidine⟩N−Boc	1	**415**	70
3	−CH₂−⟨piperidine⟩N−Boc	1	**416**	59
4	−CH₂−⟨piperidine⟩N−Me	1	**306**	43
5	CH₂CH₂N(Et)₂	2	**307**	43
6	−ξ−⟨piperidine⟩N−CH₂CF₃	2	**308**	34
7	−CH₂−⟨2-pyridyl⟩	2	**309**	55
8	−CH₂−⟨3-pyridyl⟩	2	**310**	30
9	−CH₂−⟨4-pyridyl⟩	2	**311**	19
10	−CH₂−⟨N-Me imidazol-2-yl⟩	2	**312**	43
11	H	1	**313**	64
12	Me	1	**314**	59
13	Et	2	**315**	26
14	CH₂CH₂OMe	2	**316**	49

Table 8.11: Methods and yields for amide coupling; *Reagents and conditions:* Method 1: Amine (2.5 eq.), cyanuric fluoride (0.3-0.7 eq.), pyridine (1 eq), MeCN, r.t., 18 h or Method 2: Amine (1.25 eq.), 2-chloro-1-methyl pyridinium iodide (1.1 eq.), Et₃N (2.5 eq.), CH₂Cl₂, r.t., 18 h.

The Boc-protected amines **414**-**416** were deprotected to give secondary amine targets **302**, **304** and **305** (Table 8.10).
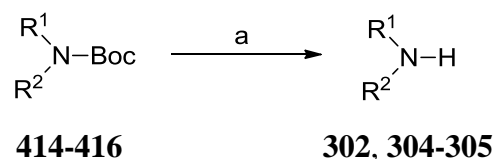
Substrate	Product	Yield %
414	302	69
415	304	85
416	305	64

Table 8.10: *Reagents and conditions:* a) TFA, DCM, Et$_3$SiH (2.5 eq.).

The Eschweiler-Clarke methylation procedure was also employed to convert **414** directly to **303** in a single step in high yield, demonstrating the utility of this process for elaboration of Boc-protected intermediates to their *N*-methylated counterparts in the final synthetic step (Scheme 8.15).
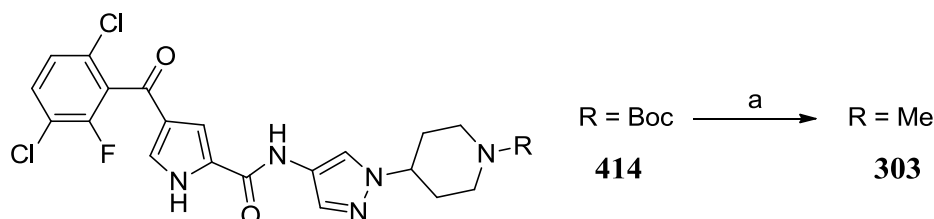
Scheme 8.15: Yields for Eschweiler-Clarke deprotection-*in situ* methylation; *Reagents and conditions:* a) HCHO (4 eq.), HCO$_2$H, 95 °C, sealed tube, 2 h, 100%.

8.6   Synthesis of Other 5-Membered Heterocyclic Amides

To access the methylated imidazole amide **320**, regioselective methylation of 4-nitroimidazole **417** was required. Alkylation of 4-nitroimidazole using Mitsunobu conditions has not previously been reported, and resulted in exclusive formation of the undesired 1-methyl-5-nitroimidazole regioisomer (**419**). This is consistent with the 1:350 ratio of **418**:**419** reported for methylation of this substrate using dimethyl sulfate under neutral conditions.[332] In the presence of sodium hydroxide the regioselectivity is reported to change, giving a **418**:**419** ratio of 3:1.[332] The use of the carcinogenic dimethyl sulfate

was undesirable, and, in preference, an alternative procedure employing dimethyl oxalate as the methylating reagent under basic conditions was identified.[333] Under these conditions a 4:1 ratio in favour of **418** was achieved (Scheme 8.16).

417 **418** **419**
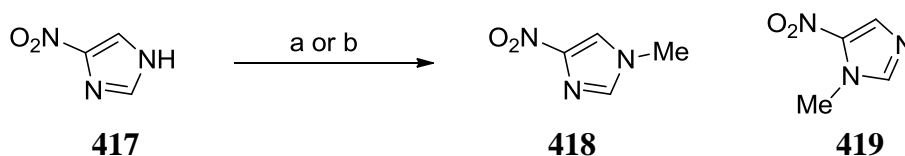
Scheme 8.16: *Reagents and conditions:* a) DEAD (1.5 eq), PPh₃ (1.5 eq.), MeOH (1 eq.), THF, r.t., 18 h, A (0%), B (50%); b) Dimethyl oxalate (1.5 eq.), KOtBu (1.5 eq.), DMF, 140 °C, 4 h, A (49%), B (12%).

The complex mechanistic factors governing the regiochemistry of this alkylation reaction have been discussed in a series of papers.[332,334,335] Two mechanistic possibilities for the reaction of **417** with electrophilic methylating reagents ($R\text{-}Me^{\delta+}$) were proposed, termed S_E2cB and S_E2':

S_E2cB mechanism

417 **418**

419
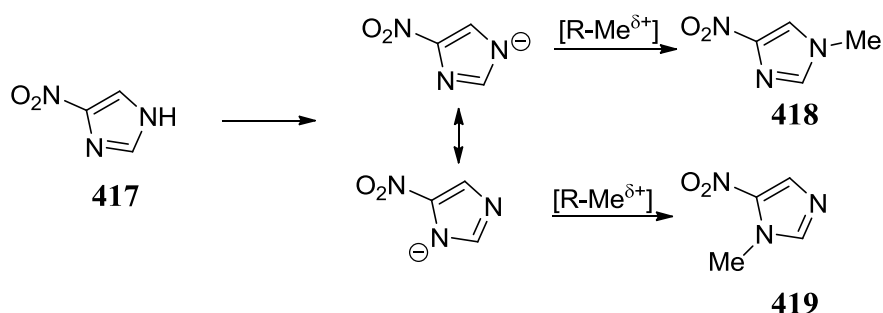
At basic pHs, the S_E2cB mechanism predominates, with the position of alkylation governed by the most nucleophilic nitrogen in the conjugate base. Nominal deprotonation of tautomer 2 leads to a more stable, less nucleophilic anion, leading to formation of **418** as the major product.[332]

S_E2' mechanism

417
Tautomer 1

419

417
Tautomer 2

418

208
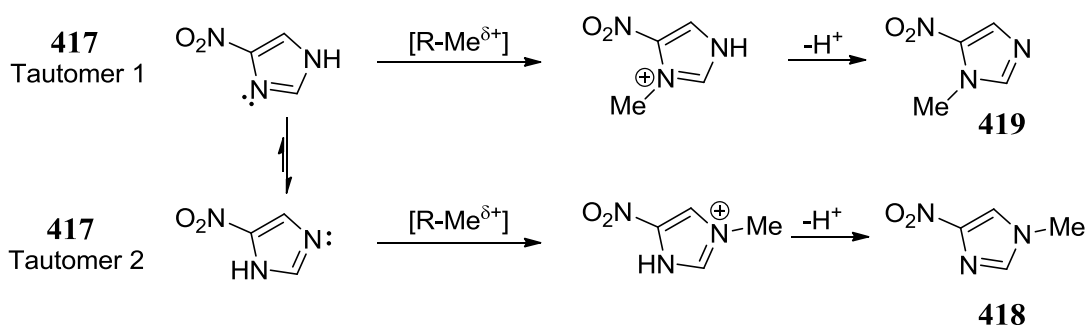
In the S_E2' mechanism a more complex situation exists with substitution occurring at the non-protonated nitrogen. The reaction outcome is affected by both the tautomeric ratio and rate of reaction of each tautomer. Under neutral conditions the tautomer ratio has been determined as 400:1 in favour of tautomer 1, and in practice near exclusive formation of 1-methyl-5-nitroimidazole regioisomer **419** is observed. Between pH 11 and pH 6 there is a transition from the S_E2cB to the S_E2'mechanism, with a subsequent change in the ratio of regioisomers formed.[332]

418 **420**
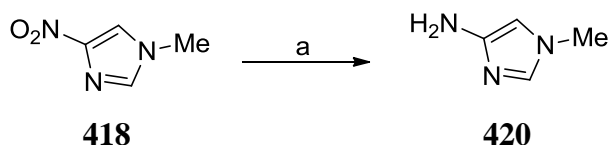
Scheme 8.17: *Reagents and conditions:* a) H_2/10% Pd/C, MeOH, EtOAc, 40 °C, 2 h, 99%,

Reduction of the nitro group gave aminoimidazole **420** (Scheme 8.17), which degraded on storage at room temperature for 48 hours. However, when progressed immediately after preparation to the amide coupling step using the PCl_3 protocol, desired analogue **320** was successfully formed (Table 8.11). A set of commercially available methylated 5-membered aromatic heterocyclic amines were also successfully coupled to pyrrole carboxylic acid **337** using the PCl_3 coupling protocol (Table 8.12).

337 **317-320**
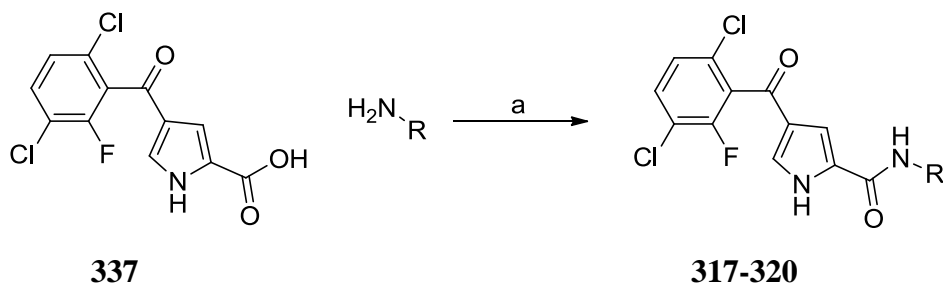
Cmpd	R	Yield %
317		34
318		40
319		67
320		24

Table 8.12: Yields for amide couplings in the synthesis of **317-320**; *Reagents and conditions*: a) Amine (3.5 eq.), PCl_3, MeCN, μW, 150 °C, 15 min.

8.7 Analogues Containing an Alternative Pyrrole 4-Substituent

A selection of the amines described above were coupled to a pyrrole carboxylic acid incorporating a methoxy substituted benzoyl group at the 4-position of the pyrrole core. Pyrrole carboxylic acid **421** was prepared by a colleague (Tristan Reuillon) using a procedure analogous to that described in scheme 8.1. The yields for the coupling reactions with this monomer are summarised in table 8.13.
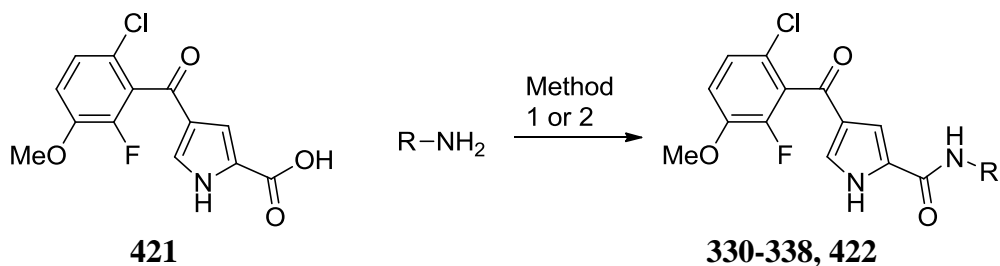
Entry	R	Amide Coupling		
		Method	Yield %	Product
1		1	50	**422**
2		2	35	**322**
3		2	60	**323**
4		2	45	**324**
9		2	43	**325**
5		2	49	**326**
6		2	45	**327**
7		2	30	**328**
8		2	26	**329**

Table 8.13: Yields for coupling of pyrrole carboxylic acid **421** with amines. *Reagents and conditions*: Method 1: Amine (2.5 eq.), cyanuric fluoride (0.3-0.7 eq.), pyridine (1 eq), MeCN, r.t., 18 h or Method 2: Amide (1.25 eq.), 2-chloro-1-methyl pyridinium iodide (1.1 eq.), Et$_3$N (2.5 eq.), CH$_2$Cl$_2$, r.t., 18 h.

Compound **422** was deprotected using the TFA/triethylsilane procedure to give **321** (Scheme 8.18).
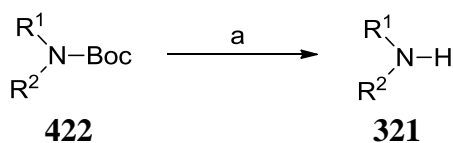
Scheme 8.18: *Reagents and conditions:* a) TFA, DCM, Et$_3$SiH (2.5 eq.), 72%.

8.8 Summary

The synthetic component of the ERK5 project has focussed on the synthesis of bespoke amine monomers to explore the SARs of the amide substituent of the pyrrole carboxylate lead. In order to rapidly build an understanding of the SARs in this position, robust routes that allowed facile analogue preparation were developed, which enabled diversification of cyclic aliphatic, and 5- and 6-membered heteroaromatic amides substituents. Nucleophilic aromatic substitution reactions allowed access to 2-substituted 5-amino-linked pyridyl and pyrimidyl amides.

Diversification of the 2-position in the 4-aminopyridine-linked series proved challenging, with the optimal route being through reaction of a pyridine *N*-oxide with PyBrOP to activate it towards nucleophilic aromatic substitution. Yields were moderate for this transformation, and further work to optimize this route would be a useful future direction to enable the synthesis of a wider range of analogues of this structural class.

Access to diverse substituted pyrazole amides was achieved through the use of Mitsunobu alkylation reaction, employing alcohol monomers.

A range of different amide coupling protocols was used, with yields often being substrate dependent. The Mukaiyama protocol emerged as the most versatile, having the advantage of requiring fewer equivalents of amine as compared to the other procedures investigated. This was particularly beneficial in cases where the amine coupling partner required a multi-step synthesis.

Chapter 9: Conclusions and Future Directions

The two medicinal chemistry programs described in this thesis encompassed diverse chemistry, biology, and stages of the drug discovery process.

9.1   The Sulfatase-2 Project

Sulf-2 has been implicated as a tumour promoter in multiple cancer cell lines, and high Sulf-2 expression is an indicator of a poor disease prognosis. The case is less certain for Sulf-1, with conflicting reports regarding its tumour promoter and tumour suppressor functions. The aim of the project was to identify tool compounds that either selectively inhibit Sulf-2, or exhibit dual Sulf-1/Sulf-2 inhibition. The Sulf-2 project was in the early target validation phase, with little prior literature on the design of inhibitors. The only known series of inhibitors were monosaccharide sulfamate mimics of the endogenous substrate, exemplified by compound **25**, which has Sulf-2 inhibitory potency above 100 μM.

Two approaches were employed in the design of potential inhibitors. The first attempted to build knowledge of the structural features present in **25** that contribute to binding, and identify areas of the template where substitution might improve potency and affect selectivity. Novel regioselective sulfamoylation chemistry was developed to allow rapid synthesis of compound **25** and a set of novel analogues, exploring variation of the 1-, 2-, 3-, and 4- positions. Derivatives **60**-**62**, and compound **105** were identified as more potent inhibitors of Sulf-2 than the lead monosaccharide **25**. A summary of the key SAR developed in the monosaccharide series is shown in figure 9.1.

Sulf-2 inhibition
maintained on deletion
of O^4 or substitution
as benzyl ether

Deletion of anomeric
substituent tolerated

Larger polar or lipophilic
groups not tolerated

Deletion of O^3 resulted
in loss of Sulf-2
inhibitory activity

Replacement with sulfonamides and
amides not tolerated, but free amine
retains Sulf-2 inhibitory activity
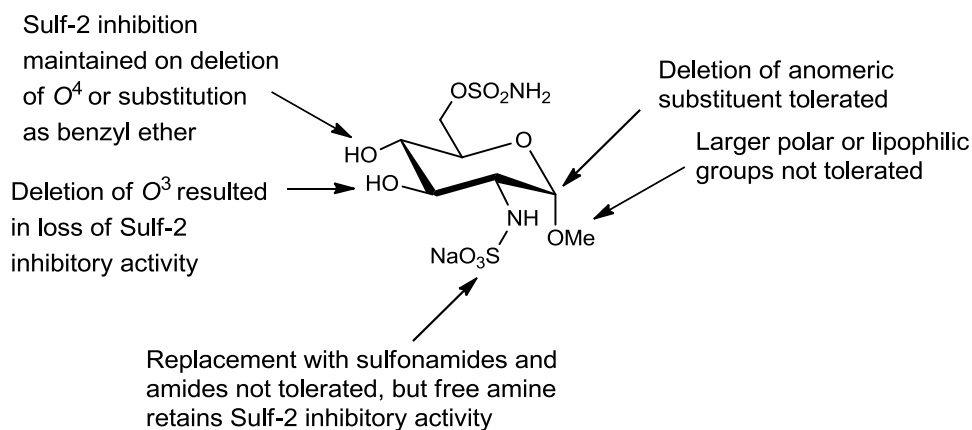
Figure 9.1: Summary of Sulf-2 inhibition SARs for analogues of compound **25**

The second approach attempted the *de novo* design of non-saccharide inhibitors based on a superposition of potential scaffolds onto the solution structure of heparin as a surrogate for the endogenous HSPG ligands. Compounds based on a biphenyl template were designed, and these compounds were synthesised by other colleagues in the group. These compounds have yet to be assayed for sulfatase inhibitory activity.

9.1.1   Potential Future Design Options

Combination of structural features present in the monosaccharide sulfamates with highest per cent inhibition of Sulf-2 may provide more potent inhibitors, and compounds such as **423** and **424** should be assessed. Introduction of alternative substituents at the O^4-position (**425**) should also be investigated.

R = e.g.
4-methoxybenzyl,
CH_2CH_2OH, CH_2CO_2H

423   **424**   **425**
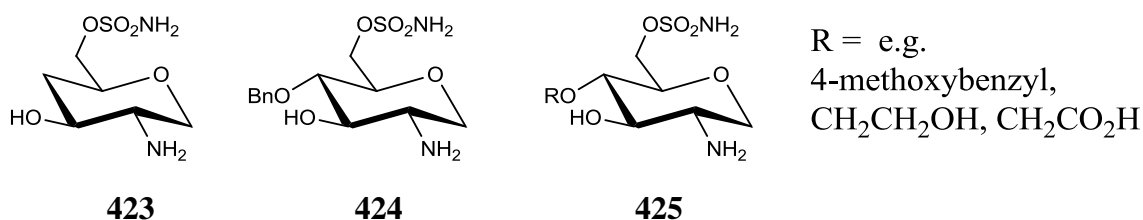
In order to improve the potency of the monosaccharide sulfamate against Sulf-2, it may be necessary to expand the template into di-, tri- or tetra-saccharides, to better mimic the key binding interactions of the endogenous substrate, for example **426**.
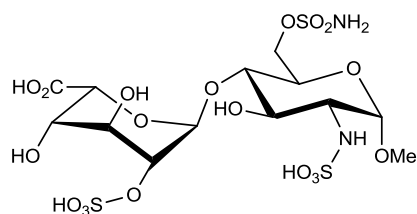
426

Alternative sulfamate isosteres could also be explored, with an initial focus on those that were active in the literature exploration of SARs for ARSC inhibitors (e.g. **427**). Incorporation of the most potent substituents from the simple phenyl sulfamate library (**68-82**) into the most promising compounds from the biaryl series, would explore whether the SAR was additive (**428**).
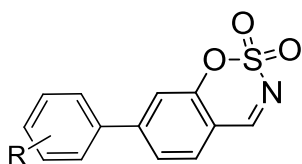
427
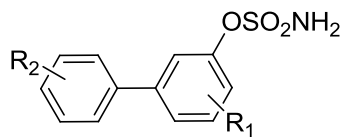
428

9.2 The ERK5 Project

The ERK5 program was a more mature project, with extensive existing knowledge of ERK5 potency SARs in the lead pyrrole carboxylate series. Two sub-classes of the series were the cyclic aliphatic amides, and the heteroaromatic amides. In this thesis, optimisation of the amide substituents of each of this class was attempted, with the aim of improving both potency and ADMET properties. The molecular properties of the lead compounds were assessed relative to the set of marketed kinase inhibitors, to inform the optimisation program, and define ideal physicochemical and structural space.

Combination of optimised amide substituents with a trisubstituted arylketone substitution pattern has provided a set of potent compounds with ERK5 inhibitory activity below 20 nM. In the class 1 aliphatic heterocyclic amides, reduction of efflux in the Caco-2 assay was achieved for **269**, with the *N*-methylpiperidine of **212** replaced by an *N*-trifluoroacetylpiperidine. However, this resulted in a 3-fold loss of ERK5 inhibitory activity relative to **212**, and this series was not pursued further.

212 ERK5; IC_{50} = 199 nM
Caco-2 ER = 9

269 ERK5; IC_{50} = 520 nM
Caco-2 ER = 1.1
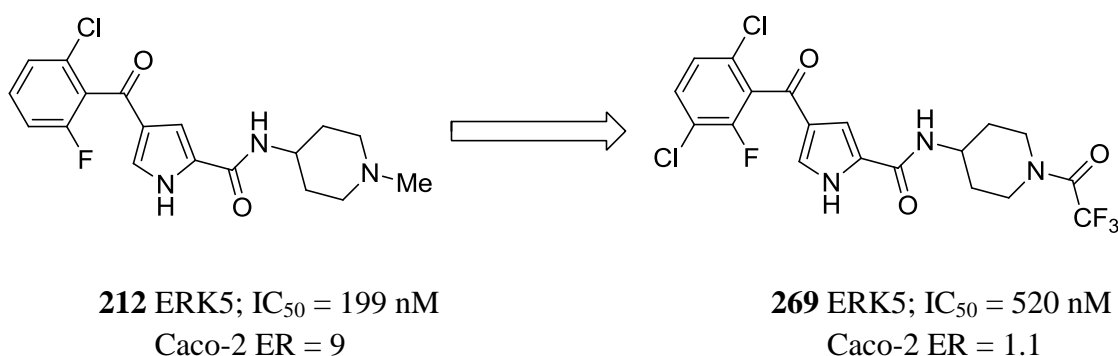
Further work in the cyclic aliphatic amide series may be warranted, to attempt to vary the electronics of the nitrogen subsituent through changes in the fluorination pattern of the amide, for example by preparation of analogues **429**-**432**.

429 R = $COCHF_2$

430 R = $COCH_2F$

431 R = $COCF_2CF_3$

432 R = CH_2CF_3
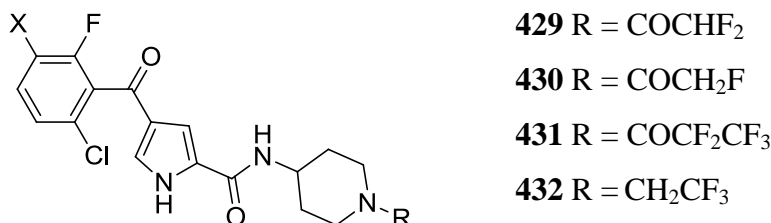
Variation of the position of the basic centre through alternative aminopiperidine regioisomers (**433**), and by adjusting the ring size (**434** and **435**), could also be investigated (Table 9.1).
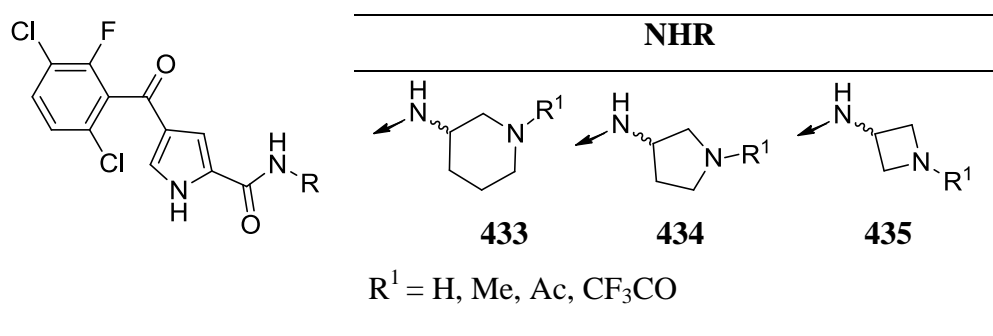
Table 9.1: Possible future analogues of **212**

Substitution on the aliphatic ring carbons could also be investigated, to prepare either bicyclic bridged analogues such as **436**, or incorporating substituents α to the ring nitrogen which may affect the pK_a of the piperidine (e.g. **437**). The aim of these targets would be to combine improved potency with low efflux in the Caco-2 membrane permeability assay.
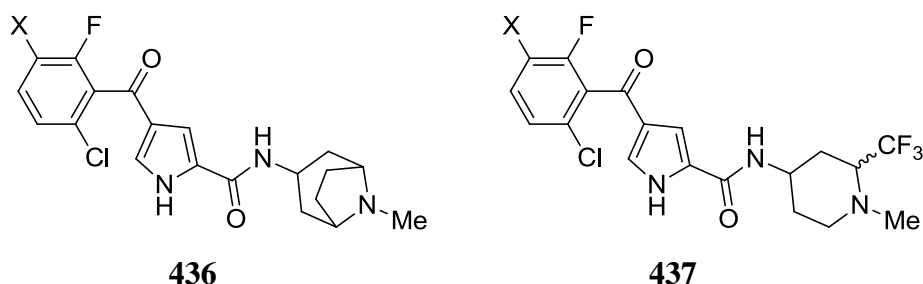
In the heteroaromatic amide series, introduction of a basic centre at the 2-position of the pyrimidine led to improved ERK5 potency. hERG inhibition and microsomal instability issues were successfully overcome, leading to the identification of piperazine **286** and 4-aminopiperidine **289** having ERK5 IC$_{50}$ values below 20 nM. However, these compounds suffered from significant efflux (ER = 30-100) in the Caco-2 membrane permeability assay. Replacement of the pyrimidine with a pyridine led to compounds with similar pharmacological and *in vitro* ADME profiles.

215 ERK5; IC$_{50}$ = 403 nM

286 ERK5; IC$_{50}$ = 13 nM
Caco-2 ER = 36

289 ERK5; IC$_{50}$ = 14 nM
Caco-2 ER = 99
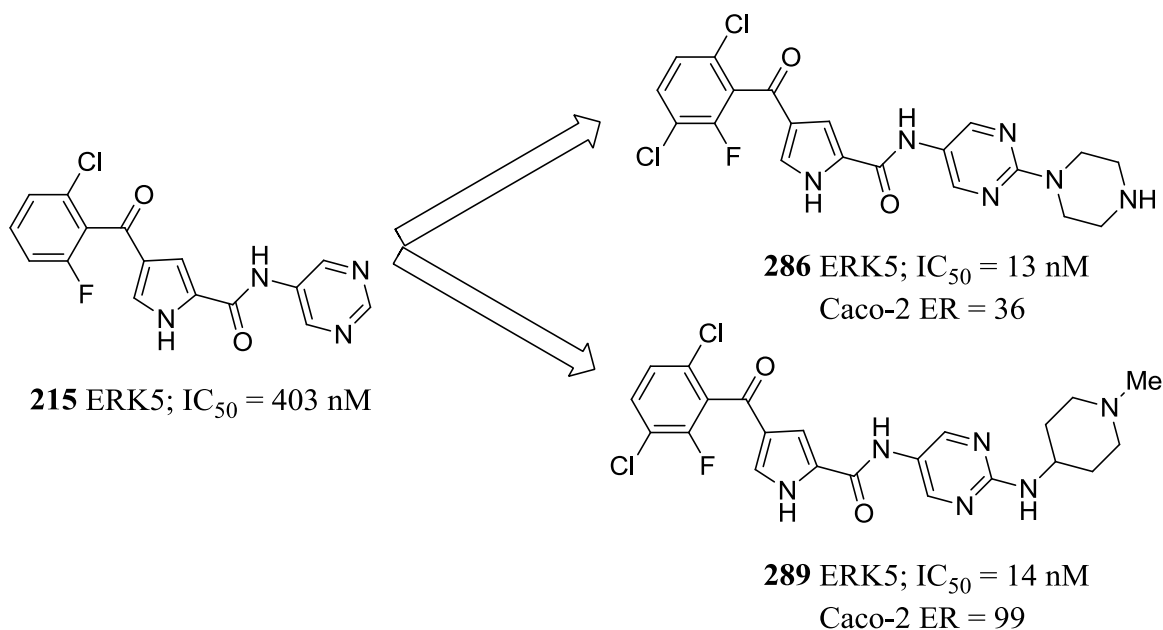
Substitution of the 2-position of 4-pyridyl amides was synthetically challenging. The *N*-methylpiperazine **299** had encouraging ERK5 inhibition, but suffered from metabolic instability and poor solubility. Development of an improved synthetic route to allow rapid exploration of this area would be of interest. Targets which may represent potent ERK5 inhibitors with superior pharmacokinetic and pharmaceutical properties, such as **438** and **439** would be of interest.

299 ERK5; IC$_{50}$ = 36 nM
MLM Cl$_{int}$ 106 μL/min/mg
Sol 3-65 μM

438 R =

439 R =
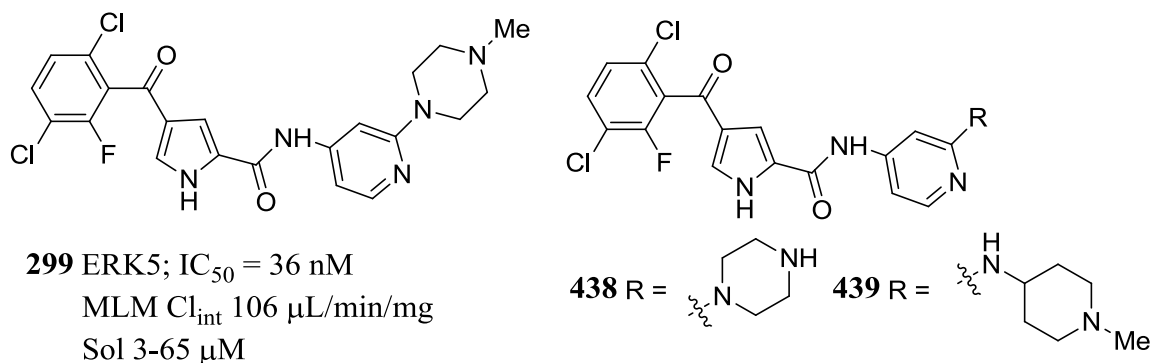
Incorporation of a pyrazole as a replacement for the pyrimidine ring allowed facile introduction of carbon linked substituents, minimising the number of hydrogen bond donor and acceptor groups in the molecule. Compound **305** proved the most potent analogue, having an ERK5 IC$_{50}$ of 7 nM. Efflux in the Caco-2 cell assay was greatly reduced (ER = 4.5) but low intrinsic flux. Related analogue **306** had poor oral bioavailability in an *in vivo* mouse PK study. Investigation of neutral pyrazole substituents led to the identification of

314 as a potent ERK5 inhibitor with high ligand efficiency. This compound had good stability in mouse liver microsomes, high solubility, and a Caco-2 efflux ratio of 0.9, which translated *in vivo* into low clearance and sufficient bioavailability to allow its use as an *in vivo* tool.
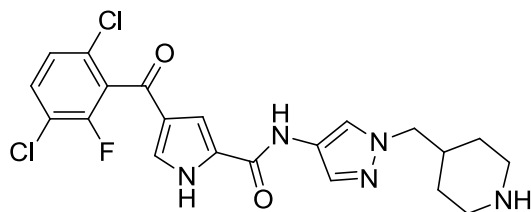
305 ERK5; IC_{50} = 7 nM
Caco-2 ER = 4.5
L.E. = 0.37
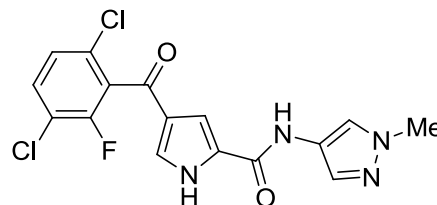
314 ERK5; IC_{50} = 27 nM
Caco-2 ER = 0.9
L.E. = 0.43
Mouse F = 42%
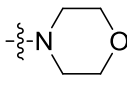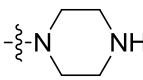
Compound **314** is currently undergoing evaluation in an *in vivo* tumour xenograft model.

Future design options in this series include incorporation of alternative non-basic pyrazole substituents such as **440**-**444**, with the aim of attaining further improvements in potency, whilst maintaining the favourable pharmacokinetic profile.

Cmpd	R
440	CH₂CH₂OH
441	CH₂CH₂SO₂Me
442	oxetane
443	tetrahydrofuran
444	tetrahydropyran

Table 9.2: Possible future pyrazole-linked analogues of **314**.

The tolerance of the benzoyl substituent at the pyrrole 4-position to alternative substituents replacing the 3'-chloro group may also be an area of the template which could be explored in more detail (Table 9.3).

Cmpd	R
445	OEt
446	CH_2CH_2OH
447	
448	
449	
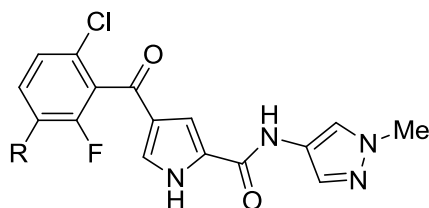
Table 9.3: Possible future analogues of **314** incorporating diversity on the benzoyl group at the pyrrole 4-position.

Thus, the work presented in this thesis has considerably extended the understanding on SARs for ERK5 inhibition in the pyrrole carboxamide series, and has highlighted structural features which improve ERK5 inhibition, and which affect ADMET properties. The key SAR developments are summarised in Figure 9.2. This has provided insights into areas of the template which may benefit from further exploration.
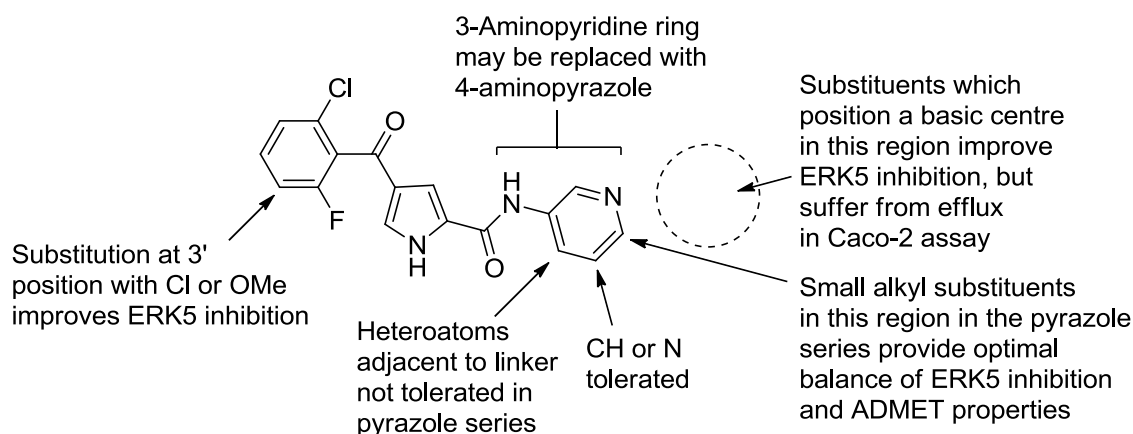
Figure 9.2: Summary of SARs for compound **212** developed or confirmed by the work contained in this thesis.

Chapter 10:   Experimental

10.1 Sulf-2 Project Experimental Procedures

The sulfatase biological assays were performed by Dr Gary Beale and Sari Alhasan.

10.1.1 Sulfatase Biological Assay Protocols

Sulf-2 Assay Protocol

Compounds were screened using 4-MUS as a substrate for Sulf-2 according to a protocol described by Morimoto-Tomita et al.[84] Briefly 293T cells were transiently transfected with pcDNA3.1Myc/His (-)-Sulf-2 DNA (Addgene) using Fugene 6 according to the manufacturers protocol. Conditioned medium containing Sulf-2 was bound to Ni-NTA agarose beads overnight at 4°C. Beads were washed with three times 15 mLs of 50 mM Hepes (pH 7.5), 10 mM $MgCl_2$, 0.05% Tween 20, followed by 15 mLs of 50 mM Hepes (pH 7.5), 10 mM $MgCl_2$. Beads were suspended in reaction buffer 50 mM Hepes (pH 7.5), 10 mM $MgCl_2$ prior to inhibition assays. 20 µLs of bead suspension was incubated with 1 mM compound (in DMSO) plus 10X reaction buffer for 1 h at 37°C. The reaction was started by the addition of 20 µLs of 20 mM 4-MUS (Final Concentration 8 mM) and incubated at 37°C for 1 h. The reaction was stopped with 140 µL 1 M Tris buffer (pH 10.4) and read at 460 nm following excitation at 355 nm in FLUOstar Omega plate reader (BMG Labtech) using Omega data analysis software.

ARSA and ARSB Assay Protocols

Compounds were screened in a 96-well black plate (Sterilin) using 4-MUS as a substrate, using 50 µl reaction mixture containing 40 ng of the commercially available enzymes (ARSA or ARSB from R & D Systems), 50 mM HEPES (pH = 4.5), 10 mM $CaCl_2$, 1 mM test compound (dissolved in DMSO; final concentration of DMSO in reaction = 2%), and H_2O (45 µL). The assay mixture was incubated for 1 h at 37 °C, followed by addition of 5 µL of 4-MUS (Km = 1.6 mM for ARSA and 612 µM for ARSB), and incubation for a further 1 h at 37 °C. The reaction was stopped with 100 µL of 1 M Tris (pH = 10.5) and

read at 460 nm following excitation at 355 nm in FLUOstar Omega plate reader (BMG Labtech) using the Omega data analysis software.

10.2 Summary of Generic Analytical and Chromatographic Conditions

All commercial reagents were obtained from Aldrich Chemical Company or Apollo Scientific Ltd and were of the highest available purity. Unless otherwise stated, chemicals were used as supplied without further purification. Anhydrous solvents were obtained from Aldrich SureSeal™ bottles and were stored under nitrogen. Petrol refers to the fraction with a boiling point between 40 and 60°C. All reactions carried out in a microwave were performed in a Biotage Initiator Sixty apparatus.

The progress of reactions was monitored by thin layer chromatography was conducted on plates pre-coated with silica gel (Merck 60F$_{254}$), NH_2F_{254}s or C18-SiO$_2$. Eluent mixture ratios are quoted as volume:volume. Visualisation was either by short wave (254 nm) ultraviolet light, or by treatment with the visualisation reagent stated. 'Flash' medium pressure liquid chromatography (MPLC) was carried out either on a Biotage SP4 automated purification system or a Varian automated purification system, using pre-packed Varian or Grace silica, amino-bonded or C18 silica cartridges. Elution gradients are quoted as per cent polar component at the start and end of the elution.

Compounds requiring semi-preparative HPLC were purified on one of the following machines: (i) Varian Prostar Modular HPLC system equipped with a binary pumping system, UV detector and fraction collector and controlled by Varian Star software. (ii) Agilent 1200 HPLC system equipped with a binary pump, autosampler, fraction collector and diode array detector and controlled by Agilent ChemStation software.

Melting points were determined with on either a Stuart Scientific SMP3 or SMP40 apparatus and are uncorrected. ^{1}H, ^{13}C and ^{19}F nuclear magnetic resonance (NMR) spectra were obtained as CD$_3$OD, CDCl$_3$, D$_2$O, or DMSO-d^6 solutions and recorded at 500 MHz, 75 MHz, and 125 MHz, respectively, on a Bruker Avance III 500 spectrometer. Where ^{13}C NMR data are not quoted, insufficient material was available or problems obtaining adequate spectra were encountered. Chemical shifts are quoted in parts per million (δ) referenced to the appropriate deuterated solvent employed. Multiplicities are indicated by s (singlet), d (doublet), t (triplet), q (quartet), quin (quintet), sept (septet), m (multiplet) or (br) broad, or combinations thereof. Coupling constant values are given in Hz.

Homonuclear and heteronuclear two dimensional NMR experiments were used where appropriate to facilitate assignment of chemical shifts. LC-MS was carried out on a Waters Acquity LC platform running either positive ion or negative ion electrospray mode, unless otherwise stated. Optical rotations were determined on an Optical Activity PolAAR 3001 polarimeter with a path length of 0.25 dm. IR spectra were recorded on either a Bio-Rad FTS 3000MX diamond ATR or an Agilent Cary 630 FTIR as a neat sample. UV spectra were obtained using a U-2001 Hitachi Spectrophotometer and performed in ethanol. High resolution mass spectra were performed by the EPSRC National Mass Spectrometry Service, University of Wales Swansea, Singleton Park, Swansea, SA2 8PP. Data were compared with literature data for compounds which had been previously reported.

10.2.1 Procedures for the Synthesis of Sulfamoyl Chloride

Method 1: Formic acid (460 μL, 550 mg, 12 mmol, 1 eq) was added dropwise to chlorosulfonyl isocyanate (1.05 mL, 1.7 g, 12 mmol, 1 eq) in anhydrous dichloromethane (5 mL) at 0 °C. Gentle gas evolution was observed. The mixture was allowed to warm to room temperature and stirred at room temperature for 3 h to give a white suspension.

Method 2: Formic acid (460 μL, 550 mg, 12 mmol, 1 eq) was added dropwise to chlorosulfonyl isocyanate (1.05 mL, 1.7 g, 12 mmol, 1 eq) at 0 °C. Gentle gas evolution was observed. The mixture was allowed to warm to room temperature and stirred at room temperature for 3 h to give a white solid. The solid was dissolved in anhydrous toluene (6 mL) to give a clear 2 M solution. Stock solutions were used immediately.

Method 3: Formic acid (460 μL, 550 mg, 12 mmol, 1 eq) was added dropwise to chlorosulfonyl isocyanate (1.05 mL, 1.7 g, 12 mmol, 1 eq) in anhydrous MeCN (5 mL) at 0 °C. Gentle gas evolution was observed. The mixture was allowed to warm to room temperature and stirred at room temperature for 3 h to give a white suspension.

10.2.2 General Procedures for Sulfamoylation of Alcohols and Phenols

Sulfamoylation Method 1: Sulfamoyl chloride (1.5-3 eq.) was added portion-wise over 30 minutes to the substrate alcohol (1 eq.) in anhydrous DMA (2 mL) at -15 °C. The reaction mixture was stirred at -15 °C for 2 h.

Sulfamoylation Method 2: Sulfamoyl chloride (1.5 eq.) was added to the substrate alcohol (1 eq.) in anhydrous DMF (4 mL/mmol) at -40 °C over 15 minutes. The mixture was stirred at -40 °C for 18 h. The reaction was quenched with water (2 mL) and extracted with EtOAc (20 mL). Saturated $NaCl_{(aq)}$ (10 mL) added to aqueous layer and further extracted with EtOAc (3×20 mL). The organic layers were combined, dried ($MgSO_4$) and the solvent was removed *in vacuo*.

Sulfamoylation Method 3: Sulfamoyl chloride (1.5 eq.) was added to the substrate alcohol (1 eq.) in anhydrous MeCN (5.4 mL) containing 600 μL DMA at room temperature. The mixture was stirred at room temperature for 15 min, quenched with EtOH (1.5 mL) and partitioned between EtOAc (2×10 mL) and H_2O (10 mL). The aqueous layer was extracted with a further 10 mL of CH_2Cl_2, the organic extracts were combined, dried over $MgSO_4$ and solvent removed *in vacuo*.

Sulfamoylation Method 4: Sulfamoyl chloride (2 eq.) was added to the substrate alcohol (1 eq.) in DMA at 0 °C. The mixture was stirred at r.t. overnight, and then quenched with water. The mixture was extracted with EtOAc (2×20 mL), washed with brine, dried over $MgSO_4$, filtered and the solvent removed *in vacuo*.

10.2.3 Sulf-2 General Synthetic Procedures

General Procedure A: Deprotection of Benzyl Carbamate using Palladium-Catalysed Flow Hydrogenation

The appropriate benzyl carbamate (1 eq.) was dissolved in MeOH (25 mL/mmol) and hydrogenated on a Thales H-cube over 10% Pd/C on full H_2 mode at 40 °C for 18 h with continuous recycling of the reaction mixture. The solvent was removed *in vacuo*.

General Procedure B: Chemoselective *N*-Sulfation

The substrate amine (1 eq.) was dissolved in de-ionised water (6 mL/mmol) and the pH of the solution was adjusted to between pH 9 and 10 with NaOH (2 M aq.). Pyridine-sulfur trioxide complex (1.1 eq.) was added portion-wise at 30 minute intervals. After each addition the pH of the solution was adjusted to pH 9-10 by the addition of 2 M aqueous NaOH. The mixture was stirred at room temperature for 2 h and the solvent removed *in vacuo*.

General Procedure C: Synthesis of Trichloroethysulfate Protected Amines

2,3-Dimethyl-1-((2,2,2-trichloroethoxy)sulfonyl)-1*H*-imidazol-3-ium tetrafluoroborate (1 eq.) was added to the substrate alcohol (1 eq.) in THF (10 mL/mmol) at r.t., and the mixture was stirred at room temperature for 18 h. The solvent was removed *in vacuo.*

10.3 Synthesis of Compounds for the Sulf-2 Project

10.3.1 Synthesis of monosaccharide sulfamates

Nomenclature

The monosaccharide sulfamates prepared below have been titled using their IUPAC names. However, NMR peaks have been assigned using the common saccharide numbering system. This allows direct comparison with NMR assignments from the carbohydrate chemistry literature for known compounds. The numbering system used for the NMR assignments is outlined on the generic structures below.
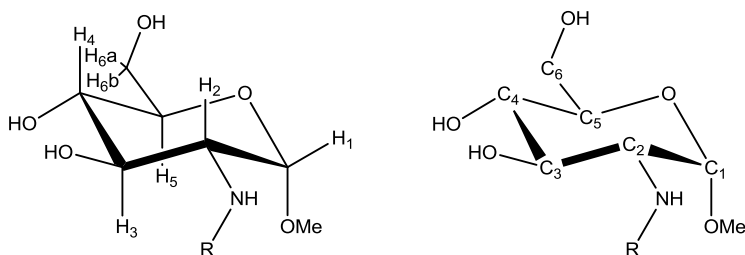
N-((3R,4S,5S,6R)-4,5-dihydroxy-6-(hydroxymethyl)-2-methoxy tetrahydro-2H-pyran-3-yl)acetamide (107)
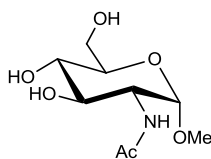
Amberlite IR120 (H$^+$) ion exchange resin (1.25 g) was added to N-acetylglucosamine (1 g, 4.5 mmol) in anhydrous MeOH (30 mL) and heated to reflux for 18 h. The mixture was allowed to cool to r.t., filtered, and the solvent removed *in vacuo*. Dowex 1X8 200-400 mesh ion exchange resin in the chloride form (400 g) was suspended in 2 volumes of water. This suspension was allowed to stand for 2 minutes and the resin decanted away from large settled particles. The suspension was then allowed to stand for a further 90 minutes, and the supernatant decanted away from resin. The remaining resin was re-suspended in 2 volumes of water and packed into a glass column (50 cm × 4 cm). The column was eluted with NaOH (2 M aq.) until the pH of the eluant reached pH 14 to convert resin to OH$^-$ form. The column was then eluted with water until the pH of eluant returned to neutral. The crude compound mixture was dissolved in water (3 mL) and eluted under gravity at a rate of 3 mL/min, collecting 15 mL fractions. Fractions were analysed for the presence of compound by spotting onto SiO$_2$ TLC plates and staining with anisaldehyde visualisation reagent. Six fractions containing compound were individually frozen and lyophilised overnight and analysed by ^{1}H NMR to determine purity and anomer composition. Fractions containing levels of β anomer below the detection limit of ^{1}H NMR were combined to give a white solid (466 mg, 44%). R_f 0.3 (40% MeOH/CH$_2$Cl$_2$, anisaldehyde); m.p. 190-192 °C; λ_{max}(EtOH)/nm < 210 nm; IR ν_{max}/cm^{-1} 3288 (br), 2928, 1645 (amide I), 1550 (amide II); ^{1}H NMR (500 MHz; CD$_3$OD) δ_H 1.88 (3H, s, CH$_3$CO), 3.25 (1H, dd, J = 9.9 and 8.9 Hz, H-4), 3.27 (3H, s, OCH$_3$), 3.53 (1H, dd, J = 10.6 and 8.9 Hz, H-3), 3.42-3.47 (1H, m, H-5), 3.59 (1H, dd, J = 11.9 and 5.7 Hz, H-6$_a$), 3.73 (1H, dd, J = 11.9 and 2.4 Hz, H-6$_b$), 3.80 (1H, dd, J = 10.6 and 3.6 Hz, H-2), 4.55 (1H, d, J = 3.6 Hz, H-1); ^{13}C NMR (125 MHz; CD$_3$OD) δ_C 22.6 (CH$_3$CO), 55.4 (CH$_3$O), 55.5 (C-2), 62.8 (C-6), 72.4 (C-4), 73.0 (C-3), 73.7 (C-5), 99.8 (C-1), 173.7 (CO); MS (ESI+) *m/z* 236.2 [M+H]$^+$.

((2*R*,3*S*,4*R*,5*R*,6*S*)-5-Acetamido-3,4-dihydroxy-6-methoxytetrahydro-2*H*-pyran-2-yl)methyl sulfamate (27)
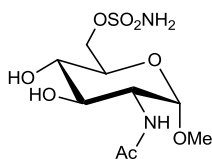
Prepared according to sulfamoylation method 1 using sulfamoyl chloride (0.6 mL, 1.0 M in toluene, 0.60 mmol, 1.5 eq.), alcohol **107** (100 mg, 0.43 mmol, 1 eq.) and DMA (2 mL) at -15 °C with stirring at -15 °C for 2 h. The reaction was quenched with water (0.3 mL) and MeOH (2 mL) and the solvent was removed *in vacuo*. The residue was azeotroped with toluene (2 × 10 mL) and purified by MPLC on SiO$_2$ with gradient elution from 2-10% MeOH/EtOAc to give a white solid (44 mg, 35%). R_f 0.2 (5% MeOH/EtOAc; anisaldehyde); m.p. 182-184 °C dec.; λ_{max}(EtOH)/nm < 210 nm; IR ν_{max}/cm^{-1} 3325, 1641 (amide I), 1542 (amide II), 1365 (SO), 1182 (SO); ^{1}H NMR (500 MHz; CD$_3$OD) δ_H 2.02 (3H, s, CH$_3$CO), 3.39 (1H, dd, *J* = 10.0 and 8.8 Hz , H-4), 3.42 (s, 3H, OCH$_3$), 3.68 (1H, dd, *J* = 10.7 and 8.8 Hz, H-3), 3.81 (1H, ddd, *J* = 10.0, 6.0 and 1.9 Hz, H-5), 3.95 (1H, dd, *J* = 10.7 and 3.6 Hz, H-2), 4.30 (1H, dd, *J* = 10.8 and 6.0 Hz, H-6$_a$), 4.45 (1H, dd, *J* = 10.8 and 1.9 Hz, H-6$_b$), 4.69 (1H, d, *J* = 3.6 Hz, H-1); ^{13}C NMR (125 MHz; CD$_3$OD) δ_C 22.6 (*C*H$_3$CO), 55.2 (C-2), 55.7 (OCH$_3$), 70.1 (C-6), 71.3 (C-5), 72.1 (C-4), 72.9 (C-3), 99.9 (C-1); HRMS calcd for C$_9$H$_{19}$N$_2$O$_8$S [M+H]$^+$ 315.0857, found 315.0860.

Two other *bis*-sulfamate by-products were also isolated from this reaction, and characterised as the following two compounds:-

((2*R*,3*R*,4*R*,5*R*,6*S*)-5-acetamido-3-hydroxy-6-methoxy-3-((aminosulfonyl)oxy)tetrahydro-2*H*-pyran-2-yl) methyl sulfamate (115)
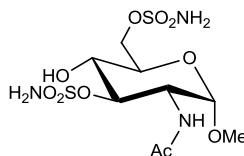
Bis-sulfamate **115** was isolated as a by-product from the synthesis of sulfamate **27** as a white solid. R_f 0.4 (5% MeOH/EtOAc, anisaldehyde); m.p. 118-120 °C; λ_{max}(EtOH)/nm <210 nm; ^{1}H NMR (500 MHz; CD$_3$OD) δ_H 1.88 (3H, s, CH$_3$CO), 3.32 (3H, s, OCH$_3$), 3.51 (1H, dd, 10.0 and 8.8 Hz, H-4), 3.77 (1H, ddd, *J* = 10.0, 5.5 and 1.9 Hz, H-5), 4.09 (1H, dd, *J* = 10.6 and 3.5 Hz, H-2), 4.21 (1H, dd, *J* = 10.9 and 5.5 Hz, H-6$_a$), 4.32 (1H, dd, *J* =

10.9 and 1.9 Hz, H-6$_b$), 4.49 (1H, dd, J = 8.8 and 10.6 Hz, H-3), 4.59 (1H, d, J = 3.5 Hz, H-1); ^{13}C NMR (125 MHz; CD$_3$OD) δ_C 22.7 (*C*H$_3$CO), 53.2 (C-2), 55.8 (OCH$_3$), 65.6 (C-6), 70.2 (C-4), 71.3 (C-5), 83.0 (C-3), 100.0 (C-1), 173.8 (CO); HRMS calcd for C$_9$H$_{18}$N$_3$O$_{10}$S$_2$ [M-H]$^-$ 392.0439, found 392.0437.

((2*R*,3*S*,4*R*,5*R*,6*S*)-5-Acetamido-4-hydroxy-6-methoxy-4-((amino sulfonyl)oxy) tetrahydro-2*H*-pyran-2-yl) methyl sulfamate (116)
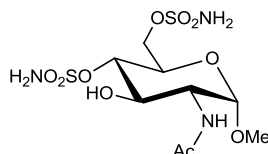
Bis-sulfamate **116** was isolated as a by-product from the synthesis of sulfamate **27** as a white solid. R_f 0.3 (5% MeOH/EtOAc, anisaldehyde); m.p. 170-174 °C; λ_{max}(EtOH)/nm <210 nm; IR ν_{max}/cm^{-1} 3288 (br), 1662 (amide I), 1540 (amide II), 1349 (SO), 1172 (SO); ^{1}H NMR (500 MHz; CD$_3$OD) δ_H 1.88 (3H, s, CH$_3$CO), 3.30 (3H, s, OCH$_3$), 3.77 (1H, dd, J = 10.9 and 8.9 Hz, H-3), 3.87 (1H, ddd, J = 10.1, 6.6 and 2.1 Hz, H-5), 3.94 (1H, dd, J =10.9 and 3.6 Hz, H-2), 4.14 (1H, dd, J =11.1 and 6.6 Hz, H-6$_a$), 4.22 (1H, dd, J = 10.1 and 8.9 Hz, H-4), 4.37 (1H, dd, J = 11.1 and 2.1 Hz, H-6$_b$), 4.59 (1H, d, J = 3.6 Hz, H-1); ^{13}C NMR (125 MHz; CD$_3$OD) δ_C 22.5 (CH$_3$CO), 55.2 (OCH$_3$), 55.9 (C-2), 69.0 (C-5), 69.4 (C-6), 71.2 (C-3), 80.3 (C-4), 99.4 (C-1), 173.8 (CO); HRMS calcd for C$_9$H$_{23}$N$_4$O$_{10}$S$_2$ [M+NH$_4$]$^+$ 411.0850, found 411.0851.

Benzyl ((3*R*,4*R*,5*S*,6*R*)-2,4,5-trihydroxy-6-(hydroxymethyl)tetrahydro-2H-pyran-3-yl)carbamate (102) [336]
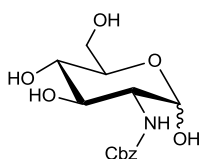
NaHCO$_{3(s)}$ (9.3 g, 110.7 mmol, 3 eq.) was added to a solution of D-glucosamine hydrochloride (7.7 g, 35.7 mmol, 1 eq.) in H$_2$O (230 mL). Benzyl chloroformate (5.60 mL, 39.3 mmol, 1.1 eq.) was added portion-wise over 30 min and the mixture was stirred at room temperature for 18 h. The white precipitate formed was filtered off, azeotroped with toluene (2 × 50 mL) and dried *in vacuo* at 45 °C to give the product mixture of anomers as a white solid (10.25 g, 92 %). R_f 0.2 (10% MeOH/CH$_2$Cl$_2$; anisaldehyde); mp 180 °C dec.; λ_{max}(EtOH)/nm < 210; IR ν_{max}/cm^{-1} 3297, 1681 (carbamate I), 1543 (carbamate II); ^{1}H NMR (500 MHz; CD$_3$OD) δ_H 3.27-3.47 (2H, m), 3.56-3.90 (4H, m), 4.59 (0.3 H, d, J =

8.2 Hz, β anomer H-1), 5.11 (2H, s, CH$_2$Ph), 5.14 (0.7 H, d, J = 3.3 Hz, α anomer H-1), 7.26-7.44 (5H, m, H-Ar); ^{13}C NMR (125 MHz; CD$_3$OD) δ$_C$ 57.7 (C-2), 67.5, 62.8, 72.5, 72.9, 73.1, 78.0, 93.0, 97.3 (C-1), 128.9 (C-Ar), 129.5 (C-Ar), 138.3 (C-Ar), 158.9 (CO); MS (ESI-) m/z 312.2 [M-H]$^-$.

Benzyl((2S,3R,4R,5S,6R)-4,5-dihydroxy-6-(hydroxymethyl)-2-methoxy tetrahydro - 2H-pyran-3-yl) carbamate (103)
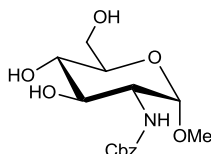
Carbamate **102** (5 g, 16 mmol) was suspended in a 1.25 M solution of HCl in methanol (40 mL) and heated to 80 °C for 18 h. The resulting solution was evaporated and the residue purified by MPLC on SiO$_2$ with a gradient elution from 2-12% MeOH/CH$_2$Cl$_2$. Product containing fractions were combined and evaporated to give a white solid (3.8 g, 73%). R_f 0.3 (10% MeOH/CH$_2$Cl$_2$; anisaldehyde); mp 159-160 °C; [α]$_D^{22.8}$ +84.8° (c = 1.0, MeOH); λ$_{max}$(EtOH)/nm 204; IR ν $_{max}$/cm^{-1} 3330 br, 1678 (carbamate I), 1539 (carbamate II); ^{1}H NMR (500 MHz; CD$_3$OD) δ$_H$ 3.36-3.40 (1H, m, H-4), 3.52-3.67 (3H, m, H-2, H-3, H-5), 3.71 (1H, dd, , J = 11.8 and 5.7 Hz, H-6$_a$), 3.84 (1H, dd, J = 11.8 and 2.1 Hz, H-6$_b$), 4.70 (1H, d, J = 3.2 Hz, H-1), 5.11 (2H, s, CH$_2$Ph), 7.28-7.41 (5H, m, H-Ar); ^{13}C NMR (125 MHz; CD$_3$OD) δ$_C$ 55.5 (OMe), 56.1 (C-2), 62.7 (C-6), 67.6 (CH$_2$Ph), 72.3 (C-4), 73.2 (C-5), 73.7 (C-3), 100.2 (C-1), 128.9 (C-Ar), 129.4 (C-Ar), 138.3 (C-Ar), 158.9 (CO); MS (ESI-) m/z 313.1[M-H]$^-$; (ESI+) m/z 315.2 [M+H]$^+$.

((2R,3S,4R,5R,6S)-5-(((Benzyloxy)carbonyl)amino)-3,4-dihydroxy-6-methoxy tetrahydro-2H-pyran-2-yl)methyl sulfamate (104)
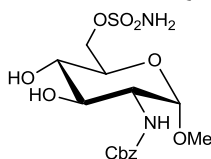
Prepared according to sulfamoylation method 2 using sulfamoyl chloride (1.0 mL, 1.0 M in toluene, 1.0 mmol, 1.65 eq.), alcohol **103** (200 mg, 0.61 mmol, 1 eq.) and DMF (4 mL) at -40 °C. The mixture was stirred at -40 °C for 18 h, quenched by cautious addition of water (2 mL) and extracted with EtOAc (20 mL). Saturated NaCl$_{(aq)}$ (10 mL) added to aqueous layer and further extracted with EtOAc (3 × 20 mL). The organic layers were combined, dried (MgSO$_4$) and the solvent was removed *in vacuo*. The residue was purified

by MPLC on SiO$_2$ with a gradient elution from 50% EtOAc/petrol to 100% EtOAc to 10% MeOH/EtOAc to give a white solid (136 mg, 55%). R_f 0.5 (5% MeOH/EtOAc; anisaldehyde); mp 104-106 °C; $[\alpha]_D^{22.6}$ +40.93° (c = 0.43, MeOH); λ_{max}(EtOH)/nm 257.5 (weak), 210; IR ν_{max}/cm^{-1} 3377, 3332, 3236, 1685 (carbamate I), 1542 (carbamate II), 1372 (SO), 1180 (SO); ^{1}H NMR (500 MHz; DMSO-d^6) δ_H 3.14 (1H, m, H-4), 3.26 (3H, s, OCH$_3$), 3.39-3.51 (2H, m, H-2 and H-3), 3.60 (1H, ddd, J = 1.6, 6.6 and 8.0 Hz, H-5), 4.08 (1H, dd, J = 6.6 and 10.6 Hz, H-6$_a$), 4.28 (1H, dd, J = 1.6 and 10.6 Hz, H-6$_b$), 4.61 (1H, d, J = 3.2 Hz, H-1), 4.91 (1H, d, J = 5.6 Hz, OH-3), 5.01 (1H, d, J = 12.5 Hz, CH_aH$_b$Ph), 5.05 (1H, d, J = 12.5 Hz, CH$_a$$H_b$Ph), 5.31 (1H, d, J = 5.7 Hz, OH-4), 7.18 (1H, d, J = 7.9 Hz, NHCO$_2$Bn), 7.29-7.41 (5H, m, H-Ar), 7.49 (2H, br s, OSO$_2$NH$_2$); ^{1}H NMR δ_H (500 MHz; CD$_3$OD) 3.36-3.44 (4H, m, OCH$_3$ and H-4), 3.58-3.68 (2H, m, H-2 and H-3), 3.79 (1H, ddd, J = 9.9, 6.0 and 1.6 Hz, H-5), 4.27 (1H, dd, J = 10.7 and 6.0 Hz, H-6$_a$), 4.42 (1H, dd, J = 10.7 and 1.6 Hz, H-6$_b$), 4.70 (1H, d, J = 3.2 Hz, H-1), 5.11 (2H, s, CH$_2$Ph), 7.29-7.41 (5H, m, H-Ar); ^{13}C NMR (125 MHz; CD$_3$OD) δ_C 55.7 (OCH$_3$), 57.1 (C-2), 67.6 (CH$_2$Ph), 70.1 (C-6), 71.3 (C-5), 72.0 (C-4), 73.1 (C-3), 100.2 (C-1), 128.9 (C-Ar), 129.0 (C-Ar), 129.5 (C-Ar), 138.3 (C-Ar), 158.9 (CO); HRMS calc. for C$_{15}$H$_{23}$N$_2$O$_9$S [M+H]$^+$ 407.1119, found 407.1119.

((2R,3S,4R,5R,6S)-5-Amino-3,4-dihydroxy-6-methoxytetrahydro-2H-pyran-2-yl)methyl sulfamate (105)

Prepared according to general procedure A using sulfamate **104** (1.525 g, 3.8 mmol), MeOH (90 mL) and CH$_2$Cl$_2$ (30 mL) for 18 h to give a white solid (1.015 g, 99%). R_f 0.05 (CH$_2$Cl$_2$/MeOH/NH$_4$OH 80:20:3; anisaldehyde); mp 104-112 °C; $[\alpha]_D^{17.1}$ +59.2° (c = 0.5, MeOH); λ_{max}(EtOH)/nm <220; IR ν_{max}/cm^{-1} 3297, 1359 (SO), 1176 (SO); ^{1}H NMR (500 MHz; CD$_3$OD) δ_H 3.17 (1H, dd, J = 10.5 and 3.7 Hz, H-2), 3.40 (1H, dd, J = 10.1 and 8.9 Hz, H-4), 3.5 (3H, s, OCH$_3$), 3.77 (1H, dd, J = 10.5 and 8.9 Hz, H-3), 3.84 (1H, ddd, J = 10.1, 5.8 and 2.0 Hz, H-5), 4.31 (1H, dd, J = 10.9 and 5.8 Hz, H-6$_a$), 4.45 (1H, dd, J = 10.9 and 2.0 Hz, H-6$_b$), 4.94 (1H, d, J = 3.7 Hz, H-1); ^{13}C NMR (125 MHz; CD$_3$OD) δ_C 55.8 (OCH$_3$), 56.2 (C-2), 69.8 (C-6), 71.5 (C-4), 71.6 (C-5), 73.6 (C-3), 99.4 (C-1); HRMS calc. for C$_7$H$_{17}$N$_2$O$_7$S [M+H]$^+$ 273.0751, found 273.0755.

Ammonium ((2*S*,3*R*,4*R*,5*S*,6*R*)-4,5-dihydroxy-2-methoxy-6-((sulfamoyloxy)methyl)tetrahydro-2*H*-pyran-3-yl)sulfamate (25)

Prepared according to general procedure B, using amine **105** (140 mg, 0.52 mmol, 1 eq.), de-ionised water (3 mL) and pyridine-sulfur trioxide complex (90 mg, 0.565 mmol, 1.1 eq.). The crude product was purified by MPLC on SiO_2 with a gradient elution from 70/30/3 to 35/65/3 CH_2Cl_2/MeOH/NH_4OH to give an off-white solid (81 mg, 0.23 mmol, 43%); (Found: C, 21.4; H, 5.1; N, 10.5; C, 21.6; H, 5.1; N, 11.1; calcd for $C_7H_{19}N_3O_{10}S_2 \cdot H_2O$: C, 21.7; H, 5.5; N, 10.9); R_f 0.1 (MeOH/NH_3 95:5; anisaldehyde); mp 125-135 °C; $[\alpha]_D^{16.9}$ +103.13° (c = 0.32, MeOH); λ_{max}(EtOH)/nm < 220; IR ν_{max}/cm^{-1} 3218, 3084, 1356 (SO), 1170 (SO); ^{1}H NMR (500 MHz; DMSO-d^6) δ_H 3.01 (1H, ddd, *J* = 3.5, 8.0 and 10.7 Hz, H-2), 3.12 (1H, ddd, *J* = 5.6, 8.5 and 9.9 Hz, H-4), 3.28 (3H, s, OCH₃), 3.40-3.46 (1H, m, H-3), 3.60 (1H, ddd, *J* = 1.6, 6.9 and 9.9 Hz, H-5), 4.08 (1H, dd, *J* = 6.9 and 10.1 Hz, H-6$_a$), 4.20 (1H, d, *J* = 8.0 Hz, NHSO₃⁻), 4.31 (1H, dd, *J* = 1.6 and 10.1 Hz, H-6$_b$), 4.69 (1H, d, *J* = 3.5 Hz, H-1), 5.24 (1H, d, *J* = 5.6 Hz, OH-4), 5.49 (1H, d, *J* = 2.2 Hz, OH-3), 7.09 (4H, br s, NH₄⁺), 7.50 (2H, br s, OSO₂NH₂); ^{1}H NMR (500 MHz; D₂O) δ_H 3.30 (1H, dd, *J* = 10.0 and 3.6 Hz, H-2), 3.47 (3H, s, OCH₃), 3.57 (1H, app t, *J* = 10.0 Hz, H-4), 3.64 (1H, app t, *J* = 10.0 Hz, H-3), 3.95 (1H, ddd, *J* = 10.0, 4.6, and 2.3 Hz, H-5), 4.47 (1H, dd, *J* = 11.2 and 4.6 Hz, H-6$_a$), 4.51 (1H, dd, *J* = 11.2 and 2.3 Hz, H-6$_b$), 5.07 (1H, d, *J* = 3.6 Hz, H-1); ^{13}C NMR (125 MHz; D₂O) δ_C 55.5 (OCH₃), 57.6 (C-2), 68.9 (C-6), 69.1 (C-5), 69.5 (C-4), 71.3 (C-3), 98.7 (C-1); HRMS calc. for $C_7H_{15}N_2O_{10}S_2$ [M-H]⁻ 351.074, found 351.074.

2,2,2-Trichloroethyl ((2*S*,3*R*,4*R*,5*S*,6*R*)-4,5-dihydroxy-2-methoxy-6-(sulfamoyloxy)methyl)tetrahydro-2*H*-pyran-3-yl)sulfamate (117)

Amine **105** (50 mg, 0.18 mmol, 1 eq.) and 2,3-dimethyl-1-((2,2,2-trifluoroethoxy)sulfonyl)-1*H*-imidazol-3-ium tetrafluoroborate (70 mg, 0.18 mmol, 1 eq.) were combined in THF and stirred at r.t. for 18 h. The solvent was removed *in vacuo* and

the residue purified by MPLC on SiO_2 with gradient elution from 60-80% EtOAc/petrol to give a clear gum (54 mg, 61%); R_f 0.55 (EtOAc; anisaldehyde); λ_{max}(EtOH)/nm <220; $[\alpha]_D^{19.5}$ +106.7° (c = 0.15, EtOH); IR ν_{max}/cm^{-1} 3281 (br), 2926, 1358 (SO), 1178 (SO); ^{1}H NMR (500 MHz; DMSO-d^6) δ_H 3.17-3.24 (2H, m, H-4 and H-2), 3.36 (3H, s, OMe), 3.49-3.55 (1H, ddd, J = 6.0, 8.7, and 10.4 Hz, H-3), 3.65 (1H, ddd, J = 1.7 , 6.5 and 9.9 Hz, H-5), 4.08-4.15 (1H, m, H-6$_a$), 4.32 (1H, dd, J = 1.7 and 10.4 Hz, H-6$_b$), 4.67 (1H, d, J = 11.2 Hz, CH_aH$_b$CCl$_3$), 4.73 (1H, d, J = 3.6 Hz, H-1), 4.91 (1H, d, J = 11.2 Hz, CH$_a$$H_bCCl_3$), 5.41-5.48 (2H, m, OH^3 and OH^4), 8.77 (1H, s, CHNH), 7.53 (2H, s, NH$_2$); ^{13}C NMR (125 MHz; DMSO-d^6) δ_C 54.7 (OMe), 58.2 (C-2), 68.3 (C-6), 69.5 (C-5), 70.2 (C-3), 70.5 (C-4), 77.4 (CH$_2$CCl$_3$), 98.1 (C-1); HRMS calcd for $C_9H_{16}N_2O_{10}S_2{}^{35}Cl_3$ [M-H]$^-$ 480.9317, found 480.9314.
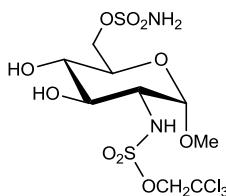
((2R,3S,4R,5R,6S)-3,4-Dihydroxy-6-methoxy-5-(methylsulfonamido) tetrahydro-2H-pyran-2-yl)methyl sulfamate (48)
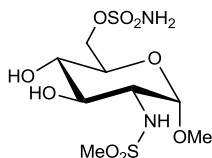
Methanesulfonyl chloride (76 μL, 0.77 mmol, 1.05 eq.) was added dropwise to amine **105** (200 mg, 0.74 mmol, 1 eq.) and *N,N*-diisopropylethylamine (192 μL, 1.1 mmol, 1.5 eq.) in anhydrous dichloromethane (2 mL) and dioxane (2 mL) at 0 °C. The mixture was stirred at 0 °C for 1 h. A further 19 μL (0.19 mmol, 0.25 eq.) of methanesulfonyl chloride was added and the mixture stirred at 0 °C for 1 h. Water was added, and the mixture extracted with CH_2Cl_2 (2 × 10 mL). The organic layer was evaporated *in vacuo* and purified by MPLC on SiO_2 with a gradient elution from EtOAc to 8% MeOH/EtOAc to give a clear gum (73 mg, 0.21 mmol, 28%). R_f 0.2 (CH_2Cl_2/MeOH 90:10; anisaldehyde); $[\alpha]_D^{22.6}$ +41.48° (c = 0.27, MeOH); λ_{max}(EtOH)/nm < 220; IR ν_{max}/cm^{-1} 3316 br, 2938, 1368 (SO), 1178 (SO); ^{1}H NMR (500 MHz; CD$_3$OD) δ_H 3.08 (3H, s, CH$_3$SO$_2$), 3.32-3.37 (2H, m, H-2 and H-4), 3.45 (1H, s, OCH$_3$), 3.64 (1H, dd, J = 10.4 and 8.8 Hz, H-3), 3.80 (1H, ddd, J = 10.1 , 5.9, and 2.0 Hz, H-5), 4.29 (1H, dd, J = 10.7 and 5.9 Hz, H-6$_a$), 4.44 (1H, dd, J = 10.7 and 2.0 Hz, H-6$_b$), 4.72 (1H, d, J = 3.6 Hz, H-1); ^{13}C NMR (125 MHz; CD$_3$OD) δ_C 41.1 (CH$_3$SO$_2$), 55.5 (OCH$_3$), 57.3 (C-2), 68.8 (C-6), 69.3 (C-5), 69.6 (C-4), 71.4 (C-3), 99.4 (C-1); HRMS calc. for $C_9H_{17}N_2O_9S_2$ [M-H]$^-$ 349.0381, found 349.0383.

((2R,3S,4R,5R,6S)-3,4-Dihydroxy-6-methoxy-5-(trifluoromethylsulfonamido) tetrahydro-2H-pyran-2-yl)methyl sulfamate (49)
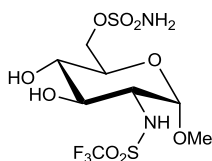
Trifluoromethanesulfonic anhydride (62 μL, 0.37 mmol, 1 eq.) was added to amine **105** (100 mg, 0.37 mmol, 1 eq.) and triethylamine (57 μL, 0.44 mmol, 1.2 eq.) in a mixture of dioxane (8 mL) and dichloromethane (2 mL) at 0 °C. The mixture was stirred at 0 °C for 1 h, and then further trifluoromethanesulfonic anhydride (31 μL, 0.18 mmol, 0.5 eq.) was added at 0 °C. The mixture was stirred at 0 °C for a further 1 h, and then quenched by the cautious addition of water. The mixture was extracted with CH_2Cl_2 (2 × 20 mL). The aqueous layer was diluted with saturated $NaCl_{(aq)}$ and extracted with further CH_2Cl_2 (2 × 20 mL). The organic layers were combined, dried over $MgSO_4$, and the solvent was removed *in vacuo*. The residue was purified by MPLC on SiO_2 with a gradient elution from 2-15% $MeOH/CH_2Cl_2$ to give a clear gum which was dissolved in EtOAc (20 mL) and washed with water (4 × 30 mL). The organic layer was dried over $MgSO_4$ and the solvent removed *in vacuo* to give a white solid (55 mg, 0.14 mmol, 37%). R_f 0.6 (CH_2Cl_2/MeOH 80:20; anisaldehyde,); mp 55-65 °C; $[\alpha]_D^{22.6}$ +95.5° (c = 0.18, MeOH); λ_{max}(EtOH)/nm <220; IR ν_{max}/cm^{-1} 3274 (br), 2923, 2851, 1363 (SO), 1178 (SO); ^{1}H NMR (500 MHz; CD_3OD) δ_H 3.35-3.42 (2H, m, H-2 and H-4), 3.46 (3H, s, OCH$_3$), 3.65 (1H, dd, J = 10.4 and 8.8 Hz, H-3), 3.81 (1H, ddd, J = 10.0 Hz, 6.0 and 2.0 Hz, H-5), 4.28 (1H, dd, J = 10.8 and 6.0 Hz, H-6$_a$), 4.44 (1H, dd, J = 10.8 and 2.0 Hz, H-6$_b$), 4.73 (1H, d, J = 3.6 Hz, H-1); ^{13}C NMR (125 MHz; CD_3OD) δ_C 59.9 (OCH$_3$), 60.3 (C-2), 69.9 (C-6), 71.2 (C-5), 72.0 (C-4), 72.5 (C-3), 100.7 (C-1), 128.3 (q, J_{CF} = 320.1 Hz, CF$_3$); ^{19}F NMR (470 MHz; CD_3OD) δ_F -79.51; HRMS calc. for $C_8H_{14}O_9N_2F_3S_2$ [M-H]$^-$ 403.0098, found 403.0100.

## ((2R,3S,4S,5R,6S)-3,4,5-Trihydroxy-6-methoxytetrahydro-2H-pyran-2-yl)methyl sulfamate (50)
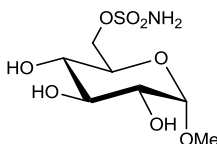
Prepared according to sulfamoylation method 2 using sulfamoyl chloride (1.85 mL, 1 M in MeCN, 1.85 mmol, 1.8 eq.), methyl-α-D-glucopyranoside (200 mg, 1.02 mmol, 1 eq.), and

DMF (7 mL). The residue was purified by MPLC on SiO_2 with a gradient elution from 2-8% MeOH/EtOAc to give a white solid (70 mg, 25%); R_f 0.25 (15% MeOH/EtOAc; anisaldehyde); mp 55-60 °C; λ_{max}(EtOH)/nm < 220; $[\alpha]_D^{18.1}$ +105.8° (c = 0.31, MeOH); IR ν_{max}/cm^{-1} 3339, 2919, 1360 (SO), 1177 (SO); ^{1}H NMR (500 MHz; CD$_3$OD) δ_H 3.32 (1H, dd, J = 9.2 and 10.0 Hz, H-4), 3.43 (1H, dd, 3.7 and 9.2 Hz, H-2), 3.45 (3H, s, OCH$_3$), 3.66 (1H, app t, J = 9.2 Hz, H-3), 3.80 (1H, ddd, J = 2.0, 5.9 and 10.0 Hz, H-5), 4.28 (1H, dd, J = 5.9 and 10.7 Hz, H-6$_a$), 4.43 (1H, dd, J = 2.0 and 10.7 Hz, H-6$_b$), 4.71 (1H, d, J = 3.7 Hz, H-1); ^{13}C NMR (125 MHz; CD$_3$OD) δ_C 68.2 (OCH$_3$), 70.1 (C-6), 71.2 (C-5), 71.5 (C-4), 73.4 (C-2), 75.1 (C-3), 101.3 (C-1); HRMS calc. for C$_7$H$_{14}$N$_1$O$_8$S$_1$ [M-H]$^-$ 272.0446, found 272.0442.

((2R,3S,4S,5S,6S)-3,4,5-Trihydroxy-6-methoxytetrahydro-2H-pyran-2-yl)methyl sulfamate (51)
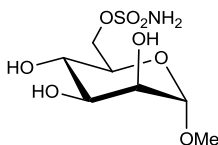
Prepared according to sulfamoylation method 2 using sulfamoyl chloride (1.85 mL, 1 M in MeCN, 1.85 mmol, 1.8 eq.), methyl-α-D-mannopyranoside (200 mg, 1.02 mmol, 1 eq.), and DMF (7 mL). The residue was purified by MPLC on SiO_2 with a gradient elution from EtOAc to 8% MeOH/EtOAc to give a white solid. This material was re-purified by MPLC on SiO_2 with a gradient elution from 5-10% MeOH/CH$_2$Cl$_2$ to give a white solid (25 mg, 9%); R_f 0.2 (5% MeOH/EtOAc; anisaldehyde); m.p. 65-70 °C; λ_{max}(EtOH)/nm < 220; $[\alpha]_D^{18.8}$ +96.8° (c = 0.28, EtOH); IR ν_{max}/cm^{-1} 3341, 1356 (SO), 1176 (SO); ^{1}H NMR (500 MHz; CD$_3$OD) δ_H 3.42 (3H, s, OCH$_3$), 3.63-3.72 (2H, m, H-3 and H-4), 3.75 (1H, ddd, J = 1.8, 6.3 and 9.6 Hz, H-5), 3.83 (1H, dd, J = 1.7 and 3.2 Hz, H-2), 4.30 (1H, dd, J = 6.3 and 10.8 Hz, H-6$_a$), 4.48 (1H, dd, J = 1.8 and 10.8 Hz, H-6$_b$), 4.67 (1H, d, J = 1.7 Hz, H-1); ^{13}C NMR (125 MHz; CD$_3$OD) δ_C 55.4 (OCH$_3$), 68.3 (C-4), 70.4 (C-6), 71.9 (C-2), 72.2 (C-5), 72.5 (C-3), 102.8 (C-1); HRMS calcd for C$_7$H$_{14}$N$_1$O$_8$S$_1$ [M-H]$^-$ 272.0446, found 272.0434.

4-(((2S,3R,4R,5S,6R)-4,5-Dihydroxy-2-methoxy-6-((sulfamoyloxy) methyl) tetrahydro-2H-pyran-3-yl)amino)-4-oxobutanoic acid (52)
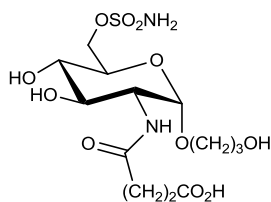
Succinic anhydride (38 mg, 0.37 mmol, 1 eq.) was added to a solution of compound **105** (100 mg, 0.37 mmol, 1 eq.) in a mixture of water (3 mL) and dioxane (3 mL), and the mixture was stirred at room temperature for 18 h. The solvent was removed *in vacuo* and purified by MPLC on SiO_2 with a gradient elution from EtOAc to 50 % MeOH/EtOAc. Product containing fractions were evaporated, and triturated with EtOAc (2 × 3 mL). The resultant solid was dried under vacuum to give a white solid (25 mg, 0.067 mmol, 18%); R_f 0.1 (40% MeOH/EtOAc; anisaldehyde); mp 87-90 °C; $[\alpha]_D^{22.6}$ +90.0° (c = 0.08, MeOH); λ_{max}(EtOH)/nm < 220; IR ν $_{max}$/cm^{-1} 3319, 1716 (carbamate I), 1636 (CO_2H), 1542 (carbamate II), 1361 (SO), 1176 (SO); ^{1}H NMR (500 MHz; CD$_3$OD) δ_H 2.55-2.68 (4H, m, CH_2CH_2CO$_2$H), 3.39 (1H, dd, J = 9.0 and 9.9 Hz, H-4), 3.42 (3H, s, OCH$_3$), 3.69 (1H, dd, J = 9.0 and 10.6 Hz, H-3), 3.82 (1H, ddd, J = 1.7, 6.0 and 9.9 Hz, H-5), 3.95 (1H, dd, J = 3.5 and 10.6 Hz, H-2), 4.29 (1H, dd, J = 6.0 and 10.7 Hz, H-6$_a$), 4.44 (1H, dd, J = 1.7 and 10.7 Hz, H-6$_b$), 4.69 (1H, d, J = 3.5 Hz, H-1); ^{13}C NMR (125 MHz; CD$_3$OD) δ_C 30.4 (CH$_2$CO$_2$H), 31.5 (CH$_2$CONH), 55.2 (C-2), 55.8 (OCH$_3$), 70.1 (C-6), 71.3 (C-5), 72.0 (C-4), 72.9 (C-3), 99.9 (C-1), 175.1 (CO), 176.5 (CO); HRMS calcd for $C_{11}H_{19}N_2O_{10}S$ [M-H]$^-$ 371.0766, found 371.0771.

Benzyl ((2R,3R,4R,5S,6R)-4,5-dihydroxy-6-(hydroxymethyl)-2-methoxy tetrahydro-2H-pyran-3-yl)carbamate (124)
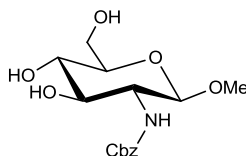
A solution of hydrogen chloride (15 mL, 1.25 M in MeOH) was added to glucosamine derivative **102** (2.0 g, 6.4 mmol, 1 eq.) and the mixture was heated to 70 °C for 1 h. The solvent was removed *in vacuo*, and the residue purified by MPLC on SiO_2 with a gradient elution from 2-15% MeOH/CH$_2$Cl$_2$ to give a white solid (430 mg, 1.31 mmol 21%, β anomer). The α anomer (**103**) was also obtained (770 mg, 2.14 mmol, 37%). Data for the β anomer **124**: R_f 0.25 (5% MeOH/EtOAc; anisaldehyde); mp 174-176 °C; λ_{max}(EtOH)/nm <

220; IR v_{max}/cm^{-1} 3297 br, 1696 (carbamate I), 1542 (carbamate II); ^{1}H NMR (500 MHz; CD$_3$OD) δ_H 3.26-3.47 (4H, m, H-2, H-3, H-4, H-5), 3.51 (3H, s, OCH$_3$), 3.72 (1H, dd, J = 5.8 and 12.0 Hz, H-6$_a$), 3.92 (1H, dd, J = 2.1 and 12.0 Hz, H-6$_b$), 4.31 (1H, d, J = 7.9 Hz, H-1), 5.13 (2H, s, CH$_2$Ph), 7.30-7.43 (5H, m, H-Ar); ^{13}C NMR (125 MHz; CD$_3$OD) δ_C 57.2 (C-2), 59.0 (OCH$_3$), 62.8 (C-6), 67.4 (CH$_2$Ph), 72.2 (C-3), 76.1 (C-5), 78.0 (C-4), 104.2 (C-1), 128.8 (C-Ar), 128.9 (C-Ar), 129.4 (C-Ar), 138.4 (C-Ar), 159.1 (CO); MS (ESI-) m/z 326.3 [M-H]$^-$.

((2R,3S,4R,5R,6R)-5-Amino-3,4-dihydroxy-6-methoxytetrahydro-2H-pyran-2-yl) methyl sulfamate (125)
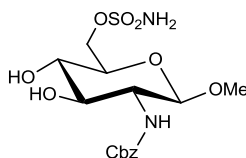
Prepared according to sulfamoylation method 1 using sulfamoyl chloride (3.75 mL, 1 M, 3.75 mmol, 3 eq.), alcohol **124** (410 mg, 1.25 mmol, 1 eq.) and DMA (3 mL) at -20 °C. The mixture was stirred at -20 °C for 1 h, and then allowed to warm to -5 °C and stirred at -5 °C for 90 minutes. The reaction was quenched by the addition of water, and extracted with EtOAc (20 mL). Saturated aqueous sodium chloride solution was added to the aqueous layer, and further extracted with CH$_2$Cl$_2$ (7 × 20 mL). The organic extracts were combined, dried over MgSO$_4$, and the solvent removed *in vacuo*. The residue was purified by MPLC on SiO$_2$ with a gradient elution from 70% EtOAc/petrol to 100% EtOAc to give a white solid. (96 mg, 0.24 mmol, 19%); R_f 0.25 (EtOAc; anisaldehyde); mp 155 °C dec.; λ_{max}(EtOH)/nm < 220; IR v_{max}/cm^{-1} 3464, 3391, 3325, 3231, 1695 (carbamate I), 1534 (carbamate II), 1369 (SO), 1180 (SO); ^{1}H NMR (500 MHz; CD$_3$OD) δ_H 3.36-3.51 (6H, m, OCH$_3$, H-2, H-3, H-4), 3.55 (1H, ddd, J = 1.9, 6.0, and 9.7 Hz, H-5), 4.28 (1H, dd, J = 6.0 and 10.9 Hz, H-6$_a$), 4.34 (1H, d, J = 7.9 Hz, H-1), 4.49 (1H, dd, J = 1.9 and 10.9 Hz, H-6$_b$), 5.13 (2H, s, CH_2Ph), 7.30-7.42 (5H, m, H-Ar); ^{13}C NMR (125 MHz; CD$_3$OD) δ_C 54.9 (OMe), 57.3 (C-2), 67.4 (CH$_2$Ph), 71.8 (C-6), 73.9 (C-5), 75.3 (C-4), 75.9 (C-3), 102.4 (C-1), 128.8 (C-Ar), 128.9 (C-Ar), 129.4 (C-Ar), 138.4 (C-Ar), 159.1 (CO); HRMS calcd for C$_{15}$H$_{21}$O$_9$N$_2$S [M-H]$^-$ 405.0973, found 405.0973.

((2R,3S,4R,5R,6R)-5-Amino-3,4-dihydroxy-6-methoxytetrahydro-2H-pyran-2-yl)methyl sulfamate (126)
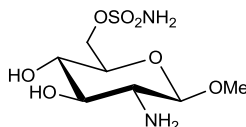
Prepared according to general procedure A using sulfamate **125** (90 mg, 0.22 mmol), MeOH (3 mL) and CH_2Cl_2 (1.5 mL) for 1 h to give a clear gum (57 mg, 0.21 mmol, 95%). R_f 0.2 (70:30:3 CH_2Cl_2/MeOH/NH_4OH; anisaldehyde); λ_{max}(EtOH)/nm < 220; IR ν_{max}/cm^{-1} 3321 br, 1358 (SO), 1176 (SO); ^{1}H NMR (500 MHz; CD_3OD) δ_H 2.62 (1H, dd, J = 8.1 and 9.6 Hz, H-2), 3.29-3.38 (2H, m, H-3 and H-4), 3.54-3.59 (4H, m, OCH_3 and H-5), 4.22 (1H, d, J = 8.1 Hz, H-1), 4.29 (1H, dd, J = 5.8 and 10.8 Hz, H-6$_a$), 4.47 (1H, dd, J = 1.9 and 10.8 Hz, H-6$_b$); ^{13}C NMR (125 MHz; CD_3OD) δ_C 57.4 (OMe), 58.2 (C-2), 69.8 (C-6), 71.5 (C-4), 75.6 (C-5), 77.1 (C-3), 105.2 (C-1); HRMS calcd for $C_7H_{15}O_7N_2S$ [M-H]$^-$ 271.0606, found 271.0606.

Ammonium ((2R,3R,4R,5S,6R)-4,5-dihydroxy-2-methoxy-6-((sulfamoyloxy)methyl)tetrahydro-2H-pyran-3-yl)sulfamate (59)
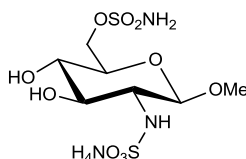
Prepared according to general procedure B, using amine **126** (50 mg, 0.18 mmol, 1 eq.) de-ionised water (2 mL) and pyridine-sulfur trioxide complex (32 mg, 0.20 mmol, 2.1 eq.). for 2 h. The crude product was purified by MPLC on SiO_2 with a gradient elution from 70:30:3 to 50:50:5 CH_2Cl_2/MeOH/NH_4OH. Product containing fractions were evaporated, dissolved in MeOH (5 mL) and filtered. The solvent was removed *in vacuo* and the residue dissolved in water, frozen and lyophilized to give a white solid (20 mg, 0.054 mmol, 29%); R_f 0.25 (70:30:3 CH_2Cl_2/MeOH/NH_4OH; anisaldehyde); mp 130 °C dec.; λ_{max}(EtOH)/nm < 220; IR ν_{max}/cm^{-1} 3372, 3261 br, 1363 (SO), 1177 (SO); ^{1}H NMR (500 MHz; CD_3OD) δ_H 3.05 (1H, dd, J = 8.2 and 9.7 Hz, H-2), 3.39 (1H, dd, J = 8.8 and 9.9 Hz, H-4), 3.54 (3H, s, OMe), 3.58 (1H, ddd, J = 1.9, 6.1 and 9.9 Hz, H-5), 3.72 (1H, dd, J = 8.8 and 9.7 Hz, H-3), 4.28 (1H, dd, J = 6.1 and 10.9 Hz, H-6$_a$), 4.41 (1H, d, J = 8.2 Hz, H-1), 4.48 (1H, dd, J = 1.9 and 10.9 Hz, H-6$_b$); ^{13}C NMR (125 MHz; CD_3OD) δ_C 57.1 (OMe), 61.6 (C-2), 70.0 (C-6), 71.5 (C-4), 75.3 (C-5), 77.3 (C-3), 103.5 (C-1); HRMS calcd for $C_7H_{15}O_{10}N_2S_2$ [M-H]$^-$ 351.0175, found 351.0174.

(2*R*,3*S*,4*R*,5*R*,6*R*)-2-(Acetoxymethyl)-5-(((benzyloxy)carbonyl)amino)-6-chloro tetrahydro-2*H*-pyran-3,4-diyl diacetate (127)
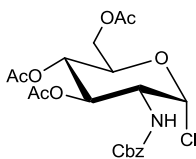
Benzyl carbamate protected glucosamine **102** (1.0 g, 3.2 mmol, 1 eq.) was suspended in acetyl chloride (3 mL), and stirred at room temperature for 48 h. The mixture was diluted with CH_2Cl_2 (20 mL) and poured onto ice. The organic layer was separated, and treated with saturated aqueous $NaHCO_3$ solution until the aqueous layer was pH 7. The organic layer was separated, the aqueous layer extracted with CH_2Cl_2. The organic layers were combined, washed with brine, dried over $MgSO_4$, and the solvent removed *in vacuo* to give a white solid (800 mg, 1.74 mmol, 55 %); R_f 0.2 (25% EtOAc/petrol; anisaldehyde); mp 116-117 °C; λ_{max}(EtOH)/nm < 220; IR v_{max}/cm^{-1} 3372, 2940, 1742, 1720, 1517; ^{1}H NMR (500 MHz; CD$_3$OD) δ_H 1.94 (3H, s, CH$_3$), 2.05 (3H, s, CH$_3$), 2.09 (3H, s, CH$_3$), 4.16 (1H, dd, *J* = 3.8 and 13.9 Hz, H-6$_a$), 4.29 (1H, dd, *J* = 3.7 and 10.6 Hz, H-2), 4.34-4.39 (2H, m, H-5 and H-6$_b$), 5.10 (1H, d, *J* = 12.5 Hz, C*H*$_a$H$_b$Ph), 5.15 (1H, app t, *J* = 9.5 Hz, H-4), 5.19 (1H, d, *J* = 12.5 Hz, CH$_a$*H*$_b$Ph), 5.37 (1H, dd, *J* = 9.5 and 10.6 Hz, H-3), 6.29 (1H, d, *J* = 3.7 Hz, H-1), 7.31-7.41 (5H, m, H-Ar); ^{13}C NMR (125 MHz; CDCl$_3$) δ_C 20.5 (*C*H$_3$CO$_2$), 20.6 (*C*H$_3$CO$_2$), 20.7 (*C*H$_3$CO$_2$), 55.3 (C-2), 61.2 (*C*H$_2$Ph), 67.1 (C-4), 67.4 (C-6), 70.1 (C-3), 70.9 (C-5), 93.8 (C-1), 128.2 (C-Ar), 128.4 (C-Ar), 128.6 (C-Ar), 138.4 (C-Ar), 158.6 (CO), 169.2 (CO), 170.5 (CO), 171.0 (CO); MS (ESI-) *m/z* 456.3 [M-H]$^-$; (ESI+) *m/z* 458.4 [M+H]$^+$.

(2*R*,3*S*,4*R*,5*S*)-2-(Acetoxymethyl)-5-(((benzyloxy)carbonyl)amino) tetrahydro-2*H*-pyran-3,4-diyl diacetate (128)
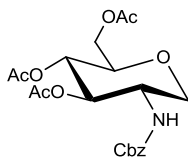
TMS$_3$SiH (1.94 mL, 6.3 mmol, 1.2 eq.) was added to a solution of chloride **127** (2.4 g, 5.2 mmol, 1 eq.) in anhydrous toluene (30 mL). A solution of AIBN (0.2 M in toluene, 1 mL, 0.2 mmol, 0.04 eq.) was added and the mixture heated to 110 °C for 1.5 h. The reaction was allowed to cool to r.t., the solvent removed *in vacuo,* and the residue purified by MPLC on SiO$_2$ with a gradient elution from 20-70% EtOAc/petrol to give a white solid

(1.85 g, 84%); R_f 0.65 (50% EtOAc/petrol; anisaldehyde); mp 115-117 °C; λ_{max}(EtOH)/nm < 220; $[\alpha]_D^{23.3}$ +31.2° (c = 0.50, EtOH); IR ν_{max}/cm^{-1} 3365, 2953, 1738, 1695, 1531; ^{1}H NMR (500 MHz; CD$_3$OD) δ_H 1.93 (3H, s, CH$_3$), 2.04 (3H, s, CH$_3$), 2.08 (3H, s, CH$_3$), 3.41 (1H, app. t, J = 11.0 Hz, H-1$_a$), 3.67 (1H, ddd, J = 2.0, 4.7 and 9.7 Hz, H-5), 3.87 (1H, app. td, J = 11.0 and 5.4 Hz, H-2), 3.97 (1H, dd, J = 5.4 and 11.0 Hz, H-1$_b$), 4.12 (1H, dd, J = 2.0 and 12.3 Hz, H-6$_a$), 4.25 (1H, dd, J = 4.7 and 12.3 Hz, H-6$_b$), 4.97 (1H, app t, J = 9.7 Hz, H-4), 5.04-5.17 (3H, m, CH_aH$_b$Ph, CH$_a$$H_b$Ph and H-3), 7.31-7.40 (5H, m, H-Ar); ^{13}C NMR (125 MHz; CD$_3$OD) δ_C 20.6 (3 × CH$_3$CO), 52.6 (C-2), 63.7 (C-6), 67.6 (CH$_2$Ph), 69.1 (C-1), 70.5 (C-4), 75.7 (C-3), 77.6 (C-5), 128.8 (C-Ar), 129.1 (C-Ar), 129.5 (C-Ar), 138.3 (C-Ar), 158.3 (PhCH$_2$$C$O), 171.4 (CH$_3$$C$O), 172.1 (CH$_3$$C$O), 172.4 (CH$_3$$C$O); HRMS calcd for C$_{20}H_{25}O_9N_1$ [M-H]$^-$ 422.1457, found 422.1450.

Benzyl ((3S,4R,5S,6R)-4,5-dihydroxy-6-(hydroxymethyl)tetrahydro-2H-pyran-3-yl)carbamate (129)

Triacetate ester **128** (100 mg, 0.24 mmol) was dissolved in methanol (3 mL) and sodium methoxide (10 mg, 0.19 mmol, 0.8 eq.) was added. The mixture was stirred at room temperature for 2 h. Three drops of 4 M HCl in dioxane were added, and the solvent was removed *in vacuo*. The material was purified by MPLC on SiO$_2$ with a gradient elution from EtOAc to 5% MeOH/EtOAc to give a white solid (50 mg, 0.17 mmol, 71%); R_f 0.15 (5% MeOH/EtOAc; anisaldehyde); mp 172-175 °C; λ_{max}(EtOH)/nm < 220; $[\alpha]_D^{16.9}$ +18.6° (c = 0.22, EtOH); IR ν_{max}/cm^{-1} 3372 br, 3301br, 2954, 2894, 2860, 1693 (carbamate I), 1543 (carbamate II); ^{1}H NMR (500 MHz; CD$_3$OD) δ_H 3.15-3.22 (2H, m, H-1$_a$ and H-5), 3.29 (1H, app t, J = 9.3 Hz, H-4), 3.36-3.42 (1H, m, H-3), 3.59 (1H, app td, J = 10.2 and 5.1 Hz, H-2), 3.66 (1H, dd, J = 6.0 and 12.0 Hz, H-6$_a$), 3.87 (1H, dd, J = 1.9 and 12.0 Hz, H-6$_b$), 3.97 (1H, dd, J = 5.1 and 11.0 Hz, H-1$_b$), 5.12 (2H, s, CH$_2$Ph), 7.30-7.42 (5H, m, H-Ar), ; ^{13}C NMR (125 MHz; CD$_3$OD) δ_C 54.6 (C-2), 63.1 (C-6), 67.6 (CH$_2$Ph), 69.5 (C-1), 72.5 (C-4), 77.1 (C-3), 82.6 (C-5), 128.9 (C-Ar), 129.0 (C-Ar), 129.5 (C-Ar); HRMS Calc for C$_{14}$H$_{20}$O$_6$N$_1$ [M+H]$^+$ 298.1285, found 298.1290.

**Note:** Unable to visualise all carbon signals by ^{13}C nmr.

((2R,3S,4R,5S)-5-(((Benzyloxy)carbonyl)amino)-3,4-dihydroxytetrahydro-2H-pyran-2-yl)methyl sulfamate (130)

Prepared according to sulfamoylation method 1 using sulfamoyl chloride (10 mL, 1 M in toluene, 10 mmol, 1.7 eq.), alcohol **129** (950 mg, 5.9 mmol, 1 eq.), and DMA (15 mL) at -20 °C. The mixture was stirred at -20 °C for 1 h. Further sulfamoyl chloride (7.6 mL, 1 M in toluene, 7.6 mmol, 1.3 eq.) was added at -20 °C and the mixture was stirred at -20 °C for 1 h. The reaction was quenched by the addition of water, and extracted with EtOAc (50 mL). Saturated aqueous sodium chloride solution was added to the aqueous layer, and further extracted with CH_2Cl_2 (5 × 30 mL). The organic extracts were combined, dried over $MgSO_4$, and the solvent removed *in vacuo*. The residue was purified by MPLC on SiO_2 with a gradient elution from 50% EtOAc/petrol to 100% EtOAc to 12 % MeOH/EtOAc to give a white solid. (200 mg, 0.53 mmol, 17%); R_f 0.25 (EtOAc; anisaldehyde); mp 158-162 °C dec.; λ_{max}(EtOH)/nm < 220; $[\alpha]_D^{16..9}$ -8.7° (c = 0.23, EtOH); IR ν_{max}/cm^{-1} 3414, 3388, 3336, 3237, 1685 (carbamate I), 1534 (carbamate II), 1374 (SO), 1182 (SO); ^{1}H NMR (500 MHz; CD$_3$OD) δ_H 3.21 (1H, app t, J = 11.2 Hz, H-1$_a$), 3.28-3.34 (1H, m, H-4), 3.38-3.46 (2H, m, H-3 and H-5), 3.60 (1H, app td, J = 11.2 and 5.3 Hz, H-2), 3.96 (1H, dd, J = 5.3 and 11.2 Hz, H-1$_b$), 4.24 (1H, dd, J = 6.0 and 10.8 Hz, H-6$_a$), 4.45 (1H, dd, J = 1.3 and 10.8 Hz, H-6$_b$), 5.12 (2H, s, CH$_2$Ph), 7.31-7.42 (5H, m, H-Ar); HRMS calcd for $C_{14}H_{19}O_8N_2S_1$ [M-H]$^-$ 375.0868 , found 379.0877.

((2R,3S,4R,5S)-5-Amino-3,4-dihydroxytetrahydro-2H-pyran-2-yl) methyl sulfamate (131)

Prepared according to general procedure A using carbamate **130** (175 mg, 0.47 mmol, 1 eq.), MeOH (15 mL) and CH_2Cl_2 (10 mL) for 3 h to give a clear gum (110 mg, 0.45 mmol, 97%); R_f 0.1 (CH$_2$Cl$_2$:MeOH:NH$_4$OH 70:30:3; anisaldehyde); λ_{max}(EtOH)/nm < 220; IR ν_{max}/cm^{-1} 3921, 2876, 1355 (SO), 1174 (SO); ^{1}H NMR (500 MHz; CD$_3$OD) δ_H 2.79 (1H, ddd, J = 5.0, 9.4 and 10.7 Hz, H-2), 3.19-3.26 (2H, m, H-1$_a$ and H-3), 3.29 (1H, app t, J = 9.4 Hz, H-4), 3.45 (1H, ddd, J = 1.8, 6.0 and 9.4 Hz, H-5), 3.95 (1H, dd, J = 5.0 and 11.3

Hz, H-1$_b$), 4.25 (1H, dd, J = 6.0 and 10.8 Hz, H-6$_a$), 4.43 (1H, dd, J = 1.8 and 10.8 Hz, H-6$_b$); ^{13}C NMR (125 MHz; CD$_3$OD) δ_C 54.1 (C-2), 70.4 (C-6), 71.2 (C-1), 71.7 (C-4), 79.9 (C-5), 80.1 (C-3); HRMS calcd for C$_6$H$_{13}$O$_6$N$_2$S$_1$ [M-H]$^-$ 241.0500, found 241.0500.

Sodium ((3S,4R,5S,6R)-4,5-Dihydroxy-6-((sulfamoyloxy)methyl)tetrahydro-2H-pyran-3-yl)sulfamate (60)

Prepared according to general procedure B, using amine **131** (130 mg, 0.54 mmol, 1 eq.), de-ionised water (3 mL) and pyridine-sulfur trioxide complex (165 mg, 1.07 mmol, 2.0 eq.) for 2 h. The crude product was purified by MPLC on SiO$_2$ with a gradient elution from 20% EtOAc/MeOH to 100% MeOH. Product containing fractions were evaporated, dissolved in MeOH (5 mL) and filtered. The solvent was removed *in vacuo* to give a pale yellow solid (42 mg, 0.13 mmol, 24%); R_f 0.15 (20% MeOH /EtOAc; anisaldehyde); mp 120-124 °C; [α]$_D^{22.2}$ +8.0° (c = 0.20, MeOH); λ$_{max}$ (EtOH)/nm < 220; IR ν $_{max}$/cm^{-1} 3290 (br), 1358 (SO), 1173 (SO); ^{1}H NMR (500 MHz; D$_2$O) δ_H 3.22-3.28 (1H, m, H-2), 3.35 (app t, J = 11.2 Hz, H-1$_a$), 3.42 (1H, app t, J = 8.5 Hz, H-3), 3.49 (1H, app t, J = 8.5 Hz, H-4), 3.59 (1H, ddd, J = 2.0, 5.0 and 8.5 Hz, H-5), 4.25 (1H, dd, J = 4.8 and 11.2 Hz, H-1$_b$), 4.33 (1H, dd, J = 5.0 and 11.2 Hz, H-6$_a$), 4.43 (1H, dd, J = 2.0 and 11.2 Hz, H-6$_b$); ^{13}C NMR (125 MHz; CD$_3$OD) δ_C 58.5 (C-2), 70.4 (C-1 and C-6), 71.9 (C-4), 78.1 (C-3), 79.7 (C-5); ^{13}C NMR (D$_2$O) δ_C 54.9 (C-2), 68.7 (C-1), 69.0 (C-6), 69.6 (C-4), 75.2 (C-3), 77.5 (C-5); HRMS calcd for C$_6$H$_{13}$N$_2$O$_9$S$_2$ [M-H]$^-$ 321.0068, found 321.0069.

Benzyl ((2S,3R,4R,5S,6R)-4,5-dihydroxy-6-(hydroxymethyl)-2-isopropoxy tetrahydro-2H-pyran-3-yl)carbamate (132)

Benzyl carbamate protected glucosamine **102** (500 mg, 1.6 mmol, 1 eq.) was dissolved in isopropyl alcohol (15 mL) and a HCl in dioxane (1.5 mL, 4 M) was added. The mixture was heated to 60 °C for 4 h, allowed to cool, and the solvent was removed *in vacuo*. The mixture was dissolved in MeOH and purified by MPLC on SiO$_2$, with a gradient elution from 2-10% MeOH/CH$_2$Cl$_2$, to give a white solid (414 mg, 1.17 mmol, 73%). R_f 0.5 (10%

MeOH/CH$_2$Cl$_2$; anisaldehyde); mp 158-159 °C; λ_{max} (EtOH)/nm < 220; $[\alpha]_D^{22.7}$ +114.1° (c = 0.27, EtOH); IR ν_{max}/cm^{-1} 3318 br, 2967, 1689 (carbamate I), 1535 (carbamate II); ^{1}H NMR (500 MHz; CD$_3$OD) δ_H 1.13 (3H, d, J = 6.2 Hz, CH$_3$), 1.25 (3H, d, J = 6.2 Hz, CH$_3$), 3.37-3.40 (1H, m, H-3), 3.59-3.75 (4H, m, H-2, H-4, H-5 and H-6$_a$), 3.83 (1H, dd, 11.0 and 1.1 Hz, H-6$_b$), 3.91 (1H, sept, J = 6.2 Hz, CH(CH$_3$)$_2$), 4.95 (1H, d, J = 2.8 Hz, H-1), 5.10 (1H, d, J = 12.5 Hz, CH_aH$_b$Ph), 5.17 (1H, d, J = 12.5 Hz, CH$_a$$H_b$Ph), 7.31-7.45 (5H, m, H-Ar); ^{13}C NMR (125 MHz; CD$_3$OD) δ_C 21.7 (CH$_3$), 23.6 (CH$_3$), 55.8 (C-2), 62.8 (C-6), 67.5 (CH$_2$Ph), 71.1 (CH(CH$_3$)$_2$), 72.4 (C-4), 73.0 (C-3), 73.8 (C-5), 97.1 (C-1), 128.9 (C-Ar), 129.0 (C-Ar), 129.4 (C-Ar), 138.4 (C-Ar), 158.8 (CO); HRMS calc. for C$_{17}$H$_{26}$O$_7$N$_1$ [M+H]$^+$ 356.1704, found 356.1708.
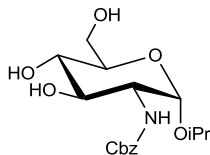
((2R,3S,4R,5R,6S)-5-((((Benzyloxy)carbonyl)amino)-3,4-dihydroxy-6-isopropoxy tetrahydro-2H-pyran-2-yl)methyl sulfamate (133)
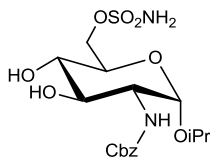

Prepared according to sulfamoylation method 1 using sulfamoyl chloride (3.3 mL, 1.0 M in toluene, 3.3 mmol, 3 eq.), alcohol **132** (390mg, 1.1 mmol, 1 eq.), and DMA (5 mL) at -20 °C. The mixture was allowed to warm to -5 °C over 1 h, and stirred at -5 °C for a further 1 h. The reaction was quenched with water, and extracted with EtOAc (20 mL). Saturated aqueous NaCl solution was added, and the mixture extracted with CH$_2$Cl$_2$ (2 × 20 mL). The organic layers were combined, dried over MgSO$_4$, and the solvent removed *in vacuo*. The residue was purified by MPLC on SiO$_2$ with a gradient elution from 70% EtOAc/Petrol to 100% EtOAc to give a white solid (148 mg, 0.32 mmol, 31%). R_f 0.4 (EtOAc; anisaldehyde); mp 166-168 °C; λ_{max}(EtOH)/nm < 220; IR ν_{max}/cm^{-1} 3336 br, 3244, 2973, 1683 (carbamate I), 1537 (carbamate II), 1371 (SO), 1178 (SO); ^{1}H NMR (500 MHz; CD$_3$OD) δ_H 1.13 (3H, d, J = 6.2 Hz, CH$_3$), 1.25 (3H, d, J = 6.2 Hz, CH$_3$), 3.35-3.41 (1H, m, H-4), 3.60 - 3.67 (2H, m, H-2 and H-3), 3.87-3.95 (2H, m, H-5 and CHMe$_2$), 4.29 (1H, dd, J = 5.9 and 10.8 Hz, H-6$_a$), 4.41 (1H, dd, J =1.7 and 10.8 Hz, H-6$_b$), 4.95 (1H, d, J = 2.4 Hz, H-1), 5.10 (1H, d, J = 12.5 Hz, CH_aH$_b$Ph), 5.16 (1H, d, J = 12.5 Hz, CH$_a$$H_b$Ph), 7.30-7.45 (5H, m, H-Ar); ^{13}C NMR (125 MHz; CD$_3$OD) δ_C 21.7 (CH$_3$), 23.6 (CH$_3$), 57.1 (C-2), 67.6 (CH$_2$Ph), 70.2 (C-6), 71.4 (C-5), 71.6 (CH(Me)$_2$), 72.1 (C-4), 72.8

(C-3), 96.0 (C-1), 128.9 (C-Ar), 129.0 (C-Ar), 129.5 (C-Ar), 138.4 (C-Ar), 158.8 (CO); HRMS calcd for $C_{17}H_{25}O_9N_2S$ [M-H]$^-$ 433.1286, found 433.1286.

### (2R,3S,4R,5R,6S)-5-Amino-3,4-dihydroxy-6-isopropoxytetrahydro-2H-pyran-2-yl)methyl sulfamate (134)

Prepared according to general procedure A using carbamate **133** (108 mg, 0.25 mmol), MeOH (4 mL) and CH_2Cl_2 (4 mL) for 1 h to give a clear oil (75 mg, 0.25 mmol, 100%); R_f 0.02 (10% MeOH/EtOAc; anisaldehyde); λ_{max}(EtOH)/nm < 220; IR ν_{max}/cm^{-1} 1368 (SO), 1179 (SO); ^{1}H NMR (500 MHz; CD$_3$OD) δ_H 1.22 (3H, d, J = 6.2 Hz, CH$_3$), 1.29 (3H, d, J = 6.2 Hz, CH$_3$), 2.69 (1H, dd, J = 3.7 and 10.0 Hz, H-2), 3.31 (1H, dd, J = 9.0 and 10.0 Hz, H-4), 3.52 (1H, dd, J = 9.0 and 10.0 Hz, H-3), 3.92 (1H, ddd, J = 1.9, 5.9 and 10.0 Hz, H-5), 3.97 (1H, sept, J = 6.2 Hz, CH(Me)$_2$), 4.28 (1H, dd, J = 5.9 and 10.7 Hz, H-6$_a$), 4.41 (1H, dd, J = 1.9 and 10.7 Hz, H-6$_b$), 4.97 (1H, d, J = 3.7 Hz, H-1); ^{13}C NMR (125 MHz; CD$_3$OD) δ_C 21.9 (CH$_3$), 23.7 (CH$_3$), 56.8 (C-2), 70.1 (C-6), 71.6 (CH(CH$_3$)$_2$), 71.8 (C-5), 71.8 (C-4), 75.5 (C-3), 98.2 (C-1); HRMS calcd for $C_9H_{19}O_7N_2S$ [M-H]$^-$ 299.0918, found 299.0914.

Ammonium ((2S,3R,4R,5S,6R)-4,5-dihydroxy-2-isopropoxy-6-((sulfamoyloxy) methyl)tetrahydro-2H-pyran-3-yl)sulfamate (56)


Prepared according to general procedure B, using amine **134** (70 mg, 0.23 mmol, 1 eq.), de-ionised water (2 mL), and pyridine-sulfur trioxide complex (41 mg, 0.26 mmol, 1.1 eq.). After 30 min further SO$_3$.pyridine complex (15 mg, 0.09 mmol, 0.4 eq.) was added, the pH of the mixture re-adjusted to pH 9-10. The mixture was stirred at room temperature for 1 h and the solvent removed *in vacuo*. The residue was purified by MPLC on SiO$_2$ with a gradient elution from 70:30:3 to 50:50:5 CH_2Cl_2/MeOH/NH$_4$OH. Product containing fractions were evaporated, dissolved in MeOH (5 mL) and filtered. The solvent was removed *in vacuo*, the residue dissolved in water (1 mL), frozen and lyophilized to give a white solid (24 mg, 27%); R_f 0.1 (70:30:3 CH_2Cl_2/MeOH/NH$_4$OH; anisaldehyde); mp 50-

70 °C; $[\alpha]_D^{22.6}$ +97.3° (c = 0.30, MeOH); λ_{max}(EtOH)/nm < 220; IR ν_{max}/cm^{-1} 3222 br, 3069, 2976, 2932, 1360 (SO), 1172 (SO); ^{1}H NMR (500 MHz; CD$_3$OD) δ_H 1.24-1.29 (6H, 2 × d, J = 6.2 Hz, 2 × CH$_3$), 3.25 (1H, dd, J = 3.7 and 10.2 Hz, H-2), 3.38 (1H, app t, J = 9.6 Hz, H-4), 3.57 (1H, dd, J = 9.6 and 10.2 Hz, H-3), 3.91 (1H, ddd, J = 1.9, 6.0 and 9.6 Hz, H-5), 3.96 (1H, sept, J = 6.2 Hz, CH(Me)$_2$), 4.28 (1H, dd, J = 6.0 and 10.6 Hz, H-6$_a$), 4.42 (1H, dd, J = 1.9 and 10.6 Hz, H-6$_b$), 5.23 (1H, d, J = 3.7 Hz, H-1); ^{13}C NMR (125 MHz; D$_2$O) δ_C 20.6 (CH$_3$), 22.3 (CH$_3$), 57.5 (C-2), 68.9 (C-6), 69.2 (C-5), 69.6 (C-4), 71.3 (C-3), 71.5 (CHMe$_2$), 95.8 (C-1); HRMS calcd for C$_9$H$_{19}$O$_{10}$N$_2$S$_2$ [M-H]$^-$ 379.0487, found 379.0484.

Benzyl ((2S,3R,4R,5S,6R)-2-(allyloxy)-4,5-dihydroxy-6-(hydroxymethyl) tetrahydro-2H-pyran-3-yl)carbamate[336] (135)

Benzyl carbamate protected glucosamine **102** (6 g, 19 mmol, 1 eq.) was dissolved in allyl alcohol (40 mL) and HCl in dioxane (5 mL, 4 M) was added. The mixture was heated to 60 °C for 4 h, allowed to cool, and the solvent removed *in vacuo*. The mixture was purified by MPLC on SiO$_2$, with a gradient elution from 0-12% MeOH/CH$_2$Cl$_2$, to give a white solid (3.53 g, 10 mmol, 52%); R_f 0.5 (10% MeOH/CH$_2$Cl$_2$; anisaldehyde); mp 135-138 °C; λ_{max}(EtOH)/nm < 220; $[\alpha]_D^{23.1}$ +17.4° (c = 0.46, EtOH); IR ν_{max}/cm^{-1} 3309, 2921, 1686 (carbamate I), 1536 (carbamate II); ^{1}H NMR (500 MHz; CD$_3$OD) δ_H 3.38-3.42 (1H, m, H-4), 3.62 (1H, ddd, J = 2.0 , 5.9 and 9.6 Hz, H-5), 3.67 (2H, m, H-2 and H-3), 3.72 (1H, dd, J = 5.9 and 12.0 Hz, H-6$_a$), 3.85 (1H, dd, J = 2.0 and 12.0 Hz, H-6$_b$), 4.03 (1H, dd, J = 6.0 and 13.1 Hz, OCH$_a$H$_b$CHCH$_2$), 4.23 (1H, dd, J = 5.0 and 13.1 Hz, OCH$_a$H$_b$CHCH$_2$), 4.88 (1H, d, J = 2.6 Hz, H-1), 5.09-5.20 (3H, m, CH$_a$H$_b$CHCH$_2$O and CH$_2$Ph), 5.34 (1H, ddd, J = 1.7, 2.6 and 17.1 Hz, CH$_a$H$_b$CHCH$_2$O), 5.90-5.99 (1H, m, OCH$_2$CHCH$_2$), 7.31-7.43 (5H, m, H-Ar); ^{13}C NMR (125 MHz; CD$_3$OD) δ_C 57.2 (C-2), 62.8 (C-6), 67.6 (CH$_2$Ph), 69.2 (CH$_2$CHCH$_2$O), 72.3 (C-4), 73.0 (C-3), 74.0 (C-5), 98.1 (C-1), 117.5 (CH$_2$CHCH$_2$O), 128.9 (C-Ar), 129.0 (C-Ar), 129.4 (C-Ar), 135.4 (C-Ar), 138.4 (CH$_2$CHCH$_2$O), 158.8 (CO$_2$Bn); HRMS calcd for C$_{17}$H$_{22}$O$_7$N$_1$ [M-H]$^-$ 352.1402, found 352.1409.

((2*R*,3*S*,4*R*,5*R*,6*S*)-6-(Allyloxy)-5-(((benzyloxy)carbonyl)amino)-3,4-dihydroxy tetrahydro-2*H*-pyran-2-yl)methyl sulfamate (137)

Prepared according to sulfamoylation method 1 using sulfamoyl chloride (11.4 mL, 1.0 M in toluene, 11.4 mmol, 2 eq.), alcohol **135** (2.0 g, 5.7 mmol, 1 eq.), and DMA (15 mL) at -20 °C. The mixture was allowed to stir at -20 °C for 1 h, and allowed to warm to 10 °C over 45 min. The reaction was cooled to -20 °C and further sulfamoyl chloride (5.7 mL, 1.0 M in toluene, 5.7 mmol, 1 eq.) was added. The reaction was allowed to warm to 10 °C over 45 min, quenched with water, and extracted with EtOAc (50 mL). Saturated aqueous NaCl solution was added, and the mixture extracted with CH_2Cl_2 (3 × 50 mL). The organics were combined, dried ($MgSO_4$), and the solvent removed *in vacuo*. The residue was purified by MPLC on SiO_2 with a gradient elution from 50% EtOAc/Petrol to 100% EtOAc to give a clear glass. (970 mg, 2.24 mmol, 40 %); R_f 0.2 (EtOAc; anisaldehyde); λ_{max}(EtOH)/nm < 220; $[\alpha]_D^{23.2}$ +83° (c = 0.51, EtOH); IR ν_{max}/cm^{-1} 3449, 3384, 3331, 3235, 2915, 1681 (carbamate I), 1538 (carbamate II), 1370 (SO), 1180 (SO); ^{1}H NMR (500 MHz; CD_3OD) δ_H 3.35-3.43 (1H, m, H-4), 3.65-3.69 (2H, m, H-2 and H-3), 3.85 (1H, ddd, *J* = 1.6, 6.0 and 10.2 Hz, H-5), 4.04 (1H, dd, *J* = 6.0 and 13.1 Hz, OC*H*$_a$H$_b$CHCH$_2$), 4.22 (1H, dd, *J* = 5.0 and 13.1 Hz, OCH$_a$*H*$_b$CHCH$_2$), 4.29 (1H, dd, *J* = 6.0 and 10.7 Hz, H-6$_a$), 4.43 (1H, dd, *J* = 1.6 and 10.7 Hz, H-6$_b$), 4.89 (1H, d, H-1), 5.11 (1H, d, *J* = 12.5 Hz, C*H*$_a$H$_b$Ph), 5.16 (1H, d, *J* = 12.5 Hz, CH$_a$*H*$_b$Ph), 5.20 (1H, dd, *J* = 1.3 and 10.6 Hz, C*H*$_a$H$_b$CHCH$_2$O), 5.27-5.37 (1H, app dq, *J* = 1.3 and 17.5 Hz, CH$_a$*H*$_b$CHCH$_2$O), 5.90-6.00 (1H, m, CH$_2$C*H*CH$_3$), 7.30-7.43 (5H, m, H-Ar); ^{13}C NMR (125 MHz; CD_3OD) δ_C 57.1 (C-2), 67.6 (*C*H$_2$Ph), 69.5 (CH$_2$CH*C*H$_2$O), 70.1 (C-6), 71.5 (C-5), 72.1 (C-4), 72.9 (C-3), 98.1 (C-1), 117.8 (*C*H$_2$CHCH$_2$O), 128.9 (C-Ar), 129.0 (C-Ar), 129.5 (C-Ar), 135.3 (CH$_2$*C*HCH$_2$O), 138.3 (C-Ar), 158.8 (CO); HRMS calcd for $C_{17}H_{23}O_9N_2S_1$ [M-H]$^-$ 431.1130, found 431.1126.
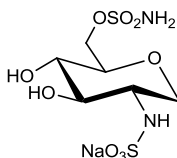
((2R,3S,4R,5R,6S)-5-Amino-3,4-dihydroxy-6-propoxytetrahydro-2H-pyran-2-yl)methyl sulfamate (138)

Prepared according to general procedure A using carbamate **137** (150 mg, 0.35 mmol), MeOH (2 mL) and CH_2Cl_2 (2 mL) for 2 h to give a clear glass (104 mg, 0.35 mmol, 100%); R_f 0.15 (CH_2Cl_2:MeOH 70:30; anisaldehyde); λ_{max}(EtOH)/nm < 220; IR ν_{max}/cm^{-1} 3348, 3299, 2965, 2932, 1359 (SO), 1176 (SO); ^{1}H NMR (500 MHz; CD_3OD) δ_H 1.02 (3H, t, J = 7.4 Hz, CH_2CH_3), 1.65-1.74 (2H, m, CH_2CH_3), 2.70 (1H, dd, J = 3.6 and 9.9 Hz, H-2), 3.32 (1H, dd, J = 9.0 and 9.9 Hz, H-4), 3.44 (1H, J = 6.4 and 9.6 Hz, $CH_3CH_2CH_aH_bO$), 3.53 (1H, dd, J = 9.0 and 9.9 Hz, H-3), 3.75 (1H, dt, J =9.6 and 6.7 Hz, $CH_3CH_2CH_aH_bO$), 3.85 (1H, ddd, J = 1.9 , 5.9 and 9.9 Hz, H-5), 4.28 (1H, dd, J = 5.9 and 10.7 Hz, H-6$_a$), 4.42 (1H, dd, J = 1.9 and 10.7 Hz, H-6$_b$), 4.84 (1H, d, J = 3.6 Hz, H-1); ^{13}C NMR (125 MHz; CD_3OD) δ_C 11.1 (CH_3), 23.8 (CH_2CH_3), 57.0 (C-2), 70.1 (C-6), 70.8 ($CH_2CH_2CH_3$), 71.7 (C-5), 71.8 (C-4), 75.7 (C-3), 99.8 (C-1); HRMS calcd for $C_9H_{19}O_7N_2S$ [M-H]$^-$ 299.0918, found 299.0913.

Ammonium ((2S,3R,4R,5S,6R)-4,5-dihydroxy-2-propoxy-6-((sulfamoyloxy)methyl)tetrahydro-2H-pyran-3-yl)sulfamate (57)

Prepared according to general procedure B, using amine **138** (100 mg, 0.33 mmol, 1 eq.), de-ionised water (4 mL) and pyridine-sulfur trioxide complex (79 mg, 0.50 mmol, 2 eq.) for 1 h. The crude product was purified by MPLC on SiO_2 with a gradient elution from 70:30:3 to 50:50:5 CH_2Cl_2/MeOH/NH_4OH. Product containing fractions were evaporated, the residue dissolved in water (1 mL) and lyophilized to give a white solid (50 mg, 0.13 mmol, 39%); R_f 0.1 (CH_2Cl_2:MeOH:NH_4OH 70:30:3; anisaldehyhde); mp 50-60 °C; $[\alpha]_D^{22.2}$ +48.0° (c = 0.10, MeOH); λ_{max}(EtOH)/nm < 220; IR ν_{max}/cm^{-1} 3224, 3085, 2968, 2937, 1359 (SO), 1171 (SO); ^{1}H NMR (500 MHz; CD_3OD) δ_H 1.01 (3H, t, J = 7.4 Hz, CH_2CH_3), 1.65-1.74 (2H, m, CH_2CH_3), 3.27 (1H, dd, J = 3.6 and 10.1 Hz, H-2), 3.40 (1H, dd, J = 8.8 and 10.0 Hz, H-4), 3.48 (1H, dt, J = 9.5 and 6.5 Hz, $CH_aH_bCH_2CH_3$), 3.60 (1H, dd, J = 8.8 and 10.1 Hz, H-3), 3.71 (1H, dt, J = 9.5 and 6.8 Hz, $CH_aH_bCH_2CH_3$), 3.84 (1H,

ddd, J = 1.9, 6.0 and 10.0 Hz, H-5), 4.29 (1H, dd, J = 6.0 and 10.7 Hz, H-6$_a$), 4.43 (1H, dd, J = 1.9 and 10.7 Hz, H-6$_b$), 5.10 (1H, d, J = 3.6 Hz, H-1); ^{13}C NMR (125 MHz; CD$_3$OD) δ_C 11.1 (CH$_2$CH$_3$), 23.8 (CH$_2$CH$_3$), 59.6 (C-2), 70.2 (C-6), 71.0 (CH$_2$CH$_2$CH$_3$), 71.1 (C-5), 72.0 (C-4), 74.1 (C-3), 99.3 (C-1); HRMS calcd for C$_9$H$_{19}$O$_{10}$N$_2$S$_2$ [M-H]$^-$ 379.0487, found 379.0489.

((2*R*,3*S*,4*R*,5*R*,6*S*)-5-((((Benzyloxy)carbonyl)amino)-3,4-dihydroxy-6-(2-hydroxyethoxy)tetrahydro-2*H*-pyran-2-yl)methyl sulfamate (139)

Allyl ether **137** (200 mg, 0.46 mmol) was dissolved in methanol (10 mL), and ozone was bubbled through the solution at -78 °C for 30 min. The mixture was allowed to stir at -78 °C to r.t. for 2 h and then NaBH$_4$ was added, and stirred for 1 h. The solvent was removed *in vacuo,* and the residue purified by MPLC on SiO$_2$ with a gradient elution from 5-12% MeOH/CH$_2$Cl$_2$ to give a white solid (140 mg, 0.32 mmol, 69%); R_f 0.5 (10% MeOH/CH$_2$Cl$_2$; anisaldehyde); λ_{max}(EtOH)/nm < 220; IR ν_{max}/cm^{-1} 3335, 3094, 2923, 1693 (carbamate I), 1535.8 (carbamate II), 1365 (SO), 1178 (SO); ^{1}H NMR (500 MHz; CD$_3$OD) δ_H 3.39 (1H, dd, J = 8.8 and 9.9 Hz, H-4), 3.48-3.55 (1H, m, CH$_a$H$_b$CH$_2$OH), 3.65-3.71 (2H, m, H-2 and H-3), 3.72-3.76 (2H, m, CH$_a$H$_b$CH$_2$OH and CH$_2$CH$_a$H$_b$OH), 3.80-3.84 (1H, m, CH$_2$CH$_a$H$_b$OH), 3.88 (1H, ddd, J = 1.9, 6.0, and 9.9 Hz, H-5), 4.29 (1H, dd, J = 6.0 and 10.9 Hz, H-6$_a$), 4.44 (1H, dd, J = 1.9 and 10.9 Hz, H-6$_b$), 4.83 (1H, d, J = 3.3 Hz, H-1), 5.13 (2H, s, CH$_2$Ph), 7.30-7.44 (5H, m, H-Ar); ^{13}C NMR (125 MHz; CD$_3$OD) δ_C 57.1 (C-2), 62.1 (CH$_2$CH$_2$OH), 67.7 (CH$_2$Ph), 70.1 (C-6), 70.5 (CH$_2$CH$_2$OH), 71.5 (C-5), 72.0 (C-4), 73.4 (C-3), 99.5 (C-1), 128.9 (C-Ar), 129.0 (C-Ar), 129.5 (C-Ar), 138.3 (C-Ar), 159.0 (CO); HRMS calcd for C$_{16}$H$_{23}$O$_{10}$N$_2$S$_1$ [M-H]$^-$ 436.1079, found 436.1085.

((2*R*,3*S*,4*R*,5*R*,6*S*)-5-Amino-3,4-dihydroxy-6-(2-hydroxyethoxy) tetrahydro-2*H*-pyran-2-yl)methyl sulfamate (140)

Prepared according to general procedure A using alcohol **139** (135 mg, 0.31 mmol), MeOH (5 mL) and CH$_2$Cl$_2$ (1 mL) for 3 h to give a clear gum (70 mg, 78%); R_f 0.2 (MeOH;

anisaldehyde); λ_{max}(EtOH)/nm < 220; IR ν_{max}/cm^{-1} 3360, 3286, 3100, 2939, 2909, 1351 (SO), 1188 (SO); ^{1}H NMR (500 MHz; CD$_3$OD) δ_H 2.70 (1H, dd, J = 3.6 and 10.0 Hz, H-2), 3.32 (1H, dd, J = 9.0 and 10.1 Hz, H-4), 4.87 (1H, d, J = 3.6 Hz, H-1), 3.53-3.59 (2H, m, H-3 and CH_aCH$_b$CH$_2$OH), 3.76 (2H, m, CH$_2$CH_2OH), 3.85 (1H, ddd, J = 3.7, 5.0 and 10.6 Hz, CH$_a$CH_bCH$_2$OH), 3.89 (1H, ddd, J = 1.9, 5.8 and 10.1 Hz, H-5), 4.29 (1H, dd, J = 5.8 and 10.7 Hz, H-6$_a$), 4.43 (1H, dd, J =1.9 and 10.7 Hz, H-6$_b$); ^{13}C NMR (125 MHz; CD$_3$OD) δ_C 57.1 (C-2), 62.1 (CH$_2$OH), 70.1 (C-6), 70.6 (CH$_2$CH$_2$OH), 71.7 (C-5), 71.8 (C-4), 75.8 (C-3), 100.4 (C-1); HRMS calcd for C$_8$H$_{17}$O$_8$N$_2$S$_1$ [M-H]$^-$ 301.0711, found 301.0705.

Sodium ((2S,3R,4R,5S,6R)-4,5-Dihydroxy-2-(2-hydroxyethoxy)-6-((sulfamoyloxy)methyl) tetrahydro-2H-pyran-3-yl)sulfamate (53)

Prepared according to general procedure B, using amine **140** (65 mg, 0.22 mmol, 1 eq.), de-ionised water (1.5 mL) and pyridine-sulfur trioxide complex (40 mg, 0.26 mmol, 1.2 eq.) for 1 h. The solvent was removed *in vacuo* and the residue was purified by MPLC on C-18 reversed phase SiO$_2$ with a gradient elution from 20-50% MeOH/H$_2$O. Product containing fractions were evaporated, dissolved in MeOH (5 mL) and filtered. The solvent was removed *in vacuo*. The residue was dissolved in water (3 mL), frozen and lyophilized to give a pale yellow solid (22 mg, 0.058 mmol, 27%); R_f 0.9 (MeOH; anisaldehyde); mp 184 °C dec.; [α]$_D^{20.6}$ +50.0° (c = 0.08, MeOH); λ_{max}(EtOH)/nm < 220; IR ν_{max}/cm^{-1} 3262 (br), 1359 (SO), 1175 (SO); ^{1}H NMR (500 MHz; CD$_3$OD) δ_H 3.30 (1H, dd, J = 3.6 and 10.2 Hz, H-2), 3.40 (1H, dd, J = 8.8 and 10.0 Hz, H-4), 3.58-3.63 (1H, m, 1H, CH_aCH$_b$CH$_2$OH), 3.65 (1H, dd, J = 8.8 and 10.2 Hz, H-3), 3.71-3.85 (3H, m, CH$_2$CH_2OH and CH$_a$CH_bCH$_2$OH), 3.89 (1H, ddd, J = 1.8, 6.0 and 10.0 Hz, H-5), 4.28 (1H, dd, J = 6.0 and 10.7 Hz, H-6$_a$), 4.44 (1H, dd, J = 1.8 and 10.7 Hz, H-6$_b$), 5.15 (1H, d, J = 3.6 Hz, H-1); ^{13}C NMR (125 MHz; CD$_3$OD) δ_C 59.6 (C-2), 62.1 (CH$_2$CH$_2$OH), 70.2 (C-6), 70.6 (CH$_2$CH$_2$OH), 71.1 (C-5), 72.0 (C-4), 73.9 (C-3), 99.3 (C-1); HRMS calcd for C$_8$H$_{17}$O$_{11}$N$_2$S$_2$ [M-H]$^-$ 381.0279, found 381.0281.

(2*R*,3*S*,4*R*,5*R*,6*S*)-2-(Acetoxymethyl)-6-(allyloxy)-5-(((benzyloxy) carbonyl) amino) tetrahydro-2*H*-pyran-3,4-diyl diacetate (141)

Alcohol **135** (500 mg, 1.41 mmol, 1 eq.) was dissolved in pyridine (3 mL) and Ac$_2$O (3 mL) was added. The mixture was stirred at room temperature for 18 h. The solvent was removed *in vacuo*, and the residue purified by MPLC on SiO$_2$ with a gradient elution from 20-80% EtOAc/petrol to give a white solid (650 mg, 1.35 mmol, 96%); R_f 0.5 (50% EtOAc/petrol; anisaldehyde); mp 67-69 °C; λ_{max}(EtOH)/nm < 220; IR ν_{max}/cm^{-1} 1742, 1514; ^{1}H NMR (500 MHz; CDCl$_3$) δ_H 1.92 (3H, CH$_3$CO), 2.04 (3H, CH$_3$CO), 2.12 (3H, CH$_3$CO), 3.97-4.12 (4H, m, H-2, H-4, H-5, H-6$_a$), 4.19 (1H, dd, *J* = 5.5 and 12.6 Hz, OC*H*$_a$H$_b$CHCH$_2$), 4.27 (1H, dd, *J* = 4.4 and 12.3 Hz, H-6$_b$), 4.94 (1H, d, *J* = 3.5 Hz, H-1), 5.03-5.18 (3H, m, CH$_2$Ph and H-4), 5.22-5.34 (3H, m, OCH$_2$CHC*H*$_2$ and H-3), 5.85-5.94 (1H, m, OCH$_2$C*H*CH$_2$), 7.31-7.41 (5H, m, H-Ar); ^{13}C NMR (125 MHz; CDCl$_3$) δ_C 20.5 (*C*H$_3$CO), 20.6 (*C*H$_3$CO), 20.7 (*C*H$_3$CO), 53.7 (C-2), 62.0 (C-6), 67.0 (*C*H$_2$Ph), 67.9 (C-5), 68.3 (C-4), 68.9 (O*C*H$_2$CHCH$_2$), 71.3 (C-3), 96.6 (C-1), 118.5 (OCH$_2$CH*C*H$_2$), 128.1 (C-Ar), 128.2 (C-Ar), 128.5 (C-Ar), 133.0 (C-Ar), 136.2 (OCH$_2$*C*HCH$_2$), 169.4 (CH$_3$*C*O), 155.8 (*C*OCH$_2$Ph), 170.7 (CH$_3$*C*O), 171.0 (CH$_3$*C*O); HRMS calcd for C$_{23}$H$_{28}$O$_{10}$N$_1$ [M-H]$^-$ 478.1719, found 478.1721.

2-(((2*S*,3*R*,4*R*,5*S*,6*R*)-4,5-Diacetoxy-6-(acetoxymethyl)-3-(((benzyloxy) carbonyl)amino)tetrahydro-2*H*-pyran-2-yl)oxy)acetic acid (142)

Allyl ether **141** (3.0 g, 6.2 mmol) was dissolved in a mixture of CH$_2$Cl$_2$:MeCN:H$_2$O (10 mL:10 mL:15 mL). NaIO$_4$ (10.7 g, 50 mmol, 8 eq.) was added, followed by RuCl$_3$ (50 mg, 0.24 mmol, 0.04 eq.) and the mixture was stirred at room temperature for 30 minutes. The reaction was quenched with water, partitioned between CH$_2$Cl$_2$ (5 × 50 mL), and water (100 mL). The organic extracts were combined, washed with brine (50 mL), dried over MgSO$_4$ and the solvent removed *in vacuo*. The residue was purified by MPLC on SiO$_2$ with a gradient elution from 90:10:1 to 75:25:2.5 CH$_2$Cl$_2$/MeOH/NH$_4$OH to give a clear

glass (1.85g 3.7 mmol, 60%); R_f 0.15 (25% MeOH/EtOAc; anisaldehyde); mp 82-85 °C; λ_{max}(EtOH)/nm < 220; IR ν_{max}/cm^{-1} 1739, 1586, 1535; ^{1}H NMR (500 MHz; CD$_3$OD) δ_H 1.85 (3H, s, CH$_3$CO), 2.03 (3H, s, CH$_3$CO), 2.09 (3H, s, CH$_3$CO), 4.02 (1H, dd, J = 3.2 and 10.4 Hz, H-2), 4.12 (1H, d, J = 12.3 Hz, CH$_a$H$_b$CO$_2$H), 4.17 (1H, app. d, J = 10.3 Hz, H-5), 4.24-4.32 (3H, m, CH$_2$Ph and CH$_a$H$_b$CO$_2$H), 5.00 (1H, d, J = 3.2 Hz, H-1), 5.02-5.10 (2H, m, H-4 and H-6$_a$), 5.18 (1H, d, J = 12.4 Hz, H-6$_b$), 5.33 (1H, app. t, J = 10.4 Hz, H-3), 7.30-7.40 (5H, m, H-Ar); ^{13}C NMR (125 MHz; CD$_3$OD) δ_C 20.6 (2 × CH$_3$CO), 20.7 (CH$_3$CO), 55.0 (C-2), 63.4 (CH$_2$CO$_2$H), 67.5 (C-6), 67.8 (CH$_2$Ph), 69.1 (C-5), 70.2 (C-4), 73.2 (C-3), 99.1 (C-1), 128.7 (C-Ar), 129.0 (C-Ar), 129.5 (C-Ar), 138.5 (C-Ar), 158.7 (COCH$_2$Ph), 171.4 (CH$_3$$C$O), 171.8 (CH$_3$$C$O), 172.4 (CH$_3$$C$O), 175.4 (CO$_2$H); HRMS calcd for C$_{22}H_{26}O_{12}N_1$ [M-H]$^-$ 496.1460, found 496.1474.
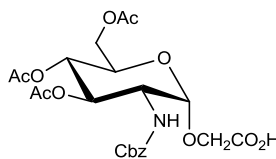
(2*R*,3*S*,4*R*,5*R*,6*S*)-2-(Acetoxymethyl)-5-(((benzyloxy)carbonyl)amino)-6-(2-methoxy-2-oxoethoxy)tetrahydro-2*H*-pyran-3,4-diyl diacetate (143)
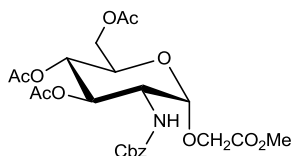
Carboxylic acid **142** (1.5 g, 3.0 mmol, 1 eq.) was dissolved in MeCN (30 mL) and Cs$_2$CO$_{3(s)}$ (1.97 g, 6.0 mmol, 2 eq.) was added followed by methyl iodide (371 μL, 6.0 mmol, 2 eq.). The mixture was stirred at room temperature for 18 h, filtered, and the solvent removed *in vacuo*. The residue was purified by MPLC on SiO$_2$ with a gradient elution from 20-80% EtOAc/Petrol, to give a clear gum, (1.19 g, 2.32 mmol, 77%); R_f 0.4 (50% EtOAc/Petrol; anisaldehyde); λ_{max}(EtOH)/nm < 220; IR ν_{max}/cm^{-1} 1739, 1518; ^{1}H NMR (500 MHz; CD$_3$OD) δ_H 1.89 (3H, s, CH$_3$CO$_2$R), 2.04 (3H, s, CH$_3$CO$_2$R), 2.09 (3H, s, CH$_3$CO$_2$R), 3.79 (3H, s, CO$_2$CH$_3$), 4.02 (1H, dd, J = 3.7 and 10.7 Hz, H-2), 4.13 (1H, dd, J = 2.2 and 12.3 Hz, H-6$_a$), 4.19 (1H, ddd, J = 2.2, 4.2, and 10.2 Hz, H-5), 4.29 (1H, dd, J = 4.2 and 12.3 Hz, H-6$_b$), 4.34 (2H, s, CH$_2$CO$_2$Me), 5.01 (1H, d, J = 3.7 Hz, H-1), 5.07 (1H, dd, J = 9.7 and 10.2 Hz, H-4), 5.10 (1H, d, J = 12.6 Hz, CH$_a$H$_b$Ph), 5.19 (1H, d, J = 12.6 Hz, CH$_a$H$_b$Ph), 5.31 (1H, dd, J = 9.7 and 10.7 Hz, H-3), 7.30-7.42 (5H, m, H-Ar); ^{13}C NMR (125 MHz; CD$_3$OD) δ_C 20.5 (CH$_3$CO), 20.6 (2 × CH$_3$CO), 52.6 (CO$_2$$CH_3$), 55.0 (C-2), 63.2 ($C$-6), 66.0 ($CH_2CO_2$Me), 67.7 ($CH_2$Ph), 69.5 (C-5), 70.0 (C-4), 72.5 (C-3), 99.6 (C-1), 128.8 (C-Ar), 129.0 (C-Ar), 129.5 (C-Ar), 138.3 (C-Ar), 158.5 (NCO$_2$CH$_2$Ph),

171.3 (CO_2R), 172.0 (CO_2R), 172.1 (CO_2R), 172.4 (CO_2Me); MS (ESI-) *m/z* 510.2 [M-H]⁻; HRMS calc for $C_{23}H_{33}N_2O_{12}$ [M+NH₄OAc]⁺ 529.2028, found 529.2039.

Methyl 2-(((2*S*,3*R*,4*R*,5*S*,6*R*)-3-(((benzyloxy)carbonyl)amino)-4,5-dihydroxy-6-(hydroxymethyl)tetrahydro-2*H*-pyran-2-yl)oxy)acetate (144)

NaOMe₍ₛ₎ (8 mg, 0.16 mmol, 0.2 eq.) was added to methyl ester **143** (400 mg, 0.78 mmol, 1 eq.) in MeOH (5 mL) at room temperature, and the mixture was stirred at room temperature for 1 h. The solvent was removed *in vacuo*, and the residue purified by MPLC on SiO₂ with a gradient elution from 0-20% MeOH/EtOAc to give a white solid (300 mg, 0.78 mmol, 100%); R_f 0.5 (5% MeOH/EtOAc; anisaldehyde); mp 150-152 °C; λ_{max}(EtOH)/nm < 220; IR ν_{max}/cm⁻¹ 3489, 3327, 3268, 2945, 2890, 1721, 1685, 1530; ¹H NMR (500 MHz; CD₃OD) δ_H 3.39 (1H, app t, *J* = 9.0 Hz, H-4), 3.65 (1H, ddd, *J* = 2.1, 5.8, and 9.8 Hz, H-5), 3.68-3.74 (3H, m, H-2, H-3 and H-6ₐ), 3.77 (3H, s, CO₂C*H₃*), 3.85 (1H, dd, *J* = 2.1 and 11.8 Hz, H-6_b), 4.25 (1H, d, *J* = 16.4 Hz, C*H_a*H_bCO₂Me), 4.31 (1H, d, *J* = 16.4 Hz, C*H_a*H_bCO₂Me), 4.93 (1H, d, *J* = 3.1 Hz, H-1), 5.11 (1H, d, *J* = 12.4 Hz, CH_a*H_b*Ph), 5.15 (1H, d, *J* = 12.4 Hz, CH_a*H_b*Ph), 7.39-7.43 (5H, m, H-Ar); ¹³C NMR (125 MHz; CD₃OD) δ_C 52.5 (CO₂*C*H₃), 57.0 (C-2), 62.7 (C-6), 65.2 (*C*H₂CO₂CH₃), 67.6 (*C*H₂Ph), 72.1 (C-4), 73.0 (C-3), 74.4 (C-5), 99.4 (C-1), 128.9 (C-Ar), 129.0 (C-Ar), 129.5 (C-Ar), 138.3 (C-Ar), 159.0 (NH*C*O₂Bn), 172.5 (*C*O₂Me); HRMS calcd for $C_{17}H_{22}N_1O_9$ [M-H]⁻ 384.1300, found 384.1305.

Methyl 2-(((2*S*,3*R*,4*R*,5*S*,6*R*)-3-(((benzyloxy)carbonyl)amino)-4,5-dihydroxy-6-((sulfamoyloxy)methyl)tetrahydro-2*H*-pyran-2-yl)oxy)acetate (145)
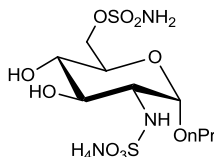

Prepared according to sulfamoylation method 2 using sulfamoyl chloride (0.78 mL, 1 M in MeCN, 0.78 mmol, 1.5 eq.), alcohol **144** (200 mg, 0.52 mmol, 1 eq.) and DMF (4 mL) at -40 °C. The residue was purified by MPLC on SiO₂ with a gradient elution from 50% EtOAc/petrol to 100% EtOAc to 7 % MeOH/EtOAc to give a white solid. (162 mg, 0.35 mmol, 67 %); R_f 0.2 (EtOAc; anisaldehyde); mp 136-137 °C; λ_{max}(EtOH)/nm < 220; IR ν

$_{max}$/cm^{-1} 3432, 3389, 3248, 3242, 1760 (CO ester), 1686 (carbamate I), 1541 (carbamate II), 1372 (SO), 1180 (SO); ^{1}H NMR (500 MHz; CD$_3$OD) δ_H 3.38-3.44 (1H, m, H-4), 3.67-3.74 (2H, m, H-2 and H-3), 3.77 (3H, s, OMe), 3.93 (1H, ddd, J = 1.7, 5.8 and 9.9 Hz, H-5), 4.244.33 (3H, m, H-6$_a$ and CH_2CO$_2$Me), 4.42 (1H, dd, J = 1.7 and 10.9 Hz, H-6$_b$), 4.93 (1H, d, J = 2.9 Hz, H-1), 5.13 (1H, d, J = 12.6 Hz, CH_aH$_b$Ph), 5.16 (1H, d, J = 12.6 Hz, CH$_a$$H_b$Ph), 7.30-7.45 (5H, m, H-Ar); ^{1}H NMR (500 MHz; DMSO-d_6) δ_H 3.16-3.24 (1H, m, H-4), 3.45-3.58 (2H, m, H-2 and H-3), 3.68 (3H, s, OMe), 3.80 (1H, ddd, J = 1.7, 6.0, and 10.1 Hz, H-5), 4.13 (1H, dd, J = 6.0 and 10.7 Hz, H-6$_a$), 4.19-4.29 (3H, m, CH$_2$CO$_2$Me and H-6$_b$), 4.89 (1H, d, J = 3.3 Hz, H-1), 4.97 (1H, d, J = 5.7 Hz, OH-3), 5.08 (2H, s, CH$_2$Ph), 5.38 (1H, d, J = 6.3 Hz, OH-4), 7.12 (1H, d, J = 8.0 Hz, NHCO$_2$Bn), 7.33-7.37 (1H, m, H-Ar), 7.38-7.43 (4H, m, H-Ar), 7.50 (2H, br s, SONH$_2$); ^{13}C NMR (125 MHz; CD$_3$OD) δ_C 52.5 (CO$_2$$CH_3$), 56.9 (C-2), 65.6 ($CH_2CO_2$Me), 67.7 (CH$_2$Ph), 70.0 (C-6), 71.8 (C-4), 71.9 (C-5), 72.9 (C-3), 99.6 (C-1), 128.9 (C-Ar), 129.0 (C-Ar), 129.5 (C-Ar), 138.3 (C-Ar), 158.9 (NHCO$_2$Bn), 172.4 (CO$_2$Me); HRMS calcd for C$_{17}$H$_{23}$O$_{11}$N$_2$S$_1$ [M-H]$^-$ 463.1028, found 463.1031.

2-(((2S,3R,4R,5S,6R)-3-((((benzyloxy)carbonyl)amino)-4,5-dihydroxy-6-((sulfamoyloxy)methyl)tetrahydro-2H-pyran-2-yl)oxy)acetic acid (148)

To methyl ester **145** (100 mg, 0.22 mmol, 1 eq.) in THF (2 mL) at room temperature was added NaOH (216 μL, 2 M aq., 0.43 mmol, 2 eq.), and the reaction was stirred at room temperature for 2 hours. HCl (324 μL, 2 M aq., 0.65 mmol, 3 eq.) was added, and the mixture extracted with EtOAc (10 mL) and CH$_2$Cl$_2$ (10 mL). The organic extracts were combined, dried (MgSO$_4$) and the solvent removed *in vacuo* to give a clear gum (80 mg, 0.18 mmol, 82%); R_f 0.15 (20% MeOH/EtOAc; ninhydrin); λ_{max}(EtOH)/nm < 220; IR ν $_{max}$/cm^{-1} 3400 br, 1693 (str, br), 1531, 1358 (SO), 1178 (SO); ^{1}H NMR (500 MHz; CD$_3$OD) δ_H 3.38-3.42 (1H, m, H-4), 3.66-3.72 (2H, m, H-2 and H-3), 3.88 (1H, ddd, J = 1.6, 5.7, and 9.9 Hz, H-5), 4.17 (1H, d, J = 16.6 Hz, CH_aH$_b$CO$_2$H), 4.24-4.31 (2H, m, H-6$_a$ and CH$_a$$H_bCO_2$H), 4.41 (1H, dd, J = 1.6 and 10.7 Hz, H-6$_b$), 4.90 (1H, d, J = 2.7 Hz, H-1), 5.12 (2H, s, CH$_2$Ph), 7.28-7.42 (5H, m, H-Ar); ^{13}C NMR (125 MHz; CD$_3$OD) δ_C 56.9 (C-2), 65.4 (CH$_2$CO$_2$H), 67.7 (CH$_2$Ph), 70.0 (C-6), 71.8 (C-5), 71.9 (C-4), 73.1 (C-3), 99.5 (C-1),
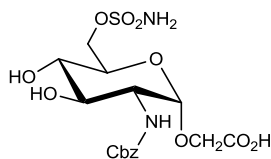
128.9 (C-Ar), 129.0 (C-Ar), 129.5 (C-Ar), 138.3 (C-Ar), 159.0 (CO$_2$Bn), 173.6 (CO$_2$H); HRMS calcd for C$_{16}$H$_{21}$O$_{11}$N$_2$S$_1$ [M-H]$^-$ 449.0872, found 449.0864.

2-(((2S,3R,4R,5S,6R)-3-amino-4,5-dihydroxy-6-((sulfamoyloxy) methyl) tetrahydro-2H-pyran-2-yl)oxy)acetic acid (149)
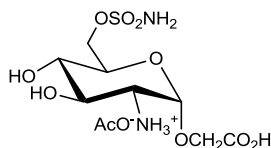
Carbamate **148** (70 mg, 0.16 mmol) was dissolved in acetic acid (5 mL) and hydrogenated on a Thales H-cube on full H$_2$ mode through 5% Pd/C catalyst cartridge at 40 °C for 3 h, with constant recycling of reaction mixture. The solvent was removed *in vacuo* to give a clear gum. (63 mg, 100%); R_f 0.3 (50:50:5 EtOAc:MeOH:NH$_4$OH; ninhydrin); λ_{max}(EtOH)/nm < 220;IR ν $_{max}$/cm^{-1} 3012, 1710, 1365 (SO), 1172 (SO); ^{1}H NMR (500 MHz; CD$_3$OD) δ$_H$ 3.20 (1H, dd, J = 3.6 and 10.6 Hz, H-2), 3.42 (1H, dd, J = 9.3 and 9.8 Hz, H-4), 3.85-3.92 (2H, m, H-3 and H-5), 4.00 (1H, d, J = 15.6 Hz, CH_aH$_b$CO$_2$H), 4.18 (1H, d, J = 15.6 Hz, CH$_a$$H_bCO_2$H), 4.33 (1H, dd, J = 5.4 and 10.9 Hz, H-6$_a$), 4.42 (1H, dd, J = 1.8 and 10.9 Hz, H-6$_b$), 5.11 (1H, d, J = 3.6 Hz, H-1); ^{13}C NMR (125 MHz; CD$_3$OD) δ$_C$ 20.9 (CH$_3$CO$_2^-$), 55.6 (C-2), 68.1 (CH$_2$CO$_2$H), 69.3 (C-6), 71.3 (C-4), 71.7 (C-3), 72.0 (C-5), 97.2 (C-1), 175.4 (CO$_2$H), 176.7 (CH$_3$CO$_2^-$); MS (ESI-) m/z 315.1 [M-H]$^-$, (ESI+) 317.2.3 [M+H]$^+$.

Disodium 2-(((2S,3R,4R,5S,6R)-4,5-dihydroxy-6-((sulfamoyloxy) methyl)-3-(sulfoamino)tetrahydro-2H-pyran-2-yl)oxy)acetate (55)

Prepared according to general procedure B, using amine **149** (70 mg, 0.18 mmol), de-ionised water (2 mL) and pyridine-sulfur trioxide complex (59 mg, 0.37 mmol, 3.7 eq.) for 18 h. The crude product was purified by MPLC on SiO$_2$ with a gradient elution from 50-80% MeOH/EtOAc. Product containing fractions were evaporated *in vacuo*. The residue was dissolved in water, frozen, and lyophilized to give a white solid (28 mg, 38%); R_f 0.7 (MeOH; ninhydrin); mp 150 °C dec.; λ_{max}(EtOH)/nm < 220; IR ν $_{max}$/cm^{-1} 3224 br, 1587, 1356 (SO), 1176 (SO); ^{1}H NMR (500 MHz; CD$_3$OD) δ$_H$ 3.29 (1H, dd, J = 3.6 and 10.1 Hz, H-2), 3.42 (1H, dd, J = 9.0 and 10.1 Hz, H-4), 3.74 (1H, dd, J = 9.0 and 10.1 Hz, H-3),

3.90 (1H, ddd, J = 1.7, 5.8, and 10.1 Hz, H-5), 4.05 (1H, d, J = 15.8 Hz, CH_aH$_b$CO$_2$H), 4.21 (1H, d, J = 15.8 Hz CH$_a$$H_bCO_2$H), 4.30 (1H, dd, J = 5.8 and 10.8 Hz, H-6$_a$), 4.42 (1H, d, J = 1.7 and 10.8 Hz, H-6$_b$), 5.11 (1H, d, J = 3.6 Hz, H-1); ^{1}H NMR (500 MHz; D$_2$O) δ_H 3.19 (1H, dd, J = 3.6 and 10.3 Hz, H-2), 3.47 (1H, dd, J = 9.2 and 10.1 Hz, H-4), 3.67 (1H, dd, J = 9.2 and 10.3 Hz, H-3), 3.89-3.95 (2H, m, H-5 and CH$_a$$H_bCO_2$H), 4.05 (1H, d, J = 15.3 Hz, CH_aH$_b$CO$_2$H), 4.36 (2H, d, J = 3.3 Hz, H-6), 5.06 (1H, d, J = 3.6 Hz, H-1); ^{13}C NMR (125 MHz; CD$_3$OD) δ_C 59.5 (C-2), 67.5 (*CH$_2$CO$_2$H*), 70.0 (C-6), 71.4 (C-5), 71.9 (C-4), 73.9 (C-3), 99.9 (C-1), 175.7 (CO$_2$H); HRMS calcd for C$_8$H$_{15}$N$_2$O$_{12}$S$_2$ [M-H]$^-$ 395.0072, found 395.0057.

(2R,3S,4R,5R,6S)-2-(acetoxymethyl)-5-(((benzyloxy)carbonyl)amino)-6-(3-hydroxypropoxy)tetrahydro-2H-pyran-3,4-diyl diacetate[337] (150)

BH$_3$.THF (1 M in THF, 4.17 mL, 4.17 mmol, 4 eq.) was added to allyl ether **141** (500 mg, 1.05 mmol, 1 eq.) in THF (50 mL) at 0 °C, and stirred at room temperature for 18 h. After the addition of phosphate buffer (pH 7.4, 8 mL), hydrogen peroxide (1 mL, 27% in water, 14 mmol, 13 eq.) was added, and the mixture was stirred at room temperature for 18 h. The mixture was extracted with CH$_2$Cl$_2$ (3 × 40 mL), washed with saturated aqueous NaCl, dried over MgSO$_4$ and solvent removed *in vacuo*. The residue was purified by MPLC on SiO$_2$ with gradient elution from 20-100% EtOAc/petrol to give a clear oil (180 mg, 35%); R_f 0.2 (50% EtOAc/petrol; anisaldehyde); λ_{max}(EtOH)/nm < 220; IR ν_{max}/cm^{-1} 1739, 1513; ^{1}H NMR (500 MHz; CD$_3$OD) δ_H 1.85-1.92 (5H, m, CH$_3$CO and CH$_2$CH_2CH$_2$OH), 2.03 (3H, s, CH$_3$CO), 2.09 (3H, s, CH$_3$CO), 3.60 (1H, dt, J = 9.9 and 6.1 Hz, CH_aH$_b$CH$_2$CH$_2$OH), 3.72 (2H, t, J = 6.1 Hz, CH$_2$CH$_2$CH_2OH), 3.87 (1H, dt, J = 9.9 and 6.1 Hz, CH$_a$$H_bCH_2CH_2$OH), 3.97 (1H, dd, J = 3.3 and 10.9 Hz, H-2), 4.05 (1H, ddd, J = 2.0 Hz, 4.7, and 9.6 Hz , H-5), 4.14 (1H, dd, J = 2.0 and 12.2 Hz, H-6$_a$), 4.29 (1H, dd, J = 4.7 and 12.2 Hz, H-6$_b$), 4.90 (1H, d, H-1), 5.00-5.09 (2H, m, H-4 and CH_aH$_b$Ph), 5.19 (1H, d, J = 12.5 Hz, CH$_a$$H_b$Ph), 5.26 (1H, app t, J = 9.8 Hz, H-3), 7.30-7.40 (5H, m, H-Ar); ^{13}C NMR (125 MHz; CD$_3$OD) δ_C 20.6 (2 × CO*C*H$_3$), 20.7 (CO*C*H$_3$), 33.2 (CH$_2$*C*H$_2$CH$_2$OH), 55.1 (C-2), 59.8 (CH$_2$CH$_2$*C*H$_2$OH), 63.4 (C-6), 66.4 (*C*H$_2$CH$_2$CH$_2$OH), 67.7 (CH$_2$Ph), 68.9 (C-5), 70.4 (C-4), 72.8 (C-3), 98.9 (C-1), 128.9 (C-Ar), 129.1 (C-Ar),

129.5 (C-Ar), 138.3 (C-Ar), 171.4 (2 × $COCH_3$), 172.4 ($COCH_3$); HRMS calcd for $C_{23}H_{31}N_1O_{11}$ [M-H]$^-$ 496.1824, found 496.1830.

Benzyl ((2S,3R,4R,5S,6R)-2-(3-(benzyloxy)propoxy)-4,5-dihydroxy-6-(hydroxymethyl)tetrahydro-2H-pyran-3-yl)carbamate (152)

Compound **102** (1.5g, 4.8 mmol), 3-benzyloxy-1-propanol (5 mL), HCl in dioxane (2 mL, 4 M) and dioxane (20 mL) were combined and heated to 75 °C for 5 h. The mixture was allowed to cool to room temperature and the solvent removed *in vacuo*. The residue was purified by MPLC on SiO_2 with a gradient elution from 0-5% MeOH/EtOAc. Product containing fractions were combined, evaporated, and re-purified by MPLC on SiO_2 with a gradient elution from 70% EtOAc/Petrol to 100% EtOAc to 8% MeOH/EtOAc to give a pale brown solid (685 mg, 1.49 mmol, 31%). R_f 0.5 (5% MeOH/EtOAc; anisaldehyde); mp 98-101 °C; λ_{max}(EtOH)/nm < 220; IR ν $_{max}$/cm^{-1} 3324, 2932, 2881, 1689 (carbamate I), 1536 (carbamate II); ^{1}H NMR (500 MHz; CDCl$_3$) δ$_H$ 1.87 (2H, quint, CH_2CH$_2$OBn), 1.98 (1H, br t, J = 5.7 Hz, C$_6$OH), 2.72 (1H, br s, OH), 2.99 (1H, br s, OH), 3.47-3.72 (6H, m, H-3, H-4, H-5, H-6$_a$, CH$_2$O), 3.75-3.86 (4H, m, CH$_2$O, H-2, H-6$_b$), 4.47 (2H, s, CH$_2$OCH_2Ph), 4.80 (1H, d, J = 3.4 Hz, H-1), 5.11 (2H, s, NCO$_2$CH_2Ph), 5.32-5.38 (1H, d, J = 8.4 Hz, NH), 7.26-7.36 (10H, m, H-Ar); ^{13}C NMR (125 MHz; CDCl$_3$) δ$_C$ 29.6 (OCH$_2$$CH_2CH_2$O), 55.4 (C-2), 62.4, 65.5 (NHCOCH$_2$Ph), 67.1, 67.5, 71.1, 73.0 (CH$_2$CH$_2$OCH$_2$Ph), 74.4, 97.5 (C-1), 127.7 (C-Ar), 128.4 (C-Ar), 128.5 (C-Ar), 128.6 (C-Ar), 138.2 (C-Ar), 157.2 (CO); HRMS calcd for $C_{24}H_{32}O_8N_1$ [M+H]$^+$ 462.2122, found 462.2119.
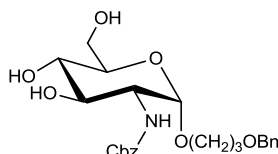
((2R,3S,4R,5R,6S)-5-(((benzyloxy)carbonyl)amino)-6-(3-(benzyloxy) propoxy)-3,4-dihydroxytetrahydro-2H-pyran-2-yl)methyl sulfamate (153)
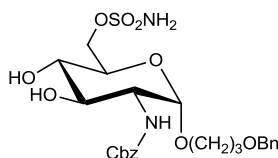
Prepared according to sulfamoylation method 2 using sulfamoyl chloride (2.1 mL, 1 M in MeCN, 2.1 mmol, 1.5 eq.), compound **152** (650 mg, 1.4 mmol, 1 eq.), and DMF (8 mL). The residue was purified by MPLC on SiO_2 with gradient elution from 50% EtOAc/petrol

to 100% EtOAc to give a white solid (435 mg, 57 %); R_f 0.2 (EtOAc; anisaldehyde); mp 137-139 °C; λ_{max}(EtOH)/nm < 220; IR ν_{max}/cm^{-1} 3336, 1684 (carbamate I), 1542 (carbamate II), 1372 (SO), 1182 (SO); ^{1}H NMR (500 MHz; CD$_3$OD) δ_H 1.86-1.95 (2H, m, OCH$_2$CH_2CH$_2$OBn), 3.36-3.42 (1H, m, H-4), 3.52-3.58 (1H, m, OCH_aH$_b$CH$_2$CH$_2$OBn), 3.61-3.68 (4H, m, H-2, H-3, OCH$_2$CH$_2$CH_2OBn), 3.81-3.89 (2H, m, H-5 and OCH$_a$H$_b$CH$_2$CH$_2$OBn), 4.28 (1H, dd, J = 5.8 and 10.7 Hz, H-6$_a$), 4.41 (1H, dd, J = 1.7 and 10.7 Hz, H-6$_b$), 4.50 (2H, s, CH$_2$OCH_2Ph), 4.83 (1H, d, J = 1.8 Hz, H-1), 5.11 (2H, s, NHCO$_2$CH_2Ph), 7.27-7.40 (10H, m, H-Ar); ^{13}C NMR (125 MHz; CD$_3$OD) δ_C 30.7 (OCH$_2$$CH_2CH_2$OBn), 57.1 (C-2), 66.2 (OCH$_2$CH$_2$CH$_2$OBn), 67.6 (NHCO$_2$$CH_2$Ph), 68.2 (OCH$_2CH_2$$CH_2$OBn), 70.1 (C-6), 71.4 (C-5), 72.0 (C-4), 73.0 (C-3), 74.1 (CH$_2$OCH$_2$Ph), 99.1 (C-1), 128.7 (C-Ar), 128.9 (C-Ar), 129.0 (C-Ar), 129.1 (C-Ar), 129.4 (C-Ar), 129.5 (C-Ar), 138.2 (C-Ar), 139.8 (C-Ar), 158.8 (CO); HRMS calcd for C$_{24}$H$_{33}$O$_{10}$N$_2$S$_1$ [M+Na]$^+$ 541.1850, found 541.1846.

(2S,3R,4R,5S,6R)-4,5-dihydroxy-2-(3-hydroxypropoxy)-6-((sulfamoyloxy)methyl) tetrahydro-2H-pyran-3-aminium acetate (154)

Compound **153** (190 mg, 0.35 mmol) was dissolved in acetic acid (9 mL) and hydrogenated on a Thales H-cube at a hydrogen pressure of 20 bar through 5% Pd/C catalyst cartridge at 20 °C for 1 h, with constant recycling of the reaction mixture at a flow rate of 1 mL/minute. The solvent was removed *in vacuo* to give a clear gum, which was triturated with Et$_2$O (4 × 5 mL). The resulting gum was dried *in vacuo* at 40 °C for 18 h to give a clear glass (110 mg, 83%); R_f 0.1 (25% MeOH/EtOAc); λ_{max}(EtOH)/nm < 220; IR ν_{max}/cm^{-1} 2939 br, 1707 w, 1539 (CO$_2^-$), 1361 (SO), 1176 (SO); ^{1}H NMR (500 MHz; CD$_3$OD) δ_H 1.91 (2H, app. quin, J = 6.2 Hz, CH$_2$CH_2CH$_2$OH), 2.00 (3H, s, CH$_3$CO$_2^-$), 3.12 (1H, dd, J = 3.1 and 10.4 Hz, H-2), 3.40 (1H, app. t, J = 9.5 Hz, H-4), 3.63 (1H, dt, J = 9.8 and 6.2 Hz, CH_aH$_b$CH$_2$CH$_2$OH), 3.69-3.80 (3H, m, H-3 and CH_2OH), 3.87 (1H, ddd, J = 1.7, 5.7, and 9.5 Hz, H-5), 3.93 (1H, dt, J = 9.8 and 6.2 Hz, CH$_a$H$_b$CH$_2$CH$_2$OH), 4.31 (1H, dd, J = 5.7 and 10.9 Hz, H-6$_a$), 4.45 (1H, dd, J = 1.7 and 10.9 Hz, H-6$_b$), 5.01 (1H, d, J = 3.1 Hz, H-1); ^{13}C NMR (125 MHz; CD$_3$OD) δ_C 22.2 (CH$_3$ acetate), 33.2 (CH$_2$$CH_2CH_2$OH), 55.8 (C-2), 59.7 (CH$_2$CH$_2$$CH_2$OH), 66.4 ($CH_2CH_2CH_2$OH), 69.6 (C-6),

71.5 (C-4), 71.8 (C-5), 72.5 (C-3), 97.5 (C-1), 177.3 (CO); HRMS calcd for $C_9H_{21}N_2O_8S_1$ $[M+H]^+$ 317.1013, found 317.1017.

Sodium ((2S,3R,4R,5S,6R)-4,5-dihydroxy-2-(3-hydroxypropoxy)-6-((sulfamoyloxy)methyl)tetrahydro-2H-pyran-3-yl)sulfamate (54)

Prepared according to general procedure B, using compound **154** (100 mg, 0.27 mmol, 1 eq.), de-ionised water (5 mL) and pyridine-sulfur trioxide complex (126 mg, 0.53 mmol, 3 eq.) for 18 h. The crude product was purified by MPLC on SiO_2 with a gradient elution from 20-40% MeOH/EtOAc. Product containing fractions were evaporated *in vacuo* to give a pale glass (43 mg, 41%); R_f 0.3 (30% MeOH/EtOAc; anisaldehyde); mp 105-110 °C; $[\alpha]_D^{18.0}$ +85.71° (c = 0.21, MeOH); λ_{max}(EtOH)/nm < 220; IR ν_{max}/cm^{-1} 3287, 2929, 1361 (SO), 1175 (SO); ^{1}H NMR (500 MHz; CD_3OD) δ_H 1.82-1.93 (2H, m, $CH_2CH_2CH_2OH$), 3.28 (1H, dd, J = 3.6 and 10.4 Hz, H-2), 3.40 (1H, dd, 9.6 and 10.1 Hz, H-4), 3.56-3.63 (2H, m, H-3 and $CH_aH_bCH_2CH_2OH$), 3.67-3.79 (2H, m, $CH_2CH_2CH_2OH$), 3.81-3.90 (1H, m, H-5), 4.44 (1H, dd, J = 2.0 and 10.8 Hz, H-6$_a$), $CH_aH_bCH_2CH_2OH$), 4.28 (1H, dd, J = 6.0 and 10.8 Hz, H-6$_b$), 5.11 (1H, d, J = 3.6 Hz H-1); ^{13}C NMR (125 MHz; CD_3OD) δ_C 33.40 ($CH_2CH_2CH_2OH$), 59.54 (C-2), 59.94 ($CH_2CH_2CH_2OH$), 66.2 ($CH_2CH_2CH_2OH$), 70.2 (C-6), 71.1 (C-5), 71.9 (C-4), 74.0 (C-3), 99.3 (C-1); HRMS calcd for $C_9H_{19}N_2O_{11}S_1$ 395.0436 $[M-H]^-$, found 495.0417.

((2R,3S,4R,5R,6S)-5-amino-6-(3-(benzyloxy)propoxy)-3,4-dihydroxytetrahydro-2H-pyran-2-yl)methyl sulfamate (155)

Compound **153** (200 mg, 0.37 mmol) was dissolved in EtOH (10 mL) and hydrogenated on a Thales H-cube at a hydrogen pressure of 20 bar through 5% Pd/C catalyst cartridge at 20 °C for 1 h, with constant recycling of the reaction mixture at a flow rate of 1 mL/minute. The solvent was removed *in vacuo* to give a clear gum, which was purified by MPLC on SiO_2 with gradient elution from 15-30% MeOH/EtOAc to give a clear gum (113 mg, 75 %); R_f 0.1 (15% MeOH/EtOAc; anisaldehyde); λ_{max}(EtOH)/nm < 220; IR ν_{max}/cm^{-1} 2931,

1363 (SO), 1178 (SO); ^{1}H NMR (500 MHz; CD$_3$OD) δ_H 1.96 (2H, m, CH_2CH$_2$OBn), 2.63 (1H, dd, J = 3.6 and 9.9 Hz, H-2), 3.31 (2H, dd, J = 9.0 and 9.9 Hz, H-4), 3.48 (1H, dd, J = 9.0 and 9.9 Hz, H-3), 3.57 (1H, app. dt, J = 9.8 and 6.2 Hz, CH_aH$_b$O), 3.65 (2H, t, J = 6.3 Hz, CH_2OBn), 3.83 (1H, ddd, J = 1.9 , 5.8, and 9.9 Hz, H-5), 3.90 (1H, app dt, J = 9.8 and 6.2 Hz, CH$_a$$H_b$O), 4.27 (1H, dd, J = 5.8 and 10.7 Hz, H-6$_a$), 4.40 (1H, dd, J = 1.9 and 10.7 Hz, H-6$_b$), 4.60 (2H, s, CH_2Ph), 4.81 (1H, d, J = 3.6 Hz, H-1), 7.29-7.34 (1H, m, H-Ar), 7.36-7.40 (4H, m, H-Ar); ^{13}C NMR (125 MHz; CD$_3$OD) δ_C 30.8 (OCH$_2$$CH_2CH_2$OBn), 57.0 (C-2), 66.1 (OCH$_2$CH$_2$CH$_2$OBn), 68.2 (OCH$_2$CH$_2$$CH_2$OBn), 70.1 (C-6), 71.7 (C-4 and C-5), 74.0 (CH$_2$Ph), 76.1 (C-3), 100.3 (C-1), 128.7 (C-Ar), 128.9 (C-Ar), 129.4 (C-Ar), 139.8 (C-Ar); HRMS calcd for C$_{16}$H$_{25}$N$_2$O$_8$S$_1$ [M-H]$^-$ 405.1337, found 405.1339.
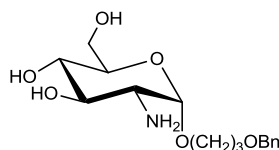
Ammonium ((2S,3R,4R,5S,6R)-2-(3-(benzyloxy)propoxy)-4,5-dihydroxy-6-((sulfamoyloxy) methyl)tetrahydro-2H-pyran-3-yl)sulfamate (58)
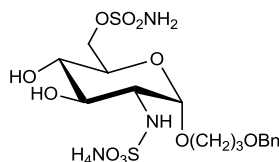
Prepared according to general procedure B, using compound **155** (100 mg, 0.25 mmol), de-ionised water (3 mL) and pyridine-sulfur trioxide complex (46 mg, 0.30 mmol, 2.2 eq.) for 18 h. The crude product was purified by MPLC on SiO$_2$ with gradient elution from 85:15:1.5 to 65:35:3.5 EtOAc:MeOH:NH$_4$OH to give a white solid (74 mg, 62%); R_f 0.2 (70:30:3 EtOAc/MeOH/NH$_4$OH; anisaldehyde); mp 85-90 °C; $[\alpha]_D^{22.7}$ +108.6° (c = 0.14, MeOH); λ_{max}(EtOH)/nm < 220; IR ν_{max}/cm^{-1} 3246, 3064, 2880, 1363 (SO), 1175 (SO); ^{1}H NMR (500 MHz; CD$_3$OD) δ_H 1.90-2.02 (2H, m, OCH$_2$CH_2CH$_2$OBn), 3.28 (1H, dd, J = 3.6 and 10.2 Hz, H-2), 3.41 (1H, dd, J = 8.9 and 10.0 Hz, H-4), 3.57-3.64 (2H, m, H-3 and OCH_aH$_b$CH$_2$CH$_2$OBn), 3.64-3.71 (2H, m, OCH$_2$CH$_2$CH_2OBn), 3.80-3.91 (2H, m, OCH$_a$$H_bCH_2CH_2$OBn and H-5), 4.27 (1H, dd, J = 6.0 and 10.7 Hz, H-6$_a$), 4.41 (1H, dd, J = 1.9 and 10.7 Hz, H-6$_b$), 4.56 (2H, s, CH_2Ph), 5.10 (1H, d, J = 3.6 Hz, H-1), 7.28-7.32 (1H, m, H-Ar), 7.35-7.41 (4H, m, H-Ar); ^{13}C NMR (125 MHz; CD$_3$OD) δ_C 30.8 (OCH$_2$$CH_2CH_2$OBn), 59.6 (C-2), 66.4 (OCH$_2$CH$_2$CH$_2$OBn), 68.4 (OCH$_2$CH$_2$$CH_2$OBn), 70.2 (C-6), 71.1 (C-5), 71.9 (C-4), 74.0 (CH$_2$Ph), 74.1 (C-3), 99.4 (C-1), 128.6 (C-Ar), 129.0 (C-Ar), 129.4 (C-Ar), 139.9 (C-Ar); HRMS calcd for C$_{16}$H$_{25}$N$_2$O$_{11}$S$_2$ [M-H]$^-$ 485.0905, found 485.0914.

Benzyl ((2R,4aR,6S,7R,8R,8aS)-8-hydroxy-6-methoxy-2-phenyl hexahydropyrano[3,2-d][1,3]dioxin-7-yl)carbamate[202] (156)

Compound **103** (200 mg, 0.6 mmol), benzaldehyde dimethyl acetal (230 μL, 1.52 mmol, 3 eq.), and *p*-toluenesulfonic acid (5 mg, cat.), were combined in DMF (5 mL) and heated to 75 °C for 3 h. The reaction mixture was diluted with EtOAc (20 mL), washed with brine (10 mL), dried over MgSO$_4$, and the solvent removed *in vacuo*. The residue was purified by MPLC on SiO$_2$ with gradient elution from 25% EtOAc/petrol to 100% EtOAc to give a white solid (197 mg, 78%); R_f 0.4 (40% EtOAc/petrol; anisaldehyde); mp 207-210 °C (lit.[338] 207-208 °C); λ_{max}(EtOH)/nm < 220; IR ν_{max}/cm^{-1} 3313, 1685 (carbamate I), 1546 (carbamate II); ^{1}H NMR (500 MHz; CDCl$_3$) δ_H 2.68 (1H, d, J = 1.8 Hz, OH), 3.42 (3H, s, OCH$_3$), 3.61 (1H, app t, J = 8.5 Hz, H-4), 3.77-3.87 (2H, m, H-6$_a$ and H-5), 3.90-4.02 (2H, m, H-2 and H-3), 4.31 (1H, dd, J = 3.5 and 9.0 Hz, H-6$_b$), 4.77 (1H, d, J = 3.6 Hz, H-1), 5.12-5.21 (3H, m, CH$_2$Ph and NH), 5.59 (1H, s, PhC*H*(OR)$_2$), 7.33-7.44 (8H, m, H-Ar), 7.49-7.55 (2H, m, H-Ar); ^{13}C NMR (125 MHz; CDCl$_3$) δ_C 55.1 (OMe), 56.0 (C-2), 62.5 (C-5), 67.1 (*C*H$_2$Ph), 68.8 (C-6), 70.8 (C-3), 81.8 (C-4), 99.5 (C-1), 102.3 (PhC*H*(O)$_2$), 126.3 (C-Ar), 127.1 (C-Ar), 128.3 (C-Ar), 128.6 (C-Ar), 129.1 (C-Ar), 129.3 (C-Ar), 136.1 (C-Ar)137.1 (C-Ar), 156.8 (CO); HRMS calcd for C$_{22}$H$_{26}$O$_7$N$_1$ [M+H]$^+$ 416.1704, found 416.1705.

Benzyl ((2R,4aR,6S,7R,8aS)-6-methoxy-2-phenylhexahydropyrano [3,2-d][1,3] dioxin-7-yl)carbamate[339] (157)

Compound **156** (500 mg, 1.20 mmol, 1 eq.) and 1,1-thiocarbonyl diimidazole (322 mg, 1.81 mmol, 1.5 eq.) were combined in toluene (12 mL), degassed, and heated at reflux for 3 h under a nitrogen atmosphere. *Tris*(trimethylsilyl) silane (743 μL, 2.40 mmol, 2 eq.) and AIBN (604 μL, 0.2 M solution in toluene, 0.12 mmol, 0.1 eq.) were added and the mixture heated at reflux for 1 h. A further 0.1 eq. of AIBN solution was added and heating continued for a further 30 minutes. The solvent was removed *in vacuo*, and the residue purified by MPLC on SiO$_2$ with a gradient elution from 5-35% EtOAc/petrol to give a

white solid (400 mg, 1.00 mmol, 83%); R_f 0.75 (40% EtOAc/Petrol; anisaldehyde); mp 180-183 °C (lit.[339] 175-176 °C); λ_{max}(EtOH)/nm < 220; IR ν_{max}/cm^{-1} 3320, 1686 (carbamate I), 1539 (carbamate II); ^{1}H NMR (500 MHz; CD$_3$OD) δ_H 1.91 (app. q, J = 11.5 Hz, H-3$_a$), 2.10 (1H, app. dt, J = 11.5 and 4.4 Hz, H-3$_b$), 3.46 (3H, s, OMe), 3.66-3.74 (2H, m, H-4 and H-5), 3.79 (1H, app. t, J = 10.0 Hz, H-6$_a$), 3.94 (1H, app. dt, J = 12.4 and 3.7 Hz, H-2), 4.23 (1H, dd, J = 4.4 and 10.0 Hz, H-6$_b$), 4.69 (1H, d, J = 3.7 Hz, H-1), 5.12 (2H, s, CH$_2$Ph), 5.64 (1H, s, PhCH(O)$_2$), 7.31-7.44 (8H, m, H-Ar), 7.46-7.51 (2H, m, H-Ar); ^{1}H NMR (500 MHz; CDCl$_3$) δ_H 1.83 (1H, app. q, J = 11.4 Hz, H-3$_a$), 2.23 (app. dt, J = 11.4 and 4.5 Hz, H-3$_b$), 3.40 (3H, s, OMe), 3.60-3.66 (1H, m, H-4), 3.69-3.77 (2H, m, H-5 and H-6$_a$), 3.98-4.06 (1H, m, H-2), 4.26 (1H, dd, J = 5.5 and 10.2 Hz, H-6$_b$), 4.63 (1H, d, J = 3.5 Hz, H-1), 5.05 (1H, d, J = 9.6 Hz, NH), 5.11 (2H, s, CH$_2$Ph), 5.54 (1H, s, PhCH(O)$_2$), 7.31-7.39 (8H, m, H-Ar), 7.46-7.49 (2H, m, H-Ar); ^{13}C NMR (125 MHz; CDCl$_3$) δ_C 31.2 (C-3), 49.3 (C-2), 55.1 (OMe), 64.0 (C-6), 67.0 (C-5), 69.3 (C-4), 98.0 (C-1), 101.8 (PhCH(O)$_2$), 126.2 (C-Ar), 128.2 (C-Ar), 128.3 (C-Ar), 128.4 (C-Ar), 128.6 (C-Ar), 129.1 (C-Ar), 136.2 (C-Ar), 137.4 (C-Ar), 155.5 (CO); HRMS calcd for C$_{22}$H$_{26}$O$_6$N$_1$ [M-H]$^-$ 400.1755, found 400.1757.

Benzyl ((2*S*,3*R*,5*S*,6*R*)-5-(benzyloxy)-6-(hydroxymethyl)-2-methoxy tetrahydro-2*H*-pyran-3-yl)carbamate (159)

BH$_3$.THF (10.2 mL, 1 M in THF, 10.2 mmol, 7 eq.) was added to a solution of compound **157** in THF (4 mL), followed by the addition of Bu$_2$BOTf (1.45 mL, 1.45 mmol, 1 eq.) at 0 °C, and the mixture was stirred at 0 °C for 1 h. Et$_3$N (1.5 mL) was added followed by cautious addition of MeOH (2 mL) until the evolution of hydrogen ceased. Further MeOH (8 mL) was added, the mixture was evaporated and purified by MPLC on SiO$_2$ with a gradient elution from 20-70% EtOAc/petrol to give a white solid (262 mg, 49%); R_f 0.1 (40% EtOAc/petrol; anisaldehyde); mp 120-122 °C; λ_{max}(EtOH)/nm < 220; IR ν_{max}/cm^{-1} 3326, 1681 (carbamate I), 1538 (carbamate II); ^{1}H NMR (500 MHz; CDCl$_3$) δ_H 1.65 (1H, app q, H-3$_b$), 1.86 (1H, dd, J = 6.0 and 6.9 Hz, C6-OH), 2.36 (1H, dt, J = 11.7 and 4.3 Hz, H-3$_a$), 3.37 (3H, s, OMe), 3.48-3.56 (2H, m, H-4 and H-5), 3.58-3.64 (1H, m, H-6$_a$), 3.70-3.77 (1H, m, H-2), 3.80-3.90 (1H, m, H-6$_b$), 4.45 (1H, d, J = 11.8 Hz, NHCO$_2$C*H*$_a$CH$_b$Ph),

4.56-4.66 (2H, m, H-1 and NHCO$_2$CH$_a$CH_bPh), 5.01 (1H, d, J = 9.5 Hz, NH), 5.10 (2H, s, CH$_2$Ph), 7.27-7.40 (10H, m, H-Ar); ^{13}C NMR (125 MHz; CD$_3$OD) δ_C 31.4 (C-3), 50.7 (C-2), 55.4 (OMe), 62.5 (C-6), 67.6 (CH$_2$Ph), 72.0 (CH$_2$Ph), 73.1 (C-4), 73.5 (C-5), 98.8 (C-1), 128.8 (C-Ar), 128.9 (C-Ar), 129.0 (C-Ar), 129.1 (C-Ar), 129.4 (C-Ar), 129.5 (C-Ar), 138.3 (C-Ar), 139.8 (C-Ar), 158.2 (CO); HRMS calcd for C$_{22}$H$_{28}$N$_1$O$_6$ [M+H]$^+$ 402.1911, found 402.1913.

((2*R*,3*S*,5*R*,6*S*)-3-(Benzyloxy)-5-(((benzyloxy)carbonyl)amino)-6-methoxy tetrahydro-2*H*-pyran-2-yl)methyl sulfamate (160)

Prepared according to sulfamoylation method 3 using sulfamoyl chloride (1.54 mL, 1 M in MeCN, 1.54 mmol, 2 eq.), compound **159** (310 mg, 0.77 mmol, 1 eq.) in MeCN (5.4 mL) containing DMA (600 μL) at room temperature. The reaction was stirred at room temperature for 15 min, quenched with EtOH (1.5 mL) and partitioned between EtOAc (2 × 10 mL) and H$_2$O (10 mL). The aqueous layer was extracted with further CH$_2$Cl$_2$ (10 mL), the organic extracts were combined, dried over MgSO$_4$ and solvent removed *in vacuo*. The residue was purified by MPLC on SiO$_2$ with gradient elution from 20-60% EtOAc/petrol to give a clear gum (270 mg, 73%); R_f 0.4 (50% EtOAc/petrol; anisaldehyde); λ_{max}(EtOH)/nm < 220; IR ν_{max}/cm^{-1} 3321, 2906, 1699 (carbamate I), 1521 (carbamate II), 1379 (SO), 1182 (SO); ^{1}H NMR (500 MHz; CD$_3$OD) δ_H 1.74 (1H, m, H-3$_a$), 2.29 (1H, m, H-3$_b$), 3.44 (3H, s, OMe), 3.54-3.62 (1H, m, H-4), 3.73-3.84 (2H, m, H-2 and H-5), 4.28-4.33 (1H, dd, J = 5.2 and 10.6 Hz, H-6$_a$), 4.38 (1H, dd, J = 1.9 and 10.6 Hz, H-6$_b$), 4.55 (1H, d, J = 11.3 Hz, CHOCH_aH$_b$Ph), 4.63-4.70 (2H, m, H-1 and CHOCH$_a$$H_b$Ph), 5.11 (2H, s, CO$_2CH_2$Ph), 7.27-7.42 (10H, m, H-Ar); ^{13}C NMR (125 MHz; CD$_3$OD) δ_C 31.3 (C-3), 50.5 (C-2), 55.6 (OMe), 67.6 (NHCO$_2$CH$_2$Ph), 70.6 (C-6), 70.9 (C-5), 72.0 (OCH$_2$Ph), 73.1 (C-4), 98.9 (C-1), 128.8 (C-Ar), 128.9 (C-Ar), 129.0 (C-Ar), 129.0 (C-Ar), 129.2 (C-Ar), 129.4 (C-Ar), 129.5 (C-Ar), 139.5 (C-Ar), 158.3 (CO); HRMS calcd for C$_{22}$H$_{27}$N$_2$O$_8$S [M-H]$^-$ 479.1494, found 479.1495.
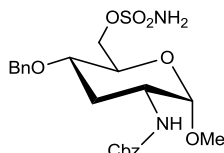
Benzyl ((2S,3R,5S,6R)-5-hydroxy-6-(hydroxymethyl)-2-methoxytetrahydro-2H-pyran-3-yl)carbamate (161)
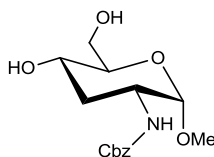
para-Toluenesulfonic acid (10 mg. cat.) was added to a solution of compound **157** (170 mg, 0.43 mmol) in CH_2Cl_2 (6 mL) and methanol (6 mL), and the mixture was heated to 80 °C under microwave irradiation for 20 min. The mixture was diluted with CH_2Cl_2 (50 mL) and washed with K_2CO_3 (2 × 20 mL, 1 M aq.). The organic layer was dried over $MgSO_4$, filtered, and evaporated. The residue was purified by MPLC on SiO_2 with a gradient elution from 80% EtOAc/petrol to 100% EtOAc to give a white solid (95 mg, 72%); R_f 0.2 (80% EtOAc/petrol; anisaldehyde); mp 109-111 °C; λ_{max}(EtOH)/nm < 220; $[\alpha]_D^{19.2}$ +52.3° (c = 0.11, MeOH); IR ν_{max}/cm^{-1} 3327, 2921, 1681 (carbamate I), 1538 (carbamate II); ^{1}H NMR (500 MHz; CD$_3$OD) 1.76 (1H, app. dt, J = 12.5 and 11.7 Hz, H-3$_a$), 2.02 (1H, app. t, J = 4.0 and 11.7 Hz, H-3$_b$), 3.40-3.50 (4H, m, H-5 and OMe), 3.57 (1H, app. td, J = 11.0 and 4.7 Hz, H-4), 3.69 (1H, dd, J = 5.8 and 11.8 Hz, H-6$_a$), 3.78 (1H, app dt, J = 12.8 and 4.0 Hz, H-2), 3.85 (1H, d, J = 2.2 and 11.8 Hz, H-6$_b$), 4.64 (1H, d, J = 4.0 Hz, H-1), 5.11 (2H, s, CH$_2$Ph), 7.30-7.42 (5H, m, H-Ar); ^{13}C NMR (125 MHz; CD$_3$OD) δ_C 34.6 (C-3), 50.9 (C-2), 55.3 (OMe), 62.8 (C-6), 66.2 (C-4), 67.4 (CH$_2$Ph), 74.5 (C-5), 98.7 (C-1), 128.9 (C-Ar), 129.0 (C-Ar), 129.5 (C-Ar), 140.8 (C-Ar), 160.7 (CO); HRMS calcd for $C_{15}H_{22}N_1O_6$ [M+H]$^+$ 312.1447, found 312.1442.

((2R,3S,5R,6S)-5-((((Benzyloxy)carbonyl)amino)-3-hydroxy-6-methoxy tetrahydro-2H-pyran-2-yl)methyl sulfamate (162)

Prepared according to sulfamoylation method 2 using sulfamoyl chloride (1.6 mL, 1 M in MeCN, 1.6 mmol, 1.5 eq.), compound **161** (330 mg, 1.06 mmol, 1 eq.), and DMF (7 mL). After 18 h further sulfamoyl chloride (320 μL, 1 M in MeCN, 0.32 mmol, 0.3 eq.) was added and the reaction mixture was stirred at -40 °C for 4 h. The mixture was allowed to warm to -20 °C and stirred at -20 °C for 2 h. The reaction was quenched with MeOH, allowed to warm to room temperature, diluted with EtOAc (30 mL) and the layers

separated. The aqueous layer was further extracted with CH_2Cl_2 (3×30 mL), the organics combined, dried over $MgSO_4$, and the solvent removed *in vacuo*. The residue was purified by MPLC on SiO_2 with a gradient elution from 65-85% EtOAc/petrol to give a white solid (150 mg, 36 %); R_f 0.7 (EtOAc; anisaldehyde); mp 45-48 °C; λ_{max}(EtOH)/nm < 220; $[\alpha]_D^{15.9}$ +103.3° (c = 0.12, MeOH); IR ν_{max}/cm^{-1} 3342, 2946, 1692 (carbamate I), 1522 (carbamate II); ^{1}H NMR (500 MHz; CD$_3$OD) δ_H 1.78 (1H, app dt, J = 12.5 and 11.7 Hz, H-3$_a$), 2.05 (1H, app dt, J = 11.7 and 4.6 Hz, H-3$_b$), 3.42 (3H, s, OCH$_3$), 3.58 (1H, app td, J = 10.7 and 4.6 Hz, H-3), 3.71 (1H, ddd, J = 1.5, 6.2, and 9.9 Hz, H-5), 3.79 (1H, app dt, J = 12.5 and 3.6 Hz, H-2), 4.25 (1H, dd, J = 6.2 and 10.6 Hz, H-6$_a$), 4.43 (1H, dd, J = 1.5 and 10.6 Hz, H-6$_b$), 4.64 (1H, d, J = 3.6 Hz, H-1), 5.11 (2H, s, CH$_2$Ph), 7.30-7.42 (5H, m, H-Ar); ^{13}C NMR (125 MHz; CD$_3$OD) δ_C 34.7 (C-3), 50.7 (C-2), 55.5 (OCH$_3$), 65.9 (C-4), 67.6 (CH$_2$Ph), 70.1 (C-6), 72.1 (C-5), 98.8 (C-1), 128.9 (C-Ar), 129.0 (C-Ar), 129.5 (C-Ar), 138.3 (C-Ar), 158.2 (CO); HRMS calc. for $C_{15}H_{23}N_2O_8S_1$ [M+H]$^+$ 391.1170, found 391.1174.

(2*S*,3*R*,5*S*,6*R*)-5-Hydroxy-2-methoxy-6-((sulfamoyloxy)methyl) tetrahydro-2*H*-pyran-3-aminium acetate (163)
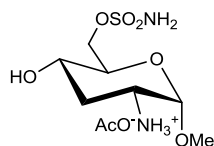
Compound **162** (145 mg, 0.37 mmol, 1 eq.), was dissolved in acetic acid (6 mL) and hydrogenated on a Thales H-cube on full H$_2$ mode through 10% Pd/C catalyst cartridge at 40 °C for 2 h, with constant recycling of reaction mixture at a flow rate of 1 mL/minute. The solvent was removed *in vacuo* to give a clear gum, which was triturated with toluene (4×5 mL), dissolved in water, frozen and lyophilised. The residue was dried *in vacuo* at 40 °C to give a clear gum. (115 mg, 98%); R_f 0.05 (20% MeOH/CH$_2$Cl$_2$; anisaldehyde); λ_{max}(EtOH)/nm < 220; $[\alpha]_D^{18.3}$ +94.3° (c = 0.14, MeOH); IR ν_{max}/cm^{-1} 1342 (SO), 1169 (SO); ^{1}H NMR (500 MHz; CD$_3$OD) δ_H 1.86 (1H, app dt, J = 12.1 and 11.7 Hz, H-3$_a$), 2.20 (1H, app dt, J = 11.7 and 4.6 Hz, H-3$_b$), 3.26-3.32 (1H, m, H-2), 3.52 (3H, s, OCH$_3$), 3.60-3.67 (1H, m, H-4), 3.76 (1H, ddd, J = 1.9 , 5.8 and 9.8 Hz, H-5), 4.27 (1H, dd, J = 5.8 and 10.9 Hz, H-6$_a$), 4.44 (1H, dd, J = 1.9 and 10.9 Hz, H-6$_b$), 4.80 (1H, d, J = 3.5 Hz, H-1); ^{13}C NMR (125 MHz; CD$_3$OD) δ_C 34.1 (C-3), 49.9 (C-2), 55.6 (OMe), 65.1 (C-4), 69.7 (C-6), 72.3 (C-5), 97.6 (C-1); MS (ESI+) *m/z* 257.3 [M+H]$^+$; (ESI-) *m/z* 255.3 [M-H]$^-$.

Sodium-((2*S*,3*R*,5*S*,6*R*)-5-Hydroxy-2-methoxy-6-((sulfamoyloxy)methyl) tetrahydro-2*H*-pyran-3-yl)sulfamate (63)
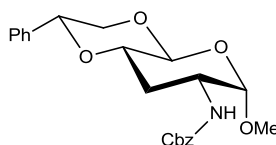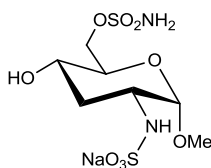
Prepared according to general procedure B, using compound **163** (110 mg, 0.35 mmol, 1 eq.), de-ionised water (5 mL) and pyridine-sulfur trioxide complex (110 mg, 0.70 mmol, 2 eq.) for 2 h. The crude product was purified by MPLC on SiO_2 with a gradient elution from 10-30% MeOH/EtOAc. Product containing fractions were evaporated *in vacuo* to give a pale glass. The material was re-purified by MPLC on SiO_2 with a gradient elution from 10-25% $MeOH/CH_2Cl_2$. Product containing fractions were evaporated, dissolved in water, frozen and lyophilized to give a yellow solid (25 mg, 21%); R_f 0.2 (20% MeOH/EtOAc; anisaldehyde); mp 130-135 °C; λ_{max}(EtOH)/nm < 220; IR ν_{max}/cm^{-1} 3283, 1368 (SO), 1173 (SO); ^{1}H NMR (500 MHz; CD_3OD) δ_H 1.68 (1H, app dt, J = 12.0 and 12.0 Hz, H-3$_a$), 2.28 (1H, app dt, J = 11.8 and 4.7 Hz, H-3$_b$), 3.43-3.49 (4H, m, OCH_3 and H-2), 3.51-3.59 (1H, ddd, J = 4.7 Hz, 9.8 and 11.2 Hz, H-4), 3.69 (1H, ddd, J = 1.8 Hz, 6.3 and 9.8 Hz, H-5), 4.24 (1H, dd, J = 6.3 and 10.7 Hz, H-6$_a$), 4.43 (1H, dd, J = 1.8 and 10.7 Hz, H-6$_b$), 4.87 (1H, d, J = 3.5 Hz, H-1); ^{13}C NMR (125 MHz; CD_3OD) δ_C 35.9 (C-3), 53.1 (C-2), 55.6 (OCH$_3$), 66.3 (C-4), 70.3 (C-6), 72.1 (C-5), 99.5 (C-1); HRMS calcd for $C_7H_{15}N_2O_9S_2$ [M-H]$^-$ 335.0224, found 335.0208.

((2*R*,3*S*,4*R*,5*R*,6*S*)-4-(Benzoyloxy)-5-((benzyloxy)carbonyl) amino)-3-hydroxy-6-methoxytetrahydro-2*H*-pyran-2-yl)methyl benzoate (164)
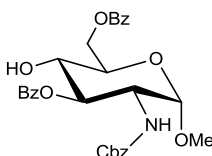
Compound **103** (1.2 g, 3.7 mmol) was dissolved in a mixture of CH_2Cl_2 (6 mL) and pyridine (6 mL) and cooled to -40 °C. Benzoyl chloride (767 μL, 6.6 mmol, 1.8 eq.) was added dropwise over 20 min, and the mixture was allowed to warm to room temperature over 90 min. The mixture was cooled to -40 °C and benzoyl chloride (170 μL, 1.5 mmol, 0.4 eq.) was added dropwise over 20 min, and the mixture was allowed to warm to room temperature over 90 min and stirred at room temperature for 1 h. The reaction was quenched with methanol, and the solvent removed *in vacuo*. The residue was dissolved in

CH$_2$Cl$_2$ (30 mL) and washed with HCl (2 × 20 mL, 2 M aq.). The organic layer was dried over MgSO$_4$, and the solvent removed *in vacuo*. The residue was purified by MPLC on SiO$_2$ with a gradient elution from 15-65% EtOAc/petrol to give a clear gum (1.05 g, 1.96 mmol, 54%); R_f 0.4 (40% EtOAc/petrol; anisaldehyde); mp 60-64 °C; λ_{max}(EtOH)/nm 229; $[\alpha]_D^{19.3}$ +93.3° (c = 0.39, MeOH); IR ν $_{max}$/cm^{-1} 3345, 1714 (br) (CO ester and carbamate I), 1603, 1518 (carbamate II); ^{1}H NMR (500 MHz; CDCl$_3$) δ_H 3.30 (1H, br s, C4-O*H*), 3.83 (1H, app. t, *J* = 9.4 Hz, H-4), 4.00 (1H, ddd, *J* = 2.1, 4.5 and 9.4 Hz, H-5), 4.21 (1H, app td, *J* = 10.3 and 3.6 Hz, H-2), 4.59 (1H, dd, *J* = 2.1 and 12.1 Hz, H-6$_a$), 4.74 (1H, dd, *J* = 4.5 and 12.1 Hz, H-6$_b$), 4.81 (1H, d, *J* = 3.6 Hz, H-1), 4.94 (1H, d, *J* = 12.3 Hz, C*H*$_a$CH$_b$Ph), 4.99 (1H, d, *J* = 12.3 Hz, CH$_a$C*H*$_b$Ph), 5.16 (1H, d, *J* = 10.3 Hz, NH), 5.33 (1H, dd, *J* = 9.4 and 10.3 Hz, H-3), 7.11-7.23 (5H, m, H-Ar), 7.39-7.49 (4H, m, H-Ar), 7.53-7.62 (2H, m, H-Ar), 8.02-8.10 (4H, m, H-Ar); ^{13}C NMR (125 MHz; CDCl$_3$) δ_C 55.4 (C-2), 60.4 (OMe), 63.4 (C-6), 66.9 (*C*H$_2$Ph), 69.5 (C-4), 70.4 (C-5), 75.4 (C-3), 98.8 (C-1), 127.8 (C-Ar), 128.1 (C-Ar), 128.4 (C-Ar), 128.5 (C-Ar), 128.5 (C-Ar), 129.3 (C-Ar), 129.7 (C-Ar), 129.8 (C-Ar), 130.1 (C-Ar), 133.3 (C-Ar), 133.5 (C-Ar), 136.1 (C-Ar), 156.0 (CO Cbz), 166.9 (CO Bz), 168.0 (CO Bz); HRMS calcd for C$_{29}$H$_{30}$N$_1$O$_9$ [M+H]$^+$ 536.1915, found 536.1904.

((2*S*,4*S*,5*R*,6*S*)-4-(Benzoyloxy)-5-(((benzyloxy)carbonyl) amino)-6-methoxy tetrahydro-2*H*-pyran-2-yl)methyl benzoate (165)
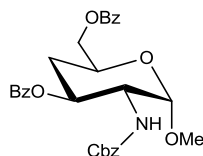
Compound **164** (150 mg, 0.28 mmol, 1 eq.) was dissolved in toluene (4 mL) and the solution degassed. 1,1'-Thiocarbonyldiimidazole (75 mg, 0.42 mmol, 1.5 eq.) was added and the mixture heated at reflux for 3 h. Tris(trimethylsilyl)silane (346 μL, 1.12 mmol, 4 eq.) was added to the hot reaction, followed by AIBN (280 μL, 0.2 M in toluene, 0.056 mmol, 0.2 eq.), and the mixture was heated at reflux for 30 min. The reaction was allowed to cool and the solvent was evaporated *in vacuo*. The residue was purified by MPLC on SiO$_2$ with a gradient elution from 10-30% EtOAc/petrol to give a white solid (116 mg, 79%); R_f 0.8 (50% EtOAc/petrol; anisaldehyde); mp 155-158 °C; λ_{max}(EtOH)/nm 229; $[\alpha]_D^{19.9}$ +125.7° (c = 0.11, MeOH); IR ν_{max}/cm^{-1} 3325, 1718 (CO ester), 1681 (carbamate I), 1535 (carbamate II); ^{1}H NMR (500 MHz; CD$_3$OD) δ_H 1.82 (1H, app dt, *J* = 12.4 and

11.8 Hz, H-4$_a$), 2.41 (1H, ddd, J = 1.9, 5.0, and 12.4 Hz, H-4$_b$), 3.47 (3H, s, OCH$_3$), 4.09 (1H, dd, J = 3.6 and 10.8 Hz, H-2), 4.30-4.37 (1H, m, H-5), 4.41-4.49 (2H, m, H-6), 4.89 (1H, d, J = 3.6 Hz, H-1), 4.99 (1H, d, J = 12.5 Hz, CH_aH$_b$Ph), 5.12 (1H, d, J = 12.5 Hz, CH$_a$$H_b$Ph), 5.38 (1H, td, J = 10.8 and 5.0 Hz, H-3), 7.15-7.23 (5H, m, H-Ar), 7.46-7.56 (4H, m, H-Ar), 7.62-7.68 (2H, m, H-Ar), 8.01-8.04 (2H, m, H-Ar), 8.07-8.11 (2H, m, H-Ar); ^{13}C NMR (125 MHz; CD$_3$OD) δ_C 34.3 (C-4), 55.7 (C-2 and OCH$_3$), 67.0 (C-5), 67.45 (CH$_2$Ph), 67.5 (C-6), 71.3 (C-3), 101.0 (C-1), 128.5 (C-Ar), 128.8 (C-Ar), 129.4 (C-Ar), 129.6 (C-Ar), 129.7 (C-Ar), 130.6 (C-Ar), 130.8 (C-Ar), 131.2 (C-Ar), 131.2 (C-Ar), 134.4 (C-Ar), 134.4 (C-Ar), 138.2 (C-Ar), 158.8 (NHCO$_2$Bn), 167.6 (PhCO$_2$), 167.7 (PhCO$_2$); HRMS calc. for C$_{29}$H$_{33}$N$_2$O$_8$ [M+NH$_4$]$^+$ 537.2231, found 537.2224.

Benzyl ((2S,3R,4S,6S)-4-hydroxy-6-(hydroxymethyl)-2-methoxy tetrahydro-2H-pyran-3-yl)carbamate (166)

Compound **165** (340 mg, 0.66 mmol) was dissolved in methanol and sodium methoxide (160 µL, 1 M in methanol, cat.) was added. The mixture was stirred at room temperature for 18 h. The solvent was evaporated *in vacuo*, the residue was purified by MPLC on SiO$_2$ with a gradient elution from 80-100% EtOAc/petrol to give a white solid (140 mg, 68%); R_f 0.1 (80% EtOAc/petrol; anisaldehyde); mp 112 °C dec.; λ_{max}(EtOH)/nm < 220; $[\alpha]_D^{20.0}$ +92.0° (c = 0.10, MeOH); IR ν_{max}/cm^{-1} 3334, 2926, 1691; ^{1}H NMR (500 MHz; CD$_3$OD) δ_H 1.46 (app dt, J = 12.8 and 12.0 Hz, H-4$_a$), 2.01 (1H, J = 2.0, 4.7, and 12.8 Hz, H-4$_b$), 3.37-3.42 (3H, s, OCH$_3$), 3.52-3.61 (3H, m, H-2 and H-6), 3.80-3.88 (2H, m, H-3 and H-5), 4.75 (1H, d, J = 3.5 Hz, H-1), 5.13 (2H, s, CH$_2$Ph), 7.30-7.43 (5H, m, H-Ar); ^{13}C NMR (125 MHz; CD$_3$OD) δ_C 37.2 (C-4), 55.5 (OCH$_3$), 58.8 (C-2), 65.8 (C-6), 67.2 (C-5), 67.6 (CH$_2$Ph), 70.0 (C-3), 100.8 (C-1), 128.9 (C-Ar), 129.0 (C-Ar), 129.5 (C-Ar), 138.4 (C-Ar), 159.0 (CO); HRMS calcd for C$_{15}$H$_{22}$N$_1$O$_6$ [M+H]$^+$ 312.1442, found 312.1447.

((2S,4S,5R,6S)-5-(((Benzyloxy)carbonyl)amino)-4-hydroxy-6-methoxy tetrahydro-2H-pyran-2-yl)methyl sulfamate (167)

430-98

Prepared according to sulfamoylation method 2 using sulfamoyl chloride (0.93 mL, 1 M in MeCN, 0.93 mmol, 1.8 eq.), alcohol **166** (160 mg, 0.51 mmol, 1 eq.), and DMF (4 mL). After stirring at -40 °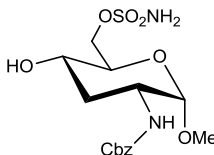C for 18 h, further sulfamoyl chloride (200 μL, 1 M in MeCN, 0.2 mmol, 0.4 eq.) was added at -40 °C over 30 min, and the reaction mixture was stirred at -40 °C for 18 h. The reaction was quenched with MeOH, allowed to warm to room temperature, diluted with water (10 mL) and EtOAc (30 mL) and the layers separated. The aqueous layer was further extracted with CH_2Cl_2 (4 × 15 mL). The organic layers were combined, dried over $MgSO_4$, and the solvent removed *in vacuo*. The residue was purified by MPLC on SiO_2 with a gradient elution from 50-90% EtOAc/petrol to give a white solid (102 mg, 51 %); R_f 0.7 (EtOAc; anisaldehyde); mp 45-48 °C; λ_{max}(EtOH)/nm <220; IR ν_{max}/cm^{-1} 3349, 2925, 1693 (carbamate I), 1527 (carbamate II), 1362 (SO), 1177 (SO); ^{1}H NMR (500 MHz; CD_3OD) δ_H 1.52 (1H, app dt, J = 12.0 and 12.0 Hz, H-4$_a$), 2.07 (1H, ddd, J = 1.7, 4.5 and 12.0 Hz, H-4$_b$), 3.40 (3H, s, OMe), 3.57 (1H, dd, J = 3.4 and 10.3 Hz, H-2), 3.86 (1H, app td, J = 10.9 and 4.7 Hz, H-3), 4.10 (1H, m, H-5), 4.13-4.17 (2H, m, H-6), 4.76 (1H, d, J = 3.4 Hz, H-1), 5.13 (2H, s, CH_2Ph), 7.30-7.44 (5H, m, H-Ar); ^{13}C NMR (125 MHz; CD_3OD) δ_C 36.9 (C-4), 55.7 (OCH_3), 58.6 (C-2), 66.9 (C-3), 67.2 (C-5), 67.6 (CH_2Ph), 72.3 (C-6), 100.8 (C-1), 128.9 (C-Ar), 129.0 (C-Ar), 129.5 (C-Ar), 138.3 (C-Ar); HRMS calc. for $C_{15}H_{26}N_3O_8S_1$ [M+NH$_4$]$^+$ 408.1435, found 408.1436.

Note: Unable to visualise all carbon signals by ^{13}C nmr.

(2S,3R,4S,6S)-4-Hydroxy-2-methoxy-6-((sulfamoyloxy)methyl) tetrahydro-2H-pyran-3-aminium acetate (168)

Compound **167** (95 mg, 0.24 mmol) was dissolved in acetic acid (4 mL) and hydrogenated on a Thales H-cube on full H_2 mode through 10% Pd/C catalyst cartridge at 40 °C for 2 h, with constant recycling of the reaction mixture at a flow rate of 1 mL/minute. The solvent

was removed *in vacuo* to give a clear gum, which was triturated with toluene (4 × 5 mL). The residue was dried *in vacuo* at 40 °C to give a clear gum (54 mg, 70%); R_f 0.05 (20% MeOH/CH$_2$Cl$_2$; anisaldehyde); λ_{max}(EtOH)/nm < 220; IR ν_{max}/cm^{-1} 3012, 1706, 1547, 1359 (SO), 1175 (SO); ^{1}H NMR (500 MHz; CD$_3$OD) δ_H 1.56 (1H, app dt, *J* = 12.6 and 11.5 Hz, H-4$_a$), 2.00 (3H, s, C*H$_3$*CO$_2$), 2.07-2.14 (1H, m, H-4$_b$), 3.03 (1H, dd, *J* = 3.5 and 10.1 Hz, H-2), 3.49 (3H, s, OCH$_3$), 4.00 (app. td, *J* = 10.9 and 4.9 Hz, H-3), 4.10-4.22 (3H, m, H-5 and H-6), 4.96 (1H, d, *J* = 3.5 Hz, H-1); ^{13}C NMR (125 MHz; CD$_3$OD) δ_C 21.8 (*C*H$_3$CO), 36.6 (C-4), 55.8 (C-2), 57.1 (OCH$_3$), 66.0 (C-3), 67.6 (C-6), 71.9 (C-5), 98.8 (C-1), 176.8 (CO acetate); HRMS calcd for C$_7$H$_{15}$N$_2$O$_6$S$_1$ [M-H]$^-$ 255.0656, found 255.0647.

Sodium-((2*S*,3*R*,4*S*,6*S*)-4-hydroxy-2-methoxy-6-((sulfamoyloxy) methyl) tetrahydro-2*H*-pyran-3-yl)sulfamate (62)

Prepared according to general procedure B, using amine **168** (50 mg, 0.16 mmol, 1 eq.), de-ionised water (3 mL) and pyridine-sulfur trioxide complex (50 mg, 0.32 mmol, 2 eq.) for 2 h. The crude product was purified by MPLC on SiO$_2$ with a gradient elution from 10-30% MeOH/EtOAc. Product containing fractions were evaporated *in vacuo* to give a pale glass. The material was re-purified by MPLC on SiO$_2$ with a gradient elution from 5-25% MeOH/CH$_2$Cl$_2$. Product containing fractions were evaporated, dissolved in water, frozen and lyophilized to give a yellow solid (4 mg, 8%); R_f 0.15 (20% MeOH/EtOAc; anisaldehyde); m.p. 144-148 °C; λ_{max}(EtOH)/nm < 220; IR ν_{max}/cm^{-1} 32729, 2936, 1361 (SO), 1173 (SO); ^{1}H NMR (500 MHz; CD$_3$OD) δ_H 1.49 (1H, app dt, *J* = 12.0 and 11.8 Hz, H-4$_a$), 2.05 (1H, ddd, *J* = 2.2 , 5.0 and 12.8 Hz, H-4$_b$), 3.19 (1H, dd, *J* = 3.6 and 9.9 Hz, H-2), 3.49 (3H, s, OCH$_3$), 3.82 (1H, ddd, *J* = 4.9 Hz, 10.0 and 11.2 Hz, H-3), 4.05-4.19 (3H, m, H-5 and H-6), 5.03 (1H, d, *J* = 3.6 Hz, H-1); ^{13}C NMR (125 MHz; CD$_3$OD) δ_C 36.3 (C-4), 55.8 (OCH$_3$), 60.8 (C-2), 66.9 (C-5), 68.0 (C-3), 72.4 (C-6), 101.1 (C-1); HRMS calcd for C$_7$H$_{15}$N$_2$O$_9$S$_2$ [M-H]$^-$ 335.0224, found 335.0210.

((2*R*,3*S*,4*R*,5*R*,6*S*)-4-(Benzoyloxy)-3-(benzyloxy)-5-(((benzyloxy) carbonyl) amino) -6-methoxytetrahydro-2*H*-pyran-2-yl)methyl benzoate (170)

Benzyl-2,2,2-trichloroacetimidate (78 µL, 0.37 mmol, 2 eq.) and trifluoromethanesulfonic acid (300 µL, 10% v/v in CH_2Cl_2, 0.02 eq.), were added to a solution of alcohol **164** (100 mg, 0.19 mmol, 1 eq.) in CH_2Cl_2 (3 mL) and the mixture stirred at room temperature for 1 h. Further benzyl-2,2,2-trichloroacetimidate (78 µL, 0.37 mmol, 2 eq.) was added and the mixture stirred at room temperature for 1 h. Further benzyl-2,2,2-trichloroacetimidate (78 µL, 0.37 mmol, 2 eq.) and trifluoromethanesulfonic acid (300 µL, 10% v/v in CH_2Cl_2, 0.02 eq.) were added and the mixture was stirred at r.t. for 18 h. The reaction was quenched by addition of $NaHCO_3$ (10% w/v aq., 5 mL), diluted with brine (10 mL) and extracted with CH_2Cl_2 (2 × 15 mL). The organic layers were combined, dried over $MgSO_4$, and the solvent removed *in vacuo*. The residue was purified by flash MPLC on SiO_2 with gradient elution from 5-25% EtOAc/petrol to give a clear gum (88 mg, 75%); R_f 0.3 (20% EtOAc/petrol; UV, anisaldehyde); mp. 99-105 °C; λ_{max}(EtOH)/nm 227; $[\alpha]_D^{18.9}$ +31.4° (c = 0.14, EtOH); IR ν $_{max}$/cm^{-1} 3364, 33187, 3241, 3186, 1692, 1617; ^{1}H NMR (500 MHz; CDCl$_3$) δ$_H$ 3.42 (3H, s, OMe), 3.70-3.94 (2H, m, H-4), 4.06 (1H, dt, *J* = 9.9 and 3.1 Hz, H-5), 4.18 (1H, td, *J* = 10.6 and 3.5 Hz, H-2), 4.46-4.62 (4H, m, H-6 and CHOC*H*$_2$Ph), 4.79 (1H, d, *J* = 3.5 Hz, H-1), 4.86-4.96 (2H, m, CO$_2$C*H*$_2$Ph), 5.12 (1H, d, *J* = 10.1 Hz, NH), 5.63 (1H, dd, *J* = 9.3 and 10.6 Hz, H-3), 7.07-7.21 (10 H, m, H-Ar), 7.42-7.52 (4H, m, H-Ar), 7.54-7.63 (2H, m, H-Ar), 8.03 - 8.08 (4H, m, H-Ar); ^{13}C NMR (125 MHz; CDCl$_3$) δ$_C$ 54.2, 55.4, 63.1, 66.8, 69.2, 74.2, 74.8, 75.7, 98.7, 127.7, 127.9, 128.0, 128.3, 128.4, 128.4, 128.5, 129.7, 129.9, 133.2, 133.3, 136.9, 156.0; HRMS calcd for $C_{36}H_{39}N_2O_9$ 643.2650 [M+NH$_4$]$^+$, found 643.2645.

Benzyl ((2*S*,3*R*,4*R*,5*S*,6*R*)-5-(benzyloxy)-4-hydroxy-6-(hydroxymethyl)-2-methoxytetrahydro-2*H*-pyran-3-yl)carbamate (171)

Lithium aluminium hydride (516 µL, 2 M in THF, 1.03 mmol, 3 eq.) was added to dibenzoate ester **170** (215 mg, 0.34 mmol, 1 eq.) in THF (5 mL) at 0 °C and the mixture

was stirred at 0 °C for 2 h. Water (60 μL) was added, followed by NaOH (15% w/v aq., 180 μL), followed by further water (60 μL). The mixture was stirred at room temperature for 30 min, filtered through Celite, and the solvent removed *in vacuo*. The residue was purified by MPLC on SiO$_2$ with gradient elution from 20-80% EtOAc/petrol to give a white solid (98 mg, 69%); R_f 0.25 (50% EtOAc/petrol; UV, anisaldehyde); mp. 101-104 °C; λ_{max}(EtOH)/nm 258; $[\alpha]_D^{18.5}$ +11.2° (c = 0.08, EtOH); IR ν_{max}/cm^{-1} 3296, 2918, 1685, 1540; ^{1}H NMR (500 MHz; DMSO-d^6) δ_H 3.28 (3H, s, OMe), 3.31-3.36 (1H, m, H-4), 3.42 (1H, m, H-5), 3.47-3.59 (2H, m, H-2 and H-6$_a$), 3.61-3.73 (2H, m, H-3 and H-6$_b$), 4.61 (1H, d, J = 11.5 Hz, CH_aH$_b$Ph), 4.64 (1H, d, J = 3.4 Hz, H-1), 4.72 (1H, t, J = 5.8 Hz, OH-6), 4.91 (1H, d, J = 11.5 Hz, CH$_a$$H_b$Ph), 5.02-5.16 (3H, m, CH$_2$Ph and OH-3), 7.19 (1H, d, J = 8.2 Hz, NH), 7.28-7.45 (10H, m, H-Ar); ^{13}C NMR (125 MHz; DMSO-d^6) δ_C 54.4 (OMe), 56.2 (C-2), 60.4 (C-6), 65.3(CH$_2$Ph), 70.8 (C-3), 71.4(C-5), 73.7 (NHCO$_2$CH$_2$Ph), 78.6 (C-4), 98.0 (C-1), 127.3 (C-Ar), 127.5 (C-Ar), 127.8 (C-Ar), 128.0 (C-Ar), 128.3 (C-Ar), 137.1 (C-Ar), 139.0 (C-Ar), 156.2 (CO); HRMS calc. for C$_{22}$H$_{28}$N$_1$O$_7$ [M+H]$^+$ 418.1860, found 418.1862.
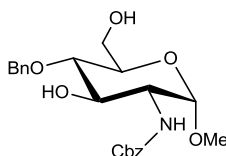
((2*R*,3*S*,4*R*,5*R*,6*S*)-3-(Benzyloxy)-5-(((benzyloxy)carbonyl)amino)-4-hydroxy-6-methoxytetrahydro-2*H*-pyran-2-yl)methyl sulfamate (172)
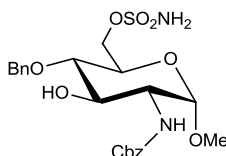
Prepared according to sulfamoylation method 2 using sulfamoyl chloride (1.15 mL, 1 M in MeCN, 1.15 mmol, 2 eq.), alcohol **171** (200 mg, 0.05 mmol, 1 eq.) and DMF (2 mL). After stirring at -40 °C for 18 h, further sulfamoyl chloride (0.20 mL, 1 M in MeCN, 0.20 mmol, 0.33 eq.) was added and the mixture was stirred at -40 °C for 4 h. The residue was purified by MPLC on SiO$_2$ with a gradient elution from EtOAc to 8% EtOAc/petrol to give a white solid (150 mg, 52%); R_f 0.3 (50% EtOAc/petrol; anisaldehyde); m.p. 46-48 °C; λ_{max}(EtOH)/nm 257; $[\alpha]_D^{19.1}$ +74.8° (c = 0.107, EtOH); IR ν_{max}/cm^{-1} 3332 (br), 2939, 1695 (carbamate I), 1523 (Carbamate II), 1365 (SO), 1181 (SO); ^{1}H NMR (500 MHz; DMSO-d^6) δ_H 3.30 (3H, s, OMe), 3.37 (1H, m, H-4), 3.53 (1H, ddd, J = 3.6, 8.5 and 10.6 Hz, H-2), 3.6 -3.76 (2H, m, H-3 and H-5), 4.20-4.28 (2H, m, H-6), 4.62 (1H, d, J = 10.9 Hz, OCH_aH$_b$Bn), 4.67 (1H, d, J = 3.5 Hz, H-1), 4.94 (1H, d, J = 10.9 Hz, OCH$_a$$H_b$Bn), 5.06 (1H, d, J = 12.6 Hz, CO$_2$OCH_aH$_b$Bn), 5.10 (1H, d, J = 12.6 Hz, CO$_2$CH$_a$$H_b$Bn), 5.23 (1H,

d, J = 7.3 Hz, OH³), 7.20-7.44 (11H, m, 10 × H-Ar and NH), 7.62 (2H, s, NH₂); ¹³C NMR (125 MHz; DMSO-d^6) δ$_C$ 54.7 (OMe), 56.0 (C-2), 65.4 (CO₂CH₂Ph), 67.8 (C-6), 68.2 (C-5), 70.7 (C-3), 73.8 (CH₂Ph), 78.1 (C-4), 98.1 (C-1), 127.4 (C-Ar), 127.7 (C-Ar), 127.8 (C-Ar), 128.1 (C-Ar), 128.3 (C-Ar), 128.6 (C-Ar), 137.0 (C-Ar), 138.6 (C-Ar), 156.2 (CO); MS (ES+) m/z 497.5 [M+H]⁺; HRMS calcd for C₂₂H₃₂N₃O₉S₁ [M+NH₄]⁺ 514.1854, found 514.1848.

((2R,3S,4R,5R,6S)-5-Amino-3-(benzyloxy)-4-hydroxy-6-methoxytetrahydro-2H-pyran-2-yl)methyl sulfamate (173)
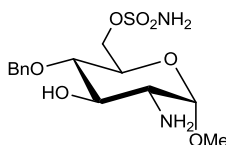
Benzyl ether **172** (220 mg, 0.44 mmol) was dissolved in methanol (5 mL) and hydrogenated on a Thales H-cube through 5% Pd/C catalyst cartridge with 10 bar H₂ at r.t. for 35 min, with constant recycling of reaction mixture at a flow rate of 1 mL/minute. The solvent was removed *in vacuo* to give a clear gum which solidified on standing (160 mg, 100%). R_f 0.25 (30% MeOH/EtOAc; anisaldehyde); m.p. 50-52 °C; λ$_{max}$(EtOH)/nm <258; [α]$_D^{19.2}$ +77.6° (c = 0.107, EtOH); IR ν $_{max}$/cm⁻¹ 3353.6 (br), 29135, 1362 (SO), 1176 (SO); ¹H NMR (500 MHz; DMSO-d^6) δ$_H$ 1.84 (2H, br, CHNH_2), 2.48-2.54 (1H, m, H-2), 3.27 (1H, dd, J = 8.8 and 9.9 Hz, H-4), 3.32 (3H, s, OMe), 3.43-3.49 (1H, m, H-3), 3.70-3.75 (1H, m, H-5), 4.20-4.27 (2H, m, H-6), 4.62 (2H, m, H-1 and CH_aH$_b$Ph), 4.93 (1H, d, J = 11.0 Hz, CH$_a$$H_b$Ph), 5.27 (1H, d, J = 5.8 Hz, OH³), 7.18-7.43 (5H, m, H-Ar), 7.61 (2H, br s, OSO₂NH₂); ¹³C NMR (125 MHz; DMSO-d^6) δ$_C$ 54.68 (OMe), 56.4 (C-2), 68.0 (C-6), 68.5 (C-5), 73.6 (CH₂Ph), 75.0 (C-3), 77.7 (C-4), 100.1 (C-1), 127.4 (C-Ar), 127.7 (C-Ar), 128.08 (C-Ar), 138.7 (C-Ar); HRMS calc. for C₁₄H₂₃N₂O₇S₁ [M+H]⁺ 363.1220, found 363.1226.

((2R,3S,4R,5R,6S)-5-(Benzyloxy)-4-hydroxy-2-methoxy-6-((sulfamoyloxy) methyl) tetrahydro-2H-pyran-3-yl)sulfamic acid (61)

Prepared according to general procedure B, using amine **173** (75 mg, 0.2 mmol, 1 eq.), de-ionised water (6 mL), THF (3 mL) and pyridine-sulfur trioxide complex (132 mg, 0.82

mmol, 4 eq.) for 2 h. The crude product was purified by MPLC on SiO_2 with a gradient elution from 10-30% MeOH/EtOAc. Product containing fractions were evaporated *in vacuo* to give a yellow solid. (23 mg, 25%); R_f 0.3 (30% MeOH/EtOAc; anisaldehyde); m.p. 195 °C dec.; λ_{max}(EtOH)/nm 258; $[\alpha]_D^{19.5}$ +80° (c = 0.15, EtOH); IR ν_{max}/cm^{-1} 3291, 2920, 1363 (SO), 1178 (SO); ^{1}H NMR (500 MHz; DMSO-d^6) δ_H 3.07-3.14 (1H, ddd, J = 3.5, 8.3 and 10.4 Hz, H-2), 3.28 (3H, s, OMe), 3.31 (1H, dd, J = 8.7 and 10.1 Hz, H-4), 3.66-3.73 (2H, m, H-3 and H-5), 4.20 (1H, dd, J = 5.0 and 10.5 Hz, H-6$_a$), 4.25 (1H, dd, J = 1.7 and 10.5 Hz, H-6$_b$), 4.38 (1H, d, J = 8.3 Hz, CHNH), 4.63 (1H, d, J = 11.0 Hz, CH_aH$_b$Ph), 4.69 (1H, d, J = 3.5 Hz, H-1), 4.96 (1H, d, J = 11.0 Hz, CH$_a$$H_b$Ph), 5.75 (1H, d, J = 2.2 Hz, OH^3), 7.26-7.40 (5H, m, H-Ar), 7.60 (2H, br s, NH$_2$); ^{13}C NMR (125 MHz; DMSO-d^6) δ_C 54.8 (OMe), 57.8 (C-2), 67.9 (C-5), 68.0 (C-6), 73.3 (C-3), 73.6 (CH$_2$Ph), 78.2 (C-4), 99.2 (C-1), 127.3 (C-Ar), 127.6 (C-Ar), 128.1 (C-Ar), 138.8 (C-Ar); HRMS calc. for $C_{14}H_{22}N_2O_{10}S_2$ [M-H]$^-$ 441.0643, found 441.0631.
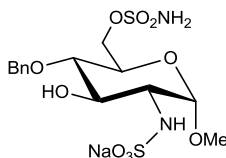
10.3.2 Synthesis of Alkyl Sulfamates

(Tetrahydro-2*H*-pyran-2-yl) methyl sulfamate (67) [147]
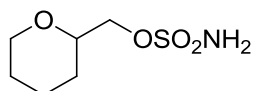
Prepared according to sulfamoylation method 4 using tetrahydropyran-2-methnol (283 μL, 2.5 mmol) and sulfamoyl chloride (2.5 mL, 0.3 M in toluene, 7.5 mmol, 3 eq) and DMA (3 mL). The crude product was purified by MPLC on SiO_2 with a gradient elution from 10-50% EtOAc/petrol to give a clear oil. Re-purification by MPLC on SiO_2 with a gradient elution from 10-60% EtOAc/petrol gave a clear oil (224 mg, 48%); R_f 0.15 (30% EtOAc/petrol; CAM); λ_{max}(EtOH)/nm 256 weak; IR ν_{max}/cm^{-1} 3409, 3303, 3117, 1345 (SO), 1175 (SO); ^{1}H NMR (500 MHz; CDCl$_3$) δ_H 1.34-1.67 (5H, m, H-pyran), 1.89-1.97 (1H, m, H-pyran), 3.49 (1H, td, J = 11.1 and 3.1 Hz, CH-O pyran), 3.65-3.71 (1H, m, CH_aH$_b$-O pyran), 4.03-4.07 (1H, m, CH$_a$$H_b$-O pyran), 4.17-4.25 (2H, m, CH_2OSO$_2$), 5.14 (2H, s, NH$_2$); ^{13}C NMR (125 MHz; DMSO-d^6) δ_C 22.3 (CCH$_2$C), 25.3 (CCH$_2$C), 27.1 (CCH$_2$C), 67.2 (CH$_2$O), 71.3 (CH$_2$O), 74.5 ((CH$_2$)HC(CH$_2$)O); HRMS ASAP calcd for $C_6H_{14}N_1O_4S_1$ [M+H]$^+$ 196.0638, found 196.0635.

4-Nitrophenethyl sulfamate (114)[340]
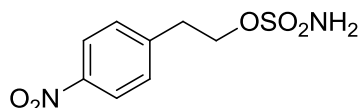
Sulfamoyl chloride (1.8 mL, 1.0 M solution in toluene, 1.8 mmol, 3 eq.) was added to 4-nitrophenethyl alcohol (100 mg, 0.6 mmol, 1 eq.) in anhydrous DMA (1 mL) at room temperature and the mixture was allowed to stir overnight. The reaction was quenched with water (10 mL), and extracted with CH_2Cl_2 (3 × 20 mL), dried over $MgSO_4$, and the solvent evaporated *in vacuo*. The residue was purified by MPLC on SiO_2 with a gradient elution from 20-80% EtOAc:petrol to give a white solid (100 mg, 68%); R_f 0.85 (5% MeOH/EtOAc); mp 128-130 °C; λ_{max}(EtOH)/nm 268; λ_{max}(EtOH)/nm 271; IR ν_{max}/cm^{-1} 3370, 3286, 1514 (NO$_2$), 1343 (SO), 1190 (SO); ^{1}H NMR (500 MHz; CD$_3$OD) δ_H 3.21 (2H, t, J = 6.4 Hz, CH$_2$Ar), 4.42 (2H, t, J = 6.4 Hz, CH_2-O-S), 7.58 (2H, d, J = 8.8 Hz, H-Ar), 8.23 (2H, d, J = 8.8 Hz, H-Ar); ^{13}C NMR (125 MHz; CD$_3$OD) δ_C 36.0 (CH$_2$Ar), 70.2 (CH$_2$OSO$_2$NH$_2$), 124.6 (CH-Ar), 131.3 (CH-Ar), 147.0 (C-Ar), 148.4 (C-Ar); HRMS Calc for C$_8$H$_9$N$_2$O$_5$S$_1$ [M-H]$^-$ 245.0238, found 245.0238.

2,2,2-Trichloroethyl 4-hydroxypiperidine-1-sulfonate (184)
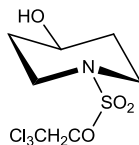
Prepared according to general procedure C using 2,3-dimethyl-1-((2,2,2-trichloroethoxy)sulfonyl)-1*H*-imidazol-3-ium tetrafluoroborate (378 mg, 0.99 mmol, 1 eq.), 4-hydroxypiperidine (100 mg, 0.99 mmol, 1 eq.), and THF (10 mL). The residue was purified by MPLC on SiO_2 with a gradient elution from 25-50% EtOAc/petrol to yield a white solid (290 mg, 94%); R_f 0.3 (50% EtOAc/petrol; KMnO$_4$;); m.p. 80-83 °C; λ_{max}(EtOH)/nm < 220; IR ν_{max}/cm^{-1} 3449, 2952, 2928, 2880, 1362 (SO), 11737 (SO); ^{1}H NMR (500 MHz; CDCl$_3$) δ_H 1.53 (1H, d, J = 3.9 Hz, OH), 1.67-1.76 (2H, m, 2 × CH_{ax}CHO), 1.95-2.02 (2H, m, 2 × CH_{eq}CHO), 3.30 (2H, ddd, J = 3.6 Hz, 8.1 and 12.2 Hz, 2 × CH$_{ax}$N), 3.69 (2H, ddd, J = 3.8, 7.6 and 12.0 Hz, 2 × CH$_{eq}$N), 3.93-4.00 (m, J = 3.8 Hz, CHOH), 4.63 (2H, s, CH$_2$CCl$_3$); ^{13}C NMR (125 MHz; CDCl$_3$) δ_C 32.8 (2 × CH$_2$CHOH), 44.0 (2 × CH$_2$N), 65.6 (CHOH), 77.8 (CH$_2$CCl$_3$), 93.7 (CCl$_3$); MS *m/z* 312.2 [M(^{35,35,35}Cl)H]$^+$, 314.2 [M(^{35,35,37}Cl)H]$^+$, 316.2 [M(^{35,37,37}Cl)H]$^+$.

1-((2,2,2-Trichloroethoxy)sulfonyl)piperidin-4-yl sulfamate (185)
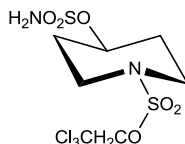
Sulfamoyl chloride (1.08 mL, 1 M in MeCN, 1.08 mmol, 2 eq.) was added to alcohol **184** (170 mg, 0.54 mmol, 1 eq.) in DMF (1 mL) containing potassium carbonate (375 mg, 2.7 mmol, 5 eq.) at -40 °C, and the mixture was stirred at -40 °C for 18 h. The reaction was quenched with methanol, allowed to warm to room temperature, and partitioned between EtOAc (3 × 20 mL) and water (15 mL). The aqueous layer was re-extracted with CH_2Cl_2 (3 × 20 mL) and EtOAc (2 × 20 mL), the organic layers combined, dried over $MgSO_4$, and the solvent removed *in vacuo*. The residue was purified by MPLC on silica with a gradient from 20-50% EtOAc/petrol to give a clear oil. (195 mg, 92%); R_f 0.4 (50% EtOAc/petrol; $KMnO_4$); m.p. 74-76 °C; λ_{max}(EtOH)/nm < 220; IR ν_{max}/cm^{-1} 3378, 3284, 2865, 1358 (SO), 1175 (SO); ^{1}H NMR (500 MHz; $CDCl_3$) δ_H 2.03-2.17 (4H, m, 2 × CH_2CHO), 3.47-3.55 (2H, m, 2 × CH$_{ax}$N), 3.56-3.63 (2H, m, 2 × CH$_{eq}$N), 4.64 (2H, s, CH_2CCl_3), 4.74-4.88 (3H, m, CHOSO$_2$NH$_2$ and NH$_2$); ^{13}C NMR δ_C (125 MHz; $CDCl_3$) 30.0 (2 × CH_2CHO), 43.3 (2 × CH_2N), 76.8 (CHOSO$_2$NH$_2$), 77.8 (CH_2CCl$_3$), 93.6 (CCl$_3$); HRMS calcd for $C_7H_{17}{}^{35}Cl_3N_3O_6S_2$ [M+NH$_4$]$^+$ 407.9619, found 407.9624.

Sodium 4-(sulfamoyloxy)piperidine-1-sulfonate (66)
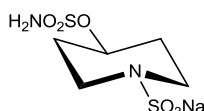
Zinc powder (238 mg, 3.63 mmol, 15 eq.) was added to sulfamate **185** (95 mg, 0.24 mmol, 1 eq.) in MeOH (4 mL) and water (4 mL) at r.t., and the mixture was stirred at r.t. for 1 h. The mixture was filtered through Celite, the Celite washed with methanol, and the solvent removed *in vacuo*. The residue was dissolved in water and run through a Dowex 50W8X-200 ion exchange resin which had previously been converted to the sodium form. Product containing fractions were frozen and lyophilised to give a white solid, which was dried *in vacuo* with P_2O_5 to give a white solid (70 mg, 99%). R_f 0.3 (30% MeOH/EtOAc; $KMnO_4$); m.p. 220 °C dec.; λ_{max}(EtOH)/nm <220; IR ν_{max}/cm^{-1} 3222 (br), 2857, 1350 (SO), 1171 (SO); ^{1}H NMR (500 MHz; DMSO-d^6) δ_H 1.64-1.73 (2H, m, 2 × CHCHOSO$_2$NH$_2$), 1.88-1.97 (2H, m, 2 × CHCHOSO$_2$NH$_2$), 2.60-2.70 (2H, m, 2 × CHN), 3.10-3.20 (2H, m, 2 ×

CHN), 4.45 (1H, tt, J = 4.3 Hz, CHOSO$_2$NH$_2$), 7.45 (2H, s, NH$_2$); ^{13}C NMR δ_C (125 MHz; CD$_3$OD) 32.1 (2 × CH$_2$CHO), 45.2 (2 × CH$_2$N), 77.9 (CHOSO$_2$NH$_2$); ^{13}C NMR (125 MHz; DMSO-d^6) δ_C 30.9 (2 × CH$_2$CHO), 43.9 (2 × CH$_2$N), 76.6 (CHOSO$_2$NH$_2$); HRMS calcd for C$_5$H$_{11}$N$_2$O$_6$S$_2$ [M-H]$^-$ 259.0064, found 259.0054.

trans- 2,2,2-Trichloroethyl-(4-hydroxycyclohexyl)sulfamate (181)
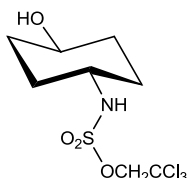
Prepared according to general procedure C using 2,3-dimethyl-1-((2,2,2-trichloroethoxy)sulfonyl)-1H-imidazol-3-ium tetrafluoroborate (331 mg, 0.87 mmol, 1 eq.), *trans*-4-aminocyclohexanol (100 mg, 0.87 mmol, 1 eq.), and THF (10 mL). The residue was purified by MPLC on SiO$_2$ with a gradient elution from 25-75% EtOAc/petrol to yield a white solid (204 mg, 73%); R_f 0.3 (50% EtOAc/petrol; KMnO$_4$); m.p. 120-123 °C; λ_{max}(EtOH)/nm <220; IR ν_{max}/cm^{-1} 34958, 3080, 2924, 2828, 1350 (SO), 1174 (SO); ^{1}H NMR (500 MHz; CDCl$_3$) δ_H 1.31-1.45 (4H, m, 2 × CH_{ax}CHOH and 2 × CH_{ax}CHNH), 1.98-2.05 (2H, m, 2 × CH_{eq}CHOH), 2.15-2.22 (2H, m, 2 × CH_{eq}CHNH), 3.40-3.50 (1H, m, CHOH), 3.60-3.68 (1H, m, CHNH), 4.42 (1H, d, J = 7.9 Hz, OH), 4.63 (2H, s, CH$_2$CCl$_3$); ^{1}H NMR (500 MHz; DMSO-d^6) δ_H 1.17-1.38 (4H, m, 2 × CH_{ax}CHOH and 2 × CH_{ax}CHNH), 1.79-1.88 (2H, m, 2 × CH_{eq}CHOH), 1.91-2.00 (2H, m, 2 × CH_{eq}CHNH), 3.14-3.22 (1H, m, CHOH), 3.31-3.45 (1H, m, CHNH), 4.59 (1H, d, J = 4.3 Hz, OH), 4.74 (2H, s, CH$_2$CCl$_3$), 8.31 (1H, br s, NH); ^{13}C NMR (125 MHz; DMSO-d^6) δ_C 30.6, 33.5, 52.7, 67.6, 77.1 (CH$_2$CCl$_3$), 94.1 (CCl$_3$); HRMS calcd for C$_8$H$_{18}$^{35}Cl$_3$N$_2$O$_4$S$_1$ [M+NH$_4$]$^+$ 343.0047, found 343.0054.

trans-(2,2,2-Trichloroethyl)(4-(sulfamoyloxy)cyclohexyl)sulfamate (182)
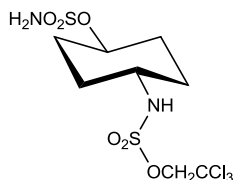
Sulfamoyl chloride (1.04 mL, 1 M in MeCN, 1.04 mmol, 2 eq.) was added to alcohol **181** (170 mg, 0.52 mmol, 1 eq.) in DMF (1 mL) containing potassium carbonate (359 mg, 2.6 mmol, 5 eq.) at -40 °C, and the mixture stirred at -40 °C for 18 h. The reaction was

quenched with methanol, allowed to warm to room temperature, and partitioned between Et$_2$O (2 × 20 mL) and water (20 mL). The organics layers were combined, dried over MgSO$_4$, and the solvent removed *in vacuo*. The residue was purified by MPLC on silica with a gradient from 20-50% EtOAc/petrol to give a clear gum (160 mg, 76%). R_f 0.5 (30% EtOAc/petrol; KMnO$_4$); m.p. 141-144 °C; λ_{max}(EtOH)/nm <220; IR ν_{max}/cm^{-1} 3283 (br), 2954, 1363 (SO), 1176 (SO); ^{1}H NMR (500 MHz; DMSO-d^6) δ_H 1.38-1.49 (2H, m, 2 × CH_{ax}CHNH), 1.52-1.63 (2H, m, 2 × CH_{ax}CHOSO$_2$NH$_2$), 1.99-2.09 (4H, m, 2 × CH_{eq}CHOSO$_2$NH$_2$ and 2 × CH_{eq}CHNH), 3.27-3.38 (1H, m, CHNH), 4.36 (1H, tt, J = 3.8 and 10.2 Hz, CHCOSO$_2$NH$_2$), 4.76 (2H, s, CH$_2$CCl$_3$), 7.43 (2H, s, NH$_2$), 8.40 (1H, s, NH); ^{13}C NMR (125 MHz; DMSO-d^6) δ_C 29.7 (2 × CH_2CHOSO$_2$NH$_2$), 29.9 (2 × CH_2CHNH), 51.3 (CHNH), 77.2 (CH_2CCl$_3$), 77.6 (CHOSO$_2$NH$_2$), 94.1 (CCl$_3$); HRMS calc. for C$_8$H$_{19}$^{35}Cl$_3$N$_3$O$_6$S$_2$ [M+NH$_4$]$^+$ 421.9779, found 421.9775.

Sodium *trans*-(4-(sulfamoyloxy)cyclohexyl)sulfamate (64)
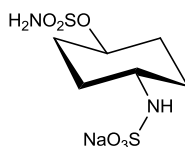
Zinc powder (230 mg, 3.5 mmol, 10 eq.) was added to sulfamate **182** (140 mg, 0.35 mmol, 1 eq.) in MeOH (4 mL) and water (4 mL) at r.t., and the mixture was stirred at r.t. for 1 h. Further zinc powder (230 mg, 3.5 mmol, 10 eq.) was added and the mixture stirred at r.t. for 1 h. The mixture was filtered through Celite, and the solvent removed *in vacuo*. The residue was dissolved in water and run through a Dowex 50W8X-200 ion exchange resin which had previously been converted to the sodium form. Product containing fractions were frozen and lyophilised to give a white solid (102 mg, 100%); R_f 0.45 (30% EtOAc/petrol; KMnO$_4$); m.p. 205-207 °C; λ_{max}(EtOH)/nm <220; IR ν_{max}/cm^{-1} 35925, 3529, 1327 (SO), 1168 (SO); ^{1}H NMR (500 MHz; DMSO-d^6) δ_H 1.14-1.25 (2H, m, 2 × CH_2CHOSO$_2$NH$_2$), 1.38-1.49 (2H, m, 2 × CH_{ax}CHOSO$_2$NH$_2$), 1.97-2.05 (4H, m, 2 × CH_{eq}CHOSO$_2$NH$_2$ and 2 × CH_{eq}CHNH), 2.88-2.97 (1H, m, CHNH), 3.21 (1H, d, J = 5.0 Hz, NH), 4.32 (1H, tt, J = 3.8 and 9.9 Hz, CHO), 7.30 (2H, s, NH$_2$); ^{13}C NMR (125 MHz; DMSO-d^6) δ_C 30.3 (2 × CH_2CHOSO$_2$NH$_2$), 30.4 (2 × CH_2CHNH), 50.5 (CHNH), 78.8 (CHOSO$_2$NH$_2$); HRMS calcd for C$_6$H$_{13}$N$_2$O$_6$S$_2$ [M-H]$^-$ 273.0221, found 273.0211.

2,2,2-Trichloroethyl 4-(hydroxymethyl)piperidine-1-sulfonate (188)
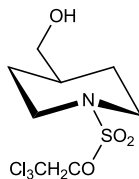
Prepared according to general procedure C using 2,3-dimethyl-1-((2,2,2-trichloroethoxy)sulfonyl)-1*H*-imidazol-3-ium tetrafluoroborate (331 mg, 0.87 mmol, 1 eq.), 4-piperidine methanol (100 mg, 0.87 mmol, 1 eq.), and THF (10 mL). The residue was purified by MPLC on SiO_2 with a gradient elution from 25-65% EtOAc/petrol to yield a clear oil (265 mg, 94%); R_f 0.2 (45% EtOAc/petrol; $KMnO_4$); λ_{max}(EtOH)/nm <220; IR ν_{max}/cm^{-1} 3352 (br), 1368 (SO), 1175 (SO); ^{1}H NMR (500 MHz; DMSO-d^6) δ_H 1.25 (2H, app qd, J = 4.2 and 12.6 Hz, 2 × CH_{ax}CH$_2$N), 1.52-1.62 (1H, m, C*H*CH$_2$OH), 1.78 (2H, app dd, J = 2.7 and 12.6 Hz, 2 × CH_{eq}CH$_2$N), 3.00 (2H, app td, J = 12.6 and 2.7 Hz, 2 × CH$_{ax}$N), 3.30 (2H, dd, J = 5.4 and 6.1 Hz, CH_2OH), 3.75 (2H, m, 2 × CH$_{eq}$N), 4.60 (1H, t, J = 5.4 Hz, OH), 4.91 (2H, s, CH$_2$CCl$_3$); ^{13}C NMR (125 MHz; DMSO-d^6) δ_C 27.6 (2 × *C*H$_2$CH$_2$N), 37.2 (*C*HCH$_2$OH), 46.5 (2 × CH$_2$N), 65.2 (CH$_2$OH), 77.7 (*C*H$_2$CCl$_3$), 94.1 (CCl$_3$); MS (ES+) *m/z* 326.3 [M(^{35,35,35}Cl)+H]$^+$, 328.3 [M(^{35,35,37}Cl)+H]$^+$, 330.3 [M(^{35,37,37}Cl)+H]$^+$.

(1-((2,2,2-Trichloroethoxy)sulfonyl)piperidin-4-yl)methyl sulfamate (189)
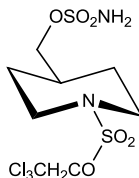
Sulfamoyl chloride (1.5 mL, 1 M in MeCN, 1.5 mmol, 2 eq.) was added to alcohol **188** (250 mg, 0.75 mmol, 1 eq.) in DMF (2 mL) containing potassium carbonate (528 mg, 3.8 mmol, 5 eq.) at -40 °C, and the mixture stirred at -40 °C for 18 h. The reaction was quenched with methanol, allowed to warm to room temperature, and partitioned between Et$_2$O (2 × 30 mL) and water (20 mL). The organics layers were combined, dried over MgSO$_4$, and the solvent removed *in vacuo*. The residue was purified by MPLC on silica with a gradient from 30-60% EtOAc/petrol to give a white crystalline solid (232 mg, 75%); R_f 0.3 (45% EtOAc/petrol; KMnO$_4$); m.p. 114-116 °C; λ_{max}(EtOH)/nm <220; IR ν_{max}/cm^{-1} 3366, 3263, 1360 (SO), 1178 (SO); ^{1}H NMR (500 MHz; DMSO-d^6) δ_H 1.37 (2H, app qd, J

= 12.4 and 4.1 Hz, 2 × CH_{ax}CH$_2$N), 1.81 (2H, app dd, J = 2.4 and 12.4 Hz, 2 × CH_{eq}CH$_2$N), 1.87-1.98 (1H, m, CHCH$_2$OH), 3.05 (2H, app td, J = 12.4 and 2.4 Hz, 2 × CH$_{ax}$N), 3.73 - 3.80 (2H, m, 2 × CH$_{eq}$N), 3.95 (2H, d, J = 6.4 Hz, CH_2OSO$_2$NH$_2$), 4.93 (2H, s, CH$_2$CCl$_3$), 7.50 (2H, s, OSO$_2$NH$_2$); ^{13}C NMR (125 MHz; DMSO-d^6) δ$_C$ 27.0 (2 × CH_2CH$_2$N), 33.9 (CHCH$_2$O), 46.0 (2 × CH$_2$N), 72.2 (CH$_2$OSO$_2$NH$_2$), 77.7 (CH_2CCl$_3$), 94.1 (CCl$_3$); MS (ES+) m/z 405.2 [M(^{35,35,35}Cl)+H]$^+$, 407.2 [M(^{35,35,37}Cl)+H]$^+$, 409.2 [M(^{35,37,37}Cl)+H]$^+$; HRMS calcd for C$_8$H$_{19}$N$_3$O$_6$^{35}Cl$_3$S$_2$ [M+NH$_4$]$^+$ 421.9775, found 421.9780.

Sodium 4-((sulfamoyloxy)methyl)piperidine-1-sulfonate (65)
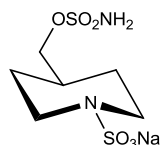
Activated zinc powder (677 mg, 1.04 mmol, 20 eq.) was added to sulfamate **189** (210 mg, 0.52 mmol, 1 eq.) in MeOH (6 mL) and water (6 mL) at r.t., and the mixture was stirred at r.t. for 1 h. The mixture was filtered through Celite, the Celite washed with methanol, and the solvent removed *in vacuo*. The residue was dissolved in water and run through a Dowex 50W8X-200 ion exchange resin which had previously been converted to the sodium form. Product containing fractions were frozen and lyophilised to give a white solid (138 mg, 90%); R_f 0.5 (30% MeOH/EtOAc; KMnO$_4$); m.p. 245 °C dec.; λ$_{max}$(EtOH)/nm <220; IR ν $_{max}$/cm^{-1} 3318, 3219, 31057, 1365 (SO), 1180 (SO); ^{1}H NMR (500 MHz; DMSO-d^6) δ$_H$ 1.12-1.23 (2H, m, 2 × CH_{ax}CH$_2$N), 1.57-1.71 (3H, m, 2 × CH_{eq}CH$_2$N and CHCH$_2$OH), 2.27 (2H, app td, J = 12.0 and 2.4 Hz, 2 × CH$_{ax}$N), 3.35-3.41 (2H, m, 2 × CH$_{eq}$N), 3.87 (2H, d, J = 6.4 Hz, CH_2OSO$_2$NH$_2$), 7.29 (2H, br s, OSO$_2$NH$_2$); ^{13}C NMR (125 MHz; DMSO-d^6) δ$_C$ 27.9 (2 × CH_2CH$_2$N), 35.0 (CHCH$_2$O), 46.1 (2 × CH$_2$N), 72.8 (CH$_2$OSO$_2$NH$_2$); HRMS calcd for C$_6$H$_{13}$N$_2$O$_6$S$_2$ [M-H]$^-$ 273.0221, found 273.0214.

10.3.3 Synthesis of Phenyl Sulfamates

Phenyl sulfamate (29)[341,210]
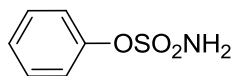
Prepared according to sulfamoylation method 4 using phenol (200 mg, 2.1 mmol, 1 eq.), sulfamoyl chloride (6.4 mL, 1 M in toluene, 6.4 mmol, 3 eq.) and DMA (8 mL). The resulting crude solid was purified by MPLC on SiO_2 with a gradient elution from 10-40% EtOAc/petrol to give a white solid (280 mg, 76%). R_f 0.5 (30% EtOAc/petrol); m.p. 82-84 °C (Lit.[341] 85 °C); λ_{max}(EtOH)/nm 202, 256, 265; IR ν_{max}/cm^{-1} 3419 (NH), 3303 (NH), 1361 (SO), 1171 (SO); ^{1}H NMR (500 MHz; DMSO-d^6) δ_H 7.27-7.36 (3H, m, H-Ar), 7.44-7.50 (2H, m, H-Ar), 7.98 (2H, s, NH$_2$); ^{13}C NMR (125 MHz; DMSO-d^6) δ_C 122.1 (C-Ar), 126.4 (C-Ar), 129.7 (C-Ar), 150.2 (C-O); MS (ESI-) m/z 172.1 [M-H]$^-$.

2-Trifluoromethylphenyl sulfamate (68)[342]
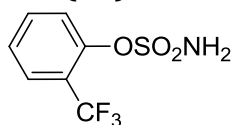
Prepared according to sulfamoylation method 4 using 2-trifluoromethylphenol (195 mg, 1.2 mmol, 1 eq.), sulfamoyl chloride (1.6 mL, 1.5 M in toluene, 2.4 mmol, 2 eq.) and DMA (2 mL). The resulting crude solid was purified by MPLC on SiO_2 with a gradient elution from 10-40% EtOAc/petrol to give a white solid (90 mg, 31%); R_f 0.1 (20% EtOAc/petrol); m.p. 102-104 °C; λ_{max}(EtOH)/nm 212.9, 262.9; IR ν_{max}/cm^{-1} 3371 (NH), 3278 (NH), 1383 (SO), 1195 (SO); ^{1}H NMR (500 MHz; CDCl$_3$) δ_H 5.02 (2H, s, NH$_2$), 7.44 (1H, t, J = 8.0 Hz, H-Ar), 7.65 (1H, td, J = 8.0 and 1.3 Hz, H-Ar), 7.69 (2H, t, J = 8.0 Hz, H-Ar); ^{13}C NMR (125 MHz; CD$_3$OD) δ_C 124.4 (q, J = 272.1 Hz, CF$_3$), 123.2 (CH-Ar), 127.0 (CH-Ar), 128.2 (q, J = 5.0 Hz, CH-C-CF$_3$), 134.7 (CH-Ar), 150.0 (C-O-S); HRMS calcd for C$_7$H$_7$F$_3$N$_1$O$_3$S$_1$ [M+H]$^+$ 242.0093, found 242.0091.

3-Trifluoromethylphenyl sulfamate (69)
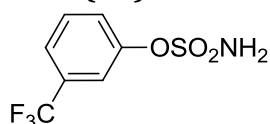
Prepared according to sulfamoylation method 4 using 3-trifluoromethylphenol (150 μL, 1.2 mmol, 1 eq.), sulfamoyl chloride (0.5 mL, 5 M in CH$_2$Cl$_2$, 2.5 mmol, 2.1 eq.) and

DMA (2 mL). The resulting crude solid was purified by MPLC on SiO$_2$ with a gradient elution from 10-50% EtOAc/petrol to give the sulfamate as a white solid (269 mg, 93%); R_f 0.8 (50% EtOAc/petrol); m.p. 103-106 °C (Lit.[343] 100-102 °C); λ_{max}(EtOH)/nm 263; IR ν_{max}/cm^{-1} 3355 (NH), 3281 (NH), 1366 (SO), 1181 (SO); ^{1}H NMR (500 MHz; DMSO-d^6) δ_H 7.60-7.62 (2H, m, H-Ar), 7.73-7.75 (2H, m, H-Ar), 8.20 (2H, s, NH$_2$); ^{13}C NMR (125 MHz; CD$_3$OD) δ_C 120.5 (q, CH-C-CF$_3$, J = 3.9 Hz), 125.0 (q, J = 271.6 Hz, CF$_3$,), 124.4 (q, J = 3.9 Hz, CH-C-CF$_3$), 127.3 (C-Ar), 131.8 (C-Ar), 133.1 (q, J = 32.9 Hz, C-CF$_3$), 152.4 (C-O-S); HRMS calcd for C$_7$H$_5$O$_3$N$_1$F$_3$S$_1$ [M-H]$^-$ 239.9948, found 239.9953.

4-Trifluoromethylphenyl sulfamate (70)[210]
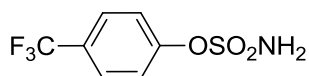
Prepared according to sulfamoylation method 4 using 4-trifluoromethylphenol (195 mg, 1.2 mmol, 1 eq.), sulfamoyl chloride (1.6 mL, 1.5 M in toluene, 2.4 mmol, 2 eq.) and DMA (2 mL). The resulting crude solid was purified by MPLC on SiO$_2$ with a gradient elution from 10-40% EtOAc/petrol to give a white solid (200 mg, 93%); R_f 0.05 (10% EtOAc/petrol); m.p. 112-113 °C (Lit.[210] 100-102 °C); λ_{max}(EtOH)/nm 219.9, 258.9; IR ν_{max}/cm^{-1} 3379 (NH), 3274 (NH), 1350 (SO), 1158 (SO); ^{1}H NMR (500 MHz; CDCl$_3$) δ_H 5.03 (2H, s, NH$_2$), 7.48 (2H, d, J = 8.4 Hz, H-Ar), 7.73 (2H, d, J = 8.4 Hz, H-Ar); ^{13}C NMR (125 MHz; CD$_3$OD) δ_C 125.0 (q, J = 271.1 Hz, CF$_3$), 123.9 (2 × C-Ar), 128.1 (q, J = 3.8 Hz, 2 × CHCCF$_3$), 129.7 (q, J = 32.8 Hz, CCF$_3$), 154.9 (C-O-S); HRMS calcd for C$_{12}$H$_{10}$O$_3$N$_1$S$_1$ [M+NH$_4$]$^+$ 216.0437, found 216.04615.

2-Cyanophenyl sulfamate (71)[344]
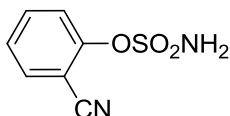
Prepared according to sulfamoylation method 4 using 2-cyanophenol (143 mg, 1.2 mmol, 1 eq.), sulfamoyl chloride (1.6 mL, 1.5 M in toluene, 2.4 mmol, 2 eq.) and DMA (3 mL). The resulting crude solid was purified by MPLC on SiO$_2$ with a gradient elution from 10-40% EtOAc/petrol to give a white solid 125 mg (26%); R_f 0.3 (30% EtOAc/petrol); m.p. 118-120 °C; λ_{max}(EtOH)/nm 230, 273 sh; IR ν_{max}/cm^{-1} 3358, 3238, 3090, 2246 (CN), 1556 (NO$_2$), 1384 (SO), 1166 (SO); ^{1}H NMR Spectrum: (500 MHz; CDCl$_3$): δ_H 5.30 (2H, s, NH$_2$), 7.46 (1H, td, J = 7.7 and 1.0 Hz, H-Ar) 7.63 (1H, dd, J = 8.3 and 0.7 Hz, H-Ar),

7.70-7.76 (2H, m, H-Ar); ^{13}C-NMR (125 MHz; CD$_3$OD) δ_C 108.7 (C-Ar), 116.3 (CN), 124.2 (C-Ar), 128.1 (C-Ar), 135.0 (C-Ar), 135.7 (C-Ar), 153.2 (C-O); HRMS calcd for C$_7$H$_{10}$O$_3$N$_3$S$_1$ [M+NH$_4$]$^+$ 216.0437, found 216.0439.

3-Cyanophenyl sulfamate (72)[343]
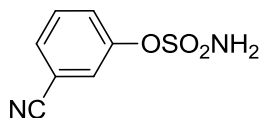
Prepared according to sulfamoylation method 4 using 3-cyanophenol (143 mg, 1.2 mmol, 1 eq.), sulfamoyl chloride (3.2 mL, 0.75 M in toluene, 2.4 mmol, 2 eq.) and DMA (3 mL). The resulting crude solid was purified by MPLC on SiO$_2$ with a gradient elution from 10-50% EtOAc/petrol to give a white solid (138 mg, 58%); R_f 0.2 (25% EtOAc/petrol); m.p. 105-107 °C (lit.[343] 101-104 °C); λ_{max}(EtOH)/nm 280; IR ν_{max}/cm^{-1} 3342 (NH), 3234 (NH), 2244, 1383 (SO), 1194 (SO); ^{1}H NMR (500 MHz; CDCl$_3$) δ_H 5.05 (s, 2H, NH$_2$), 7.58 (1H, dd, J = 8.2 and 7.9 Hz, H-Ar), 7.62-7.64 (1H, m, H-Ar), 7.65-7.68 (m, 2H, H-Ar); ^{13}C NMR (125 MHz; DMSO-d^6) δ_C 114.0 (C-Ar), 117.3 (CN), 125.8 (C-Ar), 127.0 (C-Ar), 130.96 (C-Ar), 130.99 (C-Ar), 150.1 (C-O); HRMS calcd for C$_7$H$_{10}$O$_3$N$_3$S$_1$ [M+NH$_4$]$^+$ 216.0437, found 216.04615.

4-Cyanophenyl sulfamate (73)[210]
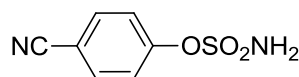
Prepared according to sulfamoylation method 4 using 4-cyanophenol (143 mg, 1.2 mmol, 1 eq.), sulfamoyl chloride (1.6 mL, 1.5 M in toluene, 2.4 mmol, 2 eq.) and DMA (3 mL). The resulting crude solid was purified by MPLC on SiO$_2$ with a gradient elution from 10-50% EtOAc/petrol to give a white solid (50 mg, 21%); R_f 0.2 (20% EtOAc/petrol); m.p. 147-148 °C (Lit.[210] 152-153 °C); λ_{max}(EtOH)/nm 229.9; IR ν_{max}/cm^{-1} 3353 (NH), 3251 (NH), 2240 (CN), 1376 (SO), 1155 (SO); ^{1}H NMR (500 MHz; CDCl$_3$) δ_H 5.04 (2H, s, NH$_2$), 7.48 (2H, dt, J = 8.8 and 2.0 Hz, H-Ar), 7.77 (2H, dt, J = 8.8 and 2.0 Hz, H-Ar); ^{13}C NMR (125 MHz; CD$_3$OD) δ_C 111.4 (*C*-CN), 119.1 (CN), 124.3 (2 × CH-Ar), 135.2 (2 × CH-Ar), 155.5 (*C*-O); HRMS calcd for C$_7$H$_5$N$_2$O$_3$S [M-H]$^-$ 197.0026, found 197.0027.

2-Nitrophenyl sulfamate (74)[345]
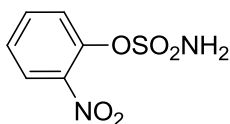
Prepared according to sulfamoylation method 4 using 2-nitrophenol (400 mg, 3.0 mmol, 1 eq.), sulfamoyl chloride (3 mL, 3 M in toluene, 9 mmol, 3 eq.) and DMA (3 mL). The resulting crude solid was purified by MPLC on SiO_2 with a gradient elution from 10-50% EtOAc/petrol to give a white solid (324 mg, 52%); R_f 0.1 (30% EtOAc/petrol); m.p. 103-104 °C (lit.[345] 102-104 °C); λ_{max}(EtOH)/nm 249.5 sh; IR ν_{max}/cm^{-1} 3402 (NH), 3263 (NH), 1600, 1512, 1355 (SO), 1174 (SO); ^{1}H NMR (500 MHz; DMSO-d^6) δ_H 7.55-7.61 (2H, m, H-Ar), 7.81-7.85 (1H, m, H-Ar) 8.06 (1H, dd, J = 8.1 and 1.6 Hz, H-Ar), 8.40 (2H, s, NH$_2$); ^{13}C NMR (125 MHz; DMSO-d^6) δ_C 126.1 (C-Ar), 126.6 (C-Ar), 128.3 (C-Ar), 135.2 (C-Ar), 144.0 (C-Ar), 145.0 (C-O-S); HRMS calcd for $C_6H_5O_5N_2S_1$ [M+NH$_4$]$^+$ 216.9925, found: 216.9924.

3-Nitrophenyl sulfamate (75)[346]
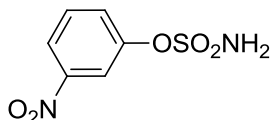
Prepared according to sulfamoylation method 4 using 3-nitrophenol (208 mg, 1.5 mmol, 1 eq.), sulfamoyl chloride (1.5 mL, 3 M in toluene, 4.5 mmol, 3 eq.) and DMA (2 mL). The resulting crude solid was purified by MPLC on SiO_2 with a gradient elution from 10-50% EtOAc/petrol to give a white solid (285 mg, 87%); R_f 0.1 (UV, 30% EtOAc/petrol); m.p. 94-96 °C; λ_{max}(EtOH)/nm 265; IR ν_{max}/cm^{-1} 3368 (NH), 3281 (NH), 1563.3, 1365 (SO), 1174 (SO); ^{1}H NMR (500 MHz; CDCl$_3$) δ_H 5.08 (2H, s, NH$_2$), 7.66 (1H, t, J = 8.1 Hz, H-Ar) 7.72 - 7.75 (1H, m, H-Ar), 8.22 - 8.27 (2H, m, H-Ar); ^{13}C NMR (125 MHz; CD$_3$OD) δ_C 118.7 (C-Ar), 122.5 (CN), 129.9 (C-Ar), 131.8 (C-Ar), 150.3 (C-Ar), 152.4 (C-O-S); HRMS calcd for $C_6H_5O_5N_2S_1$ [M+NH$_4$]$^+$ 216.9925, found: 216.9926.

4-Nitrophenyl sulfamate (76)[210]
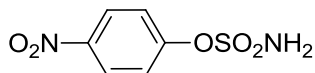
Prepared according to sulfamoylation method 4 using 4-nitrophenol (166 mg, 1.2 mmol, 1 eq.), sulfamoyl chloride (3.2 mL, 0.75 M in toluene, 2.4 mmol, 2 eq.) and DMA (3 mL). . The resulting crude solid was purified by MPLC on SiO_2 with a gradient elution from 5-

40% EtOAc/petrol to give a white solid (64 mg, 24%); R_f 0.25 (20% EtOAc/petrol); m.p. 105-107 °C (Lit.[210] 100-102 °C); λ_{max}(EtOH)/nm 215.9, 265.9; IR ν_{max}/cm^{-1} 3419.0 (NH), 3291 (NH), 1587, 1510, 1351 (SO), 1173 (SO); ^{1}H NMR (500 MHz; CDCl$_3$) δ_H 5.10 (2H, s, NH$_2$), 7.53 (2H, dt, J = 9.0 and 2.2 Hz, H-Ar), 8.35 (dt, 2H, J = 9.0 and 2.2 Hz, H-Ar); ^{13}C NMR (125 MHz; DMSO-d^6) δ_C 115.8 (C-Ar), 126.2 (C-Ar), 139.6 (C-NO$_2$), 163.9 (C-O-S); MS (ESI-) m/z: runs as phenol.

Data were inconsistent with literature[210] as the ^{13}C NMR shifts do not correspond. For further structural confirmation, crystallisation was performed using the slow evaporation of 5mg of the obtained product from MeCN over 2 weeks. X-ray crystallography confirmed the product had the desired structure.

2-Methoxyphenyl sulfamate (77)[347]
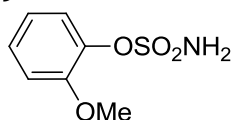
Prepared according to sulfamoylation method 4 using 2-methoxyphenol (248 mg, 2 mmol), sulfamoyl chloride (4 mL, 2 M in toluene, 6 mmol, 3 eq.) and DMA (4 mL). The resulting crude solid was purified by MPLC on SiO$_2$ with a gradient elution from 10-50% EtOAc/petrol to give a white solid (116 mg, 29%); R_f 0.25 (30% EtOAc/petrol); m.p. 84-86 °C, (lit.[347] 78 °C); λ_{max}(EtOH)/nm 218.9, 270.9 sh; IR ν_{max}/cm^{-1} 3350 (NH), 3256 (NH), 1382 (SO), 1108 (SO); ^{1}H NMR (500 MHz; CDCl$_3$) δ_H 3.94 (3H, s, OCH$_3$), 4.99 (2H, s, NH$_2$), 7.04 (2H, dd, J = 8.0 and 7.9 Hz, H-Ar), 7.31 (1H, d, J = 8.0 Hz, H-Ar), 7.38 (1H, d, J = 8.0 Hz, H-Ar); ^{13}C NMR (125 MHz; DMSO-d^6) δ_C 55.8 (OCH$_3$), 113.4 (C-Ar), 120.4 (C-Ar), 123.2 (C-Ar), 127.3 (C-Ar), 138.9 (C-Ar), 151.8 (C-O-S); HRMS calcd for C$_7$H$_8$NO$_4$S [M-H]$^-$ 202.0180, found 202.0180.

3-Methoxyphenyl sulfamate (78)[343]
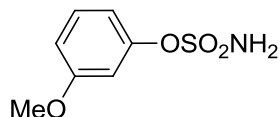
Prepared according to sulfamoylation method 4 using 3-methoxyphenol (248 mg, 2 mmol), sulfamoyl chloride (4 mL, 2 M in toluene, 6 mmol, 3 eq.) and DMA (4 mL). The resulting crude solid was purified by MPLC on SiO$_2$ with a gradient elution from 10-50% EtOAc/petrol to give an amorphous white solid (225 mg, 56%); R_f 0.25 (30%

EtOAc/petrol); λ_{max}(EtOH)/nm 219.9, 270.9 sh; IR ν_{max}/cm^{-1} 3378 (NH), 3279 (NH), 1360 (SO), 1124 (SO); ^{1}H NMR (500 MHz; CDCl$_3$) δ_H 3.84 (s, 3H, OCH$_3$), 4.97 (s, 2H, NH$_2$), 6.92 (2H, d, J = 7.6 Hz, H-Ar), 7.29 (1H, s, H-Ar), 7.34 (1H, t, J = 7.6 Hz, H-Ar); ^{13}C NMR (125 MHz; DMSO-d^6) δ_C 55.4 (OCH$_3$), 108.1 (C-Ar), 112.1 (C-Ar), 114.1 (C-Ar), 130.2 (C-Ar), 151.1 (C-O-S), 160.1 (*C*-O-Me); HRMS calcd for C$_7$H$_8$O$_4$N$_1$S$_1$ [M-H]$^-$ 202.0180, Found 202.0175.

4-Methoxyphenyl sulfamate (79)[210]
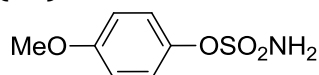
Prepared according to sulfamoylation method 4 using 4-methoxyphenol (149 mg, 1.2 mmol, 1 eq.), sulfamoyl chloride (1 mL, 2.4 M in CH$_2$Cl$_2$, 2.4 mmol, 2 eq.) and DMA (4 mL). The resulting crude solid purified by MPLC on SiO$_2$ with a gradient elution from 1-30% EtOAc/petrol to give a white solid (130 mg, 53%); R_f 0.4 (UV, 30% EtOAc/petrol); m.p. 64-67 °C (lit.[210] 62-64 °C); λ_{max}(EtOH)/nm 275; IR ν_{max}/cm^{-1} 3386 (NH), 3284 (NH), 1348 (SO), 1166 (SO); ^{1}H NMR (500 MHz; DMSO-d^6) δ_H 3.77 (s, 3H, OCH$_3$), 7.00 (2H, dd, J = 9.2 and 2.3 Hz, H-Ar), 7.20 (2H, dd, J = 9.2 and 2.3 Hz, H-Ar), 7.89 (s, 2H, NH$_2$); ^{13}C NMR (125 MHz; DMSO-d^6) δ_C 59.7 (OCH$_3$), 114.6 (C-Ar), 123.3 (C-Ar), 143.5 (C-Ar), 157.5 (C-Ar); ^{13}C NMR (125 MHz; CD$_3$OD) δ_C 56.1 (OCH$_3$), 115.6 (CH-Ar), 124.4 (CH-Ar), 145.5 (C-O-S), 159.6 (*C*-OMe); HRMS calcd for C$_7$H$_8$O$_4$N$_1$S$_1$ [M-H]$^-$ 202.0180, found 202.0185.

Data were consistent with literature values[210] except for the ^{13}C NMR chemical shift of OCH$_3$. The reported literature value is not consistent with expected value for this structure. A single crystal was grown for X-ray crystallography studies by dissolving 20mg of compound in H$_2$O (1 mL) and allowing to crystallise through slow evaporation for 2 weeks. X-ray data confirmed that the desired product has been formed.

2-Phenylphenyl sulfamate (80)[348]
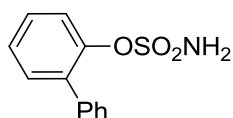
Prepared according to sulfamoylation method 4 using 2-phenylphenol (204 mg, 1.2 mmol, 1 eq.), sulfamoyl chloride (1.6 mL, 1.5 M in toluene, 2.4 mmol, 2 eq.) and DMA (2 mL). The resulting crude solid was purified by MPLC on SiO$_2$ with a gradient elution from 10-

40% EtOAc/petrol to give a white solid (200 mg, 67%); R_f 0.5 (20% EtOAc/petrol); m.p. 89-91 °C (Lit.[348] 87 °C); λ_{max}(EtOH)/nm 213.9, 240.9,; IR ν_{max}/cm^{-1} 3364, 3268, 3108, 3065, 1379 (SO), 1105 (SO); ^{1}H NMR (500 MHz; CDCl$_3$) δ_H 4.10 (2H, s, NH$_2$), 7.41-7.60 (9H, m, H-Ar); ^{13}C NMR (125 MHz; DMSO-d^6) δ_C 121.6 (C-Ar), 126.4 (C-Ar), 127.3 (C-Ar), 128.2 (C-Ar), 128.7 (C-Ar), 129.1 (C-Ar), 131.3 (C-Ar), 134.2 (C-Ar), 137.0 (C-Ar), 147.4 (C-O); MS (ESI-) m/z 248.1 [M-H]$^-$; HRMS calcd for C$_{12}$H$_{15}$O$_3$N$_2$S$_1$ [M+NH$_4$]$^+$ 267.0798, found 267.0803.

3-Phenylphenyl sulfamate (81)
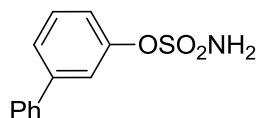
Prepared according to sulfamoylation method 4 using 3-phenylphenol (204 mg, 1.2 mmol, 1 eq.), sulfamoyl chloride (1.6 mL, 1.5 M in toluene, 2.4 mmol, 2 eq.) and DMA (2 mL). The resulting crude solid was purified by MPLC on SiO$_2$ with a gradient elution from 10-40% EtOAc/petrol to give a white solid (128 mg, 43%); R_f 0.2 (20% EtOAc/petrol); m.p. 91-93 °C; λ_{max}(EtOH)/nm 213.9, 248.9; IR ν_{max}/cm^{-1} 3359 (NH), 3263 (NH), 1353 (SO), 1147 (SO); ^{1}H NMR (500 MHz; CDCl$_3$) δ_H 4.95 (2H, s, NH$_2$), 7.30-7.70 (9H, m, H-Ar); ^{13}C NMR (125 MHz; DMSO-d^6) δ_C 120.4 (C-Ar), 121.2 (C-Ar), 124.9 (C-Ar), 126.8 (C-Ar), 128.0 (C-Ar), 129.0 (C-Ar), 130.3 (C-Ar), 139.0 (C-Ar), 142.0 (C-Ar), 150.7 (C-O); HRMS calcd for C$_{12}$H$_{10}$NO$_3$S [M-H]$^-$ 248.0387, Found 248.0391.

4-Phenylphenyl sulfamate (82)[210]
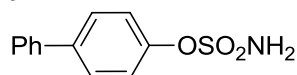
Prepared according to sulfamoylation method 4 using 4-phenylphenol (204 mg, 1.2 mmol, 1 eq.), sulfamoyl chloride (1 mL, 2.4 M in CH$_2$Cl$_2$, 2.4 mmol, 2 eq.) and DMA (4 mL). The resulting crude solid was purified by MPLC on SiO$_2$ with a gradient elution from 10-40% EtOAc/petrol to give a white solid (201 mg, 67%); R_f 0.4 (25% EtOAc/petrol); m.p. 165-167 °C (Lit.[210] 160-162 °C); λ_{max}(EtOH)/nm 250; IR ν_{max}/cm^{-1} 3421 (NH), 3299 (NH), 3078, 1362 (SO), 1176 (SO); ^{1}H NMR (500 MHz; DMSO-d^6) δ_H 7.37-7.41 (3H, m, H-Ar), 7.49 (2H, tt, J = 8.0 and 1.5 Hz, H-Ar) 7.68 (2H, dq, J = 8.0 and 1.5 Hz, H-Ar), 7.76 (2H, dt, J = 8.0 and 1.5 Hz, H-Ar), 8.06 (2H, s, NH$_2$); ^{13}C NMR (125 MHz; DMSO-d^6) δ_C 122.7 (C-Ar), 126.7 (C-Ar), 127.6 (C-Ar), 128.0 (C-Ar), 129.0 (C-Ar), 138.6 (C-

Ar), 139.2 (C-Ar), 149.6 (C-O); HRMS calcd for $C_{12}H_{10}N_1O_3S_1$ [M-H]$^-$ 248.0387, found 248.0390.

10.3.4 Synthesis of Benzylic Sulfamate Targets

4-Nitrobenzyl sulfamate (89)
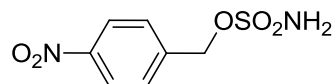
Prepared according to sulfamoylation method 4 using 4-nitrobenzyl alcohol (706 µL, 6 mmol, 1 eq.), sulfamoyl chloride (12 mL, 1.5 M in toluene, 18 mmol, 3 eq.) and DMA (12 mL). The crude material was purified by MPLC on SiO_2 with a gradient elution from 10-50% EtOAc/petrol to give a white solid (700 mg, 50%); R_f 0.3 (30% EtOAc/petrol); m.p. 113-104 °C; λ_{max}(EtOH)/nm 213.9, 266.9; IR ν_{max}/cm^{-1} 3384 (NH), 3287 (NH), 1505.6 (NO_2), 1344 (SO), 1168 (SO); ^{1}H NMR (500 MHz; CDCl$_3$) δ_H 4.82 (2H, s, NH$_2$), 5.33 (2H, s, CH$_2$), 7.62 (2H, d, J = 8.8 Hz, H-Ar), 8.29 (2H, dt, J = 8.8 and 2.2 Hz, H-Ar); ^{13}C NMR (125 MHz; DMSO-d^6) δ_C 68.6 (CH$_2$), 123.6 (2 × CH-Ar), 128.8 (2 × CH-Ar), 142.5 (C-Ar), 147.3 (C-NO$_2$); HRMS calcd for $C_7H_7O_5N_2S_1$ [M-H]$^-$ 231.0080, found: 231.0081.

4-Acetamidobenzyl alcohol (196)[83]
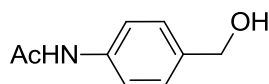
Acetic anhydride (1 mL, 10.6 mmol, 3.3 eq.) was added to 4-aminobenzyl alcohol (400 mg, 3.25 mmol, 1 eq.) in methanol (15 mL) at r.t. over 5 minutes and the mixture was stirred at r.t. for 3 h. Additional acetic anhydride (0.4 mL) was added and the mixture stirred at r.t. for 2 h. Pyridine was added and the mixture stirred at r.t. overnight. The solvent was removed *in vacuo* and the residue purified by MPLC on SiO_2 with a gradient elution from 1-10% MeOH /CH$_2$Cl$_2$ to give a brown oil. The oil was triturated with Et$_2$O to give a beige solid (350 mg, 65%); R_f 0.5 (10% MeOH/CH$_2$Cl$_2$); IR ν_{max}/cm^{-1} 3415, 3245, 3186, 1668 (amide I), 1547 (amide II); ^{1}H NMR (500 MHz; CDCl$_3$) δ_H 1.68 (1H, s, OH), 2.20 (3H, s, CH$_3$), 4.68 (2H, s, CH$_2$), 7.22 (s, 1H, NH), 7.35 (2H, d, J = 8.3 Hz, H-Ar), 7,51 (2H, d, J = 8.3Hz, H-Ar); ^{13}C NMR (125 MHz; CD$_3$OD) δ_C 23.8 (CH$_3$), 64.9 (CH$_2$), 121.1 (2 × C-Ar), 128.6 (2 × C-Ar), 138.5 (C-Ar), 139.1 (C-Ar), 171.6 (COCH$_3$); MS (ESI-) *m/z* 164.1 [M-H]$^-$.

10.4 ERK5 Project Experimental Procedures

10.4.1 ERK5 Biological Assay Protocols

The ERK5 biological assays were performed by Ms Ai Ching Wong at Cancer Research Technology Discovery research Laboratories, London, and in by Lan-Zhen Wang at the Paul O'Gorman Building, Newcastle Cancer Centre, Newcastle upon Tyne.

ERK5 IMAP™ Assay Protocol

Preparation of Assay Buffer (1x)

The 0.01% Tween®-20 5x stock was supplied as part of IMAP^{TM} FP Progressive Binding System Kit (Molecular Devices R7436), which was diluted to 1x using miliQ H$_2$O. 1 µL of a 1 M DTT stock was added for every 1 mL of 1x assay buffer to give a final concentration of 1 mM DTT.

Preparation of ERK5 Working Solution

The final dilution was dependent on activity of the enzyme batches. The initial batch (08/08/08) was used at a 1 in 1 in 350 final dilution in assay buffer. A 1:175 dilution of ERK5 stock was performed in 1x assay buffer. For 1 plate, 13 µL of ERK5 stock was added to 2262 µL of 1x assay buffer. ERK5 was expressed and purified at CRT by Leon Pang and Sue Young. Aliquots were stored at -80 °C. Batch PO080808 was used at a stock concentration of 73.4 ng/µl.

Preparation of ATP/Substrate Working Solution

For one plate, ATP disodium salt (90 µL, 20 mM) (Sigma A7699) and FAM-EGFR-derived peptide (15 µL, 100 µM) (LVEPLTPSGEAPNQ(K-5FAM)-COOH) (Molecular Devices RP7129; reconstituted in miliQ H$_2$O to a stock concentration of 100 µL; Stored at -20°C) was added to 2295 µL of 1x assay buffer.

Preparation of IMAP™ binding solution

For one plate 20.5 µL of IMAP™ binding reagent stock, 1476 µL of 1x binding buffer A (60%), and 984 µL of binding buffer B (40%) (IMAP™ FP Progressive screening express kit (Molecular Devices R8127) was added to 9819.5 µL of milliQ H_2O.

Assay Procedure

1 µL of compound (in 60:40 H_2O/DMSO) or 60:40 H_2O/DMSO (for controls and blanks) were dry-spotted into the relevant wells of a 384-well assay plate using the MATRIX PlateMate® Plus. 5 µL of ERK5 working solution was added to test and control wells, and 5 µL of 1x assay buffer added to blanks; 4 µL of ATP/substrate working solution was added to all wells using a Matrix multichannel pipette. The plate was sealed using DMSO resistant 205 clear seal and incubated for 2 h at 37 °C. 1 µL of the kinase reaction mixture from the first plate was dry spotted into a second 384-well assay plate using the MATRIX PlateMate® Plus. 9 µL of assay buffer was added, followed by 30 µL of IMAP™ binding solution using a multichannel pipette. The plate was incubated at RT in darkness for 2 h. The assay plate was then read on an Analyst HT plate reader (Molecular Devices) using the settings described below;

Measurement mode = Fluorescence polarisation; Method ID = ERK5; Integration time = 100 ms; Excitation filter = Fluorescein 485-20; Emission filter = 530-25; Dichroic mirror = 505 nm; Plate definition file = Corning 384 black fb; Z-height = 5.715 mm (middle); G-factor = 1; Attenuator = out; Detector counting = Smartread+; Sensitivity = 2.

p38α LANCE Assay Protocol

Preparation of Assay Buffer (1x)

1x assay buffer was prepared freshly in house, consisting of the following reagents; 250 mM tris(hydroxymethyl)aminomethane (Tris) pH 7.5, 25 mM $MgCl_2$, 2.5 mM ethylene glycol tetraacetic acid (EGTA), 10 mM dithiothreitol (DTT) and 0.05% Triton X100 in milliQ H_2O (NB: 1x buffer final assay concentrations were 5x lower than stated above).

Preparation of p38α/SAPK2 Working Solution

The p38α/SAPK2, active *N*-terminal GST-tagged recombinant full length protein (Millipore 14-251) was supplied as a 10 μg/4 μL stock. This was diluted to a 10 μg/40 μL (1 μM) concentration by addition of 156 μL of Tris/HCl (pH 7.5, 50 mM), NaCl (150 mM), EGTA (0.1 mM), Brij-35 surfactant (0.03%), glycerol (50%) and 0.1% 2-mercaptoethanol (0.1%). The final dilution was dependent on activity of the enzyme batches. The p38α concentration used in the assay was 1 nM. A 2x working stock solution (2 nM, 500 fold dilution of 1 μM stock) in 1x assay buffer was prepared. For one plate, 9.4 μL of p38α (1 μM) was added to 1870.6 μL of milliQ H_2O.

Preparation of ATP/Substrate working solution

For one plate, ATP disodium salt (17.5 μL, 200 mM stock), (Sigma A7699) and Ulight-MBP Peptide (50 μL, 5 μM stock) (Perkin Elmer TRF0109) was added to 400 μL of 5x assay buffer and 1532.5 μL of milliQ H_2O.

Preparation of EDTA/Antibody Detection Reagent

For one plate, 84 μL of ethylenediaminetetraacetic acid (EDTA) (0.5 M) (Sigma E4378-100G) and 27 μL of Europium-anti-phospho-MBP antibody (0.625 μM) (Perkin Elmer) was added to 420 μL of LANCE detection buffer (1x) and 3669 of milliQ H_2O.

Assay Procedure

1 μL of compound (in 80:20 H_2O/DMSO) or 80:20 H_2O/DMSO was dry-spotted into the relevant wells of a 384-well assay plate using the MATRIX PlateMate® Plus. 5 μL of p38α working solution was added to test and control wells, and 5 μL of assay buffer added to blanks; 4 μL of ATP/substrate working solution was added to all wells using a Thermo Multidrop Combi or Matrix multichannel pipette. The plate was sealed using DMSO resistant clear seal and incubated for 1 h at 37 °C. 10 μL of the EDTA/antibody working solution was added to all wells using a Thermo Multidrop Combi or Matrix multichannel pipette. The plate was incubated at RT in darkness for 2 h. The assay plate was then read on a PheraStar microplate reader using the settings described below;

Pherastar: Measurement mode = TRF; Method ID = LANCE HTRF ERK5; Optic Module: 337, 665, 620 nm. Focal Height = 6.0, Positioning delay, 0.1 sec, Number of flashes per well = 100, Integration start = 60

Hela cell-based densitometry assay protocol

HeLa cells were serum starved overnight followed by treatment with ERK5 inhibitors for 1 hr. Cells were then stimulated with 100ng/ml EGF for 10 min. The cells were harvested and lysed at 4 ^{o}C for 5-10 min in Laemmli buffer containing Halt protease and phosphate inhibitors (Pierce). The lysates were boiled for 10 min at 100 ^{o}C. A twenty microliter sample was run on a 6% tris-glycine gel and transferred to nitrocellulose. Western blotting was done with ERK5 antibody (Cell signalling #3372S). The IC$_{50}$ was calculated from densitometry of the top (phosphor-ERK) bands.

10.4.2 ERK5 General Synthetic Procedures

A number of compounds were prepared using the general procedures reported below. Quantities used and variations are recorded before the analytical data for each compound.

General procedure D: CDI amide coupling

Carbonyl diimidazole (CDI, 2 eq.) was added to a solution of the relevant carboxylic acid in THF (2 mL/mmol) and the mixture heated to 70 °C for 3 h. The relevant amine (2.5 eq.) was added and the mixture was heated at 70 °C for 2 h. The mixture was partitioned between EtOAc (2 × 20 mL) and saturated $NaHCO_{3(aq.)}$. The organic layers were combined, washed with brine (20 mL), dried over $MgSO_4$ and solvent removed *in vacuo*.

General procedure E: Cyanuric fluoride amide coupling

Cyanuric fluoride (0.7 eq.) was added to the relevant carboxylic acid (1 eq.) and pyridine (1 eq.) in MeCN (2 mL/mmol). The relevant amine (2.5 eq.) was added and the mixture was stirred at r.t. for 18 h. The reaction was diluted with EtOAc, washed with water and 0.5 M aqueous HCl, followed by further washes with saturated aqueous $NaHCO_3$ and brine. The organic layer was dried over $MgSO_4$ and the solvent removed *in vacuo*.

General procedure F: PCl₃ amide coupling[349]

The relevant carboxylic acid (1 eq.), the relevant amine (2.5 eq.) and PCl_3 (1 eq.) were combined in MeCN (4 mL/mmol) and heated under microwave irradiation to 100 °C for 30 min. The mixture was allowed to cool, 2 M $NaOH_{(aq)}$ (20 mL) was added, the mixture was stirred for 10 min, and then extracted with EtOAc (3 × 20 mL). The organic layers were combined, washed with brine, dried over $MgSO_4$ and the solvent removed *in vacuo*.

General procedure G: Boc deprotection in TFA/CH₂Cl₂

TFA (2 mL/mmol) and Et_3SiH (2.5 eq.) were added to the relevant carbamate (1 eq.) in DCM (2 mL/mmol) and the mixture was stirred at r.t. for 2 h. The solvent was removed *in vacuo*, the residues partitioned between EtOAc (5 × 30 mL) and $NaHCO_{3(aq)}$ (40 mL). The organic extracts were combined, dried over $MgSO_4$, and the solvent removed *in vacuo*.

General procedure H: Hydrogenation of heteroaromatic nitro group

The relevant nitro compound (1 eq.) was dissolved in MeOH (5 mL/mmol) and hydrogenated on a Thales H-cube over 10% Pd/C on full H_2 mode at 40 °C for 2 h with continuous recycling of the reaction mixture. The solvent was removed *in vacuo*.

General procedure I: Amine displacement of 4-nitro-2-chloropyrimidine

The relevant amine (1 eq.), 2-chloro-5-nitropyrimidine (1 eq.), and Et$_3$N (1.1 eq.) were combined in THF (5 mL/mmol) at 0 °C, and the mixture allowed to stir at r.t. for 1 h. The solvent was removed *in vacuo*, and the residue partitioned between EtOAc (2 × 30 mL) and water (20 mL). The organic layer washed with brine, dried over MgSO$_4$ and the solvent removed *in vacuo*.

General procedure J: Mitsunobu alkylation of 4-nitropyrazole

Diethylazodicarboxylate (1.5 eq.) was added dropwise to a mixture of 4-nitropyrazole (1 eq.), triphenylphosphine (1.73 g, 6.63 mmol, 1.5 eq.) and the substrate alcohol (1 eq.), in THF at 0 °C. The mixture was stirred at 0 °C for 10 min, and then allowed to stir at r.t. for 18 h. The mixture was partitioned between EtOAc (2 × 30 mL) and water (20 mL), washed with brine (20 mL), dried over MgSO$_4$ and the solvent removed *in vacuo*.

General procedure K: Eschweiler-Clarke conversion of a Boc protected amine to a methylamine

Formaldehyde (37% w/v aqueous, 4 eq.) was added to the substrate carbamate (1 eq.) in formic acid (10 mL/mmol), and the mixture was heated to 100 °C for 3 h in a sealed tube. The mixture was allowed to cool, basified with 10% K$_2$CO$_{3(aq)}$, and extracted with EtOAc (2 × 20 mL). The organic extracts were combined, washed with brine, dried over MgSO$_4$, and the solvent removed *in vacuo*.

General procedure L: Amide coupling with 2-chloro-1-methylpyridinium iodide

Pyrrole acid (1 eq.), Et$_3$N (2.5 eq.), and 2-chloro-1-methylpyridinium iodide (1.1 eq.) were combined in DCM (15 mL/mmol) and stirred at r.t. for 10 min, followed by the addition of the substrate amine (1.25 eq.) in DCM (2.5 mL/mmol). The reaction was stirred at r.t. for 18 h, the solvent evaporated, and the mixture partitioned between EtOAc (2 × 15 mL) and 10% aqueous K$_2$CO$_3$ (15 mL). The organic layers were combined, washed with brine, dried over MgSO$_4$ and the solvent removed *in vacuo*.

10.4.3 ERK5 Synthetic Procedures

Methyl 4-(2-chloro-6-fluorobenzoyl)-1*H*-pyrrole-2-carboxylate (334)
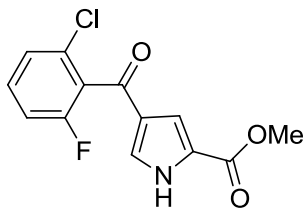
To a suspension of AlCl$_3$ (2.23 g, 16.8 mmol, 2.5 eq.) in DCM (17 mL) at 0 °C was added 2-chloro-6-fluorobenzoyl chloride (1.8 mL, 13.3 mmol, 2 eq.). The mixture was stirred at 0 °C for 10 min, and then methyl-1*H*-pyrrole-2-carboxylate (847 mg, 6.7 mmol, 1 eq.) was added. The mixture was stirred at r.t. for 18 h, cooled to 0 °C and HCl (1 M aqueous) was added until gas evolution ceased. Rochelle's salt (50 mL, saturated aq.) was added and the mixture was stirred at r.t. for 45 min. The mixture was extracted with DCM (3 × 100 mL), the organic layers combined, washed with NaHCO$_3$(100 mL, 10% aq.) and brine (100 mL), dried over MgSO$_4$, and solvent removed *in vacuo*. The residue was purified by MPLC on SiO$_2$ with a gradient elution from 0-100% EtOAc/petrol to give a white solid (1.74 g, 92%); R_f 0.5 (5% MeOH/DCM); m.p. 148-150 °C; λ_{max}(EtOH)/nm 280, 233; IR ν_{max}/cm^{-1} 3226, 1731, 1638, 1604; ^{1}H NMR (500 MHz; DMSO-d_6) δ_H 3.83 (3H, s, OMe), 7.02-7.05 (1H, m, H-3), 7.42 (1H, app td, *J* = 8.2 and 0.8 Hz, H-5'), 7.49 (1H, d, *J* = 8.2 Hz, H-3'), 7.57 (1H, dd, *J* = 1.7 and 3.3 Hz, H-5), 7.61 (1H, td, *J* = 8.2 and 6.3 Hz, H-4'), 12.94 (1H, br s, NH); ^{19}F NMR (470 MHz; DMSO-d_6) δ_F -114.43; ^{13}C NMR (125 MHz; DMSO-d_6) δ_C 51.7 (OMe), 114.6 (CH-pyrrole), 115.0 (d, J_{CF} = 21.8 Hz, C-5'), 124.5 (C-pyrrole), 125.4 (C-pyrrole), 125.9 (d, J_{CF} = 3.2 Hz, C-3'), 127.7 (d, J_{CF} = 23.2 Hz, C-1'), 130.1 (C-pyrrole), 130.3 (d, J_{CF} = 6.4 Hz, C-2'), 131.9 (d, J_{CF} = 9.1 Hz, C-4'), 158.5 (d, J_{CF} = 246.9 Hz, C-6'), 160.3 (CO-NH), 183.7 (CO); HRMS calcd for C$_{13}$H$_{10}$^{35}Cl$_1$F$_1$O$_3$N$_1$ [M+H]$^+$ 282.0328, found 282.0333.

4-(2-Chloro-6-fluorobenzoyl)-1*H*-pyrrole-2-carboxylic acid (336)
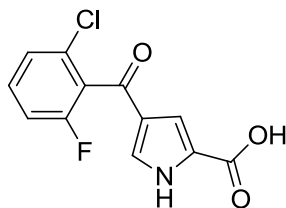
A solution of LiOH (2.9 g, 121 mmol, 20 eq.) in H$_2$O (80 mL) was added to ester **334** (1.7 g, 6.05 mmol, 1 eq.) in THF (48 mL) and heated to 65 °C for 18 h. After cooling to r.t., the

mixture was acidified to pH 3 with HCl (1 M aq.) and extracted with EtOAc (2 × 150 mL). The combined organic layers were washed with water and brine, dried over MgSO$_4$, and the solvent removed *in vacuo* to give a white solid (1.6 g, 99%); R_f 0.15 (10% MeOH/DCM); m.p. 220-222 °C; λ_{max}(EtOH)/nm 281, 232; IR ν_{max}/cm^{-1} 3313, 1637, 1553; ^{1}H NMR (500 MHz; DMSO-d_6) δ_H 6.98 (1H, br s, H-pyrrole), 7.42 (td, J = 8.2 and 0.6 Hz, H-5'), 7.47-7.51 (2H, m, H-3' and H-pyrrole), 7.61 (1H, td, J = 8.2 and 6.3 Hz, H-4'), 12.75 (1H, br s, NH-pyrrole), 12.97 (1H, br s, CO$_2$H); ^{19}F NMR (470 MHz; DMSO-d_6) δ_F -114.41; ^{13}C NMR (125 MHz; DMSO-d_6) δ_C 114.1 (CH-pyrrole), 114.9 (d, J_{CF} = 21.3 Hz, C-5'), 125.3 (C-pyrrole), 125.8 (d, J_{CF} = 3.2 Hz, C-3'), 125.9 (C-pyrrole), 127.8 (C-pyrrole), 127.9 (d, J_{CF} = 23.2 Hz, C-1'), 129.7 (C-pyrrole), 130.3 (d, J_{CF} = 6.0 Hz, C-2'), 131.8 (d, J_{CF} = 9.1 Hz, C-4'), 158.5 (d, J_{CF} = 247 Hz, C-6'), 161.3 (CO-NH), 183.7 (CO); HRMS calcd for C$_{12}$H$_6{}^{35}$Cl$_1$F$_1$N$_1$O$_3$ [M+H]$^+$ 266.0026, found 266.0018.

Methyl 4-(3,6-dichloro-2-fluorobenzoyl)-1*H*-pyrrole-2-carboxylate (335)
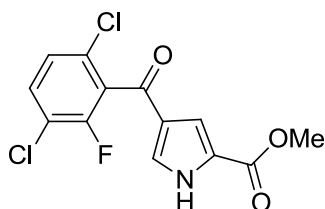
To a suspension of AlCl$_3$ (11.9 g, 89.6 mmol, 2.5 eq.) in DCM (100 mL) at 0 °C was added 3,6-dichloro-2-fluorobenzoyl chloride (16.3 mL, 71.7 mmol, 2 eq.). The mixture was stirred at 0 °C for 10 min, and then methyl-1*H*-pyrrole-2-carboxylate (4.48 g, 35.8 mmol, 1 eq.) was added. The mixture was stirred at r.t. for 18 h, cooled to 0 °C and HCl (1 M aq.) added until gas evolution ceased. Rochelle's salt (sat'd aq., 200 mL) was added and the mixture stirred at r.t. for 45 min. The mixture was extracted with DCM (4 × 150 mL), the organic layers combined, dried over MgSO$_4$, and solvent removed *in vacuo*. The residue was purified by MPLC on SiO$_2$ with a gradient elution from 0-65% EtOAc/petrol to give a white solid (10.12 g, 89%); R_f 0.8 (50/50/0.5 EtOAc/petrol/AcOH); m.p. 136-138 °C; λ_{max}(EtOH)/nm 282, 229; IR ν_{max}/cm^{-1} 3285, 3230, 1689, 1654; H NMR (500 MHz; DMSO-d_6) δ_H 3.84 (3H, s, CH$_3$), 7.12 (1H, app t, J = 1.5 Hz, H-pyrrole), 7.53 (1H, dd, J = 0.9 and 8.5 Hz, H-5'), 7.71 (1H, dd, J = 1.5 and 3.2 Hz, H-pyrrole), 7.80 (1H, app t, J = 8.5 Hz, H-4'), 12.98 (1H, s, NH-pyrrole); ^{19}F NMR (470 MHz; DMSO-d_6) δ_F -116.69; ^{13}C NMR (125 MHz; DMSO-d_6) δ_C 51.7 (CH$_3$), 114.6 (CH-pyrrole), 119.4 (d, J_{CF} = 18.1 Hz, C-3'), 124.8 (C-pyrrole), 124.9 (C-pyrrole), 126.8 (d, J_{CF} = 4.1 Hz, C-5'), 128.9 (d, J_{CF} =

22.7 Hz, C-1'), 129.1 (d, J_{CF} = 5.2 Hz, C-6'), 131.0 (C-pyrrole), 131.9 (C-4'), 153.8 (d, J_{CF} = 248.5 Hz, C-2'), 160.3 (CO_2Me), 182.5 (CO); MS (ES+) m/z 314.2 [M(^{35}Cl)+H]$^+$, 316.1 [M(^{37}Cl)+H]$^+$.

4-(3,6-Dichloro-2-fluorobenzoyl)-1*H*-pyrrole-2-carboxylic acid (337)
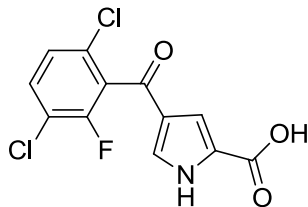
A solution of LiOH (26.6 g, 632 mmol, 20 eq.) in H_2O (140 mL) was added to ester **335** (10.0 g, 31.6 mmol, 1 eq.) in THF (180 mL) and heated to 65 °C for 48 h. After cooling to r.t., the mixture was acidified to pH 3 with HCl (1 M aq.) and extracted with EtOAc (2 × 300 mL). The combined organic layers were washed with water and brine, dried over MgSO$_4$, and the solvent removed *in vacuo* to give a white solid (9.0 g, 95%); R_f 0.25 (50/50/0.5 EtOAc/petrol/AcOH); m.p. 230-232 °C; λ_{max}(EtOH)/nm 289, 267; IR ν_{max}/cm^{-1} 3264br, 1697, 1646; ^{11}H NMR (500 MHz; DMSO-d_6) δ_H 7.07 (1H, app t, J = 1.6 Hz, H-pyrrole), 7.53 (1H, dd, J = 1.1 and 8.6 Hz, H-5'), 7.71 (1H, dd, J = 1.6 and 3.2 Hz, H-pyrrole), 7.80 (1H, app t, J = 8.6 Hz, H-4'), 12.81 (1H, br s, NH-pyrrole), 13.00 (1H, br s, CO$_2$H); ^{19}F NMR (470 MHz; DMSO-d_6) δ_F -116.71; ^{13}C NMR (125 MHz; DMSO-d_6) δ_C 114.1 (CH-pyrrole), 119.3 (d, J_{CF} = 18.1 Hz, C-3'), 124.8 (C-pyrrole), 126.1 (C-pyrrole), 126.8 (d, J_{CF} = 3.6 Hz, C-5'), 129.0 (d, J_{CF} = 23.3 Hz, C-1'), 129.1 (d, J_{CF} = 5.5 Hz, C-6'), 130.6 (C-pyrrole), 131.9 (C-4'), 153.8 (d, J_{CF} = 248.4 Hz, C-2'), 161.3 (CO$_2$H), 182.5 (CO); MS (ES+) m/z 302.1 [M(^{35}Cl)+H]$^+$, 304.1 [M(^{37}Cl)+H]$^+$.

4-(2-Chloro-6-fluorobenzoyl)-*N*-(1-isopropylpiperidin-4-yl)-1*H*-pyrrole-2-carboxamide (253)
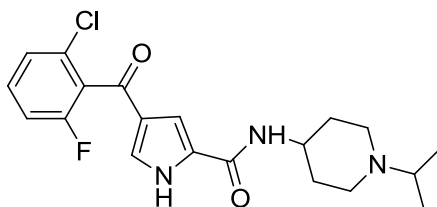
Prepared according to general procedure D using carboxylic acid **336** (100 mg, 0.37 mmol, 1 eq.), CDI (121 mg, 0.75 mmol, 2 eq.), Et$_3$N (57 μL, 0.41 mmol, 1.1 eq.) and 1-isopropylpiperidin-4-amine dihydrochloride (200 mg, 0.93 mmol, 2.5 eq.) in THF (2 mL). Purification by MPLC on aminopropyl SiO$_2$ with a gradient elution from 0-3%

MeOH/DCM to give a white solid (88 mg, 60%); R_f 0.8 (5% MeOH/DCM, NH$_2$ silica); m.p. 225 °C dec.; λ_{max}(EtOH)/nm 285, 236; IR ν_{max}/cm^{-1} 3347, 3122, 2966, 2865, 1617, 1570; ^{1}H NMR (500 MHz; DMSO-d_6) δ_H 0.99 (6H, d, J = 6.5 Hz, 2 × Me), 1.49 (2H, ddd, J = 3.6 Hz, 12.1 Hz, and 15.5 Hz, 2 × H-piperidine), 1.75-1.83 (2H, m, 2 × H-piperidine), 2.14-2.22 (2H, m, 2 × CH-N-piperidine), 2.72 (1H, sept, J = 6.5 Hz, CH(Me)$_2$), 2.77-2.84 (2H, m, 2 × CH-N-piperidine), 3.64-3.75 (1H, m, CO-NH-CH), 7.23 (1H, br s, H-3), 7.35 (1H, br s, H-5), 7.39-7.45 (1H, app t, J = 8.2 Hz, H-5'), 7.49 (1H, d, J = 8.2 Hz, H-3'), 7.60 (1H, td, J = 8.2 and 6.3 Hz, H-4'), 8.13 (1H, d, J = 8.0 Hz, CO-NH), 12.43 (1H, br s, NH-pyrrole); ^{19}F NMR (470 MHz; DMSO-d_6) δ_F -114.42; ^{13}C NMR (125 MHz; DMSO-d_6) δ_C 18.0 (2 × CH$_3$), 32.0 (2 × CH$_2$-piperidine), 47.2 (2 × CH$_2$-piperidine), 53.6 (CH(Me)$_2$), 109.9 (C-pyrrole), 114.9 (d, J_{CF} = 21.7 Hz, C-5'), 124.9 (C-pyrrole), 125.8 (d, J_{CF} = 3.2 Hz, C-3'), 128.2 (d, J_{CF} = 23.4 Hz, C-1'), 128.4 (C-pyrrole), 129.0 (C-pyrrole), 130.4 (d, J_{CF} = 6.1 Hz, C-2'), 131.7 (d, J_{CF} = 9.1 Hz, C-4'), 158.5 (d, J_{CF} = 248.8 Hz, C-6'), 159.0 (CO-NH), 183.9 (CO); MS (ES+) m/z 392.4 [M(^{35}Cl)+H]$^+$, 394.4 [M(^{37}Cl)+H]$^+$; HRMS calcd for C$_{20}$H$_{24}$^{35}Cl$_1$F$_1$N$_3$O$_2$ [M+H]$^+$ 392.1536, found 392.1540.

4-(2-Chloro-6-fluorobenzoyl)-N-(1-cyclopropylpiperidin-4-yl)-1H-pyrrole-2-carboxamide (254)
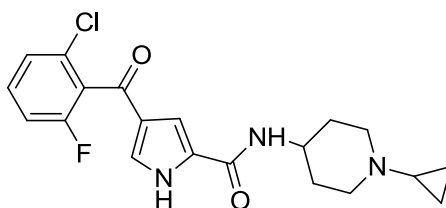
Prepared according to general procedure D using carboxylic acid **336** (95 mg, 0.36 mmol, 1 eq.), CDI (115 mg, 0.71 mmol, 2 eq.), 1-cyclopropylpiperidin-4-amine (125 mg, 0.81 mmol, 2.5 eq.) and THF (3 mL). Purification by MPLC on NH$_2$ SiO$_2$ with a gradient elution from 0-3% MeOH/CH$_2$Cl$_2$ gave a white solid (72 mg, 52%); R_f 0.25 (NH$_2$ SiO$_2$, 2% MeOH/CH$_2$Cl$_2$); m.p. 247-249 °C; λ_{max}(EtOH)/nm 284, 238; IR ν_{max}/cm^{-1} 3343, 3122, 2944, 1619, 1571; ^{1}H NMR (500 MHz; DMSO-d_6) δ_H 0.29-0.33 (2H, 2 × H-cyclopropyl), 0.41-0.46 (2H, 2 × H-cyclopropyl), 1.40-1.51 (2H, m, 2 × H-piperidine), 1.60-1.65 (1H, m, cyclopropyl-CH-N), 1.72-1.80 (2H, m, 2 × H-piperidine), 2.20-2.30 (2H, m, 2 × CH-N-piperidine), 2.92-3.00 (2H, m, 2 × CH-N-piperidine), 3.68-3.80 (1H, m, CH-NH-piperidine), 7.23 (1H, s, H-3), 7.34 (1H, s, H-5), 7.38-7.44 (1H, m, H-5'), 7.48 (1H, d, J = 8.0 Hz, H-3'), 7.60 (1H, td, J = 8.0 and 6.3 Hz, H-4'), 8.10 (1H, d, J = 7.9 Hz, CO-NH),

12.42 (1H, s, NH-pyrrole); ^{19}F NMR (470 MHz; DMSO-d_6) δ_F -114.42; ^{13}C NMR (125 MHz; DMSO-d_6) δ_C 5.9 (2 × CH$_2$-cPr), 31.5 (2 × CH$_2$-piperidine), 38.0 (CH-cPr), 46.6 (CH-NH-piperidine), 52.3 (2 × CH$_2$-N-piperidine), 109.9 (CH-pyrrole), 114.9 (d, J_{CF} = 21.3 Hz, C-5'), 124.9 (C-pyrrole), 125.8 (d, J_{CF} = 3.2 Hz, C-3'), 128.1 (C-pyrrole), 128.2 (d, J_{CF} = 23.2 Hz, C-1'), 128.9 (CH-pyrrole), 130.4 (d, J_{CF} = 6.1 Hz, C-2'), 131.7 (d, J_{CF} = 9.1 Hz, C-4'), 158.52 (d, J_{CF} = 247 Hz, C-6'), 159.02 (CO-NH), 183.87 (CO); MS (ES+) m/z 390.4 [M(^{35}Cl)+H]$^+$, 392.4 [M(^{37}Cl)+H]$^+$; HRMS calcd for C$_{20}$H$_{22}$^{35}Cl$_1$F$_1$N$_3$O$_2$ [M+H]$^+$ 390.1379, found 390.1379.

tert-Butyl 4-(4-(2-chloro-6-fluorobenzoyl)-1*H*-pyrrole-2-carboxamido) piperidine-1-carboxylate (258)
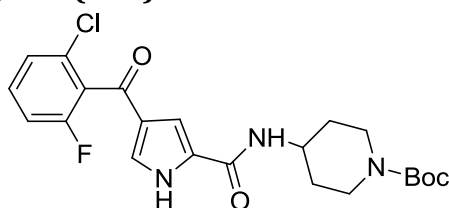
Prepared according to general procedure D using carboxylic acid **336** (500 mg, 1.87 mmol, 1 eq.), CDI (607 mg, 3.75 mmol, 2 eq.), *tert*-butyl-4-aminopiperidine-1-carboxylate (800 mg, 4.00 mmol, 2.15 eq.) and THF (10 mL). Purification by MPLC on SiO$_2$ with a gradient elution from 30-80% EtOAc/petrol gave a white solid (631 mg, 75%); R_f 0.4 (5% MeOH/DCM); m.p. 150-155 °C dec.; λ_{max}(EtOH)/nm 284, 238; IR ν_{max}/cm^{-1} 3188, 2971, 2864, 1689, 1619, 1569.6; ^{1}H NMR (500 MHz; DMSO-d_6) δ_H 1.30-1.47 (2H, m, 2 × H-piperidine), 1.44 (9H, s, *t*Bu), 1.79 (2H, dd, J = 3.2 and 12.5 Hz, 2 × H-piperidine), 2.87 (2H, br s, 2 × CH-N-piperidine), 3.89-4.02 (3H, m, 3 × C*H*-N-piperidine), 7.22 (1H, br s, H-3), 7.36 (1H, br s, H-5), 7.39-7.45 (1H, app t, J = 8.1 Hz, H-5'), 7.49 (1H, d, J = 8.1 Hz, H-3'), 7.60 (1H, td, J = 8.1 and 6.3 Hz, H-4'), 8.17 (1H, d, J = 7.9 Hz, CO-NH), 12.47 (1H, br s, NH-pyrrole); ^{19}F NMR (470 MHz; DMSO-d_6) δ_F -114.42; ^{13}C NMR (125 MHz; DMSO-d_6) δ_C 28.0 (C(*C*H$_3$)$_3$), 31.4 (2 × CH$_2$-piperidine), 45.9 (2 × CH$_2$-piperidine), 78.6 (*C*(CH$_3$)$_3$), 109.9 (CH-pyrrole), 114.9 (d, J_{CF} = 21.8 Hz, C-5'), 125.0 (C-pyrrole), 125.8 (d, J_{CF} = 3.1 Hz, C-3'), 128.1 (d, J_{CF} = 23.1 Hz, C-1'), 128.1 (C-pyrrole), 128.8 (CH-pyrrole), 130.4 (d, J_{CF} = 6.0 Hz, C-2'), 131.7 (d, J_{CF} = 9.0 Hz, C-4'), 153.9 (CO-NH), 158.3 (d, J_{CF} = 246 Hz, C-6'), 183.9 (CO); MS (ES-) m/z 448.4 [M(^{35}Cl)-H]$^-$, 450.4 [M(^{37}Cl)-H]$^-$; HRMS calcd for C$_{22}$H$_{24}$^{35}Cl$_1$F$_1$N$_3$O$_4$ [M+H]$^+$ 448.1445, found 448.1435.

4-(2-Chloro-6-fluorobenzoyl)-*N*-(piperidin-4-yl)-1*H*-pyrrole-2-carboxamide (251)
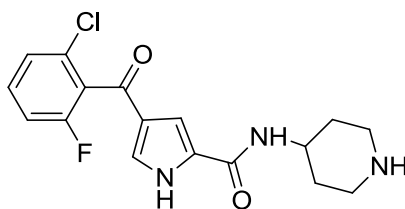
Prepared according to general procedure G using TFA (8 mL), CH$_2$Cl$_2$ (8 mL), Et$_3$SiH (533 μL, 3.34 mmol, 2.25 eq.) and carbamate **258** (600 mg, 1.33 mmol, 1 eq.) to give a white solid (460 mg, 99%); R_f 0.5 (10% MeOH/DCM, NH$_2$ silica); m.p. 160 °C dec.; λ$_{max}$(EtOH)/nm 282, 230; IR ν$_{max}$/cm^{-1} 2964 br, 1626, 1568; ^{1}H NMR (500 MHz; DMSO-*d$_6$*) δ$_H$ 1.59-1.71 (2H, m, 2 × H-piperidine), 1.91-1.99 (2H, m, 2 × H-piperidine), 2.93-3.04 (2H, m, 2 × C*H*-N-piperidine), 3.25-3.34 (2H, m, 2 × C*H*-N-piperidine), 3.96-4.07 (1H, m, CO-NH-C*H*), 7.28 (1H, br s, H-3), 7.36 (1H, br s, H-5), 7.39-7.45 (1H, app t, *J* = 8.1 Hz, H-5'), 7.49 (1H, d, *J* = 8.1 Hz, H-3'), 7.60 (1H, td, *J* = 8.1 and 6.3 Hz, H-4'), 8.00 (1H, br s, NH), 8.30 (1H, d, *J* = 7.6 Hz, CO-NH), 12.47 (1H, br s, NH-pyrrole); ^{19}F NMR (470 MHz; DMSO-*d$_6$*) δ$_F$ -114.44; ^{13}C NMR (125 MHz; DMSO-*d$_6$*) δ$_C$ 29.0 (C-piperidine), 42.7 (C-piperidine), 44.2 (C-piperidine), 110.0 (CH-pyrrole), 114.9 (d, *J*$_{CF}$ = 21.6 Hz, C-5'), 125.0 (C-pyrrole), 125.8 (d, *J*$_{CF}$ = 2.7 Hz, C-3'), 128.1 (C-1'), 128.4 (C-pyrrole), 128.6 (C-pyrrole), 130.4 (d, *J*$_{CF}$ = 6.4 Hz, C-2'), 131.7 (d, *J*$_{CF}$ = 9.3 Hz, C-4'), 159.2 (d, *J*$_{CF}$ = 247.5 Hz, C-6'), 158.9 (CO-NH), 183.85 (CO); MS (ES+) *m/z* 350.4 [M(^{35}Cl)+H]$^+$, 352.4 [M(^{37}Cl)+H]$^+$; HRMS calcd for C$_{17}$H$_{18}$^{35}Cl$_1$F$_1$O$_2$N$_3$ [M+H]$^+$ 350.1066, found 350.1072.

4-(2-Chloro-6-fluorobenzoyl)-*N*-(1-ethylpiperidin-4-yl)-1*H*-pyrrole-2-carboxamide (252)
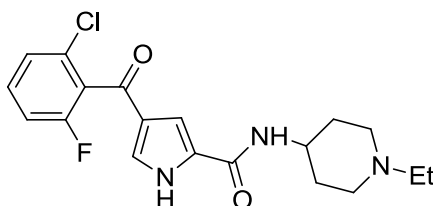
Amine **251** (120 mg, 0.34 mmol, 1 eq.), acetaladehyde (39 μL, 0.69 mmol, 2 eq.), acetic acid (39 μL, 0.69 mmol, 2 eq.) and MgSO$_4$ (150 mg) were combined in MeOH (3 mL) and stirred at r.t. for 1 h. Sodium cyanoborohydride (32 mg, 0.51 mmol, 1.5 eq) was added and the mixture was stirred at r.t. for 18 h. The reaction was quenched with water, basified with NaHCO$_3$ (10% aq.) and extracted with CH$_2$Cl$_2$ (2 × 15 mL). The organic layers were

combined, dried over MgSO$_4$, and the solvent removed *in vacuo*. The residue was purified by MPLC on SiO$_2$ with a gradient elution from 95/5/0/5 to 86/14/1.4 CH$_2$Cl$_2$/MeOH/NH$_4$OH to give a white solid (21 mg, 16%). R_f 0.15 (90/10/1 CH$_2$Cl$_2$/MeOH/NH$_4$OH); m.p. 258-260 °C dec.; λ_{max}(EtOH)/nm 287, 237; IR ν_{max}/cm^{-1} 3119, 2964, 2815, 1645, 1606, 1571; ^{1}H NMR (500 MHz; DMSO-d_6) δ_H 1.02 (3H, t, J = 7.1 Hz, N-CH$_2$C*H*$_3$), 1.52 (2H, app qd, J = 11.8 and 3.3Hz, 2 × H-piperidine), 1.74-1.81 (2H, m, 2 × H-piperidine), 1.90-1.97 (2H, m, 2 × CH-N-piperidine), 2.34 (2H, q, J = 7.1 Hz, N-C*H*$_2$CH$_3$), 2.85-2.92 (2H, m, 2 × CH-N-piperidine), 3.67-3.77 (1H, m, C*H*-NH-piperidine), 7.23 (br s, H-3), 7.35 (br s, H-5), 7.39-7.44 (1H, app t, J = 8.2 , H-5'), 7.49 (1H, d, J = 8.2 Hz, H-3'), 7.60 (1H, td, J = 8.2 and 6.3 Hz, H-4'), 8.14 (1H, d, J = 7.7 Hz, CO-NH), 12.43 (1H, s, NH pyrrole); ^{19}F NMR (470 MHz; DMSO-d_6) δ_F -114.42; ^{13}C NMR (125 MHz; DMSO-d_6) δ_C 12.3 (CH$_3$), 31.6 (2 × CH$_2$ piperidine), 46.6 (CH-NH-piperidine), 51.6 (2 × CH$_2$-N- piperidine), 51.9 (N-*C*H$_2$CH$_3$), 109.9 (CH-pyrrole), 114.9 (d, J_{CF} = 21.5 Hz, C-5'), 124.9 (C-pyrrole), 125.8 (d, J_{CF} = 2.8 Hz, C-3'), 128.1 (C-1'), 128.2 (C-pyrrole), 128.9 (CH-pyrrole), 130.4 (J_{CF} = 6.2 Hz, C-2'), 131.7 (J_{CF} = 9.1 Hz, C-4'), 158.5 (d, J_{CF} = 247 Hz, C-6'), 159.0 (CO-NH), 183.9 (CO); MS (ES+) *m/z* 378.4 [M(^{35}Cl)+H]$^+$, 380.4 [M(^{37}Cl)+H]$^+$; HRMS calcd for C$_{19}$H$_{22}$^{35}Cl$_1$F$_1$N$_3$O$_2$ [M+H]$^+$ 378.1379, found 378.1388.

N-(1-Acetylpiperidin-4-yl)-4-(2-chloro-6-fluorobenzoyl)-1*H*-pyrrole-2-carboxamide (255)
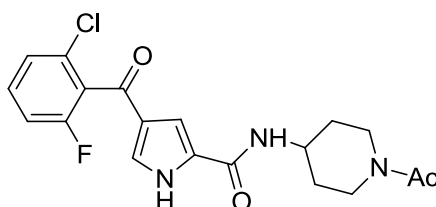
Acetyl chloride (17 μL, 0.24 mmol, 1.1 eq.) was added to amine **251** (75 mg, 0.21 mmol, 1 eq.) and Et$_3$N (36 μL, 0.26 mmol, 1.2 eq.) in DCM (2 mL) at r.t. and the mixture was stirred at r.t. for 30 min. Methanol was added and the solvent removed *in vacuo*. The residue was partitioned between EtOAc (2 × 20 mL) and H$_2$O (10 mL), washed with brine (10 mL), dried over MgSO$_4$, and the solvent removed *in vacuo*. The residue was purified by MPLC on SiO$_2$ with a gradient elution from 0-5% MeOH/DCM to give a white solid (40 mg, 48 %); R_f 0.2 (3% MeOH/EtOAc); m.p. 257-259 °C; λ_{max}(EtOH)/nm 281, 236; IR ν_{max}/cm^{-1} 3503, 3370, 1626, 1565; ^{1}H NMR (500 MHz; DMSO-d_6) δ_H 1.29-1.50 (2H, m, 2 × CH-piperidine), 1.77-1.90 (2H, m, 2 × CH-piperidine), 2.04 (3H, s, CH$_3$), 2.70 (1H, app

td, J = 12.5 and 2.5 Hz, CH-N-piperidine), 3.16 (1H, app td, J = 12.5 and 2.5Hz, CH-N-piperidine), 3.84 (1H, d, J = 13.6 Hz, CH-N-piperidine), 3.96-4.05 (1H, m, CH-NH-piperidine), 4.35 (1H, d, J = 13.6 Hz, CH-N-piperidine), 7.23 (1H, br s, H-3), 7.37 (1H, br s, H-5), 7.39-7.44 (1H, app t, J = 8.2 Hz, H-5'), 7.49 (1H, d, J = 8.2 Hz, H-3'), 7.60 (1H, td, J = 8.2 and 6.3 Hz, H-4'), 8.19 (1H, d, J = 8.1 Hz, CO-NH), 12.48 (1H, br s, NH-pyrrole); ^{19}F NMR (470 MHz; DMSO-d_6) δ_F -114.42; ^{13}C NMR (125 MHz; DMSO-d_6) δ_C 21.2 (Me), 31.9 (2 × CH$_2$-piperidine), 44.7 (2 × CH$_2$-piperidine), 46.0 (CH-NH-piperidine), 110.0 (C-pyrrole), 114.9 (d, J_{CF} = 21.8 Hz, C-5'), 125.0 (C-pyrrole), 125.8 (J_{CF} = 3.1 Hz, C-3'), 128.1 (d, J_{CF} = 23.2 Hz, C-1'), 128.2 (C-pyrrole) 128.8 (CH-pyrrole), 130.4 (d, J_{CF} = 5.9 Hz, C-2'), 131.7 (d, J_{CF} = 9.3 Hz, C-4'), 158.5 (d, J_{CF} = 246.9 Hz, C-6'), 159.0 (CO-NH), 168.0 (CO-N), 183.9 (CO); MS (ES+) m/z 392.4 [M(^{35}Cl)+H]$^+$, 394.4 [M(^{37}Cl)+H]$^+$; HRMS calcd for C$_{19}$H$_{20}$^{35}Cl$_1$F$_1$N$_3$O$_2$ [M+H]$^+$ 392.1172, found 392.1174.

4-(2-Chloro-6-fluorobenzoyl)-N-(1-(methylsulfonyl)piperidin-4-yl)-1H-pyrrole-2-carboxamide (256)
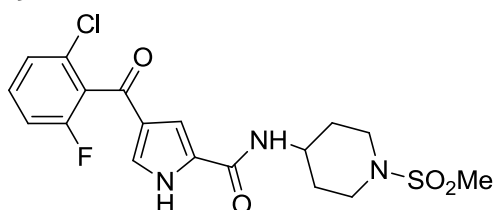
Amine **251** (100 mg, 0.29 mmol), methanesulfonyl chloride (24 µL, 0.32 mmol, 1.1 eq.) and triethylamine (48 µL, 0.34 mmol, 1.2 eq.) were combined in CH$_2$Cl$_2$ (1 mL) and stirred at r.t. for 1 h. Further methanesulfonyl chloride (20 µL, 0.27 mmol, 0.9 eq.) was added and the mixture was stirred for a further 30 min, quenched with water (5 mL) and extracted with CH$_2$Cl$_2$ (2 × 10 mL). The organic extracts were combined, washed with HCl (10 mL, 1 M aq.), dried over MgSO$_4$, and the solvent removed *in vacuo*. The residue was purified by MPLC on SiO$_2$ with a gradient elution from 40-100% EtOAc/petrol to give a white solid (33 mg, 27%). R_f 0.25 (EtOAc); m.p. 284-286 °C; λ_{max}(EtOH)/nm 285, 236; IR ν_{max}/cm^{-1} 3240, 3191, 1657, 1622, 1567, 1325 (SO), 1148 (SO); ^{1}H NMR (500 MHz; DMSO-d_6) δ_H 1.58 (1H, app qd, J = 11.7 and 4.1 Hz, 2 × H-piperidine), 1.87-1.96 (2H, m, 2 × H-piperidine), 2.84-2.95 (4H, m, 2 × CH-N-piperidine, and CH$_3$), 3.55-3.63 (2H, m, 2 × CH-N-piperidine), 3.85-3.95 (1H, m, CH-NH-piperidine), 7.23 (1H, br s, H-3), 7.38 (1H, br s, H-5), 7.42 (1H app t, J = 8.2 Hz, H-5'), 7.48 (1H, d, J = 8.2 Hz, H-3'), 7.60 (1H, td, J = 8.2 and 6.5 Hz, H-4'), 8.25 (1H, d, J = 8.2 Hz, CO-NH), 12.46 (1H, br s, NH-pyrrole);

^{19}F NMR (470 MHz; DMSO-d_6) δ_F -114.42; ^{13}C NMR (125 MHz; DMSO-d_6) δ_C 30.8 (2 × CH$_2$-piperidine), 34.2 (CH$_3$), 44.7 (2 × CH$_2$-N- piperidine), 45.4 (CH-NH-piperidine), 110.0 (CH-pyrrole), 114.9 (d, J_{CF} = 21.8 Hz, C-5'), 125.0 (C-pyrrole), 125.8 (d, J_{CF} = 3.3 Hz, C-3'), 128.1 (d, J_{CF} = 23.1 Hz, C-1'), 128.2 (C-pyrrole), 128.7 (C-pyrrole), 130.4 (J_{CF} = 6.1 Hz, C-2'), 131.7 (d, J_{CF} = 8.9 Hz, C-4'), 158.5 (d, J_{CF} = 246 Hz, C-6'), 159.1 (CO-NH), 183.9 (CO); MS (ES+) m/z 428.3 [M(^{35}Cl)+H]$^+$, 430.4 [M(^{37}Cl)+H]$^+$; HRMS calcd for C$_{18}$H$_{20}$^{35}Cl$_1$F$_1$N$_3$O$_4$S$_1$ [M+H]$^+$ 428.0842, found 428.0849.

4-(2-Chloro-6-fluorobenzoyl)-*N*-(1-(pyrimidin-2-yl)piperidin-4-yl)-1*H*-pyrrole-2-carboxamide (257)
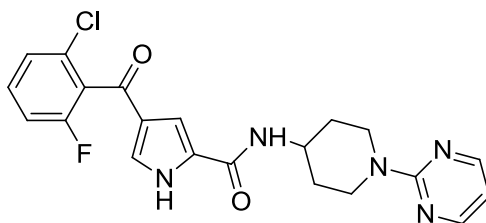
Amine **251** (70 mg, 0.20 mmol, 1 eq.), 2-chloropyrimidine (23 mg, 0.2 mmol, 1 eq.), Hunig's base (42 µL, 0.24 mmol, 1.2 eq.), and MeCN (1.5 mL) were combined and heated to 150 °C for 90 min under microwave irradiation. The mixture was partitioned between EtOAc (2 × 20 mL) and citric acid (10 mL, 10% aq.). The organic layers were washed with sodium carbonate (10 mL, 10% aq.), dried over MgSO$_4$ and the solvent removed *in vacuo*. The residue was purified by MPLC on SiO$_2$ with a gradient elution from 50-100% EtOAc/petrol to give a white solid (20 mg, 23%); R_f 0.5 (10% MeOH/CH$_2$Cl$_2$); m.p. 235-238 °C; λ_{max}(EtOH)/nm 287, 245; IR ν_{max}/cm^{-1} 3372, 3191, 3118, 2926, 2853, 1629, 1588, 1566; ^{1}H NMR (500 MHz; DMSO-d_6) δ_H 1.45 (2H, qd, J = 12.1 and 4.1 Hz, 2 × H-piperidine), 1.84-1.90 (2H, m, 2 × H-piperidine), 3.05 (2H, td, J = 12.1 and 2.4 Hz, 2 × H-N-piperidine), 4.05-4.15 (1H, m, CH-NH-piperidine), 4.63-4.69 (2H, m, 2 × CH-N-piperidine), 6.64 (1H, t, J = 4.7 Hz, H-pyrimidine), 7.20 (1H, br s, H-3), 7.35 (1H, br s, H-5), 7.40 (1H, dd, J = 1.0 and 8.4 Hz, H-Ar), 7.48 (1H, d, J = 8.4 Hz, H-Ar), 7.59 (1H, td, J = 8.4 and 6.3 Hz, H-4'), 8.16 (1H, d, J = 7.9 Hz, CONH), 8.40 (2H, d, J = 4.7 Hz, 2 × H-pyrimidine), 12.47 (1H, br s, NH-pyrrole); ^{19}F NMR (470 MHz; DMSO-d_6) δ_F -114.42; ^{13}C NMR (125 MHz; DMSO-d_6) δ_C 31.1 (2 × CH-piperidine), 42.6 (2 × CH-N-piperidine), 46.3 (CH-NH-piperidine), 109.0 (C-pyrimidine), 109.8 (CH-pyrrole), 114.9 (d, J_{CF} = 21.8 Hz, C-5'), 125.0 (C-pyrrole), 125.8 (d, J_{CF} = 2.8 Hz, C-3'), 128.1 (d, J_{CF} = 23.2 Hz, C-1'), 128.3 (C-pyrrole), 128.9 (CH-pyrrole), 130.4 (d, J_{CF} = 6.3 Hz, C-2'), 131.7 (d, J_{CF} = 9.1

Hz, C-4'), 158.0 (2 × CH-pyrimidine), 158.5 (d, J_{CF} = 246 Hz, C-6'), 159.0 (C-pyrimidine), 161.7 (CO-NH), 183.9 (CO); MS (ES+) m/z 428.4 [M(^{35}Cl)+H]$^+$, 430.4 [M(^{37}Cl)+H]$^+$; HRMS calcd for $C_{21}H_{20}{}^{35}Cl_1F_1N_5O_2$ [M+H]$^+$ 428.1284, found 428.1290.

tert-Butyl 4-(4-(3,6-dichloro-2-fluorobenzoyl)-1*H*-pyrrole-2-carboxamido) piperidine-1-carboxylate (263)
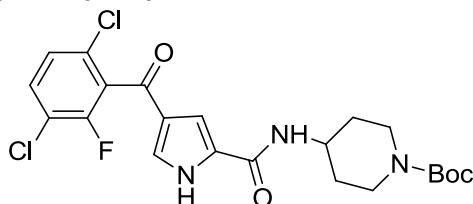
Prepared according to general procedure D using carboxylic acid **337** (350 mg, 1.16 mmol, 1 eq.), CDI (375 mg, 2.31 mmol, 2 eq.), 1-Boc-4-aminopiperidine (578 mg, 2.89 mmol, 2.5 eq) and THF (6 mL). Purification by MPLC on SiO_2 with a gradient elution from 0-5% $MeOH/CH_2Cl_2$ gave a white solid (440 mg, 79%); R_f 0.4 (2% $MeOH/CH_2Cl_2$); m.p. 221-223 °C; λ_{max}(EtOH)/nm 285, 236; IR ν $_{max}$/cm^{-1} 3367, 3179, 1698, 1625, 1569; ^{1}H NMR (500 MHz; DMSO-d_6) δ_H 1.33-1.47 (11H, m, C(CH$_3$)$_3$ and 2 × H-piperidine), 1.80 (2H, dd, J = 3.0 and 12.8 Hz, 2 × H-piperidine), 2.87 (2H, br s, 2 × CH-N-piperidine), 3.89-4.01 (2H, m, 2 × CH-N-piperidine and C*H*-NH-piperidine), 7.25 (1H, br s, H-pyrrole), 7.51 (1H, br s, H-pyrrole), 7.54 (1H, dd, J = 1.1 and 8.6 Hz, H-5'), 7.80 (1H, app t, J = 8.6 Hz, H-4'), 8.15 (1H, d, J = 8.0 Hz, CO-NH), 12.53 (1H, s, NH-pyrrole); ^{19}F NMR (470 MHz; DMSO-d_6) δ_F -116.77; ^{13}C NMR (125 MHz; DMSO-d_6) δ_C 28.1 (C(*C*H$_3$)$_3$), 31.4 (2 × CH$_2$-piperidine), 45.9 (CH-NH-piperidine), 78.6 (*C*(CH$_3$)$_3$), 109.8 (C-3-pyrrole), 119.3 (d, J = 18.1 Hz, C-3'), 124.5 (C-2 pyrrole), 126.8 (d, J_{CF} = 3.8 Hz, C-5'), 128.7 (C-pyrrole), 129.0 (C-H pyrrole), 129.2 (d, J_{CF} = 3.4 Hz, C-6'), 129.3 (d, J_{CF} = 21.6 Hz, C-1'), 131.7 (C-4'), 153.8 (d, J_{CF} = 248.4 Hz, C-2'), 153.9 (CO-carbamate), 158.9 (CO-NH), 182.5 (CO); MS (ES-) m/z 482.2 [M(^{35,35}Cl)+H]$^+$, 484.2 [M(^{35,37}Cl)+H]$^+$; HRMS calcd for $C_{22}H_{28}{}^{35}Cl_2F_1N_4O_4$ [M+NH$_4$]$^+$ 501.1466, found 501.1456.

4-(3,6-Dichloro-2-fluorobenzoyl)-*N*-(piperidin-4-yl)-1*H*-pyrrole-2-carboxamide (260)
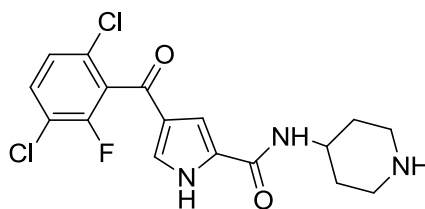
Prepared according to general procedure G using carbamate **263** (415 mg, 0.86 mmol, 1 eq.), Et$_3$SiH (342 µL, 2.14 mmol, 2.5 eq.) and CH$_2$Cl$_2$ (5 mL). Purification by MPLC on NH$_2$ SiO$_2$ with gradient elution from 0-10% MeOH/CH$_2$Cl$_2$ gave a white solid (247 mg, 75%); R_f 0.3 (5% MeOH:CH$_2$Cl$_2$; NH$_2$ SiO$_2$); m.p. 225-230 °C; λ_{max}(EtOH)/nm 286, 236; IR ν_{max}/cm^{-1} 3279, 2945, 1623, 1563; ^{1}H NMR (500 MHz; DMSO-d_6) δ_H 1.39 (2H, dq, J = 3.8 and 12.0 Hz, 2 × H-piperidine), 1.74 (2H, dd, J = 2.5 and 12.0 Hz, 2 × H-piperidine), 2.51 (2H, dd, J = 2.5 and 12.0 Hz, 2 × CH-piperidine), 2.94-3.01 (2H, m, 2 × H-piperidine), 3.75-3.85 (1H, m, C*H*-NH-CO), 4.13 (1H, br s, NH), 7.27 (1H, br s, H-pyrrole), 7.49 (1H, br s, H-pyrrole), 7.54 (1H, dd, J = 1.2 and 8.6 Hz, H-5'), 7.80 (1H, app t, J = 8.6 Hz, H-4'), 8.12 (1H, d, J = 8.0 Hz, CO-NH); ^{19}F NMR (470 MHz; DMSO-d_6) δ_F -116.76; ^{13}C NMR (125 MHz; DMSO-d_6) δ_C 33.0 (2 × CH$_2$-piperidine), 45.2 (2 × CH$_2$-N-piperidine), 46.8 (*C*H-NH-CO), 109.8 (CH-pyrrole), 119.9 (d, J_{CF} = 17.9 Hz, C-3'), 124.5 (C-pyrrole), 126.8 (d, J_{CF} = 4.1 Hz, C-5'), 129.0 (CH-pyrrole), 129.2 (d, J_{CF} = 5.7 Hz, C-6'), 129.3 (d, J_{CF} = 22.9 Hz, C-1'), 129.4 (C-pyrrole), 131.7 (C-4'), 153.8 (d, J_{CF} = 248 Hz, C-2'), 158.8 (CO-NH), 182.5 (CO); MS (ES-) *m/z* 382.1 [M(^{35,35}Cl)+H]$^+$, 383.8 [M(^{35,37}Cl)+H]$^+$; HRMS calcd for C$_{17}$H$_{17}$^{35}Cl$_2$F$_1$N$_3$O$_2$ [M+H]$^+$ 384.0676, found 384.0681.

4-(3,6-Dichloro-2-fluorobenzoyl)-*N*-(1-(methylsulfonyl) piperidin-4-yl)-1*H*-pyrrole-2-carboxamide (262)
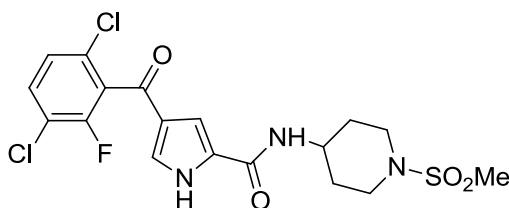
Amine **260** (80 mg, 0.21 mmol, 1 eq.), methanesulfonyl chloride (24 µL, 0.31 mmol, 1.5 eq.) and Et$_3$N (43 µL, 0.31 mmol, 1.5 eq) were combined in CH$_2$Cl$_2$ (2 mL) and stirred at r.t. for 30 min. Further Et$_3$N (1 eq) and methanesulfonyl chloride (1 eq.) were added and the mixture was stirred at r.t. for 1 h, quenched with ethanol, and partitioned between CH$_2$Cl$_2$ (3 × 20 mL) and water (10 mL). The organic extracts were combined, washed with

brine (10 mL), dried over MgSO$_4$ and the solvent removed *in vacuo*. The residue was purified by MPLC on NH$_2$ SiO$_2$ with a gradient elution from 50-100% EtOAc:petrol to give a white solid (34 mg, 35%); R_f 0.25 (NH$_2$ SiO$_2$, 2% MeOH/CH$_2$Cl$_2$); m.p. 298 °C dec.; λ_{max}(EtOH)/nm 288, 234; IR ν_{max}/cm^{-1} 3354, 3223, 1660, 1630, 1562, 1325, 1156; ^{1}H NMR (500 MHz; DMSO-d_6) δ_H 1.58 (2H, app qd, J = 3.5 and 12.5 Hz, 2 × H-piperidine), 1.92 (2H, app dd, J = 2.8 and 12.5 Hz, 2 × H-piperidine), 2.88 (2H, dd, J = 2.2 and 12.5 Hz, 2 × CH-*N*-piperidine), 2.92 (3H, s, CH$_3$), 3.56-3.63 (2H, m, 2 × CH-N-piperidine), 3.86-3.96 (1H, m, C*H*-NH-piperidine), 7.27 (1H, s, H-pyrrole), 7.52 (1H, s, H-pyrrole), 7.54 (1H, dd, J = 1.1 and 8.6 Hz, H-5'), 7.81 (1H, app t, J = 8.6 Hz, H-4'), 8.23 (1H, d, J = 7.7 Hz, CO-NH), 12.55 (1H, s, NH-pyrrole); ^{19}F NMR (470 MHz; DMSO-d_6) δ_F -116.76; ^{13}C NMR (125 MHz; DMSO-d_6) δ_C 30.9 (2 × CH$_2$-piperidine), 34.3 (CH$_3$), 44.6 (2 × CH$_2$-N-piperidine), 45.4 (C*H*-NH-piperidine), 109.9 (CH-pyrrole), 119.3 (d, J_{CF} = 18.1 Hz, C-3'), 124.5 (C-pyrrole), 126.8 (d, J_{CF} = 3.7 Hz, C-5'), 129.0 (C-6'), 129.1 (CH-pyrrole), 129.2 (C-pyrrole), 129.3 (d, J_{CF} = 18.9 Hz, C-1'), 131.8 (C-4'), 153.8 (d, J_{CF} = 248.4 Hz, C-2'), 159.1 (CO-NH), 182.6 (CO); MS (ES-) *m/z* 460.2 [M(^{35,35}Cl)+H]$^+$, 462.2 [M(^{35,37}Cl)+H]$^+$; HRMS calcd for C$_{18}$H$_{19}$^{35}Cl$_2$F$_1$N$_3$O$_4$S [M+H]$^+$ 462.0452, found 462.0448.

N-(1-Acetylpiperidin-4-yl)-4-(3,6-dichloro-2-fluorobenzoyl)-1*H*-pyrrole-2-carboxamide (261)
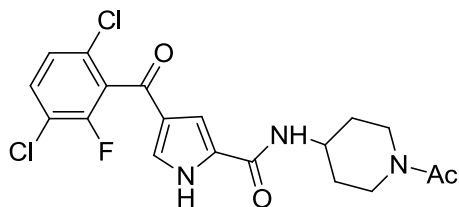
Amine **260** (75 mg, 0.2 mmol, 1 eq), acetyl chloride (15 μL, 0.22 mmol, 1.1 eq.) and Et$_3$N (33 μL, 0.24 mmol, 1.2 eq) were combined in CH$_2$Cl$_2$ (2 mL), and stirred at r.t. for 1 h. Further Et$_3$N (0.5 eq) and methanesulfonyl chloride (0.5 eq.) were added and the mixture was stirred at r.t. for 1 h, quenched with methanol, and partitioned between CH$_2$Cl$_2$ (20 mL) and HCl (10 mL, 0.5 M aq.). The organic extract was washed with brine (10 mL), dried over MgSO$_4$ and the solvent removed *in vacuo*. The residue was purified by MPLC on NH$_2$ SiO$_2$ with a gradient elution from 1-3% MeOH:CH$_2$Cl$_2$ to give a white solid (43 mg, 52%); R_f 0.7 (NH$_2$ SiO$_2$, 5% MeOH/CH$_2$Cl$_2$); m.p. 253-255 °C; λ_{max}(EtOH)/nm 281, 236; IR ν_{max}/cm^{-1} 3179, 1677, 1624, 1571; ^{1}H NMR (500 MHz; DMSO-d_6) δ_H 1.30-1.50

(2H, m, 2 × H-piperidine), 1.77-1.90 (2H, m, 2 × H-piperidine), 2.04 (3H, s, CH$_3$), 2.71 (1H, app td, J = 12.5 and 2.5 Hz, CH-N-piperidine), 3.12-3.20 (1H, m, CH-N-piperidine), 3.81-3.88 (1H, m, CH-N-piperidine), 3.96-4.06 (1H, m, CH-NH-piperidine), 4.31-4.39 (1H, m, CH-N-piperidine), 7.26 (1H, s, H-pyrrole), 7.51 (1H, s, H-pyrrole), 7.54 (1H, dd, J = 1.2 and 8.6 Hz, H-5'), 7.80 (1H, app t, J = 8.6 Hz, H-4'), 8.17 (1H, d, J = 7.9 Hz, CO-NH), 12.54 (1H, s, NH-pyrrole); ^{19}F NMR (470 MHz; DMSO-d_6) δ_F -116.76; ^{13}C NMR (125 MHz; DMSO-d_6) δ_C 21.2 (CH$_3$), 31.2 (C-piperidine), 32.0 (C-piperidine), 39.8 (C-piperidine), 44.7 (C-piperidine), 46.0 (C-piperidine), 109.9 (CH-pyrrole), 119.3 (d, J_{CF} = 18.0 Hz, C-3'), 124.5 (C-pyrrole), 128.8 (d, J_{CF}= 3.6 Hz, C-5'), 129.0 (CH-pyrrole), 129.2 (C-pyrrole), 129.2 (d, J_{CF} = 5.0 Hz, C-6'), 129.3 (d, J_{CF} = 20.0 Hz, C-1'), 131.7 (C-4'), 153.8 (d, J_{CF} = 248.4 Hz, C-2'), 159.0 (CO-NH), 168.0 (CO-N), 182.5 (CO); MS (ES-) m/z 424.3 [M(^{35,35}Cl)+H]$^+$, 426.2 [M(^{35,37}Cl)+H]$^+$; HRMS calcd for C$_{19}$H$_{19}$^{35}Cl$_2$F$_1$N$_3$O$_3$ [M+H]$^+$ 426.0782, found 426.0773.

4-(3,6-Dichloro-2-fluorobenzoyl)-*N*-(1-(2,2,2-trifluoroacetyl) piperidin-4-yl)-1*H*-pyrrole-2-carboxamide (269)
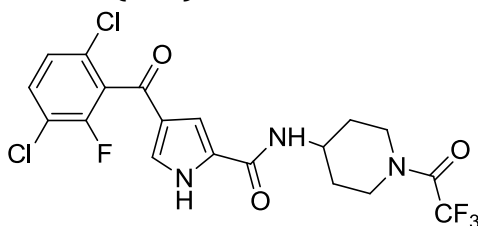
Trifluoroacetic anhydride (28 μL, 0.3 mmol, 1.5 eq.) was added to a solution of amine **260** (76 mg, 0.2 mmol, 1 eq.), and Et$_3$N (31 μL, 0.24 mol, 1.2 eq.) in CH$_2$Cl$_2$ (2 mL) and dioxane (2 mL) at 0 °C. The mixture was stirred at r.t. for 2 h, before further trifluoroacetic anhydride (54 μL, 0.6 mmol, 3 eq) and Et$_3$N (52 μL, 0.6 mmol, 2 eq.) were added. After stirring for 1 h at r.t. the reaction was partitioned between EtOAc (2 × 20 mL) and water (10 mL), the organic layers combined, washed with brine, dried over MgSO$_4$ and the solvent removed *in vacuo*. The residue was purified by MPLC on SiO$_2$ with gradient elution from 25-80% EtOAc/petrol to give a white solid (39 mg, 41%); R_f 0.1 (40% EtOAc/petrol); m.p. 200 °C dec.; λ$_{max}$(EtOH)/nm 285, 228; IR ν $_{max}$/cm^{-1} 3357, 3165, 1690, 1626, 1568; ^{1}H NMR (500 MHz; DMSO-d_6) δ_H 1.43-1.58 (2H, m, 2 × H-piperidine), 1.92-2.03 (2H, m, 2 × H-piperidine), 3.08-3.16 (1H, m, H-piperidine), 3.40-3.48 (1H, m, H-piperidine), 3.86-3.94 (1H, m, H-piperidine), 4.09-4.19 (1H, m, H-piperidine), 4.25-4.33 (1H, m, H-piperidine), 7.25 (1H, s, H-pyrrole), 7.50-7.57 (2H, m, H-pyrrole and H-5'),

7.81 (1H, app t, J = 8.4 Hz, H-4'), 8.21 (1H, d, J = 7.9 Hz, CO-NH), 12.57 (1H, s, NH-pyrrole); ^{19}F NMR (470 MHz; DMSO-d_6) δ_F -68.16, -116.77; ^{13}C NMR (125 MHz; DMSO-d_6) δ_C 30.9 (C-piperidine), 31.8 (C-piperidine), 42.2 (C-piperidine), 44.2 (C-piperidine), 45.2 (C-piperidine), 110.0 (CH-pyrrole), 116.4 (q, J_{CF} = 284.4 Hz, CF$_3$), 119.4 (d, J_{CF} = 18.4 Hz, C-3'), 124.5 (C-pyrrole), 126.8 (d, J_{CF} = 3.7 Hz, C-5'), 128.9 (CH-pyrrole), 129.1 (C-pyrrole), 129.2 (d, J_{CF} = 5.0 Hz, C-6'), 129.3 (d, J_{CF} = 23.3 Hz, C-1'), 131.8 (C-4'), 15378 (d, J_{CF} = 248.6 Hz, C-2'), 154.0 (q, J_{CF} = 35.0 Hz, COCF$_3$), 159.0 (CO-NH), 182.6 (CO); HRMS calcd for C$_{19}$H$_{19}$^{35}Cl$_2$F$_4$N$_4$O$_3$ [M+NH$_4$]$^+$ 497.0765, found 497.0758.

5-Nitro-2-(pyrrolidin-1-yl)pyrimidine (339)[350]
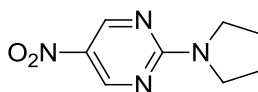
Prepared according to general procedure I using pyrrolidine (115 µL, 1.38 mmol, 1.1 eq.), 2-chloro-4-nitropyrimidine (200 mg, 1.25 mmol, 1 eq.), Et$_3$N (192 µL, 1.38 mmol, 1.1 eq.) and THF (10 mL) with stirring for 18 h to give a yellow solid (195 mg, 80%); R_f 0.65 (5% MeOH/DCM); m.p. 203 °C dec.; λ_{max}(EtOH)/nm 346; IR ν $_{max}$/cm^{-1} 2982, 2958, 2881, 1589, 1458, 1315; ^{1}H NMR (500 MHz; DMSO-d_6) δ_H 1.98-2.04 (4H, m, 2 × CH$_2$-pyrrolidine), 3.63-3.68 (4H, m, 2 × CH$_2$-N-pyrrolidine), 9.15 (2H, s, 2 × H-pyrimidine); ^{13}C NMR (125 MHz; DMSO-d_6) δ_C 24.8 (2 × CH$_2$-pyrrolidine), 47.5 (2 × CH$_2$-N-pyrrolidine), 133.1 (C-NO$_2$), 154.9 (2 × CH-N-pyrimidine), 159.5 (C-NR$_2$-pyrimidine); MS (ES+) m/z 195.3 [M+H]$^+$.

2-(Pyrrolidin-1-yl)pyrimidin-5-amine (340) [350]
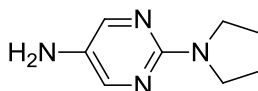
Prepared according to general procedure H using nitropyrimidine **339** (185 mg, 0.95 mmol) and MeOH (5 mL) to give a yellow solid (156 mg, 100%); R_f 0.25 (5% MeOH/DCM); m.p. 140-144 °C; λ_{max}(EtOH)/nm 255; IR ν $_{max}$/ cm^{-1} 3347, 3173, 2967, 2920, 2857, 1640, 1606; ^{1}H NMR (500 MHz; DMSO-d_6) δ_H 1.87-1.96 (4H, m, 2 × CH$_2$-pyrrolidine), 3.35-3.43 (4H, m, 2 × CH$_2$-N-pyrrolidine), 4.45 (2H br s, NH$_2$), 7.87 (2H, s, 2 × H-pyrimidine); ^{13}C NMR (125 MHz; DMSO-d_6) δ_C 25.1 (2 × CH$_2$-pyrrolidine), 46.7 (2 × CH$_2$-N-pyrrolidine), 133.0 (C-NH$_2$), 144.6 (2 × CH-pyrimidine), 155.1 (C-N-pyrimidine);

MS (ES+) m/z 165.2 [M+H]$^+$; HRMS calcd for $C_8H_{12}N_4$ [M+H]$^+$ 165.1135, found 165.1130.

4-(2-Chloro-6-fluorobenzoyl)-*N*-(2-(pyrrolidin-1-yl)pyrimidin-5-yl)-1*H*-pyrrole-2-carboxamide (274)
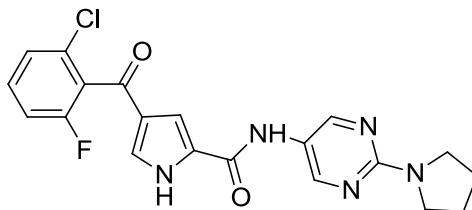
Prepared according to general procedure E using cyanuric fluoride (10 μL, 0.11 mmol, 0.7 eq.), carboxylic acid **336** (46 mg, 0.17 mmol, 1 eq.), amine **340** (70 mg, 0.43 mmol, 2.5 eq.), pyridine (14 μL, 0.17 mmol, 1 eq.), and THF (1 mL). Purification by MPLC on NH$_2$ silica with a gradient elution from 0-3% MeOH/CH$_2$Cl$_2$ gave a pale yellow solid (30 mg, 42%); R_f 0.35 (5% MeOH/CH$_2$Cl$_2$); m.p. 243-246 °C; λ_{max}(EtOH)/nm 290, 233; IR ν_{max}/cm^{-1} 3199, 2970, 2867, 1632, 1608, 1571; ^{1}H NMR (500 MHz; DMSO-d_6) δ_H 2.52-2.56 (4H, m, 2 × CH$_2$-pyrrolidine), 3.48-3.53 (4H, m, 2 × CH$_2$-N-pyrrolidine), 7.37-7.44 (2H, m, CH-pyrrole and H-Ar), 7.47-7.53 (2H, m, CH-pyrrole and H-Ar), 7.58-7.65 (1H, td, J = 8.2 and 6.3 Hz, H-4'), 8.59 (2H, s, 2 × H-pyrimidine), 10.01 (1H, br s, CO-NH), 12.69 (1H, br s, NH-pyrrole); ^{19}F NMR (470 MHz; DMSO-d_6) δ_F -114.35; ^{13}C NMR (125 MHz; DMSO-d_6) δ_C 25.0 (2 × CH$_2$-pyrrolidine), 46.5 (2 × CH$_2$-N-pyrrolidine), 111.0 (CH-pyrrole), 115.0 (d, J = 21.8 Hz, C-5'), 125.2 (C-pyrrole), 125.8 (d, J_{CF} = 2.6 Hz, C-3'), 128.1 (d, J_{CF} = 23.2 Hz, C-1'), 128.2 (C-pyrrole), 128.8 (CH-pyrrole), 130.4 (d, $J_{CF}$ = 5.9 Hz, C-2'), 131.8 (d, J_{CF} = 9.5 Hz, C-4'), 151.4 (2 × CH-pyrimidine), 157.4 (C-pyrimidine), 158.4 (CO-NH), 158.5 (d, J_{CF} = 247 Hz, C-6'), 183.9 (CO); MS (ES+) m/z 414.4 [M(^{35}Cl)+H]$^+$, 416.4 [M(^{37}Cl)+H]$^+$; HRMS calcd for $C_{20}H_{18}{}^{35}Cl_1F_1N_5O_2$ [M+H]$^+$ 414.1128, found 414.1132.

N-Methyl-5-nitropyrimidin-2-amine (341)
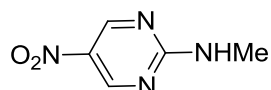
Prepared according to general procedure I using 2-chloro-5-nitropyrimidine (300 mg, 1.9 mmol, 1 eq.), methylamine hydrochloride (141 mg, 2.1 mmol, 1.1 eq.) and Et$_3$N (576 μL, 4.2 mmol, 2.2 eq) in THF (2 mL) to give a yellow solid (160 mg, 55%); R_f 0.3 (NH$_2$ SiO$_2$,

30% EtOAc/petrol); m.p. 130 °C dec.; λ_{max}(EtOH)/nm 336, 212; IR ν_{max}/cm^{-1} 3264, 1558, 1323; ^{1}H NMR (500 MHz; DMSO-d_6) δ_H 2.96 (3H, d, J = 4.9 Hz, CH$_3$), 8.75 (1H, br s, NH), 9.06 (1H, d, J = 3.3 Hz, H-pyrimidine), 9.15 (1H, d, J = 3.3 Hz, H-pyrimidine); ^{13}C NMR (125 MHz; DMSO-d_6) δ_C 28.3 (CH$_3$), 133.6 (C-5), 155.0 (C-4), 155.4 (C-6), 163.1 (C-2); MS (ES+) m/z 155.2 [M+H]$^+$. HRMS - no mass ion

N^2-Methylpyrimidine-2,5-diamine (351)
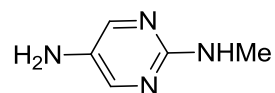
Prepared according to general procedure H using nitropyrimidine **341** (160 mg, 1.04 mmol) in MeOH (30 mL) and EtOAc (30 mL) for 3 h to give a yellow gum (128 mg, 100%); R_f 0.5 (NH$_2$ SiO$_2$, 70% EtOAc/petrol); λ_{max}(EtOH)/nm 250; IR ν_{max}/cm^{-1} 3271 (br), 1517; ^{1}H NMR (500 MHz; DMSO-d_6) δ_H 2.73 (3H, d, J = 4.7 Hz, CH$_3$), 4.41 (2H, s, NH$_2$), 6.13 (1H, q, J = 4.7 Hz, NHMe), 7.84 (2H, s, 2 × H-pyrimidine); ^{13}C NMR (125 MHz; DMSO-d_6) δ_C 28.5 (CH$_3$), 133.4 (C-5), 144.6 (C-4 and C-6), 157.2 (C-2); HRMS calc for C$_5$H$_9$N$_4$ [M+H]$^+$ 125.0822, found 125.0810.

4-(2-Chloro-6-fluorobenzoyl)-N-(2-(methylamino)pyrimidin-5-yl)-1H-pyrrole-2-carboxamide (272)
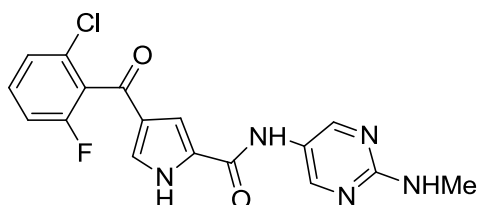
Prepared according to general procedure E using amine **351** (190 mg, 1.4 mmol, 2.5 eq.), carboxylic acid **336** (151 mg, 0.57 mmol, 1 eq.), cyanuric fluoride (34 μL, 0.40 mmol, 0.7 eq.), pyridine (46 μL, 0.57 mmol, 1 eq.) and MeCN (3 mL). Purification by MPLC on NH$_2$ SiO$_2$ with a gradient elution from 0-4% MeOH/EtOAc gave a yellow solid (43 mg, 35 %); R_f 0.55 (NH$_2$ SiO$_2$, 5% MeOH/EtOAc); m.p. 310-312 °C; λ_{max}(EtOH)/nm 285, 232; IR ν_{max}/cm^{-1} 3233, 1651, 1607; ^{1}H NMR (500 MHz; DMSO-d_6) δ_H 2.83 (3H, d, J = 4.8 Hz, Me), 7.04 (1H, q, J = 4.8 Hz, NHMe), 7.39 (1H, s, H-pyrrole), 7.43 (1H, app t, J = 8.3 Hz, H-5'), 7.48 (1H, s, H-pyrrole), 7.50, (1H, d, J = 8.3 Hz, H-3'), 7.62 (1H, qd, J = 6.2 and 8.3 Hz, H-4'), 8.53 (2H, s, 2 × H-pyrimidine), 9.98 (1H, s, CO-NH), 12.68 (1H, s, NH-pyrrole); ^{19}F NMR (470 MHz; DMSO-d_6) δ_F -114.35; ^{13}C NMR (125 MHz; DMSO-d_6) δ_C

28.1 (CH$_3$), 111.0 (CH-pyrrole), 115.0 (d, J_{CF} = 21.7 Hz, C-5'), 123.2 (C-pyrimidine), 125.2 (C-pyrrole), 125.8 (d, J_{CF} = 3.1 Hz, C-3'), 128.1 (d, J_{CF} = 23.2 Hz, C-1'), 128.2 (C-pyrrole), 128.9 (C-pyrrole), 130.4 (d, J_{CF} = 6.4 Hz, C-2'), 131.8 (d, J_{CF} = 9.1 Hz, C-4'), 151.5 (C-pyrimidine), 158.4 (CONH), 158.6 (d, J_{CF} = 247.0 Hz, C-6'), 160.0 (C-pyrimidine), 183.9 (CO); LCMS (ES-) m/z 374.3 [M(^{35,35}Cl)+H]$^+$, 376.3 [M(^{35,37}Cl)+H]$^+$; HRMS calc for C$_{17}$H$_{13}$^{35}Cl$_1$F$_1$N$_5$O$_2$ [M+H]$^+$ 374.0815, found 374.0812.

N,N-Dimethyl-5-nitropyrimidin-2-amine (342)[351]
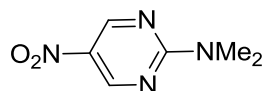
Prepared according to general procedure I using 2-chloro-5-nitropyrimidine (300 mg, 1.9 mmol, 1 eq.), Me$_2$NH (1.4 mL, 2.8 mmol, 1.5 eq., 2.0 M in THF) and Et$_3$N (288 µL, 2.1 mmol, 1.1 eq) in THF (8 mL) to give a yellow solid (275 mg, 87%); R_f 0.75 (NH$_2$ SiO$_2$, 30% EtOAc/petrol); m.p. 209-212 °C (lit.[351] 222 °C); λ_{max}(EtOH)/nm 341, 219; IR ν_{max}/cm^{-1} 1547, 1301; ^{1}H NMR (500 MHz; DMSO-d_6) δ_H 3.31 (6H, s, NMe$_2$), 9.15 (2H, s, 2 × H-pyrimidine); ^{13}C NMR (125 MHz; DMSO-d_6) δ_C 37.4 (NMe$_2$), 133.4 (C-5-pyrimidine), 154.8 (2H, s, 2 × CH-pyrimidine), 161.6 (C-2-pyrimidine); HRMS calcd for C$_6$H$_9$N$_4$O$_2$ [M+H]$^+$ 169.0720, found 169.0720.

N^2,N^2-Dimethylpyrimidine-2,5-diamine (352)[352]
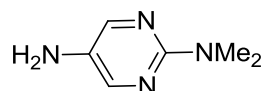
Prepared according to general procedure H using nitropyrimidine **342** (263 mg, 1.60 mmol) in MeOH (60 mL) and EtOAc (60 mL) for 4 h to give a yellow solid (215 mg, 100%); R_f 0.8 (NH$_2$ SiO$_2$, EtOAc); m.p. 68-72 °C (lit.[353] 80-84 °C); λ_{max}(EtOH)/nm 261; IR ν_{max}/cm^{-1} 3206; ^{1}H NMR (500 MHz; DMSO-d_6) δ_H 3.12 (6H, s, NMe$_2$), 4.50 (2H, s, NH$_2$), 7.01 (2H, s, 2 × CH-pyrimidine); ^{13}C NMR (125 MHz; DMSO-d_6) δ_C 37.2 (NMe$_2$), 133.2 (C-5-pyrimidine), 144.3 (2 × CH-pyrimidine), 156.7 (C-2-pyrimidine); HRMS calcd for C$_6$H$_{11}$N$_4$ [M+H]$^+$ 139.0978, found 139.0978.

4-(2-Chloro-6-fluorobenzoyl)-*N*-(2-(dimethylamino)pyrimidin-5-yl)-1*H*-pyrrole-2-carboxamide (273)
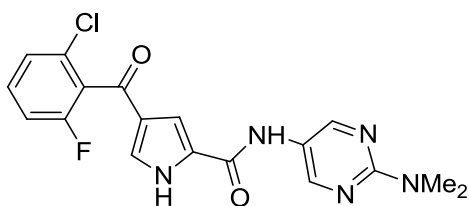
Prepared according to general procedure E using amine **352** (100 mg, 0.72 mmol, 2.5 eq.), carboxylic acid **336** (77 mg, 0.29 mmol, 1 eq.), cyanuric fluoride (25 μL, 0.20 mmol, 0.7 eq.), pyridine (23 μL, 0.29 mmol, 1 eq.) and MeCN (2 mL). Purification by MPLC on NH$_2$ SiO$_2$ with a gradient elution from 50-100% EtOAc/petrol gave a white solid (38 mg, 34 %); R_f 0.5 (NH$_2$ SiO$_2$, EtOAc); m.p. 300 °C dec.; λ_{max}(EtOH)/nm 287, 232; IR ν $_{max}$/cm^{-1} 2951, 1645, 1622; ^{1}H NMR (500 MHz; DMSO-d_6) δ$_H$ 3.15 (6H, s, NMe$_2$), 7.39 (1H, s, H-pyrrole), 7.44 (1H, app t, J = 8.4 Hz, H-5'), 7.49 (1H, s, H-pyrrole), 7.50 (1H, d, J = 8.4 Hz, H-3'), 7.62 (1H, td, J = 8.4 and 6.3 Hz, H-4'), 8.61 (2H, s, 2 × H-pyrimidine), 10.02 (1H, s, CO-NH), 12.70 (1H, s, NH); ^{19}F NMR (470 MHz; DMSO-d_6) δ$_F$ -114.35; ^{13}C NMR (125 MHz; DMSO-d_6) δ$_C$ 36.9 (NMe$_2$), 111.1 (CH-pyrrole), 115.0 (d, J_{CF} = 21.5 Hz, C-5'), 122.9 (C5-pyrimidine), 125.2 (C-pyrrole), 125.8 (d, J_{CF} = 3.2 Hz, C-3'), 128.1 (d, J_{CF} = 23.2 Hz, C-1'), 128.2 (C-pyrrole), 128.9 (CH-pyrrole), 130.4 (d, J_{CF} = 5.9 Hz, C-2'), 131.8 (d, J = 9.1 Hz, C-4'), 151.2 (2 × CH-pyrimidine), 158.4 (C-2-pyrimidine), 158.6 (d, J_{CF} = 247.0 Hz, C-6'), 159.1 (CO-NH), 183.9 (CO); LCMS (ES-) m/z 388.4 [M(^{35}Cl)+H]$^+$, 390.3 [M(^{37}Cl)+H]$^+$; HRMS calcd for C$_{18}$H$_{16}$^{35}Cl$_1$F$_1$N$_5$O$_2$ [M+H]$^+$ 388.0971, found 388.0977.

2-(4-Methylpiperazin-1-yl)-5-nitropyrimidine (343)[354]
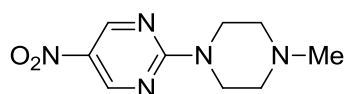
Prepared according to general procedure I using 1-methylpiperazine (382 μL, 3.45 mmol, 1.1 eq.), 2-chloro-5-nitropyrimidine (500 mg, 3.14 mmol, 1 eq.), Et$_3$N (480 μL, 3.45 mmol, 1.1 eq.) and THF (15 mL). The residue was purified by MPLC on SiO$_2$ with a gradient elution from 0-13% MeOH/EtOAc to give a yellow solid. (573 mg, 82%); R_f 0.6 (NH$_2$ SiO$_2$, Ethyl acetate); m.p. 149-152 °C; λ_{max}(EtOH)/nm 346, 332, 219; IR ν $_{max}$/cm^{-1} 1567, 1474; ^{1}H NMR (500 MHz; DMSO-d_6) δ$_H$ 2.26 (3H, s, Me), 2.41-2.46 (4H, m, H-piperazine), 3.92-3.99 (4H, m, H-piperazine), 9.15 (2H, s, H-pyrimidine); ^{13}C NMR (125 MHz; DMSO-d_6) δ$_C$ 44.0 (2 × C-piperazine), 45.5 (NMe), 54.1 (2 × C-piperazine), 133.2

(C-NO$_2$), 155.1 (2 × CH-pyrimidine), 160.8 (C-pyrimidine); MS (ES+) m/z 224.3 [M+H]$^+$; HRMS calcd for C$_9$H$_{14}$N$_5$O$_2$ [M+H]$^+$ 224.1142, found 224.1136.

2-(4-Methylpiperazin-1-yl)pyrimidin-5-amine(353)[355]
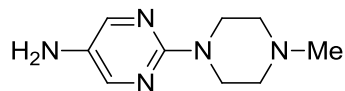
Prepared according to general procedure H using nitropyrimidine **343** (195 mg, 0.87 mmol) and MeOH (5 mL) to give a pale yellow solid (168 mg, 99%). R_f 0.5 (NH$_2$ SiO$_2$, 5% MeOH/CH$_2$Cl$_2$); m.p. 139-142 °C; λ$_{max}$(EtOH)/nm 353, 255; IR ν $_{max}$/cm^{-1} 3347, 3173, 2967, 2920, 1640, 1606; ^{1}H NMR (500 MHz; DMSO-d_6) δ$_H$ 2.22 (3H, s, NMe), 2.31-2.40 (4H, m, H-piperazine), 3.48-3.58 (4H, m, H-piperazine), 4.64 (2H, s, NH$_2$), 7.92 (2H, s, H-pyrimidine); ^{13}C NMR (125 MHz; DMSO-d_6) δ$_C$ 44.3 (2 × C-piperazine), 45.9 (NMe), 54.4 (2 × C-piperazine), 134.3 (C-NH$_2$), 144.0 (2 × CH-pyrimidine), 156.0 (C-pyrimidine); MS (ES+) m/z 194.3 [M+H]$^+$; HRMS calcd for C$_9$H$_{16}$N$_5$ [M+H]$^+$ 194.1400, found 194.1399.

4-(2-Chloro-6-fluorobenzoyl)-*N*-(2-(4-methylpiperazin-1-yl)pyrimidin-5-yl)-1*H*-pyrrole-2-carboxamide (275)
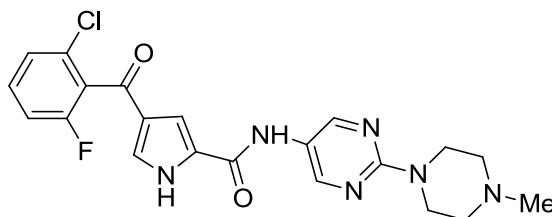
Prepared according to general procedure E using carboxylic acid **336** (150 mg, 0.78 mmol, 2.5 eq.), amine **353** (83 mg, 0.31 mmol, 1 eq.), cyanuric fluoride (19 μL, 0.22 mmol, 0.7 eq.) pyridine (25 μL, 0.31 mmol, 1 eq.) and MeCN (2 mL). Purification by MPLC on NH$_2$ SiO$_2$ with a gradient elution from 0-4% MeOH/CH$_2$Cl$_2$ gave a white solid (68 mg, 50%); R_f 0.3 (NH$_2$ SiO$_2$, 5% MeOH/CH$_2$Cl$_2$); m.p. 246 °C dec.; λ$_{max}$(EtOH)/nm 289, 231; IR ν $_{max}$/cm^{-1} 3186, 1661, 1641, 1606, 1582; ^{1}H NMR (500 MHz; DMSO-d_6) δ$_H$ 2.24 (3H, s, NMe), 2.35-2.42 (4H, m, H-piperazine), 3.68-3.76 (4H, m, H-piperazine), 7.40 (1H, s, H-pyrrole), 7.44 (1H, app t, J = 8.2 Hz, H-5'), 7.48-7.54 (2H, m, H-pyrrole and H-3'), 7.62 (1H, td, J = 8.2 and 6.3 Hz, H-4'), 8.61 (2H, s, 2 × H-pyrimidine), 10.05 (1H, s, CO-NH), 12.69 (1H, s, NH-pyrrole); ^{19}F NMR (470 MHz; DMSO-d_6) δ$_F$ -114.36; ^{13}C NMR (125 MHz; DMSO-d_6) δ$_C$ 43.6 (2 × CH$_2$ piperazine), 45.8 (NMe), 54.3 (2 × CH$_2$ piperazine),

111.1 (CH-pyrrole), 115.0 (d, J_{CF} = 21.5 Hz, C-5'), 125.2 (C-pyrrole), 125.8 (d, J_{CF} = 3.2 Hz, C-3'), 127.9 (C-pyrimidine), 128.0 (d, J_{CF} = 22.7 Hz, C-1'), 128.1 (C-pyrrole), 129.0 (CH-pyrrole), 130.4 (d, J_{CF} = 6.2 Hz, C-2'), 131.8 (d, J_{CF} = 9.1 Hz, C-4'), 151.0 (2 × CH-pyrimidine), 158.4 (CO-NH), 158.4 (C-pyrimidine), 158.5 (d, J_{CF} = 247 Hz, C-6'), 183.9 (CO); MS (ES+) m/z 443.5 [M(^{35}Cl)+H]$^+$, 445.4 [M(^{37}Cl)+H]$^+$; HRMS calcd for $C_{21}H_{21}{}^{35}Cl_1F_1N_6O_2$ [M+H]$^+$ 443.193, found 443.193.

4-(3,6-Dichloro-2-fluorobenzoyl)-*N*-(2-(4-methylpiperazin-1-yl)pyrimidin-5-yl)-1*H*-pyrrole-2-carboxamide (276)
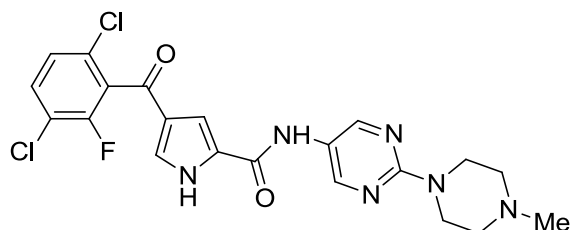
Prepared according to general procedure E using amine **353** (160 mg, 0.83 mmol, 2.5 eq.), carboxylic acid **337** (100 mg, 0.33 mmol, 1 eq.), cyanuric fluoride (20 μL, 0.23 mmol, 0.7 eq.), pyridine (27 μL, 0.33 mmol, 1 eq.) and MeCN (2 mL). Purification by MPLC on NH$_2$ SiO$_2$ with a gradient elution from 0-4% MeOH/CH$_2$Cl$_2$ gave a white solid (65 mg, 41%); R_f 0.65 (NH$_2$ SiO$_2$, 5% MeOH/EtOAc); m.p. 226-228 °C; λ_{max}(EtOH)/nm 287, 227; IR ν $_{max}$/cm^{-1} 3174, 1663, 1639, 1592; ^{1}H NMR (500 MHz; DMSO-d_6) δ$_H$ 2.25 (3H, s, CH$_3$), 2.37-2.41 (4H, m, 2 × CH$_2$-piperazine), 3.70-3.76 (4H, m, 2 × CH$_2$-piperazine), 7.44 (1H, s, H-pyrrole), 7.56 (1H, dd, J = 1.1 and 8.6 Hz, H-5'), 7.64 (1H, s, H-pyrrole), 7.82 (1H, app t, J = 8.6 Hz, H-4'), 8.64 (2H, s, 2 × H-pyrimidine), 10.07 (1H, s, CO-NH), 12.78 (1H, s, NH); ^{19}F NMR (470 MHz; DMSO-d_6) δ$_F$ -116.68; ^{13}C NMR (125 MHz; DMSO-d_6) δ$_C$ 43.6 (2 × CH$_2$-piperazine), 45.8 (CH$_3$), 54.3 (2 × CH$_2$-piperazine), 111.0 (CH-pyrrole), 119.3 (d, J_{CF} = 18.3 Hz, C-3'), 123.7 (C-pyrimidine), 124.7 (C-pyrrole), 126.9 (d, J_{CF} = 3.8 Hz, C-5'), 128.4 (C-pyrrole), 129.1 (d, J_{CF} = 22.3 Hz, C-1'), 129.2 (d, J_{CF} = 5.6 Hz, C-6'), 129.9 (CH-pyrrole), 131.8 (C-4'), 151.1 (2 × CH-pyrimidine), 153.8 (d, J_{CF} = 248.4 Hz, C-2'), 158.4 (C-pyrimidine), 158.4 (CO-NH), 182.6 (NH-pyrrole); MS (ES+) m/z 477.3 [M(^{35,35}Cl)+H]$^+$, 479.3 [M(^{35,37}Cl)+H]$^+$; HRMS calcd for $C_{21}H_{20}{}^{35}Cl_2F_1N_6O_2$ [M+H]$^+$ 477.1003, found 477.1008.

2-(4-Cyclopropylpiperazin-1-yl)-5-nitropyrimidine (344)

$$O_2N-\underset{N}{\overset{N}{\diagdown}}-N\diagdown N-\triangleleft$$
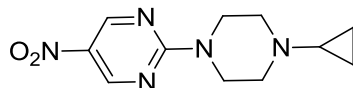
Prepared according to general procedure I using 1-cyclopropylpiperazine (250 mg, 1.98 mmol, 1 eq.), 2-chloro-5-nitropyrimidine (316 mg, 1.98 mmol, 1 eq.), Et$_3$N (304 μL, 2.18 mmol, 1.1 eq.) and THF (4 mL) with stirring for 18 h to give a yellow solid (222 mg, 95%); R_f 0.9 (EtOAc, NH$_2$ SiO$_2$); m.p. 184 °C dec.; λ$_{max}$(EtOH)/nm 339; IR ν$_{max}$/cm^{-1} 1552, 1303; ^{1}H NMR (500 MHz; DMSO-d_6) δ$_H$ 0.38-0.43(2H, m, 2 × H-cyclopropyl), 0.46-0.52 (2H, m, 2 × H-cyclopropyl), 1.68-1.74 (1H, m, N-CH-cPr), 2.63-2.69 (4H, m, 2 × CH$_2$-piperazine), 3.90-3.95 (4H, m, 2 × CH$_2$-piperazine), 9.15 (2H, s, 2 × H-pyrimidine); ^{13}C NMR (125 MHz; DMSO-d_6) δ$_C$ 5.8 (2 × CH$_2$-cyclopropyl), 37.8 (CHN-cyclopropyl), 44.1 (2 × CH$_2$-piperazine), 52.3 (2 × CH$_2$-piperazine), 133.1 (C-5-pyrimidine), 155.1 (C-4 and C-6-pyrimidine), 160.8 (C-2-pyrimidine); HRMS calc for C$_{11}$H$_{16}$N$_5$O$_2$ [M+H]$^+$ 250.1299, found 250.1294.

2-(4-Cyclopropylpiperazin-1-yl)pyrimidin-5-amine (354)

$$H_2N-\underset{N}{\overset{N}{\diagdown}}-N\diagdown N-\triangleleft$$
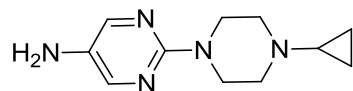
Prepared according to general procedure H using nitropyrimidine **344** (420 mg, 1.7 mmol) in MeOH (30 mL) and EtOAc (30 mL) for 3 h to give an orange solid (360 mg, 98%); R_f 0.2 (CH$_2$Cl$_2$, NH$_2$ SiO$_2$); m.p. 79-84 °C; λ$_{max}$(EtOH)/nm 256; IR ν$_{max}$/cm^{-1} 3205, 2818; ^{1}H NMR (500 MHz; DMSO-d_6) δ$_H$ 0.34-0.39 (2H, m, 2 × H-cyclopropyl), 0.43-0.49 (2H, m, 2 × H-cyclopropyl), 1.61-1.68 (1H, m, N-CH-cPr), 2.56-2.63 (4H, m, 2 × CH$_2$-piperazine), 3.46-3.54 (4H, m, 2 × CH$_2$-piperazine), 4.62 (2H, s, NH$_2$), 7.92 (2H, s, 2 × H-pyrimidine); ^{13}C NMR (125 MHz; DMSO-d_6) δ$_C$ 5.6 (2 × CH$_2$-cyclopropyl), 38.2 (CH-N-cyclopropyl), 44.4 (2 × CH$_2$-piperazine), 52.6 (2 × CH$_2$-piperazine), 134.3 (C-5-pyrimidine), 144.0 (C-4 and C-6-pyrimidine), 155.9 (C-2-pyrimidine); HRMS calc for C$_{11}$H$_{18}$N$_5$ [M+H]$^+$ 220.1557, found 220.1554.

N-(2-(4-cyclopropylpiperazin-1-yl)pyrimidin-5-yl)-4-(3,6-dichloro-2-fluorobenzoyl)-1*H*-pyrrole-2-carboxamide (287)
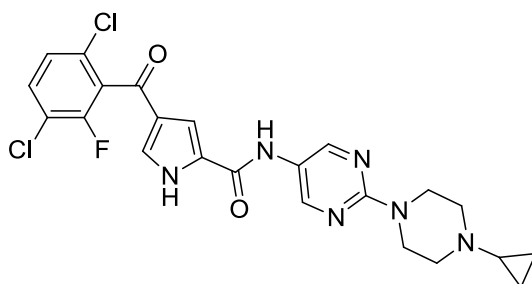
Prepared according to general procedure E using amine **354** (94 mg, 0.78 mmol, 2.5 eq.), carboxylic acid **337** (94 mg, 0.31 mmol, 1 eq.), cyanuric fluoride (8 μL, 0.09 mmol, 0.3 eq.), pyridine (25 μL, 0.31 mmol, 1 eq.) and MeCN (2 mL) with stirring at r.t. for 72 h. Purification by MPLC on SiO_2 with a gradient elution from 50-100% EtOAc/petrol gave a white solid. This solid was repurified by MPLC on NH_2 SiO_2 with gradient elution from 0-2% MeOH/CH_2Cl_2 to give a white solid (28 mg, 18%); R_f 0.3 (2% MeOH/CH_2Cl_2 , NH_2 SiO_2); m.p. 224 °C dec.; λ_{max}(EtOH)/nm 290, 236; IR ν_{max}/cm^{-1} 3180, 2937, 2843, 1657, 1637; ^{1}H NMR (500 MHz; DMSO-d_6) δ_H 0.37-0.41 (2H, m, 2 × H-cyclopropyl), 0.45-0.50 (2H, m, 2 × H-cyclopropyl), 1.65-1.71 (1H, m, N-C*H*-cPr), 2.60-2.64 (4H, m, 2 × CH_2-piperazine), 3.68-3.72 (4H, m, 2 × CH_2-piperazine), 7.43 (1H, s, H-pyrrole), 7.56 (1H, dd, *J* = 1.1 and 8.5 Hz, H-5'), 7.64 (1H, s, H-pyrrole), 7.82 (1H, app t, *J* = 8.5 Hz, H-4'), 8.64 (2H, s, 2 × H-pyrimidine), 10.07 (CO-NH), 12.78 (NH-pyrrole); ^{19}F NMR (470 MHz; DMSO-d_6) δ_F -116.68; ^{13}C NMR (125 MHz; DMSO-d_6) δ_C 5.7 (2 × CH_2-cyclopropyl), 38.1 (CHN-cyclopropyl), 43.7 (2 × CH_2-piperazine), 52.6 (2 × CH_2-piperazine), 111.0 (CH-pyrrole), 119.3 (d, J_{CF} = 18.0 Hz, C-3'), 123.6 (C-pyrimidine), 124.7 (C-pyrrole), 126.9 (d, J_{CF} = 3.6 Hz, C-5'), 128.3 (C-pyrrole), 129.2 (d, J_{CF} = 22.9 Hz, C-1'), 129.2 (d, J_{CF} = 5.4 Hz, C-6'), 129.8 (CH-pyrrole), 131.8 (C-2'), 151.1 (C-pyrimidine), 153.5 (d, J_{CF} = 248.5 Hz, C-2'), 157.4 (C-pyrimidine), 158.4 (CO-NH), 182.6 (CO); MS (ES+) *m/z* 462.4, 464.4 [M+H]$^+$; HRMS calc for $C_{23}H_{22}{}^{35}Cl_2F_1N_6O_2$ [M+H]$^+$ 503.1160, found 503.1143.

tert-Butyl 4-(5-nitropyrimidin-2-yl)piperazine-1-carboxylate (345)[356]
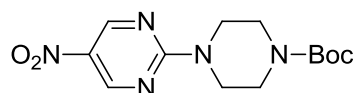
Prepared according to general procedure I using 2-chloro-5-nitropyrimidine (350 mg, 2.2 mmol, 1 eq.), 1-Boc-piperazine (450 mg, 2.4 mmol, 1.1 eq.), Et$_3$N (336 μL, 2.4 mmol, 1.1

eq) and THF (12 mL). The residue was purified by MPLC on SiO$_2$ with a gradient elution from 15-100% EtOAc/petrol to give a yellow solid (460 mg, 68%); R_f 0.4 (SiO$_2$, 20% EtOAc/petrol); m.p. 196-199 °C; λ_{max}(EtOH)/nm 339, 221; IR ν_{max}/cm^{-1} 1676, 1539, 1325; ^{1}H NMR (500 MHz; DMSO-d_6) δ_H 1.47 (9H, s, C(CH$_3$)$_3$), 3.47-4.57 (4H, m, 2 × CH$_2$-piperazine), 3.92-3.99 (4H, m, 2 × CH$_2$-piperazine), 9.17 (2H, s, 2 × H-pyrimidine); ^{13}C NMR (125 MHz; DMSO-d_6) δ_C 28.0 (C(CH$_3$)$_3$), 42.5 (2 × CH$_2$-piperazine), 43.9 (2 × CH$_2$-piperazine), 79.3 (C(CH$_3$)$_3$), 133.4 (C-5-pyrimidine), 153.8 (CO), 155.1 (C-4 and C-6-pyrimidine), 161.0 (C-2-pyrimidine); HRMS calcd for C$_{13}$H$_{20}$N$_5$O$_4$ [M+H]$^+$ 310.1510, found 310.1510.

### *tert*-Butyl 4-(5-aminopyrimidin-2-yl)piperazine-1-carboxylate (355)[357]
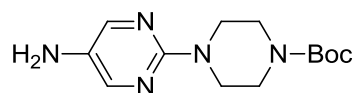
Prepared according to general procedure H using nitropyimidine **345** (440 mg, 1.42 mmol) in MeOH (75 mL) and EtOAc (75 mL) to give a yellow solid (395 mg, 99%); R_f 0.15 (NH$_2$ SiO$_2$, 70% EtOAc/petrol); m.p. 131-133 °C; λ_{max}(EtOH)/nm 252; IR ν_{max}/cm^{-1} 3336, 1676; ^{1}H NMR (500 MHz; DMSO-d_6) δ_H 1.45 (9H, s, C(CH$_3$)$_3$), 3.38-3.42 (4H, m, 2 × CH$_2$-piperazine), 3.50-3.55 (4H, m, 2 × CH$_2$-piperazine), 4.68 (2H, s, NH$_2$), 7.94 (2H, s, 2 × H-pyrimidine); ^{13}C NMR (125 MHz; DMSO-d_6) δ_C 28.1 (C(CH$_3$)$_3$), 44.2 (2 × CH$_2$-piperazine), 44.7 (2 × CH$_2$-piperazine), 78.9 (C(CH$_3$)$_3$), 134.7 (C-5-pyrimidine), 144.0 (C-4 and C-6-pyrimidine), 154.0 (CO), 155.6 (C-2-pyrimidine); HRMS calcd for C$_{13}$H$_{20}$N$_5$O$_2$ [M-H]$^-$ 278.1622, found 278.1609.

tert-Butyl 4-(5-(4-(2-chloro-6-fluorobenzoyl)-1*H*-pyrrole-2-carboxamido) pyrimidin-2-yl)piperazine-1-carboxylate (361)

Prepared according to general procedure E using amine **355** (200 mg, 0.72 mmol, 2.5 eq.), carboxylic acid **336** (76 mg, 0.29 mmol, 1 eq.), cyanuric fluoride (24 μL, 0.20 mmol, 0.7 eq.), pyridine (23 μL, 0.29 mmol, 1 eq.) and MeCN (2 mL). Purification by MPLC on NH$_2$

SiO$_2$ with a gradient elution from 50-100% EtOAc/petrol gave a white solid (74 mg, 49%); R_f 0.15 (NH$_2$ SiO$_2$, 70% EtOAc/petrol); m.p. 219-221 °C; λ_{max}(EtOH)/nm 310; IR ν_{max}/cm^{-1} 3300, 1637 (br); ^{1}H NMR (500 MHz; DMSO-d_6) δ_H 1.46 (9H, s, C(CH$_3$)$_3$), 3.41-3.48 (4H, m, 2 × CH$_2$-piperazine), 3.68-3.76 (4H, m, 2 × CH$_2$-piperazine), 7.40 (1H, s, H-pyrrole), 7.44 (1H, app t, J = 8.4 Hz, H-5'), 7.47-7.53 (2H, m, H-pyrrole and H-3'), 7.62 (1H, app dt, J = 8.4 and 6.1 Hz, H-4'), 8.67 (2H, s, 2 × H-pyrimidine), 10.10 (1H, s, CO-NH), 12.71 (1H, s, NH); ^{19}F NMR (470 MHz; DMSO-d_6) δ_F -114.35; ^{13}C NMR (125 MHz; DMSO-d_6) δ_C 28.1 (C(CH$_3$)$_3$), 43.5 (4 × CH$_2$-piperazine), 79.0 (C(CH$_3$)$_3$), 111.2 (CH-pyrrole), 115.0 (d, J_{CF} = 21.7 Hz, C-5'), 124.0 (C-pyrimidine), 125.2 (C-pyrrole), 125.9 (d, J_{CF} = 2.5 Hz, C-3'), 128.1 (C-1'), 128.1 (C-pyrrole), 129.0 (CH-pyrrole), 130.4 (d, J_{CF} = 6.8 Hz (C-2'), 131.8 (d, J_{CF} = 9.5 Hz, C-4'), 151.0 (2 × CH-pyrimidine), 152.4 (d, J_{CF} = 248.9, C-6'), 153.9 (CO-carbamate), 158.2 (C-pyrimidine), 158.5 (CO-NH), 184.1 (CO); HRMS calcd for C$_{25}$H$_{25}$^{35}Cl$_1$F$_1$N$_6$O$_3$ [M-H]$^-$ 527.1615, found 527.1615.

4-(2-Chloro-6-fluorobenzoyl)-*N*-(2-(piperazin-1-yl)pyrimidin-5-yl)-1*H*-pyrrole-2-carboxamide (285)
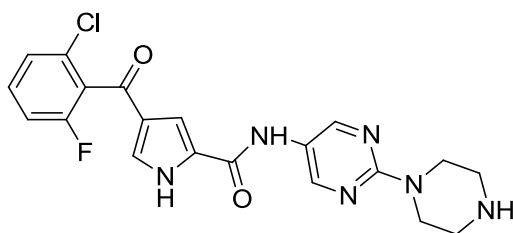
Prepared according to general procedure G using Et$_3$SiH (48 μL, 0.30 mmol, 2.5 eq.), TFA (0.6 mL), CH$_2$Cl$_2$ (0.6 mL) and carbamate **361** (64 mg, 0.12 mmol, 1 eq.) to give a white solid (27 mg, 52%); R_f 0.1 (NH$_2$ SiO$_2$, EtOAc); m.p. 311 °C dec.; λ_{max}(EtOH)/nm 291, 233; IR ν_{max}/cm^{-1} 3266, 1634, 1607, 1572; ^{1}H NMR (500 MHz; DMSO-d_6) δ_H 2.75-2.79 (4H, m, 2 × CH$_2$-piperazine), 3.64-3.68 (4H, m, 2 × CH$_2$-piperazine), 7.39 (1H, s, H-pyrrole), 7.43 (1H, app t, J = 8.4 Hz, H-5'), 7.49 (1H, s, H-pyrrole), 7.50 (1H, d, J = 8.4 Hz, H-3'), 7.62 (1H, app dt, J = 6.3 and 8.4 Hz, H-4'), 8.62 (2H, s, 2 × H-pyrimidine), 10.06 (1H, s, CO-NH); ^{19}F NMR (470 MHz; DMSO-d_6) δ_F -114.35; ^{13}C NMR (125 MHz; DMSO-d_6) δ_C 44.9 (2 × C-piperazine), , 45.4 (2 × C-piperazine), 111.1 (CH-pyrrole), 115.0 (d, J_{CF} = 21.6 Hz, C-5'), 123.4 (C-pyrimidine), 125.2 (C-pyrrole), 125.8 (d, J_{CF} = 3.2 Hz, C-3'), 129.0 (d, J_{CF} = 23.0 Hz, C-1'), 128.2 (C-pyrrole), 129.0 (CH-pyrrole), 130.4 (d, J_{CF} = 6.2 Hz, C-2'), 131.8 (d, J_{CF} = 9.1 Hz, C-4'), 151.1 (C-pyrimidine), 158.5 (CO-N),

158.5 (C-pyrimidine), 158.6 (d, J_{CF} = 247.0 Hz, C-6'), 183.9 (CO); HRMS calcd for C$_{20}$H$_{19}$^{35}Cl$_1$F$_1$N$_6$O$_2$ [M+H]$^+$ 429.1237, found 429.1232.

tert-Butyl 4-(5-(4-(3,6-dichloro-2-fluorobenzoyl)-1*H*-pyrrole-2-carboxamido)pyrimidin-2-yl)piperazine-1-carboxylate (362)
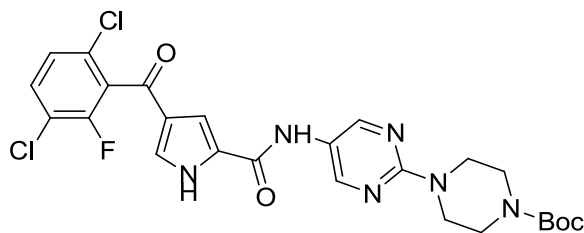
Prepared according to general procedure E using amine **355** (190 mg, 0.68 mmol, 2.5 eq.), carboxylic acid **337** (82 mg, 0.27 mmol, 1 eq.), cyanuric fluoride (16 μL, 0.19 mmol, 0.7 eq.), pyridine (22 μL, 0.27 mmol, 1 eq.) and MeCN (4 mL). Purification by MPLC on NH$_2$ SiO$_2$ with a gradient elution from 40-100% EtOAc/petrol gave a white solid (105 mg, 69%); R_f 0.25 (NH$_2$ SiO$_2$, 70% EtOAc/petrol); m.p. 211-213 °C; λ_{max}(EtOH)/nm 283, 223; IR ν $_{max}$/cm^{-1} 3199, 1637, 1573; ^{1}H NMR (500 MHz; DMSO-d_6) δ$_H$ 1.46 (9H, s, C(CH$_3$)$_3$, 3.40-3.47 (4H, m, 2 × CH$_2$-piperazine), 3.70-3.76 (4H, m, 2 × CH$_2$-piperazine), 7.44 (1H, s, H-pyrrole), 7.56 (1H, d, J = 8.6 Hz, H-5'), 7.82 (1H, app t, J = 8.6 Hz, H-4'), 8.67 (2H, s, 2 × H-pyrimidine), 10.10 (1H, s, CO-NH), 12.79 (1H, s, NH); ^{19}F NMR (470 MHz; DMSO-d_6) δ$_F$ -116.69; ^{13}C NMR (125 MHz; DMSO-d_6) δ$_C$ 28.1 (C(CH$_3$)$_3$), 43.5 (4 × CH$_2$-piperazine), 79.0 (C(CH$_3$)$_3$), 111.1 (CH-pyrrole), 119.3 (d, J_{CF} = 18.0 Hz, C-3'), 124.0 (C-pyrimidine), 124.7 (C-pyrrole), 126.9 (d, J_{CF} = 3.5 Hz, C-5'), 128.3 (C-1'), 128.3 (C-pyrrole), 129.2 (d, J_{CF} = 5.5 Hz, C-6'), 129.2 (CH-pyrrole), 131.8 (C-4'), 151.1 (2 × CH-pyrimidine), 153.8 (d, J_{CF} = 248.4 Hz, C-2'), 153.9, 158.2 (C-pyrimidine), 158.4 (CO-NH), 182.6 (C-O); HRMS calcd for C$_{25}$H$_{24}$^{35}Cl$_2$F$_1$N$_6$O$_4$ [M+H]$^+$ 563.1197, found 563.121.

### 4-(3,6-Dichloro-2-fluorobenzoyl)-*N*-(2-(piperazin-1-yl)pyrimidin-5-yl)-1*H*-pyrrole-2-carboxamide (286)
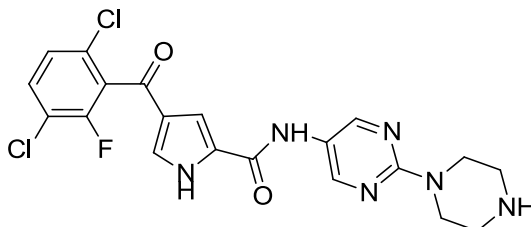
Prepared according to general procedure G using Et$_3$SiH (64 μL, 0.40 mmol, 2.5 eq.), TFA (1 mL), CH$_2$Cl$_2$ (1 mL) and carbamate **362** (90 mg, 0.16 mmol, 1 eq.) to give a white solid

(35 mg, 47%); R_f 0.2 (NH$_2$ SiO$_2$, 5% MeOH/EtOAc); m.p. 230 °C dec.; λ_{max}(EtOH)/nm 303, 225; IR ν_{max}/cm^{-1} 3275 (br), 2922, 2847, 1635; ^{1}H NMR (500 MHz; DMSO-d_6) δ_H 2.75-2.79 (4H, m, 2 × CH$_2$-piperazine), 3.64-3.69 (4H, m, 2 × CH$_2$-piperazine), 7.42 (1H, s, H-pyrrole), 7.55 (1H, d, J = 8.6 Hz, H-5'), 7.63 (1H, s, H-pyrrole), 7.82 (1H, app t, J = 8.6 Hz, H-4'), 8.62 (2H, s, 2 × H-pyrimidine), 10.05 (1H, br s, CO-NH); ^{13}C NMR (125 MHz; DMSO-d_6) δ_C 44.9 (2 × C-piperazine), 45.4 (2 × C-piperazine), 111.0 (CH-pyrrole), 119.3 (d, J_{CF} = 18.1 Hz, C-3'), 123.4 (C-pyrimidine), 124.7 (C-pyrrole), 126.9 (d, J_{CF} = 3.6 Hz), 128.4 (C-pyrrole), 129.2 (d, J_{CF} = 23.2 Hz, C-1'), 129.2, (d, J_{CF} = 5.3 Hz, C-6'), 129.9 (CH-pyrrole), 131.8 (C-4'), 151.1 (2 × CH-pyrimidine), 153.8 (d, J_{CF} = 248.7 Hz, C-2'), 158.4 (C-pyrimidine), 158.6 (CO-NH), 182.6 (CO); HRMS calcd for C$_{20}$H$_{18}$^{35}Cl$_2$F$_1$N$_6$O$_2$ [M+H]$^+$ 463.0847, found 463.0853.

4-(5-Nitropyrimidin-2-yl)morpholine (346)
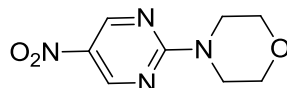
Prepared according to general procedure I using 2-chloro-5-nitropyrimidine (300 mg, 1.88 mmol, 1 eq.) morpholine (181 μL, 2.07 mmol, 1.1 eq.), Et$_3$N (288 μL, 2.07 mmol, 1.1 eq) and THF (12 mL). The residue was purified by MPLC on SiO$_2$ with a gradient elution from 20-100% EtOAc/petrol to give a yellow solid (290 mg, 73%); R_f 0.35 (SiO$_2$, 30% EtOAc/petrol); m.p. 161-164 °C (lit.[358] 165-168 °C); λ_{max}(EtOH)/nm 339, 221; IR ν_{max}/cm^{-1} 1545 (NO$_2$), 1326 (NO$_2$); ^{1}H NMR (500 MHz; DMSO-d_6) δ_H 3.71-3.75 (4H, m, 2 × CH$_2$-morpholine), 3.94-3.97 (4H, m, 2 × CH$_2$-morpholine), 2.14 (2H, s, 2 × H-pyrimidine); ^{13}C NMR (125 MHz; DMSO-d_6) δ_C 44.5 (2 × CH$_2$-morpholine), 65.8 (2 × CH$_2$-morpholine), 133.4 (C-5-pyrimidine), 155.1 (C-4 and C-6-pyrimidine), 161.0 (C-2-pyrimidine); HRMS calcd for C$_8$H$_{11}$N$_4$O$_3$ [M+H]$^+$ 211.0826, found 211.0828.

2-Morpholinopyrimidin-5-amine (356)
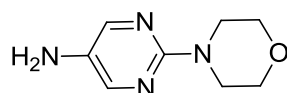
Prepared according to general procedure H using nitropyrimidine **346** (278 mg, 1.54 mmol) in MeOH (35 mL) and EtOAc (15 mL) to give a yellow solid (239 mg, 100%); R_f 0.3 (NH$_2$ SiO$_2$, 70% EtOAc/petrol); m.p. 110-113 °C (lit.[358] 99 °C); λ_{max}(EtOH)/nm 255; IR ν_{max}/cm^{-1} 3301, 3203 (NH$_2$); ^{1}H NMR (500 MHz; DMSO-d_6) δ_H 3.46-3.50 (4H, m, 2 × CH$_2$-morpholine), 3.63-3.70 (4H, m, 2 × CH$_2$-morpholine), 4.68 (2H, s, NH$_2$), 7.94 (2H, s,

2 × H-pyrimidine); ^{13}C NMR (125 MHz; DMSO-d_6) δ_C 45.0 (2 × CH$_2$-morpholine), 66.0 (2 × CH$_2$-morpholine), 134.8 (C-5-pyrimidine), 143.9 (C-4 and C-6-pyrimidine), 155.9 (C-2-pyrimidine); HRMS calcd for C$_8$H$_{13}$N$_4$O$_1$ [M+H]$^+$ 181.1084, found 181.1084.

4-(2-Chloro-6-fluorobenzoyl)-*N*-(2-morpholinopyrimidin-5-yl)-1*H*-pyrrole-2-carboxamide (279)
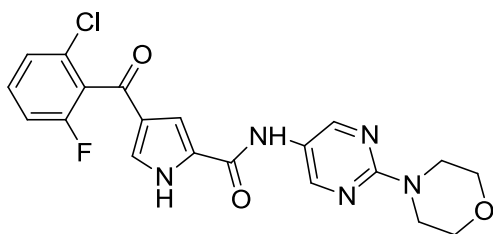
Prepared according to general procedure E using amine **356** (110 mg, 0.61 mmol, 2.5 eq.), carboxylic acid **336** (65 mg, 0.24 mmol, 1 eq.), cyanuric fluoride (15 μL, 0.17 mmol, 0.7 eq.), pyridine (20 μL, 0.24 mmol, 1 eq.) and MeCN (2 mL). Purification by MPLC on NH$_2$ SiO$_2$ with a gradient elution from 50-100% EtOAc/petrol gave a white solid (52 mg, 50%); R_f 0.4 (NH$_2$ SiO$_2$, EtOAc); m.p. 286-287 °C; λ_{max}(EtOH)/nm 292, 232; IR ν_{max}/cm^{-1} 3211, 1656, 1634; ^{1}H NMR (500 MHz; DMSO-d_6) δ_H 3.70 (8H, s, 4 × CH$_2$-morpholine), 7.41 (1H, m, H-pyrrole), 7.44 (1H, app. t, J = 8.3 Hz, H-5'), 7.48-7.52 (2H, m, H-pyrrole and H-3'), 7.62 (1H, td, J = 8.3 and 6.3 Hz, H-4'), 8.68 (2H, s, 2 × H-pyrimidine), 10.10 (CO-NH), 12.72 (NH-pyrrole); ^{19}F NMR (470 MHz; DMSO-d_6) δ_F -114.35; ^{13}C NMR (125 MHz; DMSO-d_6) δ_C 44.2 (2 × CH$_2$-morpholine), 65.9 (2 × CH$_2$-morpholine), 111.2 (CH-pyrrole), 115.0 (d, J_{CF} = 21.5 Hz, C-5'), 124.1 (C-pyrimidine), 125.2 (C-pyrrole), 125.8 (J_{CF} = 2.7 Hz, C-3'), 128.7 (d, J_{CF} = 22.7 Hz, C-1'), 128.1 (C-pyrrole), 129.0 (CH-pyrrole), 130.4 (d, J_{CF} = 6.4 Hz, C-2'), 131.8 (d, J_{CF} = 8.6 Hz, C-4'), 151.0 (2 × CH-pyrimidine), 158.4 (CO-NH and C-pyrimidine), 158.6 (d, J = 247.0 Hz, C-6'), 183.9 (CO); HRMS calcd for C$_{20}$H$_{18}$^{35}Cl$_1$F$_1$N$_5$O$_3$ [M+H]$^+$ 430.1077, found 430.1083.

4-(3,6-Dichloro-2-fluorobenzoyl)-*N*-(2-morpholinopyrimidin-5-yl)-1*H*-pyrrole-2-carboxamide(280)
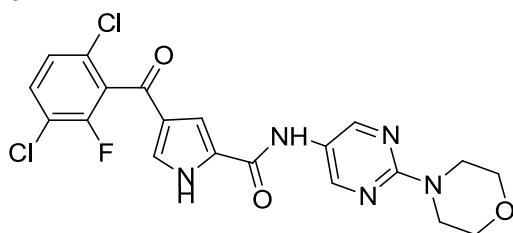
Prepared according to general procedure E using amine **356** (110 mg, 0.57 mmol, 2.5 eq.), carboxylic acid **337** (74 mg, 0.24 mmol, 1 eq.), cyanuric fluoride (15 μL, 0.17 mmol, 0.7

eq.), pyridine (20 μL, 0.24 mmol, 1 eq.) and MeCN (2 mL). Purification by MPLC on NH₂ SiO₂ with a gradient elution from 50-100% EtOAc/petrol gave a beige solid (45 mg, 40%); R_f 0.1 (NH₂ SiO₂, 70% EtOAc/petrol); m.p. 165-170 °C; λ_{max}(EtOH)/nm 285, 226; IR ν_{max}/cm⁻¹ 2922, 1635; ¹H NMR (500 MHz; DMSO-d_6) δ_H 3.70 (8H, s, 4 × CH₂-morpholine), 7.44 (1H, s, H-pyrrole), 7.56 (1H, d, J = 8.4 Hz, H-5'), 7.65 (1H, s, H-pyrrole), 7.82 (app t, J = 8.4 H, H-4'), 8.68 (2H, s, 2 × H-pyrimidine), 10.10 (1H, s, CO-NH), 12.79 (1H, s, NH); ¹⁹F NMR (470 MHz; DMSO-d_6) δ_F -116.68; ¹³C NMR (125 MHz; DMSO-d_6) δ_C 44.2 (2 × C-morpholine), 65.9 (2 × C-morpholine), 111.1 (CH-pyrrole), 119.3 (d, J_{CF} = 17.8 Hz, C-3'), 124.1 (C-pyrimidine), 124.7 (C-pyrrole), 126.9 (d, J_{CF} = 4.1 Hz, C-5'), 128.3 (C-pyrrole), 129.1 (d, J_{CF} = 23.0 Hz, C-1'), 129.2 (d, J_{CF} = 5.4 Hz, C-6'), 129.9 (CH-pyrrole), 131.8 (C-4'), 151.0 (C-pyrimidine), 153.8 (d, J_{CF} = 248.5 Hz, C-2'), 158.4 (C-pyrimidine), 158.5 (CO-NH), 182.6 (CO); HRMS calcd for C₂₀H₁₇³⁵Cl₂F₁N₅O₃ [M+H]⁺ 464.0687, found 464.0692.

## 1-(5-Nitropyrimidin-2-yl)piperidin-4-ol (347)

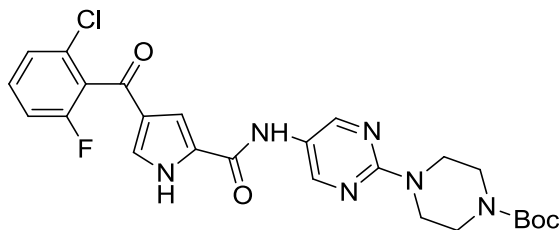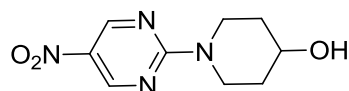Prepared according to general procedure I using 2-chloro-5-nitropyrimidine (300 mg, 1.9 mmol, 1 eq.), 4-hydroxypiperidine (209 mg, 2.1 mmol, 1.1 eq.), Et₃N (288 μL, 2.1 mmol, 1.1 eq) and THF (10 mL) to give a yellow solid (397 mg, 94%); R_f 0.25 (NH₂ SiO₂, 60% EtOAc/petrol); m.p. 178-180 °C; λ_{max}(EtOH)/nm 348, 222; IR ν_{max}/cm⁻¹ 1548.5, 1326.1; ¹H NMR (500 MHz; DMSO-d_6) δ_H 1.41-1.49 (2H, m, 2 × H-piperidine), 1.82-1.90 (2H, m, 2 × H-piperidine), 3.60-3.68 (2H, m, 2 × H-piperidine), 3.82-3.90 (1H, m, CH-OH), 4.28-4.36 (2H, m, 2 × H-piperidine), 4.89 (1H, d, J = 4.1 Hz, OH), 9.13 (2H, s, 2 × H-pyrimidine); ¹³C NMR (125 MHz; DMSO-d_6) δ_C 33.8 (2 × CH₂-piperidine), 41.7 (2 × CH₂-N-piperidine), 65.0 (CH-OH), 132.9 (C-5-pyrimidine), 155.1 (2 × CH-pyrimidine), 160.7 (C-2-pyrimidine); HRMS calcd for C₉H₁₃N₄O₃ [M+H]⁺ 225.0982, found 225.0985.

1-(5-Aminopyrimidin-2-yl)piperidin-4-ol (357)
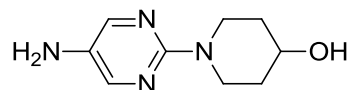
Prepared according to general procedure H using nitropyrimidine **347** (382 mg, 1.70 mmol), MeOH (40 mL) and EtOAc (40 mL) for 4 h to give a yellow gum (237 mg, 72%);

R_f 0.3 (NH$_2$ SiO$_2$, EtOAc); IR ν_{max}/cm^{-1} 3329, 3223, 2852; ^{1}H NMR (500 MHz; DMSO-d_6) δ_H 1.26 - 1.36 (2H, m, 2 × H-piperidine), 1.71 - 1.79 (2H, m, 2 × H-piperidine), 2.99 - 3.08 (2H, m, 2 × H-piperidine), 3.63 - 3.72 (1H, m, CH-OH), 4.10 - 4.18 (2H, m, 2 × H-piperidine), 4.57 (2H, s, NH$_2$), 4.66 (1H, d, J = 4.3 Hz, OH), 7.90 (2H, s, 2 × H-pyrimidine); ^{13}C NMR (125 MHz; DMSO-d_6) δ_C 33.8 (2 × CH$_2$-piperidine), 42.3 (2 × CH$_2$-N-piperidine), 66.6 (CH-OH), 133.8 (C-5-pyrimidine), 144.2 (2 × CH-pyrimidine), 155.9 (C-2-pyrimidine); MS (ES+) m/z 195.3 [M+H]$^+$.

1-(5-Nitropyrimidin-2-yl)piperidin-4-yl acetate (348)
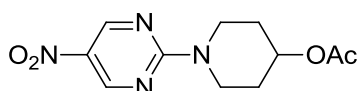
TFA (10 mL) was added to *tert*-butyl 4-acetoxypiperidine-1-carboxylate[359] (500 mg, 2.06 mmol) in DCM (10 mL) and the mixture was stirred at r.t. for 90 min. The solvent was removed *in vacuo* to give a clear oil. This oil was added to a solution of 2-chloro-5-nitropyrimidine (263 mg, 1.65 mmol, 1 eq.) and triethylamine (2.3 mL, 16.5 mmol, 10 eq.) in THF (5 mL) and the mixture was stirred at r.t. for 30 min. The mixture was partitioned between EtOAc (30 mL) and HCl (2 × 20 mL, 0.5 M aq.), washed with brine, dried over MgSO$_4$ and the solvent removed *in vacuo* to give a clear oil (1.1 g, 91%); R_f 0.2 (20% EtOAc/petrol); m.p. 177-179 °C; λ_{max}(EtOH)/nm 339; IR ν_{max}/cm^{-1} 1740, 1548, 1329; ^{1}H NMR (500 MHz; DMSO-d_6) δ_H 1.60-1.71 (2H, m, 2 × H-piperidine), 1.93-2.02 71 (2H, m, 2 × H-piperidine), 2.07 (3H, s, COCH$_3$), 3.81 (2H, ddd, J = 3.6 Hz, 8.7 and 13.6 Hz, 2 × H-piperidine), 4.24-4.32 (2H, m, 2 × H-piperidine), 4.98-5.05 (1H, m, CHOAc), 9.12 (2H, s, 2 × H-pyrimidine); ^{13}C NMR (125 MHz; DMSO-d_6) δ_C 21.0 (CH$_3$), 30.1 (2 × CH$_2$-piperidine), 41.4 (2 × CH$_2$-piperidine), 68.9 (CHOAc), 133.2 (C-2-pyrimidine), 155.1 (2 × CH-pyrimidine), 160.8 (C-5-pyrimidine), 169.8 (CO-CH$_3$); HRMS calcd for C$_{11}$H$_{15}$N$_4$O$_4$ [M+H]$^+$ 267.1088, found 267.1089.

1-(5-Aminopyrimidin-2-yl)piperidin-4-yl acetate (358)
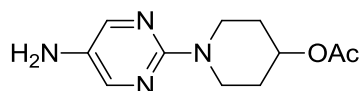
Prepared according to general procedure H using nitropyrimidine **348** (370 mg, 1.70 mmol) in EtOAc (40 mL) for 3 h to give a yellow solid (328 mg, 100%); R_f 0.15 (70% EtOAc/petrol); m.p. 119-121 °C; λ_{max}(EtOH)/nm 256, 350; IR ν_{max}/cm^{-1} 3404, 1719; ^{1}H

NMR (500 MHz; DMSO-d_6) δ_H 1.46-1.57 (2H, m, 2 × H-piperidine), 1.82-1.90 (2H, m, 2 × H-piperidine), 2.04 (3H, s, COCH_3), 3.26 (2H, ddd, J = 3.3 Hz, 9.6 and 13.4 Hz, 2 × H-piperidine), 4.01-4.10 (2H, m, 2 × H-piperidine), 4.62 (2H, s, NH_2), 4.85-4.93 (1H, m, CHOAc), 7.92 (2H, s, 2 × H-pyrimidine); ^{13}C NMR (125 MHz; DMSO-d_6) δ_C 21.0 (COCH$_3$), 29.84 (2 × CH$_2$-piperidine), 41.9 (2 × CH$_2$N-piperidine), 70.3 (CH-OAc), 134.1 (C-5-pyrimidine), 144.1 (C-4 and -6-pyrimidine), 155.7 (C-2-pyrimidine), 169.8 (COCH$_3$); HRMS calc for $C_{11}H_{17}N_4O_2$ [M+H]$^+$ 237.1346, found 237.1343.

1-(5-(4-(2-Chloro-6-fluorobenzoyl)-1H-pyrrole-2-carboxamido)pyrimidin-2-yl)piperidin-4-yl acetate (283)
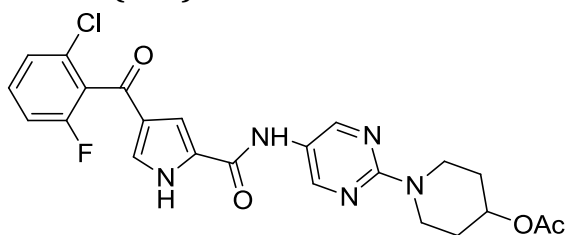
Prepared according to general procedure E using amine **358** (190 mg, 0.81 mmol, 2.5 eq.), carboxylic acid **336** (86 mg, 0.32 mmol, 1 eq.), cyanuric fluoride (19 μL, 0.23 mmol, 0.7 eq.), pyridine (26 μL, 0.32 mmol, 1 eq.) and MeCN (2 mL). Purification by MPLC on NH$_2$ SiO$_2$ with a gradient elution from 20-70% EtOAc/petrol gave a pale yellow solid (74 mg, 47%); R_f 0.55 (70% EtOAc/petrol); m.p. 279-281 °C; λ_{max}(EtOH)/nm 288, 233; IR ν $_{max}$/cm^{-1} 3224, 1710, 1639, 1572; ^{1}H NMR (500 MHz; DMSO-d_6) δ_H 1.51-1.61 (2H, m, 2 × H-piperidine), 1.88-1.95 (2H, m, 2 × H-piperidine), 2.06 (3H, s, COCH_3), 3.45-3.53 (2H, m, 2 × H-piperidine), 4.15-4.22 (2H, m, 2 × H-piperidine), 4.92-4.99 (1H, m, CHOAc), 7.40 (1H, s, H-pyrrole), 7.44 (1H, app t, J = 8.5 Hz, H-5'), 7.48-7.53 (2H, m, H-pyrrole and H-3'), 7.62 (1H, td, J = 8.5 and 6.1 Hz, H-4'), 8.64 (2H, s, 2 × H-pyrimidine), 10.07 (1H, s, CO-NH), 12.71 (1H, s, NH-pyrrole); ^{19}F NMR (470 MHz; DMSO-d_6) δ_F -114.35; ^{13}C NMR (125 MHz; DMSO-d_6) δ_C 21.0 (CH$_3$), 30.0 (2 × CH$_2$-piperidine), 41.1 (2 × CH$_2$N-piperidine), 69.9 (CHOAc), 111.1 (CH-pyrrole), 115.0 (d, J_{CF} = 21.7 Hz, C-5'), 123.6 (C-pyrimidine), 125.2 (C-pyrrole), 125.9 (C-pyrrole), 128.0 (d, J_{CF} = 18.6 Hz, C-1'), 128.1 (d, J_{CF} = 3.6 Hz, C-3'), 129.0 (CH-pyrrole), 130.4 (d, J_{CF} = 6.1 Hz, C-2'), 131.8 (d, J_{CF} = 9.1 Hz, C-4'), 151.1 (2 × CH-pyrimidine), 158.2 (C-pyrimidine), 158.4 (CO-NH), 158.6 (d, J_{CF} = 247.2 Hz, C-6'), 169.8 (CO-Me), 183.9 (CO); HRMS calc for $C_{23}H_{22}{}^{35}Cl_1F_1N_4O_4$ [M+H]$^+$ 486.1339, found 486.1329.

4-(2-Chloro-6-fluorobenzoyl)-*N*-(2-(4-hydroxypiperidin-1-yl)pyrimidin-5-yl)-1*H*-pyrrole-2-carboxamide (281)
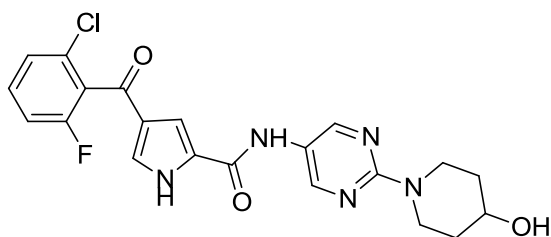
K_2CO_3 (37 mg, 0.27 mmol, 2 eq.) was added to a solution of acetate ester **283** (65 mg, 0.13 mmol, 1 eq.) in a mixture of THF (2 mL), MeOH (2 mL) and H_2O (2 mL). The mixture was stirred at r.t for 18 h, partitioned between EtOAc (2 × 25 mL) and H_2O (20 mL), washed with brine, dried over $MgSO_4$ and the solvent removed *in vacuo* to give a pale yellow solid (55 mg, 93%); R_f 0.3 (NH_2 SiO_2, 5% MeOH/EtOAc); m.p. 164-166 °C; λ_{max}(EtOH)/nm 293, 233; IR ν_{max}/cm^{-1} 3246, 2970, 1639, 1513; ^{1}H NMR (500 MHz; DMSO-*d$_6$*) δ_H 1.31-1.42 (2H, m, 2 × H-piperidine), 1.76-1.84 (2H, m, 2 × H-piperidine), 3.23-3.33 (2H, m, 2 × H-piperidine), 3.72-3.80 (1H, m, CHOH), 4.23-4.30 (2H, m, 2 × H-piperidine), 4.75 (1H, d, *J* = 4.2 Hz, OH), 7.40 (1H, s, H-pyrrole), 7.44 (1H, app t, *J* = 8.5 Hz, H-5'), 7.49 (1H, s, H-pyrrole), 8.23 (1H, d, *J* = 8.5 Hz, H-3'), 7.62 (1H, td, *J* = 8.5 and 6.1 Hz, H-4'), 8.61 (2H, s, 2 × H-pyrimidine), 10.05 (1H, s, CO-NH), 12.70 (1H, s, NH-pyrrole); ^{19}F NMR (470 MHz; DMSO-*d$_6$*) δ_F -114.35; ^{13}C NMR (125 MHz; DMSO-*d$_6$*) δ_C 33.9 (C-piperidine), 48.6 (C-piperidine), 66.2 (C-piperidine), 111.1 (CH-pyrrole), 115.0 (d, J_{CF} = 21.5 Hz, C-5'), 123.2 (C-pyrimidine), 125.2 (C-pyrrole), 125.8 (d, J_{CF} = 3.6 Hz, C-3'), 128.1 (d, J_{CF} = 22.7 Hz, C-1'), 128.1 (C-pyrrole), 128.9 (CH-pyrrole), 130.4 (d, J_{CF} = 5.4 Hz, C-2'), 131.8 (d, J_{CF} = 8.6 Hz, C-4'), 151.2 (2 × CH-pyrimidine), 158.4 (C-pyrimidine), 158.4 (CO-NH), 158.6 (d, J_{CF} = 246.8 Hz, C-2'), 183.9 (CO); HRMS calc for $C_{21}H_{20}{}^{35}Cl_1F_1N_5O_3$ [M+H]$^+$ 444.1233, found 444.1225.

1-(5-(4-(3,6-Dichloro-2-fluorobenzoyl)-1*H*-pyrrole-2-carboxamido)pyrimidin-2-yl)piperidin-4-yl acetate (284)
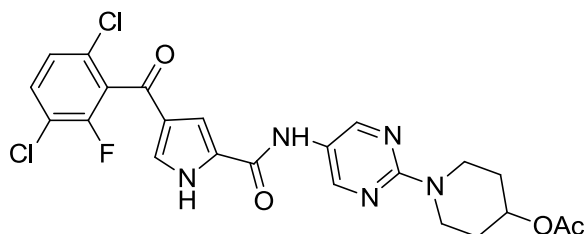
Prepared according to general procedure E using amine **358** (190 mg, 0.81 mmol, 2.5 eq.), carboxylic acid **337** (98 mg, 0.32 mmol, 1 eq.), cyanuric fluoride (19 μL, 0.23 mmol, 0.7

eq.), pyridine (26 μL, 0.32 mmol, 1 eq.) and MeCN (2 mL). Purification by MPLC on NH$_2$ SiO$_2$ with a gradient elution from 20-55% EtOAc/petrol gave a pale yellow solid (90 mg, 54%); R_f 0.3 (NH$_2$ SiO$_2$, 50% EtOAc/petrol); m.p. 252-254 °C; λ_{max}(EtOH)/nm 290, 226; IR ν_{max}/cm^{-1} 3238, 1711, 1650, 1577; ^{1}H NMR (500 MHz; DMSO-d_6) δ_H 1.50-1.61 (2H, m, 2 × H-piperidine), 1.87-1.96 (2H, m, 2 × H-piperidine), 2.06 (3H, s, COCH$_3$), 3.46-3.53 (2H, m, 2 × H-piperidine), 4.16-4.23 (2H, m, 2 × H-piperidine), 4.92-4.99 (1H, m, CHOAc), 7.44 (1H, s, H-pyrrole), 7.56 (1H, dd, J = 1.2 and 8.7 Hz, H-5'), 7.64 (1H, s, H-pyrrole), 7.82 (1H, app t, J = 8.7 Hz, H-4'), 8.65 (2H, s, 2 × H-pyrimidine), 10.07 (1H, s, CO-NH), 12.78 (1H, s, NH-pyrrole); ^{19}F NMR (470 MHz; DMSO-d_6) δ_F -116.68; ^{13}C NMR (125 MHz; DMSO-d_6) δ_C 21.0 (CH$_3$), 30.0 (2 × CH$_2$-piperidine), 41.1 (2 × CH$_2$N-piperidine), 69.9 (CH-NH-piperidine), 111.0 (CH-pyrrole), 119.3 (d, J_{CF} = 18.1 Hz, C-3'), 123.6 (C-pyrimidine), 124.7 (C-pyrrole), 126.9 (d, J_{CF} = 3.6 Hz, C-5'), 128.3 (C-pyrrole), 129.2 (d, J_{CF} = 19.4 Hz, C-1'), 129.2 (C-6'), 129.9 (CH-pyrrole), 131.8 (C-4'), 151.2 (2 × CH-pyrimidine), 153.8 (d, J_{CF} = 248.3 Hz, C-2'), 158.2 (CO-NH), 158.4 (C-pyrimidine), 169.8 (CO-acetate), 182.6 (CO); HRMS calc for C$_{23}$H$_{21}$^{35}Cl$_2$F$_1$N$_5$O$_4$ [M+H]$^+$ 520.0949, found 520.0939.

4-(3,6-Dichloro-2-fluorobenzoyl)-N-(2-(4-hydroxypiperidin-1-yl)pyrimidin-5-yl)-1H-pyrrole-2-carboxamide (282)
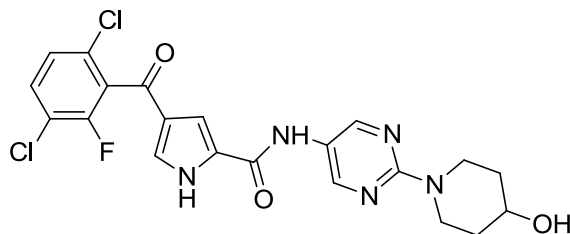
K$_2$CO$_{3(s)}$ (42 mg, 0.31 mmol, 2 eq.) was added to a solution of **284** (80 mg, 0.15 mmol, 1 eq.) in a mixture of THF (2 mL), MeOH (2 mL) and H$_2$O (2 mL). The mixture was stirred at r.t for 18 h, partitioned between EtOAc (2 × 25 mL) and H$_2$O (20 mL), washed with brine, dried over MgSO$_4$ and the solvent removed *in vacuo* to give a pale yellow solid (40 mg, 54%); R_f 0.5 (EtOAc); m.p. 200-202 °C; λ_{max}(EtOH)/nm 289, 227; IR ν_{max}/cm^{-1} 3251, 2934, 1638, 1585; ^{1}H NMR (500 MHz; DMSO-d_6) δ_H 1.31-1.41 (2H, m, 2 × H-piperidine), 1.76-1.86 (2H, m, 2 × H-piperidine), 3.28 (2H, ddd, J = 3.2 Hz, 10.0 and 13.3 Hz, 2 × CH-N piperidine), 3.72-3.80 (1H, m, CH-OH), 4.22-4.32 (2H, m, 2 × CH-N piperidine), 4.75 (1H, d, J = 4.3 Hz, OH), 7.43 (1H, s, H-pyrrole), 7.56 (1H, dd, J = 1.3 and 8.6 Hz, H-5'), 7.64 (1H, s, CH-pyrrole), 7.83 (1H, app t, J = 8.6 Hz, H-4'), 8.62 (2H, s,

2 × H-pyrimidine), 10.05 (1H, s, CO-NH), 12.77 (1H, s, NH-pyrrole); ^{19}F NMR (470 MHz; DMSO-d_6) δ_F -116.68; ^{13}C NMR (125 MHz; DMSO-d_6) δ_C 33.9 (2 × CH$_2$-piperidine), 41.5 (2 × CH$_2$-piperidine), 66.2 (CHOH), 111.0 (CH-pyrrole), 119.3 (d, J_{CF} = 18.1 Hz, C-3'), 123.2 (C-pyrimidine), 124.7 (C-pyrrole), 126.9 (d, J_{CF} = 3.6 Hz, C-5'), 128.4 (C-pyrrole), 129.2 (d, J_{CF} = 17.5 Hz, C-1'), 129.3 (C-6'), 129.9 (CH-pyrrole), 131.8 (C-4'), 151.2 (2 × CH-pyrimidine), 153.8 (d, J_{CF} = 248.4 Hz, C-2'), 158.4 (CO-NH), 158.4 (C-pyrimidine), 182.6 (CO); HRMS calc for C$_{21}$H$_{19}$^{35}Cl$_2$F$_1$N$_5$O$_3$ [M+H]$^+$ 478.0843, found 478.0834.

N-(1-Methylpiperidin-4-yl)-5-nitropyrimidin-2-amine (349)[360]
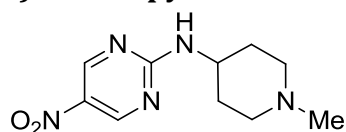
Prepared according to general procedure I using 2-chloro-5-nitropyrimidine (300 mg, 1.9 mmol, 1 eq.), 4-amino-1-methylpiperidine (259 μL, 2.1 mmol, 1.1 eq.), Et$_3$N (288 μL, 2.1 mmol, 1.1 eq) and THF (10 mL) to give a yellow solid (370 mg, 83%); R_f 0.5 (NH$_2$ SiO$_2$, EtOAc); m.p. 154-157 °C; λ_{max}(EtOH)/nm 340, 213; IR ν_{max}/cm^{-1} 3242, 1587, 1329; ^{1}H NMR (500 MHz; DMSO-d_6) δ_H 1.61 (2H, qd, J = 3.5 and 11.9 Hz, 2 × H-piperidine), 1.80-1.89 (2H, m, 2 × H-piperidine), 1.93-2.03 (2H, m, 2 × H-piperidine), 2.20 (3H, s, CH$_3$), 2.77-2.84 (2H, m, 2 × H-piperidine), 3.80-3.90 (1H, m, C*H*-NH), 8.83 (1H, d, J = 8.4 Hz, NH), 9.07 (1H, d, J = 3.4 Hz, H-pyrimidine), 9.13 (1H, d, J = 3.4 Hz, H-pyrimidine); ^{13}C NMR (125 MHz; DMSO-d_6) δ_C 30.9 (2 × CH$_2$-piperidine), 45.9 (N-CH$_3$), 48.4 (CH-NH), 54.1 (2 × CH$_2$-N-piperidine), 133.5 (C-5-pyrimidine), 155.2 (CH-pyrimidine), 155.4 (CH-pyrimidine), 162.1 (C-2-pyrimidine); HRMS calcd for C$_{10}$H$_{16}$N$_5$O$_2$ [M+H]$^+$ 238.1299, found 238.1301.

N^2-(1-Methylpiperidin-4-yl)pyrimidine-2,5-diamine (359)[360]
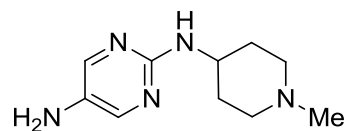
Prepared according to general procedure H using nitropyrimidine **349** (360 mg, 1.52 mmol) and MeOH (30 mL) for 2 h to give a pale yellow solid (290 mg, 92%); R_f 0.5 (NH$_2$ SiO$_2$, 5% MeOH/EtOAc); m.p. 158-161 °C; λ_{max}(EtOH)/nm 248; IR ν_{max}/cm^{-1} 3257, 2967, 2789; ^{1}H NMR (500 MHz; DMSO-d_6) δ_H 1.45 (2H, qd, J = 3.6 and 11.7 Hz, 2 × H-piperidine), 1.78-1.86 (2H, m, 2 × H-piperidine), 1.90-1.99 (2H, m, 2 × H-piperidine), 2.17

(3H, s, CH$_3$), 2.70-2.77 (2H, m, 2 × H-piperidine), 3.46-3.56 (1H, m, C*H*-NH), 4.41 (2H, s, NH$_2$), 6.02 (1H, d, J = 8.0 Hz, NH), 7.82 (2H, s, 2 × H-pyrimidine); ^{13}C NMR (125 MHz; DMSO-d_6) δ$_C$ 31.8 (2 × CH$_2$-piperidine), 46.1 (N-CH$_3$), 47.5 (CH-NH), 54.6 (2 × CH$_2$N-piperidine), 133.5 (C-5 pyrimidine), 144.6 (2 × CH-pyrimidine), 156.0 (C-2 pyrimidine); HRMS calcd for C$_{10}$H$_{18}$N$_5$ [M+H]$^+$ 208.1557, found 208.1559.

4-(2-Chloro-6-fluorobenzoyl)-*N*-(2-((1-methylpiperidin-4-yl)amino)pyrimidin-5-yl)-1*H*-pyrrole-2-carboxamide (288)
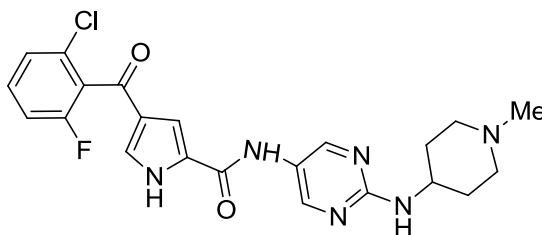
Prepared according to general procedure E using amine **359** (140 mg, 0.68 mmol, 2.5 eq.), carboxylic acid **336** (72 mg, 0.27 mmol, 1 eq.), cyanuric fluoride (16 μL, 0.19 mmol, 0.7 eq.), pyridine (22 μL, 0.27 mmol, 1 eq.) and MeCN (2 mL). Purification by MPLC on NH$_2$ SiO$_2$ with a gradient elution from 1-8% MeOH/EtOAc gave a white solid (43 mg, 35 %); R_f 0.25 (NH$_2$ SiO$_2$, 10% MeOH/EtOAc); m.p. 287 °C dec.; λ$_{max}$(EtOH)/nm 284, 233; IR ν$_{max}$/cm^{-1} 3278, 1637, 1607; ^{1}H NMR (500 MHz; DMSO-d_6) δ$_H$ 1.53 (2H, qd, J = 3.1 and 11.4 Hz, 2 × H-piperidine), 1.80-1.89 (2H, m, 2 × H-piperidine), 1.98 (2H, app t, J = 11.4 Hz, 2 × H-piperidine), 2.19 (3H, s, CH$_3$), 2.73-2.82 (2H, m, 2 × H-piperidine), 3.60-3.71 (1H, m, C*H*-NH), 7.03 (1H, d, J = 7.9 Hz, NH-piperidine), 7.39 (1H, s, H-pyrrole), 7.43 (1H, app t, J = 8.4 Hz, H-5'), 7.48 (1H, s, H-pyrrole), 7.50 (1H, d, J = 8.4 Hz, H-3'), 7.62 (1H, td, J = 8.4 and 6.3 Hz Hz, H-4'), 8.51 (2H, s, 2 × H-pyrimidine), 9.98 (1H, s, CO-NH), 12.68 (1H, s, NH-pyrrole); ^{19}F NMR (470 MHz; DMSO-d_6) δ$_F$ -114.36; ^{13}C NMR (125 MHz; DMSO-d_6) δ$_C$ 31.5 (2 × CH$_2$-piperidine), 46.0 (CH$_3$), 48.6 (CHNH-piperidine), 54.5 (2 × CH$_2$N-piperidine), 111.0 (CH-pyrrole), 115.0 (d, J_{CF} = 21.7 Hz, C-5'), 123.2 (C-pyrimidine), 125.2 (C-pyrrole), 125.8 (d, J_{CF} = 3.2 Hz, C-3'), 128.1 (d, J_{CF} = 22.98 Hz, C-1'), 128.2 (C-pyrrole), 128.9 (CH-pyrrole), 130.4 (d, J_{CF} = 6.4 Hz, C-2'), 131.8 (d, J_{CF} = 9.1 Hz, C-4'), 151.6 (2 × CH-pyrimidine), 158.4 (CO-NH), 158.5 (d, J_{CF} = 247.0 Hz, C-6), 158.9 (C-pyrimidine), 183.9 (CO); HRMS calcd for C$_{22}$H$_{23}$^{35}Cl$_1$F$_1$N$_6$O$_3$ [M+H]$^+$ 457.1550, found 457.1531.

4-(3,6-Dichloro-2-fluorobenzoyl)-*N*-(2-((1-methylpiperidin-4-yl)amino)pyrimidin -5-yl)-1*H*-pyrrole-2-carboxamide (289)
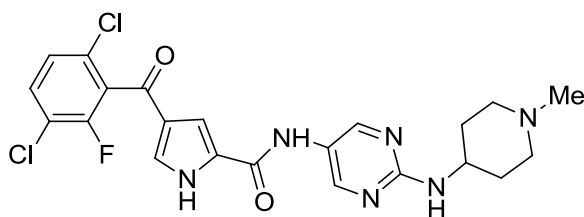
Prepared according to general procedure E using amine **359** (150 mg, 0.72 mmol, 2.5 eq.), carboxylic acid **337** (88 mg, 0.29 mmol, 1 eq.), cyanuric fluoride (21 µL, 0.24 mmol, 0.7 eq.), pyridine (23 µL, 0.29 mmol, 1 eq.) and MeCN (2 mL). Purification by MPLC on NH₂ SiO₂ with a gradient elution from 1-7% MeOH/EtOAc gave a white solid (50 mg, 35 %); R_f 0.20 (5% MeOH/EtOAc, NH₂ SiO₂); m.p. 275 °C dec.; λ_{max}(EtOH)/nm 283, 226; IR ν_{max}/cm^{-1} 3163, 1642, 1593; ^{1}H NMR (500 MHz; DMSO-d_6) δ_H 1.54 (2H, qd, J = 3.1 and 11.5 Hz, 2 × H-piperidine), 1.81-1.89 (2H, m, 2 × H-piperidine), 1.92-2.02 (2H, m, 2 × H-piperidine), 2.19 (3H, s, CH₃), 2.73-2.81 (2H, m, 2 × H-piperidine), 3.61-3.72 (1H, m, C*H*-NH-piperidine), 7.02 (1H, d, J = 7.8 Hz, NH-piperidine), 7.42 (1H, s, H-pyrrole), 7.56 (1H, d, J = 8.6 Hz, H-5'), 7.63 (1H, s, H-pyrrole), 7.82 (1H, app t, J = 8.6 Hz, H-4'), 8.51 (2H, s, 2 × H-pyrimidine), 9.98 (1H, s, CO-NH), 12.74 (1H, br s, NH-pyrrole); ^{19}F NMR (470 MHz; DMSO-d_6) δ_F -116.67; ^{13}C NMR (125 MHz; DMSO-d_6) δ_C 31.5 (2 × CH₂-piperidine), 46.0 (CH₃), 48.6 (CH-NH-piperidine), 54.5 (2 × CH₂N-piperidine), 110.9 (CH-pyrrole), 119.3 (d, J_{CF} = 18.0 Hz, C-3'), 123.2 (C-pyrimidine), 124.7 (C-pyrrole), 126.9 (d, J_{CF} = 3.6 Hz, C-5'), 128.5 (C-pyrrole), 128.8 (CH-pyrrole), 129.2 (d, J_{CF} = 22.3 Hz, C-1'), 129.2 (d. J_{CF} = 5.1 Hz, C-6'), 131.8 (C-4'), 151.6 (2 × CH-pyrimidine), 153.8 (d, J_{CF} = 248.9 Hz, C-2'), 158.4 (CO-NH), 158.9 (C-pyrimidine), 182.6 (CO); HRMS calcd for C₂₂H₂₁^{35}Cl₂F₁N₆O₂ [M+H]$^+$ 491.1160, found 491.1150.

N-(1-Cyclopropylpiperidin-4-yl)-5-nitropyrimidin-2-amine (350)

Prepared according to general procedure I using 1-cyclopropylpiperidin-4-amine (125 mg, 0.89 mmol, 1 eq.), 2-chloro-4-nitropyrimidine (142 mg, 0.89 mmol, 1 eq.), Et₃N (136 µL, 0.98 mmol, 1.1 eq.) and THF (2 mL) with stirring for 3 h to give a yellow solid (222 mg, 95%); R_f 0.8 (EtOAc, NH₂ SiO₂); m.p. 141-143 °C; λ_{max}(EtOH)/nm 348, 216; IR ν_{max}/cm^{-1} 1576, 1545, 1328; ^{1}H NMR (500 MHz; DMSO-d_6) δ_H 0.29-0.34 (2H, m, 2 × H-cPr), 0.42-

0.47 (2H, m, $2 \times$ H-cPr), 1.52 (2H, qd, J = 3.6 and 12.0 Hz, $2 \times$ H-piperidine), 1.60-1.66 (1H, m, N-CH cPr), 1.80-1.88 (2H, m, $2 \times$ H-piperidine), 2.21-2.30 (2H, m, $2 \times$ H-piperidine), 2.93-3.00 (2H, m, $2 \times$ H-piperidine), 3.84-3.94 (1H, m, CH-NH piperidine), 8.83 (1H, d, J = 7.9 Hz, NH), 9.07 (1H, d, J = 3.3 Hz, H-pyrimidine), 9.14 (1H, d, J = 3.3 Hz, H-pyrimidine); ^{13}C NMR (125 MHz; DMSO-d_6) δ_C 6.0 ($2 \times$ CH$_2$-cPr), 31.0 ($2 \times$ CH$_2$-piperdine), 38.0 (CHN-cPr), 49.0 (CHN-piperidine), 52.0 ($2 \times$ CH$_2$-piperdine), 133.5 (C-pyrimidine), 155.2 (CH-pyrimidine), 155.4 (CH-pyrimidine), 162.1 (C-pyrimidine); HRMS calcd for $C_{12}H_{18}N_5O_2$ [M+H]$^+$ 264.1455, found 264.1455.

*N*²-(1-cyclopropylpiperidin-4-yl)pyrimidine-2,5-diamine (360)
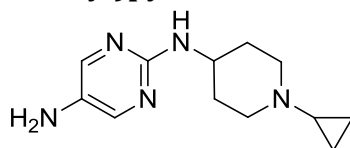
Prepared according to general procedure H using nitropyrimidine **350** (207 mg, 0.79 mmol), MeOH (20 mL) and EtOAc (20 mL) for 2 h to give an orange gum (279 mg, 100%); R_f 0.3 (EtOAc, NH$_2$ SiO$_2$); m.p. 120-122 °C; λ_{max}(EtOH)/nm 250, 228; IR ν_{max}/cm^{-1} 3285, 3204, 2932, 2789; ^{1}H NMR (500 MHz; DMSO-d_6) δ_H 0.27-0.32 (2H, m, $2 \times$ H-cPr), 0.41-0.45 (2H, m, $2 \times$ H-cPr), 1.37 (2H, qd, J = 3.2 and 11.3 Hz, $2 \times$ H-piperidine), 1.57-1.63 (1H, m, N-CH cPr), 1.78-1.85 (2H, m, $2 \times$ H-piperidine), 2.19-2.27 (2H, m, $2 \times$ H-piperidine), 2.88-2.95 (2H, m, $2 \times$ H-piperidine), 3.50-3.61 (1H, m, CH-NH piperidine), 4.40 (2H, s, NH$_2$), 6.01 (1H, d, J = 8.1 Hz, NH), 7.82 (2H, s, $2 \times$ H-pyrimidine); ^{13}C NMR (125 MHz; DMSO-d_6) δ_C 5.9 ($2 \times$ CH$_2$-cyclopropyl), 31.8 ($2 \times$ CH$_2$-piperidine), 38.1 (CHN-cyclopropyl), 48.1 (CHN-piperidine), 52.4 ($2 \times$ CH$_2$-piperidine), 133.5 (C-5-pyrimidine), 144.6 (C-4 and C-6-pyrimidine), 155.9 (C-2-pyrimidine); HRMS calc for $C_{23}H_{21}{}^{35}Cl_2F_1N_5O_4$ [M+H]$^+$ 234.1713, found 234.1710.

N-(2-((1-Cyclopropylpiperidin-4-yl)amino)pyrimidin-5-yl)-4-(3,6-dichloro-2-fluorobenzoyl)-1*H*-pyrrole-2-carboxamide (290)
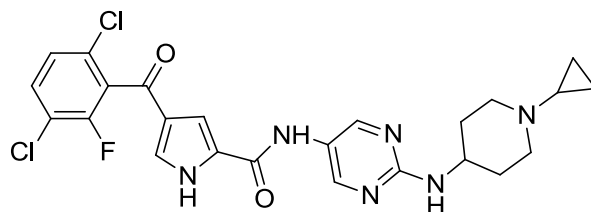
Prepared according to general procedure E using amine **360** (170 mg, 0.73 mmol, 2.5 eq.), carboxylic acid **337** (88 mg, 0.29 mmol, 1 eq.), cyanuric fluoride (7 µL, 0.09 mmol, 0.3

eq.), pyridine (23 μL, 0.29 mmol, 1 eq.) and MeCN (2 mL), with stirring for 24 h at room temperature followed by 24 h at 40 °C. Purification by MPLC on SiO_2 with a gradient elution from 4-15% MeOH/EtOAc gave a yellow solid (23 mg, 15%); R_f 0.25 (EtOAc, NH_2 SiO_2); m.p. 170 °C dec.; λ_{max}(EtOH)/nm 294, 216; IR ν_{max}/cm^{-1} 3311 (br), 1640, 1609; ^{1}H NMR (500 MHz; DMSO-d_6) δ_H 0.29-0.34 (2H, m, 2 × H-cyclopropyl), 0.41-0.46 (2H, m, 2 × H-cyclopropyl), 1.45 (2H, app qd, J = 3.6 and 11.8 Hz, 2 × H-piperidine), 1.59-1.65 (1H, m, N-CH-cyclopropyl), 1.81-1.88 (2H, m, 2 × H-piperidine), 2.25 (2H, app td, J = 11.8 and 2.0 Hz, 2 × H-piperidine), 2.90-3.00 (2H, m, 2 × H-piperidine), 3.65-3.75 (1H, m, NH-CH--piperidine), 7.03 (1H, d, J = 7.9 Hz, NH), 7.42 (1H, s, H-pyrrole), 7.56 (1H, dd, J = 1.1 and 8.5 Hz, H-4'), 7.63 (1H, s, H-pyrrole), 7.82 (1H, app t, J = 8.5 Hz, H-5'), 8.51 (2H, s, 2 × H-pyrimidine); ^{19}F NMR (470 MHz; DMSO-d_6) δ_F -116.68; ^{13}C NMR (125 MHz; DMSO-d_6) δ_C 6.0 (2 × CH$_2$-cPr), 31.500 (2 × CH$_2$-piperidine), 38.1 (CHN-cPr), 48.1 (CHN-piperidine), 52.3 (2 × CH$_2$N-piperidine), 110.9 (CH-pyrrole), 119.3 (d, J_{CF} = 18.2 Hz, C-3'), 123.1 (C-pyrimidine), 124.7 (C-pyrrole), 126.9 (d, J_{CF} = 3.6 Hz, C-5'), 128.4 (C-pyrrole), 129.2 (d, J_{CF} = 22.71 Hz, C-1'), 129.2 (d, J_{CF} = 5.2 Hz, C-6'), 129.8 (CH-pyrrole), 131.8 (C-4'), 151.6 (C-pyrimidine), 153.8 (d, J_{CF} = 248.5 Hz, C-2'), 158.4 (CO-NH), 158.9 (C-pyrimidine), 182.6 (CO); HRMS calcd for $C_{24}H_{24}{}^{35}Cl_2F_1N_6O_2$ [M+H]$^+$ 517.1319, found 517.1304.

2-Methoxy-5-nitropyrimidine (363)[361,362]
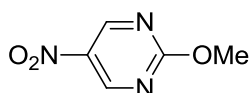
Sodium (35 mg, 1.5 mmol, 1.2 eq.) was added to methanol (5 mL) and the mixture stirred under nitrogen until the sodium had dissolved. 5-Nitro-2-chloropyrimidine (200 mg, 1.25 mmol, 1 eq.) was added and the mixture heated at reflux for 1 h. The solvent was removed *in vacuo* and the residue purified by MPLC on SiO_2 with a gradient elution from 10-20% EtOAc/petrol to give a yellow solid (115 mg, 59%); Rf 0.4 (20% EtOAc/petrol); m.p. 65-67 °C (Lit.[361] 69-70 °C); λ_{max}(EtOH)/nm 270 nm; IR ν_{max}/cm^{-1} 1567, 1474, 1404, 1315; ^{1}H NMR (500 MHz; DMSO-d_6) δ_H 4.08 (3H, s, OMe), 9.42 (2H, s, H-pyrimidine); ^{13}C NMR (125 MHz; DMSO-d_6) δ_C 56.4 (Me), 138.8 (C-NO$_2$), 156.4 (2 × CH-pyrimidine), 166.7 (*C*-O-Me); MS *m/z* (ES+) 156.2 [M+H]$^+$.

2-Methoxypyrimidin-5-amine (364)[363]
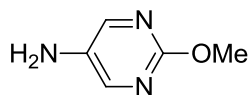
Prepared according to general procedure H using nitropyrimidine **363** (140 mg, 0.9 mmol) in MeOH (5 mL) for 90 min. The solvent was removed *in vacuo* to give a white solid (109 mg, 97%); R_f 0.1 (5% MeOH/DCM, NH$_2$ SiO$_2$); m.p. 113-116 °C (lit.[363] 119-120 °C) ; λ_{max}(EtOH)/nm 327, 237; IR ν_{max}/cm^{-1} 3304, 3180, 1648(w), 1565; ^{1}H NMR (500 MHz; DMSO-d_6) δ_H 3.78 (3H, s, OMe), 5.01 (2H, s, NH$_2$), 7.99 (s, 2H, H-pyrimidine); ^{13}C NMR (125 MHz; DMSO-d_6) δ_C 53.9 (OMe), 137.9, (C-NH$_2$), 144.3 (2 × CH-pyrimidine), 157.8 (*C*-O-Me); MS *m/z* (ES+) 126.2 [M+H]$^+$.

4-(2-Chloro-6-fluorobenzoyl)-*N*-(2-methoxypyrimidin-5-yl)-1*H*-pyrrole-2-carboxamide (271)
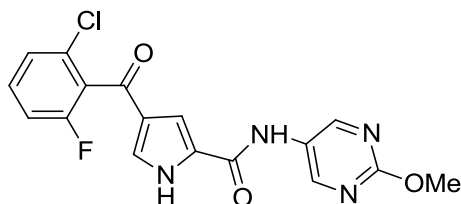
Prepared according to general procedure E using carboxylic acid **336** (86 mg, 0.32 mmol, 1 eq.), amine **364** (100 mg, 0.8 mmol, 2.5 eq.), pyridine (26 µL, 0.32 mmol, 1 eq.) and cyanuric fluoride (19 µL, 0.22 mmol, 0.7 eq.). Purification by MPLC on SiO$_2$ with a gradient elution from 0-3% MeOH/CH$_2$Cl$_2$ gave a white solid (52 mg, 43 %); R_f ; 0.15 (50% EtOAc/petrol); m.p. 258 °C dec.; λ_{max}(EtOH)/nm 267; IR ν_{max}/cm^{-1} 3337, 2961, 1649, 1616, 1583; ^{1}H NMR (500 MHz; DMSO-d_6) δ_H 3.94 (3H, s, OMe), 7.41-7.48 (2H, m, H-pyrrole and H-5'), 7.51 (1H, d, *J* = 8.3 Hz, H-3'), 7.54 (1H, br s, H-pyrrole), 7.62 (1H, td, *J* = 8.3 and 6.3 Hz, H-4'), 8.90 (2H, s, 2 × CH-pyrimidine), 10.34 (1H, s, NH), 12.78 (1H, br s, NH); ^{19}F NMR (470 MHz; DMSO-d_6) δ_F -114.34; ^{13}C NMR (125 MHz; DMSO-d_6) δ_C 54.7 (OMe), 111.6 (CH-pyrrole), 115.0 (d, J_{CF} = 21.3 Hz, C-5'), 125.3 (C-pyrrole), 125.9 (d, J_{CF} = 3.0 Hz, C-3'), 127.8 (C-pyrimidine), 128.0 (d, J_{CF} = 23.2 Hz, C-1'), 128.6 (C-pyrrole), 129.3 (CH-pyrrole), 130.4 (d, J_{CF} = 5.9 Hz, C-2'), 131.9 (d, J_{CF} = 9.1 Hz, C-4'), 151.4 (C-pyrimidine), 156.6 (d, J_{CF} = 248 Hz, C-6'), 158.55 (C-pyrimidine), 161.3 (CO-NH), 183.9 (CO); MS (ES+) *m/z* 375.3 (75.8%) [M(^{35}Cl)+H]$^+$, 377.3 (24.2%) [M(^{37}Cl)+H]$^+$; HRMS calcd for C$_{17}$H$_{12}$^{35}Cl$_1$F$_1$N$_4$O$_3$ [M+H]$^+$ 375.0655, found 375.0648.

tert-Butyl 4-(5-nitropyridin-2-yl)piperazine-1-carboxylate (366)[365]
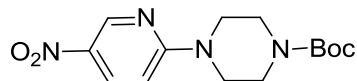
N^1-Boc-piperazine (2.35 g, 12.7 mmol, 2 eq.), 2-chloro-5-nitropyridine (1.00 g, 6.3 mmol, 1 eq.) and K_2CO_3 (1.75 g, 12.7 mmol, 2 eq.) were combined in THF (10 mL) and stirred at r.t. for 72 h. The mixture was partitioned between EtOAc (2 × 70 mL) and HCl (2 × 30 mL, 0.5 M aq.) washed with brine, dried over $MgSO_4$ and the solvent removed *in vacuo* to give an orange oil (1.85 g, 97 %); R_f 0.5 (50% EtOAc/Petrol); m.p.168-170 °C (Lit.[364] 169 °C); λ_{max}(EtOH)/nm 358, 228; IR ν_{max}/cm^{-1} 1688, 1594, 1338; ^{1}H NMR (500 MHz; DMSO-d_6) δ_H 1.46 (9H, s, C(CH_3)$_3$), 3.46-3.52 (4H, m, 4 × H-piperazine), 3.78-3.83 (4H, m, 4 × H-piperazine), 6.97 (1H, d, J = 9.6 Hz, H-3-pyridine), 8.29 (1H, dd, J = 2.8 and 9.6 Hz, H-4-pyridine), 9.01 (1H, d, J = 2.8 Hz, H-6-pyridine); ^{13}C NMR (125 MHz; DMSO-d_6) δ_C 28.0 (C(CH_3)$_3$), 44.1 (C-piperazine), 79.2 (C(CH$_3$)$_3$), 105.7 (C-3-pyridine), 132.9 (C-4-pyridine), 134.4 (C-5-pyridine), 146.0 (C-6-pyridine), 153.8 (C-2-pyridine), 160.1 (CO); HRMS calc for $C_{14}H_{21}N_4O_4$ [M+H]$^+$ 309.1557, found 309.1558.

tert-Butyl 4-(5-aminopyridin-2-yl)piperazine-1-carboxylate (368)[366]
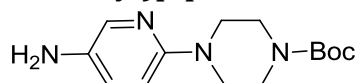
Prepared according to general procedure H using nitropyridine **366** (1.83 g, 5.9 mmol), MeOH (60 mL) and EtOAc (60 mL) for 24 h to give a beige solid (1.65 g, 100%); R_f 0.65 (EtOAc, NH$_2$ SiO$_2$); m.p. 109 °C dec.; λ_{max}(EtOH)/nm 255; IR ν_{max}/cm^{-1} 3382, 3321, 2975.8, 2820, 1685; ^{1}H NMR (500 MHz; DMSO-d_6) δ_H 1.45 (9H, s, C(CH_3)$_3$), 3.19-3.25 (4H, m, 4 × H-piperazine), 3.40-3.47 (4H, m, 4 × H-piperazine), 4.64 (2H, br s, NH$_2$), 6.68 (1H, d, J = 8.7 Hz, H-3-pyridine), 6.96 (1H, dd, J = 2.9 and 8.7 Hz, H-4-pyridine), 7.64 (1H, d, J = 2.9 Hz, H-6-pyridine); ^{13}C NMR (125 MHz; DMSO-d_6) δ_C 28.1 (C(CH_3)$_3$), 43.4 (C-piperazine), 46.3 (C-piperazine), 78.8 (C(CH$_3$)$_3$), 108.8 (C-3-pyridine), 124.4 (C-4-pyridine), 133.3 (C-5-pyridine), 137.6 (C-6-pyridine), 152.0 (C-2-pyridine), 153.9 (CO-carbamate); HRMS calc for $C_{14}H_{21}N_4O_2$ [M-H]$^-$ 277.1670, found 277.1666.

tert-Butyl 4-(5-(4-(3,6-dichloro-2-fluorobenzoyl)-1_H_-pyrrole-2-carboxamido) pyridin-2-yl)piperazine-1-carboxylate (370)
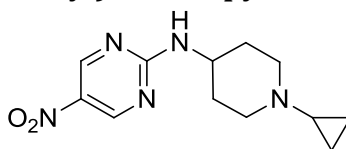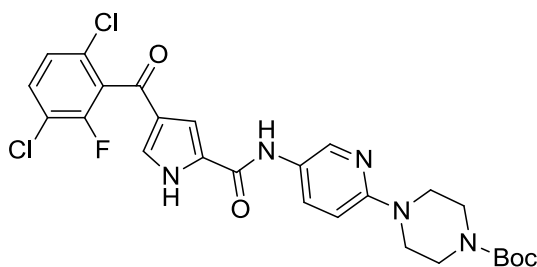

Prepared according to general procedure E using amine **368** (436 mg, 1.57 mmol, 2.5 eq.), carboxylic acid **337** (190 mg, 0.63 mmol, 1 eq.), cyanuric fluoride (16 μL, 0.19 mmol, 0.3 eq.), pyridine (51 μL, 0.63 mmol, 1 eq.) and MeCN (4 mL) with stirring at 40 °C for 18 h. Purification by MPLC on SiO_2 with a gradient elution from 20-60% EtOAc/petrol gave a grey solid (160 mg, 45%); R_f 0.5 (EtOAc, NH_2 SiO_2); m.p. 159-160 °C; λ_{max}(EtOH)/nm 293, 213; IR ν_{max}/cm^{-1} 1663, 1647; ^{1}H NMR (500 MHz; DMSO-d_6) δ_H 1.46 (9H, s, C(CH_3)$_3$), 3.34-3.38 (4H, br s, 8 × H-piperazine), 6.91 (1H, d, J = 9.0 Hz, H-3-pyridine), 7.46 (1H, br s, H-pyrrole), 7.55 (1H, dd, J = 1.3 and 8.8 Hz, H-3'), 7.61 (1H, br s, H-pyrrole), 7.82 (1H, app t, J = 8.8 Hz, H-4'), 7.90 (1H, dd, J = 2.5 and 9.0 Hz, H-4-pyridine'), 8.46 (1H, d, J = 2.5 Hz, H-6-pyridine), 10.01 (1H, s, CO-NH), 12.72 (1H, s, NH-pyrrole); ^{19}F NMR (470 MHz; DMSO-d_6) δ_F -116.67; ^{13}C NMR (125 MHz; DMSO-d_6, 110 °C) δ_C 28.7 (C(CH_3)$_3$), 43.6 (2 × CH_2-piperazine)), 45.6 (2 × CH_2-piperazine), 79.5 (C(CH$_3$)$_3$), 107.4 (C-3-pyridine), 111.4 (CH-pyrrole), 119.4 (d, J_{CF} = 18.1 Hz), 124.7 (C-pyrrole), 126.4 (C-pyridine), 126.9 (d, J_{CF} = 3.6 Hz, C-5'), 128.8 (C-pyrrole), 129.2 (d, J_{CF} = 23.2 Hz, C-1'), 129.2 (d, J_{CF} = 5.0 Hz, C-6'), 129.8 (CH-pyrrole), 131.0 (C-pyridine), 131.8 (C-4'), 140.0 (C-pyridine), 153.8 (d, J_{CF} = 248.4 Hz, C-2'), 153.9 (CO-carbamate), 155.6 (C-pyridine), 158.2 (CO-NH), 182.6 (CO); HRMS calc for $C_{26}H_{27}{}^{35}Cl_2F_1N_5O_4$ [M+H]$^+$ 562.1419, found 562.1415.

4-(3,6-Dichloro-2-fluorobenzoyl)-*N*-(6-(piperazin-1-yl)pyridin-3-yl)-1*H*-pyrrole-2-carboxamide (292)
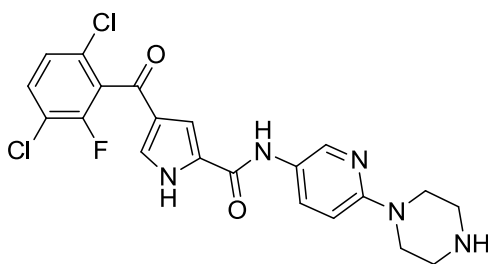
Prepared according to general procedure G using carbamate **370** (145 mg, 0.26 mmol, 1 eq.), Et$_3$SiH (102 µL, 0.64 mmol, 2.5 eq.), TFA (1.5 mL) and CH$_2$Cl$_2$ (1.5 mL). The reaction was purified by MPLC on NH$_2$ SiO$_2$ with a gradient elution from 0-4% MeOH/EtOAc gave a yellow solid 55 mg (46%); R_f 0.4 (5% MeOH/EtOAc, NH$_2$ SiO$_2$); m.p. 195 °C dec.; λ_{max}(EtOH)/nm 293, 213; IR ν_{max}/cm^{-1} 1633; ^{1}H NMR (500 MHz; DMSO-d_6) δ_H 2.78-2.84 (4H, m, 4 × H-piperazine), 3.36-3.41 (4H, m, 4 × H-piperazine), 6.85 (1H, d, *J* = 9.1 Hz, H-3-pyridine), 7.45 (1H, s, H-pyrrole), 7.55 (1H, dd, *J* = 1.2 and 8.6 Hz, H-3'), 7.61 (1H, s, H-pyrrole), 7.82 (1H, app t, *J* = 8.6 Hz, H-4'), 7.86 (1H, dd, *J* = 2.6 and 9.1 Hz, H-4-pyridine), 8.43 (1H, d, *J* = 2.6 Hz, H-6-pyridine), 9.98 (1H, s, CO-NH); ^{19}F NMR (470 MHz; DMSO-d_6) δ_F -116.66; ^{13}C NMR (125 MHz; DMSO-d_6) δ_C 45.4 (2 × CH$_2$-piperazine), 46.2 (2 × CH$_2$-piperazine), 106.6 (C-3-pyridine), 110.7 (CH-pyrrole), 119.3 (d, J_{CF} = 18.1 Hz, C-3'), 124.7 (C-pyrrole), 125.9 (C-pyridine), 126.9 (d, J_{CF} = 3.7 Hz, C-5'), 128.9 (C-pyrrole), 129.2 (d, J_{CF} = 5.1 Hz, C-6'), 129.2 (d, J_{CF} = 23.2 Hz, C-1'), 129.8 (CH-pyrrole), 130.9 (C-2-pyridine), 131.8 (C-4-pyridine), 140.1 (C-6-pyridine), 153.8 (d, J_{CF} = 248.4 Hz, C-2'), 156.3 (C-5-pyridine), 158.2 (CO-NH), 182.6 (CO); HRMS calc for C$_{21}$H$_{19}$^{35}Cl$_2$F$_1$N$_5$O$_2$ [M+H]$^+$ 462.0894, found 462.0884.

tert-Butyl 4-(5-(4-(6-chloro-2-fluoro-3-methoxybenzoyl)-1*H*-pyrrole-2-carboxamido)pyridin-2-yl)piperazine-1-carboxylate (422)

Prepared according to general procedure E using amine **368** (350 mg, 1.26 mmol, 2.5 eq.), carboxylic acid **421** (150 mg, 0.50 mmol, 1 eq.), cyanuric fluoride (30 µL, 0.35 mmol, 0.7

eq.), pyridine (41 μL, 0.50 mmol, 1 eq.) and MeCN (3 mL) with stirring at r.t. for 18 h. Purification by MPLC on SiO$_2$ with a gradient elution from 40-60% EtOAc/petrol gave a white solid (141 mg, 50%);. R_f 0.1 (40% EtOAc/petrol, SiO$_2$); m.p. 144 °C dec.; IR v_{max}/cm^{-1} 3269 br, 2975.9, 1644.8; ^{1}H NMR (500 MHz; DMSO-d_6) δ_H 1.46 (9H, s, C(CH_3)$_3$), 3.36 (8H, br s, 8 × CH-piperazine), 3.94 (3H, s OCH$_3$), 6.91 (1H, d, J = 9.1 Hz, H-3-pyridine), 7.36 (1H, app t, J = 9.0 Hz, H-4'), 7.40-7.45 (2H, m, H-pyrrole and H-3'), 7.47 (H-pyrrole), 7.90 (1H, dd, J = 2.6 and 9.1 Hz, H-4-pyridine'), 8.46 (1H, d, J = 2.6 Hz, H-6-pyridine), 10.01 (1H, s, CO-NH), 12.64 (1H, s, NH-pyrrole); ^{19}F NMR (470 MHz; DMSO-d_6) δ_F -136.15; ^{13}C NMR (125 MHz; DMSO-d_6) δ_C 28.1 (C(CH$_3$)$_3$), 44.9 (4 × CH$_2$-piperazine), 56.4 (OCH$_3$), 79.0 (C(CH$_3$)$_3$), 107.1 (C-3-pyridine), 110.9 (CH-pyrrole), 115.1 (C-4'), 120.2 (d, J_{CF} = 4.8 Hz, C-1'), 125.1 (C-pyrrole), 125.5 (d, J_{CF} = 3.6 Hz, C-5'), 126.4 (C-pyridine), 128.4 (C-6'), 128.5 (C-pyrrole), 129.0 (CH-pyrrole), 130.9 (C-4-pyridine), 140.0 (C-6-pyridine), 146.4 (d, J_{CF} = 10.7 Hz, C-3'), 147.9 (d, J_{CF} = 247.0 Hz, C-2'), 153.9 (CO-carbamate), 155.6 (C-5-pyridine), 158.2 (CO-NH), 183.6 (CO); HRMS calcd for C$_{27}$H$_{30}$^{35}Cl$_1$F$_1$N$_5$O$_5$ [M+H]$^+$ 558.1925, found 558.1911.

## 4-(6-Chloro-2-fluoro-3-methoxybenzoyl)-*N*-(6-(piperazin-1-yl)pyridin-3-yl)-1*H*-pyrrole-2-carboxamide (321)
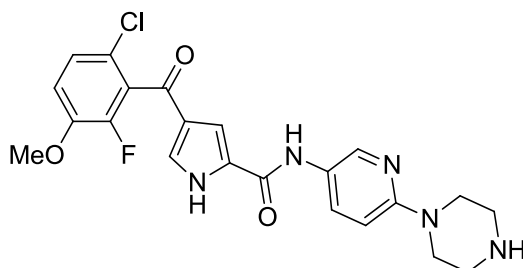
Prepared according to general procedure G using carbamate **422** (120 mg, 0.22 mmol, 1 eq.) and Et$_3$SiH (86 μL, 0.54 mmol, 2.5 eq.), TFA (1 mL) and CH$_2$Cl$_2$ (1 mL). Purification by MPLC on NH$_2$ SiO$_2$ with a gradient elution from 2-8% MeOH/CH$_2$Cl$_2$ gave a white solid (71 mg, 72%); R_f 0.3 (10% MeOH/CH$_2$Cl$_2$, NH$_2$ SiO$_2$); m.p. 184°C dec.; λ_{max}(EtOH)/nm 298, 230; IR v_{max}/cm^{-1} 3133.5 br, 2839.5, 1635.0; ^{1}H NMR (500 MHz; DMSO-d_6) δ_H 2.78-2.84 (4H, m, 4 × CH-piperazine), 3.34-3.41 (4H, m, 4 × CH-piperazine), 3.94 (3H, s OCH$_3$), 6.84 (1H, d, J = 9.1 Hz, H-3-pyridine), 7.36 (1H, app t, J = 8.9 Hz, H-4'), 7.39-7.44 (2H, m, H-pyrrole and H-3'), 7.47 (H-pyrrole), 7.85 (1H, dd, J = 2.6 and 9.1 Hz, H-4-pyridine'), 8.42 (1H, d, J = 2.6 Hz, H-6-pyridine), 9.98 (1H, s, CO-NH); ^{19}F NMR (470 MHz; DMSO-d_6) δ_F -136.15; ^{13}C NMR (125 MHz; DMSO-d_6) δ_C 45.4

(2 × CH$_2$-piperazine), 46.2 (2 × CH$_2$-piperazine), 56.4 (OCH$_3$), 106.6 (C-3-pyridine), 110.8 (CH-pyrrole), 115.1 (C-4'), 120.2 (d, J_{CF} = 4.5 Hz, C-1'), 125.1 (C-pyrrole), 125.5 (d, J_{CF} = 3.6 Hz, C-5'), 125.9 (C-pyrrole), 130.9 (C-4-pyridine), 140.1 (C-6-pyridine), 146.4 (d, J_{CF} = 10.4 Hz, C-3'), 147.9 (d, J_{CF} = 247.5 Hz, C-2'), 156.3 (C-5-pyridine), 158.2 (CO-NH), 183.6 (CO); HRMS calcd for C$_{22}$H$_{22}$^{35}Cl$_1$F$_1$N$_6$O$_3$ [M+H]$^+$ 458.1390, found 458.1382.

N-(1-Methylpiperidin-4-yl)-5-nitropyridin-2-amine (367)
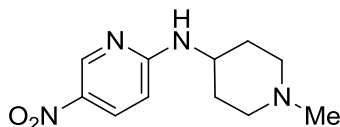
1-Methyl-4-aminopiperidine (794 μL, 6.32 mmol, 2 eq.), 2-chloro-5-nitropyridine (500 mg, 3.15 mmol, 1 eq.) and K$_2$CO$_3$ (304 μL, 2.18 mmol, 1.1 eq.) were combined in THF (10 mL) and heated to 80 °C for 3 h. The mixture was allowed to cool to r.t., partitioned between EtOAc (2 × 50 mL) and water (30 mL), washed with brine, dried over MgSO$_4$ and solvent removed *in vacuo*. The residue was purified by MPLC on SiO$_2$ with gradient elution from 50-100% EtOAc/petrol to give a yellow solid (417 mg, 56 %); R_f 0.75 (5% MeOH/CH$_2$Cl$_2$, NH$_2$ SiO$_2$); m.p. 142-145 °C; λ_{max}(EtOH)/nm 224, 362; IR ν_{max}/cm^{-1} 3357, 1600, 1278; ^{1}H NMR (500 MHz; DMSO-d_6) δ_H 1.46-1.58 (2H, m, 2 × H-piperidine), 1.85-1.93 (2H, m, 2 × H-piperidine), 1.97-2.06 (2H, m, 2 × H-piperidine), 2.20 (3H, s, CH$_3$), 2.73-2.81 (2H, m, 2 × H-piperidine), 3.85-3.97 (1H, m, CH-piperidine), 6.58 (1H, d, J = 9.4 Hz, H-3-pyridine), 8.09 (2H, m, NH and H-4-pyridine), 8.94 (1H, d, J = 2.8 Hz, H-6-pyridine); ^{13}C NMR (125 MHz; DMSO-d_6) δ_C 14.1 (2 × C-piperidine), 45.9 (CH$_3$), 48.2 (CH-piperidine), 54.0 (2 × C-piperidine), 108.5 (C-pyridine), 131.6 (C-pyridine), 134.1 (C-pyridine), 146.9 (C-pyridine), 160.7 (C-pyridine); HRMS calc for C$_{11}$H$_{17}$N$_4$O$_2$ [M+H]$^+$ 237.1346, found 237.1340.

N^2-(1-Methylpiperidin-4-yl)pyridine-2,5-diamine (369)
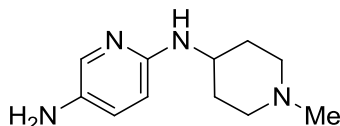
Prepared according to general procedure H using nitropyridine **367** (400 mg, 1.69 mmol) and MeOH (35 mL) for 18 h to give a pale pink solid (330 mg, 95 %); R_f 0.3 (5% MeOH/EtOAc, NH$_2$ SiO$_2$); m.p. 125-130 °C; λ_{max}(EtOH)/nm 250; IR ν_{max}/cm^{-1} 3286, 3136, 2981, 2780; ^{1}H NMR (500 MHz; DMSO-d_6) δ_H 1.37 (2H, qd, J = 11.3 and 3.5 Hz, 2 × CH-piperidine), 1.82-1.90 (2H, m, 2 × CH-piperidine), 1.93-2.01 (2H, m, 2 × CH-

piperidine), 2.18 (CH$_3$), 2.69-2.76 (2H, m, 2 × CH-piperidine), 3.42-3.52 (1H, m, CH-piperidine), 4.26 (2H, s, NH$_2$), 5.39 (1H, d, J = 5.9 Hz, NH), 6.31 (1H, d, J = 8.7 Hz, H-3-pyridine), 6.83 (1H, dd, J = 2.7 and 8.7 Hz, H-4-pyridine), 7.46 (1H, d, J = 2.7 Hz, H-6-pyridine); ^{13}C NMR (125 MHz; DMSO-d_6) δ$_C$ 32.1 (2 × CH-piperidine), 46.1 (CH$_3$), 47.4 (CHNH-piperidine), 54.5 (2 × CH-piperidine), 108.7 (C-Ar), 125.4 (C-Ar), 133.1 (C-Ar), 135.0 (C-Ar), 151.2 (C-Ar); HRMS calc for C$_{11}$H$_{19}$N$_4$ [M+H]$^+$ 207.1604, found 207.1601.

4-(3,6-Dichloro-2-fluorobenzoyl)-*N*-(6-((1-methylpiperidin-4-yl)amino) pyridin-3-yl)-1*H*-pyrrole-2-carboxamide (293)
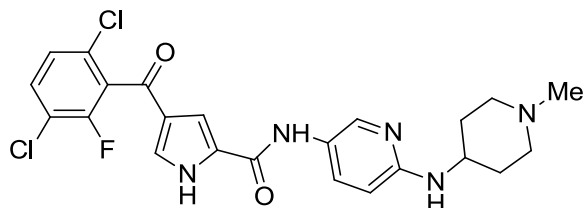
Amine **369** (150 mg, 0.73 mmol, 1.5 eq) was added to carboxylic acid **337** (147 mg, 0.48 mmol, 1 eq.), pyridine (39 μL, 0.48 mmol, 1 eq) and PyBrOP (339 mg, 0.73 mmol, 1.5 eq) in MeCN (2 mL), and the mixture was stirred at r.t. for 1 h and then partitioned between EtOAc (2 × 30 mL) and H$_2$O (20 mL). The organic layers were combined, washed with brine, dried (MgSO$_4$) and the solvent removed *in vacuo*. The residue was purified by MPLC on NH$_2$ SiO$_2$ with gradient elution from 3-15% MeOH/CH$_2$Cl$_2$ to give a beige solid, which was re-purified by MPLC on SiO$_2$ with gradient elution from 93/3/0.3 to 88/12/1.2 EtOAc/MeOH/NH$_4$OH to give a white solid (45 mg, 19%); R_f 0.15 (90/10/1 EtOAc/MeOH/NH$_4$OH); m.p. 195-200 °C; λ$_{max}$(EtOH)/nm 280, 228; IR ν$_{max}$/cm^{-1} 2944, 1639, 1593; ^{1}H NMR (500 MHz; DMSO-d_6) δ$_H$ 1.45 (2H, qd, J = 11.0 and 3.8 Hz, 2 × CH-piperidine), 1.86-1.93 (2H, m, 2 × CH-piperidine), 1.96-2.05 (2H, m, 2 × CH-piperidine), 2.19 (3H, s, CH$_3$), 2.72-2.79 (2H, m, 2 × CH-piperidine), 3.59-3.69 (1H, m, CH-NH-piperidine), 6.33 (1H, d, J = 7.8 Hz, NH-piperidine), 6.50 (1H, d, J = 8.9 Hz, H-3-pyridine), 7.42 (1H, s, H-pyrazole), 7.55 (1H, dd, J = 1.0 and 8.6 Hz, H-5'), 7.58 (1H, s, H-pyrazole), 7.63 (1H, dd, J = 2.6 and 9.0 Hz, H-4-pyridine), 7.81 (1H, app t, J = 8.6 Hz, H-4'), 8.23 (1H, d, J = 2.6 Hz, H-6-pyridine), 9.85 (1H, s, CO-NH), 12.59 (1H, br s, NH-pyrrole); ^{19}F NMR (470 MHz; DMSO-d_6) δ$_F$ -116.68; ^{13}C NMR (125 MHz; DMSO-d_6) δ$_C$ 31.8 (2 × C-piperidine), 46.1 (CH$_3$), 47.0 (CH-piperidine), 54.4 (2 × C-piperidine), 107.9 (C-3-pyridine), 110.5 (CH-pyrrole), 119.3 (d, J_{CF} = 18.3 Hz, C-3'), 124.2 (C-pyrrole), 124.7 (C-pyridine), 126.8 (d, J_{CF} = 3.6 Hz, C-5'), 129.0 (C-pyrrole), 129.2 (d, J_{CF} = 9.4 Hz, C-6'), 129.3 (d, J_{CF} = 18.7 Hz, C-1'), 129.6 (CH-pyrrole), 131.2 (C-2-pyridine), 131.8

(C-4'), 140.5 (C-6-pyridine), 153.8 (d, J_{CF} = 248.4 Hz, C-2'), 155.3 (C-5-pyridine), 158.2 (CO-NH), 182.5 (CO); HRMS calcd for $C_{23}H_{23}{}^{35}Cl_2F_1N_5O_2$ [M+H]$^+$ 490.1207, found 490.1193.

4-(6-Chloro-2-fluoro-3-methoxybenzoyl)-*N*-(6-((1-methylpiperidin-4-yl)amino)pyridin-3-yl)-1*H*-pyrrole-2-carboxamide (322)

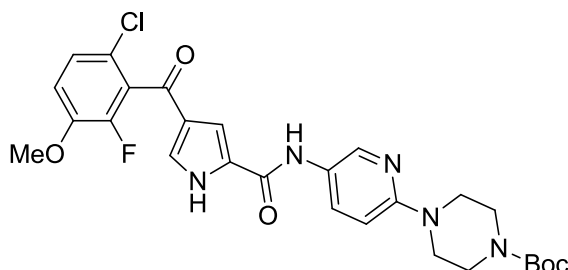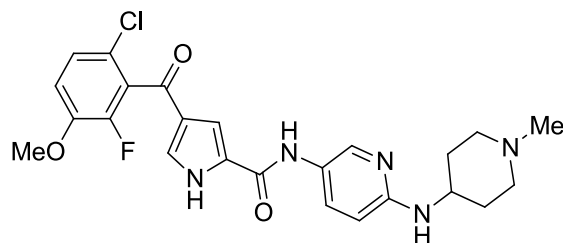Prepared according to general procedure E using amine **369** (135 mg, 0.66 mmol, 2.5 eq.), carboxylic acid **421** (78 mg, 0.26 mmol, 1 eq.), cyanuric fluoride (16 µL, 0.18 mmol, 0.7 eq.), pyridine (21 µL, 0.26 mmol, 1 eq.) and MeCN (2 mL) with stirring at r.t. for 18 h. Purification by MPLC on NH$_2$ SiO$_2$ with a gradient elution from 0-7% MeOH/CH$_2$Cl$_2$ gave a red solid. Re-purification by MPLC on SiO$_2$ with a gradient elution from 10-40% MeOH/CH$_2$Cl$_2$ gave a pale pink solid (45 mg, 35%); R_f 0.3 (5% MeOH/EtOAc, NH$_2$ SiO$_2$); m.p. 255-259 °C; λ_{max}(EtOH)/nm 304, 228; IR ν_{max}/cm^{-1} 3215.1 br, 2942.4, 1622.0 1557.8; ^{1}H NMR (500 MHz; DMSO-*d*$_6$) δ_H 1.38-1.50 (2H, m, 2 × CH-piperidine), 1.84-1.94 (2H, m, 2 × CH-piperidine), 1.96-2.05 (2H, m, 2 × CH-piperidine), 2.19 (3H, s, NCH$_3$), 2.71-2.80 (2H, m, 2 × CH-piperidine), 3.58-3.69 (1H, m, CH-NH-piperidine), 3.94 (OCH$_3$), 6.32 (1H, d, *J* = 7.7 Hz, NH-piperidine), 6.49 (1H, d, *J* = 9.0 Hz, H-3-pyridine), 7.32-7.47 (4H, m, 2 × H-pyrazole, H-4' and H-5'), 7.64 (1H, dd, *J* = 2.1 & 8.9 Hz, H-4-pyridine), 8.23 (1H, d, *J* = 2.1 Hz, H-6-pyridine), 9.84 (1H, s, CO-NH), 12.60 (1H, br s, NH-pyrrole); ^{19}F NMR (470 MHz; DMSO-*d*$_6$) δ_F -136.15; ^{13}C NMR (125 MHz; DMSO-*d*$_6$) δ_C 31.9 (2 × C-piperidine), 46.1 (NCH$_3$), 47.0 (CH-piperidine), 54.4 (2 × C-piperidine), 56.4 (OCH$_3$), 107.9 (C-3-pyridine), 110.6 (CH-pyrrole), 115.1 (C-4'), 120.2 (d, J_{CF} = 4.5 Hz, C-1'), 124.2 (C-pyrrole), 125.1 (C-pyrrole), 125.5 (d, J_{CF} = 4.5 Hz, C-5'), 128.8 (C-6'), 128.8 (CH-pyrrole), 131.2 (C-2-pyridine), 140.5 (C-6-pyridine), 146.4 (d, J_{CF} = 10.6 Hz, C-3'), 147.9 (d, J_{CF} = 246.9 Hz, C-2'), 155.2 (C-5-pyridine), 158.2 (CO-NH), 183.6 (CO); HRMS calcd for $C_{24}H_{26}{}^{35}Cl_1F_1N_5O_3$ [M+H]$^+$ 486.1703, found 486.1689.

4-Nitro-2-(pyrrolidin-1-yl)pyridine 1-oxide (372)[314]
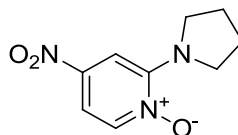
2-Chloro-4-nitropyrimidine-*N*-oxide (200 mg, 1.15 mmol, 1 eq.), pyrrolidine (96 µL, 1.15 mmol, 1 eq.) and NaHCO$_{3(s)}$ (106 mg, 1.27 mmol, 1.1 eq.) were combined in 2-propanol (5 mL) and heated at reflux for 2 h. The solvent was removed *in vacuo* and the residue partitioned between EtOAc (3 × 30 mL) and saturated aqueous NaHCO$_3$ (10 mL). The organic extracts were combined, dried over MgSO$_4$ and the solvent removed *in vacuo*. The residue was purified by MPLC on SiO$_2$ with a gradient from 0-10% MeOH/EtOAc to give a red solid (210 mg, 88%). R_f 0.4 (10% MeOH/EtOAc); m.p. 149-151 °C (lit.[367] 148.5-149.5 °C); λ$_{max}$(EtOH)/nm 400, 283, 214; IR ν$_{max}$/cm^{-1} 1613, 1519, 1497, 1442, 1336; ^{1}H NMR (500 MHz; DMSO-d_6) δ$_H$ 1.87-1.95 (4H, m, H-pyrrolidine), 3.62-3.67 (4H, m, CH-N-pyrrolidine), 7.49 (1H, d, J = 3.1 Hz, H-3), 7.57 (1H, dd, J = 3.1 and 7.2 Hz, H-5), 8.26 (1H, d, J = 7.2 Hz, H-6); ^{13}C NMR (125 MHz; DMSO-d_6) δ$_C$ 24.7 (2 × CH$_2$-pyrrolidine), 49.8 (2 × CH$_2$-N-pyrrolidine), 105.1 (C-3), 108.6 (C-5), 140.4 (C-6), 142.9 (C-4), 151.8 (C-2); HRMS calcd for C$_9$H$_{12}$N$_3$O$_3$ [M+H]$^+$ 210.0873, found 210.0869.

2-(Pyrrolidin-1-yl)pyridin-4-amine (373)
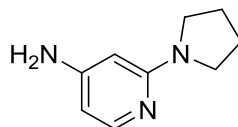
Pyridine *N*-oxide **372** was dissolved in methanol (5 mL) and hydrogenated on a Thales H-cube over 20% Pd(OH)$_2$/C at 50 bar H$_2$/t 50 °C for 3 h with continuous recycling of the reaction mixture. The solvent was removed *in vacuo* to give a white solid (230 mg, 89%). R_f 0.55 (NH$_2$ SiO$_2$, 10% MeOH/CH$_2$Cl$_2$); m.p. 171-175 °C (lit.[367] 178-179.5 °C); λ$_{max}$(EtOH)/nm 292, 233; IR ν$_{max}$/cm^{-1} 3453, 3406, 3116, 2846, 1597; ^{1}H NMR (500 MHz; DMSO-d_6) δ$_H$ 1.86-1.95 (4H, m, 2 × CH$_2$-pyrrolidine), 3.26-3.31 (4H, m, 2 × CH$_2$-N-pyrrolidine), 5.52 (1H, d, J = 1.8 Hz, H-3), 5.57 (2H, br s, NH$_2$), 5.84 (1H, dd, J = 1.8 and 5.6 Hz, H-4), 7.58 (1H, d, J = 5.6 Hz, H-5); ^{13}C NMR (125 MHz; DMSO-d_6) δ$_C$ 25.0 (2 × CH$_2$-pyrrolidine), 46.2 (2 × CH$_2$-N-pyrrolidine), 88.9 (C-3), 100.2 (C-5), 147.7 (C-6), 155.0 (C-4), 158.2 (C-2); HRMS calcd for C$_9$H$_{14}$N$_3$ [M+H]$^+$ 164.1182, found 164.1178.

4-(2-Chloro-6-fluorobenzoyl)-*N*-(2-chloropyridin-4-yl)-1*H*-pyrrole-2-carboxamide (294)
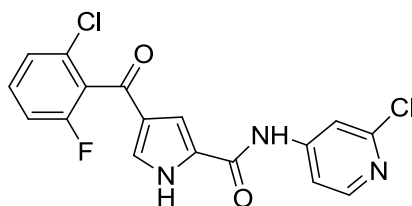
Prepared according to general procedure F using carboxylic acid **336** (360 mg, 1.35 mmol, 1 eq.), 4-amino-2-chloropyridine (434 mg, 3.4 mmol, 2.5 eq.), PCl$_3$ (117 μL, 1.35 mmol) and MeCN (5 mL). Purification by MPLC on NH$_2$ SiO$_2$ with a gradient elution from 60-100% EtOAc:petrol gave a white solid (227 mg, 45%); R_f 0.3 (NH$_2$ SiO$_2$, EtOAc); m.p. 268-270 °C; λ$_{max}$(EtOH)/nm 295; IR ν $_{max}$/cm^{-1} 3346, 2965, 2852, 1685, 1629; ^{1}H NMR (500 MHz; DMSO-d_6) δ$_H$ 7.44 (1H, app t, *J* = 8.4 Hz, H-5'), 7.51 (1H, d, *J* = 8.4 Hz, C-3'), 7.57 (1H, s, H-pyrrole), 7.58 (1H, s, H-pyrrole), 7.63 (1H, td, *J* = 8.4 and 6.3 Hz, H-4'), 7.73 (1H, dd, *J* = 1.7 and 5.7 Hz, C-5-pyridine), 7.92 (1H, d, *J* = 1.7 Hz, C-3-pyridine), 8.33 (1H, d, *J* = 5.7 Hz, C-6-pyridine), 10.55 (1H, s, CO-NH), 12.85 (1H, s, NH-pyrrole); ^{19}F NMR (470 MHz; DMSO-d_6) δ$_F$ -114.31; ^{13}C NMR (125 MHz; DMSO-d_6) δ$_C$ 112.6 (CH-pyrrole), 112.9 (C-3-pyridine), 113.1 (C-5-pyridine), 115.0 (d, J_{CF} = 21.5 Hz, C-5'), 125.4 (C-pyrrole), 125.9 (d, J_{CF} = 3.3 Hz, C-3'), 127.6 (C-pyrrole), 127.9 (d, J_{CF} = 21.5 Hz, C-1'), 130.1 (CH-pyrrole), 130.4 (d, J_{CF} = 5.9 Hz, C-2'), 131.9 (d, J_{CF} = 9.1 Hz, C-4'), 148.3 (C-2-pyridine), 150.3 (C-6-pyridine), 150.8 (C-4-pyridine), 158.6 (d, J_{CF} = 246.5 Hz, C-6'), 159.1 (CO-NH), 183.9 (CO); HRMS calcd for C$_{17}$H$_{11}$^{35}Cl$_2$F$_1$N$_3$O$_2$ [M+H]$^+$ 378.0207, found 378.0210.

4-(2-Chloro-6-fluorobenzoyl)-*N*-(2-(pyrrolidin-1-yl)pyridin-4-yl)-1*H*-pyrrole-2-carboxamide (297)
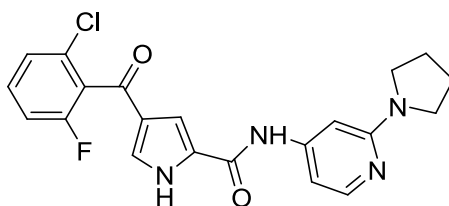
Procedure 1: Prepared according to general procedure L, using carboxylic acid **336** (61 mg, 0.23 mmol, 1 eq.), amine **373** (74 mg, 0.45 mmol, 2 eq.), 2-chloro-1-methylpyridinium iodide (64 mg, 0.25 mmol, 1.1 eq.) and triethylamine (79 μL, 0.57 mmol, 2.5 eq.) in CH$_2$Cl$_2$ (4 mL). The mixture was heated in a sealed tube at 50 °C for 2 h. The solvent was

removed *in vacuo*, and the residue was purified by MPLC on NH$_2$ SiO$_2$ with gradient elution from 0-5% MeOH/CH$_2$Cl$_2$. Product containing fractions were combined and the solvent removed *in vacuo*. The residue was re-purified by MPLC on SiO$_2$ with a gradient elution from 50:50:0.5:0.05 to 50:50:4:0.4 EtOAc/petrol/EtOH/NH$_4$OH to give a white solid (20 mg, 21%); **Procedure 2:** Chloropyridine **294** (60 mg, 0.15 mmol, 1 eq.) and pyrrolidine (20 μL, 0.30 mmol, 2 eq.) were combined in NMP (1 mL) and heated under microwave irradiation at 250 °C for 3 h. The solvent was removed *in vacuo* and the residue was purified by MPLC on NH$_2$ SiO$_2$ with gradient elution from 0-3% MeOH/CH$_2$Cl$_2$ to give a pale brown solid (27 mg, 42%); R_f 0.5 (NH$_2$ SiO$_2$, 5% MeOH/CH$_2$Cl$_2$); m.p. 198-201 °C; λ_{max}(EtOH)/nm 293, 252; IR ν $_{max}$/cm^{-1} 3352, 2958, 2854, 1634, 1571; ^{1}H NMR (500 MHz; DMSO-d_6) δ_H 1.95-2.01 (4H, m, 2 × CH$_2$ pyrrolidine), 3.36-3.42 (4H, m, 2 × CH$_2$-N-pyrrolidine), 6.89 (d, 1H, J = 1.5 Hz, H-3-pyridine), 7.02 (1H, dd, J = 1.5 and 5.7 Hz, H-5-pyridine), 7.44 (1H, app t, J = 8.4 Hz, H-5'), 7.48-7.56 (3H, m, H-3-pyrrole, H-5-pyrrole and H-3'), 7.62 (1H, td, J = 8.4 and 6.2 Hz, H-4'), 7.98 (1H, d, J = 5.7 Hz, H-6-pyridine), 10.09 (1H, s, CO-NH), 12.70 (1H, br s, NH-pyrrole); ^{19}F NMR (470 MHz; DMSO-d_6) δ_F -114.31; ^{13}C NMR (125 MHz; DMSO-d_6) δ_C 25.0. (2 × CH$_2$-pyrrolidine), 46.3 (2 × CH$_2$-N-pyrrolidine), 95.2 (C-3-pyridine), 103.0 (C-5-pyridine), 111.6 (CH-pyrrole), 115.0 (d, J_{CF} = 21.4 Hz, C-5'), 125.3 (C-pyrrole), 125.9 (d, J_{CF} = 2.7 Hz, C-3'), 128.3 (C-pyrrole), 129.5 (CH-pyrrole), 130.4 (d, J_{CF} = 6.0 Hz, C-2'), 131.9 (d, J_{CF} = 9.0 Hz, C-4'), 146.4 (C-2-pyridine), 148.4 (C-6-pyridine), 157.9 (C-4-pyridine), 158.6 (d, J_{CF} = 246.7 Hz, C-6'), 158.8 (CO-NH), 183.9 (CO); HRMS calcd for C$_{21}$H$_{19}$^{35}Cl$_1$F$_1$N$_4$O$_2$ [M+H]$^+$ 413.1175, found 413.1167.

4-(2-Chloro-6-fluorobenzoyl)-*N*-(2-(4-methylpiperazin-1-yl)pyridin-4-yl)-*1H*-pyrrole-2-carboxamide (298)
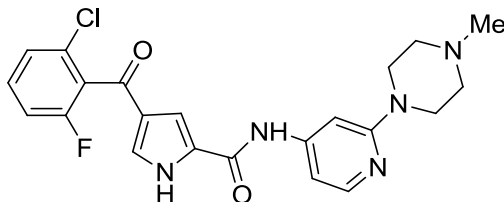
Chloropyridine **294** (60 mg, 0.16 mmol), 1-methylpiperazine (36 μL, 0.32 mmol, 2 eq.) and NMP (1 mL) were combined and heated to 250 °C under microwave irradiation for 3 h. The solvent was removed *in vacuo* and the residue was purified by MPLC on SiO$_2$ with a gradient elution from 99:1:0.1 to 95:5:0.5 EtOAc/MeOH/NH$_4$OH. Product containing fractions were combined, evaporated and the residue re-was purified by MPLC on NH$_2$

SiO$_2$ with gradient elution from 0-5% MeOH/CH$_2$Cl$_2$ to give a pale brown solid (10 mg, 14%); R_f 0.25 (NH$_2$ SiO$_2$, 5% MeOH/EtOAc); m.p. 275 °C dec.; λ_{max}(EtOH)/nm 292, 250; IR ν_{max}/cm^{-1} 3245, 1655, 1621, 1573; ^{1}H NMR (500 MHz; DMSO-d_6) δ_H 2.25 (3H, s, CH$_3$), 2.41-2.46 (4H, m, 2 × CH$_2$-piperazine), 3.43-3.49 (4H, m, 2 × CH$_2$-piperazine), 7.15 (1H, dd, J = 1.3 and 5.5 Hz, H-5-pyridine), 7.19 (1H, s, H-pyrrole), 7.44 (1H, app t, J = 8.5 Hz, H-5'), 7.48-7.58 (3H, m, H-pyrrole, H-3' and H-3-pyridine), 7.62 (1H, dt, J = 6.1 and 8.5 Hz, H-4'), 8.05 (1H, d, J = 5.5 Hz, H-6-pyridine), 10.11 (1H, s, CO-NH), 12.70 (1H, br s, NH-pyrrole); ^{19}F NMR (470 MHz; DMSO-d_6) δ_F -114.31; ^{13}C NMR (125 MHz; DMSO-d_6) δ_C 44.7 (2 × CH$_2$-piperazine), 45.8 (CH$_3$), 54.3 (2 × CH$_2$-piperazine), 96.1 (C-3-pyridine), 104.7 (C-5-pyridine), 111.7 (CH-pyrrole), 115.0 (d, J_{CF} = 21.5 Hz, C-5'), 125.3 (C-pyrrole), 125.9 (d, J_{CF} = 3.1 Hz, C-3'), 128.0 (d, J_{CF} = 23.2 Hz, C-1'), 128.2 (C-pyrrole) 130.0 (CH-pyrrole), 130.4 (d, J_{CF} = 5.9 Hz, C-2'), 131.9 (d, J_{CF} = 9.1 Hz, C-4'), 147.1 (C-2-pyridine), 148.3 (C-6-pyridine), 158.6 (d, J_{CF} = 247.0 Hz, C-6'), 158.9 (CO-NH), 160.0 (C-4-pyridine), 184.0 (CO); HRMS calc for C$_{22}$H$_{22}$^{35}Cl$_1$F$_1$N$_5$O$_2$ [M+H]$^+$ 442.1441, found 442.1430.

4-(2-Chloro-6-fluorobenzoyl)-*N*-(2-(trifluoromethyl)pyridin-4-yl)-1*H*-pyrrole-2-carboxamide (295)
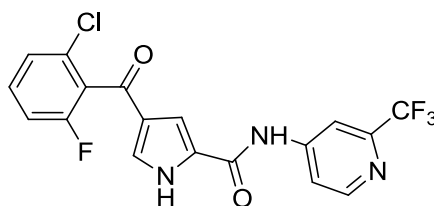
Prepared according to general procedure F using carboxylic acid **336** (112 mg, 0.42 mmol, 1 eq.), 4-amino-2-trifluoromethyl pyridine (170 mg, 1.05 mmol, 2.5 eq.), PCl$_3$ (37 μL, 0.42 mmol, 1 eq) and MeCN 2 mL). Purification by MPLC on NH$_2$ SiO$_2$ with a gradient elution from 50-100% EtOAc:petrol gave a white solid (63 mg, 45%); R_f 0.3 (NH$_2$ SiO$_2$, EtOAc); m.p. 311-313 °C; λ_{max}(EtOH)/nm 291, 272; IR ν_{max}/cm^{-1} 3238, 1623, 1592, 1555; ^{1}H NMR (500 MHz; DMSO-d_6) δ_H 7.42 (1H, app t, J = 8.2 Hz, H-5'), 7.49 (1H, d, J = 8.2 Hz, H-3'), 7.56 (1H, s, H-pyrrole), 7.57 (1H, s, H-pyrrole), 7.60 (1H, td, J = 8.2 and 6.0 Hz, H-4'), 8.03 (1H, dd, J = 1.9 and 5.6 Hz, H-5-pyridine), 8.23 (1H, d, J = 1.9 Hz, H-3-pyridine), 8.65 (1H, d, J = 5.6 Hz, H-6-pyridine), 10.67 (CO-NH), 12.85 (NH -pyrrole); ^{19}F NMR (470 MHz; DMSO-d_6) δ_F -85.76, -114.31; ^{13}C NMR (125 MHz; DMSO-d_6) δ_C 109.8 (q, 3.0 Hz, C-2 pyridine), 112.7 (CH-pyrrole), 115.0 (d, J_{CF} = 21.3 Hz, C-5'), 116.1 (C-4 pyridine), 121.6 (q, J_{CF} = 274.0 Hz, CF$_3$), 125.5 (C-pyrrole), 125.9 (d, J_{CF} = 2.7 Hz, C-3'),

127.6 (C-pyrrole), 127.9 (d, J_{CF} = 22.7 Hz, C-1'), 130.2 (CH-pyrrole), 130.4 (d, J_{CF} = 5.9 Hz, C-2'), 132.0 (d, J_{CF} = 9.2 Hz, C-4'), 147.2 (q, J_{CF} = 24.9 Hz, C-2 pyridine), 147.4 (C-pyridine), 151.1 (C-pyridine), 158.6 (d, J_{CF} = 247.0 Hz, C-6'), 159.2 (CO-NH), 184.0 (CO); HRMS calcd for $C_{18}H_{11}{}^{35}Cl_1F_4N_3O_2$ [M+H]$^+$ 412.0470, found 412.0478.

4-(2-Chloro-6-fluorobenzoyl)-*N*-(2-methoxypyridin-4-yl)-1*H*-pyrrole-2-carboxamide (296)
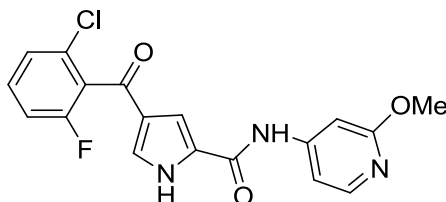
Prepared according to general procedure E using 2-methoxy-4-aminopyridine (105 mg, 0.84 mmol, 2.5 eq.), carboxylic acid **336** (90 mg, 0.34 mmol, 1 eq.), cyanuric fluoride (20 μL, 0.24 mmol, 0.7 eq.), pyridine (27 μL, 0.34 mmol, 1 eq.) and MeCN (2 mL). Purification by MPLC on SiO$_2$ with a gradient elution from 20-100% EtOAc/petrol gave a red oil which was re-purified by MPLC on NH$_2$ SiO$_2$ with gradient elution from 1-7% MeOH/CH$_2$Cl$_2$ to give a white solid (42 mg, 33%); R_f 0.15 (50% EtOAc/petrol); m.p. 232 °C dec.; λ$_{max}$(EtOH)/nm 289, 267; IR ν $_{max}$/cm^{-1} 3225, 1631, 1587; ^{1}H NMR (500 MHz; DMSO-d_6) δ$_H$ 3.86 (3H, s, CH$_3$), 7.31 (1H, s, H-pyrrole), 7.32 (1H, d, *J* = 1.6 Hz, H-3-pyridine), 7.44 (1H, app t, *J* = 8.5 Hz, H-5'), 7.49-7.57 (3H, m, H-pyrrole, H-3' and H-5-pyridine), 7.62 (1H, app dt, *J* = 6.3 and 8.5 Hz, H-4'), 8.09 (1H, d, *J* = 5.7 Hz, H-6-pyridine), 10.33 (CO-NH), 12.97 (NH-pyrrole); ^{19}F NMR (470 MHz; DMSO-d_6) δ$_F$ -114.31; ^{13}C NMR (125 MHz; DMSO-d_6) δ$_C$ 53.1 (CH$_3$), 98.9 (C-pyridine), 108.5 (C-pyridine), 112.0 (CH-pyrrole), 115.0 (d, J_{CF} = 21.8 Hz, C-5'), 125.3 (C-pyrrole), 125.9 (d, J_{CF} = 3.2 Hz, C-3'), 128.0 (C-1'), 128.0 (C-pyrrole), 129.8 (C-pyrrole), 130.4 (d, J_{CF} = 6.8 Hz, C-2'), 131.9 (d, J_{CF} = 9.5 Hz, C-4'), 147.2 (C-pyridine), 148.0 (C-pyridine), 158.6 (d, J_{CF} = 247.0 Hz, C-6'), 159.0 (CO-NH), 164.5 (C-2'), 183.9 (CO); HRMS calcd for $C_{18}H_{12}{}^{35}Cl_1F_1N_3O_3$ [M-H]$^-$ 372.0557, found 372.0549.

4-(3,6-Dichloro-2-fluorobenzoyl)-*N*-(pyridin-4-yl)-1*H*-pyrrole-2-carboxamide (377)
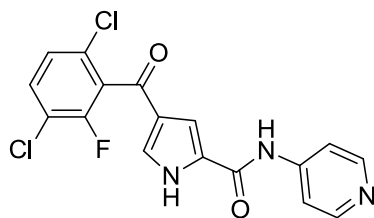
Prepared according to general procedure F using carboxylic acid **337** (500 mg, 1.65 mmol, 1 eq.), 4-aminopyridine (388 mg, 4.13 mmol, 2.5 eq), PCl$_3$ (144 µL, 1.65 mmol, 1 eq.) and MeCN (5 mL). Purification by MPLC on SiO$_2$ with a gradient elution from 2-10% MeOH/CH$_2$Cl$_2$ gave a white solid (360 mg, 58%); R_f 0.35 (70% EtOAc/Petrol); m.p. 267 °C dec.; λ_{max}(EtOH)/nm 292, 271, 211; IR ν_{max}/cm^{-1} 3242, 1641; ^{1}H NMR (500 MHz; DMSO-d_6) δ_H 7.56 (1H, dd, J = 1.3 and 8.6 Hz, H-5'), 7.61 (1H, s, H-pyrrole), 7.68-7.71 (1H, m, H-pyrrole), 7.77 (1H, dd, J = 1.5 and 4.8 Hz, 2 × H-pyridine), 7.83 (1H, app t, J = 8.6 Hz, H-4'), 8.50 (2H, dd, J = 1.5 and 4.8 Hz,, 2 × H-pyridine), 10.39 (1H, s, CO-NH), 12.87 (1H, s, NH-pyrrole); ^{19}F NMR (470 MHz; DMSO-d_6) δ_F -116.64; ^{13}C NMR (125 MHz; DMSO-d_6) δ_C 112.0 (C-3 and C-5 pyridine), 113.7 (CH-pyrrole), 119.4 (d, J_{CF} = 17.9 Hz, C-3'), 124.8 (C-pyrrole), 126.9 (d, J_{CF} = 3.6 Hz, C-5'), 128.2 (C-pyrrole), 128.9 (C-pyrrole), 129.1 (d, J_{CF} = 22.7 Hz, C-1'), 129.2 (d, J_{CF} = 7.8 Hz, C-6'), 130.7 (C-4'), 145.6 (C-2 and C-6 pyridine), 150.3 (C-4 pyridine), 153.8 (d, J_{CF} = 248.3 Hz, C-2'), 159.0 (CO-NH), 182.6 (CO); HRMS calcd for C$_{17}$H$_{11}$^{35}Cl$_1$F$_1$N$_3$O$_2$ [M+H]$^+$ 378.0207, found 378.0210.

4-(4-(3,6-Dichloro-2-fluorobenzoyl)-1*H*-pyrrole-2-carboxamido)pyridine-1-oxide (378)
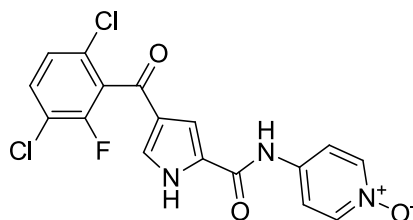
mCPBA (339 mg, 1.96 mmol, 1.5 eq.) was added to a suspension of pyridyl amide **377** (340 mg, 0.9 mmol, 1 eq.) in MeCN (8 mL), and the mixture was stirred at r.t. for 18 h. Two drops of water were added, the solvent removed *in vacuo*, and the residue was purified by MPLC on SiO$_2$ with a gradient elution from 4-15% MeOH/EtOAc to give a white solid (340 mg, 72%); R_f 0.5 (10% MeOH/CH$_2$Cl$_2$, NH$_2$ SiO$_2$); m.p. 211 °C dec.;

λ_{max}(EtOH)/nm 308, 299, 214; IR ν_{max}/cm^{-1} 3082 br, 1646, 1207 (N-oxide); ^{1}H NMR (500 MHz; DMSO-d_6) δ_H 7.54-7.58 (2H, m, H-pyrrole and H-5'), 7.69 (1H, dd, J = 1.3 and 3.3 Hz, H-pyrrole), 7.78-7.85 (3H, m, 2 × H-pyridine and H-4'), 8.17-8.21 (2H, m, 2 × H-pyridine), 10.51 (1H, s, CO-NH), 12.87 (1H, s, NH-pyrrole); ^{19}F NMR (470 MHz; DMSO-d_6) δ_F -116.64; ^{13}C NMR (125 MHz; DMSO-d_6) δ_C 111.8 (CH-pyrrole), 116.4 (C-3- and C-5-pyridine), 119.4 (d, J_{CF} = 18.1 Hz, C-3'), 124.8 (C-pyrrole), 126.9 (d, J_{CF} = 3.7 Hz, C-5'), 128.1 (C-pyrrole), 129.0 (d, J_{CF} = 23.0 Hz, C-1'), 129.2 (d, J_{CF} = 5.4 Hz, C-6'), 130.7 (C-pyrrole), 131.9 (C-4'), 136.2 (C-4-pyridine), 138.8 (C-2- and C-6-pyridine), 153.8 (d, J_{CF} = 248.8 Hz, C-2'), 158.4 (CO-NH), 182.6 (CO); HRMS calcd for $C_{17}H_{11}{}^{35}Cl_2F_1N_3O_3$ [M+H]$^+$ 394.0156, found 394.0154.

4-(3,6-Dichloro-2-fluorobenzoyl)-*N*-(2-(4-methylpiperazin-1-yl)pyridin-4-yl)-1*H*-pyrrole-2-carboxamide (299)
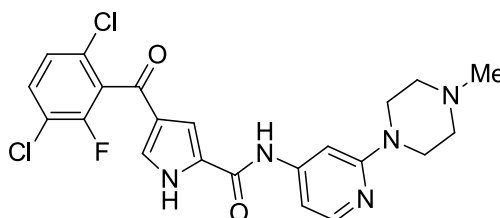
PyBrOP (154 mg, 0.33 mmol, 1.3 eq.) was added to a suspension of pyridine *N*-oxide **378** (100 mg, 0.25 mmol, 1 eq.), 1-methylpiperazine (36 μL, 0.32 mmol, 1.25 eq.) and Hunig's base (165 μL, 0.95 mmol, 3.75 eq.) in DCM (1.6 mL) and the reaction was stirred at r.t for 18 h. The mixture was partitioned between EtOAc (2 × 30 mL) and H$_2$O (20 mL), washed with brine, dried over MgSO$_4$, and the solvent removed *in vacuo*. The residue was purified by MPLC on SiO$_2$ with gradient elution from 3-8% MeOH/DCM to give impure product (52 mg). This was further purified by semi-preparative HPLC (mobile phase gradient from 95:5 to 0:100 water + 0.1% v/v formic acid:MeCN on an ACE 5 C18-AR 150 x 21.2 mm i.d. (S/No. A110809) column). Product containing fractions were evaporated, partitioned between EtOAc (2 × 30 mL) and K$_2$CO$_3$ (20 mL, 10% aq.), washed with brine, dried over MgSO$_4$, and the solvent removed *in vacuo* to give a white solid (20 mg, 17%); R_f 0.5 (5% MeOH/EtOAc, NH$_2$ SiO$_2$); m.p. 185 °C dec.; λ_{max}(EtOH)/nm 250, 222; IR ν_{max}/cm^{-1} 3112, 2932, 1641; ^{1}H NMR (500 MHz; DMSO-d_6) δ_H 2.25 (CH$_3$), 2.41-2.46 (4H, m, H-piperazine), 3.44-3.50 (4H, m, H-piperazine), 7.16 (1H, dd, J = 1.6 and 5.5 Hz, H-5-pyridine), 7.19 (H-3-pyridine), 7.53-7.58 (2H, m, H-pyrrole and H-5'), 7.68 (1H, s, H-pyrrole), 7.83 (1H, app t, J = 8.4 Hz, H-4'), 8.05 (1H, d, J = 5.7 Hz, H-6-pyridine), 10.13

(1H, s, CO-NH), 12.80 (1H, br s, NH-pyrrole); ^{19}F NMR (470 MHz; DMSO-d_6) δ_F -116.66; ^{13}C NMR (125 MHz; DMSO-d_6) δ_C 44.6 (2 × CH$_2$-piperazine), 45.8 (CH$_3$), 54.3 (2 × CH$_2$-piperazine), 96.1 (C-3-pyridine), 104.7 (C-5-pyridine), 111.6 (CH-pyrrole), 119.3 (d, J_{CF} = 18.3 Hz, C-3'), 124.8 (C-pyrrole), 126.9 (d, J_{CF} = 3.6 Hz, C-5'), 128.5 (C-pyrrole), 129.1 (d, J_{CF} = 22.7 Hz, C-1'), 129.2 (d, J_{CF} = 5.2 Hz,), 130.5 (C-pyrrole), 131.9 (C-4'), 147.1 (C-pyridine), 148.3 (C-6-pyridine), 153.8 (d, J_{CF} = 248.5 Hz, C-2'), 158.8 (CO-NH), 160.0 (C-pyridine), 182.6 (CO); HRMS calcd for C$_{22}$H$_{21}$^{35}Cl$_2$F$_1$N$_5$O$_2$ [M+H]$^+$ 476.1051, found 476.1044.

4-(3,6-Dichloro-2-fluorobenzoyl)-*N*-(2-morpholinopyridin-4-yl)-1*H*-pyrrole-2-carboxamide (300)
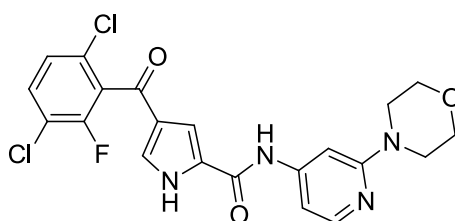
PyBrOP (154 mg, 0.33 mmol, 1.3 eq.) was added to a suspension of pyridine *N*-oxide **378** (100 mg, 0.25 mmol, 1 eq.), morpholine (28 μL, 0.37 mmol, 1.25 eq.) and Hunig's base (165 μL, 0.95 mmol, 3.75 eq.) in CH$_2$Cl$_2$ (1.6 mL) and the reaction was stirred at r.t for 18 h. The mixture was partitioned between CH$_2$Cl$_2$ (2 × 20 mL) and K$_2$CO$_3$ (20 mL, 10% aq.), washed with brine, dried over MgSO$_4$, and the solvent removed *in vacuo*. The residue was purified by MPLC on C18 reversed phase SiO$_2$ with gradient elution from 60:40:0.4 MeOH/H$_2$O/HCO$_2$H to 99.9:0.1 MeOH/HCO$_2$H. Product containing fractions were re-purified by MPLC on NH$_2$ SiO$_2$ with gradient elution from 0-4% MeOH/CH$_2$Cl$_2$ to give a white solid (16 mg, 14%); R_f 0.3 (5% MeOH/CH$_2$Cl$_2$); m.p. 136-140 °C; λ_{max}(EtOH)/nm 251, 294; IR ν_{max}/cm^{-1} 3182, 2962, 2922, 2853, 1639, 1595; ^{1}H NMR (500 MHz; DMSO-d_6) δ_H 3.41-3.45 (4H, m, H-morpholine), 3.72-3.77 (4H, m, H-morpholine), 7.18-7.22 (2H, m, H-3 pyridine and H-5-pyridine), 7.54-7.59 (2H, m, H-pyrrole and H-5'), 7.68 (1H, br s, H-pyrrole), 7.83 (1H, app t, J = 8.4 Hz, H-4'), 8.06-8.09 (1H, m, H-6-pyridine), 10.16 (1H, s, CO-NH), 12.79 (1H, br s, NH-pyrrole); ^{19}F NMR (470 MHz; DMSO-d_6) δ_F -116.65; ^{13}C NMR (125 MHz; DMSO-d_6) δ_C 45.2, 65.9, 96.0 (C-3-pyridine), 105.1 (C-5-pyridine), 111.6 (C-pyrrole), 119.3 (d, J_{CF} = 18.0 Hz, C-3'), 124.8 (C-pyrrole), 126.9 (d, J_{CF} = 3.6 Hz, C-5'), 128.4 (C-pyrrole), 129.1 (d, J_{CF} = 22.7 Hz, C-1'), 129.2 (d, J_{CF} = 5.0 Hz,), 130.5 (C-pyrrole), 131.9 (C-4'), 147.1 (C-pyridine), 148.3 (C-6-pyridine), 153.8 (d, J_{CF} =

248.4 Hz, C-2'), 158.9 (CO-NH), 160.2 (C-pyridine), 182.6 (CO); HRMS calcd for $C_{21}H_{18}{}^{35}Cl_2F_1N_4O_3$ [M+H]$^+$ 463.0735, found 463.0725.

tert-Butyl 4-(4-nitro-1H-pyrazol-1-yl)piperidine-1-carboxylate (380)[328,368]
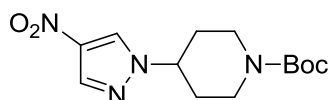
Prepared according to general procedure J using Boc-4-piperidinol (889 mg, 4.4 mmol), PPh$_3$ (1.73 g, 6.6 mmol, 1.5 eq.), 4-nitropyrazole (500 mg, 4.4 mmol, 1 eq.) and DEAD (1.04 mL, 5.3 mmol, 1.5 eq.) in THF (10 mL). The residue was purified by MPLC on SiO$_2$ with a gradient elution from 20-40% EtOAc/petrol to give a white solid (880 mg, 67%); R_f 0.5 (20% EtOAc/petrol); m.p. 116-118 °C; λ_{max}(EtOH)/nm 274; IR ν_{max}/cm^{-1} 3099, 2971, 2875, 1671, 1301; ^{1}H NMR (500 MHz; DMSO-d_6) δ_H 1.45 (9H, s, C(CH_3)$_3$), 1.85 (2H, qd, J = 4.2 and 11.6 Hz, 2 × H-piperidine), 2.04-2.11 (2H, m, 2 × H-piperidine), 2.80-3.07 (2H, m, 2 × H-piperidine), 3.99-4.19 (2H, m, 2 × H-piperidine), 4.50 (1H, tt, J = 4.2 and 11.6 Hz, CH$_2$CHCCH$_2$-piperidine), 8.32 (1H, s, H-pyrazole), 9.00 (1H, s, H-pyrazole); ^{13}C NMR (125 MHz; DMSO-d_6) δ_C 28.0 (C(CH$_3$)$_3$), 31.3 (2 × CH$_2$-piperidine), 42.4 (2 × CH$_2$-piperidine), 59.5 (CH-N-piperidine), 78.9 (C(CH$_3$)$_3$), 128.9 (C-pyrazole), 134.8 (C-pyrazole), 135.3 (C-pyrazole), 153.7 (CO); HRMS calc for $C_{13}H_{19}N_4O_4$ [M-H]$^-$ 295.1412, found 295.1408.

tert-Butyl 4-(4-amino-1H-pyrazol-1-yl)piperidine-1-carboxylate (393)[328,368]
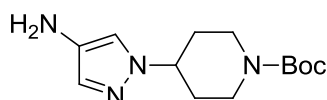
Prepared according to general procedure H using nitropyrazole **380** (310 mg, 1.05 mmol) in MeOH (15 mL) and EtOAc (15 mL) for 3 h to give a white solid (279 mg, 100%); R_f 0.4 (EtOAc, NH$_2$ SiO$_2$); m.p. 86-89 °C dec.; λ_{max}(EtOH)/nm 248; IR ν_{max}/cm^{-1} 3238, 2972, 2930, 2865, 1697, 1669; ^{1}H NMR (500 MHz; DMSO-d_6) δ_H 1.45 (9H, s, C(CH_3)$_3$), 1.71 (2H, qd, J = 4.2 and 11.7 Hz, 2 × H-piperidine), 1.90-1.97 (2H, m, 2 × H-piperidine), 2.75-3.04 (2H, m, 2 × H-piperidine), 3.80 (2H, br s, NH$_2$), 3.96-4.09 (2H, m, 2 × H-piperidine), 4.16 (1H, tt, J = 4.2 and 11.7 Hz, CH$_2$CHCCH$_2$-piperidine), 6.94 (1H, s, H-pyrazole), 7.10 (1H, s, H-pyrazole); ^{13}C NMR (125 MHz; DMSO-d_6) δ_C 28.0 (C(CH$_3$)$_3$), 31.9 (2 × CH$_2$-piperidine), 43.2 (2 × CH$_2$-piperidine), 57.6 (CHN-piperidine), 78.7 (C(CH$_3$)$_3$), 114.4 (CH-

pyrazole), 128.9 (CH-pyrazole), 131.1 (C-pyrazole), 153.8 (CO); HRMS calc for $C_{13}H_{23}N_4O_2$ [M+H]$^+$ 267.1816, found 267.1815.

tert-Butyl 4-(4-(4-(3,6-dichloro-2-fluorobenzoyl)-1*H*-pyrrole-2-carboxamido)-1*H*-pyrazol-1-yl)piperidine-1-carboxylate (414)
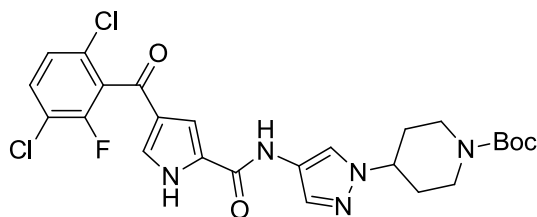
Prepared according to general procedure E using amine **393** (200 mg, 0.75 mmol, 2.5 eq.), carboxylic acid **337** (91 mg, 0.30 mmol, 1 eq.), cyanuric fluoride (18 µL, 0.21 mmol, 0.7 eq.), pyridine (24 µL, 0.30 mmol, 1 eq.) and MeCN (2 mL). Purification by MPLC on SiO$_2$ with a gradient elution from 40-70% EtOAc/petrol gave a yellow oil (125 mg, 76%); R_f 0.35 (70% EtOAc/petrol); m.p. 144 °C dec.; IR ν $_{max}$/cm^{-1} 3123 br, 2975, 1637; ^{1}H NMR (500 MHz; DMSO-d_6) δ$_H$ 1.46 (9H, s, C(CH$_3$)$_3$), 1.80 (2H, app qd, J = 4.1 and 11.6 Hz, 2 × H-piperidine), 1.97-2.04 (2H, m, 2 × H-piperidine), 2.82-3.02 (2H, m, , 2 × H-piperidine), 4.01-4.12 (2H, m, 2 × H-piperidine), 4.38 (1H, tt, J = 3.9 and 11.5 Hz, CH$_2$C*H*CCH$_2$-piperidine), 7.36 (1H, s, CH-pyrrole), 7.55 (1H, dd, J = 1.1 and 8.6 Hz, H-5'), 7.58-7.62 (2H, m, H-pyrrole and H-pyrazole), 7.82 (1H, app t, J = 8.6 Hz, H-4'), 8.02 (1H, s, H-pyrazole), 10.30 (1H, s, CO-NH), 12.67 (1H, s, NH-pyrazole); ^{19}F NMR (470 MHz; DMSO-d_6) δ$_F$ -116.66; ^{13}C NMR (125 MHz; DMSO-d_6) δ$_C$ 28.0 (C(*C*H$_3$)$_3$), 31.9 (2 × CH$_2$-piperidine), 42.8 (2 × CH$_2$-piperidine), 58.0 (CHN-piperidine), 78.8 (*C*(CH$_3$)$_3$), 110.2 (CH-pyrrole), 118.9 (CH-pyrazole), 119.3 (d, J_{CF} = 18.1 Hz, C-3'), 120.9 (C-pyrazole), 124.7 (C-pyrrole), 126.9 (d, J_{CF} = 4.1 Hz, C-5'), 128.7 (C-pyrrole), 129.2 (J_{CF} = 23.1 Hz, C-1'), 129.2 (J_{CF} = 5.1 Hz, C-6'), 129.6 (C-pyrrole), 130.0 (CH-pyrazole), 131.8 (C-4'), 153.8 (J_{CF} = 248.4 Hz, C-2'), 153.8 (CO-carbamate), 156.8 (CO-NH), 182.6 (CO); HRMS calcd for $C_{25}H_{27}{}^{35}Cl_2F_1N_5O_4$ [M+H]$^+$ 550.1419, found 550.1414.

4-(3,6-Dichloro-2-fluorobenzoyl)-*N*-(1-(piperidin-4-yl)-1*H*-pyrazol-4-yl)-1*H*-pyrrole-2-carboxamide (302)
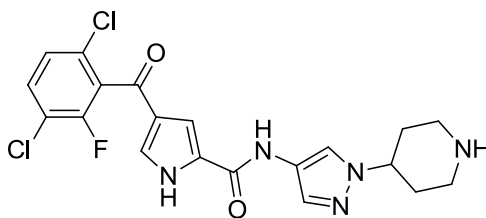
Prepared according to general procedure G using carbamate **414** (110 mg, 0.20 mmol, 1 eq.), Et$_3$SiH (80 µL, 0.50 mmol, 2.5 eq.), TFA (1 mL) and CH$_2$Cl$_2$ (1 mL). The residue was purified by MPLC on NH$_2$ SiO$_2$ with a gradient elution from 1-4% MeOH/CH$_2$Cl$_2$ to give a white solid (62 mg, 69%); R_f 0.3 (10% MeOH/CH$_2$Cl$_2$, NH$_2$ SiO$_2$); m.p. 199 °C dec.; λ_{max}(EtOH)/nm 255, 223; IR ν $_{max}$/cm^{-1} 3122 br, 2949, 1633, 1592; ^{1}H NMR (500 MHz; DMSO-*d$_6$*) δ$_H$ 1.78 (2H, app qd, *J* = 3.9 and 11.8 Hz, 2 × H-piperidine), 1.91-1.98 (2H, m, 2 × H-piperidine), 2.57-2.66 (2H, m, 2 × H-piperidine), 3.01-3.11 (2H, m, 2 × H-piperidine), 4.21 (1H, tt, *J* = 4.1 and 11.7 Hz, N-CH-piperidine), 7.35 (1H, s, H-pyrrole), 7.56 (1H, d, *J* = 8.6 Hz, H-5'), 7.57-7.61 (2H, m, H-pyrrole and H-pyrazole), 7.82 (1H, app t, *J* = 8.6 Hz, H-4'), 7.98 (1H, s, H-pyrazole), 10.27 (1H, s, CO-NH); ^{19}F NMR (470 MHz; DMSO-*d$_6$*) δ$_F$ -116.66; ^{13}C NMR (125 MHz; DMSO-*d$_6$*) δ$_C$ 33.5 (2 × CH$_2$-piperidine), 45.1 (2 × CH$_2$-piperidine), 59.0 (CHN-piperidine), 110.2 (CH-pyrrole), 118.4 (CH-pyrazole), 119.3 (d, *J$_{CF}$* = 18.0 Hz, C-3'), 120.8 (C-pyrazole), 124.7 (C-pyrrole), 126.9 (d, *J$_{CF}$* = 3.6 Hz, C-5'), 128.8 (CH-pyrrole), 129.2 (*J$_{CF}$* = 22.9 Hz, C-1'), 129.2 (*J$_{CF}$* = 4.8 Hz, C-6'), 129.7 (C-pyrrole), 130.0 (CH-pyrazole), 131.8 (C-4'), 153.8 (*J$_{CF}$* = 248.5 Hz, C-2'), 156.9 (CO-NH), 182.5 (CO); HRMS calcd for C$_{20}$H$_{19}$^{35}Cl$_2$F$_1$N$_5$O$_2$ [M+H]$^+$ 450.0894, found 450.0888.

4-(3,6-Dichloro-2-fluorobenzoyl)-*N*-(1-(1-methylpiperidin-4-yl)-1*H*-pyrazol-4-yl)-1*H*-pyrrole-2-carboxamide (303)

Prepared according to general procedure K using carbamate **414** (75 mg, 0.137 mmol), formic acid (1.5 mL), and formaldehyde (44 µL, 0.55 mmol, 4 eq.). The residue was purified by MPLC on NH$_2$ SiO$_2$ with a gradient elution from 2-6 % MeOH/EtOAc to give

a white solid (63 mg, 100%); R_f 0.25 (5% MeOH/EtOAc); m.p. 220-222 °C; λ_{max}(EtOH)/nm 252; IR ν_{max}/cm^{-1} 3121, 2938, 2788, 1631; ^{1}H NMR (500 MHz; DMSO-d_6) δ_H 1.93-2.03 (4H, m, 4 × H-piperidine), 2.09-2.21 (2H, m, 2 × H-piperidine), 2.28 (3H, s, NCH$_3$), 2.88-2.98 (2H, m, 2 × H-piperidine), 4.10-4.211 (1H, m, N-CH-piperidine), 7.36 (1H, s, H-pyrrole), 7.56 (1H, dd, J = 1.3 and 8.6 Hz, H-5'), 7.58-7.61 (2H, m, H-pyrrole and H-pyrazole), 7.82 (1H, app t, J = 8.6 Hz, H-4'), 8.01 (1H, s, H-pyrazole), 10.29 (1H, s, CO-NH), 12.67 (1H, s, NH-pyrazole); ^{19}F NMR (470 MHz; DMSO-d_6) δ_F -116.66; ^{13}C NMR (125 MHz; DMSO-d_6) δ_C 31.8 (2 × CH$_2$-piperidine), 45.5 (N-CH$_3$), 54.0 (2 × CH$_2$-piperidine), , 57.8 (CHN-piperidine), 110.1 (CH-pyrrole), 118.8 (CH-pyrazole), 119.3 (d, J_{CF} = 18.2 Hz, C-3'), 120.8 (C-pyrazole), 124.7 (C-pyrrole), 126.9 (d, J_{CF} = 3.7 Hz, C-5'), 128.7 (CH-pyrrole), 129.2 (d, J_{CF} = 23.1 Hz, C-1'), 129.2 (d, J_{CF} = 4.8 Hz, C-6'), 129.5 (C-pyrrole), 129.9 (CH-pyrazole), 131.8 (C-4'), 154.8 (d, J_{CF} = 248.5 Hz, C-2'), 156.8 (CO-NH), 182.6 (CO); HRMS calcd for C$_{21}$H$_{21}$^{35}Cl$_2$F$_1$N$_5$O$_2$ [M+H]$^+$ 464.1051, found 464.1043.

tert-Butyl 3-(4-nitro-1*H*-pyrazol-1-yl)azetidine-1-carboxylate (381)[328]
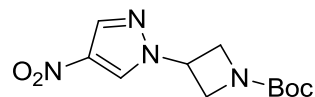
Prepared according to general procedure J using 1-Boc-3-hydroxyazetidine (766 mg, 4.42 mmol, 1 eq.), PPh$_3$ (1.74 g, 6.6 mmol, 1.5 eq.), 4-nitropyrazole (500 mg, 4.4 mmol, 1 eq.) and DEAD (1.04 mL, 6.6 mmol, 1.5 eq.) in THF (10 mL) with stirring at r.t. for 72 h. The residue was purified by MPLC on SiO$_2$ with a gradient elution from 10-40% EtOAc/petrol to give a white solid (765 mg, 63%); R_f 0.5 (40% EtOAc/petrol); m.p. 113-117 °C; λ_{max}(EtOH)/nm 276; IR ν_{max}/cm^{-1} 3117, 2973, 1675; ^{1}H NMR (500 MHz; DMSO-d_6) δ_H 1.44 (9H, s, (9H, s, C(CH$_3$)$_3$), 4.14-4.24 (2H, m, 2 × CH-azetidine), 4.29-4.39 (2H, m, 2 × CH-azetidine), 5.31 (1H, tt, J = 5.0 and 7.9 Hz, CH$_2$-C*H*-CH$_2$-azetidine), 8.43 (1H, s, H-pyrazole), 9.09 (1H, s, H-pyrazole); ^{13}C NMR (125 MHz; DMSO-d_6) δ_C 28.0 (C(*C*H$_3$)$_3$), 50.5 (C-azetidine), 79.1 (*C*(CH$_3$)$_3$), 130.8 (C-pyrazole), 135.0 (C-pyrazole), 136.3 (C-pyrazole), 155.4 (CO); HRMS calcd for C$_{11}$H$_{20}$N$_5$O$_4$ [M+NH$_4$]$^+$ 286.1510, found 286.1511.

tert-Butyl 3-(4-amino-1*H*-pyrazol-1-yl)azetidine-1-carboxylate (394)[328]
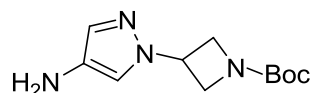
Prepared according to general procedure H using nitropyrazole **381** (250 mg, 0.93 mmol) in MeOH (20 mL) for 3 h to give a clear oil (220 mg, 99 %); R_f 0.1 (EtOAc); λ_{max}(EtOH)/nm 249; IR ν_{max}/cm^{-1} 3335 br, 2974, 1678; ^{1}H NMR (500 MHz; DMSO-d_6) δ_H 1.43 (9H, s, C(CH$_3$)$_3$), 3.93 (2H, br s, NH$_2$), 4.02-4.12 (2H, m, 2 × CH-azetidine), 4.20-4.28 (2H, m, 2 × CH-azetidine), 4.98-5.05 (1H, m, CH$_2$-C*H*-CH$_2$-azetidine), 7.07 (1H, s, H-pyrazole), 7.17 (1H, s, H-pyrazole); ^{13}C NMR (125 MHz; DMSO-d_6) δ_C 28.0 (C(CH$_3$)$_3$), 48.8 (C-azetidine), 55.8 (2 × C-azetidine), 78.8 (*C*(CH$_3$)$_3$), 115.7 (C-pyrazole), 130.5 (C-pyrazole), 131.4 (C-pyrazole), 155.5 (CO); HRMS calcd for C$_{11}$H$_{18}$N$_4$O$_2$ [M+H]$^+$ 239.1513, found 239.1503.

tert-Butyl 3-(4-(4-(3,6-dichloro-2-fluorobenzoyl)-1*H*-pyrrole-2-carboxamido)-1*H*-pyrazol-1-yl)azetidine-1-carboxylate (415)
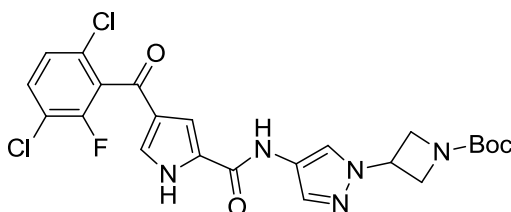
Prepared according to General procedure E using amine **394** (200 mg, 0.84 mmol, 2.5 eq.), carboxylic acid **337** (100 mg, 0.34 mmol, 1 eq.), cyanuric fluoride (20 μL, 0.24 mmol, 0.7 eq.), pyridine (27 μL, 0.34 mmol, 1 eq.) and MeCN (2 mL) with stirring at r.t. for 18 h. Purification by MPLC on SiO$_2$ with a gradient elution from 40-80% EtOAc/petrol gave a yellow solid (124 mg, 70%); R_f 0.3 (70% EtOAc/petrol); m.p. 164 °C dec.; λ_{max}(EtOH)/nm 285, 253, 223; IR ν_{max}/cm^{-1} 1627; ^{1}H NMR (500 MHz; DMSO-d_6) δ_H 1.45 (9H, s, C(CH$_3$)$_3$), 4.10-4.20 (2H, m, 2 × H-azetidine), 4.25-4.36 (2H, m, 2 × H-azetidine), 5.26 (1H, tt, J = 5.3 and 7.9 Hz, CH$_2$-C*H*-CH$_2$-azetidine), 7.37 (1H, s, H-pyrrole), 7.56 (1H, dd, J = 1.0 and 8.6 Hz, H-5'), 7.60 (1H, s, H-pyrrole), 7.71 (1H, s, H-pyrazole), 7.82 (1H, app t, J = 8.6 Hz, H-4'), 8.13 (1H, s, H-pyrazole), 10.35 (1H, s, CO-NH), 12.70 (1H, s, NH-pyrrole); ^{19}F NMR (470 MHz; DMSO-d_6) δ_F -116.66; ^{13}C NMR (125 MHz; DMSO-d_6) δ_C 28.0 (C(CH$_3$)$_3$), 49.1 (C-azetidine), 55.8 (2 × C-azetidine), 78.9 (*C*(CH$_3$)$_3$), 110.3 (CH-pyrrole), 119.3 (d, J_{CF} = 18.1 Hz, C-3'), 120.7 (C-pyrazole), 121.4 (C-pyrazole), 124.7 (C-pyrrole), 126.9 (d, J_{CF} = 4.0 Hz, C-5'), 128.6 (C-pyrrole), 129.2 (d, J_{CF} = 23.0 Hz, C-1'),

129.2 (d, J_{CF} = 5.0 Hz, C-6'), 129.6 (C-pyrrole), 131.4 (C-pyrazole), 131.8 (C-4'), 153.8 (d, J_{CF} = 248.5 Hz, C-2'), 155.6 (CO-carbamate), 156.9 (CO-NH), 182.6 (CO); HRMS calcd for $C_{23}H_{23}{}^{35}Cl_2F_1N_5O_4$ [M+H]$^+$ 522.1106, found 522.1103.

N-(1-(Azetidin-3-yl)-1*H*-pyrazol-4-yl)-4-(3,6-dichloro-2-fluorobenzoyl)-1*H*-pyrrole-2-carboxamide (304)
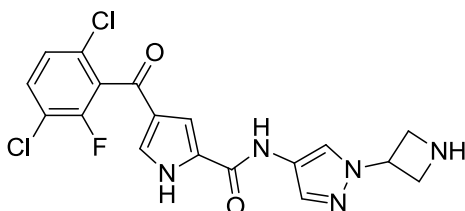
Prepared according to general procedure G using carbamate **415** (100 mg, 0.19 mmol, 1 eq.), Et$_3$SiH (76 μL, 0.48 mmol, 2.5 eq.), TFA (1 mL) and CH$_2$Cl$_2$ (1 mL). Purification by MPLC on NH$_2$ SiO$_2$ with a gradient elution from 2-8% MeOH/CH$_2$Cl$_2$ gave a white solid (69 mg, 85%); R_f 0.15 (5% MeOH/CH$_2$Cl$_2$, NH$_2$ SiO$_2$); m.p. 306-309 °C; λ_{max}(EtOH)/nm 254, 223; IR ν_{max}/cm^{-1} 3123.7 br, 2961.7, 1634.0, 1592.8, 1563.2; ^{1}H NMR (500 MHz; DMSO-d_6) δ_H 3.76 (2H, app t, J = 7.7 Hz, 2 × H-azetidine), 3.89-3.95 (2H, m, 2 ×H-azetidine), 5.21 (1H, quin, J = 7.7 Hz, CH-N-azetidine), 7.36 (1H, s, H-pyrrole), 7.56 (1H, dd, J = 1.0 and 8.5 Hz, H-5'), 7.60 (1H, s, H-pyrrole), 7.64 (1H, s, H-pyrazole), 7.83 (1H, app t, J = 8.5 Hz, H-4'), 8.13 (1H, s, H-pyrazole), 10.32 (1H, s, CO-NH); ^{19}F NMR (470 MHz; DMSO-d_6) δ_F -116.66; ^{13}C NMR (125 MHz; DMSO-d_6) δ_C 53.4 (2 × C-azetidine), 54.4(C-azetidine), 110.3 (CH-pyrrole), 119.3 (d, J_{CF} = 18.0 Hz, C-3'), 119.7 (C-pyrazole), 121.3 (C-pyrazole), 124.7 (C-pyrrole), 126.9 (d, J_{CF} = 3.5 Hz, C-5'), 128.7 (C-pyrrole), 129.2 (d, J_{CF} = 22.9 Hz, C-1'), 129.2 (d, J_{CF} = 5.3 Hz, C-6'), 129.7 (C-pyrrole), 130.5 (C-pyrazole), 131.8 (C-4'), 153.8 (d, J_{CF} = 248.6 Hz, C-2'), 156.9 (CO-NH), 182.5 (CO); HRMS calcd for $C_{18}H_{15}{}^{35}Cl_2F_1N_5O_2$ [M+H]$^+$ 422.0581, found 422.0578.

tert-Butyl 4-((4-nitro-1*H*-pyrazol-1-yl)methyl)piperidine-1-carboxylate (382)
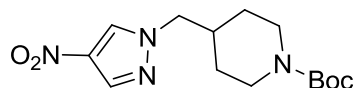
Prepared according to general procedure J using Boc-4-piperidinemethanol (951 mg, 4.4 mmol, 1 eq.), PPh$_3$ (1.74 g, 6.6 mmol, 1.5 eq.), 4-nitropyrazole (500 mg, 4.4 mmol, 1 eq.) and DEAD (1.04 mL, 6.6 mmol, 1.5 eq.) in THF (10 mL). The residue was purified by MPLC on SiO$_2$ with a gradient elution from 10-60% EtOAc/petrol to give a white solid

(1.135 g, 82%); R_f 0.35 (40% EtOAc/petrol); m.p. 158-160 °C; λ_{max}(EtOH)/nm 271; IR ν_{max}/cm^{-1} 1665, 1506, 1312.; ^{1}H NMR (500 MHz; DMSO-d_6) δ_H 1.10 (2H, qd, J = 4.1 and 12.6 Hz, 2 × H-piperidine), 1.42 (9H, s, C(CH$_3$)$_3$), 1.45-1.53 (2H, m, 2 × H-piperidine), 2.02-2.12 (1H, m, H-piperidine), 2.61-2.82 (m, 2 × CH-N-piperidine), 3.88-4.01 (2H, m, 2 × CH-N-piperidine), 4.13 (2H, d, J = 7.2 Hz, N-CH_2-CH), 8.31 (H-pyrazole), 8.92 (H-pyrazole); ^{13}C NMR (125 MHz; DMSO-d_6) δ_C 28.0 (C(CH$_3$)$_3$), 28.7 (C-piperidine), 35.9 (2 × C-piperidine), 42.8 (2 × C-piperidine), 57.2 (N-CH$_2$-CH), 78.5 (C(CH$_3$)$_3$), 130.8 (CH-pyrazole), 134.7 (C-4-pyrazole), 135.6 (CH-pyrazole), 153.8 (CO); HRMS calc for C$_{14}$H$_{21}$O$_4$N$_4$ [M-H]$^-$ 309.1568, found 309.1565.

tert-Butyl 4-((4-amino-1*H*-pyrazol-1-yl)methyl)piperidine-1-carboxylate (395)
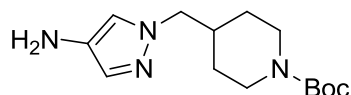
Prepared according to General procedure H using nitropyrazole **382** (1.1 g, 3.5 mmol) in MeOH (40 mL) and EtOAc (40 mL) for 5 h to give an orange solid (945 mg, 95%); R_f 0.35 (EtOAc, NH$_2$ SiO$_2$); m.p. 104-107 °C; λ_{max}(EtOH)/nm 247; IR ν_{max}/cm^{-1} 2966, 2929, 1672; ^{1}H NMR (500 MHz; DMSO-d_6) δ_H 1.04 (2H, qd, J = 4.3 and 12.3 Hz, 2 × H-piperidine), 1.42 (9H, s, C(CH$_3$)$_3$), 1.42-1.49 (2H, m, 2 × H-piperidine), 1.85-1.97 (1H, m, H-piperidine), 2.58-2.82 (m, 2 × CH-N-piperidine), 3.79-3.87 (4H, m, N-CH_2-CH and NH$_2$), 3.88-3.99 (2H, m, 2 × H-N-piperidine), 6.92 (H-pyrazole), 7.03 (H-pyrazole); ^{13}C NMR (125 MHz; DMSO-d_6) δ_C 28.1 (C(CH$_3$)$_3$), 29.0 (C-piperidine), 36.7 (2 × C-piperidine), 42.5 (2 × C-piperidine), 56.2 (N-CH$_2$-CH), 78.4 (C(CH$_3$)$_3$), 117.0 (C-2-pyrazole), 129.2 (C-4-pyrazole), 130.5 (C-3-pyrazole), 153.8 (CO); HRMS calc for C$_{14}$H$_{25}$N$_4$O$_4$ [M+H]$^+$ 281.1972, found 281.1972.

tert-Butyl 4-((4-(4-(3,6-dichloro-2-fluorobenzoyl)-1*H*-pyrrole-2-carboxamido)-1*H*-pyrazol-1-yl)methyl)piperidine-1-carboxylate (416)
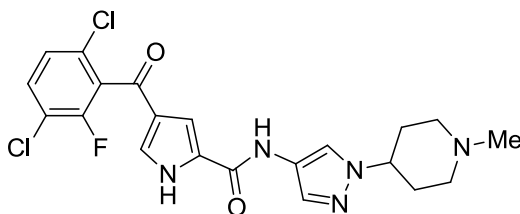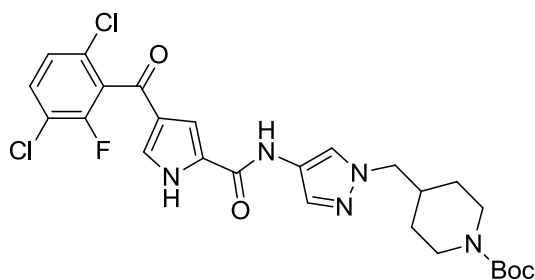

Prepared according to general procedure E using amine **395** (450 mg, 1.6 mmol, 2.5 eq.), carboxylic acid **337** (195 mg, 0.64 mmol, 1 eq.), cyanuric fluoride (18 μL, 0.21 mmol, 0.3 eq.) and pyridine (52 μL, 0.64 mmol, 1 eq.) in MeCN (2 mL) with stirring at r.t. for 18 h. Purification by MPLC on SiO$_2$ with a gradient elution from 50-100% EtOAc/petrol gave a yellow solid (214 mg, 59%); R_f 0.1 (EtOAc, NH$_2$ SiO$_2$); m.p. 211 °C dec.; λ_{max}(EtOH)/nm 254; IR ν_{max}/cm^{-1} 3126, 2977, 2932, 2860, 1645, 1592; ^{1}H NMR (500 MHz; DMSO-d_6) δ_H 1.09 (2H, qd, J = 3.6 and 12.3 Hz, 2 × CH-piperidine), 1.42 (9H, s, C(CH$_3$)$_3$), 1.44-1.52 (2H, m, 2 × H-piperidine), 1.94-2.07 (1H, m, H-piperidine), 2.60-2.80 (m, 2 × CH-N-piperidine), 3.87-4.01 (2H, m, 2 × CH-N-piperidine), 4.02 (2H, d, J = 7.1 Hz, N-C*H*$_2$-CH), 7.36 (1H, s, H-pyrrole), 7.56 (1H, dd, J = 1.3 and 8.6 Hz, H-4'), 7.58 (s, H-pyrazole), 7.60 (1H, s, H-pyrrole), 7.82 (1H, app t, J = 8.6 Hz, H-3'), 7.99 (1H, s, H-pyrazole), 10.29 (1H, s, CO-NH), 12.66 (1H, s, NH-pyrrole); ^{19}F NMR (470 MHz; DMSO-d_6) δ_F -116.65; ^{13}C NMR (125 MHz; DMSO-d_6) δ_C 28.1 (C(*C*H$_3$)$_3$), 30.0 (C-piperidine), 36.6 (2 × C-piperidine), 42.8 (2 × C-piperidine), 56.3 (N-*C*H$_2$-CH), 78.5 (*C*(CH$_3$)$_3$), 110.1 (CH-pyrrole), 119.3 (d, J_{CF} = 18.0 Hz, C-3'), 120.9 (C-pyrazole), 121.2 (C-pyrazole), 124.7 (C-pyrrole), 126.9 (d, J_{CF} = 3.8 Hz, C-5'), 128.7 (C-pyrrole), 129.2 (d, J_{CF} = 23.0 Hz, C-1'), 129.2 (d, J_{CF} = 5.1 Hz, C-6'), 129.5 (C-pyrrole), 130.2 (C-3-pyrazole), 131.8 (C-4'), 153.8 (CO-carbamate), 153.8 (d, J_{CF} = 248.5 Hz, C-2'), 156.8 (CO-NH), 182.6 (CO); HRMS calc for C$_{26}$H$_{29}$^{35}Cl$_2$F$_1$N$_5$O$_4$ [M+H]$^+$ 564.1575, found 564.1566.

4-(3,6-Dichloro-2-fluorobenzoyl)-*N*-(1-(piperidin-4-ylmethyl)-1*H*-pyrazol-4-yl)-1*H*-pyrrole-2-carboxamide (305)
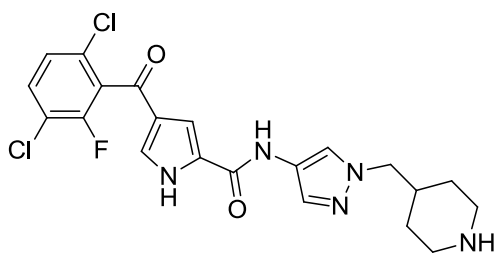
Prepared according to general procedure G using carbamate **416** (200 mg, 0.35 mmol, 1 eq.), Et$_3$SiH (283 µL, 1.77 mmol, 5 eq.), TFA (1.5 mL) and CH$_2$Cl$_2$ (1.5 mL). Purification by MPLC on NH$_2$ SiO$_2$ with a gradient elution from 3-15% MeOH/EtOAc gave a white solid (106 mg, 64%); R_f 0.05 (5% MeOH/EtOAc); m.p. 147 °C dec.; λ_{max}(EtOH)/nm 254; IR ν_{max}/cm^{-1} 2926, 1633, 1592; ^{1}H NMR (500 MHz; DMSO-d_6) δ_H 1.09 (2H, qd, J = 3.6 and 12.0 Hz, 2 × H-piperidine), 1.39-1.47 (2H, m, 2 × H-piperidine), 1.82-1.94 (1H, m, H-piperidine), 2.43 (td, J = 12.0 and 2.2 Hz, 2 × CH-N-piperidine), 2.90-2.97 (2H, m, 2 × CH-N-piperidine), 3.97 (2H, d, J = 7.1 Hz, pyrazole-CH$_2$-piperidine), 7.33 (1H, s, H-pyrrole), 7.55 (1H, dd, J = 1.3 and 8.7 Hz, H-4'), 7.57 (1H, s, H-pyrazole), 7.58 (1H, s, H-pyrrole), 7.82 (1H, app t, J = 8.7 Hz, H-3'), 7.97 (1H, s, H-pyrazole), 10.26 (1H, s, CO-NH); ^{19}F NMR (470 MHz; DMSO-d_6) δ_F -116.64; ^{13}C NMR (125 MHz; DMSO-d_6) δ_C 30.2 (C-piperidine), 37.3 (2 × C-piperidine), 45.5 (2 × C-piperidine), 57.2 (pyrazole-CH$_2$-piperidine), 110.2 (CH-pyrrole), 119.3 (d, J_{CF} = 18.2 Hz, C-3'), 120.9 (C-pyrazole), 121.1 (C-pyrazole), 124.7 (C-pyrrole), 126.8 (d, J_{CF} = 3.8 Hz, C-5'), 129.1 (C-pyrrole), 129.2 (d, J_{CF} = 11.6 Hz, C-6'), 129.2 (CH-pyrrole), 129.3 (d, J_{CF} = 20.5 Hz, C-1'), 130.0 (C-pyrazole), 131.7 (C-4'), 153.8 (d, J_{CF} = 248.86 Hz, C-2'), 157.0 (CO-NH), 182.4 (CO); HRMS calc for C$_{21}$H$_{21}$^{35}Cl$_2$F$_1$N$_5$O$_2$ [M+H]$^+$ 464.1051, found 464.1038.

1-Methyl-4-((4-nitro-1*H*-pyrazol-1-yl)methyl)piperidine (383)
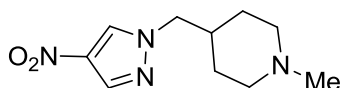
Procedure 1: Prepared according to general procedure J using 1-methyl-4-piperidinemethanol (349 µL, 2.7 mmol), PPh$_3$ (1.04 g, 4.0 mmol, 1.5 eq.), 4-nitropyrazole (300 mg, 2.7 mmol, 1 eq.) and DEAD (626 µL, 4.0 mmol, 1.5 eq.) in THF (6 mL). Purification by MPLC on NH$_2$ SiO$_2$ with a gradient elution from 30-80% CH$_2$Cl$_2$/petrol gave a white solid, containing product, reduced DEAD and Ph$_3$PO. This mixture was

dissolved in 5% MeOH/CH$_2$Cl$_2$ and passed through an SCX ion exchange column, eluting with 5% MeOH/CH$_2$Cl$_2$ followed by 80/20/2 CH$_2$Cl$_2$/MeOH/NH$_4$OH to give a beige solid (200 mg, 34%). **Procedure 2:** Prepared according to general procedure K to give a clear oil (304 mg, 84%); R_f 0.3 (CH$_2$Cl$_2$, NH$_2$ SiO$_2$); m.p. 70-73 °C; λ_{max}(EtOH)/nm 274; IR ν_{max}/cm^{-1} 3067, 2943, 2903, 2797, 1511, 1312; ^{1}H NMR (500 MHz; DMSO-d_6) δ_H 1.24 (2H, qd, J = 3.6 and 12.5 Hz, 2 × H-piperidine), 1.42-1.50 (2H, m, 2 × H-piperidine), 1.77-1.89 (3H, m, 3 × H-piperidine), 2.16 (3H, s, CH$_3$), 2.72-2.80 (2H, m, 2 × H-piperidine), 4.11 (2H, d, J = 7.3 Hz, pyrazole-CH$_2$-piperidine), 8.30 (1H, s, H-pyrazole), 8.93(1H, s, H-pyrazole); ^{13}C NMR (125 MHz; DMSO-d_6) δ_C 28.9 (2 × CH$_2$-piperidine), 35.5 (CH-piperidine), 46.0 (CH$_3$), 54.6 (2 × CH$_2$-piperidine), 57.5 (N-CH$_2$-CH), 130.8 (CH-pyrazole), 134.7 (C-pyrazole), 135.6 (CH-pyrazole); HRMS calc for C$_{10}$H$_{17}$N$_4$O$_2$ [M+H]$^+$ 225.1346, found 225.1341.

1-((1-Methylpiperidin-4-yl)methyl)-1*H*-pyrazol-4-amine (396)
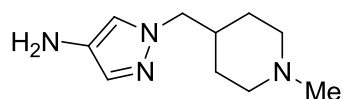
Prepared according to general procedure H using nitropyrazole **383** (190 mg, 0.85 mmol) and MeOH (20 mL) for 2 h to give a pale brown oil (150 mg, 91%); R_f 0.4 (7% MeOH/CH$_2$Cl$_2$, NH$_2$ SiO$_2$); m.p. 50-55 °C; λ_{max}(EtOH)/nm 246; IR ν_{max}/cm^{-1} 3304, 3127, 2919, 2794; ^{1}H NMR (500 MHz; DMSO-d_6) δ_H 1.18 (2H, qd, J = 12.5 and 3.7 Hz, 2 × H-piperidine), 1.39-1.47 (2H, m, 2 × H-piperidine), 1.61-1.72 (1H, m, H-piperidine), 1.74-1.84 (2H, m, 2 × H-piperidine), 2.15 (3H, s, CH$_3$), 2.70-2.78 (2H, m, 2 × H-piperidine), 3.80 (2H, d, J = 7.3 Hz, N-C*H*$_2$-CH), 6.91 (1H, s, H-pyrazole), 7.02 (1H, s, H-pyrazole); ^{13}C NMR (125 MHz; DMSO-d_6) δ_C 29.3 (2 × CH$_2$-piperidine), 36.3 (2 × CH$_2$-piperidine), 46.1 (CH$_3$), 54.9 (2 × CH$_2$-piperidine), 56.5 (N-C*H*$_2$-CH), 116.9 (CH-pyrazole), 129.0 (CH-pyrazole), 130.5 (C-pyrazole); HRMS calc for C$_{10}$H$_{18}$N$_4$ [M+H]$^+$ 195.1604, found 195.1600.

4-(3,6-Dichloro-2-fluorobenzoyl)-*N*-(1-((1-methylpiperidin-4-yl)methyl)-1*H*-pyrazol-4-yl)-1H-pyrrole-2-carboxamide (306)
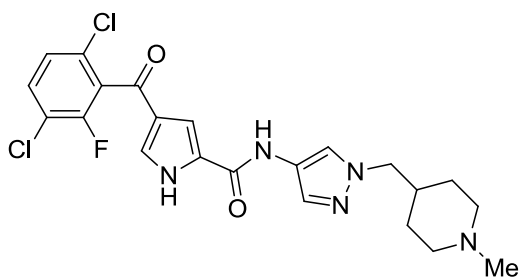
Amine **396** (140 mg, 0.43 mmol, 1.5 eq) was added to carboxylic acid **337** (87 mg, 0.29 mmol, 1 eq.), pyridine (23 μL, 0.29 mmol, 1 eq) and PyBrOP (200 mg, 0.43 mmol, 1.5 eq) in MeCN (2 mL). The mixture was stirred at r.t. for 1 h and then partitioned between EtOAc (2 × 30 mL) and H_2O (20 mL). The organic layers were combined, washed with brine, dried ($MgSO_4$) and the solvent removed *in vacuo*. Purification by MPLC on NH_2 SiO_2 with gradient elution from 1-4% MeOH/CH_2Cl_2 gave a beige solid (53 mg, 39%); R_f 0.4 (7% MeOH/CH_2Cl_2, NH_2 SiO_2); m.p. 124-128 °C; λ_{max}(EtOH)/nm 252; IR ν_{max}/cm^{-1} 2935, 1639, 1592; ^{1}H NMR (500 MHz; DMSO-d_6) δ_H 1.23 (2H, qd, *J* = 3.0 and 12.5 Hz, 2 × H-piperidine), 1.41-1.51 (2H, m, 2 × H-piperidine), 1.70-1.85 (3H, m, 3 × H-piperidine), 2.15 (CH$_3$), 2.72-2.80 (2H, m, 2 × H-piperidine), 4.00 (2H, d, *J* = 7.3 Hz, N-C*H$_2$*-CH), 7.35 (1H, s, H-pyrrole), 7.53-7.61 (3H, m, H-4', H-pyrrole and H-pyrazole), 7.82 (1H, app t, *J* = 8.4 Hz, H-3'), 7.97 (1H, s, H-pyrazole), 10.28 (1H, s, CO-NH), 12.52 (1H, br s, NH-pyrrole); ^{19}F NMR (470 MHz; DMSO-d_6) δ_F -116.65; ^{13}C NMR (125 MHz; DMSO-d_6) δ_C 29.2 (2 × C-piperidine), 36.2 (C-piperidine), 46.1 (CH$_3$), 54.8 (2 × C-piperidine), 56.7 (N-*C*H$_2$-CH), 110.5 (CH-pyrrole), 121.0 (d, J_{CF} = 29.7 Hz, C-3'), 121.3 (CH-pyrazole), 124.7 (C-pyrrole), 126.9 (d, J_{CF} = 4.1 Hz, C-5'), 128.2 (C-pyrrole), 128.7 (CH-pyrrole), 129.2 (d, J_{CF} = 21.8 Hz, C-1'), 129.2 (d, J_{CF} = 5.4 Hz, C-6'), 130.1 (C-1'), 130.5 (C-pyrazole), 131.8 (C-4'), 153.8 (d, J_{CF} = 248.2 Hz, C-2'), 156.8 (CO-NH), 182.6 (CO); HRMS calc for $C_{22}H_{23}{}^{35}Cl_2F_1N_5O_2$ [M+H]$^+$ 478.1207, found 478.1195.

4-(6-Chloro-2-fluoro-3-methoxybenzoyl)-*N*-(1-((1-methylpiperidin-4-yl)methyl)-1*H*-pyrazol-4-yl)-1*H*-pyrrole-2-carboxamide (325)
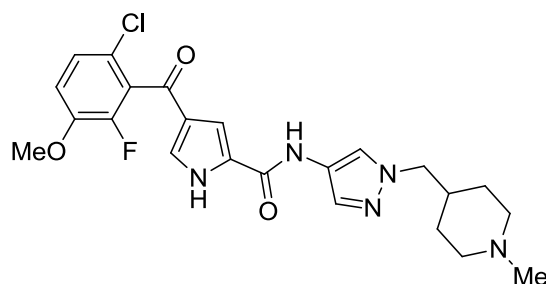
Prepared according to general procedure E using amine **396** (250 mg, 1.11 mmol, 2.5 eq.), carboxylic acid **421** (133 mg, 0.45 mmol, 1 eq.), cyanuric fluoride (27 μL, 0.31 mmol, 0.7 eq.), pyridine (36 μL, 0.45 mmol, 1 eq.) and MeCN (3 mL) with stirring at r.t. for 18 h. Purification by MPLC on NH_2 SiO_2 with a gradient elution from 0-7% MeOH/CH_2Cl_2 gave a white solid (91 mg, 43%); R_f 0.4 (5% MeOH/CH_2Cl_2, NH_2 SiO_2); m.p. 204 °C dec.; λ_{max}(EtOH)/nm 252, 227; IR ν_{max}/cm^{-1} 3124.1 br, 2951.7, 1641.1, 1602.0, 1575.4; ^{1}H NMR (500 MHz; DMSO-d_6) δ_H 1.23 (2H, qd, J = 12.0 and 3.1 Hz, 2 × CH-piperidine), 1.41-1.51 (2H, m, 2 × CH-piperidine), 1.69-1.86 (3H, m, 3 × CH-piperidine), 2.15 (3H, s, NCH$_3$), 2.72-2.79 (2H, m, 2 × CH-piperidine), 3.94 (3H, s, OCH$_3$), 3.99 (2H, d, J = 7.1 Hz, N-CH_2-CH), 7.32 (1H, s, H-pyrrole), 7.37 (1H, app t, J = 9.0 Hz, H-4'), 7.42 (1H, dd, J = 0.8 and 9.0 Hz, H-5'), 7.46 (H-pyrrole), 7.56 (H-pyrazole), 7.97 (H-pyrazole), 10.28 (CO-NH), 12.58 (1H, br s, NH-pyrrole); ^{19}F NMR (470 MHz; DMSO-d_6) δ_F -136.14; ^{13}C NMR (125 MHz; DMSO-d_6) δ_C 29.2 (2 × C-piperidine), 36.2 (C-piperidine), 46.1 (NCH$_3$), 54.8 (2 × C-piperidine), 56.4 (OCH$_3$), 56.7 (N-CH$_2$-CH), 110.3 (CH-pyrrole), 115.1 (C-4'), 120.2 (d, J_{CF} = 4.7 Hz, C-1'), 120.8 (C-pyrazole), 121.0 (CH-pyrazole), 125.1 (C-pyrrole), 125.5 (d, J_{CF} = 3.6 Hz, C-5'), 128.5 (C-6'), 128.6 (C-pyrrole) 128.8 (CH-pyrrole), 130.0 (CH-pyrazole), 146.4 (d, J_{CF} = 10.6 Hz, C-3'), 147.9 (d, J_{CF} = 247.0 Hz, C-2'), 156.8 (CO-NH), 183.6 (CO); HRMS calcd for $C_{23}H_{26}{}^{35}Cl_1F_1N_5O_3$ [M+H]$^+$ 474.1703, found 474.1691.

2,2,2-Trifluoro-1-(4-hydroxypiperidin-1-yl)ethanone (408)[369]
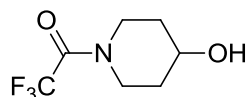
Trifluoroacetic anhydride (1.51 mL, 10.9 mmol, 1.1 eq.) was added to a mixture of 4-hydroxypiperidine (1 g, 9.9 mmol, 1 eq.) and pyridine (1.6 mL, 19.8 mmol, 2 eq.) in CH_2Cl_2 (25 mL) at 0 °C, and the reaction was stirred at r.t. for 18 h. The mixture was

washed with KHSO$_4$ (2 × 25 mL, 15% aq), followed by NaHCO$_3$ (10% aq, 20 mL). The organic layer was dried over MgSO$_4$, and the solvent removed *in vacuo*. The residue was suspended in MeOH (20 mL) and NaHCO$_3$ (10% aq, 20 mL), stirred at r.t. for 20 min and extracted with EtOAc (2 × 50 mL). The organic extracts were washed with water (20 mL) and brine (20 mL), dried over MgSO$_4$, and the solvent removed *in vacuo* to give a clear oil (910 mg, 47%); R_f 0.4 (5% MeOH/CH$_2$Cl$_2$; KMnO$_4$); λ_{max}(EtOH)/nm 208; IR ν $_{max}$/cm^{-1} 3383 br, 1673; ^{1}H NMR (500 MHz; DMSO-d_6) δ$_H$ 1.38-1.50 (2H, m, H-piperidine), 1.78-1.88 (2H, m, H-piperidine), 3.33-3.45 (2H, m, H-piperidine), 3.69-3.77 (1H, m, H-piperidine), 3.78-3.91 (2H, m, H-piperidine), 4.92 (1H, d, J = 4.0 Hz, OH); ^{19}F NMR (470 MHz; DMSO-d_6) δ$_F$ -68.11; ^{13}C NMR (125 MHz; DMSO-d_6) δ$_C$ 33.3 (C-piperidine), 34.2 (C-piperidine), 40.6 (C-piperidine), 42.6 (q, J_{CF} = 3.4 Hz, C-piperidine), 64.3 (C-OH), 116.4 (q, J_{CF} = 288.5 Hz, CF$_3$), 153.9 (q, J_{CF} = 35.6 Hz, CO); MS (ES+) *m/z* 198.2 [M+H]$^+$.

1-(2,2,2-Trifluoroethyl)piperidin-4-ol (409)[370]
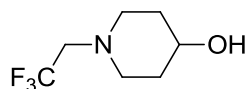
Borane.THF complex (1 M in THF, 5.25 mL, 5.25 mmol, 2.5 eq.) was added to a solution of trifluoroacetamide **408** (690 mg, 3.5 mmol, 1 eq.) in THF (10 mL) and heated at reflux for 3 h. The reaction was allowed to cool to r.t., and HCl (1 M aq.) was added until gas evolution ceased. The mixture was heated to 70 °C for 20 min, allowed to cool to r.t., and basified with NaOH (2 M aq, 10 mL). The mixture was extracted with EtOAc (2 × 30 mL), dried over MgSO$_4$, and the solvent removed *in vacuo* to give a clear oil (458 mg, 71%); R_f 0.35 (5% MeOH/CH$_2$Cl$_2$; KMnO$_4$); λ_{max}(EtOH)/nm 273 weak; IR ν $_{max}$/cm^{-1} 3337 br; ^{1}H NMR (500 MHz; DMSO-d_6) δ$_H$ 1.36-1.45 (2H, m, H-piperidine), 1.68-1.75 (2H, m, H-piperidine), 2.36-2.44 (2H, m, H-piperidine), 2.80-2.87 (2H, m, H-piperidine), 3.14 (2H, q, J_{HF} = 10.3 Hz, CH$_2$CF$_3$), 3.45-3.52 (1H, m, C*H*OH), 4.60 (1H, d, J = 4.1 Hz, OH); ^{19}F NMR (470 MHz; DMSO-d_6) δ$_F$ -67.99; ^{13}C NMR (125 MHz; DMSO-d_6) δ$_C$ 34.2 (C-piperidine), 51.3 (C-piperidine), 56.8 (q, J_{CF} = 28.9 Hz, *C*H$_2$CF$_3$), 65.4 (C-piperidine), 126.1 (q, J_{CF} = 280.4 Hz, CF$_3$); MS: No mass ion detected.

4-(4-Nitro-1*H*-pyrazol-1-yl)-1-(2,2,2-trifluoroethyl)piperidine (384)
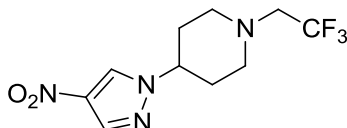
Prepared according to general procedure J using alcohol **409** (486 mg, 2.7 mmol, 1 eq.), PPh$_3$ (1.04 g, 4.0 mmol, 1.5 eq.), 4-nitropyrazole (300 mg, 2.7 mmol, 1 eq.) and DEAD (626 μL, 4.0 mmol, 1.5 eq.) in THF (5 mL) with stirring at r.t. for 18 h. The residue was purified by MPLC on SiO$_2$ with a gradient elution from 5-40% EtOAc/petrol to give a white solid (395 mg, 54%); R_f 0.25 (30% EtOAc/petrol); m.p. 94-95 °C; λ_{max}(EtOH)/nm 251; IR ν_{max}/cm^{-1} 1494, 1304; ^{1}H NMR (500 MHz; DMSO-d_6) δ_H 1.97-2.07 (4H, m, H-piperidine), 2.53-2.61 (2H, m, H-piperidine), 3.01-3.09 (2H, m, H-piperidine), 3.28 (2H, q, J_{HF} = 10.2 Hz, CH$_2$CF$_3$), 4.28-4.36 (1H, m, H-piperidine), 8.32 (H-pyrazole), 8.98 (H-pyrazole); ^{19}F NMR (470 MHz; DMSO-d_6) δ_F -68.05; ^{13}C NMR (125 MHz; DMSO-d_6) δ_C 31.2 (C-piperidine), 51.9 (C-piperidine), 56.2 (q, J_{CF} = 29.4 Hz, CH$_2$CF$_3$), 59.3 (C-piperidine), 126.1 (q, J_{CF} = 280.5 Hz, CF$_3$), 128.8 (C-pyrazole), 134.8 (C-NO$_2$), 135.2 (C-pyrazole); HRMS calcd for C$_{10}$H$_{14}$F$_3$N$_4$O$_2$ [M+H]$^+$ 279.1063, found 279.1062.

1-(1-(2,2,2-Trifluoroethyl)piperidin-4-yl)-1*H*-pyrazol-4-amine (397)
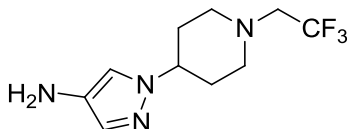
Palladium on carbon (10%, 40 mg) was added to nitropyrazole **384** (370 mg, 1.3 mmol) in MeOH (30 mL), and the mixture was stirred at r.t. under an atmosphere of hydrogen for 18 h. The reaction was filtered through Celite, and the solvent removed *in vacuo* to give a deep red solid (321 mg, 97%); R_f (5% MeOH/EtOAc); m.p. 80-83 °C; λ_{max}(EtOH)/nm 274; IR ν_{max}/cm^{-1} 3355, 3212, 2838; ^{1}H NMR (500 MHz; DMSO-d_6) δ_H 1.82-1.96 (4H, m, H-piperidine), 2.46-2.58 (2H, m, H-piperidine), 2.95-3.04 (2H, m, H-piperidine), 3.24 (2H, q, J_{HF} = 10.3 Hz, CH$_2$CF$_3$), 3.79 (2H, s, NH$_2$), 3.93-4.01 (1H, m, H-piperidine), 6.93 (1H, d, J = 0.8 Hz, H-pyrazole), 7.10 (1H, d, J = 0.8 Hz, H-pyrazole); ^{19}F NMR (470 MHz; DMSO-d_6) δ_F -68.00; ^{13}C NMR (125 MHz; DMSO-d_6) δ_C 31.9 (C-piperidine), 52.4 (C-piperidine), 56.5 (q, J_{CF} = 29.4 Hz, CH$_2$CF$_3$), 57.4 (C-piperidine), 114.3 (C-pyrazole), 126.1 (q, J_{CF} = 280.5 Hz, CF$_3$), 128.8 (C-pyrazole), 130.5 (C-pyrazole); MS (ES+) *m/z* 249.3 [M+H]$^+$; HRMS calcd for C$_{10}$H$_{16}$F$_3$N$_4$ [M+H]$^+$ 249.1322, found 249.1319.

4-(3,6-Dichloro-2-fluorobenzoyl)-*N*-(1-(1-(2,2,2-trifluoroethyl) piperidin-4-yl)-1*H*-pyrazol-4-yl)-1*H*-pyrrole-2-carboxamide (308)
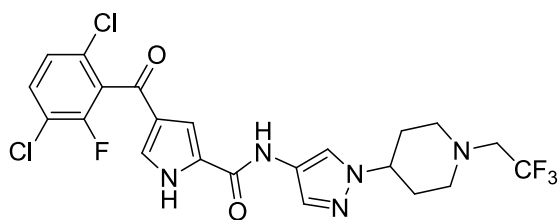
Prepared according to general procedure L using carboxylic acid **337** (100 mg, 0.33 mmol, 1 eq.), Et$_3$N (115 µL, 0.83 mmol, 2.5 eq.), and 2-chloromethylpyridinium iodide (93 mg, 0.36 mmol, 1.1 eq.) in DCM (4 mL) followed by the addition of amine **397** (102 mg, 0.41 mmol, 1.25 eq.) with stirring at r.t. for 18 h. The residue was purified by MPLC on SiO$_2$ with gradient elution from 20-45% EtOAc/petrol to give a white solid (60 mg, 34%); R_f 0.1 (30% EtOAc/petrol); m.p. 253-255 °C; λ_{max}(EtOH)/nm 253sh; IR ν_{max}/cm^{-1} 3349, 3178, 1627, 1605; ^{1}H NMR (500 MHz; DMSO-d_6) δ_H 1.90-2.03 (4H, m, H-piperidine), 2.53-2.61 (2H, m, H-piperidine), 3.01-3.08 (2H, m, H-piperidine), 3.27 (2H, q, J_{HF} = 10.2 Hz, CH$_2$CF$_3$), 4.15-4.24 (1H, m, H-piperidine), 7.36 (1H, s, H-pyrrole), 7.56 (1H, dd, J = 1.1 and 8.6 Hz, H-5'), 7.58-7.62 (2H, m, H-pyrrole and H-pyrazole), 7.82 (1H, app t, J = 8.6 Hz, H-4'), 8.02 (1H, s, H-pyrazole), 10.29 (1H, s, CO-NH), 12.67 (1H, br s, NH-pyrrole); ^{19}F NMR (470 MHz; DMSO-d_6) -67.98, -116.65; ^{13}C NMR (125 MHz; DMSO-d_6) δ_C 31.9 (C-piperidine), 52.3 (C-piperidine), 56.4 (q, J_{CF} = 29.4 Hz, CH$_2$CF$_3$), 57.8 (C-piperidine), 110.1 (CH-pyrrole), 118.7 (C-pyrazole), 119.3 (d, J_{CF} = 18.2 Hz, C-3'), 120.8 (CH-pyrazole), 121.7 (C-pyrazole), 124.7 (C-pyrrole), 125.0, 126.4 (q, J = 271.0 Hz, CF$_3$), 126.9 (d, J_{CF} = 4.1 Hz, C-5'), 128.7 (C-pyrrole), 129.2 (d, J_{CF} = 23.2 Hz, C-1'), 129.2 (d, J_{CF} = 5.1 Hz, C-6'), 129.5 (C-pyrrole), 129.9 (CH-pyrazole), 131.8 (C-4'), 153.8 (d, J_{CF} = 248.4 Hz, C-2'), 156.8 (CO-NH), 182.6 (CO); HRMS calcd for C$_{22}$H$_{20}$^{35}Cl$_2$F$_4$N$_5$O$_2$ [M+H]$^+$ 532.0925, found 532.0911.

1*H*-Pyrazol-4-amine (410)[371]
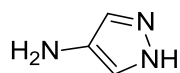
Prepared according to general procedure H using 4-nitropyrazole (500 mg, 4.40 mmol) and MeOH (30 mL) to give a red gum (360 mg, 98 %); λ_{max}(EtOH)/nm 238; IR ν_{max}/cm^{-1} 3374, 3114, 2955, 2891, 2842, 1585; ^{1}H NMR δ_H (500 MHz; DMSO-d_6) δ_H 7.03 (2H, s, 2 × H-pyrazole); ^{13}C NMR (125 MHz; DMSO-d_6) δ_C 122.5, 130.0; MS: No mass ion detected.

4-(3,6-Dichloro-2-fluorobenzoyl)-*N*-(1H-pyrazol-4-yl)-1*H*-pyrrole-2-carboxamide (313)

Prepared according to general procedure E using amine **410** (69 mg, 0.83 mmol, 2.5 eq.), carboxylic acid **337** (100 mg, 0.33 mmol, 1 eq.), cyanuric fluoride (20 μL, 0.24 mmol, 0.7 eq.), pyridine (27 μL, 0.34 mmol, 1 eq.) and MeCN (2 mL) with stirring at r.t. for 18 h. Purification by MPLC on SiO_2 with a gradient elution from 2-8% MeOH/EtOAc gave a yellow solid (78 mg, 64%); R_f 0.35 (5% MeOH/EtOAc, NH_2 SiO_2); m.p. 300-304 °C; λ_{max}(EtOH)/nm 255, 223; IR ν_{max}/cm^{-1} 3361.0, 3241.5 br, 2971.9, 1636.3, 1586.2; ^{1}H NMR (500 MHz; DMSO-d_6) δ_H 7.36 (1H, s, H-pyrrole), 7.56 (1H, dd, J = 1.1 & 8.5 Hz, H-5'), 7.60 (1H, s, H-pyrrole), 7.57 (1H, s, H-pyrazole), 7.82 (1H, app t, J = 8.5 Hz, H-4'), 7.97 (1H, s, H-pyrazole), 10.29 (1H, s, CO-NH), 12.60-12.73 (2H, m, NH-pyrrole and NH-pyrazole); ^{19}F NMR (470 MHz; DMSO-d_6) δ_F -116.66; ^{13}C NMR (125 MHz; DMSO-d_6) δ_C 110.1 (CH-pyrrole), 119.3 (d, J_{CF} = 18.1 Hz, C-3'), 120.8 (CH-pyrazole), 124.7 (C-pyrrole), 126.9 (d, J_{CF} = 4.1 Hz, C-5'), 128.8 (C-pyrrole), 129.2 (d, J_{CF} = 5.2 Hz, C-6'), 129.2 (d, J_{CF} = 22.7 Hz, C-1'), 129.5 (C-pyrrole), 131.0 (CH-pyrazole), 131.8 (C-4'), 153.8 (d, J_{CF} = 248.8 Hz, C-2'), 156.9 (CO-NH), 182.6 (CO); HRMS calcd for $C_{15}H_{10}{}^{35}Cl_2F_1N_4O_2$ [M+H]$^+$ 367.0159, found 367.0158.

1-Methyl-4-nitro-1*H*-pyrazole (385)[372]
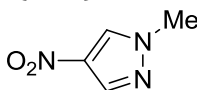
Prepared according to general procedure J using methanol (11 μL, 2.65 mmol, 1 eq.), PPh$_3$ (1.04 g, 4.0 mmol, 1.5 eq.), 4-nitropyrazole (300 mg, 2.7 mmol, 1 eq.) and DEAD (626 μL, 4.0 mmol, 1.5 eq.) in THF (5 mL) with stirring at r.t. for 18 h. The residue was purified by MPLC on SiO_2 with a gradient elution from 20-50% EtOAc/petrol to give impure product which was re-purified by MPLC on SiO_2 with a gradient elution from 10-40% EtOAc/petrol to give a white solid (227 mg, 67%); R_f 0.8 (EtOAc); m.p. 90-94 °C (Lit.^{372} 91-92 °C) ; λ_{max}(EtOH)/nm 266; IR ν_{max}/cm^{-1} 1504, 1310; ^{1}H NMR (500 MHz; DMSO-d_6) δ_H 3.92 (3H, s, CH$_3$), 8.25 (1H, s, H-pyrazole), 8.86 (1H, s, H-pyrazole); ^{13}C NMR (125

MHz; DMSO-d_6) δ_C 39.6 (CH$_3$), 131.0 (CH-pyrazole), 134.8 (CH-pyrazole), 135.5 (C-NO$_2$). MS (ES+) 128.1 [M+H]$^+$.

1-Methyl-1*H*-pyrazol-4-amine (398)
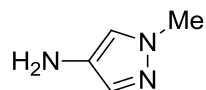
Prepared according to general procedure H using nitropyrazole **385** (200 mg, 1.57 mmol) and MeOH (10 mL) for 2 h to give an orange oil (150 mg, 98 %); R_f 0.1 (EtOAc); λ_{max}(EtOH)/nm 244; IR ν_{max}/cm^{-1} 3322, 3111; ^{1}H NMR (500 MHz; DMSO-d_6) δ_H 3.68 (3H, s, CH$_3$), 3.82 (2H, br s, NH$_2$), 6.90 (1H, d, J = 0.6 Hz, H-pyrazole), 7.01 (1H, d, J = 0.6 Hz, H-pyrazole); ^{13}C NMR (125 MHz; DMSO-d_6) δ_C 38.3 (CH$_3$), 117.2 (CH-pyrazole), 128.9 (CH-pyrazole), 131.0 (C-pyrazole); MS: No mass ion detected.

4-(3,6-Dichloro-2-fluorobenzoyl)-*N*-(1-methyl-1*H*-pyrazol-4-yl)-1*H*-pyrrole-2-carboxamide (314)
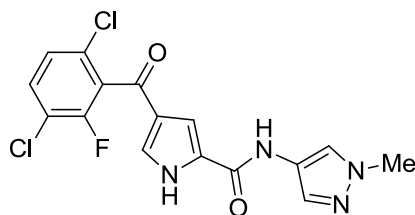
Prepared according to general procedure E using amine **398** (130 mg, 1.3 mmol, 2.5 eq.) and carboxylic acid **337** (162 mg, 0.54 mmol, 1 eq.), cyanuric fluoride (32 μL, 0.37 mmol, 0.7 eq.), pyridine (43 μL, 0.50 mmol, 1 eq.) and MeCN (2 mL) with stirring at r.t. for 18 h. Purification by MPLC on SiO$_2$ with a gradient elution from 30-60% EtOAc/petrol gave a yellow solid (120 mg, 59%); R_f 0.1 (50% EtOAc/petrol); m.p. 216-219 °C; λ_{max}(EtOH)/nm 252, 225; IR ν_{max}/cm^{-1} 3195, 3121, 2938, 1630; ^{1}H NMR (500 MHz; DMSO-d_6) δ_H 3.85 (3H, s, CH$_3$), 7.36 (1H, s, H-pyrrole), 7.54 (1H, s, H-pyrazole), 7.56 (1H, dd, J = 1.2 & 8.5 Hz, H-5'), 7.59 (1H, s, H-pyrrole), 7.82 (1H, app t, J = 8.5 Hz, H-4'), 7.98 (1H, s, H-pyrazole), 10.28 (1H, s, CO-NH), 12.68 (NH-pyrrole); ^{19}F NMR (470 MHz; DMSO-d_6) δ_F -116.66; ^{13}C NMR (125 MHz; DMSO-d_6) δ_C 38.7 (CH$_3$), 110.2 (CH-pyrrole), 119.3 (d, J_{CF} = 18.2 Hz, C-3'), 121.2 (CH-pyrazole), 121.4 (C-pyrazole), 124.7 (C-pyrrole), 126.9 (d, J_{CF} = 3.7 Hz, C-5'), 128.7 (C-pyrrole), 129.2 (d, J_{CF} = 23.2 Hz, C-1'), 129.2 (d, J_{CF} = 5.2 Hz, C-6'), 129.5 (C-pyrrole), 129.9 (CH-pyrazole), 131.8 (C-4'), 153.8 (d, J_{CF} = 248.4 Hz,

C-2'), 156.8 (CO-NH), 182.6 (CO); HRMS calcd for $C_{16}H_{12}{}^{35}Cl_2F_1N_4O_2$ [M+H]$^+$ 381.0319, found 381.0318.

4-(6-Chloro-2-fluoro-3-methoxybenzoyl)-*N*-(1-methyl-1*H*-pyrazol-4-yl)-1*H*-pyrrole-2-carboxamide (323)
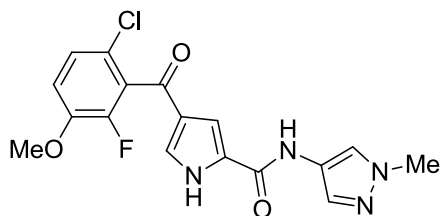
Prepared according to general procedure L using carboxylic acid **421** (150 mg, 0.51 mmol, 1 eq.), Et$_3$N (172 μL, 1.24 mmol, 2.5 eq.), and 2-chloromethylpyridinium iodide (139 mg, 0.54 mmol, 1.1 eq.) in DCM (5 mL) followed by the addition of amine **398** (60 mg, 0.62 mmol, 1.25 eq.) with stirring at r.t. for 18 h. The residue was purified by MPLC on SiO$_2$ with gradient elution from 50-80% EtOAc/petrol to give a white solid (114 mg, 60%); R_f 0.15 (75% EtOAc/petrol); m.p. 261-263 °C; λ$_{max}$(EtOH)/nm 227, 250sh; IR ν $_{max}$/cm^{-1} 3322, 3202, 1649, 1622; ^{1}H NMR (500 MHz; DMSO-d_6) δ$_H$ 3.85 (3H, s, N-CH$_3$), 3.94 (3H, s, O-CH$_3$), 7.31 (1H, s, H-pyrrole), 7.36 (1H, app t, J = 9.0 Hz, H-4'), 7.42 (1H, dd, J = 1.0 and 9.0 Hz, H-5'), 7.45 (1H, s, H-pyrrole), 7.53 (1H, s, H-pyrazole), 7.98 (1H, s, H-pyrazole), 10.27 (1H, s, CO-NH), 12.60 (1H, s, NH-pyrrole); ^{19}F NMR (470 MHz; DMSO-d_6) δ$_F$ -136.15; ^{13}C NMR (125 MHz; DMSO-d_6) δ$_C$ 38.7 (N-CH$_3$), 56.4 (O-CH$_3$), 110.3 (CH-pyrrole), 115.1 (C-4'), 120.2 (d, J = 4.9 Hz, C-1'), 121.2 (CH-pyrazole), 121.4 (C-pyrazole), 125.1 (C-pyrrole), 125.5 (d, J = 3.6 Hz, C-5'), 128.4 (C-pyrrole), 128.5 (C-6'), 128.6 (C-pyrrole), 128.8 (C-pyrrole), 129.9 (CH-pyrazole), 146.4 (d, J = 10.6 Hz, C-3'), 147.9 (d, J_{CF} = 247.0 Hz, C-2'), 156.8 (CO-NH), 183.6 (CO); HRMS calcd for $C_{17}H_{15}{}^{35}Cl_1F_1N_4O_3$ [M+H]$^+$ 377.0811, found 377.0808.

1-Ethyl-4-nitro-1*H*-pyrazole (386)
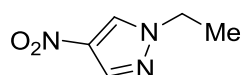
Prepared according to general procedure J using ethanol (129 μL, 2.2 mmol, 1 eq.), PPh$_3$ (869 mg, 3.3 mmol, 1.5 eq.), 4-nitropyrazole (250 mg, 2.2 mmol, 1 eq.) and DEAD (522 μL, 3.3 mmol, 1.5 eq.) in THF (3 mL) with stirring at r.t. for 18 h. The residue was purified by MPLC on SiO$_2$ with a gradient elution from 10 to 35% EtOAc/petrol to give a clear oil

(170 mg, 54%); R_f 0.3 (25% EtOAc/petrol); m.p. 62-64 °C (lit.[373] 63-64 °C); λ_{max}(EtOH)/nm 272sh; IR ν_{max}/cm^{-1} 1505, 1302; ^{1}H NMR (500 MHz; DMSO-d_6) δ_H 1.44 (3H, t, J = 7.3 Hz, CH$_3$), 4.24 (2H, q, J = 7.3 Hz, CH$_2$), 8.29 (1H, s, H-pyrazole), 8.94 (1H, s, H-pyrazole); ^{13}C NMR (125 MHz; DMSO-d_6) δ_C 14.8 (CH$_3$), 47.6 (CH$_2$), 129.8 (CH-pyrazole), 134.7 (C-NO$_2$), 135.4 (CH-pyrazole); MS (ES+) m/z 142.1 [M+H]$^+$.

### 1-Ethyl-1*H*-pyrazol-4-amine (399)[60]
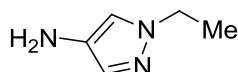
Palladium on carbon (10%, 30 mg) was added to nitropyrazole **386** (160 mg, 1.13 mmol) in MeOH (15 mL), and the mixture was stirred at r.t. under an atmosphere of hydrogen for 18 h. The reaction was filtered through Celite, and the solvent removed *in vacuo* to give a brown oil (125 mg, 100%); R_f 0.25 (10% MeOH/EtOAc); λ_{max}(EtOH)/nm 245; IR ν_{max}/cm^{-1} 3331 br, 2980; ^{1}H NMR (500 MHz; DMSO-d_6) δ_H 1.31 (3H, t, J = 7.3 Hz, CH$_3$), 3.79 (2H, br s, NH$_2$), 3.96 (2H, q, J = 7.3 Hz, CH$_2$), 6.91 (1H, s, H-pyrazole), 7.05 (1H, s, H-pyrazole); MS (ES+) m/z 112.2 [M+H]$^+$.

4-(3,6-Dichloro-2-fluorobenzoyl)-*N*-(1-ethyl-1*H*-pyrazol-4-yl)-1*H*-pyrrole-2-carboxamide (315)
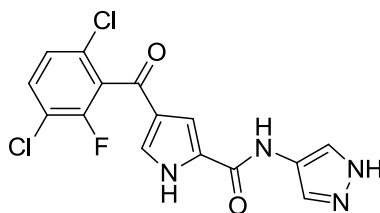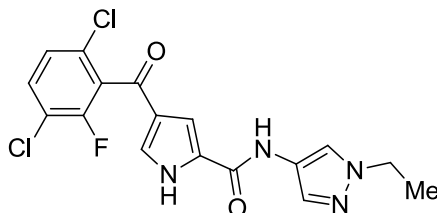

Prepared according to general procedure L using carboxylic acid **337** (100 mg, 0.33 mmol, 1 eq.), Et$_3$N (115 μL, 0.86 mmol, 2.5 eq.), and 2-chloromethylpyridinium iodide (93 mg, 0.36 mmol, 1.25 eq.) in DCM (4 mL) followed by the addition of amine **399** (46 mg, 0.41 mmol, 1.25 eq.) with stirring at r.t. for 18 h. The residue was purified by MPLC on SiO$_2$ with gradient elution from 40-70 % EtOAc/petrol to give a white solid (34 mg, 26%); R_f 0.5 (80% EtOAc/petrol); m.p. 197-201 °C; λ_{max}(EtOH)/nm 239sh; IR ν_{max}/cm^{-1} 3358, 3211, 3124, 1628, 1601; ^{1}H NMR (500 MHz; DMSO-d_6) δ_H 1.39 (3H, t, J = 7.3 Hz, CH$_3$), 4.15 (2H, q, J = 7.3 Hz, CH$_2$), 7.35 (1H, s, H-pyrrole), 7.53-7.58 (2H, m, H-5' and H-pyrazole), 7.59 (1H, s, H-pyrrole), 7.82 (1H, app t, J = 8.4 Hz, H-4'), 8.00 (1H, s, H-pyrazole), 10.27 (1H, s, CO-NH), 12.66 (1H, s, NH-pyrrole); ^{19}F NMR (470 MHz; DMSO-

*d*₆) δ_F -116.66; ¹³C NMR (125 MHz; DMSO-*d*₆) δ_C 15.5 (CH₃), 46.3 (CH₂), 110.1 (CH-pyrrole), 119.3 (d, J_{CF} = 18.1 Hz, C-3'), 120.0 (CH-pyrazole), 121.0 (C-pyrazole), 124.7 (C-pyrrole), 126.9 (d, J_{CF} = 3.7 Hz, C-5'), 128.7 (C-pyrrole), 129.2 (d, J_{CF} = 23.2 Hz, C-1'), 129.2 (d, J_{CF} = 5.3 Hz, C-6'), 129.5 (C-pyrrole), 129.9 (CH-pyrazole), 131.8 (C-4'), 153.8 (d, J_{CF} = 248.8 Hz, C-2'), 156.8 (CO-NH), 182.6 (CO); HRMS calcd for C₁₇H₁₄³⁵Cl₂F₁N₄O₂ [M+H]⁺ 395.0472, found 395.0470.

N,N-Diethyl-2-(4-nitro-1*H*-pyrazol-1-yl)ethanamine (387)[374]
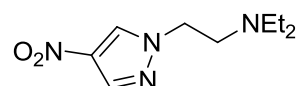
Prepared according to general procedure J using 2-(diethylamino)ethan-1-ol (47 μL, 3.54 mmol, 1 eq.), PPh₃ (1.39 g, 5.3 mmol, 1.5 eq.), 4-nitropyrazole (400 mg, 3.5 mmol, 1 eq.) and DEAD (836 μL, 5.3 mmol, 1.5 eq.) in THF (7 mL) with stirring at r.t. for 18 h. The residue was purified on an SCX cartridge eluting with MeOH followed by 10% NH₄OH/MeOH to give an orange oil which was further purified by MPLC on SiO₂ with a gradient elution from 10-50% EtOAc/petrol to give the product as a yellow gum (20 mg, 3%). Impure fractions were also obtained (300 mg, 40%) which were taken forward without further purification. R_f 0.25 (EtOAc); λ_{max}(EtOH)/nm 272; IR ν_{max}/cm⁻¹ 1506, 1307; ¹H NMR (500 MHz; DMSO-*d*₆) δ_H 0.90 (6H, t, *J* = 7.1 Hz, N-CH₂-C*H*₃), 2.49 (4H, q, *J* = 7.1 Hz, N-C*H*₂-CH₃), 2.72 (2H, t, *J* = 6.9 Hz, C*H*₂-NEt₂), 3.78 (2H, br s, NH₂), 3.97 (2H, t, *J* = 6.9 Hz, C*H*₂-CH₂-NEt₂), 6.91 (1H, d, *J* = 0.9 Hz,, H-pyrazole), 7.07 (1H, d, *J* = 0.9 Hz,, H-pyrazole); ¹³C NMR (125 MHz; DMSO-*d*₆) δ_C 11.8 (CH₃), 46.4 (*C*H₂CH₃), 51.1 (*C*H₂CH₂NEt₂), 51.5 (*C*H₂-NEt2), 130.9 (CH-pyrazole), 135.4 (CH-pyrazole), 135.9 (C-NO₂); MS: No mass ion detected.

1-(2-(Diethylamino)ethyl)-1*H*-pyrazol-4-amine (400)[374]
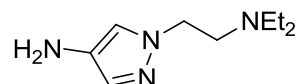
Prepared according to general procedure H using nitropyrazole **387** (300 mg, 4.40 mmol) and MeOH (15 mL) to give a brown oil (72 mg, 28 %); R_f 0.3 (90:10:1 EtOAc/MeOH/NH₄OH); λ_{max}(EtOH)/nm 246; IR ν_{max}/cm⁻¹ 3320, 2967; ¹H NMR (500 MHz; DMSO-*d*₆) δ_H 0.95 (6H, t, *J* = 7.1 Hz, N-CH₂-C*H*₃), 2.49 (4H, q, *J* = 7.1 Hz, N-C*H*₂-CH₃), 2.72 (2H, t, *J* = 6.9 Hz, C*H*₂-NEt₂), 3.78 (2H, br s, NH₂), 3.97 (2H, t, *J* = 6.9 Hz,

CH_2-CH$_2$-NEt$_2$), 6.91 (1H, d, J = 0.9 Hz,, H-pyrazole), 7.07 (1H, d, J = 0.9 Hz,, H-pyrazole); ^{13}C NMR (125 MHz; DMSO-d_6) δ_C 11.8 (2 × CH$_3$), 46.7 (2 × CH_2CH$_3$), 50.0 (CH_2-CH$_2$-NEt$_2$), 52.8 (CH_2-NEt$_2$), 116.9 (CH-pyrazole), 129.1 (CH-pyrazole), 130.5 (C-NH$_2$); MS (ES+) m/z 182.3 [M]$^+$.

4-(3,6-Dichloro-2-fluorobenzoyl)-N-(1-(2-(diethylamino)ethyl)-1H-pyrazol-4-yl)-1H-pyrrole-2-carboxamide (307)
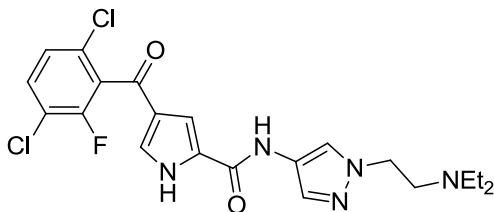
Prepared according to general procedure L using carboxylic acid **337** (80 mg, 0.26 mmol, 1 eq.), amine **400** (60 mg, 0.33 mmol, 1.25 eq.), Et$_3$N (92 µL, 0.66 mmol, 2.5 eq.), and 2-chloromethylpyridinium iodide (74 mg, 0.29 mmol, 1.1 eq.) in DCM (3 mL) with stirring at r.t. for 18 h. The residue was purified by MPLC on SiO$_2$ with gradient elution from 0-3% MeOH/DCM to give a white solid (53 mg, 43%); R_f 0.2 (2% MeOH/CH$_2$Cl$_2$, NH$_2$ SiO$_2$); m.p. 140-142 °C; λ_{max}(EtOH)/nm 254, 222; IR ν_{max}/cm^{-1} 3122, 2967, 1630; ^{1}H NMR (500 MHz; DMSO-d_6) δ_H 0.95 (6H, t, J = 7.1 Hz, N-CH$_2$-CH_3), 2.51 (4H, q, J = 7.1 Hz, N-CH_2-CH$_3$), 2.78 (2H, t, J = 6.5 Hz, CH_2-NEt$_2$), 4.14 (2H, t, J = 6.5 Hz, CH_2-CH$_2$-NEt$_2$), 7.35 (1H, s, H-pyrrole), 7.54-7.57 (2H, m, H-pyrazole and H-5'), 7.59 (1H, s, H-pyrrole), 7.82 (1H, app t, J = 8.4 Hz, H-4'), 8.03 (1H, s, H-pyrazole), 10.26 (1H, s, CO-NH), 12.66 (NH-pyrrole); ^{19}F NMR (470 MHz; DMSO-d_6) δ_F -166.65; ^{13}C NMR (125 MHz; DMSO-d_6) δ_C 11.9 (2 × CH$_3$), 46.5 (2 × CH_2CH$_3$), 50.1 (CH_2-CH$_2$-NEt$_2$), 52.5 (CH_2-CH$_2$-NEt$_2$), 110.1 (CH-pyrrole), 119.3 (d, J_{CF} = 18.2 Hz, C-3'), 120.7 (CH-pyrazole), 121.2 (C-pyrazole), 124.7 (C-pyrrole), 126.9 (d, J_{CF} = 3.7 Hz, C-5'), 128.8 (C-pyrrole), 129.2 (d, J_{CF} = 22.7 Hz, C-1'), 129.2 (d, J_{CF} = 5.1 Hz, C-6'), 129.5 (C-pyrrole), 129.9 (CH-pyrazole), 131.8 (C-4'), 153.8 (d, J_{CF} = 248.4 Hz, C-2'), 156.8 (CO-NH), 182.5 (CO); HRMS calcd for C$_{21}$H$_{23}$^{35}Cl$_2$F$_1$N$_5$O$_2$ [M+H]$^+$ 466.1207, found 466.1201.

2-((4-Nitro-1*H*-pyrazol-1-yl)methyl)pyridine (388)
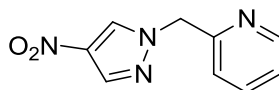
Prepared according to general procedure J using 2-pyridylmethanol (342 µL, 3.5 mmol, 1 eq.), PPh$_3$ (1.39 g, 5.3 mmol, 1.5 eq.), 4-nitropyrazole (400 mg, 3.5 mmol, 1 eq.) and DEAD (836 µL, 5.3 mmol, 1.5 eq.) in THF (7 mL) with stirring at r.t. for 18 h. The residue was purified by MPLC on NH$_2$ SiO$_2$ with a gradient elution from 10-30% EtOAc/petrol to give a white solid (599 mg, 83%); R_f 0.2 (20% EtOAc/petrol, NH$_2$ SiO$_2$); m.p. 95-101 °C; λ_{max}(EtOH)/nm 267; IR ν $_{max}$/cm^{-1} 1504, 1304; ^{1}H NMR (500 MHz; DMSO-d_6) δ_H 5.57 (2H, s, CH$_2$), 7.34 (1H, d, J = 7.4 Hz, H-pyridine), 7.39 (1H, dd, J = 5.0 and 7.4 Hz, H-pyridine), 7.83 (1H, td, J = 7.7 and 1.7 Hz, H-pyridine), 8.33 (1H, s, H-pyrrole), 8.57 (1H, d, J = 5.0 Hz, H-pyridine), 9.09 (1H, s, H-pyrrole); ^{13}C NMR (125 MHz; DMSO-d_6) δ_C 57.2 (CH$_2$), 122.2 (CH-pyridine), 123.2 (CH-pyridine), 131.5 (CH-pyrazole), 135.0 (C-NO$_2$), 136.0 (CH-pyrazole), 137.3 (CH-pyridine), 149.4 (CH-pyridine), 154.8 (C-2 pyridine); HRMS calcd for C$_9$H$_9$N$_4$O$_2$ [M+H]$^+$ 205.0720, found 205.0718.

1-(Pyridin-2-ylmethyl)-1*H*-pyrazol-4-amine (401)
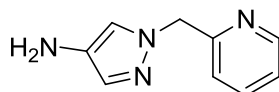
Prepared according to general procedure H using nitropyrazole **388** (580 mg, 2.84 mmol) and MeOH (20 mL), to give an orange oil (474 mg, 96 %); R_f 0.6 (EtOAc); λ_{max}(EtOH)/nm 260; IR ν $_{max}$/cm^{-1} 3314; ^{1}H NMR (500 MHz; DMSO-d_6) δ_H 3.90 (2H, br s, NH$_2$), 5.26 (2H, s, CH$_2$), 6.93 (1H, d, J = 7.8 Hz, H-pyridine), 7.01 (1H, d, J = 0.6 Hz, H-pyrazole), 7.17 (1H, d, J = 0.6 Hz, H-pyrazole), 7.32 (1H, ddd, J = 0.8, 4.9 and 7.4 Hz, H-pyridine), 7.77 (1H, td, J = 7.8 and 1.7 Hz, H-pyridine), 8.53-8.57 (1H, m, H-pyridine); ^{13}C NMR (125 MHz; DMSO-d_6) δ_C 56.6 (CH$_2$), 117.1 (C-pyrazole), 121.2 (C-pyridine), 122.5 (C-pyridine), 130.0 (C-pyrazole), 131.4 (C-NH$_2$), 137.0 (C-pyridine), 148.9 (C-pyridine), 157.6 (C-2-pyridine); HRMS calcd for C$_9$H$_11$N$_4$ [M+H]$^+$ 175.0978, found 175.0976.

4-(3,6-Dichloro-2-fluorobenzoyl)-*N*-(1-(pyridin-2-ylmethyl)-1*H*-pyrazol-4-yl)-1*H*-pyrrole-2-carboxamide (309)
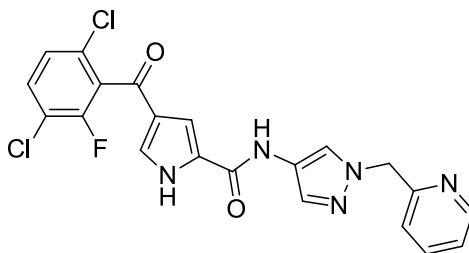
Prepared according to general procedure L using carboxylic acid **337** (100 mg, 0.33 mmol, 1 eq.), Et$_3$N (115 µL, 0.83 mmol, 2.5 eq.), and 2-chloromethylpyridinium iodide (93 mg, 0.36 mmol, 1.1 eq.) in DCM (5 mL) followed by the addition of amine **401** (72 mg, 0.41 mmol, 1.25 eq.) in DCM (1 mL) with stirring at r.t. for 18 h. The residue was purified by MPLC on SiO$_2$ with gradient elution from 60-100% EtOAc/petrol to give a white solid (83 mg, 55%); R_f 0.25 (EtOAc); m.p. 224-226 °C; λ_{max}(EtOH)/nm 256; IR ν_{max}/cm^{-1} 3123, 1631; ^{1}H NMR (500 MHz; DMSO-d_6) δ_H 5.45 (2H, s, CH$_2$), 7.07 (1H, d, J = 7.9 Hz, H-pyridine), 7.32-7.39 (2H, m, H-pyrrole and H-4'), 7.56 (1H, dd, J = 0.9 and 8.7 Hz, H-5'), 7.60 (1H, s, H-pyrrole), 7.64 (1H, s, H-pyrazole), 7.78-7.85 (2H, m, 2 × H-pyridine), 8.15 (1H, s, H-pyrazole), 8.55-8.60 (1H, m, H-pyridine), 10.35 (CO-NH), 12.68 (NH-pyrrole); ^{19}F NMR (470 MHz; DMSO-d_6) δ_F -116.64; ^{13}C ^{13}C NMR (125 MHz; DMSO-d_6) δ_C 56.7 (CH$_2$), 110.2 (CH-pyrrole), 119.3 (d, J_{CF} = 18.1 Hz, C-3'), 121.5 (C-pyrazole), 121.6 (C-pyrazole), 122.7 (C-pyridine), 124.7 (C-pyrrole), 126.9 (d, J_{CF} = 3.6 Hz, C-5'), 128.7 (C-pyrrole), 129.2 (d, J_{CF} = 23.2 Hz, C-1'), 129.2 (d, J_{CF} = 5.1 Hz, C-6'), 129.6 (C-pyrrole), 130.8 (C-pyrazole), 131.8 (C-4'), 137.1 (C-4-pyridine), 149.1 (C-pyridine), 153.8 (d, J_{CF} = 248.4 Hz, C-2'), 156.8 (CO-NH), 156.9 (C-2-pyridine), 182.6 (CO); HRMS calcd for C$_{21}$H$_{15}$^{35}Cl$_2$F$_1$N$_5$O$_2$ [M+H]$^+$ 458.0581, found 458.0579.

## 4-(6-Chloro-2-fluoro-3-methoxybenzoyl)-*N*-(1-(pyridin-2-ylmethyl)-1*H*-pyrazol-4-yl)-1H-pyrrole-2-carboxamide (327)
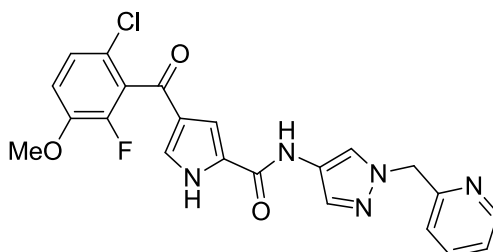
Prepared according to general procedure L using carboxylic acid **421** (100 mg, 0.34 mmol, 1 eq.), Et$_3$N (117 µL, 0.84 mmol, 2.5 eq.), and 2-chloromethylpyridinium iodide (94 mg,

0.37 mmol, 1.1 eq.) in DCM (5 mL) followed by the addition of amine **401** (73 mg, 0.42 mmol, 1.25 eq.) in DCM (1 mL) with stirring at r.t. for 18 h. The residue was purified by MPLC on SiO_2 with gradient elution from 70-100% EtOAc/petrol to give a white solid (69 mg, 45%); R_f 0.2 (EtOAc); m.p. 160 °C dec.; λ_{max}(EtOH)/nm 255, 227; IR ν_{max}/cm^{-1} 3122, 1631; ^{1}H NMR (500 MHz; DMSO-d_6) δ_H 3.94 (CH$_3$), 5.45 (2H, s, CH$_2$), 7.07 (1H, d, J = 7.9 Hz, H-pyridine), 7.30-7.40 (3H, m, H-pyrrole, H-4' and H-pyridine), 7.42 (1H, dd, J = 1.1 and 9.0 Hz, H-5'), 7.46 (1H, s, H-pyrrole), 7.63 (1H, s, H-pyrazole), 7.80 (1H, td, J = 7.7 and 1.9 Hz, H-pyridine), 8.15 (1H, s, H-pyrazole), 8.55-8.60 (1H, m, H-pyridine), 10.34 (1H, s, CO-NH), 12.61 (1H, s, NH-pyrrole); ^{19}F NMR (470 MHz; DMSO-d_6) δ_F -136.13; ^{13}C NMR (125 MHz; DMSO-d_6) δ_C 56.4 (OCH$_3$), 56.7 (CH$_2$), 110.3 (CH-pyrrole), 115.1 (C-4'), 120.2 (d, J_{CF} = 4.6 Hz, C-1'), 121.5 (C-pyrazole), 121.6 (C-pyrazole), 122.7 (C-pyridine), 125.1 (C-pyrrole), 125.5 (d, J_{CF} = 3.6 Hz, C-5'), 128.4 (C-pyrrole), 128.5 (d, J_{CF} = 20.0 Hz, C-6'), 128.8 (CH-pyrrole), 130.8 (CH-pyrazole), 137.1 (C-4-pyridine), 146.4 (d, J_{CF} = 10.7 Hz, C-3'), 147.9 (d, J_{CF} = 247.0 Hz, C-2'), 149.1 (C-6-pyridine), 156.8 (CO-NH), 156.9 (C-2-pyridine), 183.6 (CO); HRMS calcd for $C_{22}H_{18}{}^{35}Cl_1F_1N_5O_3$ [M+H]$^+$ 454.1077, found 454.1072.

3-((4-Nitro-1*H*-pyrazol-1-yl)methyl)pyridine (389)
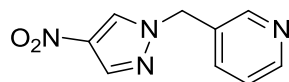
Prepared according to general procedure J using 3-pyridylmethanol (343 μL, 3.5 mmol, 1 eq.), PPh$_3$ (1.39 g, 5.3 mmol, 1.5 eq.), 4-nitropyrazole (400 mg, 3.5 mmol, 1 eq.) and DEAD (836 μL, 5.3 mmol, 1.5 eq.) in THF (7 mL) with stirring at r.t. for 18 h. The residue was purified by MPLC on NH$_2$ SiO$_2$ with a gradient elution from 10-30% EtOAc/petrol to give a clear oil, which was re-purified by MPLC on SiO_2 with a gradient elution from 30-60% EtOAc/petrol to give a clear oil (290 mg, 40%); R_f 0.3 (EtOAc); λ_{max}(EtOH)/nm 267; IR ν_{max}/cm^{-1} 1498, 1318; ^{1}H NMR (500 MHz; DMSO-d_6) δ_H 5.47 (2H, s, CH$_2$), 7.44 (1H, dd, J = 4.7 and 7.7 Hz, H-5-pyridine), 7.79 (1H, ddd, J = 1.7, 2.0 and 7.7 Hz, H-4-pyridine), 8.33 (1H, d, J = 0.6 Hz, H-pyrrole), 8.58 (1H, dd, J = 1.7 and 4.7 Hz, H-6-pyridine), 8.64 (1H, d, J = 2.0 Hz, H-2-pyridine), 9.11 (1H, s, H-pyrrole); ^{13}C NMR (125 MHz; DMSO-d_6) δ_C 53.3 (CH$_2$), 123.7 (CH-pyridine), 130.8 (CH-pyridine), 131.4 (CH-pyrazole), 135.1 (C-NO$_2$), 135.9 (CH-pyrazole), 136.2 (CH-pyridine), 149.3 (CH-

pyridine), 149.4 (C-3-pyridine); HRMS calcd for $C_9H_9N_4O_2$ [M+H]$^+$ 205.0720, found 205.0718.

## 1-(Pyridin-3-ylmethyl)-1*H*-pyrazol-4-amine (402)[375]
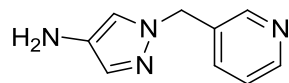
Prepared according to general procedure H using nitropyrazole **389** (270 mg, 1.32 mmol) and MeOH (15 mL), to give a brown oil (210 mg, 91%); R_f 0.2 (NH$_2$ SiO$_2$, EtOAc); λ_{max}(EtOH)/nm 255; IR ν_{max}/cm^{-1} 3321; ^{1}H NMR (500 MHz; DMSO-d_6) δ_H 3.89 (2H, s, NH$_2$), 5.21 (2H, s, CH$_2$), 6.99 (1H, d, J = 0.8 Hz, H-pyrazole), 7.17 (1H, d, J = 0.8 Hz, H-pyrazole), 7.39 (1H, ddd, J = 0.6, 4.7 and 7.7 Hz, H-5-pyridine), 7.57-7.62 (1H, m, H-6-pyridine), 8.47 (1H, d, J = 1.7 Hz, H-2-pyridine), 8.51 (1H, dd, J = 1.7 and 4.7 Hz, H-4-pyridine); ^{13}C NMR (125 MHz; DMSO-d_6) δ_C 52.2 (CH$_2$), 116.5 (C-pyrazole), 123.5 (CH-pyridine), 130.0 (CH-pyrazole), 131.5 (C-NH$_2$), 133.7 (C-3-pyridine), 135.1 (C-6-pyridine), 148.6 (C-2-pyridine), 148.7 (C-4-pyridine); HRMS calcd for $C_9H_{11}N_4$ [M+H]$^+$ 175.0978, found 175.0977.

4-(3,6-Dichloro-2-fluorobenzoyl)-*N*-(1-(pyridin-3-ylmethyl)-1*H*-pyrazol-4-yl)-1*H*-pyrrole-2-carboxamide (310)
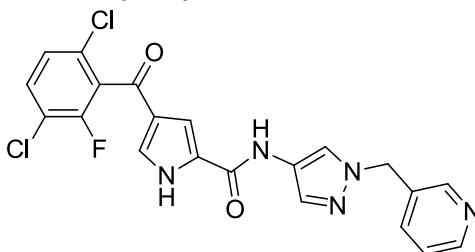
Prepared according to general procedure L using carboxylic acid **337** (125 mg, 0.41 mmol, 1 eq.), Et$_3$N (144 μL, 1.03 mmol, 2.5 eq.), and 2-chloromethylpyridinium iodide (105 mg, 0.41 mmol, 1.1 eq.) in DCM (5 mL) followed by the addition of amine **402** (90 mg, 0.52 mmol, 1.25 eq.) in DCM (1 mL) with stirring at r.t. for 18 h. The residue was purified by MPLC on SiO$_2$ with gradient elution from EtOAc to 5% MeOH/EtOAc give a white solid which was purified by MPLC on NH$_2$ SiO$_2$ with gradient elution from 0-10% MeOH/CH$_2$Cl$_2$ to give a white solid. This material was re-purified by MPLC on SiO$_2$ with gradient elution from 0-5% MeOH/EtOAc give a white solid (29 mg, 16%); R_f 0.7 (NH$_2$ SiO$_2$, 5% MeOH/CH$_2$Cl$_2$); mp 130-135 °C; λ_{max}(EtOH)/nm 256, 222; IR ν_{max}/cm^{-1} 3123,

1634; ^{1}H NMR (500 MHz; DMSO-d_6) δ_H 5.41 (2H, s, CH$_2$), 7.35 (1H, s, H-pyrrole), 7.41 (1H, ddd, J = 0.8, 4.9 and 7.9 Hz, H-5-pyridine), 7.55 (1H, dd, J = 1.3 and 8.6 Hz, H-5'), 7.60 (1H, s, H-pyrrole), 7.62 (1H, d, J = 0.6 Hz, H-pyrazole), 7.66-7.69 (1H, m, H-4-pyridine), 7.82 (1H, app t, J = 8.6 Hz, H-4'), 8.17 (1H, s, H-pyrazole), 8.52-8.56 (2H, m, H-2-pyridine and H-6-pyridine), 10.34 (1H, s, CO-NH), 12.66 (1H, br s, NH-pyrrole); ^{19}F NMR (470 MHz; DMSO-d_6) δ_F -116.65; ^{13}C NMR (125 MHz; DMSO-d_6) δ_C 52.3 (CH$_2$), 110.2 (CH-pyrrole), 119.3 (d, J_{CF} = 18.1 Hz, C-3'), 121.0 (CH-pyrazole), 121.6 (C-pyrazole), 123.6 (C-pyridine), 124.7 (C-pyrrole), 126.9 (d, J_{CF} = 3.6 Hz, C-5'), 128.6 (C-pyrrole), 129.9 (d, J_{CF} = 22.9 Hz, C-1'), 129.2 (d, J_{CF} = 5.1Hz, C-6'), 129.6 (C-pyrrole), 130.8 (C-pyrazole), 131.8 (C-4'), 133.2 (C-pyridine), 135.4 (C-pyridine), 148.9 (C-pyridine), 153.8 (d, J_{CF} = 248.4 Hz, C-2'), 156.8 (CO-NH), 182.6 (CO); HRMS calcd for C$_{21}$H$_{15}$^{35}Cl$_2$F$_1$N$_5$O$_2$ [M+H]$^+$ 458.0581, found 458.0579.

4-(6-Chloro-2-fluoro-3-methoxybenzoyl)-*N*-(1-(pyridin-3-ylmethyl)-1*H*-pyrazol-4-yl)-1*H*-pyrrole-2-carboxamide (328)
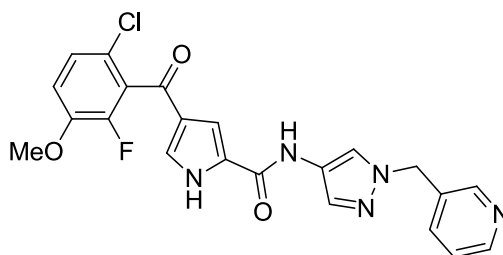
Prepared according to general procedure L using carboxylic acid **421** (123 mg, 0.41 mmol, 1 eq.), Et$_3$N (144 µL, 1.03 mmol, 2.5 eq.), and 2-chloromethylpyridinium iodide (105 mg, 0.41 mmol, 1.1 eq.) in DCM (5 mL) followed by the addition of amine **402** (90 mg, 0.52 mmol, 1.25 eq.) in DCM (1 mL) with stirring at r.t. for 18 h. The residue was purified by MPLC on SiO$_2$ with gradient elution from 0-5% MeOH/EtOAc give a white solid. This was dissolved in MeOH and passed through a SCX column eluting with MeOH (100 mL) followed by 10% NH$_4$OH/MeOH (100 mL). Product containing fraction were evaporated and purified by MPLC on NH$_2$ SiO$_2$ with gradient elution from 0-10% MeOH/CH$_2$Cl$_2$ to give a white solid (56 mg, 30%); R_f 0.6 (NH$_2$ SiO$_2$, 5% MeOH/CH$_2$Cl$_2$); mp 170 °C dec.; λ_{max}(EtOH)/nm 254, 227; IR ν_{max}/cm^{-1} 3122, 2935, 1634; ^{1}H NMR (500 MHz; DMSO-d_6) δ_H 3.94 (3H, s, CH$_3$), 5.40 (2H, s, CH$_2$), 7.31 (1H, s, H-pyrrole), 7.36 (1H, app t, J = 9.1 Hz, H-4'), 7.39-7.44 (2H, m, H-5-pyridine and H-5'), 7.46 (1H, s, H-pyrrole), 7.61 (1H, s, H-pyrazole), 7.65-7.69 (1H, m, H-4-pyridine), 8.17 (1H, s, H-pyrazole), 8.52-8.56 (2H, m,

H-2-pyridine and H-6-pyridine), 10.33 (1H, s, CO-NH), 12.60 (1H, br s, NH-pyrrole); ^{19}F NMR (470 MHz; DMSO-d_6) δ_F -136.15; ^{13}C NMR (125 MHz; DMSO-d_6) δ_C 52.3 (CH$_2$), 56.4 (OCH$_3$), 110.4 (CH-pyrrole), 115.1 (C-4'), 120.2 (d, J_{CF} = 5.0 Hz, C-1'), 120.9 (CH-pyrazole), 121.6 (C-pyrazole), 123.6 (C-pyridine), 125.1 (C-pyrrole), 125.5 (d, J_{CF} = 3.2 Hz, C-5'), 128.4 (C-pyrrole), 128.5 (C-6'), 128.8 (CH-pyrrole), 130.9 (CH-pyrazole), 133.2 (C-pyridine), 146.4 (d, J_{CF} = 10.4 Hz, C-3'), 147.9 (d, J_{CF} = 245.4 Hz, C-2'), 148.9 (C-pyridine), 156.8 (CO-NH), 183.6 (CO); HRMS calcd for $C_{22}H_{18}{}^{35}Cl_1F_1N_5O_3$ [M+H]$^+$ 454.1077, found 454.1072.

4-((4-Nitro-1H-pyrazol-1-yl)methyl)pyridine (390)[376]
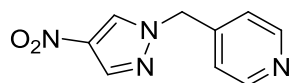
Prepared according to general procedure J using 4-pyridylmethanol (478 mg, 4.4 mmol, 1 eq.), PPh$_3$ (1.74 g, 6.6 mmol, 1.5 eq.), 4-nitropyrazole (500 mg, 4.4 mmol, 1 eq.) and DEAD (1.04 mL, 6.6 mmol, 1.5 eq.) in THF (8 mL) with stirring at r.t. for 72 h. The residue was dissolved in MeOH and passed through a 5 g SCX cartridge eluting with MeOH (100 mL) followed by 10% NH$_4$OH/MeOH (50 mL), and product containing fractions were evaporated. The residue was purified by MPLC on SiO$_2$ with a gradient elution from 25-60% EtOAc/petrol to give a white solid (495 mg, 55%); R_f 0.4 (5% MeOH/CH$_2$Cl$_2$); m.p. 87-90 °C; λ_{max}(EtOH)/nm 264; IR ν $_{max}$/cm^{-1} 1499, 1318; ^{1}H NMR (500 MHz; DMSO-d_6) δ_H 5.50 (2H, s, CH$_2$), 7.25-7.29 (2H, m, H-pyridine), 8.37 (1H, s, H-pyrazole), 8.58-8.61 (2H, m, H-pyridine), 9.12 (1H, s, H-pyrazole); ^{13}C NMR (125 MHz; DMSO-d_6) δ_C 54.5 (CH$_2$), 122.4 (C-3 and C-5-pyridine), 131.4 (CH-pyrazole), 135.2 (C-NO$_2$), 136.3 (CH-pyrazole), 144.6 (C-4-pyridine), 150.0 (C-2 and C-6-pyridine); MS (ES+) m/z 205.3 [M+H]$^+$; HRMS calcd for $C_9H_9N_4O_2$ [M+H]$^+$ 205.0720, found 205.0717.

1-(Pyridin-4-ylmethyl)-1H-pyrazol-4-amine (403)[376]
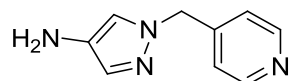
Palladium on carbon (10%, 40 mg) was added to nitropyrazole **390** (470 mg, 2.3 mmol) in MeOH (30 mL), and the mixture was stirred at r.t. under an atmosphere of hydrogen for 18 h. The reaction was filtered through Celite, and the solvent removed *in vacuo* to give a

beige solid (398 mg, 98%); R_f 0.1 (5% MeOH/EtOAc); m.p. 80-85 °C; λ_{max}(EtOH)/nm 247; IR ν_{max}/cm^{-1} 3398, 3309, 3198, 2936; ^{1}H NMR (500 MHz; DMSO-d_6) δ_H 3.93 (2H, s, NH$_2$), 5.23 (2H, s, CH$_2$), 7.03 (1H, d, J = 0.8 Hz, H-pyrazole), 7.02-7.11 (2H, m, H-pyridine), 7.17 (1H, d, J = 0.8 Hz, H-pyrazole), 8.51-8.55 (2H, m, H-pyridine); ^{13}C NMR (125 MHz; DMSO-d_6) δ_C 53.4 (CH$_2$), 117.0 (CH-pyrazole), 121.9 (C-3 and C-5-pyridine), 130.2 (CH-pyrazole), 131.5 (C-3-pyrazole), 147.3 (C-4-pyridine), 149.7 (C-2 and C-6-pyridine); HRMS calcd for C$_9$H$_{11}$N$_4$ [M+H]$^+$ 175.0978, found 175.0974.

4-(3,6-Dichloro-2-fluorobenzoyl)-*N*-(1-(pyridin-4-ylmethyl)-1*H*-pyrazol-4-yl)-1*H*-pyrrole-2-carboxamide (311)
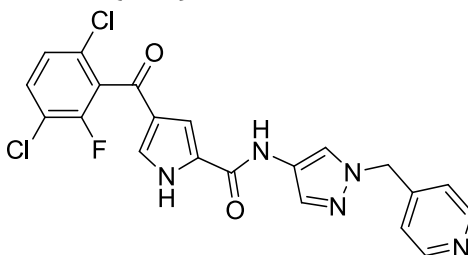
Prepared according to general procedure L using carboxylic acid **337** (100 mg, 0.33 mmol, 1 eq.), Et$_3$N (115 μL, 0.83 mmol, 2.5 eq.), and 2-chloromethylpyridinium iodide (93 mg, 0.36 mmol, 1.1 eq.) in DCM (4 mL) followed by the addition of amine **403** (72 mg, 0.41 mmol, 1.25 eq.) in DCM (1 mL) with stirring at r.t. for 18 h. The residue was purified by MPLC on SiO$_2$ with gradient elution from 80% EtOAc/petrol to 100% EtOAc give a white solid. This was further purified by MPLC on NH$_2$ SiO$_2$ with gradient elution from CH$_2$Cl$_2$ to 4% MeOH/CH$_2$Cl$_2$ to give a white solid (37 mg, 25%); R_f 0.2 (EtOAc); m.p. 165-169 °C; λ_{max}(EtOH)/nm 254sh; IR ν_{max}/cm^{-1} 3122, 2924, 1634, 1590; ^{1}H NMR (500 MHz; DMSO-d_6) δ_H 5.44 (2H, s, CH$_2$), 7.14-7.17 (2H, m, H-pyridine), 7.37 (1H, br s, H-pyrrole), 7.56 (1H, dd, J = 1.4 and 8.6 Hz, H-5'), 7.60 (1H, br s, H-pyrrole), 7.66 (1H, d, J = 0.5 Hz, H-pyrazole), 7.82 (1H, app t, J = 8.6 Hz, H-4'), 8.19 (1H, d, J = 0.5 Hz, H-pyrazole), 8.54-8.58 (2H, m, H-pyridine), 10.37 (1H, s, CO-NH), 12.69 (1H, br s, NH-pyrrole); ^{19}F NMR (470 MHz; DMSO-d_6) δ_F -116.64; ^{13}C NMR (125 MHz; DMSO-d_6) δ_C 53.6 (CH$_2$), 110.3 (CH-pyrrole), 119.3 (d, J_{CF} = 18.2 Hz, C-3'), 121.4 (CH-pyrazole), 121.6 (C-pyridine), 122.0 (C-pyrazole), 124.7 (C-pyrrole), 126.9 (d, J_{CF} = 3.6 Hz, C-5'), 128.6 (C-pyrrole), 129.2 (d, J_{CF} = 22.7 Hz, C-1'), 129.2 (d, J_{CF} = 5.0 Hz, C-6'), 129.6 (C-pyrrole), 131.1 (C-pyrazole), 131.8 (C-4'), 146.7 (C-pyridine), 149.8 (C-pyridine), 153.8 (d, J_{CF} =

248.4 Hz, C-2'), 156.9 (CO-NH), 182.6 (CO); HRMS calcd for $C_{21}H_{15}{}^{35}Cl_2F_1N_5O_2$ [M+H]$^+$ 458.0581, found 458.0575.

4-(6-Chloro-2-fluoro-3-methoxybenzoyl)-*N*-(1-(pyridin-4-ylmethyl)-1*H*-pyrazol-4-yl)-1*H*-pyrrole-2-carboxamide (329)
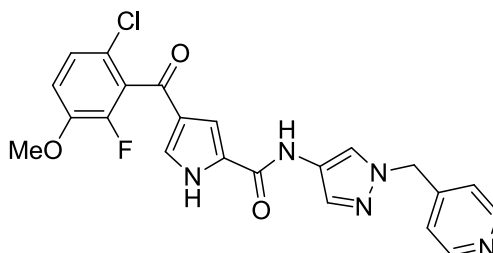
Prepared according to general procedure L using carboxylic acid **421** (800 mg, 0.27 mmol, 1 eq.), Et$_3$N (93 μL, 0.67 mmol, 2.5 eq.), and 2-chloromethylpyridinium iodide (76 mg, 0.30 mmol, 1.1 eq.) in DCM (4 mL) followed by the addition of amine **403** (58 mg, 0.34 mmol, 1.25 eq.) in DCM (1 mL) with stirring at r.t. for 18 h. The residue was purified by MPLC on SiO$_2$ with gradient elution from 0-5% MeOH/EtOAc give a white solid. This was further purified by MPLC on NH$_2$ SiO$_2$ with gradient elution from 0-4% MeOH/CH$_2$Cl$_2$ to give a white solid (32 mg, 26%); R_f 0.2 (5% MeOH/EtOAc); m.p. 190-192 °C; λ$_{max}$(EtOH)/nm 253sh, 227; IR ν$_{max}$/cm^{-1} 3332, 1626; ^{1}H NMR (500 MHz; DMSO-d_6) δ$_H$ 3.94 (3H, s, CH$_3$), 5.43 (2H, s, CH$_2$), 7.13-7.18 (2H, m, H-pyridine), 7.33 (1H, br s, H-pyrrole), 7.36 (1H, app t, J = 9.0 Hz, H-4'), 7.42 (1H, dd, J = 1.3 and 9.0 Hz, H-5'), 7.47 (1H, br s, H-pyrrole), 7.65 (1H, d, J = 0.5 Hz, H-pyrazole), 8.18 (1H, d, J = 0.5 Hz, H-pyrazole), 8.53-8.58 (2H, m, H-pyridine), 10.36 (1H, s, CO-NH), 12.61 (1H, br s, NH-pyrrole); ^{19}F NMR (470 MHz; DMSO-d_6) δ$_F$; -136.14; ^{13}C NMR (125 MHz; DMSO-d_6) δ$_C$ 53.6 (CH$_2$), 56.4 (OCH$_3$), 110.4 (CH-pyrrole), 115.1 (C-4'), 120.2 (d, J_{CF} = 4.8 Hz, C-1'), 121.4 (CH-pyrazole), 121.7 (C-pyrazole), 122.0 (C-pyridine), 125.1 (C-pyrrole), 125.5 (d, J_{CF} = 3.6 Hz, C-5'), 128.4 (C-pyrrole), 128.5 (C-6'), 128.9 (C-pyrrole), 131.0 (C-pyrazole), 146.4 (d, J_{CF} = 10.4 Hz, C-3'), 146.7 (C-pyridine), 147.9 (d, J_{CF} = 247.5 Hz, C-2'), 149.8 (C-pyridine), 156.9 (CO-NH), 183.6 (CO); HRMS calcd for $C_{22}H_{18}{}^{35}Cl_1F_1N_5O_3$ [M+H]$^+$ 454.1077, found 454.1067.

4-(6-Chloro-2-fluoro-3-methoxybenzoyl)-*N*-(1-(1-(2,2,2-trifluoroethyl) piperidin-4-yl)-1*H*-pyrazol-4-yl)-1*H*-pyrrole-2-carboxamide (326)
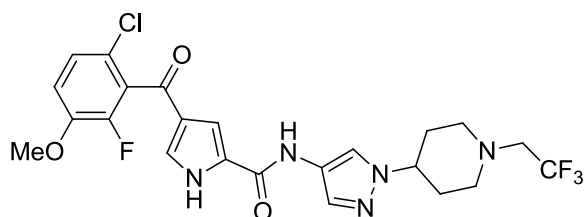
Prepared according to general procedure L using carboxylic acid **421** (80 mg, 0.27 mmol, 1 eq.), Et$_3$N (93 μL, 0.67 mmol, 2.5 eq.), and 2-chloromethylpyridinium iodide (76 mg, 0.30 mmol, 1.1 eq.) in DCM (4 mL) followed by the addition of amine **397** (83 mg, 0.34 mmol, 1.25 eq.) with stirring at r.t. for 18 h. The residue was purified by MPLC on SiO$_2$ with gradient elution from 40-80% EtOAc/petrol to give a white solid (70 mg, 49%); R_f 0.1 (60% EtOAc/petrol); m.p. 236-239 °C; λ_{max}(EtOH)/nm 252 sh, 227; IR ν $_{max}$/cm^{-1} 3353, 3204, 3123, 2951, 1630, 1602; ^{1}H NMR (500 MHz; DMSO-d_6) δ$_H$ 1.93-2.01 (4H, m, H-piperidine), 2.53-2.60 (2H, m, H-piperidine), 3.00-3.07 (2H, m, H-piperidine), 3.27 (2H, q, J_{HF} = 10.3 Hz, CH$_2$CF$_3$), 3.94 (3H, s, OCH$_3$), 4.14-4.23 (1H, m, H-piperidine), 7.32 (1H, s, H-pyrrole), 7.36 (1H, app t, J = 9.0 Hz, H-4'), 7.42 (1H, dd, J = 1.3 and 9.0 Hz, H-5'), 7.46 (1H, s, H-pyrrole), 7.59 (1H, s, H-pyrazole), 8.01 (1H, s, H-pyrazole), 10.28 (1H, s, CO-NH), 12.59 (1H, br s, NH-pyrrole); ^{19}F NMR (470 MHz; DMSO-d_6) -67.98, -136.15; ^{13}C NMR (125 MHz; DMSO-d_6) δ$_C$ 31.9 (C-piperidine), 52.3 (C-piperidine), 56.4 (q, J_{CF} = 29.1 Hz, *C*H$_2$CF$_3$), 56.4 (OMe), 57.8 (C-piperidine), 110.3 (CH-pyrrole), 115.1 (C-4'), 118.7 (CH-pyrazole), 120.2 (d, J_{CF} = 5.0 Hz, C-1'), 120.9 (C-pyrazole), 125.1 (C-pyrrole), 125.5 (d, J_{CF} = 3.6 Hz, C-5'), 125.6 (q, J = 294.0 Hz, CF$_3$), 127.2, 128.4 (C-pyrazole), 128.5 (C-6'), 128.6 (C-pyrrole), 128.8 (CH-pyrrole), 129.9 (CH-pyrazole), 146.4 (d, J_{CF} = 10.9 Hz, C-3'), 147.9 (d, J_{CF} = 247.3 Hz, C-2'), 156.9 (CO-NH), 183.6 (CO); HRMS calcd for C$_{23}$H$_{23}$^{35}Cl$_1$F$_4$N$_5$O$_3$ [M+H]$^+$ 528.1420, found 528.1406.

1-(2-Methoxyethyl)-4-nitro-1*H*-pyrazole (391)[377]
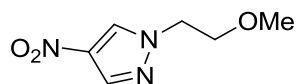
Prepared according to general procedure J using 2-methoxyethanol (244 μL, 3.1 mmol, 1 eq.), PPh$_3$ (1.22 g, 4.6 mmol, 1.5 eq.), 4-nitropyrazole (350 mg, 3.1 mmol, 1 eq.) and DEAD (731 μL, 4.6 mmol, 1.5 eq.) in THF (6 mL) with stirring at r.t. for 18 h. The residue

was purified by MPLC on SiO$_2$ with a gradient elution from 20-60% EtOAc/petrol to give a clear oil (450 mg, 85%); R_f 0.75(EtOAc); λ_{max}(EtOH)/nm 272; IR ν_{max}/cm^{-1} 1506, 1297; ^{1}H NMR (500 MHz; DMSO-d_6) δ_H 3.27 (3H, s, OMe), 3.76 (2H, d, J = 5.2 Hz, CH$_2$CH$_2$OMe), 4.38 (2H, d, J = 5.2 Hz, CH$_2$CH$_2$OMe), 8.31 (1H, s, H-pyrazole), 8.89 (1H, s, H-pyrazole); ^{13}C NMR (125 MHz; DMSO-d_6) δ_C 52.1 (CH$_2$), 57.9 (Me), 69.4 (CH$_2$), 130.9 (C-pyrazole), 134.8 (C-NO$_2$), 135.6 (C-pyrazole); MS (ES+) m/z 172.2 [M+H]$^+$.

1-(2-Methoxyethyl)-1*H*-pyrazol-4-amine (404)[377]
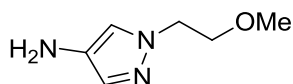
Palladium on carbon (10%, 40 mg) was added to nitropyrazole **391** (440 mg, 2.6 mmol) in MeOH (30 mL), and the mixture was stirred at r.t. under an atmosphere of hydrogen for 18 h. The reaction was filtered through Celite, and the solvent removed *in vacuo* to give a brown oil (330 mg, 91%); R_f 0.1 (5% MeOH/EtOAc); λ_{max}(EtOH)/nm 246; IR ν_{max}/cm^{-1} 3332, 2933; ^{1}H NMR (500 MHz; DMSO-d_6) δ_H 3.25 (3H, s, OMe), 3.62 (2H, d, J = 5.5 Hz, CH$_2$CH$_2$OMe), 3.80 (2H, s, NH$_2$), 4.08 (2H, d, J = 5.5 Hz, CH$_2$CH$_2$OMe), 6.93 (1H, s, H-pyrazole), 7.05 (1H, s, H-pyrazole); ^{13}C NMR (125 MHz; DMSO-d_6) δ_C 50.9 (CH$_2$), 57.9 (Me), 70.9 (CH$_2$), 116.9 (C-pyrazole), 129.2 (C-pyrazole), 130.7 (C-NH$_2$); MS (ES+) m/z 142.2 [M+H]$^+$.

4-(3,6-Dichloro-2-fluorobenzoyl)-*N*-(1-(2-methoxyethyl)-1*H*-pyrazol-4-yl)-1*H*-pyrrole-2-carboxamide (316)
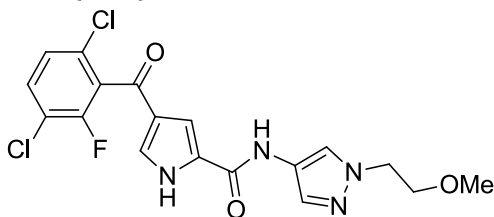
Prepared according to general procedure L using carboxylic acid **337** (150 mg, 0.50 mmol, 1 eq.), Et$_3$N (173 μL, 1.24mmol, 2.5 eq.), and 2-chloromethylpyridinium iodide (139 mg, 0.54 mmol, 1.1 eq.) in DCM (5 mL) followed by the addition of amine **404** (87 mg, 0.62 mmol, 1.25 eq.) with stirring at r.t. for 18 h. The residue was purified by MPLC on SiO$_2$ with gradient elution from 40% EtOAc/petrol to 100% EtOAc give a white solid. (102 mg, 49%); R_f 0.3 (EtOAc); m.p.155-160 °C; λ_{max}(EtOH)/nm 253sh, 224; IR ν_{max}/cm^{-1} 3194, 3124, 2929, 1628, 1591; ^{1}H NMR (500 MHz; DMSO-d_6) δ_H 3.27 (3H, s, CH$_3$), 3.70 (2H, t,

J = 5.3 Hz, CH$_2$-N), 4.27 (2H, t, J = 5.3 Hz, CH$_2$-O), 7.35 (1H, s, H-pyrrole), 7.56 70 (1H, dd, J = 1.2 and 8.5 Hz, H-5'), 7.58 (1H, s, H-pyrazole), 7.60 (1H, s, H-pyrrole), 7.82 (1H, app t, J = 8.5 Hz, H-4'), 8.00 (1H, s, H-pyrazole), 10.28 (1H, s, CO-NH), 12.67 (1H, s, NH-pyrrole); ^{19}F NMR (470 MHz; DMSO-d_6) δ_F -116.65; ^{13}C NMR (125 MHz; DMSO-d_6) δ_C 51.2 (CH$_2$-O), 57.9 (CH$_3$), 70.6 (CH$_2$-N), 110.1 (CH-pyrrole), 119.3 (d, J_{CF} = 18.1 Hz, C-3'), 121.0 (CH-pyrazole), 121.2 (C-pyrazole), 124.7 (C-pyrrole), 126.9 (d, J_{CF} = 3.6 Hz, C-5'), 128.7 (C-pyrrole), 129.2 (d, J_{CF} = 22.7 Hz, C-1'), 129.2 (d, J_{CF} = 5.1 Hz, C-6'), 129.6 (C-pyrrole), 130.2 (CH-pyrazole), 131.8 (C-4'), 153.8 (d, J_{CF} = 248.4 Hz, C-2'), 156.8 (CO-NH), 182.6, (CO); HRMS calcd for C$_{18}$H$_{16}$^{35}Cl$_2$F$_1$N$_4$O$_3$ [M+H]$^+$ 425.0578, found 425.0573.

4-(6-Chloro-2-fluoro-3-methoxybenzoyl)-*N*-(1-(2-methoxyethyl)-1*H*-pyrazol-4-yl)-1*H*-pyrrole-2-carboxamide (324)
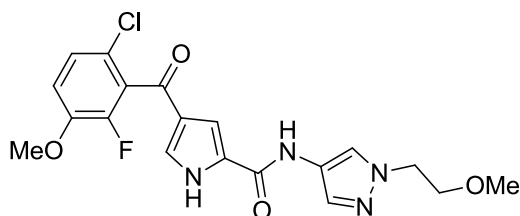
Prepared according to general procedure L using carboxylic acid **421** (125 mg, 0.42 mmol, 1 eq.), Et$_3$N (146 μL, 1.05mmol, 2.5 eq.), and 2-chloromethylpyridinium iodide (118 mg, 0.46 mmol, 1.1 eq.) in DCM (4 mL) followed by the addition of amine **404** (74 mg, 0.52 mmol, 1.25 eq.) with stirring at r.t. for 18 h. The residue was purified by MPLC on SiO$_2$ with gradient elution from 40% EtOAc/petrol to 100% EtOAc give a white solid. (80 mg, 45%); R_f 0.25 (EtOAc); m.p. 217-221 °C; λ_{max}(EtOH)/nm 252 sh, 224; IR ν_{max}/cm^{-1} 3354, 3208, 3115, 1636, 1615, 1592; ^{1}H NMR (500 MHz; DMSO-d_6) δ_H 3.27 (3H, s, CH$_2$-O-C*H*$_3$), 3.70 (2H, t, J = 5.3 Hz, CH$_2$-N), 3.94 (1H, s, Ar-O-CH$_3$), 4.27 (2H, t, J = 5.3 Hz, CH$_2$-O), 7.32 (1H, s, H-pyrrole), 7.36 (1H, app t, J = 8.9 Hz, H-4'), 7.42 (1H, dd, J = 1.0 Hz and 8.9 Hz, H-5'), 7.46 (1H, s, H-pyrrole), 7.57 (1H, s, H-pyrazole), 8.00 (1H, s, H-pyrazole), 10.28 (1H, s, CO-NH), 12.60 (1H, s, NH-pyrrole); ^{19}F NMR (470 MHz; DMSO-d_6) δ_F -136.15; ^{13}C NMR (125 MHz; DMSO-d_6) δ_C 51.2 (CH$_2$-O), 56.4 (Ar-O-CH$_3$)57.9 (CH$_2$-O-C*H*$_3$), 70.6 (CH$_2$-N), 110.3 (CH-pyrrole), 115.1 (d, J_{CF} = 18.1 Hz, C-4'), 120.2 (d, J_{CF} = 4.8 Hz, C-1'), 121.0 (CH-pyrazole), 121.1 (C-pyrazole), 125.0 (C-pyrrole), 125.5 (d, J_{CF} = 3.6 Hz, C-5'), 128.4 (C-pyrrole), 128.5 (C-6'), 128.6 (CH-pyrrole and C-pyrrole), 146.4 (d, J = 10.6 Hz, C-3'), 147.9 (d, J_{CF} = 246.9 Hz, C-2'), 156.8 (CO-NH), 183.6 (CO);

MS (ES+) m/z 421.4 $[M^{35,35}Cl+H]^+$, 423.4 $[M^{35,37}Cl+H]^+$; HRMS calcd for $C_{19}H_{19}{}^{35}Cl_1F_1N_4O_4$ $[M+H]^+$ 421.1073, found 421.1067.

1-((1-Methyl-1*H*-imidazol-2-yl)methyl)-4-nitro-1*H*-pyrazole (392)
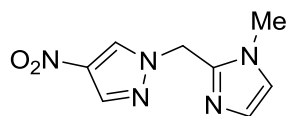
Prepared according to general procedure J using 1-methyl-2-hydroxymethylimidazole (298 mg, 2.65 mmol, 1 eq.), PPh$_3$ (1.04 g, 4.0 mmol, 1.5 eq.), 4-nitropyrazole (300 mg, 2.65 mmol, 1 eq.) and DEAD (1.04 mL, 4.0 mmol, 1.5 eq.) in THF (4 mL) with stirring at r.t. for 18 h. The residue was dissolved in MeOH and run through a 20 g SCX cartridge eluting with MeOH (100 mL) followed by 20% NH$_4$OH/MeOH (50 mL). Product containing fractions were evaporated and purified by MPLC on SiO$_2$ with a gradient elution from 80-100% EtOAc/petrol to give a clear oil (98 mg, 18%); R_f 0.2 (5% MeOH/EtOAc); m.p. 128-132 °C; λ_{max}(EtOH)/nm 271; IR ν_{max}/cm^{-1} 1509, 1312; ^{1}H NMR (500 MHz; DMSO-d_6) δ_H 3.73 (3H, s, CH$_3$), 5.55 (1H, s, CH$_2$), 6.89 (1H, d, J = 1.2 Hz, H-imidazole), 7.20 (1H, d, J = 1.2 Hz, H-imidazole), 8.31 (1H, d, J = 0.5 Hz, H-pyrazole), 8.97 (1H, d, J = 0.5 Hz, H-pyrazole); ^{13}C NMR (125 MHz; DMSO-d_6) 32.7 (CH$_3$), 47.8 (CH$_2$), 122.8 (CH-imidazole), 127.2 (CH-imidazole), 130.6 (CH-pyrazole), 135.0 (C-NO$_2$), 135.9 (CH-pyrazole), 141.3 (C-2-imidazole); HRMS calcd for $C_8H_{10}N_5O_2$ $[M+H]^+$ 208.0829, found 208.0825.

1,1'-1,2-Dimethyl-4,5-dihydro-1*H*-imidazole-4,5-diyl)*bis*(4-nitro-1*H*-pyrazole) (411)
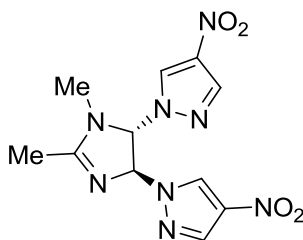
Compound **411** was obtained as a by-product from the above synthesis of **392**, and isolated as a white solid (154 mg, 18%); R_f 0.5 (EtOAc); m.p. 187-191 °C; λ_{max}(EtOH)/nm ; IR ν_{max}/cm^{-1} 1599, 1497, 1407, 1293; ^{1}H NMR (500 MHz; DMSO-d_6) δ_H 2.12 (3H, d, J = 0.9 Hz, Me), 2.84 (3H, s, N-Me), 6.24 (1H, d, J = 3.3 Hz, CH-dihydroimidazole), 6.32 (1H, d, J = 0.9 and 3.3 Hz, CH-dihydroimidazole) , 8.42 (1H, s, H-pyrazole), 8.51 (1H, s, H-pyrazole), 9.00 (1H, d, J = 0.6 Hz, H-pyrazole), 9.5 (1H, d,, J = 0.6 Hz, H-pyrazole); ^{13}C NMR (125 MHz; DMSO-d_6) 14.0 (Me), 29.7 (N-Me), 82.3 (CH-dihydroimidazole), 85.4

(CH-dihydroimidazole), 129.8 (C-pyrazole), 131.0 (C-pyrazole), 135.1 (C-pyrazole), 135.2 (C-pyrazole), 136.5 (C-pyrazole), 137.4 (C-pyrazole), 167.7 (C-2 dihydroimidazole); MS (ES+) m/z 208.3 $[M-C_3N_3O_2H]^+$.

1-((1-Methyl-1*H*-imidazol-2-yl)methyl)-1*H*-pyrazol-4-amine (405)
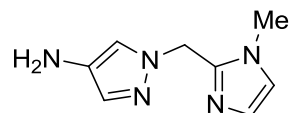
Palladium on carbon (10%, 30 mg) was added to nitropyrazole **392** (90 mg, 0.43 mmol) in MeOH (10 mL), and the mixture was stirred at r.t. under an atmosphere of hydrogen for 18 h. The reaction was filtered through Celite, and the solvent removed *in vacuo* to give a brown oil (74 mg, 96%); R_f 0.35 (5% MeOH/EtOAc; NH$_2$ SiO$_2$); λ_{max}(EtOH)/nm 245; IR ν_{max}/cm^{-1} 3325 br, 3112, 1613; ^{1}H NMR (500 MHz; DMSO-d_6) δ_H 3.61 (3H, s, CH$_3$), 3.87 (2H, br s, NH$_2$), 5.22 (1H, s, CH$_2$), 6.84 (1H, d, J = 1.2 Hz, H-imidazole), 6.94 (1H, d, J = 0.8 Hz, H-pyrazole), 6.98 (1H, d, J = 0.8 Hz, H-pyrazole), 7.12 (1H, d, J = 1.2 Hz, H-imidazole); ^{13}C NMR (125 MHz; DMSO-d_6) 32.5 (CH$_3$), 47.1 (CH$_2$), 116.0 (CH-pyrazole), 122.4 (CH-imidazole), 126.7 (CH-imidazole), 129.5 (CH-pyrazole), 131.4 (C-NH$_2$), 143.1 (C-2-imidazole); HRMS calcd for C$_8$H$_{12}$N$_5$ $[M+H]^+$ 178.1087, found 178.1083.

4-(3,6-Dichloro-2-fluorobenzoyl)-*N*-(1-((1-methyl-1*H*-imidazol-2-yl)methyl)-1*H*-pyrazol-4-yl)-1*H*-pyrrole-2-carboxamide (312)
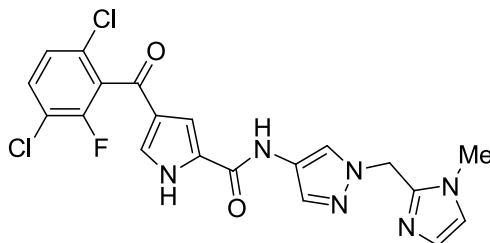
Prepared according to general procedure L using carboxylic acid **337** (82 mg, 0.27 mmol, 1 eq.), Et$_3$N (94 μL, 0.68 mmol, 2.5 eq.), and 2-chloromethylpyridinium iodide (76 mg, 0.30 mmol, 1.25 eq.) in DCM (4 mL) followed by the addition of amine **405** (60 mg, 0.34 mmol, 1.25 eq.) with stirring at r.t. for 18 h. The residue was purified by MPLC on NH$_2$ SiO$_2$ with gradient elution from 0-4% MeOH/EtOAc to give a yellow solid (54 mg, 43%); R_f 0.5 (5% MeOH/EtOAc; NH$_2$ SiO$_2$); m.p. 285 °C dec.; λ_{max}(EtOH)/nm 254sh; IR ν_{max}/cm^{-1} 3159, 1657, 1634, 1592; ^{1}H NMR (500 MHz; DMSO-d_6) δ_H 3.67 (3H, s, CH$_3$), 5.42 (2H, s, CH$_2$), 6.87 (1H, s, H-imidazole), 7.16 (1H, s, H-imidazole), 7.34 (1H, s, H-

pyrrole), 7.55 (1H, d, J = 8.5 Hz, H-4'), 7.57-7.64 (2H, m, H-pyrazole and H-pyrrole), 7.81 (1H, app t, J = 8.5 Hz, H-4'), 8.00 (1H, s, H-pyrazole), 10.32 (1H, s, CO-NH), 12.68 (1H, br s, NH-pyrrole); ^{19}F NMR (470 MHz; DMSO-d_6) δ_F -116.65; ^{13}C NMR (125 MHz; DMSO-d_6) δ_C 32.6 (CH$_3$), 47.2 (CH$_2$), 110.2 (CH-pyrrole), 119.3 (d, J_{CF} = 18.0 Hz, C-3'), 120.5 (CH-pyrazole), 121.5 (CH-imidazole), 122.5 (CH-imidazole), 124.7 (C-pyrrole), 126.8 (d, J_{CF} = 4.1 Hz, C-5'), 128.6 (C-pyrrole), 129.2 (d, J_{CF} = 23.2 Hz, C-1'), 129.2 (d, J_{CF} = 5.3 Hz, C-6'), 129.6 (CH-pyrrole), 130.4 (CH-pyrazole), 131.8 (C-4'), 142.7 (C-2-imidazole), 153.8 (d, J_{CF} = 248.9 Hz, C-2'), 156.8 (CO-NH), 182.5 (CO); HRMS calcd for C$_{20}$H$_{16}$^{35}Cl$_2$F$_1$N$_6$O$_2$ [M+H]$^+$ 461.0690, found 461.0683.

4-(3,6-Dichloro-2-fluorobenzoyl)-*N*-(3-methylisoxazol-5-yl)-1*H*-pyrrole-2-carboxamide (317)
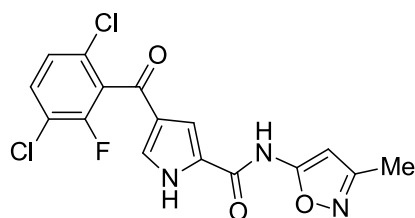
Prepared according to general procedure F using carboxylic acid **337** (75 mg, 0.25 mmol, 1 eq.), 5-amino-3-methylisoxazole (85 mg, 0.87 mmol, 3.5 eq.), PCl$_3$ (22 μL, 0.25 mmol, 1 eq.) and MeCN (1 mL). Purification by MPLC on SiO$_2$ with a gradient elution from 10-40% EtOAc:petrol gave a white solid (32 mg, 34%); R_f 0.6 (40% EtOAc/petrol); m.p. 228 °C dec.; λ_{max}(EtOH)/nm 294, 240; IR ν_{max}/cm^{-1} 3253, 3126, 3055, 1680, 1640; ^{1}H NMR (500 MHz; DMSO-d_6) δ_H 2.25 (3H, s, CH$_3$), 6.29 (1H, s, H-isoxazole), 7.57 (1H, dd, J = 1.3 and 8.4 Hz, H-3'), 7.62 (1H, br s, H-pyrrole), 7.74 (1H, s, H-pyrrole), 7.83 (1H, app t, J = 8.6 Hz, H-4'), 11.80 (1H, s, CO-NH), 12.94 (1H, s, NH-pyrrole); ^{19}F NMR (470 MHz; DMSO-d_6) δ_F -116.62; ^{13}C NMR (125 MHz; DMSO-d_6) δ_C 11.3 (CH$_3$), 89.2 (CH-isoxazole), 113.0 (CH-pyrrole), 119.3 (d, J_{CF} = 18.0 Hz, C-3'), 124.9 (C-pyrrole), 126.9 (d, J_{CF} = 3.8 Hz, C-5'), 127.1 (C-pyrrole), 129.0 (d, J_{CF} = 23.0 Hz, C-1'), 129.2 (d, J_{CF} = 5.1 Hz, C-6'), 130.7 (C-pyrrole), 131.9 (C-4'), 153.8 (d, J_{CF} = 248.4 Hz, C-2'), 156.3 (CO-NH), 160.7 (C-isoxazole), 161.1 (C-isoxazole), 182.6, (CO); HRMS calcd for C$_{16}$H$_{11}$^{35}Cl$_2$F$_1$N$_3$O$_3$ [M+H]$^+$ 382.0156, found 382.0153.

4-(3,6-Dichloro-2-fluorobenzoyl)-*N*-(5-methylisoxazol-3-yl)-1*H*-pyrrole-2-carboxamide (318)
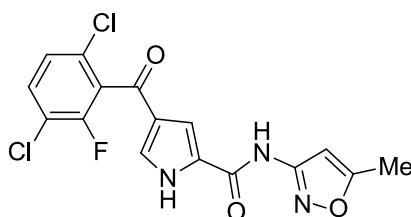
Prepared according to general procedure F using carboxylic acid **337** (100 mg, 0.33 mmol, 1 eq.), 3-amino-5-methylisoxazole (113 mg, 1.16 mmol, 3.5 eq.), PCl$_3$ (29 μL, 0.33 mmol, 1 eq.) and MeCN (1.5 mL). Purification by MPLC on SiO$_2$ with a gradient elution from 10-35% EtOAc:petrol gave a white solid (50 mg, 40%); R_f 0.6 (40% EtOAc/petrol); m.p. 255 °C dec.; λ_{max}(EtOH)/nm 288, 240; IR ν $_{max}$/cm^{-1} 3423, 3129, 3081, 1654, 1619; ^{1}H NMR (500 MHz; DMSO-d_6) δ_H 2.44 (3H, d, J = 0.7 Hz, CH$_3$), 6.76 (1H, d, J = 0.7 Hz, H-isoxazole), 7.56 (1H, dd, J = 1.4 and 8.4 Hz, H-3'), 7.64 (1H, br s, H-pyrrole), 7.69 (1H, s, H-pyrrole), 7.82 (1H, app t, J = 8.6 Hz, H-4'), 11.20 (1H, s, CO-NH), 12.83 (1H, s, NH-pyrrole); ^{19}F NMR (470 MHz; DMSO-d_6) δ_F -116.64; ^{13}C NMR (125 MHz; DMSO-d_6) δ_C 12.1 (CH$_3$), 96.7 (CH-isoxazole), 112.9 (CH-pyrrole), 119.2 (d, J_{CF} = 18.0 Hz, C-3'), 124.8 (C-pyrrole), 126.9 (d, J_{CF} = 4.1 Hz, C-5'), 127.5 (C-pyrrole), 129.1 (d, J_{CF} = 23.0 Hz, C-1'), 129.2 (d, J_{CF} = 5.1 Hz, C-6'), 130.3 (C-pyrrole), 131.8 (C-4'), 153.8 (d, J_{CF} = 248.5 Hz, C-2'), 158.0 (CO-NH), 158.1 (C-isoxazole), 169.4 (C-isoxazole), 182.6, (CO); MS (ES+) *m/z* 382.3 [M^{35,35}Cl+H]$^+$, 384.3 [M^{35,37}Cl+H]$^+$; HRMS calcd for C$_{16}$H$_{11}$^{35}Cl$_2$F$_1$N$_3$O$_3$ [M+H]$^+$ 382.0156, found 382.0155.

## 4-(3,6-Dichloro-2-fluorobenzoyl)-*N*-(1-methyl-1*H*-pyrazol-3-yl)-1*H*-pyrrole-2-carboxamide (319)
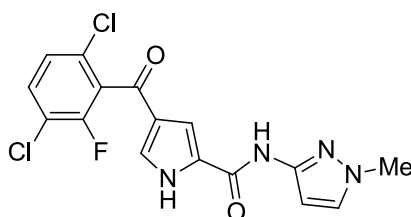
Prepared according to general procedure F using carboxylic acid **337** (100 mg, 0.33 mmol, 1 eq.), 3-amino-5-methylpyrazole (113 mg, 1.16 mmol, 3.5 eq.), PCl$_3$ (29 μL, 0.33 mmol, 1 eq.) and MeCN (1.5 mL). Purification by MPLC on SiO$_2$ with a gradient elution from 50-80% EtOAc:petrol gave a white solid which was re-purified by MPLC on NH$_2$ SiO$_2$ with a gradient elution from 50-80% EtOAc/petrol to give a white solid (85 mg, 67%); R_f

0.3 (75% EtOAc/petrol); m.p. 240-242 °C; λ_{max}(EtOH)/nm 254sh; IR ν_{max}/cm^{-1} 3200, 3131, 1636, 1574; ^{1}H NMR (500 MHz; DMSO-d_6) δ_H 3.81 (3H, s, CH$_3$), 6.57 (1H, d, J = 2.2 Hz, H-pyrazole), 7.55 (1H, dd, J = 1.4 and 8.6 Hz, H-5'), 7.56 (1H, br s, H-pyrrole), 7.60 (1H, br s, H-pyrrole), 7.62 (1H, d, J = 2.2 Hz, H-pyrazole), 7.81 (1H, app t, J = 8.6 Hz, H-4'), 10.75 (1H, s, CO-NH), 12.64 (1H, br s, NH-pyrrole); ^{19}F NMR (470 MHz; DMSO-d_6) δ_F -116.63; ^{13}C NMR (125 MHz; DMSO-d_6) δ_C 38.3 (CH$_3$), 97.2 (C-4-pyrazole), 111.5 (CH-pyrrole), 119.2 (d, J_{CF} = 18.2 Hz, C-3'), 124.7 (C-pyrrole), 126.8 (d, J_{CF} = 3.6 Hz, C-5'), 128.5 (CH-pyrrole), 129.2 (d, J_{CF} = 5.1 Hz, C-6'), 129.3 (d, J_{CF} = 23.2 Hz, C-1'), 129.6 (C-pyrrole), 130.9 (C-5-pyrazole), 131.7 (C-4'), 146.6 (C-3-pyrazole), 153.8 (d, J_{CF} = 248.4 Hz, C-2'), 157.4 (CO-NH), 170.3, 182.5 (CO); HRMS calcd for C$_{16}$H$_{12}$^{35}Cl$_2$F$_1$N$_4$O$_2$ [M+H]$^+$ 381.0316, found 381.0313.

1-Methyl-4-nitro-1*H*-imidazole (418)
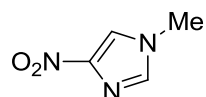
Dimethyl oxalate (522 mg, 4.42 mmol, 1 eq.) was added to 4-nitroimidazole (500 mg, 4.42 mmol, 1 eq.) and KO^{t}Bu (496 mg, 4.42 mmol, 1 eq.) in DMF (13 mL) and the mixture was heated at 140 °C for 2 h. Further dimethyl oxalate (261 mg, 2.21 mmol, 0.5 eq.) and KO^{t}Bu (248 mg, 2.21 mmol, 0.5 eq.) were added and the mixture heated at 140 °C for a further 2 h. The solvent was removed *in vacuo*, the residue partitioned between EtOAc (2 × 30 mL) and K$_2$CO$_3$ (20 mL, 10% aq.). The organic layers were combined, dried over MgSO$_4$, and the solvent removed *in vacuo*. The crude mixture was purified by MPLC on NH$_2$ SiO$_2$ with a gradient elution from 30-70% EtOAc/petrol to give a white solid (275 mg, 49%); R_f 0.5 (50% EtOAc/petrol, NH$_2$ SiO$_2$); m.p. 132-135 °C (lit.[378] 134 °C); λ_{max}(EtOH)/nm 285; IR ν_{max}/cm^{-1} 1523, 1316; ^{1}H NMR (500 MHz; CDCl$_3$) δ_H 3.81 (3H, s, CH$_3$), 7.41 (1H, s, H-imidazole), 7.74 (1H, s, H-imidazole); ^{13}C NMR (125 MHz; DMSO-d_6) δ_C 34.6 (CH$_3$), 120.1 (C-5-imidazole), 136.6 (C-2-imidazole), 148.2 (C-NO$_2$); MS (ES+) *m/z* 128.1 [M+H]$^+$.

1-Methyl-1*H*-imidazol-4-amine (420)

H_2N —⟨imidazole⟩— N—Me
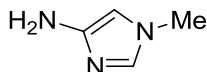
Prepared according to general procedure H using nitroimidazole **418** (250 mg, 1.97 mmol) in MeOH (10 mL) and EtOAc (10 mL) to give a brown oil (190 mg, 99%); R_f 0.1 (15% MeOH/EtOAc); λ_{max}(EtOH)/nm 232, 283; IR ν_{max}/cm^{-1} 3298 br; ^{1}H NMR (500 MHz; CDCl$_3$) δ_H 3.56 (3H, CH$_3$), 6.18 (1H, s, H-imidazole), 7.04 (1H, s, H-imidazole); ^{13}C NMR not obtained due to chemical instability; MS: no mass ion detected.

4-(3,6-Dichloro-2-fluorobenzoyl)-*N*-(1-methyl-1*H*-imidazol-4-yl)-1*H*-pyrrole-2-carboxamide (320)
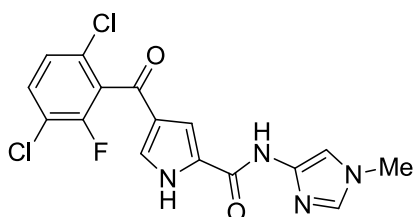
Prepared according to general procedure F using carboxylic acid **337** (125 mg, 0.33 mmol, 1 eq.), amine **420** (100 mg, 1.03 mmol, 3 eq.), PCl$_3$ (29 μL, 0.33 mmol, 1 eq.) and MeCN (1.5 mL). Purification by MPLC on NH$_2$ SiO$_2$ with a gradient elution from 0-4% MeOH/EtOAc gave a white solid (30 mg, 24%); R_f 0.7 (5% MeOH/EtOAc); m.p. 258-260 °C; λ_{max}(EtOH)/nm 227, 250 sh; IR ν_{max}/cm^{-1} 3262, 3122, 1657, 1637; ^{1}H NMR (500 MHz; DMSO-d_6) δ_H 3.68 (3H, CH$_3$), 7.33 (1H, s, H-imidazole), 7.47 (1H, s, H-imidazole), 7.52-7.60 (3H, m, H-5' and 2 × H-pyrrole), 7.81 (1H, app t, J = 8.3 Hz, H-4'), 10.67 (1H, s, CO-NH), 12.61 (1H, s, NH-pyrrole); ^{19}F NMR (470 MHz; DMSO-d_6) δ_F -116.15; ^{13}C NMR (125 MHz; DMSO-d_6) δ_C 33.1 (CH$_3$), 108.2 (CH-imidazole), 111.2 (CH-pyrrole), 119.2 (d, J_{CF} = 18.3 Hz, C-3'), 124.7 (C-pyrrole), 126.8 (d, J_{CF} = 3.6 Hz, C-5'), 128.5 (CH-pyrrole), 129.2 (d, J_{CF} = 5.4 Hz, C-6'), 129.3 (d, J_{CF} = 22.7 Hz, C-1'), 131.7 (C-4'), 133.9 (CH-imidazole), 137.6 (C-imidazole), 153.8 (d, J_{CF} = 248.4 Hz, C-2'), 156.6 (CO-NH), 182.6 (CO); HRMS calcd for C$_{16}$H$_{12}$^{35}Cl$_2$F$_1$N$_4$O$_2$ [M+H]$^+$ 381.0316, found 381.0315.

References

1. Stratton, M. R.; Campbell, P. J.; Futreal, P. A., The cancer genome. *Nature* **2009**, *458*, 719-724.

2. Futreal, P. A.; Coin, L.; Marshall, M.; Down, T.; Hubbard, T.; Wooster, R.; Rahman, N.; Stratton, M. R., A census of human cancer genes. *Nat. Rev. Cancer* **2004**, *4*, 177-183.

3. Haber, D. A.; Settleman, J., Cancer: Drivers and passengers. *Nature* **2007**, *446*, 145-146.

4. Hanahan, D.; Weinberg, R. A., The Hallmarks of Cancer. *Cell* **2000**, *100*, 57-70.

5. Hanahan, D.; Weinberg, Robert A., Hallmarks of Cancer: The Next Generation. *Cell* **2011**, *144*, 646-674.

6. Loeb, L. A., Human cancers express mutator phenotypes: origin, consequences and targeting. *Nat. Rev. Cancer* **2011**, *11*, 450-457.

7. Talbot, S. J.; Crawford, D. H., Viruses and tumours – an update. *Eur. J. Cancer* **2004**, *40*, 1998-2005.

8. De Palma, M.; Hanahan, D., The biology of personalized cancer medicine: Facing individual complexities underlying hallmark capabilities. *Mol. Oncol.* **2012**, *6*, 111-127.

9. Horne, S. D.; Stevens, J. B.; Abdallah, B. Y.; Liu, G.; Bremer, S. W.; Ye, C. J.; Heng, H. H. Q., Why imatinib remains an exception of cancer research. *J. Cell. Physiol.* **2013**, *228*, 665-670.

10. Visvader, Jane E.; Lindeman, Geoffrey J., Cancer Stem Cells: Current Status and Evolving Complexities. *Cell Stem Cell* **2012**, *10*, 717-728.

11. DeVita, V. T.; Chu, E., A History of Cancer Chemotherapy. *Cancer Res.* **2008**, *68*, 8643-8653.

12. Colvin, O. M., An overview of cyclophosphamide development and clinical applications. *Curr. Pharm. Des.* **1999**, *5*, 555-560.

13. Heidelberger, C.; Chaudhuri, N. K.; Danneberg, P.; Mooren, D.; Griesbach, L.; Duschinsky, R.; Schnitzer, R. J.; Pleven, E.; Scheiner, J., Fluorinated Pyrimidines, A New Class of Tumour-Inhibitory Compounds. *Nature* **1957**, *179*, 663-666.

14. Jolivet, J.; Cowan, K. H.; Curt, G. A.; Clendeninn, N. J.; Chabner, B. A., The Pharmacology and Clinical Use of Methotrexate. *New Engl. J. Med.* **1983**, *309*, 1094-1104.

15. Huennekens, F. M., The methotrexate story: A paradigm for development of cancer chemotherapeutic agents. *Adv. Enzyme Regul.* **1994**, *34*, 397-419.

16. Wright, D. E. Pyrazole derivatives. US3102890, **1963**.

17. Rosenberg, B.; Van Camp, L.; Krigas, T., Inhibition of Cell Division in Escherichia coli by Electrolysis Products from a Platinum Electrode. *Nature* **1965**, *205*, 698-699.

18. Chabner, B. A.; Roberts, T. G., Chemotherapy and the war on cancer. *Nat. Rev. Cancer* **2005**, *5*, 65-72.

19. Himes, R. H.; Kersey, R. N.; Heller-Bettinger, I.; Samson, F. E., Action of the Vinca Alkaloids Vincristine, Vinblastine, and Desacetyl Vinblastine Amide on Microtubules in Vitro. *Cancer Res.* **1976**, *36*, 3798-3802.

20. Wagstaff, A.; Ward, A.; Benfield, P.; Heel, R., Carboplatin. *Drugs* **1989**, *37*, 162-190.

21. Chari, R. V. J., Targeted Cancer Therapy: Conferring Specificity to Cytotoxic Drugs. *Acc. Chem. Res.* **2007**, *41*, 98-107.

22. Marks, A. M.; Packer, R. J., A Review of Secondary Central Nervous System Tumors After Treatment of a Primary Pediatric Malignancy. *Seminars in Pediatric Neurology* **2012**, *19*, 43-48.

23. Masui, K.; Gini, B.; Wykosky, J.; Zanca, C.; Mischel, P. S.; Furnari, F.; Cavenee, W., A Tale of Two Approaches: Complementary Mechanisms of Cytotoxic and Targeted Therapy Resistance May Inform Next Generation Cancer Treatments. *Carcinogenesis* **2013**.

24. Jordan, V. C., Tamoxifen: a most unlikely pioneering medicine. *Nat. Rev. Drug Discov.* **2003**, *2*, 205-213.

25. Barrett-Connor, E., Raloxifene: Risks and Benefits. *Ann. N. Y. Acad. Sci.* **2001**, *949*, 295-303.

26. Cui, Q.; Ma, Y.; Jaramillo, M.; Bari, H.; Awan, A.; Yang, S.; Zhang, S.; Liu, L.; Lu, M.; O'Connor-McCourt, M.; Purisima, E. O.; Wang, E., A map of human cancer signaling. *Mol. Syst. Biol.* **2007**, *3*.

27. Brognard, J.; Hunter, T., Protein kinase signaling networks in cancer. *Curr. Opin. Genet. Dev.* **2011**, *21*, 4-11.

28. Guardavaccaro, D.; Clevers, H., Wnt/β-Catenin and MAPK Signaling: Allies and Enemies in Different Battlefields. *Sci. Signal.* **2012**, *5*, pe15-.

29. Natarajan, M.; Lin, K.-M.; Hsueh, R. C.; Sternweis, P. C.; Ranganathan, R., A global analysis of cross-talk in a mammalian cellular signalling network. *Nat. Cell. Biol.* **2006**, *8*, 571-580.

30. Moser, C.; Lang, S. A.; Stoeltzing, O., Heat-shock Protein 90 (Hsp90) as a Molecular Target for Therapy of Gastrointestinal Cancer. *Anticancer Res.* **2009**, *29*, 2031-2042.

31. Wakeling, A. E., Epidermal growth factor receptor tyrosine kinase inhibitors. *Curr. Opin. Pharmacol.* **2002**, *2*, 382-387.

32. Force, T.; Krause, D. S.; Van Etten, R. A., Molecular mechanisms of cardiotoxicity of tyrosine kinase inhibition. *Nat. Rev. Cancer* **2007**, *7*, 332-344.

33. Garber, K., Drugging the Wnt Pathway: Problems And Progress. *J. Natl. Cancer Inst.* **2009**, *101*, 548-550.

34. Villanueva, J.; Vultur, A.; Lee, J. T.; Somasundaram, R.; Fukunaga-Kalabis, M.; Cipolla, A. K.; Wubbenhorst, B.; Xu, X.; Gimotty, P. A.; Kee, D.; Santiago-Walker, A. E.; Letrero, R.; D'Andrea, K.; Pushparajan, A.; Hayden, J. E.; Brown, K. D.; Laquerre, S.; McArthur, G. A.; Sosman, J. A.; Nathanson, K. L.; Herlyn, M., Acquired Resistance to BRAF Inhibitors Mediated by a RAF Kinase Switch in Melanoma Can Be Overcome by Cotargeting MEK and IGF-1R/PI3K. *Cancer Cell* **2010**, *18*, 683-695.

35. Kim, E. K.; Choi, E.-J., Pathological roles of MAPK signaling pathways in human diseases. *Biochim. Biophys. Acta* **2010**, *1802*, 396-405.

36. Nithianandarajah-Jones, G. N.; Wilm, B.; Goldring, C. E. P.; Müller, J.; Cross, M. J., ERK5: Structure, regulation and function. *Cell. Signal.* **2012**, *24*, 2187-2196.

37. Cargnello, M.; Roux, P. P., Activation and Function of the MAPKs and Their Substrates, the MAPK-Activated Protein Kinases. *Microbiol. Mol. Biol. Rev.* **2011**, *75*, 50-83.

38. Aronov, A. M.; Tang, Q.; Martinez-Botella, G.; Bemis, G. W.; Cao, J.; Chen, G.; Ewing, N. P.; Ford, P. J.; Germann, U. A.; Green, J.; Hale, M. R.; Jacobs, M.; Janetka, J. W.; Maltais, F.; Markland, W.; Namchuk, M. N.; Nanthakumar, S.; Poondru, S.; Straub, J.; ter Haar, E.; Xie, X., Structure-Guided Design of Potent

and Selective Pyrimidylpyrrole Inhibitors of Extracellular Signal-Regulated Kinase (ERK) Using Conformational Control. *J. Med. Chem.* **2009**, *52*, 6362-6368.

39.   Pratilas, C. A.; Solit, D. B., Targeting the Mitogen-Activated Protein Kinase Pathway: Physiological Feedback and Drug Response. *Clin. Cancer. Res.* **2010**, *16*, 3329-3334.

40.   Huang, P.; Han, J.; Hui, L., MAPK signaling in inflammation-associated cancer development. *Protein Cell* **2010**, *1*, 218-226.

41.   De Luca, A.; Maiello, M. R.; D'Alessio, A.; Pergameno, M.; Normanno, N., The RAS/RAF/MEK/ERK and the PI3K/AKT signalling pathways: role in cancer pathogenesis and implications for therapeutic approaches. *Expert Opin. Ther. Targets* **2012**, *16*, S17-S27.

42.   Wan, P. T. C.; Garnett, M. J.; Roe, S. M.; Lee, S.; Niculescu-Duvaz, D.; Good, V. M.; Project, C. G.; Jones, C. M.; Marshall, C. J.; Springer, C. J.; Barford, D.; Marais, R., Mechanism of Activation of the RAF-ERK Signaling Pathway by Oncogenic Mutations of B-RAF. *Cell* **2004**, *116*, 855-867.

43.   Kudchadkar, R. R.; Smalley, K. S. M.; Glass, L. F.; Trimble, J. S.; Sondak, V. K., Targeted therapy in melanoma. *Clinics in Dermatology* **2013**, *31*, 200-208.

44.   Wilhelm, S. M.; Adnane, L.; Newell, P.; Villanueva, A.; Llovet, J. M.; Lynch, M., Preclinical overview of sorafenib, a multikinase inhibitor that targets both Raf and VEGF and PDGF receptor tyrosine kinase signaling. *Mol. Cancer Ther.* **2008**, *7*, 3129-3140.

45.   Brown, A.; Carlson, T. G.; Loi, C.-M.; Graziano, M., Pharmacodynamic and toxicokinetic evaluation of the novel MEK inhibitor, PD0325901, in the rat following oral and intravenous administration. *Cancer Chemother. Pharmacol.* **2007**, *59*, 671-679.

46.   Boasberg, P.; Redfern, C.; Daniels, G.; Bodkin, D.; Garrett, C.; Ricart, A., Pilot study of PD-0325901 in previously treated patients with advanced melanoma, breast cancer, and colon cancer. *Cancer Chemother. Pharmacol.* **2011**, *68*, 547-552.

47.   Patel, S. P.; Kim, K. B., Selumetinib (AZD6244; ARRY-142886) in the treatment of metastatic melanoma. *Expert Opin. Invest. Drugs* **2012**, *21*, 531-539.

48.   Roskoski Jr, R., ERK1/2 MAP kinases: Structure, function, and regulation. *Pharm. Res.* **2012**, *66*, 105-143.

49. Ohori, M.; Kinoshita, T.; Yoshimura, S.; Warizaya, M.; Nakajima, H.; Miyake, H., Role of a cysteine residue in the active site of ERK and the MAPKK family. *Biochem. Biophys. Res. Commun.* **2007**, *353*, 633-637.

50. Sawyers, C., Targeted cancer therapy. *Nature* **2004**, *432*, 294-297.

51. Galmarini, D.; Galmarini, C. M.; Galmarini, F. C., Cancer chemotherapy: A critical analysis of its 60 years of history. *Crit. Rev. Oncol./Hematol.* **2012**, *84*, 181-199.

52. O'Hare, T.; Deininger, M. W. N.; Eide, C. A.; Clackson, T.; Druker, B. J., Targeting the BCR-ABL Signaling Pathway in Therapy-Resistant Philadelphia Chromosome-Positive Leukemia. *Clin. Cancer. Res.* **2011**, *17*, 212-221.

53. Capdeville, R.; Buchdunger, E.; Zimmermann, J.; Matter, A., Glivec (STI571, imatinib), a rationally developed, targeted anticancer drug. *Nat. Rev. Drug Discov.* **2002**, *1*, 493-502.

54. Dagher, R.; Cohen, M.; Williams, G.; Rothmann, M.; Gobburu, J.; Robbie, G.; Rahman, A.; Chen, G.; Staten, A.; Griebel, D.; Pazdur, R., Approval Summary: Imatinib Mesylate in the Treatment of Metastatic and/or Unresectable Malignant Gastrointestinal Stromal Tumors. *Clin. Cancer. Res.* **2002**, *8*, 3034-3038.

55. Price, K. E.; Saleem, N.; Lee, G.; Steinberg, M., Potential of ponatinib to treat chronic myeloid leukemia and acute lymphoblastic leukemia. *OncoTargets and Therapy* **2013**, *6*, 1111-1118.

56. Maemondo, M.; Inoue, A.; Kobayashi, K.; Sugawara, S.; Oizumi, S.; Isobe, H.; Gemma, A.; Harada, M.; Yoshizawa, H.; Kinoshita, I.; Fujita, Y.; Okinaga, S.; Hirano, H.; Yoshimori, K.; Harada, T.; Ogura, T.; Ando, M.; Miyazawa, H.; Tanaka, T.; Saijo, Y.; Hagiwara, K.; Morita, S.; Nukiwa, T., Gefitinib or Chemotherapy for Non–Small-Cell Lung Cancer with Mutated EGFR. *New Engl. J. Med.* **2010**, *362*, 2380-2388.

57. Shepard, H. M.; Jin, P.; Slamon, D. J.; Pirot, Z.; Maneval, D. C., Herceptin. In *Therapeutic Antibodies*, Chernajovsky, Y.; Nissim, A., Eds. Springer Berlin Heidelberg2008; Vol. 181, pp 183-219.

58. Adams, J.; Kauffman, M., Development of the Proteasome Inhibitor Velcade™ (Bortezomib). *Cancer Invest.* **2004**, *22*, 304-311.

59. Tsukamoto, S.; Yokosawa, H., Targeting the proteasome pathway. *Expert Opin. Ther. Targets* **2009**, *13*, 605-621.

60. Jung, F. H.; Ple, P. Quinoline Derivatives. WO2007099326, **2007**.

61.   Federico, M.; Bagella, L., Histone Deacetylase Inhibitors in the Treatment of Hematological Malignancies and Solid Tumors. *J. Biomed. Biotechnol.* **2011**, *2011*.

62.   Ho, C., New Drugs Approved by US FDA in 2006. *Trends In Bio/Pharmaceutical Industry* **2007**, 13.

63.   Kaminskas, E.; Farrell, A. T.; Wang, Y.-C.; Sridhara, R.; Pazdur, R., FDA Drug Approval Summary: Azacitidine (5-azacytidine, Vidaza™) for Injectable Suspension. *The Oncologist* **2005**, *10*, 176-182.

64.   Blum, W.; Klisovic, R. B.; Hackanson, B.; Liu, Z.; Liu, S.; Devine, H.; Vukosavljevic, T.; Huynh, L.; Lozanski, G.; Kefauver, C.; Plass, C.; Devine, S. M.; Heerema, N. A.; Murgo, A.; Chan, K. K.; Grever, M. R.; Byrd, J. C.; Marcucci, G., Phase I Study of Decitabine Alone or in Combination With Valproic Acid in Acute Myeloid Leukemia. *J. Clin. Oncology* **2007**, *25*, 3884-3891.

65.   Fenaux, P.; Mufti, G. J.; Hellstrom-Lindberg, E.; Santini, V.; Finelli, C.; Giagounidis, A.; Schoch, R.; Gattermann, N.; Sanz, G.; List, A.; Gore, S. D.; Seymour, J. F.; Bennett, J. M.; Byrd, J.; Backstrom, J.; Zimmerman, L.; McKenzie, D.; Beach, C. L.; Silverman, L. R., Efficacy of azacitidine compared with that of conventional care regimens in the treatment of higher-risk myelodysplastic syndromes: a randomised, open-label, phase III study. *Lancet Oncol.* **2009**, *10*, 223-232.

66.   Poulikakos, P. I.; Persaud, Y.; Janakiraman, M.; Kong, X.; Ng, C.; Moriceau, G.; Shi, H.; Atefi, M.; Titz, B.; Gabay, M. T.; Salton, M.; Dahlman, K. B.; Tadi, M.; Wargo, J. A.; Flaherty, K. T.; Kelley, M. C.; Misteli, T.; Chapman, P. B.; Sosman, J. A.; Graeber, T. G.; Ribas, A.; Lo, R. S.; Rosen, N.; Solit, D. B., RAF inhibitor resistance is mediated by dimerization of aberrantly spliced BRAF(V600E). *Nature* **2011**, *480*, 387-390.

67.   Basanta, D.; Gatenby, R.; Anderson, A., Exploiting evolution to treat drug resistance: Combination therapy and the double bind. In *Nature precedings*2011.

68.   Hamburg, M. A.; Collins, F. S., The Path to Personalized Medicine. *New Engl. J. Med.* **2010**, *363*, 301-304.

69.   Marsh, S.; McLeod, H. L., Pharmacogenomics: from bedside to clinical practice. *Hum. Mol. Genet.* **2006**, *15*, R89-R93.

70.   Ong, F. S.; Das, K.; Wang, J.; Vakil, H.; Kuo, J. Z.; Blackwell, W.-L. B.; Lim, S. W.; Goodarzi, M. O.; Bernstein, K. E.; Rotter, J. I.; Grody, W. W., Personalized

medicine and pharmacogenetic biomarkers: progress in molecular oncology testing. *Expert Rev. Mol. Diagn.* **2012**, *12*, 593-602.

71.   Manallack, D. T.; Prankerd, R. J.; Yuriev, E.; Oprea, T. I.; Chalmers, D. K., The significance of acid/base properties in drug discovery. *Chem. Soc. Rev.* **2013**, *42*, 485-496.

72.   Whittaker, P. A., The role of bioinformatics in target validation. *Drug Discov. Today: Technologies* **2004**, *1*, 125-133.

73.   Hann, M. M., Molecular obesity, potency and other addictions in drug discovery. *MedChemComm* **2011**, *2*, 349-355.

74.   Fotouhi, N.; Gillespie, P.; Goodnow, J. R., Lead generation: reality check on commonly held views. *Expert Opin. Drug Discovery* **2008**, *3*, 733-744.

75.   Orita, M.; Ohno, K.; Warizaya, M.; Amano, Y.; Niimi, T., Chapter fifteen - Lead Generation and Examples: Opinion Regarding How to Follow Up Hits. In *Methods Enzymol.*, Lawrence, C. K., Ed. Academic Press2011; Vol. Volume 493, pp 383-419.

76.   Frye, S. V., The art of the chemical probe. *Nat. Chem. Biol.* **2010**, *6*, 159-161.

77.   Bleicher, K. H.; Bohm, H.-J.; Muller, K.; Alanine, A. I., Hit and lead generation: beyond high-throughput screening. *Nat. Rev. Drug Discov.* **2003**, *2*, 369-378.

78.   Blagg, J.; Abraham, D. J., Structural Alerts for Toxicity. In *Burger's Medicinal Chemistry and Drug Discovery*, John Wiley & Sons, Inc.2003.

79.   Korfmacher, W. A., Advances in the integration of drug metabolism into the lead optimization paradigm. *Mini-Rev. Med. Chem.* **2009**, *9*, 703-716.

80.   Bray, F.; Jemal, A.; Grey, N.; Ferlay, J.; Forman, D., Global cancer transitions according to the Human Development Index (2008–2030): a population-based study. *Lancet Oncol.* **2012**, *13*, 790-801.

81.   Lai, J.-P.; Thompson, J. R.; Sandhu, D. S.; Roberts, L. R., Heparin Degrading Sulfatases in Hepatocellular Cancer: roles in pathogenesis and therapy targets. *Future Oncol.* **2008**, *4*, 803-814.

82.   Hanson, S. R.; Best, M. D.; Wong, C.-H., Sulfatases: Structure, Mechanism, Biological Activity, Inhibition, and Synthetic Utility. *Angew. Chem., Int. Ed.* **2004**, *43*, 5736-5763.

83.   Diez-Roux, G.; Ballabio, A., Sulfatases and human disease. *Ann. Rev. Genomics Hum. Genet.* **2005**, *6*, 355-379.

84. Morimoto-Tomita, M.; Uchimura, K.; Werb, Z.; Hemmerich, S.; Rosen, S. D., Cloning and Characterization of Two Extracellular Heparin-degrading Endosulfatases in Mice and Humans. *J. Biol. Chem.* **2002**, *277*, 49175-49185.

85. Hur, K.; Han, T.-S.; Jung, E.-J.; Yu, J.; Lee, H.-J.; Kim, W. H.; Goel, A.; Yang, H.-K., Up-regulated expression of sulfatases (SULF1 and SULF2) as prognostic and metastasis predictive markers in human gastric cancer. *J. Pathol.* **2012**, *228*, 88-98.

86. Iozzo, R. V., Heparan sulfate proteoglycans: intricate molecules with intriguing functions. *J. Clin. Invest.* **2001**, *108*, 165-167.

87. Varki, A.; Cummings, R.; Esko, J.; Freeze, H.; Hart, G.; Marth, J., *Essentials of Glycobiology.* Cold Spring Harbor Laboratory Press 1999.

88. Saad, O. M.; Ebel, H.; Uchimura, K.; Rosen, S. D.; Bertozzi, C. R.; Leary, J. A., Compositional profiling of heparin/heparan sulfate using mass spectrometry: assay for specificity of a novel extracellular human endosulfatase. *Glycobiology* **2005**, *15*, 818-826.

89. Lindahl, U.; Kusche-Gullberg, M.; Kjellén, L., Regulated Diversity of Heparan Sulfate. *J. Biol. Chem.* **1998**, *273*, 24979-24982.

90. Rosen, S. D.; Lemjabbar-Alaoui, H., Sulf-2: an extracellular modulator of cell signaling and a cancer target candidate. *Expert Opin. Ther. Targets* **2010**, *14*, 935-949.

91. Lamanna, W. C.; Frese, M.-A.; Balleininger, M.; Dierks, T., Sulf Loss Influences *N*-, 2-*O*-, and 6-*O*-Sulfation of Multiple Heparan Sulfate Proteoglycans and Modulates Fibroblast Growth Factor Signaling. *J. Biol. Chem.* **2008**, *283*, 27724-27735.

92. Grigoriadis, A.; Mackay, A.; Reis-Filho, J.; Steele, D.; Iseli, C.; Stevenson, B.; Jongeneel, C. V.; Valgeirsson, H.; Fenwick, K.; Iravani, M.; Leao, M.; Simpson, A.; Strausberg, R.; Jat, P.; Ashworth, A.; Neville, A. M.; O'Hare, M., Establishment of the epithelial-specific transcriptome of normal and malignant human breast cells based on MPSS and array expression data. *Breast Cancer Res.* **2006**, *8*, R56.

93. Morimoto-Tomita, M.; Uchimura, K.; Bistrup, A.; Lum, D. H.; Egeblad, M.; Boudreau, N.; Werb, Z.; Rosen, S. D., Sulf-2, a Proangiogenic Heparan Sulfate Endosulfatase, Is Upregulated in Breast Cancer. *Neoplasia* **2005**, *7*, 1001-1010.

94. Lee, J.; Chu, I. S.; Heo, J.; Calvisi, D. F.; Sun, Z.; Roskams, T.; Durnez, A.; Demetris, A. J.; Thorgeirsson, S. S., Classification and prediction of survival in

hepatocellular carcinoma by gene expression profiling. *Hepatology* **2004**, *40*, 667-676.

95.   Lemjabbar-Alaoui, H.; van Zante, A.; Singer, M. S.; Xue, Q.; Wang, Y.-Q.; Tsay, D.; He, B.; Jablons, D. M.; Rosen, S. D., Sulf-2, a heparan sulfate endosulfatase, promotes human lung carcinogenesis. *Oncogene* **2010**, *29*, 635-646.

96.   Phillips, J. J.; Huillard, E.; Robinson, A. E.; Ward, A.; Lum, D. H.; Polley, M.-Y.; Rosen, S. D.; Rowitch, D. H.; Werb, Z., Heparan sulfate sulfatase SULF2 regulates PDGFRα signaling and growth in human and mouse malignant glioma. *J. Clin. Invest.* **2012**, *122*, 911-922.

97.   Lui, N. S.; van Zante, A.; Rosen, S. D.; Jablons, D. M.; Lemjabbar-Alaoui, H., SULF2 expression by immunohistochemistry and overall survival in oesophageal cancer: a cohort study. *BMJ Open* **2012**, *2*.

98.   Nawroth, R.; van Zante, A.; Cervantes, S.; McManus, M.; Hebrok, M.; Rosen, S. D., Extracellular sulfatases, elements of the Wnt signaling pathway, positively regulate growth and tumorigenicity of human pancreatic cancer cells. *PLoS One* **2007**, *2*, e392.

99.   Dai, Y.; Yang, Y.; MacLeod, V.; Yue, X.; Rapraeger, A. C.; Shriver, Z.; Venkataraman, G.; Sasisekharan, R.; Sanderson, R. D., HSulf-1 and HSulf-2 are potent inhibitors of myeloma tumor growth in vivo. *J. Biol. Chem.* **2005**, *280*, 40066-40073.

100.   Lai, J.; Chien, J.; Staub, J.; Avula, R.; Greene, E. L.; Matthews, T. A.; Smith, D. I.; Kaufmann, S. H.; Roberts, L. R.; Shridhar, V., Loss of HSulf-1 Up-regulates Heparin-binding Growth Factor Signaling in Cancer. *J. Biol. Chem.* **2003**, *278*, 23107-23117.

101.   Gill, R. B. S.; Day, A.; Barstow, A.; Liu, H.; Zaman, G.; Dhoot, G. K., Sulf2 gene is alternatively spliced in mammalian developing and tumour tissues with functional implications. *Biochem. Biophys. Res. Commun.* **2011**, *414*, 468-473.

102.   Mohammadi, M.; Olsen, S. K.; Ibrahimi, O. A., Structural basis for fibroblast growth factor receptor activation. *Cytokine Growth Factor Rev.* **2005**, *16*, 107-137.

103.   Turner, N.; Grose, R., Fibroblast growth factor signalling: from development to cancer. *Nat. Rev. Cancer* **2010**, *10*, 116-129.

104.   Nu Nguyen, T. K.; Raman, K.; Tran, V. M.; Kuberan, B., Investigating the mechanism of the assembly of FGF1-binding heparan sulfate motifs. *FEBS Lett.* **2011**, *585*, 2698-2702.

105. Staples, G. O.; Shi, X.; Zaia, J., Glycomics Analysis of Mammalian Heparan Sulfates Modified by the Human Extracellular Sulfatase HSulf2. *PLoS One* **2011**, *6*, e16689.

106. Eisenmann, D. M., Wnt signaling: The C. elegans Research Community, WormBook, doi/10.1895/wormbook.1.7.1, http://www.wormbook.org.; Greenwald, I., Ed.2005.

107. Moon, R. T.; Kohn, A. D.; Ferrari, G. V. D.; Kaykas, A., WNT and β-catenin signalling: diseases and therapies. *Nat. Rev. Genet.* **2004**, *5*, 691-701.

108. Klaus, A.; Birchmeier, W., Wnt signalling and its impact on development and cancer. *Nat. Rev. Cancer* **2008**, *8*, 387-398.

109. Yao, H.; Ashihara, E.; Maekawa, T., Targeting the Wnt/β-catenin signaling pathway in human cancers. *Expert Opin. Ther. Targets* **2011**, *15*, 873-887.

110. Nishisho, I.; Nakamura, Y.; Miyoshi, Y.; Miki, Y.; Ando, H.; Horii, A.; Koyama, K.; Utsunomiya, J.; Baba, S.; Hedge, P., Mutations of chromosome 5q21 genes in FAP and colorectal cancer patients. *Science* **1991**, *253*, 665-669.

111. Wei, W.; Chua, M.-S.; Grepper, S.; So, S., Blockade of Wnt-1 signaling leads to anti-tumor effects in hepatocellular carcinoma cells. *Mol. Cancer* **2009**, *8*, 76.

112. Mikami, I.; You, L.; He, B.; Xu, Z.; Batra, S.; Lee, A.; Mazieres, J.; Reguart, N.; Uematsu, K.; Koizumi, K.; Jablons, D., Efficacy of Wnt-1 monoclonal antibody in sarcoma cells. *BMC Cancer* **2005**, *5*, 53.

113. Kar, S.; Deb, M.; Sengupta, D.; Shilpi, A.; Bhutia, S. K.; Patra, S. K., Intricacies of hedgehog signaling pathways: A perspective in tumorigenesis. *Exp. Cell Res.* **2012**, *318*, 1959-1972.

114. Zhang, F.; McLellan, J. S.; Ayala, A. M.; Leahy, D. J.; Linhardt, R. J., Kinetic and Structural Studies on Interactions between Heparin or Heparan Sulfate and Proteins of the Hedgehog Signaling Pathway. *Biochemistry* **2007**, *46*, 3933-3941.

115. Cirrone, F.; Harris, C. S., Vismodegib and the Hedgehog Pathway: A New Treatment for Basal Cell Carcinoma. *Clin. Ther.* **2012**, *34*, 2039-2050.

116. Ji, W.; Yang, J.; Wang, D.; Cao, L.; Tan, W.; Qian, H.; Sun, B.; Qian, Q.; Yin, Z.; Wu, M.; Su, C., hSulf-1 Gene Exhibits Anticancer Efficacy through Negatively Regulating VEGFR-2 Signaling in Human Cancers. *PLoS One.* **2011**, *6*, e23274.

117. Yang, J. D.; Sun, Z.; Hu, C.; Lai, J.; Dove, R.; Nakamura, I.; Lee, J.-S.; Thorgeirsson, S. S.; Kang, K. J.; Chu, I.-S.; Roberts, L. R., Sulfatase 1 and

sulfatase 2 in hepatocellular carcinoma: Associated signaling pathways, tumor phenotypes, and survival. *Genes, Chromosomes Cancer* **2011**, *50*, 122-135.

118. Forner, A.; Llovet, J. M.; Bruix, J., Hepatocellular carcinoma. *Lancet*.

119. Taura, K.; Ikai, I.; Hatano, E.; Yasuchika, K.; Nakajima, A.; Tada, M.; Seo, S.; Machimoto, T.; Uemoto, S., Influence of coexisting cirrhosis on outcomes after partial hepatic resection for hepatocellular carcinoma fulfilling the Milan criteria: an analysis of 293 patients. *Surgery* **2007**, *142*, 685-694.

120. Avila, M. A.; Berasain, C.; Sangro, B.; Prieto, J., New Therapies for Hepatocellular Carcinoma. *Oncogene* **2006**, *25*, 3866-3884.

121. Lang, L., FDA approves sorafenib for patients with inoperable liver cancer. *Gastroenterology* **2008**, *134*, 379.

122. Llovet, J.; Ricci, S.; Mazzaferro, V.; Hilgard, P.; Gane, E.; Blanc, J. F.; de Oliveira, A. C.; Santoro, A.; Raoul, J. L.; Forner, A.; Schwartz, M.; Porta, C.; Zeuzem, S.; Bolondi, L.; Greten, T. F.; Galle, P. R.; Seitz, J. F.; Borbath, I.; Häussinger, D.; Giannaris, T.; Shan, M.; Moscovici, M.; Voliotis, D.; Bruix, J., Sorafenib in advanced hepatocellular carcinoma. *N. Engl. J. Med.* **2008**, *359*, 378-390.

123. Frese, M.-A.; Milz, F.; Dick, M.; Lamanna, W. C.; Dierks, T., Characterization of the Human Sulfatase Sulf1 and Its High Affinity Heparin/Heparan Sulfate Interaction Domain. *J. Biol. Chem.* **2009**, *284*, 28033-28044.

124. Ghosh, D., Human sulfatases: A structural perspective to catalysis. *Cell. Mol. Life Sci* **2007**, *64*, 2013-2022.

125. Uhlhorn-Dierks, G.; Kolter, T.; Sandhoff, K., How Does Nature Cleave Sulfuric Acid Esters? A Novel Posttranslational Modification of Sulfatases. *Angew. Chem., Int. Ed.* **1998**, *37*, 2453-2455.

126. Boltes, I.; Czapinska, H.; Kahnert, A.; von Bülow, R.; Dierks, T.; Schmidt, B.; von Figura, K.; Kertesz, M. A.; Usón, I., 1.3 Å Structure of Arylsulfatase from Pseudomonas aeruginosa Establishes the Catalytic Mechanism of Sulfate Ester Cleavage in the Sulfatase Family. *Structure* **2001**, *9*, 483-491.

127. Buono, M.; P, C. M., Sulfatase activities towards the regulation of cell metabolism and signaling in mammals. *Cell. Mol. Life Sci.* **2010**, *67*, 769-780.

128. Sardiello, M.; Annunziata, I.; Roma, G.; Ballabio, A., Sulfatases and sulfatase modifying factors: an exclusive and promiscuous relationship. *Hum. Mol. Genet.* **2005**, *14*, 3203-3217.

129. Ghosh, D., Three-dimensional structures of sulfatases. *Methods Enzymol.* **2005**, *400*, 273-293.

130. Ai, X.; Do, A.-T.; Kusche-Gullberg, M.; Lindahl, U.; Lu, K.; Emerson, C. P., Substrate Specificity and Domain Functions of Extracellular Heparan Sulfate 6-*O*-Endosulfatases, QSulf1 and QSulf2. *J. Biol. Chem.* **2006**, *281*, 4969-4976.

131. Myette, J. R.; Soundararajan, V.; Shriver, Z.; Raman, R.; Sasisekharan, R., Heparin/Heparan Sulfate 6-*O*-Sulfatase from Flavobacterium heparinum. *J. Biol. Chem.* **2009**, *284*, 35177-35188.

132. Schelwies, M.; Brinson, D.; Otsuki, S.; Hong, Y.-H.; Lotz, M. K.; Wong, C.-H.; Hanson, S. R., Glucosamine-6-sulfamate Analogues of Heparan Sulfate as Inhibitors of Endosulfatases. *ChemBioChem* **2010**, *11*, 2393-2397.

133. Zheng, X.; Gai, X.; Han, S.; Moser, C. D.; Hu, C.; Shire, A. M.; Floyd, R. A.; Roberts, L. R., The human sulfatase 2 inhibitor 2,4-disulfonylphenyl-tert-butylnitrone (OKN-007) has an antitumor effect in hepatocellular carcinoma mediated via suppression of TGFB1/SMAD2 and Hedgehog/GLI1 signaling. *Genes Chromosomes Cancer* **2012**, 225-236.

134. Floyd, R. A.; Kopke, R. D.; Choi, C.-H.; Foster, S. B.; Doblas, S.; Towner, R. A., Nitrones as therapeutics. *Free Radical Biol. Med.* **2008**, *45*, 1361-1374.

135. Howarth, N. M.; Purohit, A.; Reed, M. J.; Potter, B. V. L., Estrone sulfamates: potent inhibitors of estrone sulfatase with therapeutic potential. *J. Med. Chem.* **1994**, *37*, 219-221.

136. Woo, L. W. L.; Purohit, A.; Reed, M. J.; Potter, B. V. L., Oestrone 3-*O*-(*N*-acetyl)sulphamate, a potential molecular probe of the active site of oestrone sulphatase. *Bioorg. Med. Chem. Lett.* **1997**, *7*, 3075-3080.

137. Howarth, N. M.; Purohit, A.; Reed, M. J.; Potter, B. V. L., Estrone sulfonates as inhibitors of estrone sulfatase. *Steroids* **1997**, *62*, 346-350.

138. Poirier, D.; Ciobanu, L. C.; Maltais, R., Steroid sulfatase inhibitors. *Expert Opin. Ther. Pat.* **1999**, *9*, 1083-1099.

139. Woo, L. W. L.; Lightowler, M.; Purohit, A.; Reed, M. J.; Potter, B. V. L., Heteroatom-substituted analogues of the active-site directed inhibitor estra-1,3,5(10)-trien-17-one-3-sulphamate inhibit estrone sulphatase by a different mechanism. *J. Steroid Biochem. Mol. Biol.* **1996**, *57*, 79-88.

140. Schreiner, E. P.; Billich, A., Estrone formate: a novel type of irreversible inhibitor of human steroid sulfatase. *Bioorg. Med. Chem. Lett.* **2004**, *14*, 4999-5002.

141.   Reed, J. E.; Lawrence Woo, L. W.; Robinson, J. J.; Leblond, B.; Leese, M. P.; Purohit, A.; Reed, M. J.; Potter, B. V. L., 2-Difluoromethyloestrone 3-*O*-sulphamate, a highly potent steroid sulphatase inhibitor. *Biochem. Biophys. Res. Comm.* **2004**, *317*, 169-175.

142.   Woo, L. W. L.; Purohit, A.; Malini, B.; Reed, M. J.; Potter, B. V. L., Potent active site-directed inhibition of steroid sulphatase by tricyclic coumarin-based sulphamates. *Chem. Biol.* **2000**, *7*, 773-791.

143.   Stanway, S. J.; Purohit, A.; Woo, L. W. L.; Sufi, S.; Vigushin, D.; Ward, R.; Wilson, R. H.; Stanczyk, F. Z.; Dobbs, N.; Kulinskaya, E.; Elliott, M.; Potter, B. V. L.; Reed, M. J.; Coombes, R. C., Phase I Study of STX 64 (667 Coumate) in Breast Cancer Patients: The First Study of a Steroid Sulfatase Inhibitor. *Clin. Cancer Res.* **2006**, *12*, 1585-1592.

144.   Huang, Z.; Fasco, M. J.; Kaminsky, L. S., Inhibition of estrone sulfatase in human liver microsomes by quercetin and other flavonoids. *J. Steroid Biochem. Mol. Biol.* **1997**, *63*, 9-15.

145.   Nussbaumer, P.; Geyl, D.; Horvath, A.; Lehr, P.; Wolff, B.; Billich, A., Nortropinyl-Arylsulfonylureas as novel, reversible inhibitors of human steroid sulfatase. *Bioorg. Med. Chem. Lett.* **2003**, *13*, 3673-3677.

146.   Lopez, M.; Trajkovic, J.; Bornaghi, L. F.; Innocenti, A.; Vullo, D.; Supuran, C. T.; Poulsen, S.-A., Design, Synthesis, and Biological Evaluation of Novel Carbohydrate-Based Sulfamates as Carbonic Anhydrase Inhibitors. *J. Med. Chem.* **2011**, *54*, 1481-1489.

147.   Maryanoff, B. E.; Nortey, S. O.; Gardocki, J. F.; Shank, R. P.; Dodgson, S. P., Anticonvulsant *O*-Alkyl Sulfamates *J. Med. Chem.* **1987**, *30*, 880-887.

148.   Maryanoff, B. E.; Costanzo, M. J.; Nortey, S. O.; Greco, M. N.; Shank, R. P.; Schupsky, J. J.; Ortegon, M. P.; Vaught, J. L., Structure−Activity Studies on Anticonvulsant Sugar Sulfamates Related to Topiramate. Enhanced Potency with Cyclic Sulfate Derivatives. *J. Med. Chem.* **1998**, *41*, 1315-1343.

149.   Hossain, M. M.; Hosono-Fukao, T.; Tang, R.; Sugaya, N.; van Kuppevelt, T. H.; Jenniskens, G. J.; Kimata, K.; Rosen, S. D.; Uchimura, K., Direct detection of HSulf-1 and HSulf-2 activities on extracellular heparan sulfate and their inhibition by PI-88. *Glycobiology* **2010**, *20*, 175-186.

150.   Kaur, I. P.; Smitha, R.; Aggarwal, D.; Kapil, M., Acetazolamide: future perspective in topical glaucoma therapeutics. *Int. J. Pharm.* **2002**, *248*, 1-14.

151. Kossoff, Eric H.; Pyzik, Paula L.; Furth, Susan L.; Hladky, Heather D.; Freeman, John M.; Vining, Eileen P. G., Kidney Stones, Carbonic Anhydrase Inhibitors, and the Ketogenic Diet. *Epilepsia* **2002**, *43*, 1168-1171.

152. Hinderling, P. H., Red Blood Cells: A Neglected Compartment in Pharmacokinetics and Pharmacodynamics. *Pharmacol. Rev.* **1997**, *49*, 279-295.

153. Kodadek, T., Rethinking screening. *Nat. Chem. Biol.* **2010**, *6*, 162-165.

154. Lindsay, M. A., Target discovery. *Nat. Rev. Drug Discov.* **2003**, *2*, 831-838.

155. Prinz, F.; Schlange, T.; Asadullah, K., Believe it or not: how much can we rely on published data on potential drug targets? *Nat. Rev. Drug Discov.* **2011**, *10*, 712-712.

156. Hopkins, A. L.; Groom, C. R., The druggable genome. *Nat. Rev. Drug Discov.* **2002**, *1*, 727-730.

157. Bunnage, M. E.; Chekler, E. L. P.; Jones, L. H., Target validation using chemical probes. *Nat. Chem. Biol.* **2013**, *9*, 195-199.

158. Workman, P.; Collins, I., Probing the Probes: Fitness Factors For Small Molecule Tools. *Chem. Biol.* **2010**, *17*, 561-577.

159. Hanson, S. R.; Whalen, L. J.; Wong, C.-H., Synthesis and evaluation of general mechanism-based inhibitors of sulfatases based on (difluoro)methyl phenyl sulfate and cyclic phenyl sulfamate motifs. *Bioorg. Med. Chem.* **2006**, *14*, 8386-8395.

160. Rudd, T. R.; Yates, E. A.; Hricovini, M., Spectroscopic and Theoretical Approaches for the Determination of Heparin Saccharide Structure and the Study of Protein-Glycosaminoglycan Complexes in Solution. *Curr. Med. Chem.* **2009**, *16*, 4750-4766.

161. Mulloy, B.; Forster, M. J., Conformation and dynamics of heparin and heparan sulfate. *Glycobiology* **2000**, *10*, 1147-1156.

162. Mulloy, B.; Forster, M. J.; Jones, C.; Davies, D. B., N.m.r. and molecular-modelling studies of the solution conformation of heparin. *Biochem. J.* **1993**, *293*, 849-858.

163. Sears, P.; Wong, C.-H., Carbohydrate Mimetics: A New Strategy for Tackling the Problem of Carbohydrate-Mediated Biological Recognition. *Angew. Chem., Int. Ed.* **1999**, *38*, 2300-2324.

164. Quiocho, F. A.; Spurlino, J. C.; Rodseth, L. E., Extensive features of tight oligosaccharide binding revealed in high-resolution structures of the maltodextrin

transport/chemosensory receptor. *Structure (London, England : 1993)* **1997**, *5*, 997-1015.

165. Cardin, A.; Weintraub, H., Molecular modeling of protein-glycosaminoglycan interactions. *Arterioscler. Thromb. Vasc. Biol.* **1989**, *9*, 21-32.

166. Capila, I.; Linhardt, R. J., Heparin–Protein Interactions. *Angew. Chem., Int. Ed.* **2002**, *41*, 390-412.

167. Mulloy, B.; Linhardt, R. J., Order out of complexity - protein structures that interact with heparin. *Curr. Opin. Struct. Biol.* **2001**, *11*, 623-628.

168. Moon, A. F.; Edavettal, S. C.; Krahn, J. M.; Munoz, E. M.; Negishi, M.; Linhardt, R. J.; Liu, J.; Pedersen, L. C., Structural Analysis of the Sulfotransferase (3-*O*-Sulfotransferase Isoform 3) Involved in the Biosynthesis of an Entry Receptor for Herpes Simplex Virus 1. *J. Biol. Chem.* **2004**, *279*, 45185-45193.

169. pK_a values were calculated using ACD labs pK_a prediction software.

170. Patel, C. K.; Galisson, K. J.; James, K.; Owen, C. P.; Ahmed, S., Structure-activity relationship determination within a group of substituted phenyl sulfamate based compounds against the enzyme oestrone sulfatase. *J. Pharm. Pharm.* **2003**, *55*, 211-218.

171. Manetti, F.; Cappello, V.; Botta, M.; Corelli, F.; Mongelli, N.; Biasoli, G.; Lombardi Borgia, A.; Ciomei, M., Synthesis and binding mode of heterocyclic analogues of suramin inhibiting the human basic fibroblast growth factor. *Bioorg. Med. Chem.* **1998**, *6*, 947-958.

172. Raiber, E.-A.; Wilkinson, J. A.; Manetti, F.; Botta, M.; Deakin, J.; Gallagher, J.; Lyon, M.; Ducki, S. W., Novel heparin/heparan sulfate mimics as inhibitors of HGF/SF-induced MET activation. *Bioorg. Med. Chem. Lett.* **2007**, *17*, 6321-6325.

173. Yoffe, A. D., Thermal Decomposition and Explosion of Azides. *Proc. Royal Soc. London. Ser. A, Math. Phys. Sci.* **1951**, *208*, 188-199.

174. Hassner, A.; Stern, M.; Gottlieb, H. E.; Frolow, F., Synthetic methods. 33. Utility of a polymeric azide reagent in the formation of di- and triazidomethane. Their NMR spectra and the x-ray structure of derived triazoles. *J. Org. Chem.* **1990**, *55*, 2304-2306.

175. Lukkarila, J. L.; da Silva, S. R.; Ali, M.; Shahani, V. M.; Xu, G. W.; Berman, J.; Roughton, A.; Dhe-Paganon, S.; Schimmer, A. D.; Gunning, P. T., Identification of NAE Inhibitors Exhibiting Potent Activity in Leukemia Cells: Exploring the

Structural Determinants of NAE Specificity. *ACS Med. Chem. Lett.* **2011**, *2*, 577-582.

176. Gao, F.; Yan, X.; Shakya, T.; Baettig, O. M.; Ait-Mohand-Brunet, S.; Berghuis, A. M.; Wright, G. D.; Auclair, K., Synthesis and Structure−Activity Relationships of Truncated Bisubstrate Inhibitors of Aminoglycoside 6'-*N*-Acetyltransferases. *J. Med. Chem.* **2006**, *49*, 5273-5281.

177. Karplus, M., Vicinal Proton Coupling in Nuclear Magnetic Resonance. *J. Am. Chem. Soc.* **1963**, *85*, 2870-2871.

178. Neuberger, A.; Wilson, B. M., The separation of glycosides on a strongly basic ion-exchange resin: An interpretation in terms of acidity. *Carbohydr. Res.* **1971**, *17*, 89-95.

179. Appel, R.; Berger, G., Hydrazinsulfonsäure-amide, I. Über das Hydrazodisulfamid. *Chem. Ber.* **1958**, *91*, 1339-1341.

180. Fry, A., A Tracer Study of the Reaction of Isocyanates with Carboxylic Acids1,2. *J. Am. Chem. Soc.* **1953**, *75*, 2686-2688.

181. Modesti, M.; Baldoin, N.; Simioni, F., Formic acid as a co-blowing agent in rigid polyurethane foams. *European Polym. J.* **1998**, *34*, 1233-1241.

182. Schuemacher, A. C.; Hoffmann, R. W., Condensation between isocyanates and carobxylic acids in the presence of DMAP, a mild and efficient synthesis of amides. *Synthesis* **2001**, 243-246.

183. Okada, M.; Iwashita, S.; Koizumi, N., Efficient general method for sulfamoylation of a hydroxyl group. *Tetrahedron Lett.* **2000**, *41*, 7047-7051.

184. Schwarz, S.; Thieme, I.; Richter, M.; Undeutsch, B.; Henkel, H.; Elger, W., Synthesis of estrogen sulfamates: Compounds with a novel endocrinological profile. *Steroids* **1996**, *61*, 710-717.

185. Hasuoka, A.; Nishikimi, Y.; Nakayama, Y.; Kamiyama, K.; Nakao, M.; Miyagawa, K. I.; Nishimura, O.; Fujino, M., Total synthesis of novel antibiotics pyloricidin A, B and C and their application in the study of pyloricidin derivatives. *J. Antibiot.* **2002**, *55*, 191-203.

186. Warner, D. T.; Coleman, L. L., Selective Sulfonation of Amino Groups in Amino Alcohols. *J. Org. Chem.* **1958**, *23*, 1133-1135.

187. Pearson, A. G.; Kiefel, M. J.; Ferro, V.; von Itzstein, M., Synthesis of simple heparanase substrates. *Org. Biomol. Chem.* **2011**, *9*, 4614-4625.

188. Baumgarten, P., Über N-Pyridinium-sulfonsäure. (II. Mitteilung über den Abbau des Pyridins zu Glutaconsäure-dialdehyd). *Ber. Dtsch. Chem. Ges.* **1926**, *59*, 1166-1171.

189. Atkins, G. M.; Burgess, E. M., The reactions of an *N*-sulfonylamine inner salt. *J. Am. Chem. Soc.* **1968**, *90*, 4744-4745.

190. Armitage, I.; Berne, A. M.; Elliott, E. E.; Fu, M.; Hicks, F.; McCubbin, Q.; Zhu, L., *N*-(tert-Butoxycarbonyl)-*N*-[(triethylenediammonium)sulfonyl]azanide: A Convenient Sulfamoylation Reagent for Alcohols. *Org. Lett.* **2012**, *14*, 2626-2629.

191. Williams, J. M.; Richardson, A. C., Selective acylation of pyranoside-I.: Benzoylation of methyl α-D-glycopyranosides of mannose, glucose and galactose. *Tetrahedron* **1967**, *23*, 1369-1378.

192. Bamford, M. J.; Pichel, J. C.; Husman, W.; Patel, B.; Storer, R.; Weir, N. G., Synthesis of 6-, 7- and 8-carbon sugar analogues of potent anti-influenza 2,3-didehydro-2,3-dideoxy-*N*-acetylneuraminic acid derivatives. *J. Chem. Soc. Perkin Trans. 1* **1995**, 1181-1187.

193. Harrowven, D. C.; Curran, D. P.; Kostiuk, S. L.; Wallis-Guy, I. L.; Whiting, S.; Stenning, K. J.; Tang, B.; Packard, E.; Nanson, L., Potassium carbonate-silica: a highly effective stationary phase for the chromatographic removal of organotin impurities. *Chem. Commun.* **2010**, *46*, 6335-6337.

194. Chatgilialoglu, C., Organosilanes as radical-based reducing agents in synthesis. *Accounts of Chemical Research* **1992**, *25*, 188-194.

195. Zemplen, G., Saponification of acetylated carbohydrates. *Matematikai es Termeszettudomanyi Ertesito* **1937**, *55*, 432-439.

196. Marshall, J. A.; Garofalo, A. W., Oxidative cleavage of mono-, di-, and trisubstituted olefins to methyl esters through ozonolysis in methanolic sodium hydroxide. *J. Org. Chem.* **1993**, *58*, 3675-3680.

197. Griffith, W. P.; Shoair, A. G.; Suriaatmaja, M., Ruthenium-Catalysed Cleavage of Alkenes and Alkynes to Carboxylic Acids. *Synth. Commun.* **2000**, *30*, 3091-3095.

198. Brown, H. C.; Knights, E. F.; Scouten, C. G., Hydroboration. XXXVI. Direct route to 9-borabicyclo[3.3.1]nonane via the cyclic hydroboration of 1,5-cyclooctadiene. 9-Borabicyclo[3.3.1]nonane as a uniquely selective reagent for the hydroboration of olefins. *J. Am. Chem. Soc.* **1974**, *96*, 7765-7770.

199. Foley, D.; Pieri, M.; Pettecrew, R.; Price, R.; Miles, S.; Lam, H. K.; Bailey, P.; Meredith, D., The in vitro transport of model thiodipeptide prodrugs designed to target the intestinal oligopeptide transporter, PepT1. *Org. Biomol. Chem.* **2009**, *7*.

200. Sajiki, H.; Hirota, K., A novel type of PdMC-catalyzed hydrogenation using a catalyst poison: Chemoselective inhibition of the hydrogenolysis for *O*-benzyl protective group by the addition of a nitrogen-containing base. *Tetrahedron* **1998**, *54*, 13981-13996.

201. Lünse, C. E.; Schmidt, M. S.; Wittmann, V.; Mayer, G. n., Carba-sugars Activate the glmS-Riboswitch of Staphylococcus aureus. *ACS Chemical Biology* **2011**, *6*, 675-678.

202. Barton, D. H. R.; Augy-Dorey, S.; Camara, J.; Dalko, P.; Delaumény, J. M.; Géro, S. D.; Quiclet-Sire, B.; Stütz, P., Synthetic methods for the preparation of basic D- and L-pseudo-sugars. Synthesis of carbocyclic analogues of *N*-acetyl-muramyl-L-alanyl-D-isoglutamine (MDP). *Tetrahedron* **1990**, *46*, 215-230.

203. Barton, D. H. R.; McCombie, S. W., A new method for the deoxygenation of secondary alcohols. *J. Chem. Soc. Perkin Trans. 1* **1975**, 1574-1585.

204. Barton, D. H. R.; Crich, D.; Löbberding, A.; Zard, S. Z., On the mechanism of the deoxygenation of secondary alcohols by the reduction of their methyl xanthates by tin hydrides. *Tetrahedron* **1986**, *42*, 2329-2338.

205. Daragics, K.; Fügedi, P., Regio- and chemoselective reductive cleavage of 4,6-*O*-benzylidene-type acetals of hexopyranosides using BH_3·THF–TMSOTf. *Tetrahedron Lett.* **2009**, *50*, 2914-2916.

206. Jiang, L.; Chan, T.-H., Borane Bu_2BOTf: A mild reagent for the regioselective reductive ring opening of benzylidene acetals in carbohydrates. *Tetrahedron Lett.* **1998**, *39*, 355-358.

207. Karst, N.; Jacquinet, J.-C., Chemical synthesis of β-D-GlcpA(2SO_4)-(1-3)-D-GalpNAc(6SO_4), the disaccharide repeating unit of shark cartilage chondroitin sulfate D, and of its methyl β-D-glycoside derivative. *J. Chem. Soc. Perkin Trans. 1* **2000**, 2709-2717.

208. Iversen, T.; Bundle, D. R., Benzyl trichloroacetimidate, a versatile reagent for acid-catalysed benzylation of hydroxy-groups. *J. Chem. Soc., Chem. Commun.* **1981**, 1240-1241.

209.   Sanders, W. J.; Manning, D. D.; Koeller, K. M.; Kiessling, L. L., Synthesis of sulfated trisaccharide ligands for the selectins. *Tetrahedron* **1997**, *53*, 16391-16422.

210.   Winum, J.-Y.; Vullo, D.; Casini, A.; Montero, J.-L.; Scozzafava, A.; Supuran, C. T., Carbonic Anhydrase Inhibitors. Inhibition of Cytosolic Isozymes I and II and Transmembrane, Tumor-Associated Isozyme IX with Sulfamates Including EMATE Also Acting as Steroid Sulfatase Inhibitors. *J. Med. Chem.* **2003**, *46*, 2197-2204.

211.   Endicott, J. A.; Noble, M. E. M.; Johnson, L. N., The Structural Basis for Control of Eukaryotic Protein Kinases. *Annu. Rev. Biochem.* **2012**, *81*, 587-613.

212.   Blume-Jensen, P.; Hunter, T., Oncogenic kinase signalling. *Nature* **2001**, *411*, 355-365.

213.   Barouch-Bentov, R.; Sauer, K., Mechanisms of drug resistance in kinases. *Expert Opin. Invest. Drugs* **2011**, *20*, 153-208.

214.   Manning, G.; Whyte, D. B.; Martinez, R.; Hunter, T.; Sudarsanam, S., The Protein Kinase Complement of the Human Genome. *Science* **2002**, *298*, 1912-1934.

215.   Ang, A.; Lang, Y. Protein Kinases. http://chem3513-2007.pbworks.com/w/page/15648440/Protein%20Kinases (Aug 2013).

216.   Schwartz, P. A.; Murray, B. W., Protein kinase biochemistry and drug discovery. *Bioorg. Chem.* **2011**, *39*, 192-210.

217.   Norman, R. A.; Toader, D.; Ferguson, A. D., Structural approaches to obtain kinase selectivity. *Trends Pharmacol. Sci.* **2012**, *33*, 273-278.

218.   Nagar, B.; Bornmann, W. G.; Pellicena, P.; Schindler, T.; Veach, D. R.; Miller, W. T.; Clarkson, B.; Kuriyan, J., Crystal Structures of the Kinase Domain of c-Abl in Complex with the Small Molecule Inhibitors PD173955 and Imatinib (STI-571). *Cancer Res.* **2002**, *62*, 4236-4243.

219.   Zhang, J.; Yang, P. L.; Gray, N. S., Targeting cancer with small molecule kinase inhibitors. *Nat. Rev. Cancer* **2009**, *9*, 28-39.

220.   Gavrin, L. K.; Saiah, E., Approaches to discover non-ATP site kinase inhibitors. *MedChemComm* **2013**, *4*, 41-51.

221.   Hui, L.; Zatloukal, K.; Scheuch, H.; Stepniak, E.; Wagner, E. F., Proliferation of human HCC cells and chemically induced mouse liver cancers requires JNK1-dependent p21 downregulation. *J. Clin. Invest.* **2008**, *118*, 3943-3953.

222.   Hui, L.; Bakiri, L.; Mairhorfer, A.; Schweifer, N.; Haslinger, C.; Kenner, L.; Komnenovic, V.; Scheuch, H.; Beug, H.; Wagner, E. F., p38α suppresses normal

and cancer cell proliferation by antagonizing the JNK-c-Jun pathway. *Nat. Genet.* **2007**, *39*, 741-749.

223. Zhou, G.; Bao, Z. Q.; Dixon, J. E., Components of a New Human Protein Kinase Signal Transduction Pathway. *J. Biol. Chem.* **1995**, *270*, 12665-12669.

224. Nakamura, K.; Uhlik, M. T.; Johnson, N. L.; Hahn, K. M.; Johnson, G. L., PB1 Domain-Dependent Signaling Complex Is Required for Extracellular Signal-Regulated Kinase 5 Activation. *Mol. Cell. Biol.* **2006**, *26*, 2065-2079.

225. Yan, L.; Carr, J.; Ashby, P.; Murry-Tait, V.; Thompson, C.; Arthur, J. S., Knockout of ERK5 causes multiple defects in placental and embryonic development. *BMC Dev. Biol.* **2003**, *3*, 11.

226. Montero, J. C.; Ocaña, A.; Abad, M.; Ortiz-Ruiz, M. J.; Pandiella, A.; Esparís-Ogando, A., Expression of Erk5 in Early Stage Breast Cancer and Association with Disease Free Survival Identifies this Kinase as a Potential Therapeutic Target. *PLoS One* **2009**, *4*, e5565.

227. Mehta, P. B.; Jenkins, B. L.; McCarthy, L.; Thilak, L.; Robson, C. N.; Neal, D. E.; Leung, H. Y., MEK5 overexpression is associated with metastatic prostate cancer, and stimulates proliferation, MMP-9 expression and invasion. *Oncogene* **2003**, *22*, 1381-1389.

228. Zen, K.; Yasui, K.; Nakajima, T.; Zen, Y.; Zen, K.; Gen, Y.; Mitsuyoshi, H.; Minami, M.; Mitsufuji, S.; Tanaka, S.; Itoh, Y.; Nakanuma, Y.; Taniwaki, M.; Arii, S.; Okanoue, T.; Yoshikawa, T., ERK5 is a target for gene amplification at 17p11 and promotes cell growth in hepatocellular carcinoma by regulating mitotic entry. *Genes, Chromosomes Cancer* **2009**, *48*, 109-120.

229. McCracken, S. R. C.; Ramsay, A.; Heer, R.; Mathers, M. E.; Jenkins, B. L.; Edwards, J.; Robson, C. N.; Marquez, R.; Cohen, P.; Leung, H. Y., Aberrant expression of extracellular signal-regulated kinase 5 in human prostate cancer. *Oncogene* **2007**, *27*, 2978-2988.

230. Kato, Y.; Tapping, R. I.; Huang, S.; Watson, M. H.; Ulevitch, R. J.; Lee, J.-D., Bmk1/Erk5 is required for cell proliferation induced by epidermal growth factor. *Nature* **1998**, *395*, 713-716.

231. Perez-Madrigal, D.; Finegan, K. G.; Paramo, B.; Tournier, C., The extracellular-regulated protein kinase 5 (ERK5) promotes cell proliferation through the down-regulation of inhibitors of cyclin dependent protein kinases (CDKs). *Cell. Signal.* **2012**, *24*, 2360-2368.

232. Lochhead, P. A.; Gilley, R.; Cook, S. J., ERK5 and its role in tumour development. *Biochem. Soc. Trans.* **2012**, *40*, 251-256.

233. Ramsay, A. K.; McCracken, S. R. C.; Soofi, M.; Fleming, J.; Yu, A. X.; Ahmad, I.; Morland, R.; Machesky, L.; Nixon, C.; Edwards, D. R.; Nuttall, R. K.; Seywright, M.; Marquez, R.; Keller, E.; Leung, H. Y., ERK5 signalling in prostate cancer promotes an invasive phenotype. *Br. J. Cancer* **2011**, *104*, 664-672.

234. Castro, N.; Lange, C., Breast tumor kinase and extracellular signal-regulated kinase 5 mediate Met receptor signaling to cell migration in breast cancer cells. *Breast Cancer Res.* **2010**, *12*, R60.

235. Carvajal-Vergara, X.; Tabera, S.; Montero, J. C.; Esparís-Ogando, A.; López-Pérez, R.; Mateo, G.; Gutiérrez, N.; Parmo-Cabañas, M.; Teixidó, J.; San Miguel, J. F.; Pandiella, A., Multifunctional role of Erk5 in multiple myeloma. *Blood* **2005**, *105*, 4492-4499.

236. Wang, X.; Merritt, A. J.; Seyfried, J.; Guo, C.; Papadakis, E. S.; Finegan, K. G.; Kayahara, M.; Dixon, J.; Boot-Handford, R. P.; Cartwright, E. J.; Mayer, U.; Tournier, C., Targeted Deletion of mek5 Causes Early Embryonic Death and Defects in the Extracellular Signal-Regulated Kinase 5/Myocyte Enhancer Factor 2 Cell Survival Pathway. *Mol. Cell. Biol.* **2005**, *25*, 336-345.

237. Roberts, O. L.; Holmes, K.; Müller, J.; Cross, D. A. E.; Cross, M. J., ERK5 is required for VEGF-mediated survival and tubular morphogenesis of primary human microvascular endothelial cells. *J. Cell Sci.* **2010**, *123*, 3189-3200.

238. Song, H.; Jin, X.; Lin, J., Stat3 upregulates MEK5 expression in human breast cancer cells. *Oncogene* **2004**, *23*, 8301-8309.

239. Lee, J. D.; Ulevitch, R. J.; Han, J. H., Primary Structure of BMK1: A New Mammalian MAP Kinase. *Biochem. Biophys. Res. Commun.* **1995**, *213*, 715-724.

240. Nishimoto, S.; Nishida, E., MAPK signalling: ERK5 versus ERK1/2. *EMBO Rep* **2006**, *7*, 782-786.

241. Sturla, L.-M.; Cowan, C. W.; Guenther, L.; Castellino, R. C.; Kim, J. Y. H.; Pomeroy, S. L., A Novel Role for Extracellular Signal-Regulated Kinase 5 and Myocyte Enhancer Factor 2 in Medulloblastoma Cell Death. *Cancer Res.* **2005**, *65*, 5683-5689.

242. Sohn, S. J.; Li, D.; Lee, L. K.; Winoto, A., Transcriptional Regulation of Tissue-Specific Genes by the ERK5 Mitogen-Activated Protein Kinase. *Mol. Cell. Biol.* **2005**, *25*, 8553-8566.

243. Morimoto, H.; Kondoh, K.; Nishimoto, S.; Terasawa, K.; Nishida, E., Activation of a C-terminal Transcriptional Activation Domain of ERK5 by Autophosphorylation. *J. Biol. Chem.* **2007**, *282*, 35449-35456.

244. Lu, C.; Shen, Q.; DuPre, E.; Kim, H.; Hilsenbeck, S.; Brown, P. H., cFos is critical for MCF-7 breast cancer cell growth. *Oncogene* **2005**, *24*, 6516-6524.

245. Deng, X.; Yang, Q.; Kwiatkowski, N.; Sim, T.; McDermott, U.; Settleman, J. E.; Lee, J.-D.; Gray, N. S., Discovery of a benzo[e]pyrimido-[5,4-b][1,4]diazepin-6(11*H*)-one as a Potent and Selective Inhibitor of Big MAP Kinase 1. *ACS Med. Chem. Lett.* **2011**, *2*, 195-200.

246. Tatake, R. J.; O'Neill, M. M.; Kennedy, C. A.; Wayne, A. L.; Jakes, S.; Wu, D.; Kugler Jr, S. Z.; Kashem, M. A.; Kaplita, P.; Snow, R. J., Identification of pharmacological inhibitors of the MEK5/ERK5 pathway. *Biochem. Biophys. Res. Commun.* **2008**, *377*, 120-125.

247. Elkins, J. M.; Wang, J.; Deng, X.; Pattison, M. J.; Arthur, J. S. C.; Erazo, T.; Gomez, N.; Lizcano, J. M.; Gray, N. S.; Knapp, S., X-ray Crystal Structure of ERK5 (MAPK7) in Complex with a Specific Inhibitor. *J. Med. Chem.* **2013**.

248. Yang, Q.; Deng, X.; Lu, B.; Cameron, M.; Fearns, C.; Patricelli, M. P.; Yates Iii, J. R.; Gray, N. S.; Lee, J.-D., Pharmacological Inhibition of BMK1 Suppresses Tumor Growth through Promyelocytic Leukemia Protein. *Cancer Cell* **2010**, *18*, 258-267.

249. Molecular Devices http://www.moleculardevices.com/products/assay-kits/enzymes/imap-assays.html (10-08-2013).

250. de Groot, M. J.; Wakenhut, F.; Whitlock, G.; Hyland, R., Understanding CYP2D6 interactions. *Drug Discov. Today* **2009**, *14*, 964-972.

251. Lewis, D. F. V.; Dickins, M., Substrate SARs in human P$_{450}$s. *Drug Discov. Today* **2002**, *7*, 918-925.

252. Bawn, R. Development of Small Molecule Inhibitors of ERK5 for the Treatment of Cancer. Newcastle University, Newcastle upon Tyne, **2011**.

253. Myers, S. M. The Discovery and Optimization of ERK5 Inhibitors. Newcastle University, Newcastle upon Tyne, **2012**.

254. Lave, T.; Dupin, S.; Schmitt, C.; Chou, R. C.; Jaeck, D.; Coassolo, P., Integration of *in vitro* data into allometric scaling to predict hepatic metabolic clearance in man: Application to 10 extensively metabolized drugs. *J. Pharm. Sci.* **1997**, *86*, 584-590.

255. Riley, R. J.; Parker, A. J.; Trigg, S.; Manners, C. N., Development of a Generalized, Quantitative Physicochemical Model of CYP3A4 Inhibition for Use in Early Drug Discovery. *Pharm. Res.* **2001**, *18*, 652-655.

256. Jones, G.; Willett, P.; Glen, R. C., Molecular recognition of receptor sites using a genetic algorithm with a description of desolvation. *J. Mol. Biol.* **1995**, *245*, 43-53.

257. O'Hare, T.; Walters, D. K.; Stoffregen, E. P.; Jia, T.; Manley, P. W.; Mestan, J.; Cowan-Jacob, S. W.; Lee, F. Y.; Heinrich, M. C.; Deininger, M. W. N.; Druker, B. J., In vitro Activity of Bcr-Abl Inhibitors AMN107 and BMS-354825 against Clinically Relevant Imatinib-Resistant Abl Kinase Domain Mutants. *Cancer Res.* **2005**, *65*, 4500-4505.

258. Khoury, H. J.; Cortes, J. E.; Kantarjian, H. M.; Gambacorti-Passerini, C. B.; Baccarani, M.; Kim, D.-W.; Zaritskey, A.; Countouriotis, A.; Besson, N.; Leip, E.; Kelly, V.; Brummendorf, T. H., Bosutinib is active in chronic phase chronic myeloid leukemia after imatinib and dasatinib and/or nilotinib therapy failure. *Blood* **2012**.

259. European Medicines Agency Tasigna EPAR product information: EMEA/H/C/000798 -II/0058. http://www.ema.europa.eu/ema/index.jsp?curl=pages/medicines/human/medicines/000798/human_med_001079.jsp&mid=WC0b01ac058001d124 (July 2013).

260. Zhou, T.; Commodore, L.; Huang, W.-S.; Wang, Y.; Thomas, M.; Keats, J.; Xu, Q.; Rivera, V. M.; Shakespeare, W. C.; Clackson, T.; Dalgarno, D. C.; Zhu, X., Structural Mechanism of the Pan-BCR-ABL Inhibitor Ponatinib (AP24534): Lessons for Overcoming Kinase Inhibitor Resistance. *Chem. Biol. Drug Des.* **2011**, *77*, 1-11.

261. Sebastian, S.; Settleman, J.; Reshkin, S. J.; Azzariti, A.; Bellizzi, A.; Paradiso, A., The complexity of targeting EGFR signalling in cancer: From expression to turnover. *Biochim. Biophys. Acta - Reviews on Cancer* **2006**, *1766*, 120-139.

262. Kosaka, T.; Yatabe, Y.; Endoh, H.; Yoshida, K.; Hida, T.; Tsuboi, M.; Tada, H.; Kuwano, H.; Mitsudomi, T., Analysis of Epidermal Growth Factor Receptor Gene Mutation in Patients with Non–Small Cell Lung Cancer and Acquired Resistance to Gefitinib. *Clin. Cancer. Res.* **2006**, *12*, 5764-5769.

263. Barker, A. J.; Gibson, K. H.; Grundy, W.; Godfrey, A. A.; Barlow, J. J.; Healy, M. P.; Woodburn, J. R.; Ashton, S. E.; Curry, B. J.; Scarlett, L.; Henthorn, L.; Richards, L., Studies leading to the identification of ZD1839 (iressa™): an orally

active, selective epidermal growth factor receptor tyrosine kinase inhibitor targeted to the treatment of cancer. *Bioorg. Med. Chem. Lett.* **2001**, *11*, 1911-1914.

264. Ward, W. H. J.; Cook, P. N.; Slater, A. M.; Davies, D. H.; Holdgate, G. A.; Green, L. R., Epidermal growth factor receptor tyrosine kinase: Investigation of catalytic mechanism, structure-based searching and discovery of a potent inhibitor. *Biochem. Pharmacol.* **1994**, *48*, 659-666.

265. MacFarlane, R. J.; Gelmon, K. A., Lapatinib for breast cancer: a review of the current literature. *Expert Opin. Drug Saf.* **2011**, *10*, 109-121.

266. Hoelder, S.; Clarke, P. A.; Workman, P., Discovery of small molecule cancer drugs: Successes, challenges and opportunities. *Mol. Oncol.* **2012**, *6*, 155-176.

267. Duda, D. G.; Batchelor, T. T.; Willett, C. G.; Jain, R. K., VEGF-targeted cancer therapy strategies: current progress, hurdles and future prospects. *Trends Mol. Med.* **2007**, *13*, 223-230.

268. Amir, E.; Mandoky, L.; Blackhall, F.; Thatcher, N.; Klepetko, W.; Ankersmit, H. J.; Reza Hoda, M. A.; Ostoros, G.; Dank, M.; Dome, B., Antivascular agents for non-small-cell lung cancer: current status and future directions. *Expert Opin. Invest. Drugs* **2009**, *18*, 1667-1686.

269. Wilhelm, S.; Carter, C.; Lynch, M.; Lowinger, T.; Dumas, J.; Smith, R. A.; Schwartz, B.; Simantov, R.; Kelley, S., Discovery and development of sorafenib: a multikinase inhibitor for treating cancer. *Nat. Rev. Drug Discov.* **2006**, *5*, 835-844.

270. Strumberg, D.; Schultheis, B., Regorafenib for cancer. *Expert Opin. Invest. Drugs* **2012**, *21*, 879-889.

271. Patson, B.; B Cohen, R.; Olszanski, A. J., Pharmacokinetic evaluation of axitinib. *Expert Opin. Drug Metab. Toxicol.* **2012**, *8*, 259-270.

272. Traynor, K., Cabozantinib approved for advanced medullary thyroid cancer. *Am. J. Health-Syst. Pharm.* **2013**, *70*, 88.

273. Yakes, F. M.; Chen, J.; Tan, J.; Yamaguchi, K.; Shi, Y.; Yu, P.; Qian, F.; Chu, F.; Bentzien, F.; Cancilla, B.; Orf, J.; You, A.; Laird, A. D.; Engst, S.; Lee, L.; Lesch, J.; Chou, Y.-C.; Joly, A. H., Cabozantinib (XL184), a Novel MET and VEGFR2 Inhibitor, Simultaneously Suppresses Metastasis, Angiogenesis, and Tumor Growth. *Mol. Cancer Ther.* **2011**, *10*, 2298-2308.

274. Flaherty, K. T.; Yasothan, U.; Kirkpatrick, P., Vemurafenib. *Nat. Rev. Drug Discov.* **2011**, *10*, 811-812.

275. Forde, P. M.; Rudin, C. M., Crizotinib in the treatment of non-small-cell lung cancer. *Expert Opin. Pharmacother.* **2012**, *13*, 1195-1201.

276. Cui, J. J.; Tran-Dubé, M.; Shen, H.; Nambu, M.; Kung, P.-P.; Pairish, M.; Jia, L.; Meng, J.; Funk, L.; Botrous, I.; McTigue, M.; Grodsky, N.; Ryan, K.; Padrique, E.; Alton, G.; Timofeevski, S.; Yamazaki, S.; Li, Q.; Zou, H.; Christensen, J.; Mroczkowski, B.; Bender, S.; Kania, R. S.; Edwards, M. P., Structure Based Drug Design of Crizotinib (PF-02341066), a Potent and Selective Dual Inhibitor of Mesenchymal–Epithelial Transition Factor (c-MET) Kinase and Anaplastic Lymphoma Kinase (ALK). *J. Med. Chem.* **2011**, *54*, 6342-6363.

277. Deisseroth, A.; Kaminskas, E.; Grillo, J.; Chen, W.; Saber, H.; Lu, H. L.; Rothmann, M. D.; Brar, S.; Wang, J.; Garnett, C.; Bullock, J.; Burke, L. B.; Rahman, A.; Sridhara, R.; Farrell, A.; Pazdur, R., U.S. Food and Drug Administration Approval: Ruxolitinib for the Treatment of Patients with Intermediate and High-Risk Myelofibrosis. *Clin. Cancer. Res.* **2012**, *18*, 3212-3217.

278. Ni, H.; Moe, S.; Myint, K. T.; Htet, A., Oral Janus Kinase Inhibitor for the Treatment of Rheumatoid Arthritis: Tofacitinib. *ISRN Rheumatology* **2013**, *2013*, 9.

279. Leeson, P. D.; Springthorpe, B., The influence of drug-like concepts on decision-making in medicinal chemistry. *Nat. Rev. Drug Discov.* **2007**, *6*, 881-890.

280. Ryckmans, T.; Edwards, M. P.; Horne, V. A.; Correia, A. M.; Owen, D. R.; Thompson, L. R.; Tran, I.; Tutt, M. F.; Young, T., Rapid assessment of a novel series of selective CB2 agonists using parallel synthesis protocols: A Lipophilic Efficiency (LipE) analysis. *Bioorg. Med. Chem. Lett.* **2009**, *19*, 4406-4409.

281. NDA 21-588 Review - Imatinib, Clinical Pharmacology and Biopharmaceutics Review. FDA2002.

282. NDA 21-986 Review - Dasatinib, Clinical Pharmacology Pharmacometrics Review. FDA2006.

283. NDA 22-068 - Nilotinib, Summary Review. FDA2007.

284. NDA 203-341 Review – Bosutinib, 203341Clinical Pharmacology Review. FDA, Ed.2012.

285. NDA203469Orig1s000 - Ponatinib, Pharmacology Review. FDA2012.

286. NDA21-399 - Geftinib, Pharmacology Review. FDA2003.

287. NDA 24-713 Erlotinib, Pharmacology Review. FDA2004.

288. NDA 22-059 Lapatinib, Clinical Pharmacology and Biopharmaceutic Review. FDA2007.

289. NDA-21 938 Sunitinib, clinical Pharmacology and Biopharmaceutic Review. FDA2005.

290. NDA 21 923 - Sorafenib, Clinical Pharmacology and Bipharmaceutic Review. FDA2005.

291. NDA 203085Orig1s000 - Regorafenib, Clinical Pharmacology and Biopharmaceutic Review. FDA2012.

292. NDA 202324Orig1s000 - Axitinib, Clinical Pharmacology and Biopharmaceutics Review. FDA2012.

293. NDA 22-465 - Pazopanib, Clinical Pharmacology and Biopharmaceutics Review. FDA2008.

294. NDA 022405Orig1s000 - Vandetanib, Clinical Pharmacology and Biopharmaceutics Review. FDA2010.

295. NDA 202429Orig1s000 - Vemurafenib, Clinical Pharmacology and Biopharmaceutics Review. FDA2011.

296. NDA 202570Orig1s000 - Crizotinib, Clinical Pharmacology and Biopharmaceutics Review. FDA2011.

297. Lipinski, C. A.; Lombardo, F.; Dominy, B. W.; Feeney, P. J., Experimental and computational approaches to estimate solubility and permeability in drug discovery and development settings. *Adv. Drug Del. Rev.* **1997**, *23*, 3-25.

298. Wenlock, M. C.; Austin, R. P.; Barton, P.; Davis, A. M.; Leeson, P. D., A Comparison of Physiochemical Property Profiles of Development and Marketed Oral Drugs. *J. Med. Chem.* **2003**, *46*, 1250-1256.

299. Ertl, P.; Rohde, B.; Selzer, P., Fast Calculation of Molecular Polar Surface Area as a Sum of Fragment-Based Contributions and Its Application to the Prediction of Drug Transport Properties. *J. Med. Chem.* **2000**, *43*, 3714-3717.

300. Hou, T.; Wang, J.; Zhang, W.; Xu, X., ADME Evaluation in Drug Discovery. 6. Can Oral Bioavailability in Humans Be Effectively Predicted by Simple Molecular Property-Based Rules? *J. Chem. Inf. Model.* **2007**, *47*, 460-463.

301. Peng, B.; Lloyd, P.; Schran, H., Clinical Pharmacokinetics of Imatinib. *Clin. Pharmacokinet.* **2005**, *44*, 879-894.

302. European Medicines Agency Iclusig EPAR product information: EMEA/H/C/002695.

http://www.ema.europa.eu/ema/index.jsp?curl=pages/medicines/human/medicines/002695/human_med_001656.jsp&mid=WC0b01ac058001d124 (July 2013).

303. Chouhan, J. D.; Zamarripa, D. E.; Lai, P. H.; Oramasionwu, C. U.; Grabinski, J. L., Sunitinib (Sutent®): A novel agent for the treatment of metastatic renal cell carcinoma. *J. Oncol. Pharm. Pract.* **2007**, *13*, 5-15.

304. Rose, J.; Castagnoli, N., The metabolism of tertiary amines. *Med. Res. Rev.* **1983**, *3*, 73-88.

305. Maubon, N.; Le Vee, M.; Fossati, L.; Audry, M.; Le Ferrec, E.; Bolze, S.; Fardel, O., Analysis of drug transporter expression in human intestinal Caco-2 cells by real-time PCR. *Fund. Clin. Pharmacol.* **2007**, *21*, 659-663.

306. Seelig, A., A general pattern for substrate recognition by P-glycoprotein. *Eur. J. Biochem.* **1998**, *251*, 252-261.

307. Hitchcock, S. A., Structural Modifications that Alter the P-Glycoprotein Efflux Properties of Compounds. *J. Med. Chem.* **2012**, *55*, 4877-4895.

308. Alex, A.; Millan, D. S.; Perez, M.; Wakenhut, F.; Whitlock, G. A., Intramolecular hydrogen bonding to improve membrane permeability and absorption in beyond rule of five chemical space. *MedChemComm* **2011**, *2*, 669-674.

309. Palm, K.; Stenberg, P.; Luthman, K.; Artursson, P., Polar Molecular Surface Properties Predict the Intestinal Absorption of Drugs in Humans. *Pharm. Res.* **1997**, *14*, 568-571.

310. Kuduk, S. D.; Di Marco, C. N.; Chang, R. K.; Wood, M. R.; Schirripa, K. M.; Kim, J. J.; Wai, J. M. C.; DiPardo, R. M.; Murphy, K. L.; Ransom, R. W.; Harrell, C. M.; Reiss, D. R.; Holahan, M. A.; Cook, J.; Hess, J. F.; Sain, N.; Urban, M. O.; Tang, C.; Prueksaritanont, T.; Pettibone, D. J.; Bock, M. G., Development of Orally Bioavailable and CNS Penetrant Biphenylaminocyclopropane Carboxamide Bradykinin B1 Receptor Antagonists. *J. Med. Chem.* **2006**, *50*, 272-282.

311. Miller, D. C.; Klute, W.; Calabrese, A.; Brown, A. D., Optimising metabolic stability in lipophilic chemical space: The identification of a metabolically stable pyrazolopyrimidine CRF-1 receptor antagonist. *Bioorg. Med. Chem. Lett.* **2009**, *19*, 6144-6147.

312. Cerny, M. A.; Hanzlik, R. P., Cyclopropylamine inactivation of cytochromes P_{450}: Role of metabolic intermediate complexes. *Arch. Biochem. Biophys.* **2005**, *436*, 265-275.

313. Hagmann, W. K., The Many Roles for Fluorine in Medicinal Chemistry. *J. Med. Chem.* **2008**, *51*, 4359-4369.

314. Owen, D. R.; Rodriguez-Lens, M.; Corless, M. D.; Gaulier, S. M.; Horne, V. A.; Kinloch, R. A.; Maw, G. N.; Pearce, D. W.; Rees, H.; Ringer, T. J.; Ryckmans, T.; Stammen, B. L. C., 2,4-Diaminopyridine δ-opioid receptor agonists and their associated hERG pharmacology. *Bioorg. Med. Chem. Lett.* **2009**, *19*, 1702-1706.

315. Blizzard, T. A.; Chen, H.; Gude, C.; Hermes, J. D.; Imbriglio, J. E.; Kim, S.; Wu, J. Y.; Ha, S.; Mortko, C. J.; Mangion, I.; Rivera, N.; Ruck, R. T.; Shelvin, M. Beta-lactamase inhibitors. WO2009091856, **2009**.

316. Huang, H.; Iwasawa, N.; Mukaiyama, T., A convenient method for the construction of beta-lactam compounds from beta-aminoacids using 2-chloro-1-methylpyridinium iodide as condensing reagent. *Chem. Lett.* **1984**, *13*, 1465-1466.

317. Beletskaya, I. P.; Cheprakov, A. V., The Complementary Competitors: Palladium and Copper in *C–N* Cross-Coupling Reactions. *Organometallics* **2012**, *31*, 7753-7808.

318. Wolfe, J. P.; Tomori, H.; Sadighi, J. P.; Yin, J.; Buchwald, S. L., Simple, Efficient Catalyst System for the Palladium-Catalyzed Amination of Aryl Chlorides, Bromides, and Triflates. *J. Org. Chem.* **2000**, *65*, 1158-1174.

319. Maiti, D.; Fors, B. P.; Henderson, J. L.; Nakamura, Y.; Buchwald, S. L., Palladium-catalyzed coupling of functionalized primary and secondary amines with aryl and heteroaryl halides: two ligands suffice in most cases. *Chem. Sci.* **2011**, *2*, 57-68.

320. Surry, D. S.; Buchwald, S. L., Dialkylbiaryl phosphines in Pd-catalyzed amination: a user's guide. *Chem. Sci.* **2011**, *2*, 27-50.

321. Yaunner, R. S.; Barros, J. C.; da Silva, J. F. M., Microwave-promoted piperidination of halopyridines: a comparison between Ullmann, Buchwald–Hartwig and uncatalysed S_NAr reactions. *Appl. Organomet. Chem.* **2012**, *26*, 273-276.

322. Keegstra, M. A.; Peters, T. H. A.; Brandsma, L., Copper(I) halide catalysed synthesis of alkyl aryl and alkyl heteroaryl ethers. *Tetrahedron* **1992**, *48*, 3633-3652.

323. Corcoran, R. C.; Bang, S. H., Iodopyridines from bromo- and chloropyridines. *Tetrahedron Lett.* **1990**, *31*, 6757-6758.

324. Yin, J.; Xiang, B.; Huffman, M. A.; Raab, C. E.; Davies, I. W., A General and Efficient 2-Amination of Pyridines and Quinolines. *J. Org. Chem.* **2007**, *72*, 4554-4557.

325. Londregan, A. T.; Jennings, S.; Wei, L., Mild Addition of Nucleophiles to Pyridine-*N*-Oxides. *Org. Lett.* **2011**, *13*, 1840-1843.

326. Londregan, A. T.; Jennings, S.; Wei, L., General and Mild Preparation of 2-Aminopyridines. *Org. Lett.* **2010**, *12*, 5254-5257.

327. Austin, M. W.; Blackborow, J. R.; Ridd, J. H.; Smith, B. V., The kinetics and mechanism of heteroaromatic nitration. Part II. Pyrazole and imidazole. *J. Chem. Soc.* **1965**, 1051-1057.

328. Zabierek, A. A.; Konrad, K. M.; Haidle, A. M., A practical, two-step synthesis of 1-alkyl-4-aminopyrazoles. *Tetrahedron Lett.* **2008**, *49*, 2996-2998.

329. Eschweiler, W., Ersatz von an Stickstoff gebundenen Wasserstoffatomen durch die Methylgruppe mit Hülfe von Formaldehyd. *Ber. Dtsch. Chem. Ges.* **1905**, *38*, 880-882.

330. Clarke, H. T.; Gillespie, H. B.; Weisshaus, S. Z., The Action of Formaldehyde on Amines and Amino Acids 1. *J. Am. Chem. Soc.* **1933**, *55*, 4571-4587.

331. Kawasaki, I.; Osaki, T.; Tsunoda, K.; Watanabe, E.; Matsuyama, M.; Sanai, A.; Khadeer, A.; Yamashita, M.; Ohta, S., Double nucleophilic reaction of amines to the imidazole nucleus and selective synthesis of 5-aminoimidazoles. *Tetrahedron* **2004**, *60*, 6639-6648.

332. Ridd, J. H.; Smith, B. V., The mechanisms of *N*-substitution in glyoxaline derivatives. Part III. Factors determining the orientation of *N*-methylation in substituted glyoxalines and benzimidazoles. *J. Chem. Soc. (Resumed)* **1960**, 1363-1369.

333. Bergman, J.; Sand, P., A new simple procedure for alkylation of nitrogen heterocycles using dialkyl oxalates and alkoxides. *Tetrahedron Lett.* **1984**, *25*, 1957-1960.

334. Grimison, A.; Ridd, J. H.; Smith, B. V., The mechanisms of *N*-substitution in glyoxaline derivatives. Part I. Introduction, and study of prototropic equilibria involving 4(5)-nitroglyoxaline. *J. Chem. Soc. (Resumed)* **1960**, 1352-1356.

335. Grimison, A.; Ridd, J. H.; Smith, B. V., The mechanisms of *N*-substitution in glyoxaline derivatives. Part II. The methylation of 4(5)-nitroglyoxaline by methyl sulphate. *J. Chem. Soc. (Resumed)* **1960**, 1357-1362.

336. Kamst, E.; Zegelaar-Jaarsveld, K.; van der Marel, G. A.; van Boom, J. H.; Lugtenberg, B. J. J.; Spaink, H. P., Chemical synthesis of N-acetylglucosamine derivatives and their use as glycosyl acceptors by the Mesorhizobium loti chitin oligosaccharide synthase NodC. *Carbohydrate Res.* **1999**, *321*, 176-189.

337. Sixta, G.; Hofinger, A.; Kosma, P., Synthesis of spacer-containing chlamydial disaccharides as analogues of the α-Kdop-(2-8)-α-Kdop-(2-4)-α-Kdop trisaccharide epitope. *Carbohydrate Res.* **2007**, *342*, 576-585.

338. Saito, K.; Nishimura, Y.; Kondo, S.; Takeuchi, T., Synthesis of Carbocyclic Lignan Variants Related to Podophyllotoxin. *Chem. Lett.* **1988**, *17*, 1235-1238.

339. Vatèle, J.-M.; Hanessian, S., Design and reactivity of organic functional groups - preparation and nucleophilic displacement reactions of imidazole-1-sulfonates (imidazylates). *Tetrahedron* **1996**, *52*, 10557-10568.

340. Zhang, J.; Hong Chan, P. W.; Che, C.-M., Enantioselective intramolecular amidation of sulfamate esters catalyzed by chiral manganese(III) Schiff-base complexes. *Tetrahedron Lett.* **2005**, *46*, 5403-5408.

341. Hedayatullah, M.; Guy, A., A Convenient Synthesis of Aryl Sulfamates. *Synthesis* **1978**, *1978*, 357-357.

342. Ban, H.; Asano, S. Preparation of heterocycle- and benzene-containing sulfonamide derivatives as LDL receptor agonists. EP1736467, **2005**.

343. Lo, Y. S.; Nolan, J. C.; Walsh, D. A.; Welstead, W. J. J. Preparation of sulfamate esters for use against arthritis and osteoporosis. US5194446, **1993**.

344. Kamal, A.; Rao, M. V.; Rao, A. B., *Heterocycles* **1990**, *31*, 577.

345. Woo, L. W. L.; Howarth, N. M.; Purohit, A.; Hejaz, A. M.; Reed, M. J.; Potter, B. V. L., Steroidal and Nonsteroidal Sulfamates as Potent Inhibitors of Steroid Sulfatase. *J. Med. Chem.* **1998**, *41*, 1068.

346. Denehy, E.; White, J. M.; Williams, S. J., Ground state structures of sulfate monoesters and sulfamates reveal similar reaction coordinates for sulfuryl and sulfamyl transfer. *Chem. Commun.* **2006**, *3*, 314-316.

347. Otto, E.; Muschaweck, R. Sulfamic acid esters DE2418217, **1975**.

348. Hetayatullah, M.; Guy, A., A convenient synthesis of aryl sulfamates. *Synthesis* **1978**, 357.

349. Colombo, M.; Bossolo, S.; Aramini, A., Phosphorus Trichloride-Mediated and Microwave-Assisted Synthesis of a Small Collection of Amides Bearing Strong

Electron-Withdrawing Group Substituted Anilines. *J. Comb. Chem.* **2009**, *11*, 335-337.

350. Baindur, N.; Gaul, M. D.; Kreutter, K. D.; Baumann, C. A.; Kim, A. J.; Xu, G.; Tuman, R. W.; Johnson, D. L. Alkylquinoline and alkylquinazoline kinase modulators. US2006281772, **2006**.

351. Rahamin, Y.; Sharvit, J.; Mandelbaum, A.; Sprecher, M., Electron impact-induced methyl migration in dimethylaminoheteroaromatic systems. *J. Org. Chem.* **1967**, *32*, 3856-3859.

352. Nara, S. J.; Jha, M.; Brinkhorst, J.; Zemanek, T. J.; Pratt, D. A., A Simple Cu-Catalyzed Coupling Approach to Substituted 3-Pyridinol and 5-Pyrimidinol Antioxidants. *J. Org. Chem.* **2008**, *73*, 9326-9333.

353. Krchňák, V.; Arnold, Z., Novel pyrimidine derivatives, reactions and ultraviolet spectra. *Collect. Czech. Chem. Commun.* **1975**, *40*, 1396-1402.

354. Axten, J. M.; Betancourt, T. J. R. M.; Johnson, N. W.; Semone, M. Anthranilamides. WO2008147831, **2008**.

355. Tsou, H.-R.; Otteng, M.; Tran, T.; Floyd, M. B.; Reich, M.; Birnberg, G.; Kutterer, K.; Ayral-Kaloustian, S.; Ravi, M.; Nilakantan, R.; Grillo, M.; McGinnis, J. P.; Rabindran, S. K., 4-(Phenylaminomethylene)isoquinoline-1,3(2H,4H)-diones as Potent and Selective Inhibitors of the Cyclin-Dependent Kinase 4 (CDK4). *J. Med. Chem.* **2008**, *51*, 3507-3525.

356. Bolin, D. R.; Cheung, A. W.-H.; FIirooznia, F.; Hamilton, M. M.; McDermott, L. A.; Qian, Y.; Tan, J.; Yun, W. Diacylglycerol Acyltransferase Inhibitors. **2008**.

357. Qian, Y.; Wertheimer, S. J.; Ahmad, M.; Cheung, A. W.-H.; Firooznia, F.; Hamilton, M. M.; Hayden, S.; Li, S.; Marcopulos, N.; McDermott, L.; Tan, J.; Yun, W.; Guo, L.; Pamidimukkala, A.; Chen, Y.; Huang, K.-S.; Ramsey, G. B.; Whittard, T.; Conde-Knape, K.; Taub, R.; Rondinone, C. M.; Tilley, J.; Bolin, D., Discovery of Orally Active Carboxylic Acid Derivatives of 2-Phenyl-5-trifluoromethyloxazole-4-carboxamide as Potent Diacylglycerol Acyltransferase-1 Inhibitors for the Potential Treatment of Obesity and Diabetes. *J. Med. Chem.* **2011**, *54*, 2433-2446.

358. Hurst, D. T.; Christophides, J., The Synthesis of Some 2-Substituted 5-Nitropyrimidines. *Heterocycles* **1977**, *6*, 1999-2004.

359. Ammala, C.; Briscoe, C. Gpr119 agonists for the treatment of diabetes and related disorders WO2008008895, **2008**.

360. DiMauro, E. F.; Newcomb, J.; Nunes, J. J.; Bemis, J. E.; Boucher, C.; Chai, L.; Chaffee, S. C.; Deak, H. L.; Epstein, L. F.; Faust, T.; Gallant, P.; Gore, A.; Gu, Y.; Henkle, B.; Hsieh, F.; Huang, X.; Kim, J. L.; Lee, J. H.; Martin, M. W.; McGowan, D. C.; Metz, D.; Mohn, D.; Morgenstern, K. A.; Oliveira-dos-Santos, A.; Patel, V. F.; Powers, D.; Rose, P. E.; Schneider, S.; Tomlinson, S. A.; Tudor, Y.-Y.; Turci, S. M.; Welcher, A. A.; Zhao, H.; Zhu, L.; Zhu, X., Structure-Guided Design of Aminopyrimidine Amides as Potent, Selective Inhibitors of Lymphocyte Specific Kinase: Synthesis, Structure–Activity Relationships, and Inhibition of *in Vivo* T Cell Activation. *J. Med. Chem.* **2008**, *51*, 1681-1694.

361. Brown, D. J.; Sugimoto, T., Aza-analogues of pteridine. Part II. The novel use of silver oxide in transetherification of alkoxy-1,2,4,6,8-penta-azanaphthalenes, alkoxynitropyrimidines, and related systems. *J. Chem. Soc. C* **1970**, *0*, 2661-2666.

362. Cherkasov, V. M.; Remennikov, G. Y.; Kisilenko, A. A.; Romanenko, E. A., Sigma complexes in the pyrimidine series. 2. σ Complexes of 5-nitropyrimidine and methoxy-substituted 5-nitropyrimidines with the acetone anion. *Chem. Heterocycl. Compd.* **1980**, *16*, 179-182.

363. Krchňák, V.; Arnold, Z., Novel pyrimidine derivatives, reactions and ultraviolet spectra. *Collect. Czech. Chem. Commun* **1975**, *40*, 1396-1402.

364. Dodic, N. Bioisosteric benzamide derivatives and their use as apob-100 secretion inhibitors US2004009988, **2004**.

365. Adjabeng, G.; Bifulco, N.; Davis-Ward, R. G.; Dickerson, S. H.; Donaldson, K. H.; Harris, P. A.; Hornberger, K.; Petrov, K.; Rheaul, T. R.; Schaaf, G.; Stellwagen, J.; Uehling, D. E.; Waterson, A. G. Thiazole and oxazole kinase inhibitors. WO2009032667, **2009**.

366. Spencer, J.; Patel, H.; Callear, S. K.; Coles, S. J.; Deadman, J. J., Synthesis and solid state study of pyridine- and pyrimidine-based fragment libraries. *Tetrahedron Lett.* **2011**, *52*, 5905-5909.

367. Sazonov, N. V.; Safonova, T. S.; Minakova, S. M.; Chernov, V. A., Diethylenimides of 3-pyridyl- and 4-pyridylamidophosphoric acids. *Pharm. Chem. J.* **1972**, *6*, 146-149.

368. Barlamm, B. C.; Foote, K. M.; Ple, P. Pyridine Compounds. WO2009153589, **2009**.

369. Wessig, P.; Möllnitz, K., Nanoscale Molecular Rods with a New Building Block for Solubility Enhancement. *J. Org. Chem.* **2008**, *73*, 4452-4457.

370. Bailey, J. M.; Booth, H.; Al-Shirayda, H. A. R. Y.; Trimble, M. L., Ring inversion equilibria in 4-chloro-, 4-bromo-, and 4-methoxy-1-alkylpiperidines in a non-polar solvent. *J. Chem. Soc. Perkin Trans. 2* **1984**, *0*, 737-743.

371. Park, S.; Lee, I. S.; Park, J., A magnetically separable gold catalyst for chemoselective reduction of nitro compounds. *Org. Biomol. Chem.* **2013**, *11*, 395-399.

372. Ravi, P.; Gore, G. M.; Sikder, A. K.; Tewari, S. P., Silica-Sulfuric Acid Catalyzed Nitrodeiodination of Iodopyrazoles. *Synth. Commun.* **2012**, *42*, 3463-3471.

373. Chang, K.; Grimmett, M. R.; Ward, D. D.; Weavers, R. T., The Nitration of Brominated Pyrazoles in Aqueous Sulfuric Acid. *Aust. J. Chem.* **1979**, *32*, 1727-1734.

374. Ramsden, N.; Harrison, R. J.; Oxenford, S.; Bell, K.; Piton, N.; Dagostin, C.; Boussard, C.; Ratcliffe, A. Heterocyclyl pyrazolopyrimidine analogues as JAK inhibitors WO2011/48082, **2011**.

375. Castro Pichel, J.; Fernandez Menendez, R.; Fernandez Velando, E. P.; Gonzalez del Valle, S.; Mallo-Rubio, A. WO2012/49161. **2012**.

376. Boyer, S. J.; Gao, D. A.; Guo, X.; Kirrane, T. M. J.; Sarko, C. R.; Snow, R. J.; Soleymanzadeh, F.; Zhang, Y. Heteroccyclic compounds containing an indole core WO2011/71716 **2011**.

377. Jung, F. H.; Ple, P. Quinoline Derivatives. WO2007099326, **2007**.

378. Matthews, H. R.; Rapoport, H., Differentiation of 1,4- and 1,5-disubstituted imidazoles. *J. Am. Chem. Soc.* **1973**, *95*, 2297-2303.

Appendices

Crystal Data for 4-Nitrophenyl Sulfamate 76

Chemical formula (moiety)	$C_6H_6N_2O_5S$
Chemical formula (total)	$C_6H_6N_2O_5S$
Formula weight	218.19
Temperature	150(2) K
Radiation, wavelength	MoKα, 0.71073 Å
Crystal system, space group	monoclinic, $P12_1/n1$
Unit cell parameters	a = 9.9376(4) Å $\quad$ $\alpha = 90°$
	b = 6.9353(2) Å $\quad$ $\beta = 98.447(4)°$
	c = 12.2078(5) Å $\quad$ $\gamma = 90°$
Cell volume	832.24(5) Å^3
Z	4
Calculated density	1.741 g/cm^3
Absorption coefficient μ	0.388 mm^{-1}
F(000)	448
Crystal colour and size	colourless, $0.30 \times 0.10 \times 0.10$ mm^3
Reflections for cell refinement	3865 (θ range 2.9 to 28.0°)
Data collection method	Xcalibur, Atlas, Gemini ultra
	thick-slice ω scans
θ range for data collection	2.9 to 28.0°
Index ranges	h -13 to 9, k -9 to 8, l -13 to 16
Completeness to $\theta = 26.0°$	99.9 %
Reflections collected	5672
Independent reflections	1860 (R_{int} = 0.0258)
Reflections with $F^2 > 2\sigma$	1678
Absorption correction	semi-empirical from equivalents
Min. and max. transmission	0.8926 and 0.9623
Structure solution	direct methods
Refinement method	Full-matrix least-squares on F^2
Weighting parameters a, b	0.0297, 0.4072
Data / restraints / parameters	1860 / 0 / 136
Final R indices [$F^2 > 2\sigma$]	R1 = 0.0284, wR2 = 0.0702
R indices (all data)	R1 = 0.0328, wR2 = 0.0731
Goodness-of-fit on F^2	1.087
Extinction coefficient	0.0047(13)
Largest and mean shift/su	0.001 and 0.000
Largest diff. peak and hole	0.27 and -0.38 e Å^{-3}

Crystal Data for 4-Methoxyphenyl Sulfamate 79

Chemical formula (moiety) $C_7H_9NO_4S$
Chemical formula (total) $C_7H_9NO_4S$
Formula weight   203.21
Temperature   150(2) K
Radiation, wavelength   MoKα, 0.71073 Å
Crystal system, space group   orthorhombic, $P2_12_12_1$
Unit cell parameters   a = 4.9653(2) Å $\alpha = 90°$
        b = 7.0222(4) Å $\beta = 90°$
        c = 25.0707(12) Å $\gamma = 90°$
Cell volume   874.15(7) Å^3
Z   4
Calculated density   1.544 g/cm^3
Absorption coefficient μ 0.351 mm^{-1}
F(000) 424
Crystal colour and size   colourless, $0.50 \times 0.10 \times 0.10$ mm^3
Reflections for cell refinement   1742 (θ range 2.9 to 27.9°)
Data collection method   Xcalibur, Atlas, Gemini ultra
                thick-slice ω scans
θ range for data collection   3.0 to 28.0°
Index ranges   h −1 to 6, k −6 to 9, l −31 to 24
Completeness to $\theta = 26.0°$ 99.9 %
Reflections collected 2200
Independent reflections   1651 ($R_{int} = 0.0171$)
Reflections with $F^2 > 2\sigma$ 1579
Absorption correction semi-empirical from equivalents
Min. and max. transmission   0.8439 and 0.9657
Structure solution   direct methods
Refinement method   Full-matrix least-squares on F^2
Weighting parameters a, b   0.0408, 0.1032
Data / restraints / parameters 1651 / 0 / 128
Final R indices [$F^2 > 2\sigma$]   R1 = 0.0270, wR2 = 0.0707
R indices (all data)   R1 = 0.0288, wR2 = 0.0723
Goodness-of-fit on F^2 1.066
Absolute structure parameter −0.14(8)
Extinction coefficient 0.007(2)
Largest and mean shift/su   0.000 and 0.000
Largest diff. peak and hole   0.21 and −0.30 e Å^{-3}

Crystal data and structure refinement for Monosaccharide 48.

Identification code	rjg60
Chemical formula (moiety)	$C_8H_{18}N_2O_9S_2$
Chemical formula (total)	$C_8H_{18}N_2O_9S_2$
Formula weight	350.36
Temperature	150(2) K
Radiation, wavelength	MoKα, 0.71073 Å
Crystal system, space group	orthorhombic, $P2_12_12_1$
Unit cell parameters	$a = 7.9595(3)$ Å $\quad\alpha = 90°$
	$b = 9.8112(3)$ Å $\quad\beta = 90°$
	$c = 17.7254(6)$ Å $\quad\gamma = 90°$
Cell volume	1384.22(8) Å^3
Z	4
Calculated density	1.681 g/cm^3
Absorption coefficient μ	0.433 mm^{-1}
F(000)	736
Crystal colour and size	colourless, $0.40 \times 0.30 \times 0.30$ mm^3
Reflections for cell refinement	4135 (θ range 3.3 to 28.5°)
Data collection method	Xcalibur, Atlas, Gemini ultra thick-slice ω scans
θ range for data collection	3.3 to 28.5°
Index ranges	h −8 to 10, k −11 to 13, l −22 to 14
Completeness to $\theta = 25.0°$	99.6 %
Reflections collected	6200
Independent reflections	2944 ($R_{int} = 0.0194$)
Reflections with $F^2 > 2\sigma$	2850
Absorption correction	semi-empirical from equivalents
Min. and max. transmission	0.8458 and 0.8810
Structure solution	direct methods
Refinement method	Full-matrix least-squares on F^2
Weighting parameters a, b	0.0372, 0.2774
Data / restraints / parameters	2944 / 0 / 213
Final R indices [$F^2 > 2\sigma$]	R1 = 0.0259, wR2 = 0.0647
R indices (all data)	R1 = 0.0275, wR2 = 0.0666
Goodness-of-fit on F^2	1.049
Absolute structure parameter	0.03(6)
Extinction coefficient	0.0022(9)
Largest and mean shift/su	0.001 and 0.000
Largest diff. peak and hole	0.24 and −0.29 e Å^{-3}

Crystal data and structure refinement for 411

Empirical formula	$C_{11}H_{12}N_8O_4$
Formula weight	320.29
Temperature/K	100.0
Crystal system	monoclinic
Space group	$P2_1/n$
a/Å	8.3770(9)
b/Å	10.2686(11)
c/Å	17.1922(18)
α/°	90
β/°	100.9530(19)
γ/°	90
Volume/Å^3	1451.9(3)
Z	4
ρ_{calc}mg/mm^3	1.465
m/mm^{-1}	0.991
F(000)	664.0
Crystal size/mm^3	$0.2 \times 0.08 \times 0.05$
Radiation	Cu Kα ($\lambda = 1.54178$)
2Θ range for data collection	10.082 to 132.6°
Index ranges	$-8 \leq h \leq 9, -11 \leq k \leq 12, -20 \leq l \leq 20$
Reflections collected	14908
Independent reflections	2406[R(int) = 0.0350]
Data/restraints/parameters	2406/0/210
Goodness-of-fit on F^2	1.070
Final R indexes [I>=2σ (I)]	$R_1 = 0.0355$, $wR_2 = 0.0901$
Final R indexes [all data]	$R_1 = 0.0364$, $wR_2 = 0.0915$
Largest diff. peak/hole / e Å^{-3}	0.24/-0.23